

**ANNUAL REPORTS ON  
NMR SPECTROSCOPY**

Volume 20

**ANNUAL REPORTS ON**

**NMR SPECTROSCOPY**

This Page Intentionally Left Blank

# ANNUAL REPORTS ON NMR SPECTROSCOPY

Edited by

**G. A. WEBB**

*Department of Chemistry, University of Surrey, Guildford, Surrey, England*

**VOLUME 20**

1988



**ACADEMIC PRESS**

*Harcourt Brace Jovanovich, Publishers*

London · San Diego · New York  
Boston · Sydney · Tokyo · Toronto

ACADEMIC PRESS LIMITED  
24/28 Oval Road,  
LONDON NW1 7DX

*U.S. Edition Published by*

ACADEMIC PRESS INC.  
San Diego, CA 92101

Copyright © 1988 by ACADEMIC PRESS LIMITED

*All Rights Reserved*

No part of this book may be reproduced or transmitted in any form or by any means, electronic or mechanical, including photocopy, recording, or any information storage and retrieval system without permission in writing from the publisher

**British Library Cataloguing in Publication Data**

Annual reports on NMR Spectroscopy, Vol. 20

1. Nuclear magnetic resonance spectroscopy  
—periodicals

541.2'8 QD96.N8.

ISBN 0-12-505320-7

ISSN 0066-4103

Typeset by EJS Chemical Composition, Midsomer Norton, Bath  
and printed in Great Britain by St Edmundsbury Press, Bury St Edmunds, Suffolk

# List of Contributors

Dr Peter P. Edwards, *University Chemical Laboratory, Lensfield Road, Cambridge, CB2 1EW, UK.*

Dr Ahmed Ellaboudy, *University Chemical Laboratory, Lensfield Road, Cambridge CB2 1EW, UK.*

Dr Dolores M. Holton, *University Chemical Laboratory, Lensfield Road, Cambridge CB2 1EW, UK.*

Dr P. G. Morris, *Department of Biochemistry, University of Cambridge, Tennis Court Road, Cambridge CB2 1QW, UK.*

Dr Nicholas C. Pyper, *University Chemical Laboratory, Lensfield Road, Cambridge CB2 1EW, UK.*

Dr A. R. Siedle, *Corporate Research Laboratories/3M, 3M Center, P.O. Box 33221, St Paul, Minnesota 55133-3221, USA.*

Professor B. Wrackmeyer, *Laboratorium für Anorganische Chemie, Universität Bayreuth, Postfach 10 12 51, D-8580 Bayreuth, Federal Republic of Germany.*

This Page Intentionally Left Blank

# Preface

Volume 20 of *Annual Reports on NMR Spectroscopy* consists of accounts covering three main areas of molecular science. NMR of living systems is covered, for the first time in this series, by Dr P. G. Morris. Various aspects of boron NMR are dealt with in two, largely complementary, chapters by Professor B. Wrackmeyer and Dr A. R. Siedle. This topic has previously been reviewed in Volume 12 of this series. The third area to be reported on is that of NMR studies of alkali anions in non-aqueous solvents by Drs P. P. Edwards, A. Ellaboudy, D. M. Holton and N. C. Pyper. It is a great pleasure for me to record my thanks to all of the contributors for their considerable efforts in the preparation of their reports.

*University of Surrey  
Guildford, Surrey  
England*

G. A. WEBB

This Page Intentionally Left Blank

# Contents

List of Contributors . . . . .	v
Preface . . . . .	vii

## NMR Spectroscopy in Living Systems

PETER G. MORRIS

I. Introduction . . . . .	1
II. Sample preparation . . . . .	2
A. Cells . . . . .	2
B. Isolated organs . . . . .	7
C. Intact animals . . . . .	12
III. Localization methods . . . . .	13
A. Introduction . . . . .	13
B. Localized spectroscopy . . . . .	14
C. Spectroscopic imaging . . . . .	19
IV. Measurement of intracellular cations . . . . .	21
A. Introduction . . . . .	21
B. Calcium and zinc indicators . . . . .	22
C. Magnesium indicators . . . . .	26
D. Sodium and potassium measurement . . . . .	28
E. Intracellular pH measurement . . . . .	30
F. Applications . . . . .	33
V. Enzyme kinetics . . . . .	41
A. Introduction . . . . .	41
B. Introduction to magnetization-transfer methods . . . . .	42
C. Saturation-transfer methods . . . . .	43
D. Inversion-transfer experiments . . . . .	46
E. Two-dimensional exchange experiments . . . . .	47
F. Applications and practical difficulties of magnetization-transfer methods . . . . .	49
References . . . . .	51

# Nuclear Magnetic Resonance Spectroscopy of Boron Compounds Containing Two-, Three- and Four-Coordinate Boron

BERND WRACKMEYER

I. Introduction . . . . .	61
II. Experimental . . . . .	63
A. General procedures, referencing . . . . .	63
B. Nuclear-spin relaxation . . . . .	65
III. $^{11}\text{B}$ nuclear magnetic resonance . . . . .	68
A. Chemical shifts, $\delta^{11}\text{B}$ . . . . .	68
B. Substituent effects on $^{11}\text{B}$ -chemical shifts, $\delta^{11}\text{B}$ . . . . .	71
C. Indirect nuclear spin-spin couplings $^nJ(^{11}\text{B}\text{X})$ . . . . .	160
IV. NMR of nuclei other than $^{11}\text{B}$ and $^1\text{H}$ . . . . .	168
A. $^6\text{Li}$ and $^7\text{Li}$ NMR . . . . .	168
B. $^9\text{Be}$ NMR . . . . .	168
C. $^{10}\text{B}$ , $^{27}\text{Al}$ and $^{71}\text{Ga}$ NMR . . . . .	168
D. $^{13}\text{C}$ NMR . . . . .	169
E. $^{29}\text{Si}$ , $^{119}\text{Sn}$ and $^{207}\text{Pb}$ NMR . . . . .	174
F. $^{14}\text{N}$ and $^{15}\text{N}$ NMR . . . . .	175
G. $^{31}\text{P}$ NMR . . . . .	178
H. $^{17}\text{O}$ - and $^{77}\text{Se}$ NMR . . . . .	178
I. $^{19}\text{F}$ , $^{35}\text{Cl}$ and $^{37}\text{Cl}$ NMR . . . . .	180
J. NMR of transition-metal nuclei . . . . .	181
Acknowledgments . . . . .	181
References . . . . .	182

## $^{11}\text{B}$ NMR Spectroscopy

A. R. SIEDLE

I. Introduction . . . . .	205
II. Spectroscopic techniques and general results . . . . .	206
III. Analytical applications . . . . .	208
IV. One-boron compounds . . . . .	209
A. Analogues of pharmacologically active compounds . . . . .	209
B. Cationic boron compounds . . . . .	209
C. Compounds with multiple bonds to boron and small-ring boron compounds . . . . .	212
D. Pyrazaboles . . . . .	217
E. Boron-containing heterocycles . . . . .	219
F. Alkylboranes and related compounds . . . . .	225
G. Other one-boron compounds . . . . .	229

V. Polyboranes and carboranes . . . . .	233
A. B <sub>2,3</sub> boranes and carboranes . . . . .	233
B. B <sub>4</sub> boranes and carboranes . . . . .	235
C. B <sub>5</sub> boranes and carboranes . . . . .	237
D. B <sub>6,8,9</sub> boranes and carboranes . . . . .	240
E. B <sub>10,11,12</sub> boranes and carboranes . . . . .	251
VI. Metalloboranes and metallocarboranes . . . . .	254
A. B <sub>1</sub> metalloboranes and metallocarboranes . . . . .	254
B. B <sub>2,3,4</sub> metalloboranes and metallocarboranes . . . . .	259
C. B <sub>5,7,8</sub> metalloboranes and metallocarboranes . . . . .	263
D. B <sub>9</sub> metalloboranes and metallocarboranes . . . . .	275
E. B <sub>10</sub> and larger metalloboranes and metallocarboranes . . . . .	285
VII. Coupled boranes and carboranes . . . . .	294
VIII. Transition-metal complexes of boron-containing heterocycles . . . . .	299
IX. <sup>11</sup> B NMR studies of solids . . . . .	302
Acknowledgments . . . . .	305
References . . . . .	306

## NMR Studies of Alkali Anions in Non-Aqueous Solvents

PETER P. EDWARDS, AHMED ELLABOUDY,  
DOLORES M. HOLTON and NICHOLAS C. PYPER

I. Introduction . . . . .	315
II. Nuclear shielding in the alkali anions . . . . .	318
A. Assignment of the resonance . . . . .	318
B. Experimental nuclear shieldings relative to gaseous neutral atoms . . . . .	326
C. Reliable calculations of nuclear-shielding differences for gaseous alkali ions . . . . .	327
D. Deduction of the nature of M <sup>-</sup> in solution . . . . .	331
E. Summary . . . . .	332
III. Solution structure of Na <sup>-</sup> probed by relaxation measurements . . . . .	332
A. Experimental results . . . . .	332
B. Theoretical considerations . . . . .	334
C. Quadrupolar relaxation . . . . .	338
D. Summary . . . . .	346
IV. Chemical dynamics in alkali-metal solutions . . . . .	348
A. The sodium anion . . . . .	348
B. Caesium-based species . . . . .	357
V. Overall conclusions . . . . .	362
References . . . . .	364
Index . . . . .	367
Cumulative Indexes for Authors and Subjects, Volumes 11–20 . . . . .	373

This Page Intentionally Left Blank

# NMR Spectroscopy in Living Systems

PETER G. MORRIS

*Department of Biochemistry, University of Cambridge, Tennis Court Road,  
Cambridge CB2 1QW, UK*

I. Introduction . . . . .	1
II. Sample preparation . . . . .	2
A. Cells . . . . .	2
B. Isolated organs . . . . .	7
C. Intact animals . . . . .	12
III. Localization methods . . . . .	13
A. Introduction . . . . .	13
B. Localized spectroscopy . . . . .	14
C. Spectroscopic imaging . . . . .	19
IV. Measurement of intracellular cations . . . . .	21
A. Introduction . . . . .	21
B. Calcium and zinc indicators . . . . .	22
C. Magnesium indicators . . . . .	26
D. Sodium and potassium measurement . . . . .	28
E. Intracellular pH measurement . . . . .	30
F. Applications . . . . .	33
V. Enzyme kinetics . . . . .	41
A. Introduction . . . . .	41
B. Introduction to magnetization-transfer methods . . . . .	42
C. Saturation-transfer methods . . . . .	43
D. Inversion-transfer experiments . . . . .	46
E. Two-dimensional exchange experiments . . . . .	47
F. Applications and practical difficulties of magnetization-transfer methods . . . . .	49
References . . . . .	51

## 1. INTRODUCTION

*In vivo* spectroscopy emerged as a viable technique in 1973 when it was demonstrated that well-resolved  $^{31}\text{P}$  NMR spectra could be recorded from suspensions of intact red blood cells.<sup>1</sup> In the following year similar spectra were recorded from intact tissue—a freshly excised muscle from the hind limb of a rat.<sup>2</sup> At the same time, NMR imaging techniques were being developed by Lauterbur<sup>3</sup> in SUNY at Stonybrook and by Mansfield<sup>4</sup> in Nottingham. These techniques were to develop within a decade into

arguably the most powerful diagnostic modality of the 1980s<sup>5</sup>—magnetic-resonance imaging or MRI. *In vivo* spectroscopy too has developed into a full-blown clinical diagnostic technique. However, the main thrust of scientific endeavour in this case has been concerned with the development of a biochemical understanding of normal and pathological states. These more fundamental objectives have meant that isolated tissue and animal models have retained their importance. Indeed, interest in them is increasing rapidly, stimulated by possible future clinical applications. The development of MRI and *in vivo* spectroscopy (sometimes referred to by clinicians as magnetic-resonance spectroscopy or MRS) have proceeded in parallel, with rather little in the way of cross-fertilization. Thus on several occasions scientists developing MRI methods have rediscovered (and generally renamed) pulse sequences well known to high-resolution spectroscopists. Equally, the value of selective excitation methods for conventional NMR is only just beginning to be appreciated with the advent of the first generation of high-resolution spectrometers equipped with this capability.

In the first three years since “NMR of Living Systems” was reported on in the Royal Society of Chemistry’s Specialist Reports on NMR, the volume of literature (MRI and spectroscopy taken together) has doubled each year, eventually necessitating a narrowing of the field of review to exclude clinical MRI. The policy that has been adopted for the present review is to concentrate exclusively on *in vivo* spectroscopy. MRI is discussed only in cases where it is directed towards this end, i.e. chemical-shift imaging. For those interested in gaining an understanding of MRI techniques, several books are available.<sup>6–11</sup> Literature searches, including clinical applications, can be most productively conducted on the MEDLINE database. The emphasis in this chapter is on descriptions of techniques with more selective examples of their application. Greater accent is given to important emerging techniques, e.g. new methods for intracellular cation measurement, and to topics that have not themselves been subject to recent review. A comprehensive account of NMR studies in living systems is not intended: such an undertaking would require a work of several volumes. For those wishing to keep abreast of the rapidly expanding literature in this area, the SPRs on NMR are recommended.

Of the NMR nuclei that are of biomedical importance, <sup>31</sup>P remains the most popular by far, both for animal studies, and for clinical applications.<sup>12,13</sup> <sup>13</sup>C methods continue to be widely used in the elucidation of biochemical pathways and in the measurement of fluxes through them.<sup>14</sup> This is particularly the case for microorganisms, where uncertainty in this area still remains. Such methods have been used less widely *in vivo*,<sup>15</sup> where the high cost of labelled compounds and the relatively low sensitivity of <sup>13</sup>C

have proved prohibitive. Indirect observation via coupling to  $^1\text{H}$  offers some improvement,<sup>16</sup> at least in the latter respect.

Perhaps the biggest growth area in this field is in the direct application of  $^1\text{H}$  NMR. The attraction here is clearly the high inherent sensitivity and universality of this nucleus. What has held back its development so far has been the concern over spectral complexity and, more importantly, a major dynamic-range problem. Thus it is often necessary to observe metabolites at concentrations  $<1\text{ mM}$ , in the presence of  $100\text{ M}$  water, a dynamic-range problem of some five orders of magnitude. Sophisticated solvent-suppression methods<sup>17</sup> are making some inroads, particularly when combined with spin-echo techniques.<sup>18,19</sup> However, there is a second suppression problem, which arises from the broad  $-\text{CH}_2-$  resonance of mobile lipids present at concentrations up to  $1\text{ M}$ . This is a particularly thorny problem since this spectral region includes many resonances that are of interest. Suppression techniques therefore need to be very "clean". The complexity of  $^1\text{H}$  NMR spectra is now seen as less of an embarrassment. However, spectral editing techniques are available if required.<sup>18,20</sup> Since these rely on difference methods, they also serve to alleviate the solvent-suppression problems.

It is likely that there will be sustained growth throughout the field of "NMR of Living Systems", with  $^1\text{H}$  studies figuring more prominently once the dynamic-range problems are successfully overcome.

## II. SAMPLE PREPARATION

### A. Cells

For biological systems, the only acceptable means of combatting the fundamental insensitivity of the NMR technique are to work at high field and to use large samples. Ideally, the largest volume consistent with adequate resolution should be employed. The sample also needs to be in its most "concentrated" form: in the case of cellular systems this means high cell densities, typically in the range  $10^7$ – $10^{12}\text{ cells ml}^{-1}$ . Maintaining such a "sludge" of cells *in situ* and in a viable condition are difficult problems, which have not yet been resolved entirely to everyone's satisfaction, as evidenced by the continually growing literature on the subject.

Three basic requirements have to be met: (i) the cells must be kept in uniform suspension throughout the NMR-sensitive volume; (ii) they must be suitably perfused so that nutrients are delivered and waste products eliminated; (iii) in the case of aerobic cells, adequate oxygenation must also

be ensured. It is of course important that the medium chosen be appropriate to the cell type under study and that adequate pH buffering be provided.

Various techniques have been suggested for preventing sedimentation. Gentle stirring with a motor-driven propeller works reasonably well.<sup>21</sup> (See Fig. 1 and refs 22 and 23 for a description of hardware developed for tissue superfusion but which is also useful for cell studies.) A gentle cyclic pump

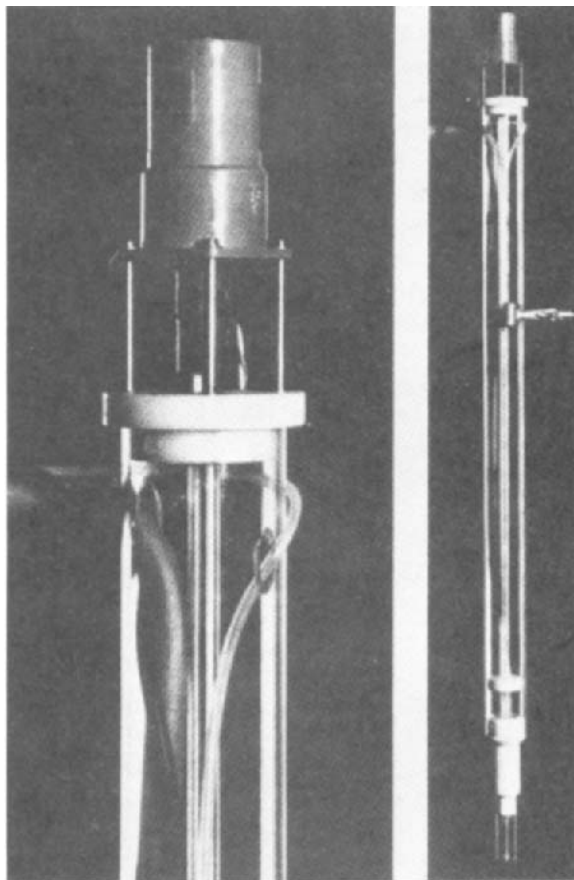


FIG. 1. Tissue superfusion apparatus. Tissue slices are maintained in uniform suspension in the 25 mm NMR tube (lower right) by a combination of the upward current from circulating perfusate and gentle stirring with a motor-driven paddle. Perfusate is introduced via a water-jacketed line (detail, left side) and is removed at a higher level by suction through a second unjacketed line (detail, right). A perforated PTFE disc safeguards against accidental loss of tissue. The PTFE plug retaining the NMR tube mimics a conventional spinner, enabling the assembly to be used with a conventional 25 mm probehead. From ref. 23.

action is also efficacious. One good solution recently described is the use of density-matching techniques.<sup>24</sup> Addition to the suspension medium of the polysaccharide arabinogalactan has been demonstrated to be effective. If the cell suspension is to be studied under aerobic conditions, the simplest procedure is to gas the cells *in situ* with O<sub>2</sub> (or 95% O<sub>2</sub>:5% CO<sub>2</sub> if a bicarbonate buffer is employed). This has the benefit of keeping the cells in suspension. However, streams of bubbles can adversely affect the field homogeneity and often, though not invariably, present problems. Smaller bubbles are generally less disruptive, and so fine jets or sinters are the order of the day. Another possibility is to gate the bubbling so that it takes place outside the period of signal acquisition.<sup>25</sup> Fluid-logic needle valves and solenoids are especially useful for setting this up.

If medium- or long-term studies are envisaged (and the lack of sensitivity normally makes them necessary), some form of perfusion system will be required. Given that this is the case, it is then sensible to conduct the oxygenation in a region remote from the cell chamber. If there is no sample limitation (large numbers of cells are readily available), it is possible to circulate the entire cell suspension. Provided this is done sufficiently rapidly that the contents of the sensitive volume are exchanged on a timescale short compared with the  $T_1$ s of the species under study, sensitivity advantages also accrue.

Usually cells are not available in such abundance and it is necessary to circulate the medium through the cell suspension. The problem is then one of constraining the cells. Several ingenious solutions have been advanced. Dialysis fibre bundles are extremely efficient<sup>26,27</sup> and can conveniently be obtained from kidney-dialysis fibre mats. However, cellulose acetate fibres are rather delicate and prone to fracture. They should therefore be used with caution; leakage protection should always be provided. An extra level-maintaining suction line is a suitable security device. For anchorage-dependent cells it is possible to culture the cells on polymeric membrane tubes through which the perfusate is circulated.<sup>28</sup> See ref. 29 for a general review of tissue culture by perfusion through artificial capillaries. An alternative strategy for anchorage dependent cells is to attach them to autoclaved microcarrier beads.<sup>30,31</sup> After growth to the required cell density, the beads are transferred to the NMR chamber and are held in place during perfusion with fine-mesh screens. Another strategy, applicable to a wider range of cells systems, including surface-independent cultures, is the use of agarose gel threads.<sup>32-35</sup> Cells are mixed with low-gelling-temperature agarose solution at 37°C and are then coextruded under mild pressure through Teflon tubes immersed in an ice/water bath. Cell concentrations comparable to those of dense cell suspensions can be achieved and the small diameter (0.5 mm) of the threads ensures proper

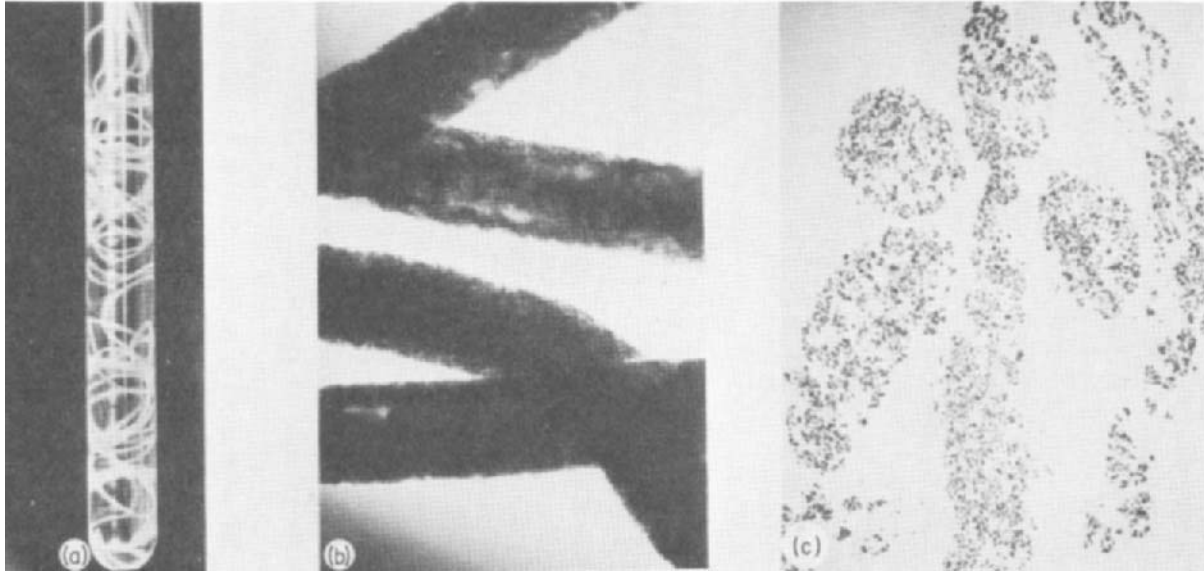


FIG. 2. (a) The gel threads containing the cells were extruded through thin tubing into the growth medium containing 20 mM Hepes buffer, which was maintained at pH 7.35–7.40. (b) Phase-contrast microscopy ( $\times 100$ ) of the gel threads, showing a high density of fibroblasts throughout the gel matrix. (c) Paraffin-block sections ( $7\text{--}8\mu\text{m}$ ) of the gel threads, fixed with Bouin's stain. Intact nuclei with prominent nucleoli in the cells are visible. From ref. 35.

perfusion. Diffusion of nutrients to the centre of the thread typically requires about 1 min. The spaghetti-like nature of this preparation is illustrated in Fig. 2. The technique has been successfully demonstrated both with yeast<sup>33</sup> and with mammalian cells (chinese hamster lung fibroblasts<sup>35</sup>).

## B. Isolated organs

### 1. Non-perfusion techniques

Isolated organs are well-suited to NMR study since specialist equipment is not essential and it is often possible to make use of conventional probeheads by replacing the NMR sample tube with a suitably equipped organ bath.

The simplest possible way in which to conduct an NMR experiment on an intact organ is to surgically remove it and place it in an NMR tube, perhaps surrounded by medium. Indeed, a simple <sup>31</sup>P NMR study of excised muscle was the experiment that first drew the attention of the scientific world to the possibilities of the technique.<sup>2</sup> Such crude methods are generally not very useful since, deprived of the normal provision of oxygen and nutrients through the vascular system, the organ quickly perishes. Amphibian muscle, however, is a notable and very useful exception. Frog gastrocnemius muscles excised under refrigerated conditions and placed in Ringer maintained at 4 °C remain viable for many hours. With a stimulation system and a force transducer for measuring developed tension, such muscles can be studied during anaerobic exercise. Pioneering work<sup>36-38</sup> on frog muscle with the apparatus illustrated in Fig. 3 (now in the London Science Museum but still functional and occasionally called into service!) demonstrated the benefits of combining <sup>31</sup>P NMR determinations of bioenergetic status and intracellular pH (see Section IV) with standard physiological measurements.

Simple bathing of an intact organ in Ringer is, as discussed, not generally appropriate if one is seeking to preserve normal physiological and metabolic status. However, it is entirely appropriate for model studies of transplant organs, such as the kidney, where it is precisely the time course of this deterioration that is of interest.<sup>39,40</sup> It is also useful for tissues that are naturally poorly perfused (e.g. the eye lens<sup>41,42</sup>) and thin (e.g. the retina<sup>43</sup>) or for whole intact organisms of a predominantly single tissue type that can be studied *in vivo*. An example of the latter case, which gives beautifully resolved <sup>31</sup>P NMR spectra, is the liver fluke *Fasciola hepatica*.<sup>44-47</sup>

Tissues can often be maintained in good condition using superfusion techniques in which oxygenated medium (e.g. Krebs-Henseleit buffer<sup>48</sup>) is circulated around the tissues (rather than through the vascular system in a true perfusion experiment). This works well for naturally thin tissues or for

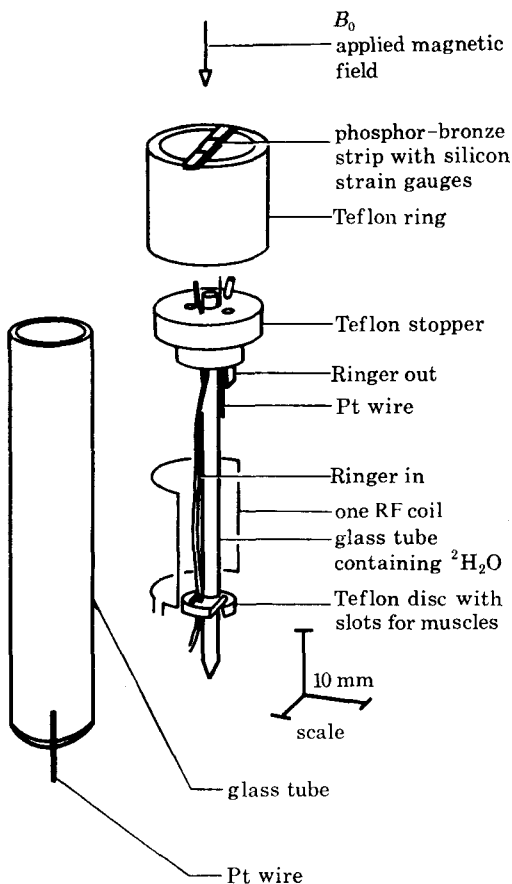


FIG. 3. Design of experimental chamber for isolated-skeletal-muscle studies. The volume in which the NMR measurement is made is roughly defined by the two single-turn radio-frequency (RF) coils, only one of which is shown in the diagram. From ref. 36.

tissue slices. The latter have been widely used in the study of brain metabolism, for which there is no suitable perfusion model. Slices are typically cut to a thickness of 0.3 mm to give the best compromise between adequate oxygenation and minimal tissue damage.<sup>49</sup> Slices remain metabolically active for many hours (typically >10) and are capable of electrophysiological response. Suitable superfusion apparatus for NMR study is illustrated in Fig. 1.<sup>22,23</sup> A similar superfusion arrangement, which recirculates air-saturated medium at rates of about  $2.5\text{--}3\text{ ml min}^{-1}$  has also been described<sup>50</sup> and used for studies of higher plant tissues.<sup>51</sup>

## 2. *Perfusion techniques for the heart*

Perfusion techniques enable a wider range of organs to be studied. A useful source of reference is the book by Ross.<sup>52</sup> Many of the classic methods described therein can be used for NMR studies with little modification other than an extension of the "umbilical" lines, which is necessary to keep the ferromagnetic perfusion hardware away from the magnet!

The first NMR perfusion experiments were conducted on isolated rat hearts<sup>53-56</sup> at about the same time as the first muscle studies. The heart is now by far the most commonly studied organ. Almost invariably, Langendorff perfusion methods are employed. These involve cannulation of the aorta and retrograde circulation of oxygenated medium. The aortic valve is maintained shut by the perfusion pressure and medium is forced through the coronary arteries. It is vitally important to ensure that the flow rates are sufficiently high. Inadequate perfusion manifests itself in poor phosphocreatine-to-ATP ratios.<sup>57-60</sup> In guinea-pig hearts, for example, this ratio increases from 0.64 at a perfusion rate of 0.6 ml min<sup>-1</sup>, reaching a plateau value of 1.82 at 3.8 ml min<sup>-1</sup>.<sup>60</sup> We find that a good guide is to perfuse at a rate of 4 ml min<sup>-1</sup> (g wet wt)<sup>-1</sup>.<sup>57</sup> Equally, excessive perfusion pressure is to be avoided. All workers to date have perfused with Ringer solution rather than with whole blood. The use of whole blood or the addition of albumin or the polysaccharide dextran to the perfusion medium has occasionally been advocated as a means of reducing the imbalance in osmotic pressure. Oedema is certainly very noticeable over the timescale of most NMR studies. Problems with frothing during oxygenation have led the majority of researchers to work with the simple medium, however. To achieve stable preparations, great care is necessary to ensure the complete removal of debris by using a suitable filter cascade. Bubbles are also a problem, and it is essential to include a bubble trap. Temperature regulation also requires attention. The normal gas-flow system supplied with high-resolution spectrometers is woefully inadequate and quite unable to cope with a flow-through situation. Water-jacketed perfusion lines solve the problem, delivering the perfusate at working temperature. Heating downstream of the bubble trap is to be avoided.

Very often it is desirable to monitor the left-ventricular pressure. This can be conveniently achieved with the aid of a balloon catheter and pressure transducer.<sup>54</sup> If pacing is required and conventional wire electrodes are to be used then RF filters will generally (though not always) be needed to avoid interference with the RF channel.<sup>57</sup> Alternatively, high-impedance lines can be sewn onto the heart. NMR preparations differ from conventional ones in that it is normal practice to immerse the heart in medium, maintaining the level well above the height of the receiver coil with a suitable suction line.

This greatly reduces the magnetic-field perturbation. (A tissue/medium interface represents less of a magnetic-susceptibility mismatch than a tissue/gas one). Shimming using the  $^1\text{H}$  FID from the perfusate is then a relatively straightforward matter, even with a single-coil probe tuned to some other nucleus (e.g.  $^{31}\text{P}$ ).<sup>61</sup> The  $^1\text{H}$  signal is normally so great that the gross RF mismatch does not cause problems. Should it do so, a transmission-line circuit can be used to retune to the new frequency.<sup>62</sup> Quantitation is the perennial problem in *in vivo* NMR. It can be addressed with the aid of external standards, preferably sealed within the organ bath. Suitable compounds for  $^{31}\text{P}$  studies have been advocated.<sup>58,59</sup>

To obtain spectra synchronous with the cardiac cycle, it is possible to gate the NMR acquisition from the ECG or from the systolic pressure wave.<sup>63</sup> Such methods allow NMR acquisition to remain in step with irregularly beating hearts. However, variable interpulse intervals can be problematic if spectra are not acquired under fully relaxed conditions. An alternative arrangement is to drive the heart using trigger pulses generated from the host computer of the NMR spectrometer.<sup>57</sup> To achieve low stimulation rates by this method, it is necessary to destroy the main endogenous pacemaker activity by crushing or removing the sino-atrial node.

To look at the response of the preparation to different conditions simply requires a switch over of perfusion media. If necessary, these changes can be automated. Such methods have been used to follow the response to carefully controlled periods of anoxia.<sup>64</sup> As discussed, the vast majority of NMR cardiac studies are conducted on Langendorff preparations. Other heart preparations are available, however, and have been used to vary the work load to which the heart is subjected.<sup>63,65</sup>

### 3. *Perfusion techniques for other organs*

Of the mammalian organs, other than the heart, the liver is perhaps the next simplest to perfuse,<sup>66</sup> involving only portal venous and venous cannulation. (It is important to avoid metal cannulae—PTFE is suitable.) A typical arrangement for perfusion of the isolated rat liver is illustrated in Fig. 4.<sup>67</sup> Several other preparations have been described.<sup>66-71</sup> For the liver, it is necessary to perfuse with blood: Iles *et al.*<sup>67</sup> used expired human erythrocytes resuspended in Krebs-Henseleit buffer containing 3% of bovine serum albumin to give a final packed cell volume of approx. 0.17. Stringent safeguards against perfusion leaks are essential! In wider-bore magnets it is also possible to perfuse the liver *in situ*.

Kidney perfusions are slightly more difficult to set up. NMR kidney studies were pioneered by the Oxford group under Professor Radda in the

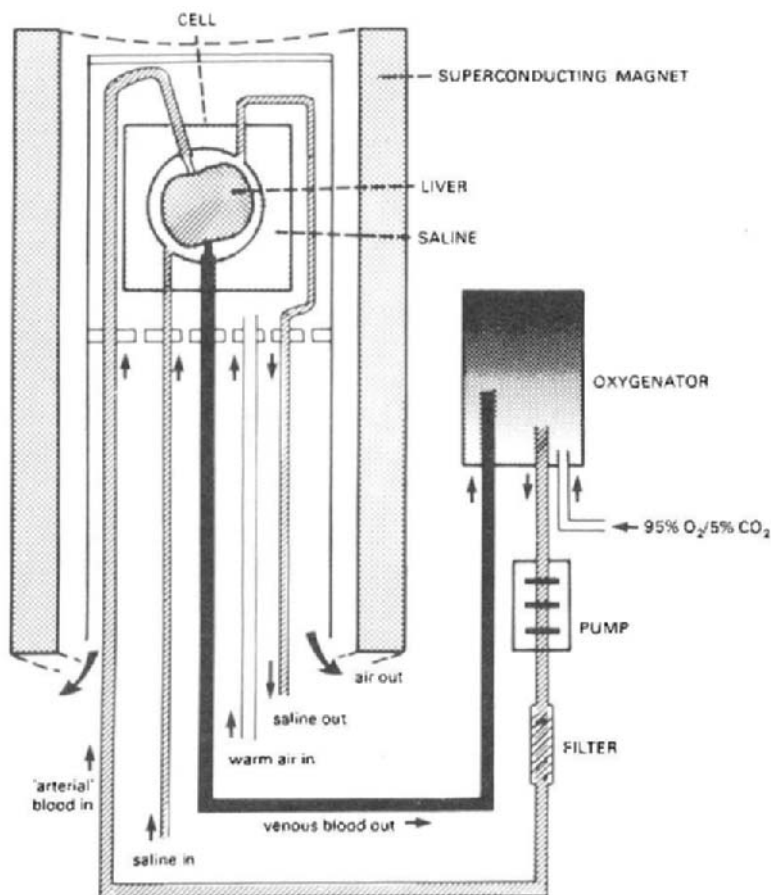


FIG. 4. Circuit for perfusion of the rat liver in the NMR spectrometer. The perfusion medium consisted of Krebs buffer pH 7.4 containing erythrocytes (packed cell volume 17%) and albumin (3%). The interior of the probe was maintained at 37°C, and the oxygenator and filter were contained in a Perspex box maintained at 39°C. The flow rate was  $7\text{--}8\text{ ml min}^{-1}$  ( $100\text{ g body wt}^{-1}$ ). From ref. 67.

early 1980s.<sup>72–75</sup> See ref. 76 for a diagram of one of their kidney-perfusion systems. Other kidney studies have since been reported.<sup>77,78</sup> Cannulation of the ureter enables physiological function to be monitored simultaneously with metabolism.

Mammalian muscle presents something of a problem. Generally it is studied *in situ*. Only one perfusion system suitable for NMR studies has been

described.<sup>79</sup> Arterial perfusion was used to compare <sup>31</sup>P NMR spectra from cat biceps brachii (>75% fast twitch, glycolytic) and soleus (>92% slow twitch, oxidative). Higher phosphocreatine/*P<sub>i</sub>* ratios were observed in the biceps, where the free ADP concentration was estimated to be <1 μM compared with 14 μM in the soleus. (These estimates are made by determining the concentration of the remaining species participating in the creatine kinase reaction, which is assumed to be at equilibrium.) Intracellular pH measurements (see Section IV) gave a value of 7.0 in both systems. Small muscles (e.g. mouse or immature rat soleus muscles) can be studied by superfusion methods.<sup>80</sup> Smooth muscle, including the uterus, has also been studied by this method.<sup>81</sup>

### C. Intact animals

Perfused-organ studies are extremely valuable: they are relatively simple to conduct and give information on the metabolism and function of an organ free from its normal complex regulatory system. Nevertheless, it is important to show that the *in vitro* observations can also be demonstrated *in vivo*. Ideally, the animal should be monitored in as natural a state as possible, with no surgical intervention. Such experiments require NMR localization techniques to select the region of interest. (These are discussed in the subsequent section.) Even in this case, however, restraint and anaesthesia are generally required, and it should be recognized that this in itself can alter metabolic behaviour, particularly in the brain.<sup>49</sup> See ref. 82 for an NMR example of the metabolic consequences of exposure to 1% halothane.

Surface coils offer a simple non-invasive means of studying brain metabolism *in vivo*<sup>83-87</sup> They are also widely used for skeletal muscles and for liver.<sup>88-89</sup> However, in the latter case, it is common practice to open the animal's abdomen and place the surface coil directly on the liver (with a non-conducting film interposed) to ensure that all signal originates from it alone. Alternatively, chronically implanted coils can be used.<sup>90</sup> For *in vivo* heart studies, localization is more of a problem, and both open-chest procedures,<sup>91</sup> with the heart placed in a solenoidal coil, and implanted coils<sup>92</sup> have been described. An interesting elliptical catheter receiver coil has also been reported.<sup>93</sup> It can be passed through peripheral blood vessels and has been used to obtain <sup>31</sup>P spectra of acceptable *S/N* in <7 min from defined regions within a canine heart.

For clinical studies, even minor surgical intervention is generally unacceptable. Careful attention to proper localization schemes is thus essential.

### III. LOCALIZATION METHODS

#### A. Introduction

As discussed in Section II, studies of isolated organs present no major difficulties, and, with relatively minor modification, it is possible to make use of conventional probeheads. Since samples do not need to be exchanged or spun, and homogeneity requirements are less severe, it is not necessary to adhere to the usual saddle arrangement for receiver coils. At low frequencies, transverse solenoids offer a  $\sqrt{3}$  sensitivity advantage,<sup>94,95</sup> while at high frequency, cavity or hybrid designs come into their own. Of course, it is possible to record NMR spectra from intact biological systems in the same simple fashion as used for isolated organs. However, such studies are rarely informative, giving metabolic profiles averaged in a meaningless way over the disparate tissues of the organism. Controlled localization is clearly essential. Many suitable methods have been advocated, ranging from the simple localization afforded by the geometry of the receiver coil to four-dimensional chemical-shift-imaging schemes. Before entering into detailed discussion of these different techniques, a list of desirable features is given. Thus, in rough order of priority one might hope for:

- (1) the highest NMR sensitivity per unit time, per unit volume;
- (2) the minimum experiment time;
- (3) accuracy of localization:
  - (i) location,
  - (ii) shape of sensitive volume;
- (4) ease of implementation.

Note that feature (2) may simply be the signal averaging time required to achieve acceptable  $S/N$ . In this circumstance it will be dictated by (1). However, this is not necessarily the case, particularly for imaging schemes that require multiple FIDs to be recorded with different combinations of field gradients in order to achieve their spatial discrimination. In this situation one often speaks of a minimum performance time for the localization procedure.<sup>11,96</sup> Accuracy of localization has two distinct aspects. First, there is the question of where the sensitive volume is located, and secondly, what its shape is. For imaging schemes the relevant parameter is spatial resolution. This at first sight appears to be a simple concept, but the detailed distribution of signal over the pixel and "leakage" into adjacent pixels needs to be taken into account in a proper treatment.<sup>97</sup> Ease of implementation includes both the hardware requirements and simplicity of use. Other factors that it might be important to take into account include the necessity for the presence of switched field gradients, which give rise to deleterious

eddy-current effects in the bore of a superconducting magnet, and the possibilities for combining the method with other NMR spectroscopic techniques, in order, for example, to measure enzyme kinetics by magnetization transfer (see Section V).

Simple volume-selection techniques were the first to be used for *in vivo* spectroscopy. Thus surface coils, originally introduced by Morse and Singer in 1970<sup>98</sup> for flow measurement, were adapted for *in vivo* use in 1980.<sup>99</sup> High-resolution <sup>31</sup>P spectra were obtained from skeletal muscle and brain in anaesthetized rats. A roughly contemporary development was the method of topical magnetic resonance, TMR (Greek *τοπος* = place).<sup>100</sup> This is a static field profiling technique essentially similar to Damadian's FONAR (field focusing nuclear magnetic resonance) method of NMR imaging.<sup>101</sup> Many of the other standard NMR imaging methods can be modified to retain chemical-shift information. Thus, as early as 1975, Lauterbur *et al.*<sup>102</sup> were able to demonstrate a projection- reconstruction-based chemical-shift-imaging system. Many other schemes have been reported including those for sensitive point<sup>103</sup> and echo-planar<sup>104</sup> imaging methods. However, the method lending itself most naturally to chemical-shift studies is Fourier imaging. Maudsley *et al.*<sup>105</sup> described the appropriate extension of Fourier imaging in 1979. However, the extra dimension was used in their case to record the variable frequency of a single resonance in order to generate a magnetic-field map. Many Fourier-based schemes now exist in both conventional and rotating-frame guises, giving one-, two- or even three-dimensional spatial resolution.

The discussion of localization techniques has been divided into two sections, the first dealing with schemes that look at a single volume element (localized spectroscopy) and the second with schemes that give one or more dimensions of localization by applying imaging methods. All available spectroscopic imaging methods as of 1985 have been evaluated and critically reviewed elsewhere.<sup>106</sup> Only those methods that are widely used or that have particular benefits to commend them are discussed here.

## B. Localized spectroscopy

### 1. Surface coils

There is little mystery surrounding the construction and practical use of a surface coil. In its simplest form it consists of a single loop of copper wire that is placed over the organ of interest. To a first approximation, it will receive signal from a hemispherical region lying immediately beneath it. Unfortunately this apparent simplicity is deceptive and is not borne out by theoretical analysis. In reality,  $B_1$  varies considerably over the hemi-

spherical region (see ref. 11, p.193 for field expressions), falling rapidly with axial distance from the coil centre. Thus as the RF pulse length is increased, the selected volume changes, penetrating more deeply into the sample.<sup>107</sup> Equally, if the pulse rate is varied, the degree of saturation will alter, and this again will lead to a change in the shape of the excited volume.<sup>107-109</sup>

Surface coils are extremely effective when applied in the right context, i.e. to peripheral tissues such as skeletal muscle, liver or brain. Even in such favourable situations, they must be used with caution, however. For example, *in vivo* <sup>31</sup>P spectra purporting to originate from human brain<sup>110,111</sup> have been shown to contain significant contributions from facial muscle.<sup>112,113</sup> It should be noted, however, that paediatric brain studies, which have been so successful in assessing the severity in cases of birth asphyxia, are relatively free from such problems. The main reason is that facial tissue represents only a very small fraction of the volume observed (large surface coils are used). Additionally, some protection can be achieved by setting the flip angle to 180° at the centre of the coil.

Any unwanted contribution from surface muscle in <sup>31</sup>P liver spectra is immediately apparent because muscle has phosphocreatine present at typically 20 mm whereas it is absent in liver. Often this fact has been used as a tissue marker or "aid to navigation"—there is no phosphocreatine present, so I must be looking at the liver! While such a strategy is acceptable at the development stage, it does not fulfil one's criteria for accuracy of location—it is greatly preferable to be able to state "I am looking at the liver and there is no phosphocreatine."

If used with care, the humble surface coil is extremely effective. Much of the popularity and success it enjoys derives from the excellent sensitivity it affords. This is due in part to the fact that the noise originates only from that volume of tissue which contributes signal. This is in contrast with the situation with larger coils, where noise originates from the entire volume even though the signal may derive from a small region within it.

With proper calibration using phantoms, it is possible to estimate absolute concentrations.<sup>114</sup> The method involves the use of multiply tuned surface coils to compare the X nucleus signal with the <sup>1</sup>H signal from water. *T*<sub>1</sub> determinations are possible and pose no particular problems provided that full three-parameter fitting is employed.<sup>115</sup> Saturation<sup>116,117</sup> or even inversion<sup>118</sup> transfer using depth pulses (see below) or DANTE trains (see Section V) of composite pulses can also be accommodated.

For all their simplicity in use, the volume excited by a surface coil is complex in nature and difficult to move about. Deeper penetration can be achieved by increasing the pulsewidth, and Faraday shields can sometimes help,<sup>119</sup> but the situation really calls for greater control. This has often been achieved by combining the use of surface coils with other techniques. Some

of the more potent of these combinations are discussed below. The most successful means of improving the spatial response of the surface coil itself is through the use of "depth pulses". These were introduced by Bendall and Gordon in 1983<sup>120</sup> and utilize the inhomogeneity of the  $B_1$  field. They select the volume corresponding to a particular  $B_1$  value by averaging out signals from all regions where  $B_1$  differs from this value, using sophisticated phase-cycling schemes, the first of which were based on the EXORCYCLE scheme of Bodenhausen *et al.*<sup>121</sup> The simplest depth pulse consists of a  $\theta$  pulse followed, after a short interval, by a phase-cycled  $2\theta$  pulse. When four echoes of the full phase cycle are summed, enhanced signal is obtained from regions where the pulse angle is a multiple of  $90^\circ$ . Outside these regions it is suppressed. In this simple case the dependence on pulse angle is squared relative to that of a single pulse. More sophisticated depth-pulse schemes<sup>112-126</sup> give greater selectivity, for example to  $\pm 16\%$  of the optimum flip for a 24-pulse sequence and  $\pm 9\%$  for an 80-pulse variant.

Schemes using composite pulses<sup>127,128</sup> have been suggested for the improvement of the spatial response of surface coils. In the NOBLE (*n*arrowband for *l*ocalization of *e*xcitation) method of Tycho and Pines<sup>129</sup> only two acquisitions are required. In one, a composite  $180^\circ$  pulse precedes the normal excitation pulse, giving inversion in a selected region of the sample. This signal can be subtracted from a normal FID (the second acquisition) to leave signal originating predominantly from the selected region. Shaka and Freeman<sup>130</sup> have suggested similar schemes using composite pulses with phase cycling. A further composite-pulse selective scheme has recently been contributed by Hetherington *et al.*<sup>131</sup> Bendall and Pegg<sup>132</sup> have shown that these composite-pulse schemes are formally related to the earlier depth-pulse sequences and in their present form do not offer significant advantages over them.

## 2. Topical magnetic resonance

Topical magnetic resonance is a method of magnetic field profiling developed specifically for *in vivo* spectroscopy by Oxford Research Systems.<sup>100</sup> In essence, it achieves localization through the application of high-order field gradients (typically  $z^2$  and  $z^4$ ) to degrade the homogeneity of the static magnetic field outside a small central homogenous volume. See the review by Gordon *et al.*<sup>133</sup> for a detailed description.

Spectra recorded from a TMR system consist of two components: a well-resolved spectrum from the central "sweet spot" and a broad one from the surrounding inhomogeneous region. The latter can be removed using convolution difference methods, which were originally suggested for NMR

use by Campbell *et al.*,<sup>134</sup> see also the reviews by Lindon and Ferrige<sup>135</sup> and Gordon *et al.*<sup>133</sup> for more sophisticated variants.

The gradients that give the localization are generated by special profiling coils. High current densities are required, and although some adjustment of sensitive volume is possible, systems are normally designed with a particular volume in mind. A further restriction stems from the fact that the location of the sensitive volume is fixed; it is therefore necessary to ensure that the region of interest is moved to coincide with it.

TMR has been useful in the study of deep-seated organs. It can also be used in combination with surface coils but is nowadays losing ground in its popularity to imaging-based methods.

### 3. Volume-selective excitation

Volume-selective excitation, as the name implies, makes use of selective pulses to achieve localization. Selective pulses were originally proposed by Garroway, Grannell and Mansfield in 1974.<sup>136</sup> The logic behind their development is illustrated in Fig. 5. In (a) a "hard" broadband pulse, as used in conventional high-resolution NMR, excites a wide spectrum, ideally in a uniform manner. The extent of this excitation is inversely related to the pulsewidth. Thus a 1  $\mu$ s pulse leads to an excitation bandwidth of about 1 MHz. In order to restrict the excitation bandwidth, longer pulses can be used. Thus a 10 ms pulse would give a 100 kHz bandwidth (b). However, the excitation is far from uniform. In fact, it approximates to the Fourier transform of the "top-hat" pulse and is therefore sinc-shaped. The final step in the argument is simply to reverse this situation; i.e. a sinc-shaped RF pulse is applied in the hope of achieving a square excitation profile (c). If this procedure is carried out in the presence of a magnetic field gradient, frequency selection will correspond to spatial selection (see the discussion in ref. 11 for details). Unfortunately, the spin system does not respond in a linear fashion, though it approximates this behaviour for small flip angles. Sinc pulses therefore do not generate perfectly square profiles. Nevertheless, they can be improved by modification<sup>137-139</sup> and have been widely applied for plane selection in NMR imaging.

Such pulses can also be used in combination with surface coils,<sup>140</sup> greatly improving the control over localization that can be achieved. To a first approximation, selective pulses can be thought of as isolating a plane within the hemispherical volume defined by the surface coil. This method, dubbed DRESS (*depth-resolved surface-coil spectroscopy*) is effective and has been used for human *in vivo* studies of brain and heart.<sup>141</sup> A multiplanar version, known as SLITDRESS, has also been proposed.<sup>142</sup>

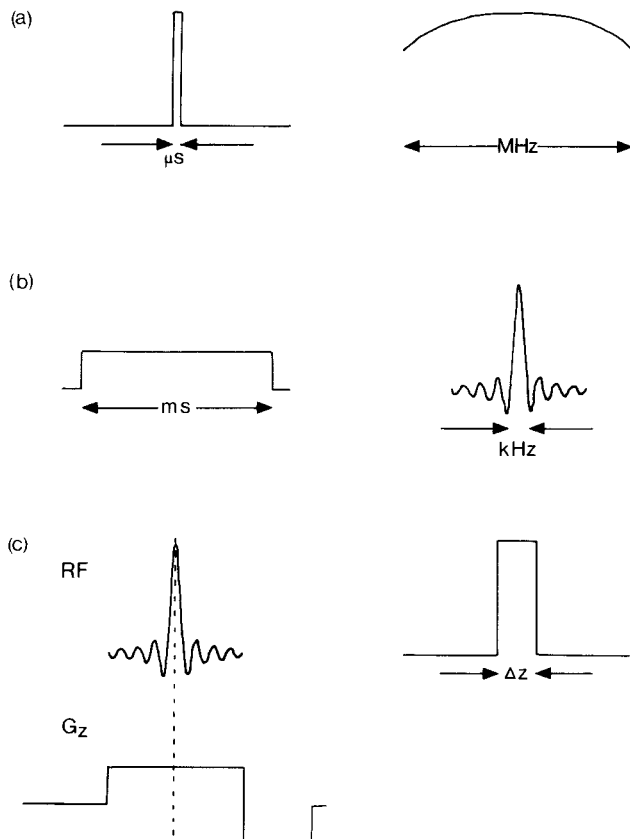


FIG. 5. Selective pulses and their Fourier transforms: (a) hard pulse; (b) soft pulse; (c) sinc pulse.

In order to select a volume element using selective excitation alone, three such pulses need to be applied, corresponding to spatial restriction in each dimension. Post *et al.*<sup>143</sup> have reported useful composite selective pulses consisting of a selective  $45^\circ$ , broadband  $90^\circ$ , phase-shifted by  $180^\circ$  relative to the selective pulse, selective  $45^\circ$  sandwich. In the selected slice spins are nutated through  $45^\circ$  by the first selective pulse, switched to  $-45^\circ$  by the hard  $90^\circ$  pulse and restored to the  $z$ -direction by the final selective pulse. Outside the selected slice, spins are unaffected by the selective pulses, but are nutated into the  $(x,y)$ -plane by the broadband pulse. This magnetization rapidly dephases in the applied field gradients. Two such composite pulses, applied consecutively, will result in a strip or line of spins with non-zero

z-magnetization. (If the same selective pulses and gradients are applied in the two dimensions, a "line" of square cross-section will result.) The addition of a third selective pulse restricts the magnetization to a single volume element, which can then be selectively excited using a simple broadband pulse. This is the volume-selective excitation method of Aue.<sup>144</sup> Pulse schemes that compensate for  $B_1$  inhomogeneity, and which can therefore be used with surface coils, have been developed.<sup>145,146</sup> They require a minimum of two FIDs to be acquired. This method works reasonably well. However, since the magnetization outside the selected volume is destroyed, multiple-volume excitation is not possible.

An alternative volume-selective scheme has been developed by Ordidge *et al.*<sup>147,148</sup> Known as ISIS (*image selective in vivo spectroscopy*), it utilizes selective  $180^\circ$  pulses. Different combinations of mutually orthogonal selective  $180^\circ$  pulses are applied in succession. The ensuing data set consisting of acquisitions from eight such pulse combinations is summed to give a signal that originates exclusively from the selected volume. This method avoids the need for an accurate hard pulse. If the complex inversion pulses proposed by Silver<sup>149</sup> are employed and the power is sufficiently high, the excitation scheme is not degraded by RF inhomogeneity effects. This makes it easy to set up and apply. Its use has been demonstrated in phantoms and also in the human leg, from which  $^1\text{H}$  ISIS spectra have been obtained.<sup>148</sup> It has been suggested that, in common with many other difference methods, it may be prone to motional artefact.<sup>106</sup>

### C. Spectroscopic imaging

Fourier imaging methods<sup>150,151</sup> when used with gradient amplitude encoding<sup>152</sup> are particularly suited to the retention of chemical-shift information since gradients need only be applied during phase encoding and can be switched off during acquisition. Simple two- and three-dimensional schemes are illustrated in Fig. 6. (See also the discussion in ref. 11, for example.)

Early studies demonstrated the application of the method in one (spatial) dimension,<sup>153,154</sup> but two and three-dimensional methods were also soon proposed.<sup>155–157</sup> In the latter case, processing entails a four-dimensional Fourier transform, and the time needed to acquire the necessary data sets can become prohibitive (typically several tens of minutes). Thus most studies are one- or two-dimensional.

Haselgrove *et al.*<sup>154</sup> were the first to demonstrate the *in vivo* application of a one-dimensional Fourier chemical-shift-imaging technique. They used their method to obtain depth-resolved  $^{31}\text{P}$  spectra in rat limbs and in the head of a gerbil whose right carotid artery had been occluded to give

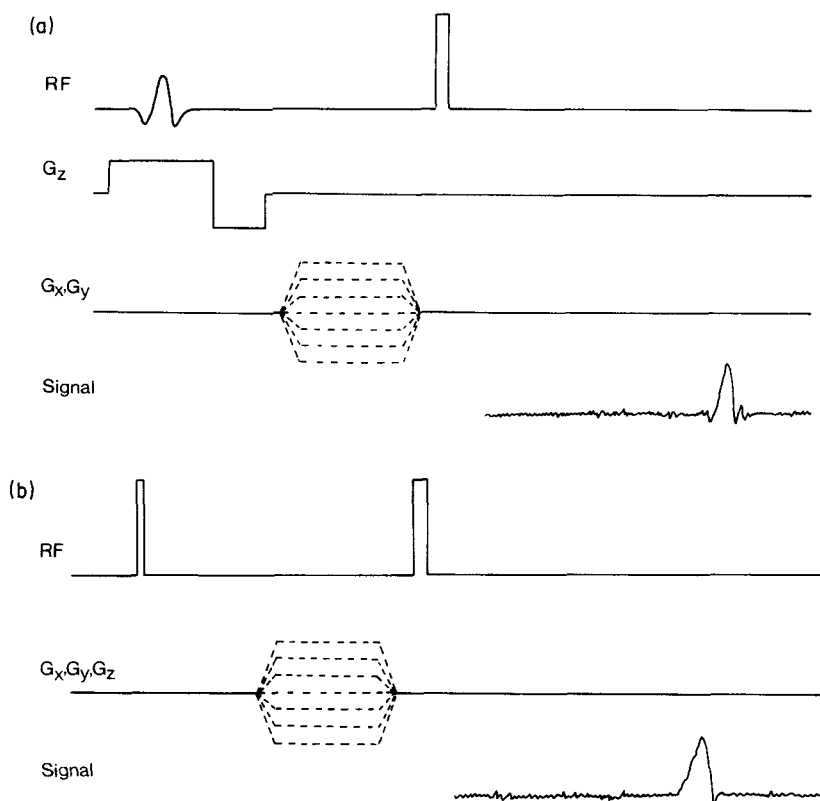


FIG. 6. Three- (a) and four-dimensional (b) chemical-shift imaging schemes, giving spectra over a plane and a volume respectively.

unilateral ischaemia. Loss of phosphocreatine and a concomitant increase in inorganic phosphate were demonstrated in the ischaemic hemisphere, but, owing to the long spin-echo time involved (50 ms), no ATP was observed.

Similar methods can be applied in the rotating frame.<sup>158</sup> Fortunately, the  $B_1$  field generated by surface coils falls off with axial distance from the coil centre in an approximately linear fashion. This  $B_1$  gradient can thus be used to generate depth-resolved images.<sup>159</sup> Recently, Fourier-series window methods have been demonstrated that reduce the number of FIDS that need to be acquired in such an experiment.<sup>160-162</sup> Their use has been demonstrated *in vivo*.<sup>162</sup>

*In vivo* applications of two- and three-dimensional static-field Fourier

methods have not been widely reported. Pykett and Rosen<sup>155</sup> used a two-dimensional Fourier method to obtain  $^1\text{H}$  chemical-shift images of a human forearm and a cat head, in which separate resonances from water and lipid were observed. Maudsley *et al.*<sup>156</sup> have reported similar  $^1\text{H}$  studies of cat heads, identifying resonances from water,  $-\text{CH}_2-$  and  $\text{CH}_3$  groups.

Until recently, little success has been achieved with  $^{31}\text{P}$  chemical-shift imaging. In the last year, however, excellent *in vivo* results have been obtained from human brain,<sup>163</sup> and it is certain that there will be very considerable and rapid growth in this area over the next few years.

#### IV. MEASUREMENT OF INTRACELLULAR CATIONS

##### A. Introduction

The determination of the intracellular free concentrations of cations is of great current interest because of their implication in the control of key biological processes. The role of  $\text{Ca}^{2+}$  in initiating muscular contraction is well known, and numerous examples exist of enzyme systems that are pH-regulated. Substantial pH deviations (typically of 0.5 units) are observed on fertilization of sea urchin eggs<sup>164</sup> and during the emergence from dormancy of several other cryptobiotic systems.<sup>165</sup> Calcium and pH signals are the first events to be observed following mitogenic stimulation.<sup>166</sup> It is assumed that they are responsible in a way as yet undetermined for the cell leaving the quiescent phase and entering the cell cycle.

Although most attention has been focused on  $\text{Ca}^{2+}$  and pH,  $\text{Na}^+$ ,  $\text{K}^+$  and  $\text{Mg}^{2+}$  levels have also been the subjects of recent studies.

Various non-NMR techniques have been applied to the measurement of intracellular cations. These methods include flame-emission photometry, atomic absorption spectrometry, ion-sensitive microelectrodes, optical indicators such as photoproteins, dyes and fluorescent probes, radioisotope tracers and, in the case of pH measurement, the distribution of weak acids. Intracellular pH has been the subject of a Ciba Foundation Symposium.<sup>167</sup> Methods for the measurement of other cations, including direct NMR observation have been reviewed by Tsien.<sup>168</sup> An early review on NMR metal-ion measurement is also available.<sup>169</sup>

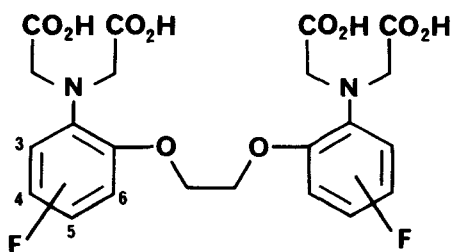
The principal advantage of NMR over other methods is that it can be applied to intact tissues in a non-destructive manner. It is equally applicable to small cell types into which insertion of microelectrodes is difficult. As always, its main disadvantage is a lack of sensitivity. However, since spectral resolution is not normally critical, large samples can be used to overcome this difficulty. In the case of the fluorinated NMR cation indicators

described below, the cellular concentrations can generally be kept at or under those required for single cell studies using comparable fluorescent indicators.

It is not usually the total amount of a particular cation that is of interest. Rather, it is the free concentration within the cell that is of importance. Thus it is necessary to distinguish the cytosolic pool from the extracellular one. This has been accomplished through the use of membrane-impermeable anionic hyperfine-shift reagents,<sup>170,171</sup> notably chelates of the lanthanides dysprosium and thallium. For  $\text{Na}^+$  and  $\text{K}^+$ , intra- and extracellular concentrations differ by more than an order of magnitude and accurate quantitation is not always straightforward. In the case of  $\text{Ca}^{2+}$ , the difference is some four orders of magnitude and direct observation of intracellular calcium would not be possible even for 100% enriched  $^{43}\text{Ca}$ . Some  $^{43}\text{Ca}$  NMR studies have nevertheless been reported.<sup>172</sup> A much better approach is indirect NMR observation using fluorinated indicators. These have now been reported for  $\text{Ca}^{2+}$ ,<sup>173,174</sup>  $\text{Mg}^{2+}$ ,<sup>175</sup>  $\text{Na}^+$ <sup>176</sup> and pH.<sup>174</sup>

## B. Calcium and zinc indicators

A new family of fluorescence indicators of intracellular calcium was proposed and developed by Tsien in the early 1980s.<sup>177,178</sup> They are tetracarboxylic acid chelators obtained by addition of fluorescence reporter groups to the basic EGTA structure, which is well-known to bind  $\text{Ca}^{2+}$  with high specificity. NMR indicators have been derived from the prototype indicator 1,2-bis(*o*-aminophenoxy)ethane-*N,N,N',N'*-tetraacetic acid (BAPTA) by symmetric fluorination:<sup>173</sup>



The indicator with the most suitable properties is 5FBAPTA. On binding  $\text{Ca}^{2+}$ , the  $^{19}\text{F}$  resonance shifts some 4.4 ppm downfield. Under normal operating conditions the system is in slow exchange<sup>179,180</sup> and so, in the presence of non-saturating  $\text{Ca}^{2+}$ , two  $^{19}\text{F}$  NMR resonances are observed (Fig. 7). The apparent dissociation constant of  $\text{Ca}$ -5FBAPTA is 708 nM, so the free calcium concentration is given by  $[\text{Ca}^{2+}] = 708 A_B/A_F$  nM,

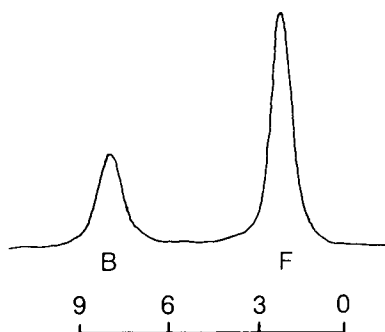


FIG. 7.  $^{19}\text{F}$  NMR spectrum of 5FBAPTA with  $\text{Ca}^{2+}$  in molar ratio 3 : 1, recorded at  $37^\circ\text{C}$  and 188.3 MHz. Chemical shifts are given downfield from 6-fluorotryptophan. From ref. 173.

where  $A_B$  and  $A_F$  are the areas of the bound and free indicator peaks respectively. The range over which calcium concentrations can be measured is limited by the accuracy with which the relative peak areas can be determined. Thus if  $S/N$  is sufficient for quantitation of the less abundant species (whether free or bound) at one tenth the area of the more abundant species, the range is approximately  $70\text{ nM}$ – $70\text{ }\mu\text{M}$ . This comfortably encompasses normal basal  $[\text{Ca}^{2+}]_i$  levels whilst permitting substantial transients to be monitored. No control is required; the method is self-calibrating. Note the sensitivity enhancement over direct NMR methods. It is the chelator (typical concentration range  $0.01$ – $1\text{ mM}$ ) that is observed, rather than the free calcium (typical concentration  $100\text{ nM}$ ) with which it is in equilibrium. There is no interference from other abundant cations ( $\text{Na}^+$ ,  $\text{K}^+$ ,  $\text{Mg}^{2+}$ ) over their normal physiological ranges. Minor cations with high affinity for 5FBAPTA (e.g.  $\text{Zn}^{2+}$ ,  $\text{Cu}^{2+}$ ,  $\text{Mn}^{2+}$ ,  $\text{Fe}^{2+}$ ) “announce their presence” through their distinct chemical shifts and do not interfere with the calcium measurement. In some cases it has proved possible to measure the concentration of the minor cation, e.g.  $\text{Zn}^{2+}$  in Ehrlich Ascites Tumour cells.<sup>174</sup>

The free indicator is not membrane-soluble. In order to load it into tissue/cells, the four carboxyl groups are masked by acetoxymethyl esterifying groups.<sup>181</sup> These render the indicator temporarily membrane-soluble. On entering the cytoplasm, endogenous esterases hydrolyse the acetyl-ester linkage and formaldehyde is spontaneously released to give the free indicator, which then remains trapped within the cell by virtue of its ionic charge. This procedure is particularly beneficial from the NMR viewpoint because the ester is virtually insoluble in water and gives a very broad resonance, which is not normally detected. Thus there is no background

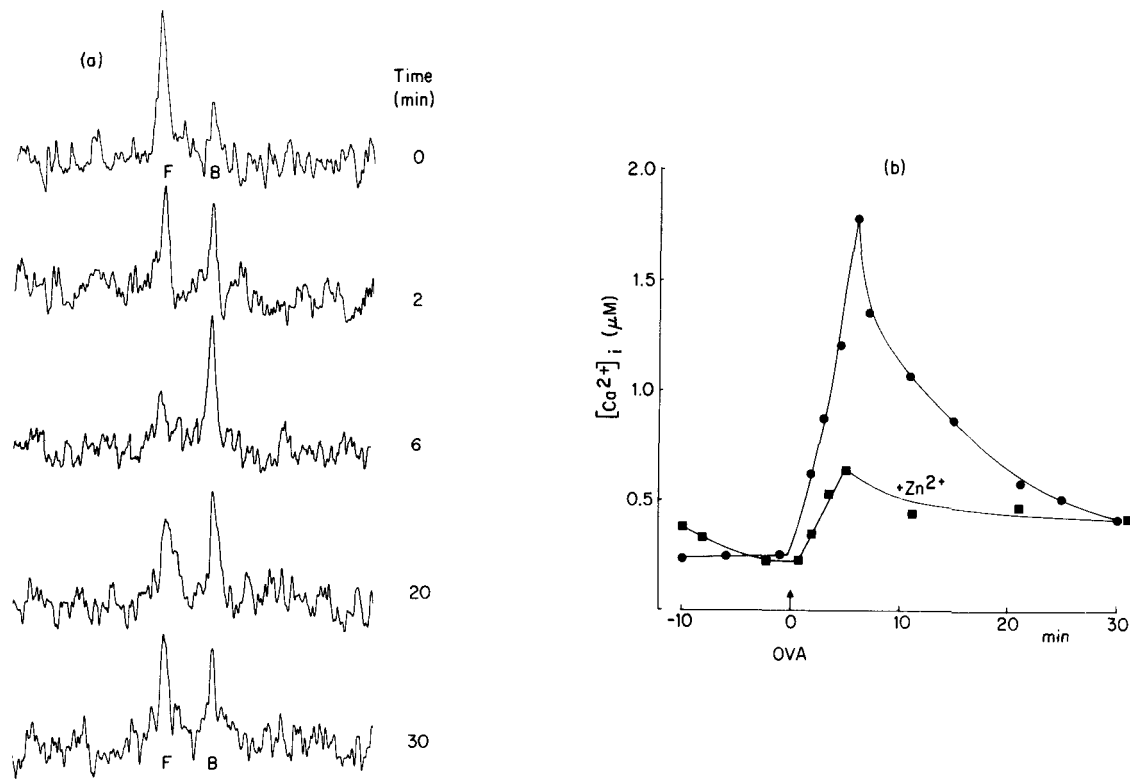


FIG. 8. (a)  $^{19}\text{F}$  NMR spectra for 2H3 cells loaded with 5FBAPTA. Each spectrum corresponds to 2 min data acquisition. Antigen (ovalbumin) was added at 0 min. (b)  $[\text{Ca}^{2+}]_i$  calculated from spectra in (a). The partial block of the Ca signal by  $0.1 \text{ mM Zn}^{2+}$  is also shown (■). From ref. 174.

signal to be subtracted and the indicator is only NMR-visible when it is *in situ* and activated.

5FBAPTA has been used to monitor both resting calcium levels and calcium transients with a time resolution approaching 10 s. Figure 8 shows the response to addition of ovalbumin to 2H3 rat basophil leukaemic cells sensitized with a monoclonal IgE antibody to ovalbumin. An initial rapid rise in  $[Ca^{2+}]_i$  is seen, followed by a slower decline (10–20 min). The time course correlates well with the release of histamine from intracellular granules by exocytosis. A partial block of the calcium signal occurs in the presence of 0.1 mM  $Zn^{2+}$ .

5FBAPTA can also be used in the study of intact tissues. The tetraester, dissolved in DMSO, can be infused into the perfusion line, preferably downstream of the aeration system to avoid precipitation. Resting calcium levels have been measured in Langendorff-perfused hearts.<sup>174</sup> It is also possible to follow the cardiac calcium transient.<sup>175</sup> To obtain the data shown in Fig. 9, sixteen FIDs were consecutively acquired with low-angle RF pulses immediately following a cardiac pacing pulse. Parallel accumulation yielded spectra corresponding to sixteen phases of the cardiac cycle. Although the basal  $[Ca^{2+}]_i$  is substantially higher than expected, for reasons not yet fully understood, the calcium transient is clearly evident.

It is certainly possible to improve on 5FBAPTA as an NMR calcium indicator. For example, replacement of the single fluorine atoms with

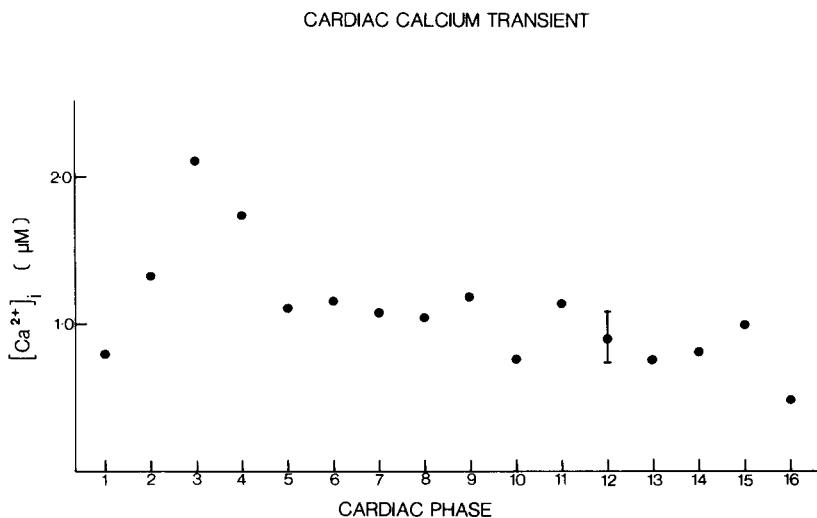


FIG. 9. Cardiac calcium transient measured in a Langendorff-perfused ferret heart using 5FBAPTA. The cardiac cycle of 0.8 s has been divided into 16 phases, each of 50 ms duration.

trifluoromethyl groups would give an immediate threefold improvement in sensitivity. However, care has to be taken in the molecular design to ensure that an adequate chemical shift is preserved between bound and free forms and that the calcium dissociation constant is appropriate.

### C. Magnesium indicators

$^{25}\text{Mg}$  has been used in biological NMR experiments.<sup>182</sup> However, it is a low-abundance low- $\gamma$  quadrupolar nucleus and most attempts to measure intracellular magnesium concentrations have involved indirect observation. Endogenous  $\text{Mg}^{2+}$  chelators have proved especially useful. Thus  $\text{Mg}^{2+}$  is by far the most abundant cation in living systems and the bulk of ATP is Mg-bound. Binding occurs principally via the  $\beta$ - and  $\gamma$ -phosphates and is reflected in changes in the  $^{31}\text{P}$  chemical shifts of these groups, an effect first noted by Cohn and Hughes in 1962.<sup>183</sup> The most sensitive resonance is that of the  $\beta$ -phosphate. Its shift is normally measured relative to that of the least sensitive  $\alpha$ -phosphate in order to determine  $[\text{Mg}^{2+}]$ .<sup>184</sup> In the fast-exchange limit, which applies,  $[\text{Mg}^{2+}]_i$  is given by

$$[\text{Mg}^{2+}]_i = K_D^{\text{MgATP}} \left( \frac{1}{\phi} - 1 \right),$$

where

$$\phi = \frac{\delta_{\alpha\beta}^{\text{cell}} - \delta_{\alpha\beta}^{\text{MgATP}}}{\delta_{\alpha\beta}^{\text{ATP}} - \delta_{\alpha\beta}^{\text{MgATP}}}.$$

The method requires a knowledge of the Mg-ATP dissociation constant,  $K_D^{\text{MgATP}}$ , under appropriate cellular conditions. This is not straightforward and has led to some confusion in the literature,<sup>185</sup> with different  $[\text{Mg}^{2+}]_i$  levels being derived from essentially similar data. Gupta *et al.*<sup>186,187</sup> have now resolved the discrepancy and report a reliable value for  $K_D^{\text{MgATP}}$  of  $50 \pm 10 \mu\text{M}$ . This value is rather low when compared with typical  $[\text{Mg}^{2+}]_i$  levels of about 0.5 mM. It means that most chemical-shift measurements are made in the asymptotic region of the titration curve, where the opportunity for error is greatest. Nevertheless, with care, the method is useful, and it has been widely applied in for example erythrocytes,<sup>184,188</sup> lymphocytes,<sup>189</sup> skeletal<sup>190</sup> and cardiac<sup>185,187</sup> muscle. Almost universally, a value of about  $0.5 \pm 0.3 \text{ mM}$  is found.

$\text{Mg}^{2+}$  is a weak antagonist of  $\text{Ca}^{2+}$  and has been described as "nature's physiological calcium blocker".<sup>191</sup> Certainly Mg depletion is a well-known cause of hypertension. The relationship between diastolic blood pressure

and  $[Mg^{2+}]_i$  has been studied in control and hypertensive patients using  $^{31}P$  NMR methods.<sup>192</sup>

Citrate is another metabolite that is known to bind  $Mg^{2+}$ . Cohen<sup>193</sup> noticed that the  $^{13}C$  chemical shift of its methylene groups is sensitive to  $Mg^{2+}$  binding and used this as a means to determine a value of  $[Mg^{2+}]_i$  in perfused rat liver of  $0.46 \pm 0.5$  mM. The determination proceeds along essentially the same lines as the  $^{31}P$  ATP method, but in the case of citrate the magnesium dissociation constant fortuitously has the highly appropriate value of  $0.38 \pm 0.01$  mM.

Recently, an  $^{19}F$   $Mg^{2+}$  indicator has been developed based on fluorocitrate.<sup>176</sup> Fluorocitrate is a potent inhibitor of aconitase.<sup>194</sup> However, the inhibition is highly stereospecific and the purified (+) isomer has proved to be a highly effective non-toxic Mg indicator. As with the Ca indicator, 5FBAPTA, it is normally loaded into cells as the acetoxymethyl ester. However, unlike 5FBAPTA, fluorocitrate operates in the fast-exchange limit and the  $Mg^{2+}$  concentration is derived from the  $^{19}F$  chemical shift. Fluorocitrate has been used to determine a value for  $[Mg^{2+}]_i$  of 0.6 mM in pig lymphocytes<sup>195</sup> and of 0.87 mM in Langendorff-perfused ferret heart<sup>175</sup> (see Fig. 10). Gating techniques have been used in order to look for a cardiac

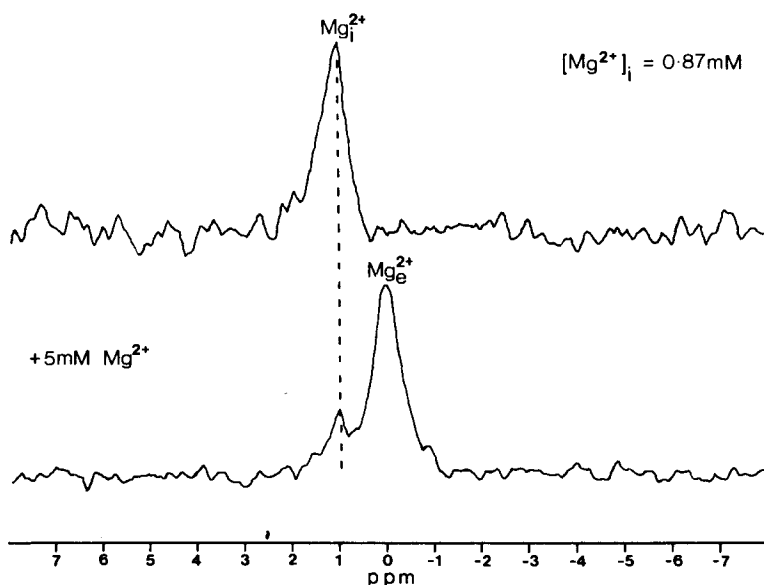


FIG. 10. Measurement of intracellular magnesium  $[Mg^{2+}]_i$  in a Langendorff-perfused ferret heart using fluorocitrate (Fcit). In the lower spectrum 5 mM  $Mg^{2+}$  and 0.5 mM sodium fluorocitrate have been added to allow calibration of the shift measurement.

Mg transient. As expected, none was observed, nor did changes in the extracellular  $\text{Mg}^{2+}$  concentration in the range 0–10 mM lead to any change in  $[\text{Mg}^{2+}]_i$ , at least in the short term (tens of minutes).

It appears to be a common feature of all systems studied to date that  $[\text{Mg}^{2+}]_i$  is very tightly regulated at a value somewhere in the range 0.3–1.0 mM.

#### D. Sodium and potassium measurement

Sodium and potassium can be monitored directly using  $^{23}\text{Na}$  and  $^{39}\text{K}$  NMR respectively. Early studies have been reviewed.<sup>196</sup> Two recent developments have led to an upsurge of interest in  $^{23}\text{Na}$  NMR:  $^{23}\text{Na}$  NMR imaging techniques and the application of membrane-impermeable shift reagents to separate intra- from extracellular sodium signals.<sup>170,171</sup>

Several anionic hyperfine shift reagents have been suggested for  $^{23}\text{Na}$  studies, including  $\text{Dy}^{3+}(\text{P}_3\text{O}_{10}^{5-})_2$ ,<sup>170</sup>  $\text{Dy}^{3+}(\text{N}(\text{CH}_2\text{CO}_2)_3^-)_2$ ,<sup>171</sup> and  $\text{Tm}^{3+}\text{TTHA}^{6-}$ ,<sup>197</sup> which give upfield shifts, and  $\text{Dy}^{3+}\text{TTHA}^{6-}$  and  $\text{Tm}^{3+}(\text{P}_3\text{O}_{10}^{5-})_2$ ,<sup>197</sup> which give downfield shifts where  $\text{TTHA}^{6-}$  is the triethylenetetraminehexaacetate ligand  $(\text{O}_2\text{CH}_2)_2\text{N}(\text{CH}_2)_2\text{N}(\text{CH}_2\text{CO}_2)-(\text{CH}_2)_2\text{N}(\text{CH}_2\text{CO}_2)(\text{CH}_2)_2\text{N}(\text{CH}_2\text{CO}_2)_2^{6-}$ . Of these,  $\text{Dy}^{3+}(\text{P}_3\text{O}_{10}^{5-})_2$  or  $\text{Dy}(\text{PPP})_2^{7-}$  gives the greatest shift (about 3 ppm for 1 mM reagent) and appears to be the least toxic.<sup>169</sup>

In the presence of the shift reagent, two  $^{23}\text{Na}$  resonances are observed, corresponding to intra- and extracellular  $\text{Na}^{23}$  (see Fig. 11). Under fully relaxed conditions the areas of these two peaks are proportional to the amounts of NMR-visible  $^{23}\text{Na}$  in intra- and extracellular pools. Calibration against a suitable standard and a determination of haematocrit (in the case of cell suspensions) yields the corresponding concentrations.<sup>169,198</sup> Note that in addition to the many conventional methods for determining cell volume, including centrifugation, radioisotope dilution etc., a  $^{59}\text{Co}$  NMR method has been applied to the study of human erythrocytes.<sup>199</sup> A  $^{31}\text{P}$  NMR method based on the use of dimethyl methylphosphonate (DMMP) has also been described.<sup>200</sup>

Shift reagents have been applied to the study of sodium transport in erythrocytes,<sup>170,198,201</sup> normal and leukaemic lymphocytes,<sup>170</sup> myocytes,<sup>202,203</sup> amphibian oocytes<sup>169</sup> and yeast.<sup>171,204</sup> Typically, values of  $[\text{Na}^+]_i$  in the range 4–20 mM are obtained.  $^{39}\text{K}$  NMR has also been used in conjunction with shift reagents in studies of potassium transport in erythrocytes<sup>205</sup> and yeast.<sup>204</sup> Intra- and extracellular lithium has been discriminated in yeast using  $^7\text{Li}$  NMR.<sup>171</sup>  $^{23}\text{Na}$  and  $^{39}\text{K}$  NMR spectra have been obtained from beating rat hearts in the presence of  $\text{Dy}^{3+}\text{TTHA}^{6-}$ , and responses to ouabain and low external  $\text{K}^+$  have been demonstrated.<sup>206</sup>

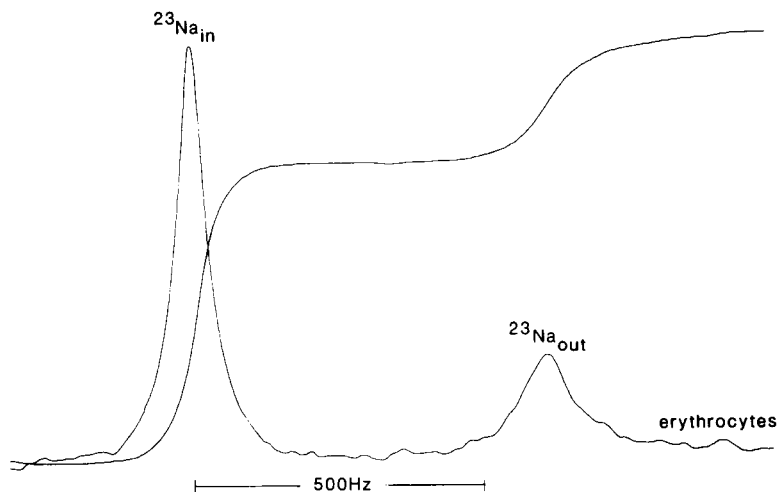


FIG. 11.  $^{23}\text{Na}$  NMR spectrum of well-packed human erythrocytes in a physiological medium containing 4 mM  $\text{Dy}(\text{PPP}_i)_2^{7-}$ . From ref. 169.

In the latter experiments less than 20% of the expected  $[\text{Na}^+]_i$  was observed by NMR.

The interest in  $^{23}\text{Na}$  NMR from the point of view of clinical magnetic-resonance imaging arises from the enormous change in sodium level (and hence in image contrast) following Na/K pump failure. For example, in a canine model of myocardial ischaemia, a 300–400% increase in sodium signal was observed.<sup>207</sup> The origin of the sodium signal has been the object of some discussion. It now seems that, in the early reports in which long spin-echo times  $\text{TE} > 30$  ms were used, the signal was exclusively extracellular. Recent experiments with TE reduced to 3.5 ms have demonstrated a dramatic increase in signal intensity.<sup>208</sup> This is ascribed to intracellular sodium, which has a short  $T_2$ , in the range 0.7–3 ms.

The use of NMR shift reagents has removed the ambiguity in the assignment of intra- and extracellular signals, but the approach is hampered by the sometimes unstable and toxic nature of the agents and the presence of a dominant, albeit shifted, extracellular signal. There is also a further important question regarding the percentage of the intracellular sodium signal that is observed by NMR. For the majority of tissues, with the notable exception of erythrocytes, early workers in the field were only able to observe about 40% of the sodium signal intensity expected on the basis of flame photometry, atomic absorption or NMR measurement following ashing. One possible explanation put forward was that the unobserved

portion was tightly bound and hence invisible. However, since most tissues showed the same fractional loss, irrespective of the protein fraction present, this explanation was considered improbable. The favoured interpretation is now in terms of a very small bound fraction that exhibits a strong quadrupolar interaction and that is in rapid exchange with the free pool. The quadrupolar interaction leads to the loss of 60% of the intensity into unobserved wings corresponding to the  $M = -\frac{3}{2}$  to  $-\frac{1}{2}$  and  $\frac{1}{2}$  to  $\frac{3}{2}$  transitions.<sup>196,209</sup> Recently, however, it has been claimed that, as for the case of erythrocytes, the full intracellular sodium signal intensity is observed in cardiac myocytes.<sup>203</sup> This assertion is based on the agreement of NMR shift-reagent-determined values with those obtained from selective ion-probe or flame-photometric measurements.

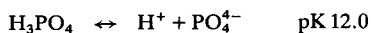
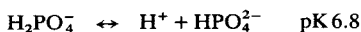
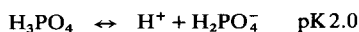
The situation regarding the NMR visibility of intracellular sodium remains unclear. Even in the simplest case of erythrocytes, controversy reigns.<sup>198,201</sup>

Recently, the development of a  $\text{Na}^+$  chelator has been described<sup>176</sup> that has appropriate properties for an indicator of  $[\text{Na}^+]_i$ . The molecule, Fcryp-1, is derived from a 2:2:1 cryptand structure and incorporates the same  $^{19}\text{F}$  reporter group as the calcium indicator, 5FBAPTA. It is loaded as the acetoxymethyl ester and operates in the fast-exchange regime. In an experiment to demonstrate the application of this indicator a value of  $13.8 \pm 1.8 \text{ mM}$  was obtained for  $[\text{Na}^+]_i$  in quiescent pig lymphocytes. With refinement of loading techniques and general availability of the indicator, it is to be hoped that the situation regarding the NMR visibility of tissue sodium will be clarified.

## E. Intracellular pH measurement

### 1. $^{31}\text{P}$ NMR techniques

There are numerous examples of NMR resonances that titrate over the physiological range of pH and that, in principle, could be used to determine intracellular pH ( $\text{pH}_i$ ). The first example to be described in the literature was the use of  $^{31}\text{P}$  NMR to monitor the shift of the inorganic phosphate,  $P_i$ , resonance in erythrocytes.<sup>1</sup> This method has survived the test of time and remains the most popular.  $P_i$  is subject to the following equilibria:



Thus, under normal physiological conditions, inorganic phosphate exists primarily as  $\text{H}_2\text{PO}_4^-$  and  $\text{HPO}_4^{2-}$ . These species have  $^{31}\text{P}$  chemical shifts

relative to phosphocreatine of 3.29 and 5.81 ppm respectively. They are in rapid chemical exchange and so the pH can be determined from the following expression:

$$\text{pH} = 6.8 + \log \left( \frac{3.29 - \delta}{\delta - 5.81} \right),$$

where  $\delta$  is the observed  $^{31}\text{P}$  shift of the inorganic-phosphate peak. More commonly, an empirically determined titration curve is used to read off pH from the observed shift (see e.g. ref. 210). It is important that this calibration be performed under intracellular conditions: a medium containing 150 mM  $\text{K}^+$ , 5 mM  $\text{Na}^+$  and 1 mM  $\text{Mg}^{2+}$  is commonly used.<sup>210</sup> In practice, the titration curve is little shifted, even by substantial changes in these concentrations.<sup>211</sup> However, such effects contribute to an uncertainty in the absolute  $\text{pH}_i$  of perhaps 0.1 units. pH changes can be measured to rather higher accuracy, normally better than 0.05 units.

There are three potential difficulties with the method:

- (i) it requires a suitable chemical-shift reference;
- (ii) uncertainty concerning cellular location;
- (iii) sensitivity (low concentration in some tissues).

For most animal tissues it has been shown that *Pi*-shift measurements reflect the cytoplasmic pH. Splitting indicative of multiple compartments has rarely been observed. Chemical shifts are measured with respect to the phosphagen phosphocreatine, if it is naturally present. In cases where it is not, e.g. in the liver, it may be necessary to resort to a suitable internal reference introduced into the perfusate. Alternatively  $^{31}\text{P}$  reference standards may be employed. Suitable compounds have been discussed.<sup>211,212</sup> These shift standards can also be used to enable quantitation of the observed signals. Provided the tissue/cell mass can be determined, this procedure yields absolute concentrations of metabolites. Such methods work quite effectively for perfused organ studies, where the tissue mass under study is well defined, but are less satisfactory for surface-coil studies.

One of the most important early findings of  $^{31}\text{P}$  NMR studies on intact tissues is the often very low concentration of inorganic phosphate when adequate perfusion is provided. In such circumstances there is some concern that the *Pi* resonance observed is due to a small percentage of damaged tissue. Equally, there is the possibility that it could reflect a high concentration of *Pi* in a less abundant cell type within the intact tissue. Such microscopic heterogeneity is difficult to exclude.

The validity of the *Pi* measurement of  $\text{pH}_i$  is now very widely accepted. Nevertheless, it is important that independent checks be made wherever possible. Phosphomonoesters generally titrate over the physiological pH

range (see e.g. the titration curves on p. 105 of ref. 210) and, if naturally present, can yield useful confirmation of  $P_i$ -determined values. In perfusion studies  $P_i$  is normally included in the medium. Although its  $^{31}\text{P}$  resonance is normally shifted relative to the intracellular one (medium pH 7.4), it may be of sufficient intensity to partially obscure the intracellular signal. In some circumstances perfusion with phosphate-free medium has been shown to be acceptable<sup>57</sup>—in other situations it can lead to washout of tissue  $P_i$  (see ref. 210 for details). In their pioneering experiment Moon and Richards<sup>1</sup> were able to confirm their pH measurements by using the two  $^{31}\text{P}$  resonances of 2,3-diphosphoglycerate. It has been pointed out,<sup>213</sup> however, that, in fresh blood, the  $P_i$  signal is weak and overlaps the 2-P signal of 2,3-diphosphoglycerate. Further, the shifts of the latter depend not only on pH but also on the degree of association with haemoglobin.<sup>214</sup>

It is possible to introduce artificial pH probes. These must, of course, have some pH-dependent NMR property, usually chemical shift, and should not perturb normal cellular metabolism. The phosphate analogue methylphosphonate has been suggested<sup>213</sup> as a suitable alternative exogenous pH probe for erythrocytes. It has a  $\text{pK}$  of about 7.5, is sensitive ( $\Delta\text{pH}/\Delta\delta = 0.460 \text{ pH ppm}^{-1}$ ) and readily enters cells.

Phosphates themselves are not very membrane-permeable. However, sugars are readily taken up by tissues, and their phosphorylated derivatives can be useful if they can be made to accumulate. The best known example is 2-deoxyglucose, which is phosphorylated by hexokinase to give 2-deoxyglucose-6-phosphate. This is not a substrate for glucose-phosphate isomerase, however, and so accumulates. Bailey *et al.*<sup>215</sup> have made use of this to confirm the cytoplasmic origin of the cardiac  $P_i$  resonance.

## 2. Other NMR $\text{pH}_i$ probes

Many  $^1\text{H}$  resonances show suitable titration behaviour for use as pH indicators. However, there are few reports of their use *in vivo*. Carnosine and histidine, which are both important as intracellular buffers in some tissues, have been identified as having suitable properties. Carnosine has been used to measure  $\text{pH}_i$  in intact freshly excised frog muscles.<sup>216</sup> Campbell and coworkers have reported<sup>217</sup> the use of the histidine  $^1\text{H}$  resonances of haemoglobin to measure  $\text{pH}_i$  in erythrocytes.

Comparatively few examples of titratable  $^{13}\text{C}$  resonances exist. The C2 histidine resonance represents one possibility.

$^{19}\text{F}$  indicators are attractive because of the lack of natural background. Deutsch *et al.*<sup>218</sup> have advocated the use of difluoromethylalanine. This is not readily transported into cells, requiring incubation times of several hours at  $37^\circ\text{C}$ . Again the trick required to achieve good loading is to supply

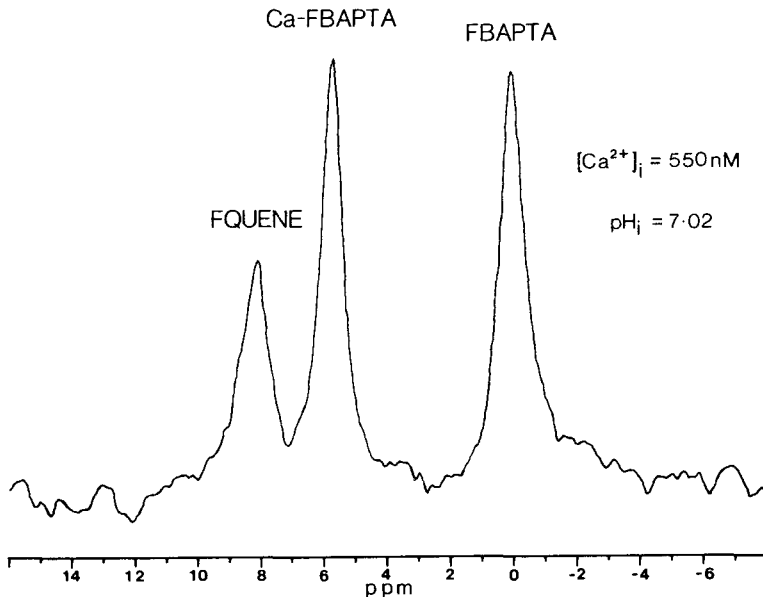


FIG. 12. Simultaneous  $[\text{Ca}^{2+}]_i$  and  $\text{pH}_i$  measurement in isolated Langendorff-perfused ferret heart.

the indicator in ester form. The free indicator is released by endogenous esterases. By this means, loading to 3 mM was rapidly achieved on incubation with 1 mM ester. The  $^{19}\text{F}$  spectrum (at 188 MHz) is an AB quartet. The separation of the centre lines reflects the degree of protonation of the amino group ( $\text{p}K = 7.2$ ).

The other successful  $^{19}\text{F}$  pH indicator to have been described is Fquene.<sup>174</sup> This is derived by simple modification of the fluorescence pH indicator quene 1,<sup>219</sup> which is itself a development of quin 2.<sup>168</sup> Fquene has a  $\text{p}K$  of 6.8. It operates in the fast-exchange limit, so that the  $\text{pH}_i$  value is determined from the observed chemical shift. It has been used both for cellular studies and for intact tissues, including heart and liver.<sup>220</sup> If desired, it can be coloaded with other  $^{19}\text{F}$  cation indicators, e.g. 5FBAPTA, to give simultaneous calcium measurement. This procedure also has the advantage of providing an internal chemical-shift reference (see Fig. 12).

## F. Applications

### 1. Proton pumps

The energy derived by living systems from the transfer of electrons to  $\text{O}_2$  is used in aerobic systems to generate proton electrochemical gradients. These

gradients are used directly to drive transport and also to produce ATP, the cell's universal energy currency. This proton-gradient coupling between oxidation and phosphorylation is known as the Mitchell hypothesis.<sup>221</sup> It is universally accepted and widely supported by experiment. ATP can also be produced anaerobically via glycolysis and used to generate a transmembrane  $\Delta\text{pH}$  in a reversal of the aerobic process. In eukaryotic systems the site of oxidative phosphorylation is the mitochondrion. However, in the simpler prokaryotic systems, such as *E. coli*, the proton gradient is generated across the plasma membrane (Fig. 13). <sup>31</sup>P NMR can be used to give a beautiful illustration of the energy-generation procedure, since both the ATP levels and the pH gradient can be observed.<sup>222-228</sup> Figure 14 illustrates the production of proton gradients in a suspension of *E. coli*.<sup>224</sup> In (a) conditions are anaerobic. There is no glucose in the medium prior to time zero, so there is no energy charge (ATP not visible in the <sup>31</sup>P NMR spectrum). Hence no pH gradient is generated, and a single Pi resonance corresponding to the pH of the extracellular medium is observed. At time

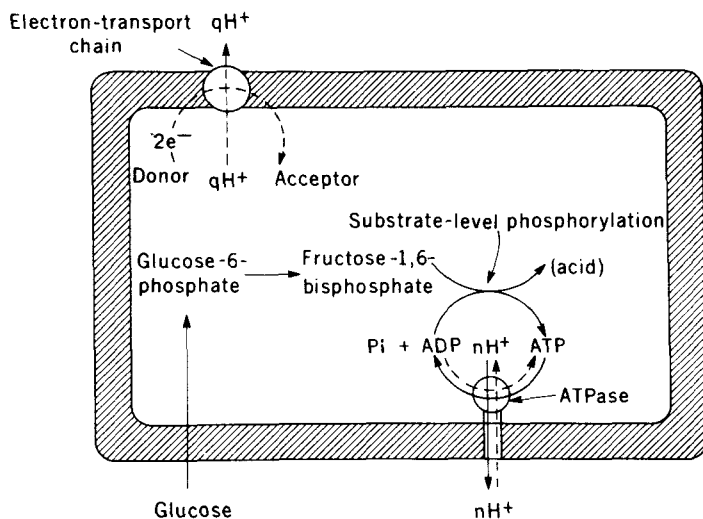


FIG. 13. Schematic view of an *E. coli* cell, demonstrating the linkage between substrate-level phosphorylation, oxidative phosphorylation and the enzyme ATPase. The ATP formed during glycolysis by substrate-level phosphorylation can be hydrolysed by the membrane-bound ATPase to pump protons out and thus form a proton electrochemical gradient. The electrochemical gradient can be formed independently by the electron-transport chain, during which electrons are transferred to an acceptor, usually  $O_2$ . Under these circumstances, the ATPase that is coupled to the electrochemical gradient can synthesize ATP with the energy obtained from transporting protons down the gradient. From ref. 227.

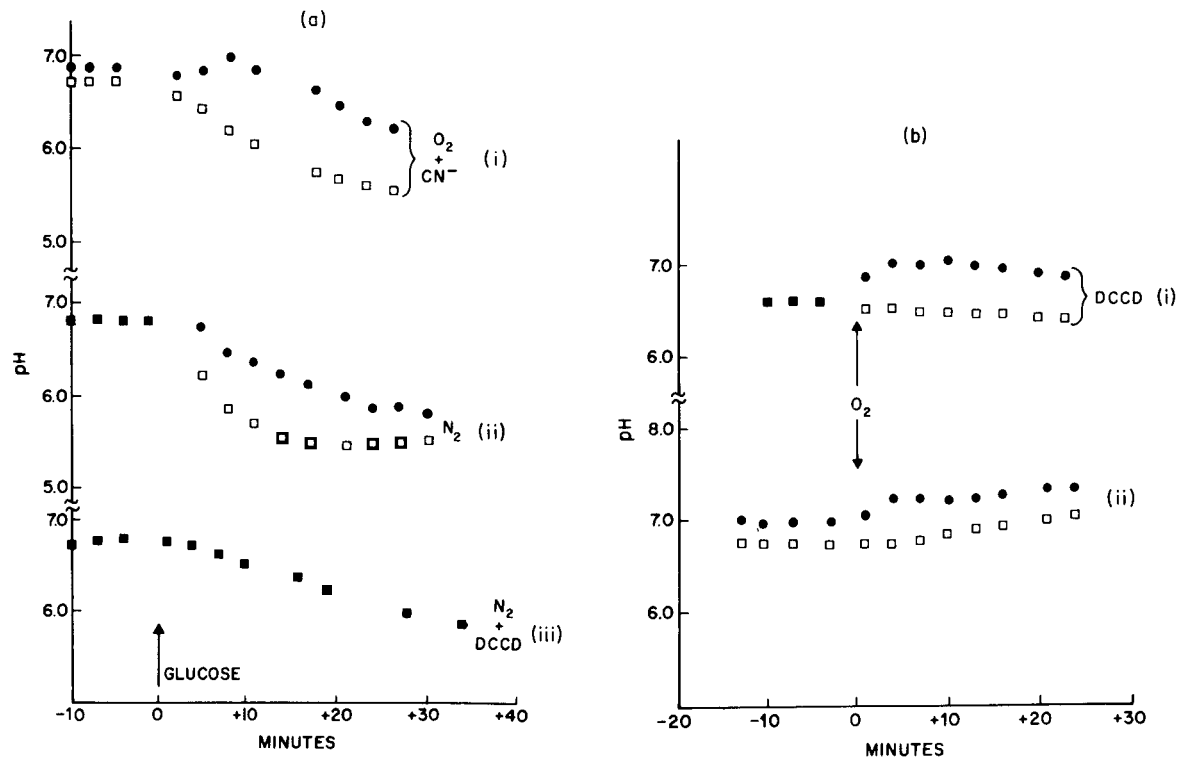


FIG. 14. (a) *E. coli* grown on M9 medium with 16 mM succinate as a carbon source were centrifuged and resuspended in M9 containing 20 mM phosphate and 50 mM Bis-Tris buffer pH 6.8. Glucose was added at time zero to make a concentration of 20 mM (i) 1 mM KCN was added before centrifugation and the rate of  $O_2$  bubbling was  $18 \text{ ml min}^{-1}$  (iii) 1 mM dicyclohexylcarbodiimide (DCCD) was added before centrifugation. The rate of  $N_2$  bubbling in curves (ii) and (iii) was  $6.4 \text{ ml min}^{-1}$ . Circles are  $pH_i$  and squares  $pH_e$ . Experiments were done at  $20^\circ\text{C}$ . (b) Same conditions as in (a) for cells grown in succinate-enriched M9 medium and resuspended in buffer. Oxygen bubbling at  $18 \text{ ml min}^{-1}$  was started at time zero.  $\bullet$ ,  $pH_i$ ;  $\square$   $pH_e$ . From ref. 222.

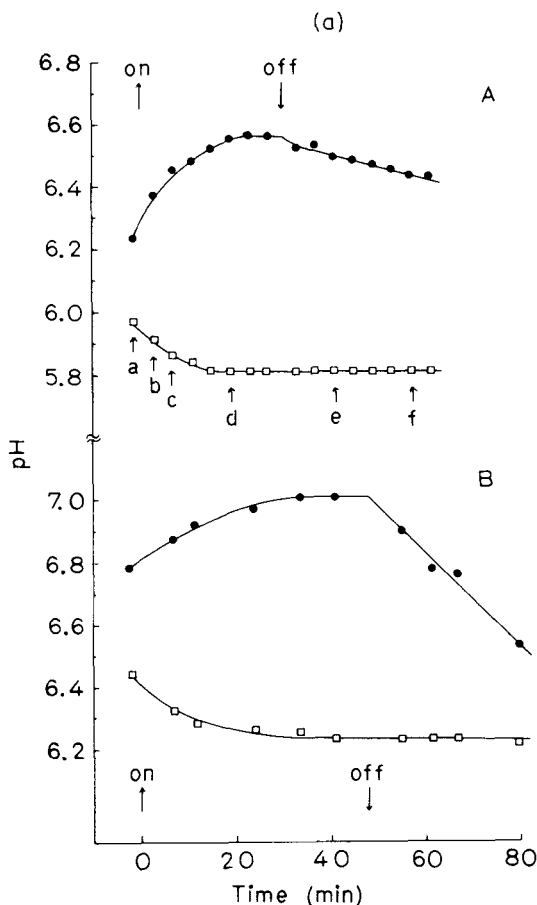
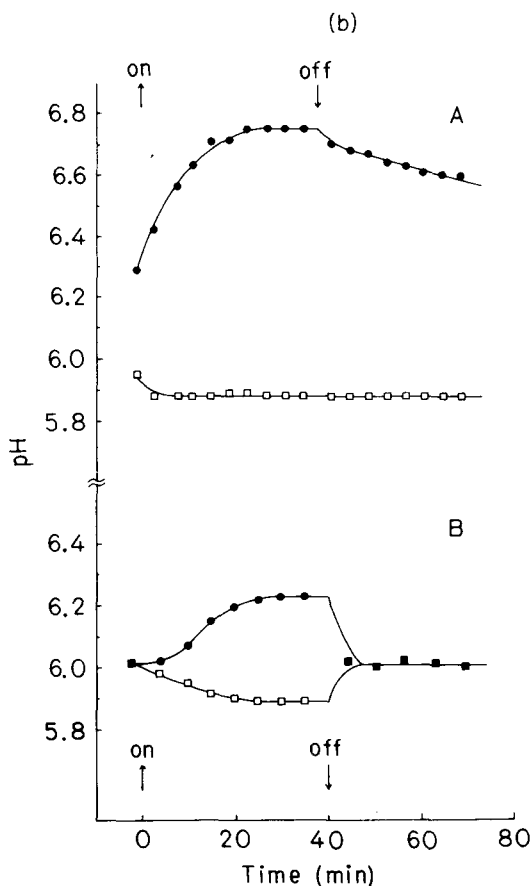


FIG. 15. (a) Light-induced intracellular (●) and extracellular (□) pH in cell suspensions of *Rhodopseudomonas sphaeroides* determined from the  $^{31}\text{P}$  chemical shift of  $P_i$  resonances. In the lower trace (B),  $\text{MgSO}_4$  was omitted from the medium. (b) The effects of ionophores: (A)  $20\mu\text{M}$  valinomycin added 15 min prior to illumination; (B)  $10\mu\text{M}$  *p*-trifluoromethoxyphenylhydrazine added 15 min prior to illumination. From ref. 229.

zero glucose is added and, even under anaerobic conditions, ATP is generated, enabling protons to be expelled and a gradient generated (ii). Essentially similar results are obtained when  $\text{O}_2$  is supplied in the presence of cyanide, which blocks the electron-transport chain at the final stage (i). However, if the ATP-ase inhibitor dicyclohexylcarbodiimide (DCCD) is added, the ATP generated by glycolysis cannot be used to establish a proton gradient (iii). Under aerobic conditions (b), with glycolysis suppressed, the



electron-transport chain establishes the proton gradient (ii), and so DCCD has no effect (i).

A second illustration concerns the phototropic bacterium *Rhodospseudomonas sphaeroides*.<sup>229</sup> When a suspension of these cells is exposed to light, they respond by generating a substantial pH gradient (Fig. 15a). This effect can be accentuated in the presence of  $20\mu\text{M}$  valinomycin, a  $\text{K}^+$  ionophore (Fig. 15(b)A). Addition of  $10\mu\text{M}$  of the uncoupler carbonyl-cyanide *p*-trifluoromethoxy phenylhydrazone (FCCP), a proton ionophore, suppresses the gradient (Fig. 15(b)B) in the absence of light.

## 2. pH homeostasis and compartmentation

It is well known that living systems have the capacity to maintain stable intracellular conditions in the presence of a changing extracellular

environment.  $^{31}\text{P}$  NMR studies of the inorganic phosphate resonance afford an excellent means for studying pH homeostasis. Thus in suspensions of Ehrlich Ascites Tumour (EAT) cells it has been shown<sup>230</sup> that the intracellular pH is maintained constant at 7.2 in the presence of an extracellular pH varying over the range  $6.6 < \text{pH}_e < 7.2$ . In this study an independent check was performed using 2-deoxyglucose-6-phosphate. This method also enabled accurate measurements to be made in the region where  $\text{pH}_i$  and  $\text{pH}_e$   $\text{Pi}$  resonances overlapped. In a similar series of experiments, Deutsch *et al.*<sup>218</sup> have used their fluorinated pH probe (see above) to demonstrate pH regulation in human peripheral blood lymphocytes. The intracellular pH was maintained constant over a similar range to that observed for the EAT cells. The same  $\alpha$ -difluoromethylalanine probe has been used to demonstrate that  $[\text{H}^+]$  does not play a role in mediating the stimulation of urea and glucose production by the hormonal effectors glucagon and adrenenergic agonists in isolated rat hepatocytes.<sup>231</sup>

Resonances whose chemical shifts are pH-sensitive also afford the opportunity to distinguish between different intracellular compartments.<sup>232</sup> The best, and really the only completely unequivocal example occurs in plant cells and tissues where the highly acidic nature of vacuoles enables the vacuolar  $\text{Pi}$  resonance to be clearly identified. Phosphate movements between cytoplasmic and vacuolar compartments can be followed. Thus Fig. 16 shown the distribution of  $\text{Pi}$  in cultured sycamore (*Acer pseudoplatanus*) cells incubated in a medium containing 45 mM  $\text{Pi}$ . The cytoplasmic pool remains roughly constant for the duration of the experiment, and loading occurs into the vacuolar pool, clearly identifiable as the upfield (acidic)  $\text{Pi}$  resonance.<sup>233, 234</sup> Many similar examples exist in systems such as suspension cultures of rye grass (*Lolium multiflorum*),<sup>235</sup> parsley cells (*Petroclinum hortense*),<sup>236</sup> *H. lupus* cells,<sup>237</sup> *Catharanthus roseus* cells, both freely suspended and immobilized,<sup>238-240</sup> *Nicotiana tabacum* cells,<sup>241</sup> in corn root tips,<sup>242</sup> in the root nodules of soybean, stem segments of sunflower and the pollen grains of tobacco.<sup>243</sup>

From time to time claims have been made concerning the visibility of  $\text{Pi}$  pools in the mitochondrial matrix. For example, Cohen *et al.*<sup>244</sup> were able to observe mitochondrial  $\text{Pi}$  in hepatocytes to which valinomycin had been added to swell the mitochondria and accentuate the  $\Delta\text{pH}$  to give a mitochondrial pH of 7.6. Among the more substantial evidence that exists is the observation of two intracellular  $\text{Pi}$  signals with corresponding pHs of 7.0 and 7.38 in perfused rat hearts.<sup>245</sup> The most alkaline compartment is ascribed to the mitochondrial matrix. Two intracellular  $\text{Pi}$  resonances have also been resolved in the slime mould *Dictostelium discoideum*.<sup>246, 247</sup> The more alkaline pool (pH 7.7) is suggested to be mitochondrial. Similarly, two intracellular compartments have been observed in the green alga

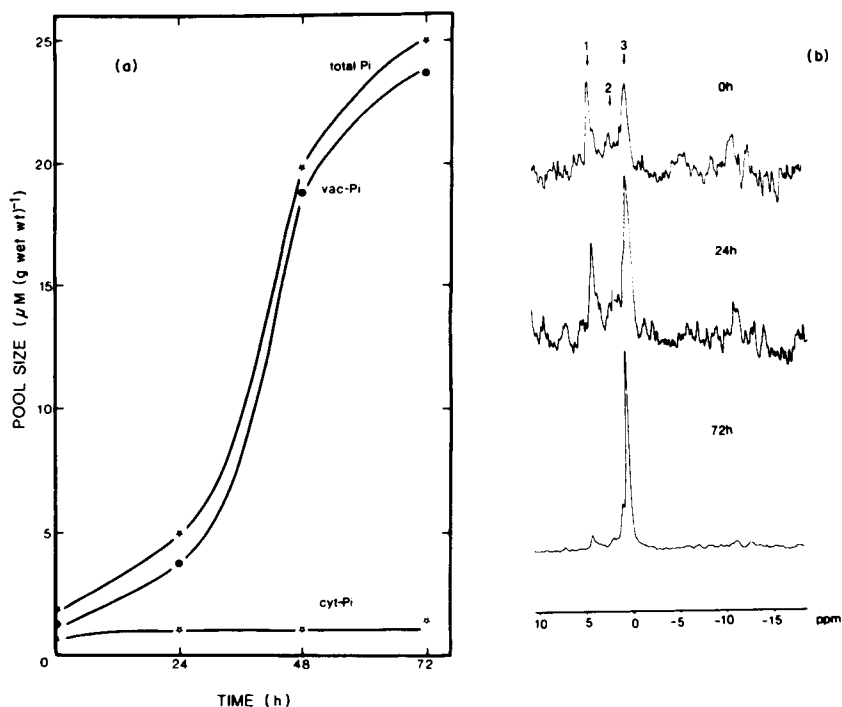


FIG. 16. Time course of  $P_i$  diffusion in the cytoplasm and in the vacuole of sycamore cells. Sycamore cells harvested from culture medium were incubated at time zero in flasks containing buffered culture medium at pH 6–6.5, plus 45 mM  $P_i$ . At various times total  $P_i$  was measured by a phosphomolybdic acid method and vacuolar and cytoplasmic  $P_i$  contents were calculated from NMR spectra. (a) Time evolution of total  $P_i$ , cytoplasmic  $P_i$  and vacuolar  $P_i$ . (b) NMR spectra recorded at time 0, 24 and 72 h; each spectrum was recorded after 1800 scans with a repetition time of 1.36 s; peaks 1, 2 and 3 were assigned respectively to glucose-6-P, cytoplasmic  $P_i$  and vacuolar  $P_i$ . The 72 h spectrum was more attenuated (eightfold) than the 0 and 24 h spectra. From ref. 234.

*Chlorella fusca*.<sup>248,249</sup> These were assigned to the cytoplasm and the stroma of the chloroplasts. On exposure to light the chloroplastic pH became more alkaline while the cytoplasmic pH became more acidic (see also Section IV.F.1 above).

### 3. pH measurement in tissues

Clinical magnetic-resonance spectroscopy is a technique of growing importance. The recent contributions to this area of the pioneering Oxford group have been reviewed.<sup>250,251</sup> The measurement of  $\text{pH}_i$  has proved

especially useful and can often be diagnostic. Thus in spectra recorded from human skeletal muscle exercising under ischaemic (anaerobic) conditions, a failure to observe any lactic acidosis concomitant with phosphocreatine breakdown could indicate an enzymatic lesion in the glycolytic chain. The accumulation of a phosphorylated intermediate would give the site of the lesion. Thus in a patient with phosphofructokinase deficiency Chance *et al.*<sup>252</sup> observed a rapid build-up of its substrate fructose-1-phosphate under ischaemic exercise conditions. (It is also possible to detect patients with partial blocks.)<sup>253</sup> If no accumulation of glycolytic intermediates is observed, the block is presumably at the level of glycogen breakdown. Such a patient with a phosphorylase-a deficiency (McArdle's Syndrome) was the first to be diagnosed by  $^{31}\text{P}$  clinical spectroscopy.<sup>254</sup> In this condition, far from lactic acidosis occurring, a mild alkalosis of typically 0.1 pH units to give pH 7.2 is observed. Similar behaviour has been noted in the stimulated

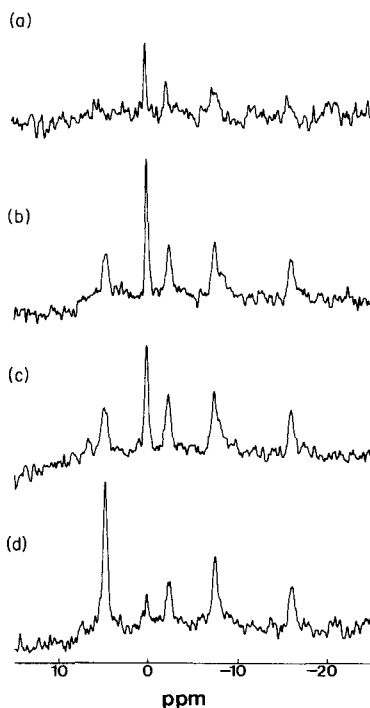


Fig. 17. (a)  $^{31}\text{P}$  NMR spectrum of perfused ferret heart obtained from a single scan. Line-broadening 12 Hz. (b)–(d) Blocks of sixty 1 s scans, as control (b) and after 2 min (c) and 10 min (d) exposure to 2 mM NaCN. Sweepwidth 6 kHz, size 4 K, pulse width  $20\mu\text{s}$  ( $40^\circ$  pulse), line-broadening 12 Hz. From ref. 57.

skeletal muscles of I strain mice,<sup>255</sup> which are also unable to breakdown muscle glycogen (as a result of phosphorylase kinase deficiency). In perfused ferret hearts, rendered effectively anoxic by treatment with cyanide, a transient alkalosis is often observed prior to the sustained and much more substantial acidosis<sup>256,257</sup> (see Fig. 17). Such studies, in which the development of force can be compared with  $\text{pH}_i$ , enable theories of muscular contraction to be tested. Thus the transient alkalosis alone can account for the observed transient positive inotropy on the basis that the reduced number of protons are less effective at competing for the  $\text{Ca}^{2+}$  binding sites of troponin. However pH effects are unable to account entirely for the subsequent contractile failure.

<sup>31</sup>P NMR has proved to be extremely useful in assessing the extent of brain damage due to birth asphyxia in neonates.<sup>258-263</sup> The  $\text{PCr}/\text{Pi}$  ratio proves diagnostic, decreasing from its normal value of about 1.7 to 0.2–1.0 in cases of severe birth asphyxia. This ratio has been shown to correlate with an increased pH.<sup>264</sup>

Recent *in vivo* <sup>31</sup>P studies of human tumours have demonstrated great diversity in their metabolic behaviour.<sup>265</sup> However, a common feature appears to be an elevation of intracellular pH. This is contrary to one's *a priori* expectation of predominantly glycolytic and hence acidotic tissue. One suggested explanation is an increase in  $\text{Na}^+/\text{H}^+$  exchange activity in the activated cells.

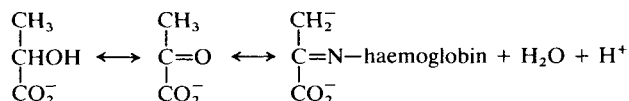
## V. ENZYME KINETICS

### A. Introduction

Several NMR methods are available for studying enzyme kinetics *in vitro*. Only magnetization-transfer techniques have been widely applied *in vivo*, however.<sup>266</sup> For reactions far from equilibrium, i.e. those that are essentially irreversible, it is sometimes possible to obtain unidirectional rate constants by following the rate of conversion of substrate to product directly. Campbell's group have used <sup>1</sup>H spin-echo NMR to study the NAD-dependent conversion of malate to lactate and to estimate the free NAD concentration at  $<25\mu\text{M}$  in intact erythrocytes.<sup>267</sup> Their paper should be consulted for an example of the extreme care that needs to be taken when studying enzyme kinetics *in situ*.

Under equilibrium conditions, isotope-exchange methods can be used to advantage if the rates are sufficiently slow. For example, in erythrocytes the rate of the lactate dehydrogenase (LDH) reaction can be determined by observing the loss of the lactate methyl-proton signal when  $\text{D}_2\text{O}$  is used as

solvent.<sup>268</sup> This occurs because the pyruvate, which interconverts with lactate in the reaction catalysed by LDH, exchanges a methyl proton with the solvent. This probably takes place via a Schiff's base formed with the  $\alpha$ -NH<sub>2</sub> groups of haemoglobin:



Exchange of <sup>15</sup>N label has been used to study the creatine kinase equilibrium and confirm the correctness of the two-site exchange model assumed in most magnetization-transfer studies. A novel <sup>31</sup>P/<sup>15</sup>N double-resonance spin-echo experiment was used to conduct these experiments, in which phase modulation was observed of the <sup>31</sup>P signal via spin coupling to <sup>15</sup>N.<sup>269</sup>

When interconversion occurs at an intermediate rate relative to the difference in chemical shifts of the two interconverting species, lifetime broadening of the NMR resonances is observed. Linewidth measurements then enable rates to be determined. Such methods have been quite widely used *in vitro*. For example, Campbell *et al.*<sup>270</sup> have followed the kinetics of proton transfer in the carbonic anhydrase reaction using this technique. However, linewidth measurements are much less useful *in vivo*, where many factors may contribute to line-broadening.

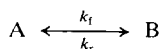
## B. Introduction to magnetization-transfer methods

Magnetization-transfer methods involve the use of magnetic rather than isotopic labels. The key realization that the nuclear spin state would be preserved during chemical reaction was made by McConnell in 1958.<sup>271</sup> He used this idea to explain his NMR studies of proton exchange in saturated ammonium nitrate solutions.<sup>272</sup> A full theoretical description of saturation-transfer experiments, in which the magnetization of one of the exchanging species is saturated (reduced to zero) was given by Forsen and Hoffman<sup>273-275</sup> in the early 1960s. The introduction of Fourier-transform techniques in the 1970s enabled more sophisticated pulse experiments to be conducted. Dahlquist *et al.*<sup>276</sup> suggested the use of a selective 180° pulse, and the method of inversion transfer was born.<sup>277,278</sup> Campbell *et al.*<sup>279</sup> provided theoretical descriptions for these pulsed Fourier-transform experiments, and used a combination of saturation- and inversion-transfer experiments to determine all the rate constants and *T*<sub>1</sub>s involved in an isomerization reaction of valium.

The first *in vivo* application to be described was a determination of *Pi* consumption in a suspension of *E. coli* cells.<sup>280</sup> This rate was shown to be equivalent to the rate of dicyclohexylcarbodiimide-sensitive ATP synthesis.

### C. Saturation-transfer methods

Consider two compounds A and B, between which a chemical group, let us say phosphate, is interchanged. The reaction can be written



where  $k_f$  and  $k_r$  are the forward and reverse psuedo-first-order rate constants. (Even if the reaction is not first-order, the forward flux would still be given by  $k_f[A]$ , but  $k_f$  would not be a true constant—if the reaction were second-order, for example, it would be proportional to  $[A]$ .) Under equilibrium conditions, we should expect in the above example to see separate  $^{31}\text{P}$  NMR signals from the phosphate groups in A and in B. If, immediately prior to the observation pulse, one of these resonances, let us say B, is saturated then its signal will be destroyed and only resonance A will be observed. If the length of the saturating pulse is increased so that it is applied for a time  $\tau$  prior to the observation pulse (see Fig. 18) then any

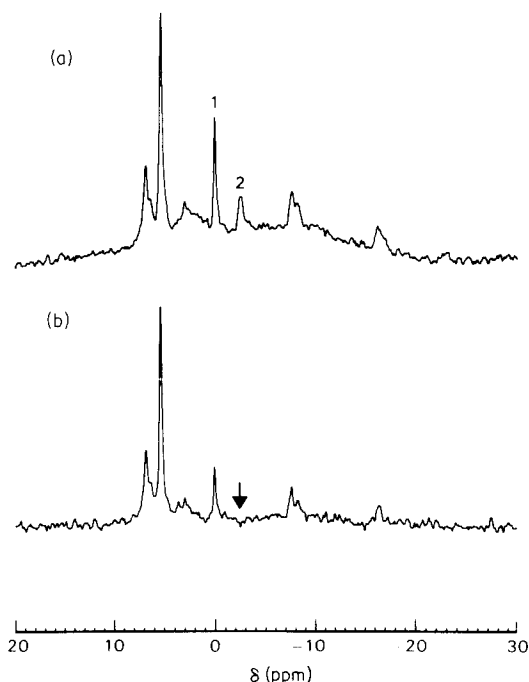


FIG. 18. Determination of the forward rate of creatine phosphotransferase in superfused cerebral tissue. (a), (b) spectra of cerebral tissue superfused in medium containing 10 mM glucose obtained after irradiation of the tissue for 0.005 s (a) or 8 s (b). The frequency of the irradiation is indicated in (b). From ref. 281.

exchange between A and B will result in a loss of intensity for the A resonance. As the period of presaturation is increased there is more time for exchange to occur and resonance A is further diminished. This results in an increasing departure from the Boltzman equilibrium magnetization, which  $T_1$  relaxation processes will tend to restore. In the limit of saturation for an infinite time, the magnetization is determined by the balance between these competing effects. The modified Bloch equations in the presence of exchange are

$$\frac{dM_A}{dt} = -k_f M_A + k_r M_B + \frac{M_A^0 - M_A}{T_{1A}},$$

$$\frac{dM_B}{dt} = k_f M_A - k_r M_B + \frac{M_B^0 - M_B}{T_{1B}},$$

where  $M_A$  and  $M_B$  are the magnetizations of A and B and superscript 0 denotes a Boltzman equilibrium value. When B is saturated so that  $M_B = 0$  we have

$$\frac{dM_A}{dt} = -k_f M_A + \frac{M_A^0 - M_A}{T_{1A}},$$

which can be integrated to give

$$M_A(t) = \frac{M_A^0}{1 + k_f T_{1A}} \left\{ 1 + k_f T_{1A} \exp \left[ - \left( k_f + \frac{1}{T_{1A}} \right) t \right] \right\} \quad (1)$$

when appropriate boundary conditions are applied. The steady-state magnetization  $M_A^s$  is given by

$$M_A^s = M_A(\infty) = \frac{M_A^0}{1 + k_f T_{1A}}, \quad (2)$$

and is approached at a rate

$$R_A = k_f + 1/T_{1A}. \quad (3)$$

As discussed above,  $M_A^s$  is determined by the balance between exchange and relaxation processes. Thus as  $t$  tends to  $\infty$

$$\frac{dM_A}{dt} = -k_f M_A + \frac{M_A^0 - M_A}{T_{1A}} = 0,$$

(exchange) (relaxation)

from which the above expression for  $M_A^s$  is quickly recovered. Note that  $T_{1A}$  refers to the natural  $T_1$  for compound A, i.e. in the absence of any chemical

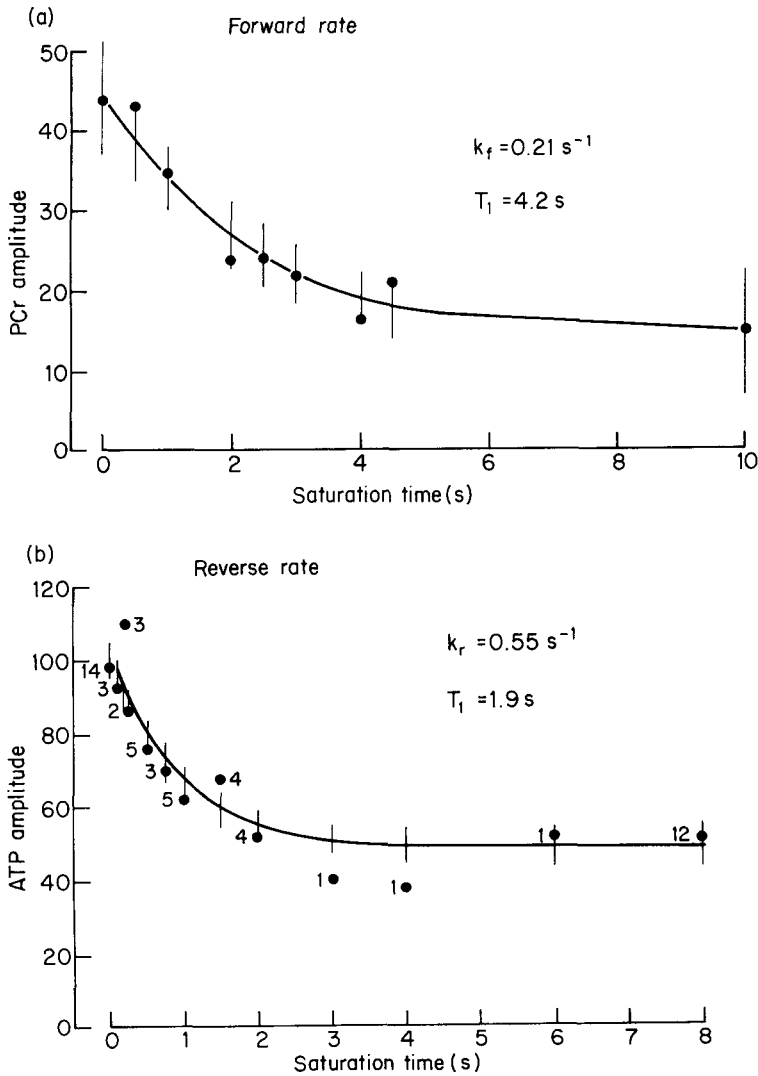


FIG. 19 (a) Determination of the forward rate of creatine phosphotransferase in superfused cerebral tissue. Amplitude of the phosphocreatine resonance plotted as a function of the duration of the  $\gamma$ ATP saturation pulse; duration times were randomly scrambled throughout the experiment. Individual data points are plotted and the bars represent the 95% confidence limits of the fitted exponential function. (b) Determination of the reverse rate of creatine phosphotransferase in superfused cerebral tissue. Amplitude of the  $\gamma$ ATP resonance plotted as a function of the duration of the phosphocreatine saturation pulse; duration times were randomly scrambled throughout the experiment. The points are the means of the numbers of individual normalized values shown. From ref. 281.

exchange. If a full time course is performed (time-dependent saturation transfer) then both  $M_A^s$  and  $R_A$  can be determined by curve-fitting. It is then a simple matter to extract  $k_f$  and  $T_{1A}$  from (2) and (3). By irradiating resonance A rather than B,  $k_r$  and  $T_{1B}$  are obtained in exactly analogous fashion. A time course is illustrated in Fig. 19 for the case of a superfused brain-slice preparation. Details of computer simulation methods for saturation and inversion transfer experiments have been given<sup>282</sup> with particular reference to the creatine kinase reaction.

If  $T_{1A}$  is known, or is determined in a separate experiment, then endpoint measurements (i.e. a measurement with no saturating pulse and another with the pulse continuously applied except during acquisition) will yield  $k_f$  from (2). This is often referred to as steady-state (rather than time-dependent) saturation-transfer NMR. In general the two methods agree well. The steady-state method is much faster, but has to be used with care since it can mask systematic errors or situations where there is multiexponential behaviour.

Saturation transfer gives measurable effects provided that  $k$  and  $1/T_1$  are of the same order of magnitude. If  $k \gg 1/T_1$  then  $M^s$  approaches zero (complete transfer of saturation), whereas if  $k \ll 1/T_1$  then  $M^s \approx M^0$  (relaxation keeps pace with transfer of saturation). Since most biological  $T_1$ s are in the range 0.1–10 s, magnetization-transfer methods usefully complement isotope-exchange (too slow) and lineshape measurements (too fast) for the determination of rate constants in this intermediate range.

#### D. Inversion-transfer experiments

Inversion transfer is similar in principle to saturation transfer, except that one of the resonances is selectively inverted, rather than saturated. This is not trivial: ideally a tailored frequency-selective pulse is applied;<sup>139</sup> more usually, high-resolution spectrometers are not equipped with linear RF amplifiers and can only generate "hard" pulses. In this case a suitably chosen train of hard pulses can serve.<sup>283</sup> Dubbed the DANTE sequence,<sup>284</sup> care must be taken to set the pulse-train parameters correctly (see Fig. 20). Thus the pulse-train duration,  $T$  should be appropriate for the required frequency selectivity (no adjacent peaks directly irradiated by the central lobe). The number of pulses  $n$  should be chosen so that the first of the excitation sidebands, which occur at frequency intervals of  $n/T$ , lies well outside the spectral region of interest. For solution studies good clean selective inversion can be achieved. However, in perfused organs or *in vivo* this is rarely the case, with 90% inversion normally considered good and 75% acceptable. Fortunately these imperfections do not materially affect the analysis.

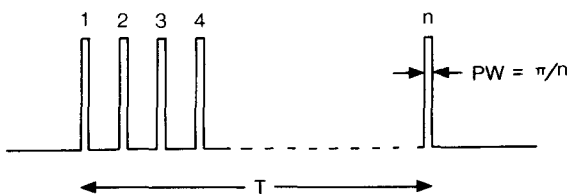


FIG. 20. DANTE pulse sequence for selective inversion.

The solutions of the modified Bloch equations that govern the inversion-transfer experiment are considerably more complex than those for saturation transfer. This is because the state of the magnetic label, which is introduced, is not held during the time in which exchange occurs but is allowed to evolve. The behaviour of the magnetization of both exchanging species is observed as a function of the time between selective inversion and observation pulses. The curves are each double exponential and contain all four kinetic parameters, viz  $T_{1A}$ ,  $T_{1B}$ ,  $k_f$  and  $k_r$ .

Helpful suggestions regarding computer modelling are given in ref. 282. It is sometimes possible to examine the short-time behaviour of the system, permitting considerable simplification in analysis.<sup>279,282</sup> The larger excursion from equilibrium makes inversion transfer a potentially more sensitive technique than saturation transfer and has the advantage that all parameters are determined in a single experiment.<sup>285</sup> It is, however, more difficult to implement and to analyse, leading many workers to favour the latter method.

### E. Two-dimensional exchange experiments

Two-dimensional NMR experiments have been developed for measuring chemical exchange.<sup>286-288</sup> A suitable pulse sequence is illustrated in Fig. 21. Exchange during the mixing period is detected as off-diagonal cross peaks—see Fig. 22 for an example. Balaban and Ferretti<sup>289</sup> have discussed the application of 2D methods to enzyme catalysis and have demonstrated their application *in vivo*, measuring the unidirectional rate constant for conversion of phosphocreatine (PCr) to ATP in rat muscle and brain.<sup>290</sup> Similar measurements in perfused rat heart have also been reported.<sup>291</sup>

2D exchange spectroscopy clearly identifies sites of chemical exchange (via the cross-peaks) and is thus extremely useful where these are uncertain. It is, however, a very time-consuming technique and has not been widely applied.

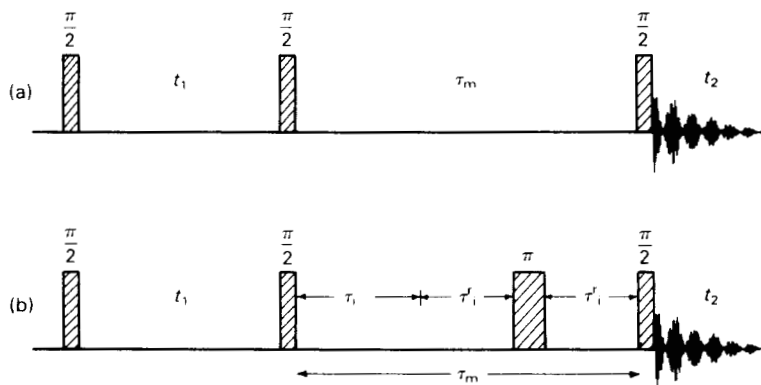


FIG. 21. (a) Basic pulse sequence for 2D exchange spectroscopy and (b) sequence with a  $\pi$ -pulse inserted in the mixing period  $\tau_m$ . The effective zero-quantum precession interval is restricted to  $\tau_i$ , since the chemical shifts are refocused in the remaining intervals  $\tau'_i = \frac{1}{2}(\tau_m - \tau_i)$ . From ref. 288.

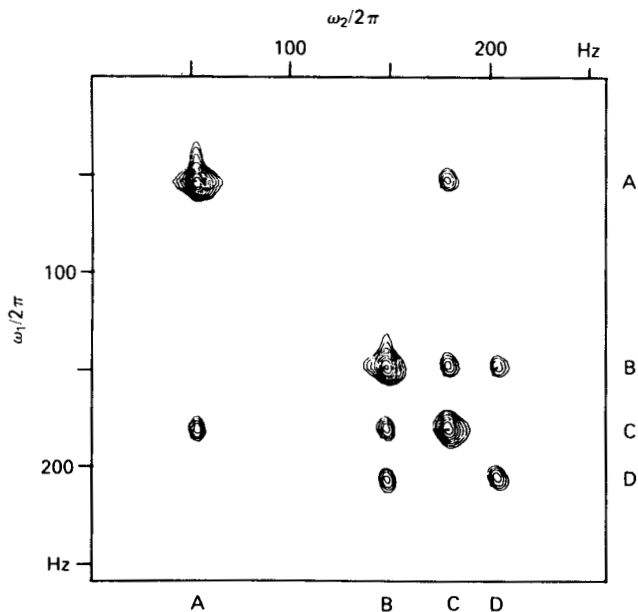
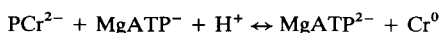


FIG. 22. Two-dimensional exchange spectrum of the protons in heptamethylbenzenonium ion in 9.4 M  $\text{H}_2\text{SO}_4$ . From ref. 288.

## F. Applications and practical difficulties of magnetization-transfer methods

### 1. Creatine kinase studies

Saturation- and to a lesser extent inversion-transfer experiments have been widely applied to the study of enzyme kinetics in living systems. The vast majority of this effort has been directed towards  $^{31}\text{P}$  measurements of the creatine kinase equilibrium:



for which the exchanging species PCr and ATP are present in relatively high concentrations (typically  $>5\text{ mM}$ ) and for which the relaxation times and exchange rates are of the same order of magnitude and so give measurable magnetization-transfer effects. Most of the remaining studies have been concerned with the unidirectional rate of  $P_i$  consumption, which is often equated, rightly or wrongly, with the net rate of ATP synthesis.

One of the earliest detailed studies was performed using anaerobic frog gastrocnemius muscles maintained at  $4^\circ\text{C}$ .<sup>292</sup> Under resting conditions equal forward and reverse fluxes of  $1.6\text{ mM s}^{-1}$  were determined. In contracting muscle, in which there was a net breakdown of PCr of  $0.85\text{ mM s}^{-1}$ , a corresponding reduction of  $0.85\text{ mM s}^{-1}$  was observed in the reverse flux, the forward flux remaining constant.

The situation in the heart appears to be substantially more complex. From the earliest saturation-transfer experiments in this organ,<sup>293–297</sup> discrepancies have been observed between forward and reverse fluxes, the forward flux being anything up to a factor of four greater. Note that the results of Matthews *et al.*<sup>296</sup> indicate that the apparent imbalance increases with workload, an observation that has been confirmed and expanded in more recent studies.<sup>298,299</sup> A number of reported values are given in Table 1. Two explanations have been advanced for this discrepancy: compartmentation<sup>294</sup> and the participation of ATP in other reactions. The question of compartmentation arises partly as a consequence of the observation of different PCr isozymes, one of which is associated with the myofibrils and a second with the outer face of the inner mitochondrial membrane. This has led to the “shuttle” hypothesis,<sup>296,300</sup> in which the ATP generated in the mitochondrial matrix is used to generate phosphocreatine, which then transfers its high-energy phosphate to ADP at the myofibrils, enabling contraction to be fuelled. As well as leading to anomalous fluxes, the shuttle effect could also manifest itself in the multiexponential behaviour of time-dependent saturation and inversion-transfer experiments. Some evidence for such behaviour has been presented.<sup>298</sup> The alternative explanation of the participation in other reactions is perhaps the more

TABLE 1

Creatine kinase rate constants and fluxes in perfused hearts.

Animal	Method	Comments	$k_t$	$k_r$	$F_t/F_r$	Ref.
Rabbit	ST <sup>a</sup>		$0.52 \pm 0.01$	$0.70 \pm 0.1$	2.33	294
Rat	ST		$0.52 \pm 0.02$			295
Rat	ST	arrested	$0.27 \pm 0.04$	$0.43 \pm 0.06$	$1.0 \pm 0.3$	296
		70 cm <sup>c</sup>	$0.42 \pm 0.03$	$0.38 \pm 0.03$	$1.2 \pm 0.06$	296
		140 cm <sup>c</sup>	$0.46 \pm 0.05$	$0.23 \pm 0.06$	$1.8 \pm 0.5$	296
Rat	ST		$0.34 \pm 0.02$	$0.39 \pm 0.03$	$1.79 \pm 0.1$	297
Rat	MST <sup>b</sup>		$0.30 \pm 0.02$	$0.61 \pm 0.04$	$0.97 \pm 0.07$	297

<sup>a</sup> Saturation transfer.<sup>b</sup> Multiple saturation transfer.<sup>c</sup> Hydrostatic perfusion pressure.

favoured currently. In measuring the reverse rate (ATP → PCr) by saturation transfer, the PCr resonance is saturated and an effect observed on the  $\gamma$  phosphate of ATP. If the latter is exchanging with other species, for example with  $P_i$ , under the influence of the many ATPases, then the effect of the transferred saturation will be diluted into the other pools, leading to a smaller apparent transfer of saturation and hence to an underestimate of  $k_r$ . Only if  $k_r \gg$  rate constants for exchange with other pools, will a correct value be obtained.

Various attempts have been made to assess the rate of ATP consumption. In a stable preparation it is presumably balanced by ATP resynthesis and, if a P:O ratio is assumed (typically 3), can be estimated from oxygen-consumption measurements.<sup>295</sup> Additional corrections can be made for glycolytic ATP synthesis.

Similar discrepancies between forward and reverse fluxes have been noted in *in vivo* studies of rat brain.<sup>301</sup> However, in *in vitro* studies of superfused guinea-pig brain slices these are equal to within experimental error.<sup>281</sup> It may be that in the latter case it is the much lower APTase activity due to lack of electrical stimulation that leads to a better estimate of  $k_r$ .

## 2. Multiple saturation transfer

Ugurbil<sup>297,302,303</sup> has recently extended the basic saturation-transfer experiment to enable rates to be determined in the presence of competing reactions. The procedure requires the saturation of the other pools that are in exchange with the species to be monitored. In the case of the creatine kinase equilibrium this means continuous saturation of the  $P_i$  resonance. Using such a multiple saturation-transfer experiment in the perfused rat

heart, Ugurbil<sup>297</sup> calculated a much higher  $k_r$ , leading to a forward to reverse flux ratio approaching unity (see entry in Table 1). It has recently been suggested<sup>304</sup> that  $Pi/\gamma$ ATP exchange catalysed by glyceraldehyde-3-phosphate dehydrogenase and phosphoglycerate kinase could also account for the discrepancy. A three-site exchange model was used to demonstrate this possibility.

### 3. $Pi/\gamma$ ATP exchange

A measurement of the unidirectional rate of consumption of  $Pi$  in *E. coli* was the first *in vivo* saturation-transfer experiment to be reported.<sup>280</sup> Alger *et al.*<sup>305</sup> have made similar but more detailed measurements in respiration-competent suspensions of yeast (*Saccharomyces cerevisiae*), which has both mitochondrial and plasma ATPases. Oligomycin is a potent inhibitor of the former and has been used to demonstrate that some 90% of the total  $Pi$  consumption of  $3.0 \pm 0.3 \mu\text{M s}^{-1}$  (g wet cells)<sup>-1</sup> is due to the mitochondrial  $F_0$ - $F_1$  ATPase.

The unidirectional rate of  $Pi$  consumption is often equated with the rate of net ATP synthesis. Evidence for this comes in the perfused heart from P : O ratios calculated on this basis of about 3. See, for example, ref. 295, where a ratio of  $3.5 \pm 0.8$  was determined after correction for glycolytic substrate-level phosphorylation. Such interpretation requires that the  $F_0$ - $F_1$  ATPase is operating far from equilibrium, so that the reverse flux is negligible. There are also problems regarding which pools of phosphate (mitochondrial/cytoplasmic) are observed. The experiments are contentious. More recent determinations<sup>306</sup> have yielded P : O ratios close to 6. This may be due to non-negligible reverse flux through mitochondrial  $F_0$ - $F_1$  ATPase. Certainly it has been suggested<sup>266</sup> that in yeast the  $F_0$ - $F_1$  ATPase must be close to equilibrium because a P : O ratio of 87 was calculated on the assumption of a unidirectional synthetic flux! Alternatively the activities of glyceraldehyde-3-phosphate dehydrogenase and phosphoglycerate kinase may be implicated<sup>304</sup> (see above).

## REFERENCES

1. R. B. Moon and J. H. Richards, *J. Biol. Chem.*, 1973, **248**, 7276.
2. D. I. Hoult, S. J. W. Busby, D. G. Gadian, G. K. Radda, R. E. Richard and P. J. Seeley, *Nature*, 1974, **252**, 285.
3. P. C. Lauterbur, *Nature*, 1973, **242**, 190.
4. P. Mansfield and P. K. Grannell, *J. Phys.*, 1973, **C6**, L422.
5. E. R. Andrew, *Brit. Med. Bull.*, 1984, **40**, 115.
6. L. Kaufman, L. E. Crooks and A. R. Margulls (eds), *Nuclear Magnetic Resonance (NMR) in Medicine*, Igaku-Shoin, New York and Tokyo, 1981.

7. P. Mansfield and P. G. Morris, *NMR Imaging in Biomedicine*, Academic Press, New York, 1982.
8. C. L. Partain, A. E. James, F. D. Rolls and R. R. Price (eds), *Nuclear Magnetic Resonance (NMR) Imaging*, W. B. Saunders, Philadelphia, 1983.
9. K. Roth, *NMR-Tomography and Spectroscopy in Medicine: Introduction*, Springer-Verlag, Berlin, 1984.
10. S. W. Young, *Nuclear Magnetic Resonance Imaging: Basic Principles*, Raven Press, New York, 1984.
11. P. G. Morris, *NMR Imaging in Medicine and Biology*, Oxford University Press, 1986.
12. B. D. Ross, D. M. Freeman and L. Chan, *Adv. Exp. Med. Biol.*, 1984, **178**, 455.
13. G. K. Radda, *Adv. Biosci.*, 1986, **54**, 29.
14. A. I. Scott, *J. Nat. Prod.*, 1985, **48**, 689.
15. J. R. Alger and R. G. Shulman, *Brit. Med. Bull.*, 1984, **40**, 160.
16. J. R. Alger, L. O. Sillerud, K. L. Behar, R. J. Gillies, R. G. Shulman, R. G. Gordon, D. Shaw and P. Hanley, *Science*, 1981, **214**, 660.
17. P. J. Hore, *J. Magn. Reson.*, 1983, **55**, 283.
18. D. L. Rothman, K. Behar, H. P. Hetherington and R. G. Shulman, *Proc. Natl. Acad. Sci. USA*, 1984, **81**, 6330.
19. S. R. Williams, D. G. Gadian, E. Proctor, D. B. Sprague, D. F. Talbot, I. R. Young and F. F. Brown, *J. Magn. Reson.*, 1985, **63**, 406.
20. S. R. Williams, D. G. Gadian, E. Proctor, D. B. Sprague, D. F. Talbot, F. F. Brown and I. R. Young, *Biochem. Soc. Trans.*, 1985, **13**, 839.
21. R. S. Balaban, D. G. Gadian, G. K. Radda and G. G. Wong, *Anal. Biochem.*, 1981, **116**, 450.
22. D. W. G. Cox, P. G. Morris, J. Feeney and H. S. Bachelard, *Biochem. J.*, 1983, **212**, 365.
23. H. S. Bachelard, D. W. G. Cox, J. Feeney and P. G. Morris, *Biochem. Soc. Trans.*, 1985, **13**, 835.
24. R. J. Labotka, J. A. Warth, V. Winecki and A. Omachi, *Anal. Biochem.*, 1985, **147**, 75.
25. G. Navon, S. Ogawa, R. G. Shulman and T. Yamane, *Proc. Natl. Acad. Sci. USA*, 1977, **74**, 888.
26. G. S. Karczmar, A. P. Koretsky, M. J. Bissell, M. P. Klein and W. M. Weiner, *J. Magn. Reson.*, 1983, **53**, 123.
27. J. C. Metcalfe, T. R. Hesketh and G. A. Smith, *Cell Calcium*, 1985, **6**, 183.
28. R. Gonzalez-Mendez, D. Wemmer, G. Hahn and N. Wade-Jardetzky, *Biochim. Biophys. Acta*, 1982, **720**, 274.
29. P. M. Guilloino and R. A. Knazek, *Methods Enzymol.*, 1979, **58**, 178.
30. K. Ugurbil, D. L. Guernsey, T. R. Brown, P. Glynn, N. Tobkes and I. S. Edelman, *Proc. Natl. Acad. Sci. USA*, 1981, **78**, 4843.
31. M. H. Melner, S. T. Sawyer, W. T. Evanochko, T. C. Ng, J. D. Glickson and D. Puett, *Biochemistry*, 1983, **2**, 2039.
32. L. Jacobson and J. S. Cohen, *Biosci. Rep.*, 1981, **1**, 141.
33. D. L. Foxall and J. S. Cohen, *J. Magn. Reson.*, 1983, **52**, 346.
34. D. L. Foxall, J. S. Cohen and J. B. Mitchell, *Exp. Cell. Res.*, 1984, **154**, 521.
35. R. H. Knop, C. W. Chen, J. B. Mitchell, A. Russo, S. McPherson and J. S. Cohen, *Biochim. Biophys. Acta*, 1984, **804**, 275.
36. M. J. Dawson, D. G. Gadian and D. R. Wilkie, *J. Physiol.*, 1977, **267**, 703.
37. M. J. Dawson, D. G. Gadian and D. R. Wilkie, *Nature*, 1978, **274**, 861.
38. M. J. Dawson, D. G. Gadian and D. R. Wilkie, *Proc. R. Soc. Lond.*, 1980, **B289**, 445.
39. P. J. Bore, L. Chan, D. G. Gadian, G. K. Radda, B. D. Ross, P. Styles and D. Taylor, in *Intracellular pH: Its Measurement, Regulation and Utilization in Cellular Functions*, Alan R. Liss, New York, 1982, pp. 527-535.

40. G. K. Radda, L. Chan, P. B. Bore, D. G. Gadian, B. D. Ross, P. Styles and D. Taylor, in *NMR Imaging: Proceedings of an International Symposium on NMR Imaging* (R. L. Witcofski, N. Karstaedt and C. L. Partain, (eds), Bowman Gray School of Medicine, Wake Forest University, Winston-Salem, North Carolina, 1982, pp. 159-169.
41. T. Glonek and S. J. Kopp, *Magn. Reson. Imaging*, 1985, **9**, 359.
42. J. V. Greiner, S. J. Kopp and T. Glonek, *Surv. Ophthalmol.*, 1985, **30**, 189.
43. D. Chapman, C. M. Kemp, P. G. Morris and M. Pons, *FEBS Lett.*, 1982, **143**, 293.
44. T. E. Mansour, P. G. Morris, J. Feeney and G. C. K. Roberts, *Biochem. Biophys. Acta*, 1982, **721**, 336.
45. A. G. M. Tielens, K. Nicolay and S. G. Van den Bergh, *Mol. Biochem. Parasitol.*, 1982, **6**, 175.
46. P. M. Matthews, L. Shen, D. Foxall and T. E. Mansour, *Biochem. Biophys. Acta*, 1985, **845**, 178.
47. P. M. Matthews, D. Foxall, L. Shen and T. E. Mansour, *Mol. Pharmacol.*, 1986, **29**, 65.
48. H. A. Krebs and K. Henseleit, *Hoppe-Seyler's Z. Physiol. Chem.*, 1932, **210**, 33.
49. H. McIlwain and H. S. Bachelard, *Biochemistry and the Central Nervous System*, 5th edition, Churchill Livingstone, Edinburgh, 1985.
50. R. B. Lee and R. G. Ratcliffe, *J. Exp. Bot.*, 1983, **34**, 1213.
51. R. B. Lee and R. G. Ratcliffe, *J. Exp. Bot.*, 1983, **34**, 1222.
52. B. D. Ross, *Perfusion Techniques in Biochemistry*, Clarendon Press, Oxford, 1972.
53. W. E. Jacobus, G. J. Taylor, D. P. Hollis and R. L. Nunnally, *Nature*, 1977, **265**, 756.
54. D. P. Hollis, R. L. Nunnally, G. T. Taylor, M. L. Weisfeldt and W. E. Jacobus, *J. Magn. Reson.*, 1978, **29**, 319.
55. P. B. Garlick, G. K. Radda, P. J. Seeley and B. Chance, *Biochem. Biophys. Res. Commun.*, 1977, **74**, 1256.
56. P. B. Garlick, G. K. Radda and P. J. Seeley, *Biochem. J.*, 1978, **170**, 103.
57. P. G. Morris, D. G. Allen and C. H. Orchard, *Adv. Myocardiol.*, 1985, **5**, 27.
58. J. K. Gard, *Diss. Abstr.*, 1985, **B45**, 3409.
59. J. K. Gard, G. M. Kichura, B. E. Sobel and R. W. Gross, *Biophys. J.*, 1985, **48**, 803.
60. W. M. Brooks, L. J. Haseler, K. Clarke and R. J. Willis, *Mol. Cell. Cardiol.*, 1986, **18**, 149.
61. J. J. H. Ackerman, D. G. Gadian, G. K. Radda and G. G. Wong, *J. Magn. Reson.*, 1981, **42**, 498.
62. R. E. Gordon and W. E. Timms, *J. Magn. Reson.*, 1982, **42**, 322.
63. E. T. Fossel, H. E. Morgan and J. S. Ingwall, *Proc. Natl Acad Sci. USA*, 1980, **77**, 3654.
64. R. L. Barbour, C. H. Sotak, G. C. Levy and S. H. P. Chan, *Biochemistry*, 1984, **23**, 6053.
65. D. G. Renlund, E. G. Lakatta, E. D. Mellits, G. Gerstenblith, *Circ. Res.*, 1985, **57**, 876.
66. R. D. Cohen, R. A. Iles and M. H. Lloyd, in *Isolated Organ Perfusion* (H. D. Ritchie and J. D. Hardcastle, eds), Staples Press, London, 1973, pp. 120-134.
67. R. A. Iles, J. R. Griffiths, A. N. Stevens, D. G. Gadian and R. R. Porteous, *Biochem. J.*, 1980, **192**, 191.
68. S. M. Cohen, *J. Biol. Chem.*, 1983, **258**, 14294.
69. S. M. Cohen, *Fed. Proc. Fed. Am. Soc. Exp. Biol.*, 1984, **43**, 2657.
70. K. Albert, G. Knippa, K. P. Zeller, E. Bayer and F. Hartman, *Z. Naturforsch.*, 1984, **39**, 859.
71. M. A. Pass, Y. Geoffrion, R. Deslauriers, K. W. Butler and I. C. P. Smith, *J. Biochem. Biophys. Methods*, 1984, **10**, 135.
72. G. K. Radda, J. J. H. Ackerman, P. Bore, P. Sehr, G. G. Wong, B. D. Ross, Y. Green, S. D. Bartlett and M. Lowry, *Int. J. Biochem.*, 1980, **12**, 277.
73. J. J. H. Ackerman, M. Lowry, G. K. Radda, B. D. Ross and G. G. Wong, *J. Physiol.*, 1981, **319**, 65.

74. D. Freeman, M. Lowry, G. K. Radda and B. Ross, *Biochem. Soc. Trans.*, 1982, **10**, 399.
75. D. Freeman, S. Bartlett, G. K. Radda and B. Ross, *Biochem. Biophys. Acta*, 1983, **762**, 325.
76. J. J. H. Ackerman, P. J. Bore, D. G. Gadian, T. H. Grove and G. K. Radda, *Phil. Trans. R. Soc. Lond.*, 1980, **B289**, 425.
77. A. M. Kumar, A. Spitzer and R. K. Gupta, *Kidney Int.*, 1986, **29**, 747.
78. B. M. Rayson and R. K. Gupta, *J. Biol. Chem.*, 1985, **260**, 7276.
79. R. A. Meyer, T. R. Brown and M. J. Kushmerick, *Am. J. Physiol.*, 1985, **248**, C279.
80. H. L. Kirschenlohr, R. Maxwell, A. N. Stevens, H. W. Hofer, J. R. Griffiths and P. G. Morris, *Biol. Chem. Hoppe-Seyler*, 1985, **336**, 811.
81. M. J. Dawson and S. Wray, *J. Physiol*, 1983, **336**, 19.
82. T. Yuasa, T. Miyatake, T. Kuwabara, M. Umeda and K. Eguchi, *Brain Nerve*, 1983, **35**, 1089.
83. S. Naruse, S. Tanaka, I. Koczika and H. Watari, *Jpn J. Physiol.*, 1983, **33**, 19.
84. E. A. Shoubridge, R. W. Briggs and G. K. Radda, *FEBS Lett.*, 1982, **140**, 288.
85. P. A. Bottomley, K. Kogure, R. Namon and O. F. Alonso, *Magn. Reson. Imaging*, 1982, **1**, 81.
86. J. W. Pritchard, J. R. Alger, K. L. Behar, O. A. C. Petroff and R. G. Shulman, *Proc. Natl Acad. Sci. USA.*, 1983, **80**, 2748.
87. J. W. Pritchard and R. G. Shulman, *Ann. Rev. Neurosci.*, 1986, **9**, 61.
88. P. Y. Shkarin, A. A. Samoitenko and L. A. Sibel'dina, *Biofizika*, 1983, **28**, 122.
89. N. V. Reo, B. A. Siegfried and J. J. H. Ackerman, *J. Biol. Chem.*, 1984, **259**, 13664.
90. M. E. Stromski, F. Anas-Mendoza, J. R. Alger and R. G. Shulman, *Magn. Reson. Med.*, 1986, **3**, 24.
91. K. J. Neurohr, E. J. Barrett and R. G. Shulman, *Proc. Natl Acad. Sci. USA*, 1983, **80**, 1603.
92. A. P. Koretsky, S. Wang, M. P. Klein, T. J. James and M. W. Weirer, *Biochemistry*, 1986, **25**, 77.
93. H. L. Kantor, R. W. Briggs and R. S. Balaban, *Circ. Res.*, 1984, **55**, 261.
94. D. I. Hoult and R. E. Richards, *J. Magn. Reson.*, 1976, **24**, 71.
95. E. Oldfield and M. Meadows, *J. Magn. Reson.*, 1978, **32**, 327.
96. P. Brunner and R. R. Ernst, *J. Magn. Reson.*, 1979, **33**, 83.
97. A. A. Maudsley, *J. Magn. Reson.*, 1986, **68**, 636.
98. O. C. Morse and J. R. Singer, *Science*, 1970, **170**, 440.
99. J. J. H. Ackerman, T. H. Grove, G. Wong, G. Gadian and G. K. Radda, *Nature*, 1980, **283**, 167.
100. R. E. Gordon, P. E. Hanley, D. Shaw, D. G. Gadian, P. Styles, P. J. Bore and L. Chan, *Nature*, 1980, **287**, 367.
101. R. Damadian, L. Minkoff, M. Goldsmith, M. Stanford and J. Koutcher, *Physiol. Chem. Phys.*, 1976, **8**, 61.
102. P. C. Lauterbur, D. M. Kramer, W. V. House and C.-H. Chen, *J. Am. Chem. Soc.*, 1975, **97**, 6866.
103. P. A. Bottomley, *J. Magn. Reson.*, 1982, **50**, 335.
104. P. Mansfield, *J. Phys.*, 1983, **D16**, L235.
105. A. A. Maudsley, A. Oppelt and A. Ganssen, *Siemens Forsch.*, 1979, **8**, 326.
106. W. P. Aue, *Rev. Magn. Reson. Med.*, 1986, **1**, 21.
107. J. V. Evelhoch, M. G. Crowley and J. J. H. Ackerman, *J. Magn. Reson*, 1986, **56**, 110.
108. A. Haase, W. Haenicke and J. Frahm, *J. Magn. Reson.*, 1984, **56**, 401.
109. M. Descorps, M. Laval, S. Comfort and J. J. Chaillout, *J. Magn. Reson.*, 1985, **61**, 418.

110. P. Bottomley, H. R. Hart, W. A. Edelstein, J. F. Schenck, L. S. Smith, W. M. Leue, O. M. Mueller and R. W. Redington, *Radiology*, 1984, **150**, 441.
111. P. Bottomley, H. R. Hart, W. A. Edelstein, J. F. Schenck, L. S. Smith, W. M. Leue, O. M. Mueller and R. W. Redington, *Lancet*, 1983, **ii**, 273.
112. P. S. Tofts, E. B. Cady, D. T. Delpy, A. M. Costello, P. L. Hope, E. O. Reynolds, D. R. Wilkie, S. J. Gould and D. Edwards, *Lancet*, 1984, **i**, 459.
113. J. W. Pettegrew, N. J. Minshew, J. Diehl, T. Smith, S. J. Kopp and T. Glonek, *Lancet*, 1983, **ii**, 913.
114. K. R. Thulborn and J. J. H. Ackerman, *J. Magn. Reson.*, 1983, **55**, 357.
115. J. L. Evelhoch and J. J. H. Ackerman, *J. Magn. Reson.*, 1983, **53**, 52.
116. G. B. Matson, T. Schleich, C. Serdahl, G. Acosta and J. A. Willis, *J. Magn. Reson.*, 1984, **56**, 200.
117. M. G. Crowley, J. L. Evelhoch and J. J. H. Ackerman, *J. Magn. Reson.*, 1985, **61**, 418.
118. R. Gonzalez-Mendez, M. E. Moseley, J. Murphy-Boesch, W. M. Chew, L. Litt and T. L. James, *J. Magn. Reson.*, 1985, **65**, 526.
119. T. C. Ng, W. Evanochko and J. D. Glickson, *J. Magn. Reson.*, 1982, **49**, 526.
120. M. R. Bendall and R. E. Gordon, *J. Magn. Reson.*, 1983, **53**, 365.
121. G. Bodenhausen, R. Freeman and D. L. Turner, *J. Magn. Reson.*, 1977, **27**, 511.
122. M. R. Bendall and W. P. Aue, *J. Magn. Reson.*, 1983, **54**, 149.
123. M. R. Bendall, *Magn. Reson. Med.*, 1984, **1**, 105.
124. M. R. Bendall, *J. Magn. Reson.*, 1984, **59**, 406.
125. M. R. Bendall and D. T. Pegg, *Magn. Reson. Med.*, 1985, **2**, 91.
126. M. R. Bendall, J. M. McKendry, I. D. Cresshull and R. J. Ordidge, *J. Magn. Reson.*, 1984, **60**, 473.
127. M. H. Levitt and R. Freeman, *J. Magn. Reson.*, 1981, **43**, 65.
128. M. H. Levitt and R. Freeman, *J. Magn. Reson.*, 1983, **55**, 247.
129. R. Tycko and A. Pines, *J. Magn. Reson.*, 1984, **60**, 156.
130. A. J. Shaka and R. Freeman, *J. Magn. Reson.*, 1984, **59**, 169.
131. H. P. Hetherington, D. Wishart, S. M. Fitzpatrick, P. Cole and R. G. Shulman, *J. Magn. Reson.*, 1986, **66**, 313.
132. M. R. Bendall and D. T. Pegg, *J. Magn. Reson.*, 1985, **63**, 494.
133. R. E. Gordon, P. E. Hanley and D. Shaw, *Prog. NMR Spectrosc.*, 1982, **15**, 1.
134. I. D. Campbell, C. M. Dobson, R. J. P. Williams and A. V. Xavier, *J. Magn. Reson.*, 1973, **11**, 172.
135. J. C. Lindon and A. G. Ferrige, *Prog. NMR Spectrosc.*, 1980, **14**, 27.
136. A. N. Garroway, P. K. Grannell and P. Mansfield, *J. Phys.*, 1974, **C7**, L457.
137. P. R. Locher, *Phil. Trans. R. Soc. Lond.*, 1980, **B289**, 519.
138. J. T. Ngo and P. G. Morris, *Biochem. Soc. Trans.*, 1986, **14**, 1271.
139. J. T. Ngo and P. G. Morris, *Magn. Reson. Med.*, 1987, **5**, 217.
140. P. A. Bottomley, T. B. Foster and R. D. Darrow, *J. Magn. Reson.*, 1984, **59**, 338.
141. P. A. Bottomley, *Science*, 1985, **229**, 769.
142. P. A. Bottomley, L. S. Smith, W. M. Leue and C. Charles, *J. Magn. Reson.*, 1985, **64**, 347.
143. H. Post, *Bruker Internal Report*.
144. W. P. Aue, S. Mueller, T. A. Cross and J. Seelig, *J. Magn. Reson.*, 1984, **56**, 350.
145. S. Mueller, W. P. Aue and J. Seelig, *J. Magn. Reson.*, 1985, **63**, 530.
146. S. Mueller, W. P. Aue and J. Seelig, *J. Magn. Reson.*, 1985, **65**, 332.
147. R. J. Ordidge, in *Proc. 4th Annual Meeting, Society of Magnetic Resonance in Medicine*, 1985, pp. 131-132.

148. R. J. Ordidge, A. Connelly and J. A. B. Lohman, *J. Magn. Reson.*, 1986, **66**, 283.
149. M. S. Silver, R. I. Joseph and D. I. Hoult, *J. Magn. Reson.*, 1984, **59**, 349.
150. A. Kumar, D. Welte and R. R. Ernst, *J. Magn. Reson.*, 1975, **18**, 69.
151. A. Kumar, D. Welte and R. R. Ernst, *Naturwissenschaften*, 1975, **62**, 34.
152. W. A. Edelstein, J. M. S. Hutchison, G. Johnson and T. Redpath, *Phys. Med. Biol.*, 1980, **25**, 751.
153. T. R. Brown, B. M. Kincaid and K. Ugurbil, *Proc Natl Acad. Sci. USA*, 1982, **79**, 3523.
154. J. C. Haselgrove, V. Subramanian, J. S. Leigh, L. Gyulai and B. Chance, *Science*, 1983, **220**, 1170.
155. I. L. Pykett and B. R. Rosen, *Radiology*, 1983, **149**, 197.
156. A. A. Maudsley, S. K. Hilal, W. H. Perman and H. E. Simon, *J. Magn. Reson.*, 1983, **51**, 147.
157. L. D. Hall and S. Sukumar, *J. Magn. Reson.*, 1984, **56**, 314.
158. D. I. Hoult, *J. Magn. Reson.*, 1979, **33**, 183.
159. S. Cox and P. Styles, *J. Magn. Reson.*, 1980, **40**, 209.
160. J. Pekar, J. S. Leigh and B. Chance, *J. Magn. Reson.*, 1985, **64**, 115.
161. K. R. Metz and R. W. Briggs, *J. Magn. Reson.*, 1985, **64**, 172.
162. M. Garwood, T. Schleich, B. D. Ross, G. B. Matson and W. D. Winters, *J. Magn. Reson.* 1985, **65**, 239.
163. B. D. Ross, personal communication.
164. M. W. Winkler, G. B. Matson, J. W. B. Hershey and E. Morton Bradbury, *Exp. Cell Res.*, 1982, **139**, 217.
165. W. B. Busa, in *Intracellular pH: Its Measurement, Regulation and Utilization in Cellular Functions*, Alan R. Liss, New York, 1982, pp. 417-426.
166. *Calcium, Drugs and Hormones* (P. F. Baker and J. C. Metcalfe, eds), *Brit. Med. Bull.*, 1986, **42**(4).
167. *Metabolic Acidosis* (R. Porter and G. Lawrenson, eds), *Ciba Found. Symp.*, 1982.
168. R. Y. Tsien, *Ann. Rev. Biophys. Bioengng*, 1983, **12**, 91.
169. R. K. Gupta and P. Gupta, *Ann. Rev. Biophys. Bioengng*, 1984, **13**, 221.
170. R. K. Gupta and P. Gupta, *J. Magn. Reson.*, 1982, **47**, 344.
171. J. A. Balschi, V. P. Cirillo and C. S. Springer, *Biophys. J.*, 1982, **38**, 323.
172. E. T. Fossel, in *Works in Progress*, Society of Magnetic Resonance in Medicine, 1983.
173. G. A. Smith, T. R. Hesketh, J. C. Metcalfe, J. Feeney and P. G. Morris, *Proc. Natl Acad. Sci. USA*, 1983, **80**, 7178.
174. J. C. Metcalfe, T. R. Hesketh and G. A. Smith, *Cell Calcium*, 1985, **6**, 183.
175. P. G. Morris, G. A. Smith, J. C. Metcalfe and G. C. Rodrigo, in *Works in Progress*, Society of Magnetic Resonance in Medicine, 1987.
176. G. A. Smith, P. G. Morris and T. R. Hesketh, *Biochim. Biophys. Acta*, 1986, **899**, 72.
177. R. Y. Tsien, *Biochemistry*, 1980, **19**, 2396.
178. R. Y. Tsien, T. Pozzan and T. J. Rink, *Nature*, 1982, **295**, 68.
179. J. Sandstrom, *Dynamic NMR Spectroscopy*, Academic Press, London, 1982.
180. J. L. Kaplan and G. Fraenkel, *NMR of Chemically Exchanging Systems*, Academic Press, New York, 1980.
181. R. Y. Tsien, *Nature*, 1981, **290**, 527.
182. D. M. Rose, P. A. Tovo, R. G. Bryant, M. L. Bleam, and M. T. Record, in *Biochemical Structure Determination by NMR* (A. A. Bothner-By, J. D. Glickson and B. D. Sykes, eds), Dekker, New York, 1982, pp. 53-64.
183. M. Cohn and T. R. Hughes, *J. Biol. Chem.* 1962, **237**, 176.
184. R. K. Gupta, J. L. Benovic and Z. B. Rose, *J. Biol. Chem.*, 1978, **253**, 6172.
185. S. T. Wu, G. M. Pieper, J. M. Salhany and R. S. Eliot, *Biochemistry*, 1981, **20**, 7399.

186. R. K. Gupta, P. Gupta, W. D. Yushok and Z. B. Rose, *Biochem. Biophys. Res. Commun.*, 1983, **117**, 210.
187. R. K. Gupta, P. Gupta, W. D. Yushok and Z. B. Rose, *Physiol. Chem. Phys.*, 1983, **15**, 265.
188. A. M. Wyrwicz, J. C. Schofield and C. T. Burt, in *Non-Invasive Probes of Tissue Metabolism*, (J. S. Cohen, ed.), Wiley, 1982, pp. 149–171.
189. T. J. Rink, R. Y. Tsien and T. Pozzan, *J. Cell. Biol.*, 1982, **95**, 189.
190. R. K. Gupta and R. D. Moore, *J. Biol. Chem.*, 1980, **255**, 3987.
191. L. T. Iseri and J. H. French, *Am. Heart J.*, 1984, **108**, 188.
192. L. M. Resnick, R. K. Gupta and J. H. Laragh, *Proc. Natl Acad. Sci. USA*, 1984, **81**, 6511.
193. S. M. Cohen, *J. Biol. Chem.*, 1983, **258**, 14294.
194. R. Peters, *Endeavour*, 1954, **13**, 147.
195. G. A. Smith, A. N. Corps, M. B. Stelmach, P. G. Morris, T. R. Hesketh and J. C. Metcalfe (submitted).
196. M. M. Civan and M. Shporer, in *Biological Magnetic Resonance*, Vol. 1 (L. J. Berliner and J. Reuben, eds), Plenum Press, New York, 1978, pp. 1–30.
197. S. Chu, M. M. Pike, E. T. Fossel, T. W. Smith, J. A. Balschi and C. S. Springer, *J. Magn. Reson.*, 1984, **56**, 33.
198. M. M. Pike, E. T. Fossel, T. W. Smith and C. S. Springer, *Am. J. Physiol.*, 1984, **246**, c528.
199. H. Shinar and N. Gil, *FEBS Lett.*, 1985, **193**, 25.
200. K. Kirk and P. W. Kuchel, *J. Magn. Reson.*, 1985, **62**, 568.
201. Y. Boulanger, P. Vinay and M. Desroches, *Biophys. J.*, 1985, **47**, 553.
202. R. K. Gupta and B. A. Wittenberg, *Fed. Proc.*, 1983, **42**, 2065.
203. B. A. Wittenberg and R. K. Gupta, *J. Biol. Chem.*, 1985, **260**, 2031.
204. T. Ogino, J. A. Den Hollander and R. G. Shulman, *Proc. Natl Acad. Sci. USA*, 1983, **80**, 5185.
205. P. J. Brophy, M. K. Hayer and F. G. Riddell, *Biochem. J.*, 1983, **210**, 961.
206. M. M. Pike, J. C. Frazer, D. F. Dedrick, J. S. Ingwall, P. D. Allen, C. S. Springer and T. W. Smith, *Biophys. J.*, 1985, **48**, 159.
207. A. A. Maudsley and S. K. Hilal, *Brit. Med. Bull.*, 1984, **40**, 165.
208. S. K. Hilal, J. B. Ra, I. K. Mun and A. J. Silver, *Soc. Magn. Reson. Med. Abstracts*, 1985, pp. 797–798.
209. H. J. C. Berendsen and H. T. Edzes, *Ann. NY Acad. Sci.*, 1973, **204**, 459.
210. R. A. Iles, A. N. Stevens and J. R. Griffiths, *Prog. NMR Spectrosc.*, 1982, **15**, 49.
211. M. Batley and J. W. Redmond, *J. Magn. Reson.*, 1982, **49**, 172.
212. J. K. Gard and J. J. H. Ackerman, *J. Magn. Reson.*, 1983, **51**, 124.
213. R. J. Labotka and R. A. Kleps, *Biochemistry*, 1983, **22**, 6089.
214. W. H. Huestis and M. A. Raftery, *Biochem. Biophys. Res. Commun.*, 1972, **49**, 428.
215. I. A. Bailey, S. R. Williams, G. K. Radda and D. G. Gadian, *Biochem. J.*, 1981, **196**, 171.
216. Y. Seo, K. Yoshizaki and T. Morimoti, *Jpn J. Physiol.*, 1983, **33**, 721.
217. F. F. Brown, I. D. Campbell, P. W. Kuchel and D. C. Rabenstein, *FEBS Lett.*, 1977, **82**, 12.
218. C. Deutsch, J. S. Taylor and D. F. Wilson, *Proc. Natl Acad. Sci. USA*, 1982, **79**, 7944.
219. J. Rogers, T. R. Hesketh, G. A. Smith and J. C. Metcalfe, *J. Biol. Chem.*, 1983, **258**, 5994.
220. J. S. Beech and R. A. Iles, *Biochem Soc. Trans.*, 1987, **15**, 871.
221. P. Mitchell, *Nature*, 1961, **191**, 144.
222. G. Navon, S. Ogawa, R. G. Shulman and T. Yamane, *Proc. Natl Acad. Sci. USA*, 1977, **74**, 888.

223. T. R. Brown, K. Ugurbil and R. G. Shulman, *Proc. Natl Acad. Sci. USA*, 1977, **74**, 5551.
224. S. Ogawa, R. G. Shulman, P. Glynn, T. Yamane and G. Navon, *Biochim. Biophys. Acta*, 1978, **502**, 45.
225. K. Ugurbil, H. Rottenberg, P. Glynn and R. G. Shulman, *Proc. Natl Acad. Sci. USA*, 1978, **75**, 2244.
226. K. Ugurbil, T. R. Brown, J. A. den Hollander, P. Glynn and R. G. Shulman, *Proc. Natl Acad. Sci. USA*, 1978, **75**, 3742.
227. R. G. Shulman, T. R. Brown, K. Ugurbil, S. Ogawa, S. M. Cohen and J. A. den Hollander, *Science*, 1979, **205**, 160.
228. R. G. Shulman, *Sci. Am.*, 1983, **1**, 76.
229. K. Nicolay, R. Kaptein, K. J. Hellingswerf and W. N. Konings, *Eur. J. Biochem.*, 1981, **116**, 191.
230. R. J. Gillies, T. Ogini, R. G. Shulman and D. C. Ward, *J. Cell Biol.*, 1982, **95**, 24.
231. C. J. Deutsch, T. Kashiwagura, J. Taylor, D. F. Wilson and M. Erecuiska, *J. Biol. Chem.*, 1985, **260**, 6808.
232. P. S. Belton and R. G. Ratcliffe, *Prog. NMR Spectrosc.*, 1985, **17**, 241.
233. J. B. Martin, R. Bligny, F. Rebeille, R. Douce, J. J. Leguay, Y. Mathieu and J. Guern, *Plant Physiol.*, 1982, **70**, 1156.
234. F. Rebeille, R. Bligny, J. B. Martin and R. Douce, *Arch Biochim. Biophys.*, 1983, **225**, 143.
235. A. Schibeci, R. J. Henry, B. A. Stone and R. T. C. Brownlee, *Biochem. Int.*, 1983, **6**, 837.
236. H. Strasser, K. H. Tietjen, K. Himmelsbach and U. Matern, *Plant Cell Rep.*, 1983, **2**, 140.
237. R. J. Robins and R. G. Ratcliffe, *Plant Cell Rep.*, 1984, **3**, 234.
238. J. J. Vogel and P. Brodelius, *J. Biotechnol.*, 1984, **1**, 3.
239. P. Brodelius and H. J. Vogel, *J. Biol. Chem.*, 1985, **260**, 3556.
240. P. Brodelius and H. J. Vogel, *Ann. NY Acad. Sci.*, 1984, **434**, 496.
241. V. Wray, O. Schiel, J. Berlin and L. Wite, *Arch. Biochem. Biophys.*, 1985, **236**, 731.
242. F. H. Andrade, *Commun. Biol.*, 1985, **4**, 15.
243. F. Mitsumori, T. Yoneyama and O. Ito, *Plant. Sci.*, 1985, **38**, 87.
244. S. M. Cohen, S. Ogawa, H. Rottenberg, P. Glynn, T. Yamane, T. R. Brown, R. G. Shulman and J. R. Williamson, *Nature*, 1978, **273**, 554.
245. P. B. Garlick, T. R. Brown, R. H. Sullivan and K. Ugurbil, *J. Mol. Cell Cardiol.*, 1983, **15**, 855.
246. M. Satre and J. B. Martin, *Biochem. Biophys. Res. Commun.*, 1985, **132**, 140.
247. J. E. Jentoft and C. D. Town, *J. Cell. Biol.*, 1985, **101**, 778.
248. F. Mitsumori and O. Ito, *FEBS Lett.*, 1984, **174**, 248.
249. F. Mitsumori and O. Ito, *J. Magn. Reson.*, 1984, **60**, 106.
250. G. K. Radda, *Biochem. Soc. Trans.*, 1986, **14**, 517.
251. G. K. Radda, *Science*, 1986, **233**, 640.
252. B. Chance, S. Elaff, W. Bank, J. S. Leigh and R. Warnell, *Proc. Natl Acad. Sci. USA*, 1982, **79**, 7714.
253. Z. Argov, W. J. Bank, B. Boden, Y. I. Ro and B. Chance, *Arch. Neurol.*, 1987, **44**, 614.
254. B. D. Ross, G. K. Radda, D. G. Gadian, G. Rocker, M. Esiri and J. Falconer-Smith, *New Engl. J. Med.*, 1981, **304**, 1338.
255. A. N. Stevens, G. Lutaya, P. G. Morris, R. A. Iles and J. R. Griffiths, *Biochem. Soc. Trans.*, 1983, **11**, 92.
256. D. G. Allen, P. G. Morris and C. H. Orchard, *J. Physiol.*, 1983, **343**, 58P.
257. D. G. Allen, P. G. Morris, C. H. Orchard and J. S. Pirolo, *J. Physiol.*, 1985, **361**, 185.
258. B. Chance, D. Younkin, S. Eleff, R. Warnell and M. Delivonia-Pappadopoulos, *Pediat. Res.*, 1983, **17**, 307a.

259. E. B. Cady, A. M. De L. Costello, M. J. Dawson, D. J. Delpy, P. L. Hope, E. O. R. Reynolds, P. S. Tofts and D. R. Wilkie, *Lancet*, 1983, **i**, 1059.
260. P. L. Hope and E. O. Reynolds, *Lancet*, 1984, **ii**, 292.
261. P. L. Hope, A. M. Costello, E. B. Cady, D. T. Delpy, P. S. Tofts, A. Chu, P. A. Hamilton, E. O. Reynolds and D. R. Wilkie, *Lancet*, 1984, **ii**, 366.
262. P. L. Hope and E. O. Reynolds, *Clin. Perinatol.*, 1985, **12**, 261.
263. D. P. Younkin, M. Delivonia-Papadopoulos, J. C. Leonard, V. H. Subramanian, S. Eleff, J. S. Leigh and B. Chance, *Ann. Neurol.*, 1984, **16**, 581.
264. O. A. Petroff and J. W. Prichard, *Lancet*, 1983, **ii**, 105.
265. R. D. Oberhaensli, D. Hilton-Jones, P. J. Bore, L. J. Hands, R. P. Rampling and G. K. Radda, *Lancet*, 1986, **ii**, 8.
266. J. R. Alger and R. G. Shulman, *Q. Rev. Biophys.*, 1982, **171**, 83.
267. R. J. Simpson, K. M. Brindle and I. D. Campbell, *Biochim. Biophys. Acta.* 1982, **707**, 191.
268. K. M. Brindle, F. F. Brown, I. D. Campbell, D. L. Foxall and R. J. Simpson, *Biochem. Soc. Trans.*, 1980, **8**, 646.
269. K. M. Brindle, R. Porteous and G. K. Radda, *Biochem. Biophys. Acta*, 1984, **786**, 18.
270. I. D. Campbell, S. Lindskog and A. I. White, *J. Mol. Biol.*, 1974, **90**, 469.
271. H. M. McConnell, *J. Chem. Phys.*, 1958, **28**, 430.
272. H. M. McConnell and D. D. Thompson, *J. Chem. Phys.*, 1957, **26**, 958.
273. S. Forsen and R. A. Hoffman, *J. Chem. Phys.*, 1963, **39**, 2892.
274. S. Forsen and R. A. Hoffman, *J. Chem. Phys.*, 1964, **40**, 1189.
275. R. A. Hoffman and S. Forsen, *J. Chem. Phys.*, 1966, **45**, 2049.
276. F. W. Dahlquist, K. J. Langmuir and R. B. DuVernet, *J. Magn. Reson.*, 1977, **27**, 455.
277. T. R. Brown and S. Ogawa, *Proc. Natl Acad. Sci. USA*, 1977, **74**, 3627.
278. J. R. Alger and J. H. Prestgard, *J. Magn. Reson.*, 177, **27**, 127.
279. I. D. Campbell, C. M. Dobson, R. G. Ratcliffe and R. J. P. Williams, *J. Magn. Reson.*, 1978, **29**, 397.
280. T. R. Brown, K. Ugurbil and R. G. Shulman, *Proc. Natl Acad. Sci. USA*, 1977, **74**, 5551.
281. P. G. Morris, J. Feeney, D. W. G. Cox and H. S. Bachelard, *Biochem. J.*, 1985, **227**, 777.
282. R. R. DeFuria, M. K. Dygert and G. M. Alachi, *J. Theor. Biol.*, 1985, **114**, 75.
283. R. Freeman and H. D. W. Hill, *J. Magn. Reson.*, 1973, **4**, 366.
284. G. A. Morris and R. Freeman, *J. Magn. Reson.*, 1978, **29**, 433.
285. H. Degani, M. Laughlin, S. Campbell and R. G. Shulman, *Biochemistry*, 1985, **24**, 5510.
286. J. Jeener, B. H. Meier, P. Bachman and R. R. Ernst, *J. Chem. Phys.*, 1979, **71**, 4546.
287. B. H. Meier and R. R. Ernst, *J. Am. Chem. Soc.*, 1979, **101**, 6441.
288. R. R. Ernst, G. Bodenhausen and A. Wokaun, *Principles of Nuclear Magnetic Resonance in One and Two Dimensions*, Oxford University Press, 1987.
289. R. S. Balaban and J. A. Ferretti, *Proc. Natl Acad. Sci. USA*, 1983, **80**, 1241.
290. R. S. Balaban, H. L. Kantor and J. A. Ferretti, *J. Biol. Chem.*, 1983, **258**, 12787.
291. P. B. Garlick and C. J. Turner, *J. Magn. Reson.*, 1983, **51**, 536.
292. D. G. Gadian, G. K. Radda, T. R. Brown, E. M. Chance, M. J. Dawson and D. R. Wilkie, *Biochem. J.*, 1981, **194**, 215.
293. T. R. Brown, D. G. Gadian, P. B. Garlick, G. K. Radda, P. J. Seeley and P. Styles, *Front. Biol. Energetics*, 1978, **2**, 1341.
294. R. L. Nunnally and D. P. Hollis, *Biochemistry*, 1979, **18**, 3642.
295. P. M. Matthews, J. L. Brand, D. G. Gadian and G. K. Radda, *Biochem. Biophys. Res. Commun.*, 1981, **103**, 1052.
296. P. M. Matthews, J. L. Brand, D. G. Gadian and G. K. Radda, *Biochim. Biophys. Acta.*, 1982, **721**, 312.

297. K. Ugurbil, *Circulation*, 1985, **72**, Suppl. 4, 94.
298. V. V. Kupriyanov, A. Y. Shteinshneider, E. Ruunge, V. I. Kapel'ko, M. Y. Zueva, V. L. Lakomkin, V. N. Smirnov and V. A. Saks, *Biochim. Biophys Acta*, 1984, **805**, 319.
299. J. A. Bittl and J. S. Ingwall, *J. Biol. Chem.*, 1985, **260**, 3512.
300. V. A. Saks, L. V. Rosenshtaukh, V. N. Smirnov and E. I. Chazov, *Can. J. Physiol. Pharmacol.*, 1978, **56**, 591.
301. E. A. Shoubridge, R. W. Briggs and G. K. Radda, *FEBS Lett.*, 1982, **140**, 288.
302. K. Ugurbil, *J. Magn. Reson.*, 1985, **64**, 207.
303. K. Ugurbil, M. Petain, R. Maiden and S. Michurski, *Biochemistry*, 1986, **251**, 100.
304. K. M. Brindle and G. K. Radda, *Biochim. Biophys. Acta*, 1987, **928**, 45.
305. J. R. Alger, J. A. den Hollander and R. G. Shulman, *Biochemistry*, 1982, **21**, 2957.
306. P. Kingsley-Hickman, E. Y. Sako, P. A. Andreone, J. A. St Cyr, S. Michurski, J. E. Foker, A. H. L. From, M. Petein and K. Ugurbil, *FEBS Lett.*, 1986, **198**, 159.

# Nuclear Magnetic Resonance Spectroscopy of Boron Compounds Containing Two-, Three- and Four-Coordinate Boron

BERND WRACKMEYER

*Laboratorium für Anorganische Chemie der Universität Bayreuth  
Postfach 10 12 51, D-8580 Bayreuth, FRG*

I. Introduction . . . . .	61
II. Experimental . . . . .	63
A. General procedures, referencing . . . . .	63
B. Nuclear-spin relaxation . . . . .	65
III. $^{11}\text{B}$ nuclear magnetic resonance . . . . .	68
A. Chemical shifts, $\delta^{11}\text{B}$ . . . . .	68
B. Substituent effects on $^{11}\text{B}$ -chemical shifts, $\delta^{11}\text{B}$ . . . . .	71
C. Indirect nuclear spin-spin couplings $^nJ(^{11}\text{BX})$ . . . . .	160
IV. NMR of nuclei other than $^{11}\text{B}$ and $^1\text{H}$ . . . . .	168
A. $^6\text{Li}$ and $^7\text{Li}$ NMR . . . . .	168
B. $^9\text{Be}$ NMR . . . . .	168
C. $^{10}\text{B}$ , $^{27}\text{Al}$ and $^{71}\text{Ga}$ NMR . . . . .	168
D. $^{13}\text{C}$ NMR . . . . .	169
E. $^{29}\text{Si}$ , $^{119}\text{Sn}$ and $^{207}\text{Pb}$ NMR . . . . .	174
F. $^{14}\text{N}$ and $^{15}\text{N}$ NMR . . . . .	175
G. $^{31}\text{P}$ NMR . . . . .	178
H. $^{17}\text{O}$ and $^{77}\text{Se}$ NMR . . . . .	178
I. $^{19}\text{F}$ , $^{35}\text{Cl}$ and $^{37}\text{Cl}$ NMR . . . . .	180
J. NMR of transition-metal nuclei . . . . .	181
Acknowledgments . . . . .	181
References . . . . .	182

## I. INTRODUCTION

The influence of boron chemistry on various areas of research in inorganic, organic and theoretical chemistry is well documented.<sup>1,2</sup> In fact, many models presently employed to describe chemical bonding in general can be traced to attempts to understand bonding in boranes.<sup>3</sup> The confirmation of many theoretical predictions in boron chemistry relies on direct and indirect

structural information provided by various physical methods that—fortunately—became available almost at the same rate as that with which the interest in boron compounds was growing. Clearly, there has always been a strong link between the interest in synthesis and the application of physical methods. As in many other areas of chemistry, developments in boron chemistry have been greatly accelerated by NMR.  $^{11}\text{B}$  NMR has been at the centre of interest from the beginning,<sup>4,5</sup> accompanied by routine  $^1\text{H}$  NMR measurements,<sup>4</sup> and occasional  $^{14}\text{N}$ ,  $^{19}\text{F}$  and  $^{31}\text{P}$  NMR work.<sup>5</sup> In the last 12 years, we have seen an increasing number of  $^{13}\text{C}$  NMR studies of boron compounds. The availability of “multinuclear” facilities for PFT NMR spectrometers stimulates the measurement of the NMR spectra of other nuclei, like  $^{29}\text{Si}$ ,  $^{119}\text{Sn}$  or other metals, in order to obtain additional information.

$^{11}\text{B}$  NMR data have been reviewed several times.<sup>4-9</sup> Reference 10 deals with early  $^{13}\text{C}$  NMR studies of boron compounds. Reference 7, on the application of “multinuclear” NMR, is closely connected with the synthesis and characterization of organoboron compounds. Recently, boron chemistry has been extended into a number of fascinating new areas (e.g. two-coordinate boron compounds,<sup>11</sup> polyhedral boron halides<sup>12</sup> and new carbaboranes<sup>13</sup> and metallacarbaboranes<sup>14-16</sup>). All of this work, and many other new studies in well-established areas, have been supported by the application of NMR spectroscopy. Therefore the present review is intended to serve several purposes: (i) to update previous reviews on  $^{11}\text{B}$  NMR of boron compounds, (ii) to demonstrate some applications of multinuclear NMR to boron chemistry; (iii) to attempt to incorporate new NMR parameters into the known data set; and (iv) to summarize the experimental facts required for obtaining the maximum information from NMR studies on boron compounds.

In order to keep this chapter at a manageable size, extensive discussions and tables of  $^1\text{H}$  NMR data have been omitted. Similarly,  $^{13}\text{C}$  NMR data are not covered in detail. Tables of  $^{11}\text{B}$  NMR data have been designed in order to avoid extensive overlap with previous reviews. This means that  $\delta^{11}\text{B}$  values of derivatives of a well-known class of boron compounds may not be cited, except for a significant deviation from comparable data. Most of the NMR measurements of nuclei other than boron are cited together with  $\delta^{11}\text{B}$  values in the tables. Since our understanding of the trends in nuclear shieldings or couplings is still poor when heavy nuclei are involved, all data for any new combination of nuclei may provide important information. Solid-state NMR work is not included, although there are a number of promising applications of  $^{11}\text{B}$  NMR, for example in borates,<sup>804,805</sup> in boron-sulphur and boron-selenium phases,<sup>789</sup> in boron carbides<sup>807</sup>, also of  $^{13}\text{C}$  NMR in boron carbides<sup>806,807</sup> and carbaboranes,<sup>808</sup> to name just a few references.

## II. EXPERIMENTAL

### A. General procedures, referencing

#### 1. $^{11}\text{B}$ NMR

Since  $^{11}\text{B}$  NMR spectra of reaction solutions are readily obtained, they frequently provide the first information about the number of products, their principal structural units as far as the boron is concerned, and about possible dynamical processes. Therefore a few brief remarks on the experimental techniques are in order.

The experimental techniques for obtaining  $^{11}\text{B}$  NMR spectra using pulse FT spectroscopy<sup>23</sup> are similar to those for other quadrupolar nuclei that possess a fast quadrupolar relaxation rate (see below). In most cases where the linewidth at half-height  $\Delta\nu_{1/2} > 50$  Hz a low digital resolution can be used together with short acquisition and pulse-repetition time when  $90^\circ$  pulses are employed. Zero-filling before the Fourier transformation ensures a sufficiently accurate measurement of  $\delta^{11}\text{B}$  (about  $\pm 0.3$  ppm or better). The influence of inert solvents on  $\delta^{11}\text{B}$  values of most boron compounds is small ( $< \pm 0.3$  ppm). However, for some polyhedral boranes, and, in particular, for metallaboranes and metallacarboranes, noticeable solvent shifts ( $\leq 4$  ppm) have been observed.<sup>703</sup> In the case of tetracoordinate boron there are many examples for a fairly slow quadrupolar relaxation rate, and therefore spin-spin coupling to other nuclei may also be resolved. This requires a more careful setting of the instrument parameters in order to avoid saturation effects and to obtain reproducible values  $J(^{11}\text{BX})$ . Thus it appears that diverging values, e.g. for  $^1J(^{11}\text{B}^1\text{H})$ , reported for the same compound result from inadequate experimental parameters rather than from the influence of the solvent, concentration, temperature, etc. The use of a high magnetic-field strength  $B_0$  is advantageous. In addition to the inherent gain in sensitivity (which is not crucial in  $^{11}\text{B}$  NMR), resolution of broad overlapping signals can be achieved. Other techniques for increasing the resolution, such as partially relaxed FT NMR,<sup>17</sup> and measuring at high temperatures (in order to slow down the quadrupolar relaxation rate), are not generally applicable. However, the use of nonviscous solvents (like pentane, methylene chloride and ether) and of moderately concentrated solutions is always advisable in order to reduce the linewidth in routine  $^{11}\text{B}$  NMR spectra.

For very dilute samples and/or in the case of broad  $^{11}\text{B}$  resonances ( $\Delta\nu_{1/2} > 500$  Hz) background signals arising from the tube and probehead material may hamper a correct interpretation as far as the intensities and the linewidths of the  $^{11}\text{B}$  resonances are concerned. This is a general problem found with the broad resonances of quadrupolar nuclei (e.g.  $^{14}\text{N}$ ,

$^{17}\text{O}$ ,  $^{27}\text{Al}$ ,  $^{59}\text{Co}$ ) when considering the various causes for background signals.

## 2. $^{13}\text{C}$ NMR

The well-known procedures for  $^{13}\text{C}$  NMR<sup>18,23</sup> are applicable for investigating the carbon-containing part of boron compounds.  $^{13}\text{C}$  resonances of carbon atoms linked directly to the  $^{11}\text{B}$  nucleus are in general severely broadened owing to scalar relaxation of the second kind (see below). This effect is rapidly attenuated by intervening atoms. A small broadening with respect to other  $^{13}\text{C}$  signals may be observed and assigned (provided that the digital resolution is sufficient) to the neighbourhood of the quadrupolar boron nucleus two or three bonds removed.<sup>71</sup> Since the partially relaxed coupling  $^nJ(^{13}\text{C}^{11}\text{B})$  is responsible for this broadening, the magnitude of  $^nJ(^{13}\text{C}^{11}\text{B})$  and the quadrupolar relaxation rate of the  $^{11}\text{B}$  nucleus are involved. The latter influence is controlled by the experimental conditions. Therefore the amount of broadening depends on the nature of the solvent, upon the temperature and the solute concentration.<sup>71</sup> Heteronuclear decoupling experiments like  $^{13}\text{C}\{^{11}\text{B}\}$  confirm the origin of the broadening

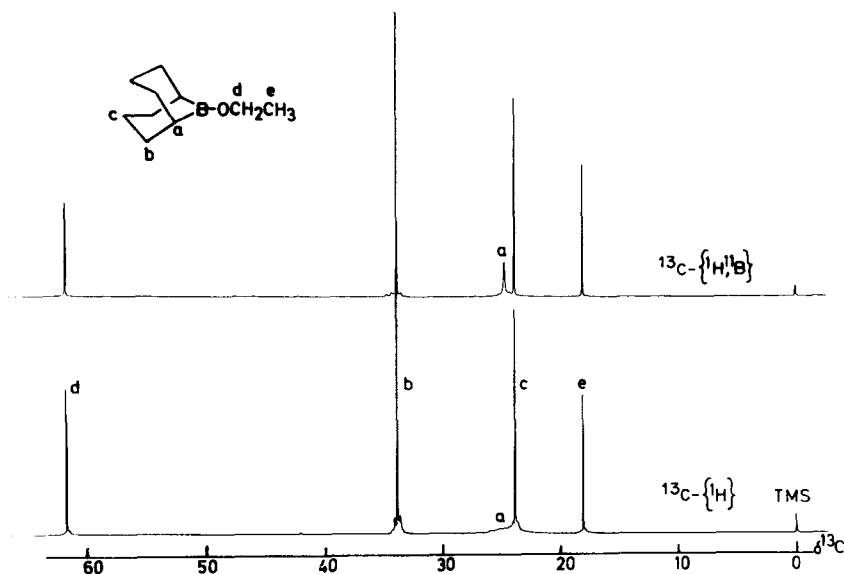


FIG. 1. 50.3 MHz  $^{13}\text{C}$  NMR spectra of 9-ethoxy-9-borabicyclo[3.3.1]nonane, showing the broad  $^{13}\text{C}(\text{BC})$  resonance and the influence of  $^{11}\text{B}$  decoupling (the same result can be achieved by measuring the  $^{13}\text{C}$  NMR spectra at low temperature, e.g.  $-50^\circ\text{C}$ ).

of the  $^{13}\text{C}$  signals (see Fig. 1) and, in some cases, enable  $^{13}\text{C}$  resonances to be detected, or they prove the connectivity between  $^{13}\text{C}$  and a specific boron site (e.g. in carbaboranes).<sup>700-702</sup>

### 3. Other nuclei

NMR measurements of quadrupolar nuclei such as  $^{14}\text{N}$ ,  $^{17}\text{O}$  and  $^{27}\text{Al}$  are straightforward when following the advice given for the  $^{11}\text{B}$  nucleus. Background signals ( $^{27}\text{Al}$ ) or a rolling baseline ( $^{14}\text{N}$ ,  $^{17}\text{O}$ ) may constitute a serious problem.

Spin- $\frac{1}{2}$  nuclei with high natural abundance ( $^{19}\text{F}$ ,  $^{31}\text{P}$ ) are observed by routine procedures. The observation of other spin- $\frac{1}{2}$  nuclei with low natural abundance may be extremely difficult owing to the broadening of the resonances and—frequently—to inefficient nuclear-spin relaxation (e.g.  $^{15}\text{N}$ ,  $^{29}\text{Si}$ ). Spin-polarization-transfer techniques based on the INEPT pulse sequence<sup>19-21</sup> have greatly improved this situation. Even for  $^{15}\text{N}$  in natural abundance, it has been shown that meaningful spectra of boron–nitrogen compounds can be obtained within a few hours or less.<sup>22</sup>

### 4. Referencing

Table 1 contains a list of the nuclear properties of the isotopes of the various nuclei frequently encountered in boron compounds. The final column shows the frequencies  $\Xi$  that can be used as external references. Since the frequencies of resonance signals can be readily determined using pulse-FT spectrometers, their conversion to the  $\delta$  scale provides a convenient and reproducible way of referencing. Of course, this does not replace the internal reference ( $\text{Me}_4\text{Si}$ ) in the case of  $^1\text{H}$  and  $^{13}\text{C}$  (and possibly  $^{29}\text{Si}$ ), but it appears to be a reliable method for those nuclei for which an external reference is needed anyhow. This concept is also seen in the case of  $\delta^{103}\text{Rh}$  or  $\delta^{195}\text{Pt}$ , where arbitrary frequencies have been proposed as external references in order to circumvent the influence of temperature and concentration upon the resonance frequency of a distinct compound (e.g.  $\text{Na}_2[\text{PtCl}_6]$  in  $\text{H}_2\text{O}/\text{D}_2\text{O}$  for  $\delta^{195}\text{Pt}$ ).

## B. Nuclear-spin relaxation

For the majority of boron compounds the longitudinal relaxation time  $T_1(^{11}\text{B})$  is of the order of  $10^{-3}$  s and the relaxation mechanism is dominated by the quadrupolar term.<sup>25</sup> Therefore  $T_1(^{11}\text{B}) = T_2(^{11}\text{B}) = T_2^0(^{11}\text{B})$  and, assuming that  $T_1$  is frequency-independent in the motional-narrowing

TABLE 1

Nuclear properties and referencing for nuclei frequently encountered in boron compounds.<sup>a</sup>

Nucleus	Natural abundance (%)	Spin $I$	Magnetogyric ratio ( $\text{rad s}^{-1} \text{T}^{-1}$ )	Relative sensitivity <sup>b</sup> $D^C$ ( $^{13}\text{C} = 1$ )	Resonance frequencies at 2.301 T	Electric quadrupole moment $Q$ ( $10^{-28} \text{m}^2$ )	Reference compound	$\Xi$ (Hz)
$^1\text{H}$	99.98	$\frac{1}{2}$	$2.676 \times 10^8$	$5.68 \times 10^3$	100.00	—	$\text{Me}_4\text{Si}$	100 000 000
$^7\text{Li}$	92.58	$\frac{3}{2}$	$1.0398 \times 10^8$		38.86	-0.045	$\text{LiCl}/\text{H}_2\text{O}$	
$^{10}\text{B}$	18.83	3	$2.875 \times 10^7$		10.53	0.074	$\text{F}_3\text{B}-\text{OEt}_2$	10 743 656
$^{11}\text{B}$	81.17	$\frac{3}{2}$	$8.582 \times 10^7$		32.08	0.0355	$\text{F}_3\text{B}-\text{OEt}_2$	32 083 972
$^{13}\text{C}$	1.11	$\frac{1}{2}$	$6.725 \times 10^7$	1.00	25.14	—	$\text{Me}_4\text{Si}$	25 145 004
$^{14}\text{N}$	99.64	1	$1.933 \times 10^7$		7.22	0.02	$\text{CH}_3\text{NO}_2$ (neat)	
$^{15}\text{N}$	0.36	$\frac{1}{2}$	$-2.711 \times 10^7$	$2.19 \times 10^{-2}$	10.13	—	$\text{CH}_3\text{NO}_2$ (neat)	10 136 757
$^{17}\text{O}$	0.037	$\frac{5}{2}$	$-3.628 \times 10^7$		13.57	-0.03	$\text{H}_2\text{O}$	
$^{19}\text{F}$	100.00	$\frac{1}{2}$	$2.517 \times 10^8$	$4.73 \times 10^3$	94.08	—	$\text{CFCl}_3$	94 093 795
$^{27}\text{Al}$	100.00	$\frac{5}{2}$	6.9706		26.06	0.149	$[\text{Al}(\text{H}_2\text{O})_6]^{3+}$	
$^{29}\text{Si}$	4.7	$\frac{1}{2}$	$-5.314 \times 10^7$	2.09	19.87	—	$\text{Me}_4\text{Si}$	19 867 184
$^{31}\text{P}$	100.00	$\frac{1}{2}$	$1.082 \times 10^8$	$3.77 \times 10^2$	40.48	—	$\text{H}_3\text{PO}_4$ (85%)	40 480 790
$^{33}\text{S}$	0.76	$\frac{3}{2}$	$2.051 \times 10^7$		7.67	0.064		
$^{35}\text{Cl}$	75.53	$\frac{3}{2}$	$2.621 \times 10^7$		9.60	-0.0797	$\text{Cl}^-$	
$^{59}\text{Co}$	100.00	$\frac{7}{2}$	6.3171		23.61	0.40	$[\text{Co}(\text{CN})_6]^{3-}$	
$^{77}\text{Se}$	7.58	$\frac{1}{2}$	$5.109 \times 10^7$	2.98	19.10	—	$\text{Me}_2\text{Se}$	19 071 523
$^{103}\text{Rh}$	100.00	$\frac{1}{2}$	$0.842 \times 10^7$	0.18	3.16	—	—	3 160 000
$^{119}\text{Sn}$	8.58	$\frac{1}{2}$	$-9.971 \times 10^7$	25.2	37.27	—	$\text{Me}_4\text{Sn}$	37 290 662
$^{125}\text{Te}$	6.99	$\frac{1}{2}$	$-8.453 \times 10^7$	12.5		—	$\text{Me}_2\text{Te}$	31 549 802
$^{195}\text{Pt}$	33.8	$\frac{1}{2}$	$5.7505 \times 10^7$	19.1	21.4	—	—	21 400 000
$^{207}\text{Pb}$	21.1	$\frac{1}{2}$	$5.59 \times 10^7$	11.8	20.9	—	$\text{Me}_4\text{Pb}$	20 920 597

<sup>a</sup> Data from Ref. 24;  $\Xi$  values from Ref. 24 or from own measurements.<sup>b</sup> A direct comparison of the  $D^C$  values for nuclei with  $I = \frac{1}{2}$  assumes same values of  $T_1$ .

limit,  $T_2(^{11}\text{B})$  is given by

$$T_2 = (\pi\Delta\nu_{1/2})^{-1}. \quad (1)$$

Since  $T_2 = T_Q$ , the linewidths  $\Delta\nu_{1/2}$  are given by

$$\Delta\nu_{1/2} = \frac{3\pi}{10} \frac{2I+3}{I^2(2I-1)} \chi^2 (1 + \frac{1}{3}\eta^2) \tau_C, \quad (2)$$

where  $\chi$  is the nuclear quadrupole coupling constant,  $\eta$  is the asymmetry parameter ( $0 < \eta < 1$ ) for the electric-field gradient,  $I$  is the nuclear spin and  $\tau_C$  is the rotational correlation time. From (2) it is apparent that the linewidth of  $^{10}\text{B}$  NMR signals is smaller (by a factor of about 0.65) than for  $^{11}\text{B}$  signals. However, this is compensated by the greater magnetic moment of the  $^{11}\text{B}$  nucleus ( $\gamma(^{11}\text{B})/\gamma(^{10}\text{B}) \approx 3$ ). Furthermore, it is evident from (2) that the small linewidths of  $^{11}\text{B}$  NMR signals are related to a symmetrical charge distribution around the  $^{11}\text{B}$  nucleus ( $\chi$  is small). Apart from an increase in the  $\chi$  values, greater linewidths are caused by a decrease in  $\tau_C$  (slower molecular tumbling), which can be attributed to increasing molecular size (or association) or greater viscosity of the solution (e.g. measurement at low temperature).

The important message from the linewidths of  $^{11}\text{B}$  NMR signals concerns the direct information on  $T_Q(^{11}\text{B})$  since, in most cases, inhomogeneity contributions to  $\Delta\nu_{1/2}$  are negligible in comparison with  $(T_Q)^{-1}$ . The values  $T_Q(^{11}\text{B})$  can be used to qualitatively predict the appearance of the NMR spectra of spin-coupled nuclei X, with  $I = \frac{1}{2}$ , if the order of magnitude of  $J(^{11}\text{B}X)$  is known. The X resonance exhibits a well resolved 1:1:1:1 quartet if  $2\pi |J(^{11}\text{B}X)| T_Q(^{11}\text{B}) \gg 1$ , a partially relaxed quartet for  $5 > 2\pi |J(^{11}\text{B}X)| T_Q(^{11}\text{B}) > 1$  and a single more or less broadened line (linewidth at half-height  $\Delta\nu_B$ ) for  $2\pi |J(^{11}\text{B}X)| T_Q(^{11}\text{B}) < 1$ .<sup>25</sup> Thus, once the origin of the relative broadening ( $\Delta\nu_B$ ) of the single X resonance is known, the constant for scalar relaxation of the second kind,  $T_2^{\text{SC}}(X)$ , can be evaluated and a range for the  $J(^{11}\text{B}X)$  value can be deduced.<sup>26</sup>

$$(T_2^{\text{SC}})^{-1} = \frac{1}{2} (T_1^{\text{SC}})^{-1} + \frac{4}{3} \pi^2 [J(^{11}\text{B}X)]^2 I(I+1) T_Q(^{11}\text{B}). \quad (3)$$

Neglecting the contribution from  $T_2^{\text{SC}}(X)$ , the broadening  $\Delta\nu_B$  of the X-resonance is related to  $J(^{11}\text{B}X)$  and  $T_Q(^{11}\text{B})$  according to

$$\Delta\nu_B = 5\pi [J(^{11}\text{B}X)]^2 T_Q(^{11}\text{B}). \quad (4)$$

Of course, analogous considerations apply to other quadrupolar nuclei that may be present in boron compounds. There are a few examples where spin-spin coupling between  $^{11}\text{B}$  and another quadrupolar nucleus (e.g.  $^2\text{H}$ ,  $^{10}\text{B}$ ,  $^{11}\text{B}$ ,  $^{14}\text{N}$ ) is partly resolved. The appearance of these spectra depends in a predictable manner on the respective quadrupolar relaxation rates.

In the case of nuclei X, with  $I = \frac{1}{2}$ , the contributions from the various mechanisms contributing to longitudinal relaxation,

$$(T_1)^{-1} = (T_1^{\text{DD}})^{-1} + (T_1^{\text{SC}})^{-1} + (T_1^{\text{SR}})^{-1} + (T_1^{\text{CSA}})^{-1}, \quad (5)$$

(DD = dipole-dipole interactions, SC = scalar interactions, SR = spin-rotation processes, CSA = chemical-shielding anisotropy) are distinguished in the normal way.<sup>18,25</sup> The evaluation of the significance of the dominant contribution helps to select the optimum spectral parameters for recording the X NMR spectra.

### III. <sup>11</sup>B NUCLEAR MAGNETIC RESONANCE

#### A. Chemical shifts, $\delta^{11}\text{B}$

##### 1. General

The nuclear screening constant  $\sigma$  is expressed as the sum of diamagnetic ( $\sigma_d$ ) and paramagnetic ( $\sigma_p$ ) components:<sup>86</sup>

$$\sigma = \sigma_d + \sigma_p. \quad (6)$$

Using Ramsey's terminology,<sup>88</sup>  $\sigma_d$  and  $\sigma_p$  are molecular terms that are large and of opposite sign. A quantitative theoretical treatment of  $\sigma$  is difficult, as can be seen by considering the sometimes crude approximations that are involved in the description of the molecular excited states and the dependence of  $\sigma$  upon the choice of origin. People's MO treatment<sup>89</sup> of  $\sigma$  simplifies some of these problems by assuming the dominance of local terms  $\sigma_d^{\text{loc}}$  and  $\sigma_p^{\text{loc}}$ , and this approach can be further simplified by using an average excitation energy ( $\text{AEE} = \Delta E$ ) instead of summing over all excited states. Although this semiempirical approach has several shortcomings (for example, in the description of the influence on  $\sigma$  exerted by heavy nuclei) it adds to the qualitative understanding of physical effects underlying the phenomenon of nuclear shielding. We have

$$\sigma_{p(A)}^{\text{loc}} = - \frac{\mu_0 \mu_B^2}{2\pi} (\Delta E)^{-1} \langle r^{-3} \rangle_{2p} \sum_B Q_{AB}, \quad (7)$$

where  $\mu_0$  is the permeability of free space,  $\mu_B$  is the Bohr magneton,  $r$  is the distance of the 2p electron from nucleus A,  $\sum_B Q_{AB}$  are bond-order charge-density terms and the summation over all atoms B includes A.

In contrast with  $\sigma_d$ , in the general approach of Ramsey the local term  $\sigma_d^{\text{loc}}$  may be regarded as fairly constant and changes in the nuclear shielding are

mainly assigned to changes in the term  $\sigma_p^{loc}$ . The term  $\Delta E$  in (7) results from the fact that the external field  $B_0$  mixes excited states with the ground state. The distance term reflects individual nuclear properties and may undergo changes induced by strongly electronegative or electropositive substituents. The latter influence is also reflected by the sum  $\sum_B Q_{AB}$ . It is also evident that the influence of electronegative or electropositive ligands on the shielding of the nucleus A may be difficult to predict since the changes induced in  $\Delta E$  and in the distance term or the  $Q_{AB}$  terms can be of opposite sign. Therefore relationships between calculated atomic charge densities (either total charge densities or, if appropriate,  $\pi$ -charge densities) and nuclear shielding must be met with some caution bearing in mind the complex dependence of  $\sigma_p^{loc}$  on various contributions.

## 2. Local symmetry, coordination number

At first sight a qualitative analysis of trends in nuclear shielding may appear even more complicated when the anisotropic quality of  $\sigma$  is taken into account (e.g. for linear and symmetric top molecules, (8), or for less symmetrical molecules, (9)):

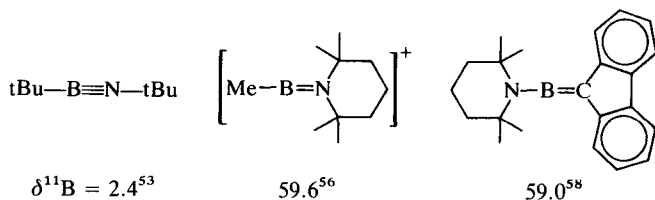
$$\sigma = \frac{1}{3}(\sigma_{\parallel} + 2\sigma_{\perp}), \quad \Delta\sigma = \sigma_{\parallel} - \sigma_{\perp}, \quad (8)$$

$$\sigma = \frac{1}{3}(\sigma_{\alpha\alpha} + \sigma_{\beta\beta} + \sigma_{\gamma\gamma}), \quad \Delta\sigma = \sigma_{\alpha\alpha} - \frac{1}{2}(\sigma_{\beta\beta} + \sigma_{\gamma\gamma}), \quad (9)$$

where  $\Delta\sigma$  is the screening anisotropy,  $\sigma_{\parallel}$  and  $\sigma_{\perp}$  are the screening components parallel and perpendicular to the molecular axis respectively, and  $\sigma_{\alpha\alpha}$ ,  $\sigma_{\beta\beta}$ ,  $\sigma_{\gamma\gamma}$  are the three principal tensor components, with the convention that  $\sigma_{\alpha\alpha} > \sigma_{\beta\beta} > \sigma_{\gamma\gamma}$ . However, experimental and calculated<sup>91</sup> data for the screening components in (8) and (9) show that changes in the isotropic value of  $\sigma$  may be traced mainly to changes in the magnitude of a single component or that there are changes of opposite sign in the magnitude of two or all three screening components.

Thus it has been found in the case of  $^{13}\text{C}$  NMR of different linear molecules that  $\sigma_{\parallel}(^{13}\text{C})$  is remarkably constant.<sup>91</sup> This indicates (i) that the paramagnetic contribution to  $\sigma_{\parallel}$  vanishes since there is no  $B_0$ -induced paramagnetic charge circulation about the  $C_{\infty}$  or  $D_{\infty}$  axis, and (ii) that the diamagnetic contribution to  $\sigma_{\parallel}$  remains fairly constant. If there are substituents off the molecular axis at one or at both ends of the molecule (e.g. in  $\text{CH}_2=\text{C}=\text{O}$ ,  $\text{CH}_2=\text{C}=\text{CH}_2$ ) the central  $^{13}\text{C}$  atom will be deshielded by strong paramagnetic currents about and perpendicular to the molecular axis, as shown by  $^{13}\text{C}$  solid-state NMR.<sup>91</sup> Clearly, a similar situation

will be found for  $\sigma(^{11}\text{B})$  in the case of iminoboranes(2) (e.g.  $\text{R}^1\text{—B}\equiv\text{N—R}^2$ <sup>52,53,109</sup>) and in aminoboron(1+) cations (e.g.  $[\text{R}^1\text{—B=NR}_2]^+$ <sup>42</sup>):



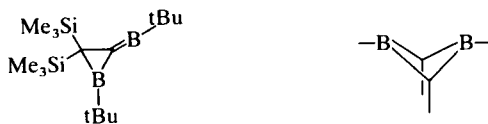
This leads to boron atoms with the coordination number 3 and a trigonal planar environment. Again it is useful to refer to the solid-state  $^{13}\text{C}$  NMR, for example of alkenes and of carbonyl compounds.<sup>90</sup> There it has been shown that the smallest principal  $\sigma_p$  tensor component (i.e. the highest shielding) is directed perpendicularly to the molecular plane. This is consistent with the picture of  $B_0$ -induced paramagnetic currents involving only  $\sigma \rightarrow \sigma^*$  transitions, which are of high energy and therefore contribute little to the isotropic paramagnetic term  $\sigma_p$  (note that  $\pi \rightarrow \pi^*$  transitions are magnetically inactive). Thus the strong deshielding frequently found for nuclei in a trigonal planar surround (e.g. boranes(3)) is caused by paramagnetic circulations related to  $\pi \rightarrow \sigma^*$ , or  $\sigma \rightarrow \pi^*$  transitions, as shown by INDO calculations for  $\sigma(^{11}\text{B})$  in trimethylborane.<sup>93</sup>

Boron compounds containing boron atoms with coordination number four are borane adducts or borates and similar compounds in which the boron atom is in a tetrahedral, or distorted tetrahedral surrounding. In general, the shielding of the  $^{11}\text{B}$  nuclei is increased in comparison with boranes(3). This may be traced to the absence of low-energy paramagnetic currents of the  $\pi \leftrightarrow \sigma$  type, leading to an overall reduction of paramagnetic contributions.

The tendency of boron atoms to increase their coordination number to  $>3$  is reflected by the amazing structural variety of polyboranes, carbaboranes, metallaboranes, etc. Although there are many  $\delta^{11}\text{B}$  data available for these compounds,<sup>4,6-9</sup> their interpretation is not straightforward. In many cases the complexity of the electronic structures precludes the assignment of changes in nuclear shielding to a particular effect. In metallaboranes one should consider the electronic structure of the metal fragment, which may entail changes in  $^{11}\text{B}$  nuclear shielding. Frequently, so-called "antipodal" effects<sup>95</sup> are useful for assignment purposes, and there are various other empirical rules<sup>96-98</sup> to account for the  $\delta^{11}\text{B}$  values.

Several systems have become available with a bonding situation that may be described as an intermediate between a carbaborane with "nonclassical" bonding and a borane with "classical" bonding. Typical examples are the

borylidene–boriranes<sup>99</sup> and the 1,3-dihydro-1,3-diborettes:<sup>43,54,59</sup>



In general, the  $^{11}\text{B}$  nuclear shielding in the “nonclassical” systems is increased with respect to that of “classical” systems.

In the last decade a large number of boranes(3) or borates(3) have found application as  $\pi$  ligands in transition-metal chemistry.<sup>15,16</sup> Since the  $\delta^{11}\text{B}$  values of the free ligands are available (or can be estimated), the complexation-shift  $\Delta^{11}\text{B}$  is an interesting quantity for discussing the metal–boron interactions. The  $\delta^{11}\text{B}$  values may be discussed in a similar way to the  $\delta^{13}\text{C}$  values of cyclopentadienyl or benzene metal complexes, for which some solid-state  $^{13}\text{C}$  NMR spectra have been studied in order to analyse the components of the shielding tensor.<sup>100</sup> These studies have shown that there are significant changes in the anisotropy of the screening constant  $\Delta\sigma$  (see (9)) and that this is the result of metal–ligand  $\pi$  interactions.

Various boranes(3) may function also as bridging ligands. In this case the formal coordination number of the boron atom is further increased. For the examples available, this is always connected with an increase in  $^{11}\text{B}$  nuclear shielding: for example<sup>101</sup>

	$\delta^{11}\text{B}$	$\delta^{11}\text{B}$
	66.0	L 30.0
	= L	Co
		L 14.0
		Co
		L 30.0

### B. Substituent effects on $^{11}\text{B}$ -chemical shifts, $\delta^{11}\text{B}$

The magnitude of substituent effects on  $^{11}\text{B}$  chemical shifts depends on the local symmetry and on the coordination number of boron. The changes in the electronic structure of boron compounds induced by different substituents may be separated into changes in the  $\sigma$ - and  $\pi$ -bonding framework where appropriate. However, since there is no simple relationship between  $\sigma$ - or  $\pi$ -charge density, or  $(\sigma + \pi)$ -charge densities at the boron atom and the  $\delta^{11}\text{B}$  values for all boron compounds,<sup>662</sup> it is advisable to discuss substituent effects for each class of boron compounds separately.

## 1. Two-coordinate boron

Although iminoboranes(2) (Table 2) are a fairly recent development in boron chemistry, there is already some variation of the substituents at the

TABLE 2  
 $\delta^{11}\text{B}$  and  $\delta^{14}\text{N}$  values of some iminoboranes(2).

Compound	$\delta^{11}\text{B}$	Solvent	$\delta^{14}\text{N}$	Ref.
$\text{Et}-\text{B}\equiv\text{N}-\text{tBu}$	3.3		-251	49
$\text{Pr}-\text{B}\equiv\text{N}-\text{tBu}$	2.9		-250	49
$\text{Bu}-\text{B}\equiv\text{N}-\text{tBu}$	2.3		-250	49
$\text{tBuB}\equiv\text{N}-\text{iPr}$	3.3		-254	248
$\text{tBu}-\text{B}\equiv\text{N}-\text{tBu}$	2.4	$\text{CDCl}_3$	-254	53
$\text{CHMe}_2\text{CMe}_2-\text{B}\equiv\text{N}-[(2,6\text{-iPr}_2)-\text{C}_6\text{H}_3]$	14.9	$\text{CDCl}_3$	-267	109
$\text{C}_6\text{F}_5-\text{B}\equiv\text{N}-\text{tBu}$	3.0		—	52
$(\text{Me}_3\text{Si})_3\text{C}-\text{B}\equiv\text{N}-\text{SiMe}_3$	21.0		-262.4	57, 342
$(\text{Me}_3\text{Si})_3\text{Si}-\text{B}\equiv\text{N}-\text{SiMe}_3$	21.9		-218.3	57, 342
$\text{iPr}_2\text{N}-\text{B}\equiv\text{N}-\text{tBu}$	5.8	$\text{C}_6\text{D}_6$	—	775
$\text{tBu}_2\text{N}-\text{B}\equiv\text{N}-\text{tBu}$	5.2	$\text{C}_6\text{D}_6$	—	775
$\text{tmp}-\text{B}\equiv\text{N}-\text{tBu}$	5.6	$\text{C}_6\text{D}_6$	-269 (N—tBu) -312 (TMP)	50
$\text{tmp}-\text{B}\equiv\text{N}-(2,4,6\text{-Me}_3)\text{C}_6\text{H}_2$	12.8	$\text{C}_6\text{D}_6$	—	774
$\text{tmp}-\text{B}\equiv\text{N}-(2,6\text{-iPr}_2)\text{C}_6\text{H}_3$	12.1	$\text{C}_6\text{D}_6$	—	775
$\text{tmp}-\text{B}\equiv\text{N}-(2,4,6\text{-tBu}_3)\text{C}_6\text{H}_2$	13.2	$\text{C}_6\text{D}_6$	—	774
$\text{tmp}-\text{B}\equiv\text{N}-\text{SiMe}_3$	17.4	$\text{C}_7\text{D}_8$	—	775
$\text{tmp}-\text{B}\equiv\text{N}-\text{SiPr}_3$	16.8	$\text{C}_6\text{D}_6$	—	775
$\text{tmp}-\text{B}\equiv\text{N}-\text{PtBu}_2$	16.6	$\text{C}_6\text{D}_6$	—	775
$\text{tmp}-\text{B}\equiv\text{N}-\text{AsBu}_2$	17.5	$\text{C}_6\text{D}_6$	—	775

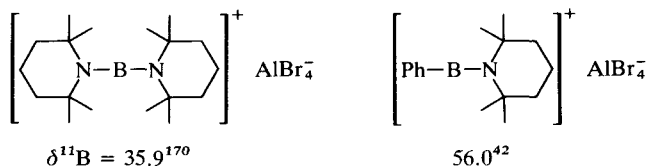
site of the imino nitrogen atom. For the boron atom there are various organyl groups, amino groups and a single example with a B—Si bond.<sup>57,342</sup> The trend in the  $\delta^{11}\text{B}$  data corresponds closely to that observed for  $\delta^{13}\text{C}$  of similarly substituted alkynes; for example

$\text{R}_2\text{N}-\text{B}\equiv\text{N}-\text{R}$		$\text{R} = \text{tBu}$	$\text{SiMe}_3$
	$\delta^{11}\text{B}$	5.6	17.4
$\text{Me}-\overset{\alpha}{\text{C}}\equiv\text{C}-\text{R}$	$\delta^{13}\text{C}(\alpha)$	73.3	103.1

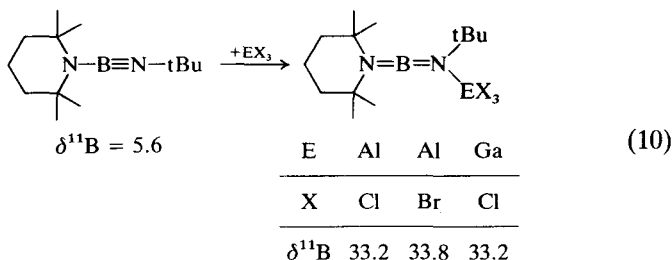
Thus the electronic structure of the  $\text{B}\equiv\text{N}$  bond is influenced by substituents in a distinct way, similar to that of the  $\text{C}\equiv\text{C}$  triple bonds in alkynes. Other NMR parameters ( $^1J(\text{NB})$ ,  $\delta^{14}\text{N}$  and the  $^{14}\text{N}$  linewidth, see Section IV.F.1 below) also support the usefulness of comparing the properties of isoelectronic compounds.

Bis(amido)boron(1+)<sup>42,55,56,108,144,170,437</sup> and a few amidoboron(1+)

cations<sup>42,56</sup> constitute another class of two-coordinate boron compounds. The  $\delta^{11}\text{B}$  values of the bis(amido)boron(1+) cations cover a narrow range between  $\delta^{11}\text{B}$  35–39, depending on the solvent and the counterion. It appears that most of the deshielding of the  $^{11}\text{B}$  nucleus in these compounds, with respect to the aminoiminoboranes, results from the change in symmetry (see Section III.A.2 above) rather than because of the positive charge. The  $^{11}\text{B}$  nuclear shielding decreases further from the bis(amido)boron(1+) to the (amido)boron(1+) cations; for example

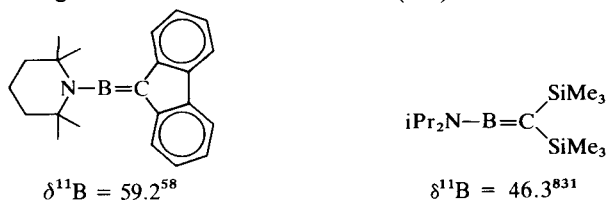


A few examples are known where the coordination number of boron prevails after the addition of certain halides  $\text{EX}_3$  to an aminoiminoborane(2):<sup>169</sup>

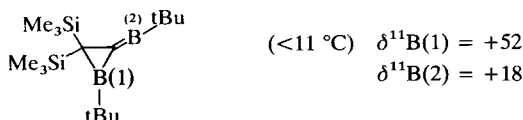


The  $\delta^{11}\text{B}$  values correspond closely to those of the bis(amido)boron(1+) cations.

Neutral amino(methylene)boranes containing a  $\text{B}=\text{C}$  double bond, isosteric with allenes, have been described.<sup>58,831</sup> Their  $\delta^{11}\text{B}$  values are found in the same range as that for the amidoboron(1+) cations:



Finally,  $\delta^{11}\text{B}$  values for a borirane-2-ylideneborane(2) are available:<sup>99</sup>



The original assignment has been confirmed by appropriate selective  $^{13}\text{C}\{^1\text{H}, ^{11}\text{B}\}$  heteronuclear triple-resonance experiments.<sup>102</sup> However, the original arguments for the assignment have to be reconsidered in the light of MO calculations,<sup>103</sup> which support significant contributions of a delocalized structure.

## 2. Three-coordinate boron

Substituent effects on  $^{11}\text{B}$  nuclear shielding in trigonal boranes have been discussed repeatedly.<sup>5</sup> An empirical treatment on the basis of pairwise-additive parameters<sup>104,105</sup> gives poor results for a larger set of  $\delta^{11}\text{B}$  data.<sup>7</sup> Attempts at relating the  $\delta^{11}\text{B}$  data to calculated  $\pi$ -electron charge densities  $q^{(\pi)}_{\text{B}}$  are promising.<sup>106</sup> However, the theoretical background of this approach is questionable, especially in the absence of experimental data on the tensor components of the nuclear screening constant. Furthermore, new  $\delta^{11}\text{B}$  data on diboranes(4), silylboranes(3) and related compounds indicate that the electron-density distribution in the whole bonding framework, in particular in the  $\sigma$ -bonds, has to be considered. This is also confirmed by NMR parameters of nuclei linked to boron in trigonal boranes. Clearly, the  $\delta^{11}\text{B}$  values of trigonal boranes reflect  $\pi$  interactions between the formally empty  $p_z$  orbital at boron and the filled orbitals of appropriate symmetry in the neighbourhood. On the other hand, the separation of  $\sigma$  and  $\pi$  effects<sup>107</sup> is still a formidable problem. Therefore the attempt at interpreting changes in  $\delta^{11}\text{B}$  values solely in terms of  $\pi$  interactions leads to a gross simplification. Even in those cases where all the evidence indicates that changes in  $\delta^{11}\text{B}$  values are related entirely to  $\pi$  interactions, the quantitative assessment of these interactions remains difficult.

(a) *Triorganylboranes.* There is a fairly large range of  $\delta^{11}\text{B}$  values for those triorganylboranes (Tables 3–7) with weak or negligible  $\text{BC}(\text{pp})\pi$  interactions. For trialkylboranes, we note the influence of the ring size. The  $^{11}\text{B}$ -nuclear shielding is significantly decreased (approx. 5–8 ppm) if the boron atom is incorporated into a five-membered ring. This effect is also evident for B-organyl groups other than alkyl in boracyclopentanes and also in boracyclopentenenes (cf. Tables 3–5). Clearly, this is an effect that originates from the nature of the B—C  $\sigma$  bonds in the somewhat strained five-membered ring.

The increase in  $^{11}\text{B}$ -nuclear shielding that is observed with an increasing number of aryl, alkenyl or alkynyl groups attached to boron can be interpreted in various ways: (i) an increase of  $\pi$ -electron density  $q^{\pi}_{\text{B}}$  at the boron atom leads to increased shielding; (ii) the greater electronegativity of  $\text{sp}^2$ - or  $\text{sp}$ -hybridized carbon atoms (with respect to  $\text{sp}^3$  carbon) stabilizes the

(Continued p. 118)



TABLE 3 (cont.)

 $\delta^{11}\text{B}$  values of some representative triorganylborananes (site of unsaturation removed from boron).

Compound	$\delta^{11}\text{B}$	Solvent	Ref.	Other nuclei	Ref.
$(\text{CH}_2=\text{CH}-\text{CH}_2\text{CH}_2)_3\text{B}$	84.9		5	—	
$\text{Et}_2\text{B}-\text{CH}(\text{Ph})\text{Et}$	81.7	THF	473	—	
$(\text{PhCH}_2)_3\text{B}$	82.0	$\text{CCl}_4$	5	$^{13}\text{C}$	778
	82.8	$\text{Et}_2\text{O}$	651		

<sup>a</sup>  $\text{C}_8\text{H}_{14}\text{B}$  = 9-borabicyclo[3.3.1]nonyl.<sup>b</sup>  $\delta^{13}\text{C}(2,8,9) = 39.4$ ;  $\delta^{13}\text{C}(3,5,7) = 46.1$ ;  $\delta^{13}\text{C}(4,6,10) = 38.1$ .

TABLE 4

 $\delta^{11}\text{B}$  values of some representative triorganylborananes with *B*-alkenyl groups.

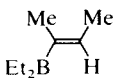
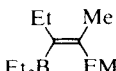
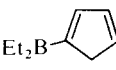
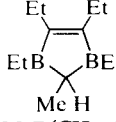
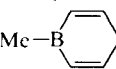
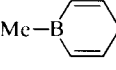
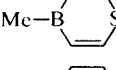
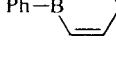
Compound	$\delta^{11}\text{B}$	Solvent	Ref.	Other nuclei	Ref.
$\text{Me}_2\text{B}-\text{CH}=\text{CH}_2$	74.5	—	5	$^{13}\text{C}$	687
	75.7	—	5	—	
	80.0	Neohexane	5	$^{13}\text{C}$ , $^{29}\text{Si}$	71
	83.3	$\text{C}_6\text{D}_6$	31	$^{13}\text{C}$ , $^{119}\text{Sn}$	71
	83.5	$\text{C}_6\text{D}_6$	41	$^{13}\text{C}$	7, 503
	71.4	$\text{CCl}_4$	5	—	
	69.6		5	—	
$\text{MeB}(\text{CH}=\text{CH}_2)_2$	64.4	—	5	$^{13}\text{C}$	714
	52.8	$\text{CDCl}_3$	64	—	
	58.3	$\text{CDCl}_3$	60	$^{13}\text{C}$	60
	60.9	$\text{C}_6\text{D}_6$	65, 66	$^{13}\text{C}$ , $^{119}\text{Sn}$	65
	49.0	—	5	—	

TABLE 4 (cont.)

 $\delta^{11}\text{B}$  values of some representative triorganylboranates with *B*-alkenyl groups.

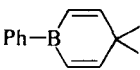
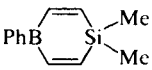
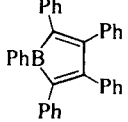
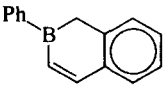
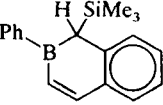
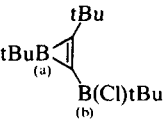
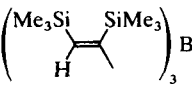
Compound	$\delta^{11}\text{B}$	Solvent	Ref.	Other nuclei	Ref.
	53.7	$\text{C}_6\text{D}_6$	30	—	
	52.7	$\text{C}_6\text{D}_6$	30	—	
	55.0	$\text{C}_6\text{H}_6$	63, 67	—	
	68.5	$\text{CDCl}_3$	142	—	
	64.0	$\text{CDCl}_3$	142	—	
	43.0 (a) 72.0 (b)		68	$^{13}\text{C}$	68
$(\text{CH}_2=\text{CH})_3\text{B}$	56.4	$\text{C}_6\text{H}_6$	69	$^{13}\text{C}$	69
$[\text{CH}_2=\text{O}(\text{iPr})]_3\text{B}$	68.9		5	—	
	68.7	$\text{CDCl}_3$	70, 71	$^{13}\text{C}, ^{29}\text{Si}$	71

TABLE 5

 $\delta^{11}\text{B}$  values of some representative triorganylboranates with *B*-aryl and *B*-heteroaryl groups.

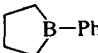
Compound	$\delta^{11}\text{B}$	Solvent	Ref.	Other nuclei	Ref.
$\text{Me}_2\text{B}-\text{Ph}$	77.6	$\text{CH}_2\text{Cl}_2$	5	—	
	84.5	$\text{CH}_2\text{Cl}_2$	5	$^{13}\text{C}$	36

TABLE 5 (cont.)

 $\delta^{11}\text{B}$  values of some representative triorganylborananes with *B*-aryl and *B*-heteroaryl groups.

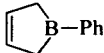
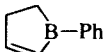
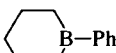
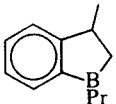
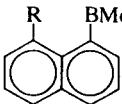
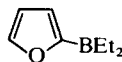
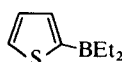
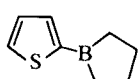
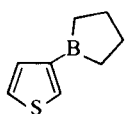
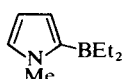
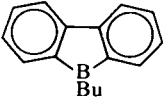
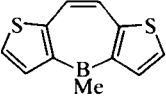
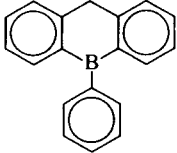
Compound	$\delta^{11}\text{B}$	Solvent	Ref.	Other nuclei	Ref.
 B-Ph	86.2	—	82, 345	$^{13}\text{C}$	345
 B-Ph	74.0	$\text{CD}_2\text{Cl}_2$	83, 345	$^{13}\text{C}$	345
 B-Ph	77.5	$\text{CH}_2\text{Cl}_2$	38	$^{13}\text{C}$	36
$\text{C}_8\text{H}_{14}\text{B}-\text{Ph}^a$	80.9 80.4	$\text{C}_6\text{D}_6$ $\text{C}_6\text{D}_6$	41 490	$^{13}\text{C}$	7, 490, 712
 B-Pr	82.6	$\text{CDCl}_3$	36	$^{13}\text{C}$	36
 <div style="display: inline-block; vertical-align: middle; margin-left: 10px;">           R = H            Me            I            SMe            SiMe<sub>3</sub> </div>	80.0	$\text{CD}_2\text{Cl}_2$	141	—	
	81.0	$\text{CD}_2\text{Cl}_2$	263	—	
	70.0	$\text{CD}_2\text{Cl}_2$	263	—	
	16.2	$\text{C}_7\text{D}_8$	263	—	
	74.6	$\text{CD}_2\text{Cl}_2$	263	—	
 BEt <sub>2</sub>	67.6	$\text{CH}_2\text{Cl}_2$	35	—	
 BEt <sub>2</sub>	70.4	$\text{CH}_2\text{Cl}_2$	35	—	
	76.0	$\text{CH}_2\text{Cl}_2$	35	$^{13}\text{C}$	36
	79.0	$\text{CH}_2\text{Cl}_2$	35	—	
 BEt <sub>2</sub>	66.4	$\text{CH}_2\text{Cl}_2$	35	$^{13}\text{C}$ $^{14}\text{N}$	36 35
MeBPh <sub>2</sub>	70.6	$\text{CH}_2\text{Cl}_2$	35		
EtB[(2,4,6-Me <sub>3</sub> )C <sub>6</sub> H <sub>2</sub> ] <sub>2</sub>	85.0	$\text{CDCl}_3$	33, 708	$^{13}\text{C}$	708

TABLE 5 (cont.)

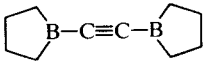
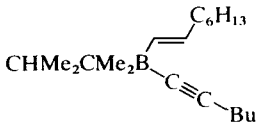
 $\delta^{11}\text{B}$  values of some representative triorganylborananes with *B*-aryl and *B*-heteroaryl groups.

Compound	$\delta^{11}\text{B}$	Solvent	Ref.	Other nuclei	Ref.
	60.0	$\text{CH}_2\text{Cl}_2$	5	—	
$(\text{Me}_3\text{Si})_3\text{C}-\text{BPh}_2$	77.5	$\text{C}_6\text{D}_6$	62	—	
$\left(\text{2-thienyl}\right)_2\text{BMe}$	57.0	$\text{CH}_2\text{Cl}_2$	35	$^{13}\text{C}$	36
	52.6	—	34	—	
$\left(\text{2-pyridyl}\right)_2\text{BEt}$	54.7	$\text{CH}_2\text{Cl}_2$	35	$^{13}\text{C}$	36
$\text{Ph}_3\text{B}$	68.0	$\text{CH}_2\text{Cl}_2$	36, 146	$^{13}\text{C}$	7, 10
	68.0	$\text{C}_6\text{D}_6$	490		
$[(2,4,6\text{-Me}_3)\text{-C}_6\text{H}_2]_3\text{B}$	79.0	$\text{CDCl}_3$	708	$^{13}\text{C}$	708
	58.0	$\text{C}_6\text{D}_6$	32	—	
$\left(\text{2-naphthyl}\right)_3\text{B}$	72.7	$\text{Et}_2\text{O}$	651	—	
$\left(\text{2-furyl}\right)_3\text{B}$	35.0	$\text{CH}_2\text{Cl}_2$	35	$^{13}\text{C}$	36
$\left(\text{2-thienyl}\right)_3\text{B}$	47.3	$\text{CH}_2\text{Cl}_2$	35	—	
$\left(\text{2-pyridyl}\right)_3\text{B}$	44.3	$\text{CH}_2\text{Cl}_2$	35	$^{13}\text{C}$	36

<sup>a</sup>  $\text{C}_8\text{H}_{14}\text{B}$  = 9-borabicyclo[3.3.1]nonyl.

TABLE 6

 $\delta^{11}\text{B}$  values of some representative triorganylborananes with a *B*-alkynyl group.

Compound	$\delta^{11}\text{B}$	Solvent	Ref.	Other nuclei	Ref.
$\text{Me}_2\text{B}-\text{C}\equiv\text{C}-\text{Me}$	71.7	$\text{C}_6\text{H}_6$	85	$^{13}\text{C}$	524
$\text{Me}_2\text{B}-\text{C}\equiv\text{C}-\text{Ph}$	71.0	$\text{C}_6\text{H}_6$	38	—	
$\text{Me}_2\text{B}-\text{C}\equiv\text{C}-\text{BMe}_2$	73.5	$\text{C}_6\text{H}_6$	85	—	
$\text{Et}_2\text{B}-\text{C}\equiv\text{C}-\text{Me}$	73.2	—	27	—	
$\text{C}_8\text{H}_{14}\text{B}-\text{C}\equiv\text{CtBu}^a$	72.0	$\text{C}_6\text{H}_6$	86, 87	—	
	76.3	$\text{C}_6\text{H}_6$	85	—	
	62.0	$\text{CDCl}_3$	51	—	
$\text{PhB}(\text{C}\equiv\text{C}-\text{Me})_2$	40.0	$\text{CH}_2\text{Cl}_2$	85	—	

<sup>a</sup>  $\text{C}_8\text{H}_{14}\text{B}$  = 9-borabicyclo[3.3.1]nonyl.

TABLE 7

 $\delta^{11}\text{B}$  values of miscellaneous triorganylborananes, *neutral* and *anionic*.

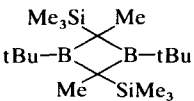
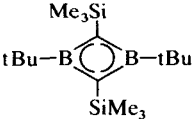
Compound	$\delta^{11}\text{B}$	Solvent	Ref.	Other nuclei	Ref.
$\text{Bu}_2\text{BCH}(\text{SiMe}_3)\text{Bu}$	83.0		260	—	
$\text{C}_8\text{H}_{14}\text{BCH}_2-\text{SiMe}_3$	85.9	$\text{CDCl}_3$	257	$^{13}\text{C}$	257
$\text{B}(\text{CH}_2\text{SiMe}_3)_3$	78.4	pentane	41	$^{13}\text{C}$	41
	81.0	$\text{C}_6\text{D}_6$	110	$^{13}\text{C}$	110
	42.0	$\text{C}_6\text{D}_6$	110	$^7\text{Li}$ , $^{13}\text{C}$	110
$\text{HC}(\text{BEt}_2)_3$	82.0	—	72		

TABLE 7 (cont.)

 $\delta^{11}\text{B}$  values of miscellaneous triorganylboranes, *neutral and anionic*.

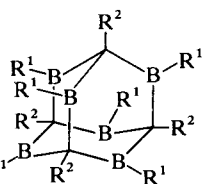
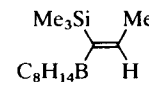
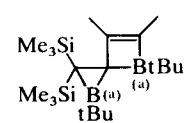
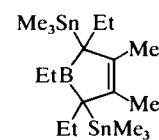
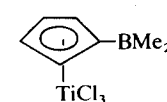
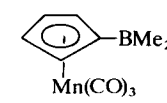
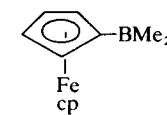
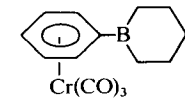
Compound	$\delta^{11}\text{B}$	Solvent	Ref.	Other nuclei	Ref.												
	<table><thead><tr><th>R<sup>1</sup></th><th>R<sup>2</sup></th><th><math>\delta^{11}\text{B}</math></th></tr></thead><tbody><tr><td>Me</td><td>H</td><td>63.2</td></tr><tr><td>Et</td><td>H</td><td>67.0</td></tr><tr><td>Et</td><td>Me</td><td>65.0</td></tr></tbody></table>	R <sup>1</sup>	R <sup>2</sup>	$\delta^{11}\text{B}$	Me	H	63.2	Et	H	67.0	Et	Me	65.0	— CCl <sub>4</sub> C <sub>7</sub> D <sub>8</sub>	73 72 74	<sup>13</sup> C	74
R <sup>1</sup>	R <sup>2</sup>	$\delta^{11}\text{B}$															
Me	H	63.2															
Et	H	67.0															
Et	Me	65.0															
	79.3	CDCl <sub>3</sub>	257	<sup>13</sup> C	257												
	+83.0 (a) +34.5 (b)		75	<sup>13</sup> C	75												
CH <sub>2</sub> {B[(2,4,6-Me <sub>3</sub> )—C <sub>6</sub> H <sub>2</sub> ] <sub>2</sub> }	80.0	CDCl <sub>3</sub>	76	<sup>13</sup> C	76												
	64.0	CDCl <sub>3</sub>	77	<sup>13</sup> C, <sup>119</sup> Sn	77												
	74.3		78	—													
	72.0	CS <sub>2</sub>	29	—													
	71.6	CS <sub>2</sub>	29	—													
	73.2	C <sub>6</sub> H <sub>6</sub>	28	—													
{[(2,4,6-Me <sub>3</sub> )—C <sub>6</sub> H <sub>2</sub> ] <sub>2</sub> BCH <sub>2</sub> } <sup>-</sup> Li <sup>+</sup>	41.0 40.4	diglyme THF	79 828	— —													

TABLE 7 (cont.)

 $\delta^{11}\text{B}$  values of miscellaneous triorganylboranes, *neutral and anionic*.

Compound	$\delta^{11}\text{B}$	Solvent	Ref.	Other nuclei	Ref.
$\left[\text{PhB} \begin{array}{c} \text{C}_6\text{H}_5 \end{array} \right]^- \text{Li}^+$	27.0	THF	80	—	
$\left[\text{PhB} \begin{array}{c} \text{C}_6\text{H}_5 \end{array} \right]^- \text{Tl}^+$	33.8	DMSO	81	$^{13}\text{C}$	81
$\left[ \begin{array}{c} \text{Ph} \\ \text{Ph} \end{array} \text{B} \begin{array}{c} \text{Ph} \\ \text{Ph} \end{array} \right]^{2-} 2\text{K}^+$	29.0	THF	67	—	
$\text{Ph}_3\text{P}-\text{C}(\text{Me})-\text{B}(\text{c-C}_5\text{H}_9)_2$	56.0	$\text{C}_6\text{D}_6$	61	$^{31}\text{P}$	61
$\left[ \begin{array}{c} \text{tBu} \\ \text{Me}_3\text{Si} \end{array} \text{B} \begin{array}{c} \text{H} \\ \text{SiMe}_3 \end{array} \right]^- \text{K}^+$	40.4	$\text{C}_6\text{D}_6$	110	$^{13}\text{C}$	110

TABLE 8

 $\delta^{11}\text{B}$  values of some diorganylboronhydrides  $\text{R}_2\text{BH}$ .

Compound	$\delta^{11}\text{B}$	Solvent	Ref.	Other nuclei	Ref.
$(\text{Me}_2\text{CHCMe}_2)_2\text{BH}$	81.1	THF	114	—	
$[\text{EtCH}(\text{SiMe}_3)]_2\text{BH}$	83.0	THF	276	—	
$\text{tBu}(\text{C}_6\text{H}_{11})\text{BH}$	82.1	$\text{Et}_2\text{O}$	371	—	
$(\text{Me}_3\text{Si})_2\text{CH}-\text{C} \begin{array}{c} \text{tBu} \\ \text{B} \\ \text{H} \end{array}$	27.0	$\text{CDCl}_3$	151	$^{13}\text{C}$	151

TABLE 9

 $\delta^{11}\text{B}$  values of some diorganylboronhalides  $\text{R}_2\text{BX}$ .

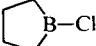
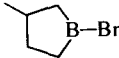
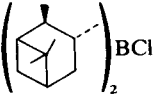
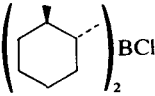
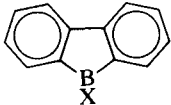
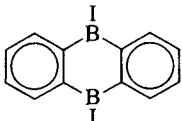
Compound	$\delta^{11}\text{B}$	Solvent	Ref.	Other nuclei	Ref.
$\text{Me}_2\text{BF}$	59.0	—	107	$\left\{ \begin{array}{l} {}^{13}\text{C} \\ {}^{19}\text{F} \\ {}^{13}\text{C} \\ {}^{35}\text{Cl} \end{array} \right.$	7
$\text{Me}_2\text{BCl}$	77.2	—	107		526, 766
$\text{Me}_2\text{BBr}$	78.8	$\text{CCl}_4$	336		7
$\text{Me}_2\text{BI}$	79.1	—	337		335
$\text{Et}_2\text{BF}$	59.6	—	107	${}^{19}\text{F}$	526, 766
$\text{Et}_2\text{BCl}$	78.0	—	107	${}^{13}\text{C}$	7
$\text{Et}_2\text{BBr}$	81.9	—	337	${}^{13}\text{C}$	7
$\text{Et}_2\text{BI}$	84.4	—	337	—	—
	82.6	$\text{C}_6\text{H}_6$	5	—	—
	85.2	$\text{CH}_2\text{Cl}_2$	5	—	—
$i\text{Pr}_2\text{BF}$	59.0	$\text{C}_6\text{D}_6$	145	${}^{13}\text{C}$	143
$i\text{Pr}_2\text{BCl}$	77.8	$\text{C}_6\text{D}_6$	145	${}^{13}\text{C}$	143
$i\text{Pr}_2\text{BBr}$	82.4	—	143	${}^{13}\text{C}$	143
$i\text{Pr}_2\text{BI}$	86.1	—	143	—	—
$\text{C}_8\text{H}_{14}\text{B}-\text{X}^a$	X = Cl	78.6	338	${}^{13}\text{C}$	7
	Br	82.2	338	—	—
	I	84.2	338	—	—
$t\text{Bu}_2\text{BF}$	57.5	—	143	${}^{13}\text{C}$	143
$t\text{Bu}_2\text{BCl}$	77.7	—	143	${}^{13}\text{C}$	143
$t\text{Bu}_2\text{BBr}$	82.4	—	143	${}^{13}\text{C}$	143
$t\text{Bu}_2\text{BI}$	87.7	—	143	${}^{13}\text{C}$	143
	74.0	$\text{Et}_2\text{O}$	372	—	—
	78.0	$\text{Et}_2\text{O}$	372	—	—
$(\text{C}_5\text{Me}_5)_2\text{BCl}$	74.2	$\text{CD}_2\text{Cl}_2$	284	—	—
$\text{Ph}_2\text{BF}$	47.4	—	337	—	—
$\text{Ph}_2\text{BCl}$	61.0	—	107	${}^{13}\text{C}$	10
$\text{Ph}_2\text{BBr}$	66.7	—	337	${}^{13}\text{C}$	10
	64.8	—	343	—	—
$\text{Ph}_2\text{BI}$	69.1	—	337	—	—

TABLE 9 (cont.)

 $\delta^{11}\text{B}$  values of some diorganylboronhalides  $\text{R}_2\text{BX}$ .

Compound		$\delta^{11}\text{B}$	Solvent	Ref.	Other nuclei	Ref.
	X = Cl	61.5		138	$^{13}\text{C}$	7
	Br	65.8		138	—	
	I	64.0		138	—	
		65.9	$\text{CS}_2$	339	—	
$(\text{CH}_2=\text{CH})_2\text{BF}$		42.4		69	$^{13}\text{C}$	69
$(\text{CH}_2=\text{CH})_2\text{BCl}$		56.7		69	$^{13}\text{C}$	69
$(\text{CH}_2=\text{CH})_2\text{BBr}$		60.1		69	$^{13}\text{C}$	69

<sup>a</sup>  $\text{C}_8\text{H}_{14}\text{B}$  = 9-borabicyclo[3.3.1]nonyl.

TABLE 10

 $\delta^{11}\text{B}$  values of some diorganylboron-oxygen compounds.<sup>a</sup>

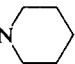
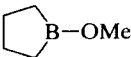
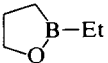
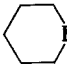
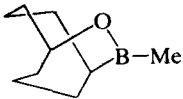
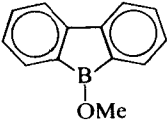

Compound	$\delta^{11}\text{B}$	Solvent	Ref.	Other nuclei	Ref.
$\text{Me}_2\text{BOMe}$	53.0	—	107	$^{13}\text{C}$	205
$\text{Me}_2\text{BOiPr}$	52.1	—	262	$^{17}\text{O}$	350
$\text{Me}_2\text{BOTtBu}$	50.8	—	115	—	
$\text{Me}_2\text{B}-\text{O}-\text{N}$ 	52.7	$\text{CH}_2\text{Cl}_2$	229	$^{13}\text{C}$	229
$\text{Me}_2\text{B}-\text{OSiMe}_3$	51.6	—	115	—	
$(\text{Me}_2\text{B})_2\text{O}$	52.0	—	7	—	
$\text{Et}_2\text{BOMe}$	53.6	—	107	$\begin{cases} ^{13}\text{C} \\ ^{17}\text{O} \end{cases}$	7 350
$(\text{Et}_2\text{B})_2\text{O}$	53.3	—	116	$\begin{cases} ^{13}\text{C} \\ ^{17}\text{O} \end{cases}$	116 350
$(\text{Et}_2\text{BOAlCl}_2)_2$	60.6	$\text{C}_7\text{D}_8$	266	$^{13}\text{C}, ^{17}\text{O}, ^{27}\text{Al}$	266
	60.8	$\text{C}_6\text{D}_6$	117	$\begin{cases} ^{13}\text{C} \\ ^{17}\text{O} \end{cases}$	7 350
	57.0	$\text{C}_7\text{D}_8$	117	$\begin{cases} ^{13}\text{C} \\ ^{17}\text{O} \end{cases}$	7 117

TABLE 10 (cont.)

 $\delta^{11}\text{B}$  values of some diorganylboron-oxygen compounds.<sup>a</sup>

Compound	$\delta^{11}\text{B}$	Solvent	Ref.	Other nuclei	Ref.
 B-OMe	52.2	$\text{CDCl}_3$	257	$^{13}\text{C}$	257
$\text{C}_6\text{H}_{14}\text{B}-\text{OR}^{b,c}$ R = H	58.8	$\text{CDCl}_3$	117	$\begin{cases} ^{13}\text{C} \\ ^{17}\text{O} \end{cases}$	$\begin{matrix} 7 \\ 117 \end{matrix}$
Me	56.3	$\text{C}_6\text{D}_6$	117	$\begin{cases} ^{13}\text{C} \\ ^{17}\text{O} \end{cases}$	$\begin{matrix} 7 \\ 117, \\ 350 \end{matrix}$
tBu	55.7	$\text{C}_7\text{D}_8$	117	$\begin{cases} ^{13}\text{C} \\ ^{17}\text{O} \end{cases}$	$\begin{matrix} 7 \\ 117 \end{matrix}$
$\text{SiMe}_3$	58.9	$\text{C}_6\text{D}_6$	117	$\begin{cases} ^{13}\text{C} \\ ^{17}\text{O} \end{cases}$	$\begin{matrix} 7 \\ 117 \end{matrix}$
$\text{BC}_8\text{H}_{14}$	59.3	$\text{C}_6\text{D}_6$	117	$^{17}\text{O}$	117
$\text{CH}_2\text{CF}_2\text{CF}_2\text{H}$	59.0	$\text{CDCl}_3$	436	$^{13}\text{C}, ^{17}\text{O}$	436
$\text{CH}_2\text{CH}_2\text{C}_6\text{F}_{13}$	57.8	$\text{CDCl}_3$	436	$^{13}\text{C}, ^{17}\text{O}$	436
 B-Me	54.7	$\text{CDCl}_3$	257	$^{13}\text{C}$	257
tBu(Me)BOiPr	52.9	—	262	—	—
tBu <sub>2</sub> BOMe	51.0	$\text{CH}_2\text{Cl}_2/\text{C}_6\text{D}_6$	143	$^{13}\text{C}$	143
Ph(iPr)BOiPr	48.6	—	262	—	—
Ph <sub>2</sub> BOMe	45.7	—	146	—	—
Ph <sub>2</sub> BOEt	45.1	—	119	—	—
 OMe	46.0	$\text{CDCl}_3$	138	—	—
$(\text{Ph}_2\text{B})_2\text{O}$	46.0	—	7	$^{13}\text{C}$	10
$[(\text{CH}_2=\text{CH})_2\text{B}]_2\text{O}$	39.0	—	120	$^{13}\text{C}$	120
 MeO-B-OMe	35.0	—	340	—	—

<sup>a</sup> For more data see Refs 5 and 7.<sup>b</sup>  $\text{C}_6\text{H}_{14}\text{B}$  = 9-borabicyclo[3.3.1]nonyl.<sup>c</sup> For  $\delta^{11}\text{B}$  values of other *B*-(alkoxy)-9-borabicyclo[3.3.1]nonanes see Ref. 375.

TABLE 11

 $\delta^{11}\text{B}$  values of some diorganylboron-sulphur and -selenium compounds.

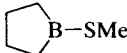
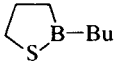
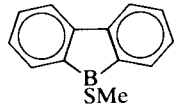
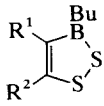
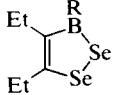
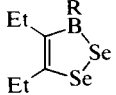
Compound	$\delta^{11}\text{B}$	Solvent	Ref.	Other nuclei	Ref.
$\text{Me}_2\text{BSMe}$	73.6	—	121	$^{13}\text{C}$	205
$\text{Me}_2\text{BSeMe}$	79.4	$\text{CS}_2$	5, 7	—	
$(\text{Me}_2\text{B})_2\text{S}_2$	75.4	—	121	—	
$(\text{Me}_2\text{B})_2\text{Se}_2$	79.7	$\text{CS}_2$	5, 7	—	
$(\text{Me}_2\text{B})_2\text{S}$	78.7	—	121	—	
$\text{Et}_2\text{BSMe}$	75.4	—	5, 7	—	
 B-SMe	80.5	$\text{CH}_2\text{Cl}_2$	5	—	
 B-Bu	80.0	—	122	—	
$\text{C}_8\text{H}_{14}\text{B-SMe}$	76.0	$\text{C}_6\text{H}_6$	123	—	
$\text{Ph}_2\text{BSMe}$	67.0	$\text{CH}_2\text{Cl}_2$	124	—	
$[(2,4,6\text{-Me}_3)\text{C}_6\text{H}_2]_2\text{BSR}$	70–73	$\text{CDCl}_3$	125	$^{13}\text{C}$	125
$[(2,4,6\text{-Me}_3)\text{C}_6\text{H}_2]_2\text{BSeMe}$	79.5	$\text{CDCl}_3$	126	$^{13}\text{C}$	125
 B-SMe	61.9	$\text{C}_6\text{D}_6$	138	—	
	59–62	$\text{CH}_2\text{Cl}_2$	207	$^{13}\text{C}$	207
 R = Me	69.6	$\text{CH}_2\text{Cl}_2$	206	$^{13}\text{C}$	206
 R = Bu	71.9	$\text{CH}_2\text{Cl}_2$	206	$^{13}\text{C}$ , $^{77}\text{Se}$	206

TABLE 12

 $\delta^{11}\text{B}$  values of some representative amino-diorganylboranates.

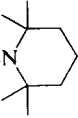
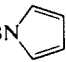
Compound	$\delta^{11}\text{B}$	Solvent	Ref.	Other nuclei	Ref.
$\text{Me}_2\text{BNH}_2$	47.1	—	127	$\begin{cases} {}^{13}\text{C} \\ {}^{15}\text{N} \end{cases}$	153 7
$\text{Me}_2\text{BNHMe}$	45.7	—	107	$\begin{cases} {}^{13}\text{C} \\ {}^{14}\text{N} \end{cases}$	153 128
$\text{Me}_2\text{BNMe}_2$	45.0	—	107	$\begin{cases} {}^{13}\text{C} \\ {}^{14}\text{N} \end{cases}$	205 128
$\text{Me}_2\text{BNEt}_2$	44.9	—	107	$\begin{cases} {}^{13}\text{C} \\ {}^{14}\text{N} \end{cases}$	153 128
	49.6	$\text{CDCl}_3$	368	${}^{13}\text{C}$	368
$\text{Me}_2\text{BN}(\text{H})\text{Ph}$	48.0	—	128	$\begin{cases} {}^{14}\text{N} \\ {}^{15}\text{N} \end{cases}$	128 182
$\text{Me}_2\text{BN}(\text{Me})\text{Ph}$	46.5	—	128	${}^{14}\text{N}$	128
$\text{Me}_2\text{BNPh}_2$	49.6	$\text{CCl}_4$	129	—	—
	56.2	$\text{CH}_2\text{Cl}_2$	152	$\begin{cases} {}^{13}\text{C}, {}^{15}\text{N} \\ {}^{14}\text{N} \end{cases}$	779 152
$\text{Me}_2\text{BN}(\text{tBu})\text{SSMe}$	56.0	$\text{CH}_2\text{Cl}_2$	285	—	—
$\text{Me}_2\text{BN}(\text{Me})\text{SO}_2\text{Me}$	54.0	$\text{CH}_2\text{Cl}_2$	5, 7	—	—
	55.8	—	279	—	—
$\text{Me}_2\text{BN}(\text{H})\text{NMe}_2$	45.5	—	130	${}^{14}\text{N}$	128
$\text{Me}_2\text{BN}(\text{Me})\text{PMe}_2$	53.0	—	131	${}^{31}\text{P}$	131
$\text{Me}_2\text{BN}(\text{H})\text{SiMe}_3$	51.6	—	132	$\begin{cases} {}^{13}\text{C} \\ {}^{14}\text{N} \end{cases}$	153 132
$\text{Me}_2\text{BN}(\text{Me})\text{SiMe}_3$	51.4	—	132	$\begin{cases} {}^{13}\text{C} \\ {}^{14}\text{N} \end{cases}$	153 132
$\text{Me}_2\text{BN}(\text{OSiMe}_3)\text{SiMe}_3$	50.5	—	225	—	—
$\text{Me}_2\text{BN}(\text{OBMe}_2)\text{SiMe}_3$	47.9(\text{BN})	—	—	—	—
	54.5(\text{BO})	$\text{CH}_2\text{Cl}_2$	230	—	—
$\text{Me}_2\text{BN}(\text{SiMe}_3)_2$	59.5	—	132	$\begin{cases} {}^{13}\text{C} \\ {}^{14}\text{N} \end{cases}$	153 132
$\text{Me}_2\text{BN}(\text{SnMe}_3)_2$	53.4	$\text{CH}_2\text{Cl}_2$	133	$\begin{cases} {}^{13}\text{C}, {}^{14}\text{N}, \\ {}^{119}\text{Sn} \end{cases}$	133
$(\text{Me}_2\text{B})_2\text{NH}$	56.1	—	134	${}^{14}\text{N}$	7
$(\text{Me}_2\text{B})_2\text{NMe}$	58.5	—	134	${}^{14}\text{N}$	7
$(\text{Me}_2\text{B})_2\text{NSnMe}_3$	58.4	$\text{CH}_2\text{Cl}_2$	135	${}^{14}\text{N}$	135
$(\text{Me}_2\text{B})_3\text{N}$	61.5	$\text{CH}_2\text{Cl}_2$	135	${}^{14}\text{N}$	135, 182
$\text{Me}_2\text{BNMeLi}$	44.0	$\text{Et}_2\text{O}$	136	—	—
$\text{Me}_2\text{BN}(\text{Li})\text{NMe}_2$	42.6	THF	272	—	—

TABLE 12 (cont.)

 $\delta^{11}\text{B}$  values of some representative amino-diorganylborananes.

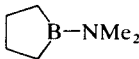
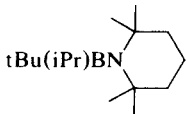
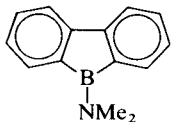
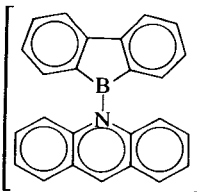
Compound	$\delta^{11}\text{B}$	Solvent	Ref.	Other nuclei	Ref.
$\text{Me}_2\text{BNMe}_2\text{—AlCl}_3$	74.3	$\text{CH}_2\text{Cl}_2/\text{C}_6\text{D}_6$	148	$^{14}\text{N}$	148
$\text{Et}_2\text{BNH}_2$	48.7	—	128	$\begin{cases} ^{13}\text{C} \\ ^{14}\text{N} \end{cases}$	153 128
$\text{Et}_2\text{BNMe}_2$	45.7	—	107	$\begin{cases} ^{13}\text{C} \\ ^{14}\text{N} \end{cases}$	153 128
$\text{Et}_2\text{BN}(\text{SnMe}_3)_2$	54.7	$\text{CH}_2\text{Cl}_2$	268	$^{13}\text{C}, ^{14}\text{N}, ^{119}\text{Sn}$	268
$(\text{Et}_2\text{B})_2\text{NtBu}$	59.1	$\text{CCl}_4$	49	—	—
 $\text{B—NMe}_2$	51.3	$\text{CH}_2\text{Cl}_2$	153	$^{13}\text{C}, ^{14}\text{N}$	153
$\text{iPr}_2\text{BNH}_2$	49.5	—	143	$^{13}\text{C}, ^{14}\text{N}$	143
$\text{iPr}_2\text{BNMe}_2$	45.6	—	143	$^{13}\text{C}, ^{14}\text{N}$	143
$\text{iPr}_2\text{BN}(\text{SnMe}_3)_2$	55.0	$\text{CH}_2\text{Cl}_2$	268	$^{13}\text{C}, ^{14}\text{N}, ^{119}\text{Sn}$	268
$\text{C}_8\text{H}_{14}\text{BNMe}_2^a$	47.0	$\text{C}_6\text{D}_6$	154	—	—
$(\text{C}_8\text{H}_{14}\text{B})_3\text{N}^a$	67.0	THF	155	$^{13}\text{C}, ^{14}\text{N}$	155
 $\text{tBu}(\text{iPr})\text{BN}$	67.7	$\text{CDCl}_3$	812	$^{13}\text{C}$	812
$\text{tBu}_2\text{BNH}_2$	48.7	—	143	$^{13}\text{C}, ^{14}\text{N}$	143
$\text{tBu}_2\text{BNMe}_2$	49.9	—	143	$^{13}\text{C}, ^{14}\text{N}$	143
$(\text{CF}_3)_2\text{BNMe}_2$	30.2	$\text{CDCl}_3$	218	$^{13}\text{C}, ^{19}\text{F}$	218
$\text{Ph}_2\text{BNMe}_2$	41.8	$\text{C}_6\text{H}_6$	128	$\begin{cases} ^{13}\text{C} \\ ^{14}\text{N} \end{cases}$	10 128
$[(2,4,6\text{-Me}_3)\text{C}_6\text{H}_2]_2\text{BNRR}'$	43–49	$\text{CDCl}_3$	156	$^{13}\text{C}$	156
 $\text{B—NMe}_2$	38.5	$\text{CDCl}_3$	138	—	—
 $\left[ \text{AlCl}_4 \right]^-$	43.5	$\text{CH}_2\text{Cl}_2$	256	$^{27}\text{Al}$	256
$\text{Ph}_2\text{BN}_3$	50.6	$\text{CDCl}_3$	217	—	—
$[(2,4,6\text{-Me}_3)\text{C}_6\text{H}_2]_2\text{BN}_3$	54.3	$\text{CCl}_4$	217	—	—
$(\text{CH}_2=\text{CH})_2\text{BNMe}_2$	37.0	—	35	—	—

TABLE 12 (cont.)

 $\delta^{11}\text{B}$  values of some representative amino-diorganylboranes.

Compound	$\delta^{11}\text{B}$	Solvent	Ref.	Other nuclei	Ref.
	28.4	Hexane	157	—	
 R = alkyl	25.0		150	$^{13}\text{C}$ , $^{29}\text{Si}$	150
	33.9	MeCN	139	$^{13}\text{C}$	139
	33.0	pyridine	139	$^{13}\text{C}$	139
	33.0	$\text{C}_6\text{D}_6$	43	$^{13}\text{C}$	43
	29.0	THF	158	—	
$(\text{HC}\equiv\text{C})_2\text{BNMe}_2$	22.0	$\text{CH}_2\text{Cl}_2$	85	—	
	22.0	THF	84, 161	$^{13}\text{C}$	162
	44.0	$\text{CD}_2\text{Cl}_2$	162	$^{13}\text{C}$	162
	31.4	$\text{CDCl}_3$	646	$^{13}\text{C}$	646

TABLE 12 (cont.)

 $\delta^{11}\text{B}$  values of some representative amino-diorganylboranates.

Compound	$\delta^{11}\text{B}$	Solvent	Ref.	Other nuclei	Ref.
$\left[ \begin{array}{c} \text{Me}_3\text{Si} \\ \diagup \quad \diagdown \\ \text{iPr}_2\text{N}-\text{B} \quad \text{B}-\text{NiPr}_2 \\ \diagdown \quad \diagup \\ \text{C} \\ \diagup \quad \diagdown \\ \text{SiMe}_3 \end{array} \right]^{2-}$	12.0	$\text{C}_6\text{D}_6$	646	$^{13}\text{C}, ^{29}\text{Si}$	646
$\begin{array}{c} \text{Me}_3\text{Si} \quad \text{R} \\ \diagup \quad \diagdown \\ \text{iPr}_2\text{N}-\text{B} \quad \text{B}-\text{NiPr}_2 \\ \diagdown \quad \diagup \\ \text{C} \\ \diagup \quad \diagdown \\ \text{R} \quad \text{SiMe}_3 \end{array}$	$\text{R} = \text{H} \quad 43.5$ $\text{Me} \quad 48.7$	$\text{CDCl}_3$ $\text{C}_6\text{D}_6$	646 646	$^{13}\text{C}, ^{29}\text{Si}$ $^{13}\text{C}$	646 646
$\begin{array}{c} \text{Me}_3\text{Si} \quad \text{SiMe}_3 \\ \diagup \quad \diagdown \\ \text{iPr}_2\text{N}-\text{B} \quad \text{B}-\text{NiPr}_2 \\ \diagdown \quad \diagup \\ \text{C} \\ \diagup \quad \diagdown \\ \text{Ph}_3\text{PAu} \quad \text{AuPPh}_3 \end{array}$	45.9	$\text{C}_6\text{D}_6$	646	$^{31}\text{P}$	646

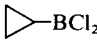
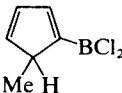
<sup>a</sup>  $\text{C}_8\text{H}_{14}\text{B} = 9\text{-borabicyclo}[3.3.1]\text{nonyl}$ .

TABLE 13

 $\delta^{11}\text{B}$  values of some halogeno-organylboranates  $\text{RBX}_2$ <sup>a</sup>

Compound	$\delta^{11}\text{B}$	Solvent	Ref.	Other nuclei	Ref.
$\text{MeBF}_2$	28.2(76)	—	180	$^{19}\text{F}$	526, 766
$\text{EtBF}_2$	28.7(81)	—	107	$^{13}\text{C}$	153
$\text{tBuBF}_2$	29.9	$\text{C}_6\text{D}_6$	118	$^{13}\text{C}$	118
$\triangle\text{-BF}_2$	28.3	—	177	$^{13}\text{C}$	275
	28.5	—	275		
$\text{PhBF}_2$	25.5(62)	Methyl-cyclohexane	178	$\begin{cases} ^{13}\text{C} \\ ^{19}\text{F} \end{cases}$	$\begin{cases} 36 \\ 526, 766 \end{cases}$
$\text{CH}_2=\text{CHBF}_2$	22.6		69	$^{13}\text{C}$	69
$\text{MeBCl}_2$	62.3		180	$^{35}\text{Cl}$	335
$\text{EtBCl}_2$	63.4		107	—	

TABLE 13 (*cont.*) $\delta^{11}\text{B}$  values of some halogeno-organylboranes  $\text{RBX}_2$ .

Compound	$\delta^{11}\text{B}$	Solvent	Ref.	Other nuclei	Ref.
$\text{CHMe}_2\text{CMe}_2\text{BCl}_2$	65.2	—	376	—	
	65.4	$\text{CH}_2\text{Cl}_2$	376	—	
	64.9	$\text{Et}_2\text{O}$	376	—	
 $\text{BCl}_2$	59.4		177	—	
$\text{PhBCl}_2$	54.8		107	$^{13}\text{C}$	36
$\text{CH}_2=\text{CHBCl}_2$	52.4		179	—	
 $\text{BCl}_2$	48.9	$\text{CCl}_4$	281	—	
$\text{Cl}_2\text{B}-\text{C}_5\text{H}_4-\text{TiCl}_3$	50.6	$\text{CH}_2\text{Cl}_2$	78	$^{13}\text{C}$	78
$\text{Cl}_2\text{B}-\text{C}_5\text{H}_4-\text{Mn}(\text{CO})_3$	50.6	$\text{CS}_2$	29	—	
$\text{Cl}_2\text{B}-\text{C}_5\text{H}_4-\text{Fecp}$	50.5	$\text{CS}_2$	29	—	
$\text{Cl}_2\text{B}-\text{C}_5\text{Me}_5$	59.9		78	—	
$(\text{Cl}_2\text{B})_2\text{C}_5\text{H}_4$	50.8	$\text{CCl}_4$	283	—	
$\text{CH}_2(\text{BCl}_2)_2$	59.3	$\text{CDCl}_3$	194	—	
$\text{MeBBBr}_2$	62.5		180	—	
$\text{EtBBBr}_2$	65.6		180	—	
$\text{Et}(\text{Pr})\text{CHBBBr}_2$	67.0	$\text{CDCl}_3$	140	—	
$\text{PhBBBr}_2$	57.7	Methyl-cyclohexane	178	$^{13}\text{C}$	36
	56.2	$\text{CDCl}_3$	343	—	
$\text{CH}_2=\text{CHBBBr}_2$	54.7		69	—	
$\text{MeBI}_2$	50.5		180	—	
$\text{EtBI}_2$	55.9		180	—	
$\text{tBuBI}_2$	60.0	$\text{C}_6\text{D}_6$	118	$^{13}\text{C}$	118
$\text{PhBI}_2$	48.2		180	$^{13}\text{C}$	36
$\text{C}_5\text{H}_4(\text{BI}_2)_2$	36.8	$\text{CCl}_4$	283	$^{13}\text{C}$	283
$(\text{CO})_3\text{MnC}_5\text{H}_4\text{BI}_2$	31.7	$\text{CS}_2$	29	—	
$\text{cpFeC}_5\text{H}_4\text{BI}_2$	26.1	$\text{CS}_2$	29	—	
$\text{CH}_2(\text{BI}_2)_2$	45.5	$\text{CDCl}_3$	194	—	
$\text{MeB}(\text{F})\text{Cl}$	43.8(100)		181	$^{19}\text{F}$	181
$\text{PhB}(\text{F})\text{Cl}$	40.9(93)	Methyl-cyclohexane	178	$^{19}\text{F}$	178
$\text{MeB}(\text{F})\text{Br}$	45.2(112)		181	$^{19}\text{F}$	181
$\text{PhB}(\text{F})\text{Br}$	42.6(92)	Methyl-cyclohexane	178	$^{19}\text{F}$	178
$\text{MeB}(\text{Cl})\text{Br}$	61.5		181	—	
$\text{PhB}(\text{Cl})\text{Br}$	56.0		181	—	

<sup>a</sup>  $^1J(^{19}\text{F}^{11}\text{B})$  in Hz in parentheses.

TABLE 14

 $\delta^{11}\text{B}$  values of some organylboron-oxygen compounds.

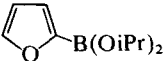
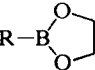
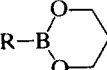
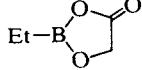
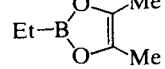
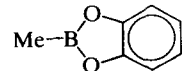
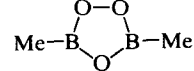
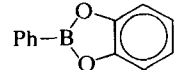
Compound	$\delta^{11}\text{B}$	Solvent	Ref.	Other nuclei	Ref.
$\text{MeB}(\text{OH})_2$	31.9	$\text{D}_2\text{O}$	193	—	
$\text{MeB}(\text{OMe})_2$	29.5	—	108	$\begin{Bmatrix} ^{13}\text{C} \\ ^{17}\text{O} \end{Bmatrix}$	205 350
$\text{MeB}(\text{OiPr})_2$	30.2	—	193	—	
$\text{EtB}(\text{OMe})_2$	31.5	—	108	$\begin{Bmatrix} ^{13}\text{C} \\ ^{17}\text{O} \end{Bmatrix}$	7 350
$\text{tBuB}(\text{OiPr})_2$	29.5		262	—	
$\text{PhB}(\text{OH})_2$	28.8	THF	195	—	
$\text{PhB}(\text{OMe})_2$	28.6	$\text{C}_6\text{H}_6$	182	$^{13}\text{C}$	36
$\text{PhB}(\text{OMe})_2$					
$(1E)\text{-1-octenyl-B}(\text{OMe})_2$	27.8	—	196	—	
$\text{HC}\equiv\text{C-B}(\text{OMe})_2$	21.6	—	183	—	
 $\text{B}(\text{OiPr})_2$	23.3	—	262	—	
$(\text{Me}_3\text{Si})_3\text{CB}(\text{OMe})_2$	31.0	$\text{CCl}_4$	184	—	
$\text{R} = \text{Me}$	34.2		650	—	
 $\text{R} = \text{Et}$	35.0	Neohexane	185	$\begin{Bmatrix} ^{13}\text{C} \\ ^{17}\text{O} \end{Bmatrix}$	7 117
$\text{R} = \text{Ph}$	31.2	$\text{CH}_3\text{CN}$	187	$^{13}\text{C}$	36
	31.2	$\text{CDCl}_3$	56		
 $\text{R} = \text{Et}$	30.5	Neohexane	185	$\begin{Bmatrix} ^{13}\text{C} \\ ^{17}\text{O} \end{Bmatrix}$	7 117
$\text{tBu}$	31.1		650	—	
$\text{exo-norbornyl-CH}_2$	30.5	—	278	—	
$\text{Ph-CH}_2$	30.5	THF	261	—	
	38.6	$\text{C}_7\text{D}_8$	117	$\begin{Bmatrix} ^{13}\text{C} \\ ^{17}\text{O} \end{Bmatrix}$	7 117
	34.4	$\text{C}_7\text{D}_8$	117	$\begin{Bmatrix} ^{13}\text{C} \\ ^{17}\text{O} \end{Bmatrix}$	7 117
	35.5	$\text{CDCl}_3$	188	$^{13}\text{C}$	188
	35.5		186	—	
	31.9	$\text{CS}_2$	189	—	

TABLE 14 (cont.)

 $\delta^{11}\text{B}$  values of some organylboron-oxygen compounds.

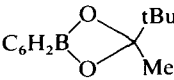
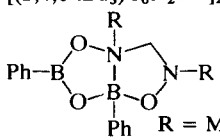
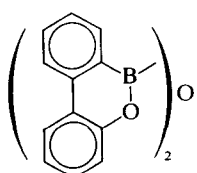
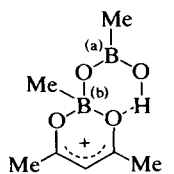
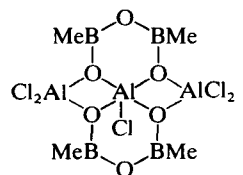
Compound	$\delta^{11}\text{B}$	Solvent	Ref.	Other nuclei	Ref.
	33.5	—	277	—	
$[(2,4\text{-tBu}_2)\text{C}_6\text{H}_3\text{-BO}]_2$	33.0	—	277	—	
$[(2,4,6\text{-tBu}_3)\text{C}_6\text{H}_2\text{BO}]_2$	32.4	—	277	—	
	R = Me 21.8 C <sub>6</sub> H <sub>11</sub> 22.0	CDCl <sub>3</sub>	287	—	
(single resonances)					
(MeBO) <sub>3</sub>	32.5	C <sub>6</sub> H <sub>6</sub>	264	{ <sup>13</sup> C <sup>17</sup> O	7
	32.5	CDCl <sub>3</sub>	190		350
(EtBO) <sub>3</sub>	33.5	C <sub>6</sub> D <sub>6</sub>	117	{ <sup>13</sup> C <sup>17</sup> O	7
(PhBO) <sub>3</sub>	30.4	C <sub>6</sub> D <sub>6</sub>	117		117
(CH <sub>2</sub> =CHBO) <sub>3</sub>	28.0	C <sub>6</sub> D <sub>6</sub>	120	—	
	27.5	CH <sub>2</sub> Cl <sub>2</sub>	269	—	
	31.8(a) 7.3(b)	C <sub>7</sub> H <sub>8</sub>	264	<sup>13</sup> C, <sup>17</sup> O	264
	31.8	C <sub>7</sub> D <sub>8</sub>	265	<sup>13</sup> C, <sup>17</sup> O, <sup>27</sup> Al	265
MeB(F)OMe	29.7(85.0)	Pentane	191	—	
MeB(Cl)OMe	42.0	Pentane	107	—	

TABLE 15

 $\delta^{11}\text{B}$  values of some organylboron-sulphur and -selenium compounds.

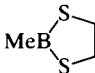
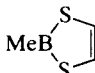
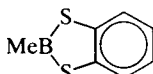
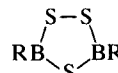
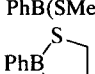
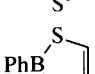
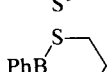
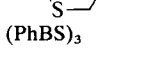
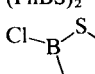
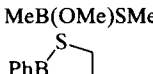
Compound	$\delta^{11}\text{B}$	Solvent	Ref.	Other nuclei	Ref.
$\text{MeB}(\text{SMe})_2$	66.3	$\text{C}_6\text{H}_6$	197	$^{13}\text{C}$	205
$\text{MeB}(\text{SCF}_3)_2$	66.7	—	198	$^{19}\text{F}$	198
$\text{MeB}(\text{SSiMe}_3)_2$	70.5	—	199	$^{29}\text{Si}$	199
	69.6	$\text{CH}_2\text{Cl}_2$	124	—	
	61.5	$\text{CH}_2\text{Cl}_2$	200	$^{13}\text{C}$	200
	62.2	$\text{CH}_2\text{Cl}_2$	188	$^{13}\text{C}$	188
	70.6	—	201	$^{13}\text{C}$	7
	75.1	—	286	—	
$\text{PhB}(\text{SMe})_2$	65.0	$\text{CH}_2\text{Cl}_2$	124	$^{13}\text{C}$	273
	66.2	$\text{CH}_2\text{Cl}_2$	36	$^{13}\text{C}$	36
	59.1	$\text{CH}_2\text{Cl}_2$	200	$^{13}\text{C}$	36, 200
	58.7	$\text{CDCl}_3$	273	$^{13}\text{C}$	273
$(\text{PhBS})_3$	58.3	$\text{CH}_2\text{Cl}_2$	124	—	
	63.8	$\text{CDCl}_3$	258	—	
$(\text{PhBS})_2$	45.7	THF	258	$^{13}\text{C}$	258
	72.5	$\text{CDCl}_3$	203	—	
$\text{MeB}(\text{OMe})\text{SMe}$	48.5	—	191		
	47.7	—	204	—	
$\text{MeB}(\text{SeMe})_2$	73.0	$\text{CH}_2\text{Cl}_2$	205	$\begin{cases} ^{13}\text{C} \\ ^{77}\text{Se} \end{cases}$	$\begin{matrix} 205 \\ 182 \end{matrix}$
	77.2	$\text{CS}_2$	5, 7	—	
$\text{PhB}(\text{SeMe})_2$	70.3	$\text{CS}_2$	5, 7	—	

TABLE 16

 $\delta^{11}\text{B}$  values of some noncyclic organylboron–nitrogen compounds.

Compound	$\delta^{11}\text{B}$	Solvent	Ref.	Other nuclei	Ref.
$\text{MeB}(\text{NHMe})_2$	31.7	—	128	$^{14}\text{N}$	128
$\text{MeB}(\text{NMe}_2)_2$	33.5	—	107	$\begin{Bmatrix} ^{13}\text{C} \\ ^{14}\text{N} \end{Bmatrix}$	205
$\text{MeB}(\text{NEt}_2)_2$	33.8	—	107		128
$\text{MeB}\left(\text{N} \begin{array}{c} \text{C}_5\text{H}_5 \end{array} \right)_2$	34.8	$\text{CH}_2\text{Cl}_2$	152	$^{14}\text{N}$	152
$\text{MeB}(\text{NHNMe}_2)_2$	30.8	$\text{C}_6\text{H}_6$	130	$^{14}\text{N}$	128
$\text{MeB}[\text{N}(\text{Me})\text{SiMe}_3]_2$	41.2	—	132	$^{14}\text{N}$	132
(a) (b)					
$\text{MeB}[\text{N}(\text{Me})\text{BMe}_2]_2$	36.5(a) 61.3(b)	$\text{CH}_2\text{Cl}_2$	208	$^{14}\text{N}$	208
$\text{MeB} \begin{array}{c} \text{NMe}_2 \\ \diagup \quad \diagdown \\ \text{NMe}_2 - \text{AlCl}_3 \end{array}$	38.5	$\text{C}_7\text{D}_8$	148	$^{14}\text{N}$	148
$\text{EtB}(\text{NHMe})_2$	33.1	—	107	$^{14}\text{N}$	128
$\text{EtB}(\text{NMe}_2)_2$	34.2	—	107	$^{14}\text{N}$	128
$\text{EtB}\left(\text{N} \begin{array}{c} \text{C}_5\text{H}_5 \end{array} \right)_2$	39.4	—	152	$\begin{Bmatrix} ^{13}\text{C} \\ ^{14}\text{N} \end{Bmatrix}$	779 128
$\text{iPrB}(\text{NMe}_2)\text{N} \begin{array}{c} \diagup \quad \diagdown \\ \text{C}_6\text{H}_{11} \end{array}$	40.2	$\text{CDCl}_3$	812	$^{13}\text{C}$	812
$\text{tBuB}(\text{NMe}_2)_2$	36.4	—	5, 7	$^{13}\text{C}$	7
$\text{CF}_3\text{B}(\text{NMe}_2)_2$	26.3	$\text{CDCl}_3$	218	$^{13}\text{C}, ^{14}\text{N}$	218
$\text{PhB}(\text{NHMe})_2$	30.4	—	128	$\begin{Bmatrix} ^{13}\text{C} \\ ^{14}\text{N} \end{Bmatrix}$	273
$\text{PhB}(\text{NMe}_2)_2$	32.4	—	128		128
$\text{PhB}\left(\text{N} \begin{array}{c} \text{C}_5\text{H}_5 \end{array} \right)_2$	37.0	$\text{CH}_2\text{Cl}_2$	152	$\begin{Bmatrix} ^{13}\text{C} \\ ^{14}\text{N} \end{Bmatrix}$	36 128
$\text{PhB}(\text{NHNMe}_2)_2$	31.2	$\text{C}_6\text{H}_6$	130	—	
$\text{CH}_2=\text{CHB}(\text{NMe}_2)_2$	30.2	—	35	—	
$\text{Me}-\text{C}\equiv\text{C}-\text{B}(\text{NMe}_2)_2$	23.8	$\text{C}_6\text{H}_6$	85	$^{13}\text{C}$	10
$\text{EtB}(\text{N}_3)\text{N}(\text{tBu})\text{SiMe}_3$	42.9	$\text{CCl}_4$	49	—	
$\text{MeB}(\text{H})\text{NMe}_2$	42.1	—	127	—	
$\text{MeB}(\text{F})\text{NMe}_2$	31.6	—	127	—	
$\text{MeB}(\text{Cl})\text{NMe}_2$	38.5	—	107	—	
$\text{tBuB}(\text{Cl})\text{NHtBu}$	40.4	$\text{CCl}_4$	234	—	
$\text{MeB}(\text{Br})\text{NMe}_2$	37.8	—	127	—	

TABLE 16 (*cont.*) $\delta^{11}\text{B}$  values of some noncyclic organylboron–nitrogen compounds.

Compound	$\delta^{11}\text{B}$	Solvent	Ref.	Other nuclei	Ref.
MeB(I)NMe <sub>2</sub>	34.7	C <sub>6</sub> H <sub>6</sub>	191	—	
MeB(OMe)NMe <sub>2</sub>	31.8	—	152	$\begin{cases} {}^{13}\text{C} \\ {}^{14}\text{N} \end{cases}$	71 152
MeB(SMe)NMe <sub>2</sub>	43.6	—	152	$\begin{cases} {}^{13}\text{C} \\ {}^{14}\text{N} \end{cases}$	71 152
MeB(SiMe <sub>3</sub> )NMe <sub>2</sub>	50.2	—	202	—	

TABLE 17

 $\delta^{11}\text{B}$  values of some cyclic organylboron–nitrogen compounds.

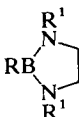
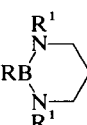
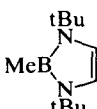
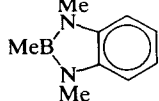
Compound		$\delta^{11}\text{B}$	Solvent	Ref.	Other nuclei	Ref.	
	R	R <sup>1</sup>					
	Me	Me	31.6	—	209	<sup>13</sup> C, <sup>14</sup> N	245
	Me	Ph	33.4	C <sub>6</sub> D <sub>6</sub>	210	—	
	tBu	Me	32.6		211	—	
	CF <sub>3</sub>	Me	24.9	CDCl <sub>3</sub>	218	<sup>13</sup> C, <sup>19</sup> F	218
	Ph	Me	32.2		211	<sup>13</sup> C	
	CH <sub>2</sub> =CH	Me	29.9		212	<sup>14</sup> N	
	MeC≡C	Me	24.9		85	—	
	Me	Me <sub>3</sub> Si	38.2		132	—	
	Me	Me <sub>2</sub> B	45.7	CH <sub>2</sub> Cl <sub>2</sub>	213	<sup>14</sup> N	213
	(MeB)	60.6					
	(Me <sub>2</sub> B)						
	R	R <sup>1</sup>					
	Me	Me	29.2		214	<sup>13</sup> C	273
	Ph	Me	29.5		215	<sup>13</sup> C	273
			26.2	CDCl <sub>3</sub>	219	—	
			31.1	CDCl <sub>3</sub>	188	<sup>13</sup> C	188

TABLE 17 (cont.)

 $\delta^{11}\text{B}$  values of some cyclic organylboron–nitrogen compounds.


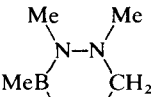
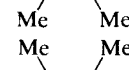
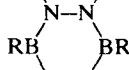
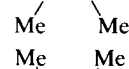
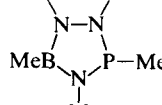
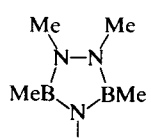
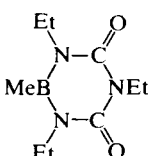
Compound	$\delta^{11}\text{B}$	Solvent	Ref.	Other nuclei	Ref.
					
R    R <sup>1</sup> R <sup>2</sup>					
Me    Me    Me	26.8	—	216	—	
Me    Ph    Ph	26.9	—	216	—	
Et    tBu    Ph	26.6	CCl <sub>4</sub>	49	—	
Et    tBu    Me <sub>3</sub> Si	28.7	CCl <sub>4</sub>	49	—	
Mes    Mes    BMes <sub>2</sub>	29.6	CDCl <sub>3</sub>	217	—	
	52.5				
	(BMes) <sub>2</sub>				
	28.0	CH <sub>2</sub> Cl <sub>2</sub>	221	<sup>13</sup> C	221
					
	R = Me    32.2	—	222		
	Ph    32.3	CH <sub>2</sub> Cl <sub>2</sub>	231	<sup>13</sup> C	36
					
	31.4	CH <sub>2</sub> Cl <sub>2</sub>	223	<sup>31</sup> P	223
	31.3	CH <sub>2</sub> Cl <sub>2</sub>	220	—	
	34.8	CDCl <sub>3</sub>	232, 233	<sup>13</sup> C	232, 233

TABLE 17 (cont.)

 $\delta^{11}\text{B}$  values of some cyclic organylboron–nitrogen compounds.

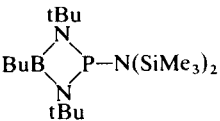
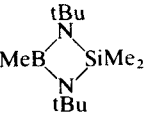
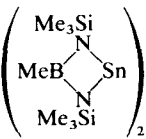
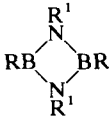
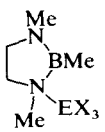
Compound	$\delta^{11}\text{B}$	Solvent	Ref.	Other nuclei	Ref.																																																					
	36.1	—	224	$^{13}\text{C}, ^{31}\text{P}$	224																																																					
	36.4	—	226	—																																																						
	43.5	Pentane	274	$^{119}\text{Sn}$	274																																																					
	<table><tr><th>R</th><th>R<sup>1</sup></th></tr><tr><td>Me</td><td>tBu</td></tr><tr><td>tBu</td><td>iPr</td></tr><tr><td>tBu</td><td>tBu</td></tr><tr><td>tBu</td><td>Me<sub>3</sub>Si</td></tr><tr><td>Ph</td><td>tBu</td></tr></table>	R	R <sup>1</sup>	Me	tBu	tBu	iPr	tBu	tBu	tBu	Me <sub>3</sub> Si	Ph	tBu	<table><tr><td>CH<sub>2</sub>Cl<sub>2</sub></td></tr><tr><td>CDCl<sub>3</sub></td></tr><tr><td>CCl<sub>4</sub></td></tr><tr><td>CDCl<sub>3</sub></td></tr><tr><td>CH<sub>2</sub>Cl<sub>2</sub></td></tr></table>	CH <sub>2</sub> Cl <sub>2</sub>	CDCl <sub>3</sub>	CCl <sub>4</sub>	CDCl <sub>3</sub>	CH <sub>2</sub> Cl <sub>2</sub>	<table><tr><td>227</td></tr><tr><td>228</td></tr><tr><td>53</td></tr><tr><td>228</td></tr><tr><td>227</td></tr></table>	227	228	53	228	227	<table><tr><td><math>^{13}\text{C}, ^{14}\text{N}</math></td></tr><tr><td><math>^{13}\text{C}</math></td></tr><tr><td>—</td></tr><tr><td><math>^{13}\text{C}, ^{29}\text{Si}</math></td></tr><tr><td><math>^{13}\text{C}, ^{14}\text{N}</math></td></tr></table>	$^{13}\text{C}, ^{14}\text{N}$	$^{13}\text{C}$	—	$^{13}\text{C}, ^{29}\text{Si}$	$^{13}\text{C}, ^{14}\text{N}$	<table><tr><td>227</td></tr><tr><td>228</td></tr><tr><td></td></tr><tr><td>228</td></tr><tr><td>227</td></tr></table>	227	228		228	227																					
R	R <sup>1</sup>																																																									
Me	tBu																																																									
tBu	iPr																																																									
tBu	tBu																																																									
tBu	Me <sub>3</sub> Si																																																									
Ph	tBu																																																									
CH <sub>2</sub> Cl <sub>2</sub>																																																										
CDCl <sub>3</sub>																																																										
CCl <sub>4</sub>																																																										
CDCl <sub>3</sub>																																																										
CH <sub>2</sub> Cl <sub>2</sub>																																																										
227																																																										
228																																																										
53																																																										
228																																																										
227																																																										
$^{13}\text{C}, ^{14}\text{N}$																																																										
$^{13}\text{C}$																																																										
—																																																										
$^{13}\text{C}, ^{29}\text{Si}$																																																										
$^{13}\text{C}, ^{14}\text{N}$																																																										
227																																																										
228																																																										
228																																																										
227																																																										
	<table><tr><th>E</th><th>X</th></tr><tr><td>B</td><td>Cl</td></tr><tr><td>B</td><td>Br</td></tr><tr><td>B</td><td>I</td></tr><tr><td>Al</td><td>Cl</td></tr><tr><td>Al</td><td>Br</td></tr><tr><td>Ga</td><td>Cl</td></tr></table>	E	X	B	Cl	B	Br	B	I	Al	Cl	Al	Br	Ga	Cl	<table><tr><td>38.1</td></tr><tr><td>9.4</td></tr><tr><td>(BCl<sub>3</sub>)</td></tr><tr><td>38.0</td></tr><tr><td>-4.7</td></tr><tr><td>(BBr<sub>3</sub>)</td></tr><tr><td>37.6</td></tr><tr><td>-55.1</td></tr><tr><td>(BI<sub>3</sub>)</td></tr><tr><td>38.3</td></tr><tr><td>38.2</td></tr><tr><td>37.6</td></tr></table>	38.1	9.4	(BCl <sub>3</sub> )	38.0	-4.7	(BBr <sub>3</sub> )	37.6	-55.1	(BI <sub>3</sub> )	38.3	38.2	37.6	<table><tr><td>CD<sub>2</sub>Cl<sub>2</sub></td></tr><tr><td>CD<sub>2</sub>Cl<sub>2</sub></td></tr><tr><td>CD<sub>2</sub>Cl<sub>2</sub></td></tr><tr><td>C<sub>6</sub>D<sub>6</sub></td></tr><tr><td>C<sub>6</sub>D<sub>6</sub></td></tr><tr><td>C<sub>6</sub>D<sub>6</sub></td></tr></table>	CD <sub>2</sub> Cl <sub>2</sub>	CD <sub>2</sub> Cl <sub>2</sub>	CD <sub>2</sub> Cl <sub>2</sub>	C <sub>6</sub> D <sub>6</sub>	C <sub>6</sub> D <sub>6</sub>	C <sub>6</sub> D <sub>6</sub>	<table><tr><td>245</td></tr><tr><td></td></tr><tr><td>245</td></tr><tr><td>245</td></tr><tr><td>246</td></tr><tr><td>246</td></tr><tr><td>246</td></tr></table>	245		245	245	246	246	246	<table><tr><td><math>^{13}\text{C}, ^{14}\text{N}</math></td></tr><tr><td><math>^{13}\text{C}, ^{14}\text{N}</math></td></tr><tr><td><math>^{13}\text{C}, ^{14}\text{N}</math></td></tr><tr><td><math>^{13}\text{C}, ^{27}\text{Al}</math></td></tr><tr><td><math>^{13}\text{C}, ^{27}\text{Al}</math></td></tr><tr><td><math>^{13}\text{C}</math></td></tr></table>	$^{13}\text{C}, ^{14}\text{N}$	$^{13}\text{C}, ^{14}\text{N}$	$^{13}\text{C}, ^{14}\text{N}$	$^{13}\text{C}, ^{27}\text{Al}$	$^{13}\text{C}, ^{27}\text{Al}$	$^{13}\text{C}$	<table><tr><td>245</td></tr><tr><td></td></tr><tr><td>245</td></tr><tr><td>245</td></tr><tr><td>246</td></tr><tr><td>246</td></tr><tr><td>246</td></tr></table>	245		245	245	246	246	246
E	X																																																									
B	Cl																																																									
B	Br																																																									
B	I																																																									
Al	Cl																																																									
Al	Br																																																									
Ga	Cl																																																									
38.1																																																										
9.4																																																										
(BCl <sub>3</sub> )																																																										
38.0																																																										
-4.7																																																										
(BBr <sub>3</sub> )																																																										
37.6																																																										
-55.1																																																										
(BI <sub>3</sub> )																																																										
38.3																																																										
38.2																																																										
37.6																																																										
CD <sub>2</sub> Cl <sub>2</sub>																																																										
CD <sub>2</sub> Cl <sub>2</sub>																																																										
CD <sub>2</sub> Cl <sub>2</sub>																																																										
C <sub>6</sub> D <sub>6</sub>																																																										
C <sub>6</sub> D <sub>6</sub>																																																										
C <sub>6</sub> D <sub>6</sub>																																																										
245																																																										
245																																																										
245																																																										
246																																																										
246																																																										
246																																																										
$^{13}\text{C}, ^{14}\text{N}$																																																										
$^{13}\text{C}, ^{14}\text{N}$																																																										
$^{13}\text{C}, ^{14}\text{N}$																																																										
$^{13}\text{C}, ^{27}\text{Al}$																																																										
$^{13}\text{C}, ^{27}\text{Al}$																																																										
$^{13}\text{C}$																																																										
245																																																										
245																																																										
245																																																										
246																																																										
246																																																										
246																																																										
(MeBNH) <sub>3</sub>		34.5	—	107	<table><tr><td><math>^{13}\text{C}</math></td></tr><tr><td><math>^{14}\text{N}</math></td></tr></table>	$^{13}\text{C}$	$^{14}\text{N}$	<table><tr><td>153</td></tr><tr><td>249</td></tr></table>	153	249																																																
$^{13}\text{C}$																																																										
$^{14}\text{N}$																																																										
153																																																										
249																																																										
(MeBNMe) <sub>3</sub>		35.9	—	107	<table><tr><td><math>^{13}\text{C}</math></td></tr><tr><td><math>^{14}\text{N}</math></td></tr></table>	$^{13}\text{C}$	$^{14}\text{N}$	<table><tr><td>153</td></tr><tr><td>249</td></tr></table>	153	249																																																
$^{13}\text{C}$																																																										
$^{14}\text{N}$																																																										
153																																																										
249																																																										
(MeBNtBu) <sub>3</sub>		36.7	CH <sub>2</sub> Cl <sub>2</sub>	227	$^{13}\text{C}, ^{14}\text{N}$	227																																																				



TABLE 17 (*cont.*) $\delta^{11}\text{B}$  values of some cyclic organylboron–nitrogen compounds.

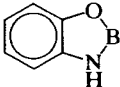
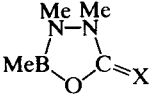
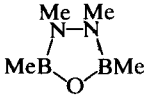
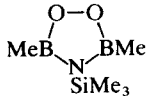
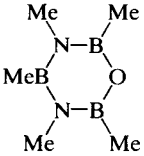
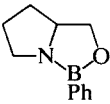
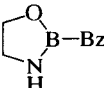
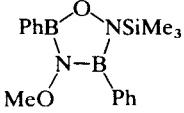
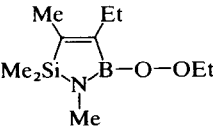
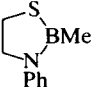
Compound	$\delta^{11}\text{B}$	Solvent	Ref.	Other nuclei	Ref.
	34.4	$\text{CH}_2\text{Cl}_2$	188	$^{13}\text{C}$	271
 <div style="display: inline-block; vertical-align: middle; margin-left: 10px;"> <math>\text{X} = \text{O}</math>  <math>\text{S}</math> </div>	31.7	$\text{CH}_2\text{Cl}_2$	231	—	
	31.4	$\text{CH}_2\text{Cl}_2$	231	—	
	31.5	$\text{CH}_2\text{Cl}_2$	237	—	
	38.3	$\text{CH}_2\text{Cl}_2$	238	—	
	32.8 ( $\text{BN}_2$ )		239	$^{13}\text{C}, ^{14}\text{N}$	239
	34.6 (BON)				
	32.0	$\text{C}_6\text{D}_6$	240	$^{13}\text{C}$	240
	33.6	$\text{CCl}_4$	192	—	
	32.2 (single broad signal)	$\text{CH}_2\text{Cl}_2$	230	$^{13}\text{C}$	230
	30.0	$\text{C}_7\text{D}_8$	236	$^{13}\text{C}, ^{14}\text{N}, ^{17}\text{O}, ^{29}\text{Si}$	236
	46.8	$\text{CH}_2\text{Cl}_2$	124	—	

TABLE 17 (cont.)

 $\delta^{11}\text{B}$  values of some cyclic organylboron–nitrogen compounds.

Compound	$\delta^{11}\text{B}$	Solvent	Ref.	Other nuclei	Ref.
	45.1	$\text{CH}_2\text{Cl}_2$	188	$^{13}\text{C}$	188
R —————					
Ph	51.5	$\text{CDCl}_3$	241	$^{13}\text{C}$ , $^{14}\text{N}$ , $^{29}\text{Si}$	241
$\text{SiMe}_3$	52.6	$\text{CCl}_4$	242	$^{13}\text{C}$ , $^{29}\text{Si}$	242
	40.0	$\text{CH}_2\text{Cl}_2$	231	—	
	54.2	$\text{CH}_2\text{Cl}_2$	244	—	
	39.3	$\text{CH}_2\text{Cl}_2$	231, 244	—	
	43.8	$\text{CH}_2\text{Cl}_2$	207	$^{13}\text{C}$	207
	42.0	$\text{CDCl}_3$	243	—	
X = S	46.3	$\text{CDCl}_3$	270	$^{13}\text{C}$ , $^{14}\text{N}$	270
Se	50.1	$\text{CDCl}_3$	270	$^{13}\text{C}$ , $^{14}\text{N}$ , $^{77}\text{Se}$	270

TABLE 18

 $\delta^{11}\text{B}$  values of some trigonal boranes ( $\text{BX}_3$ ; X = halogen, O, S, Se, N) without B—C bonds.

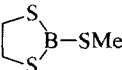
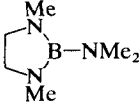
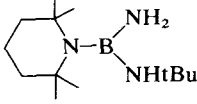
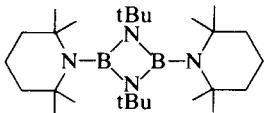
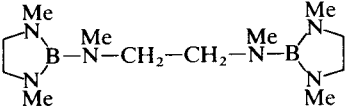
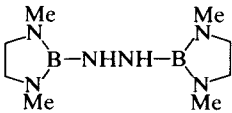
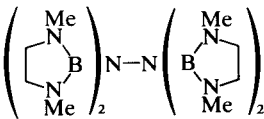
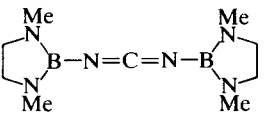
Compound	$\delta^{11}\text{B}$	Solvent	Ref.	Other nuclei	Ref.
$\text{BF}_3$	10.0	Methyl-cyclohexane	254	$^{19}\text{F}$	526, 766
$\text{BCl}_3$	46.5	Methyl-cyclohexane	254	$^{35}\text{Cl}$	335
$\text{BBr}_3$	38.7	Methyl-cyclohexane	254	—	
$\text{BI}_3$	-7.9	Methyl-cyclohexane	254	—	
$\text{B}(\text{OH})_3$	2.0–19.6	$\text{H}_2\text{O}$ , pH-dependent	255, 472	$^{17}\text{O}$	350
$\text{B}(\text{OMe})_3$	18.3	—	107	$^{17}\text{O}$	350
$\text{B}(\text{OtBu})_3$	15.6	—	5	$^{17}\text{O}$	350
$\text{B}(\text{OPh})_3$	16.5	—	5	—	
$\text{B}[\text{OC}(\text{CF}_3)_3]_3$	13.4	—	5	—	
$\text{B}(\text{OTeF}_5)_3$	14.0	$\text{CFCl}_3$	5	—	
$\text{B}[\text{ON}(\text{C}_2\text{H}_5)_2]_3$	22.6	—	5	—	
$(\text{MeOBO})_3$	17.3	$\text{C}_6\text{H}_6$	5	$^{17}\text{O}$	350
$\text{B}(\text{SMe})_3^a$	60.7	$\text{C}_6\text{H}_6$	5	—	
	64.6	$\text{CH}_2\text{Cl}_2$	5	—	
$\text{B}(\text{SeMe})_3^a$	65.5	$\text{CS}_2$	5	—	
$\text{B}(\text{NHMe})_3$	24.6	—	107	$\begin{cases} ^{14}\text{N} \\ ^{15}\text{N} \end{cases}$	$\begin{matrix} 128 \\ 690 \end{matrix}$
$\text{B}(\text{NMe}_2)_2$	27.3	—	107	$^{14}\text{N}$	128
$\text{B}\left(\text{N} \begin{array}{c} \diagup \diagdown \\ \diagdown \diagup \end{array} \right)_3$	27.8	$\text{C}_6\text{H}_6$	152	$\begin{cases} ^{13}\text{C} \\ ^{14}\text{N} \end{cases}$	$\begin{matrix} 779 \\ 152 \end{matrix}$
$\text{B}[\text{N}(\text{SCF}_3)_2]_3$	36.2	$\text{CCl}_3\text{F}$	293	$^{19}\text{F}$	293
$\text{B}(\text{NHNMe}_2)_3$	23.1	$\text{C}_6\text{H}_6$	130	—	
$(\text{iPr}_2\text{N})_2\text{BN}_3$	29.0	$\text{C}_6\text{D}_6$	295	—	
	26.5	$\text{C}_6\text{H}_6$	152	$^{13}\text{C}$	153
	26.0		297	$^{13}\text{C}$	297
$(2,4,6\text{-tBu}_3)\text{C}_6\text{H}_2\text{B}(\text{NH}_2)_2$	24.6		299	—	

TABLE 18 (*cont.*)

 $\delta^{11}\text{B}$  values of some trigonal boranes ( $\text{BX}_3$ ; X = halogen, O, S, Se, N) without B—C bonds.

Compound	$\delta^{11}\text{B}$	Solvent	Ref.	Other nuclei	Ref.
	26.4	$\text{CH}_2\text{Cl}_2$	152	$^{14}\text{N}$	152
	24.6	—	296, 794	$^{13}\text{C}$ , $^{14}\text{N}$	296
	25.7	$\text{CDCl}_3$	296	$^{13}\text{C}$ , $^{14}\text{N}$	296
	27.0		290	$^{13}\text{C}$	290
	23.3	$\text{C}_6\text{D}_6$	295	—	
	25.2	$\text{CH}_2\text{Cl}_2$	288	—	
	22.1	$\text{C}_6\text{H}_6$	289	$^{13}\text{C}$	349
	26.5	$\text{C}_6\text{D}_6$	291	$^{13}\text{C}$	291
	27.2	$\text{CH}_2\text{Cl}_2/\text{C}_6\text{D}_6$	292	$^{13}\text{C}$ , $^{14}\text{N}$ , $^{29}\text{Si}$	292

TABLE 18 (*cont.*) $\delta^{11}\text{B}$  values of some trigonal boranes ( $\text{BX}_3$ ; X = halogen, O, S, Se, N) without B—C bonds.

Compound	$\delta^{11}\text{B}$	Solvent	Ref.	Other nuclei	Ref.
	36.8	$\text{CDCl}_3$	294	$^{13}\text{C}$	294
	27.0 27.4	$\text{C}_6\text{D}_6$ —	298 794	$^{13}\text{C}, ^{14}\text{N}$ $^{13}\text{C}$	298 794
	22.4	$\text{C}_6\text{H}_6$	300	$^{13}\text{C}$	300
	26.3	$\text{CH}_2\text{Cl}_2$	301	$^{13}\text{C}$	301
	21.4	$\text{CDCl}_3$	344	—	

<sup>a</sup> Solid-state  $^{11}\text{B}$  NMR techniques have been used to study phases in the systems B—S, B—Se, B—S—Se and B—Te; there is no binary B—Te compound; there are  $\text{B}_2\text{S}_3$ ,  $\text{BS}_2$  and  $\text{BSe}_2$  but no  $\text{B}_2\text{Se}_3$ ; all these phases contain three-coordinate boron.<sup>78,9</sup>

TABLE 19

$\delta^{11}\text{B}$  values of some trigonal boranes ( $\text{BX}_2\text{Y}$ ,  $\text{BX}_2\text{Y}_2$ ,  $\text{BX}_2\text{YZ}$ ; X = H, halogen, O, S, Se, N, P, As, Sb) without B—C bonds.

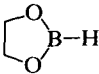
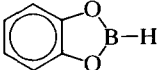
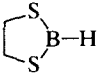
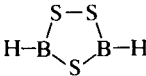
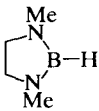
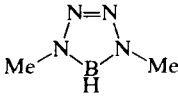
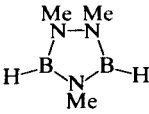
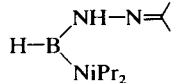
Compound	$\delta^{11}\text{B}$	Solvent	Ref.	Other nuclei	Ref.
$\text{HBF}_2$	22.0	—	5	$^{19}\text{F}$	526, 766
$\text{HB(OMe)}_2$	26.1	—	5	—	—
	28.1	$\text{CH}_2\text{Cl}_2$	302	—	—
	29.9	$\text{C}_6\text{D}_6$	188	$\begin{cases} ^{13}\text{C} \\ ^{17}\text{O} \end{cases}$	$\begin{matrix} 188 \\ 117 \end{matrix}$
	61.3	$\text{C}_6\text{H}_6$	302	—	—
	61.0	$\text{C}_6\text{D}_6$	154	—	—
$\text{H}_2\text{BNMe}_2$	37.9	Melt	127	—	—
$\text{H}_2\text{BN}(\text{SiMe}_3)\text{tBu}$	41.6	—	303	—	—
$\text{H}_2\text{BN}(\text{SiMe}_3)_2$	46.7	—	303	—	—
$\text{HB(NMe}_2)_2$	28.6	—	107	—	—
$\text{HB[N(tBu)CH}_2\text{Ph]}_2$	30.8	$\text{CH}_2\text{Cl}_2$	304	$^{13}\text{C}$	304
	28.3	—	209	—	—
	20.9	—	316	—	—
	29.5	$\text{CH}_2\text{Cl}_2$	318	—	—
$(\text{HBNH})_3$	29.1	—	5	$^{14}\text{N}$	699
$(\text{HBNMe})_3$	31.7	—	317	$\begin{cases} ^{13}\text{C} \\ ^{14}\text{N} \end{cases}$	$\begin{matrix} 153 \\ 249 \end{matrix}$
	27.6	$\text{C}_6\text{D}_6$	295	$^{13}\text{C}$	295

TABLE 19 (cont.)

$\delta^{11}\text{B}$  values of some trigonal boranes ( $\text{BX}_2\text{Y}$ ,  $\text{BXY}_2$ ,  $\text{BXYZ}$ ; X = H, halogen, O, S, Se, N, P, As, Sb) without B—C bonds.

Compound	$\delta^{11}\text{B}$	Solvent	Ref.	Other nuclei	Ref.
	21.5	$\text{C}_6\text{D}_6$	305	$^{13}\text{C}$	305
$[\text{Me}_2\text{NBH}]_2\text{O}$	29.0		306	—	
	37.0	THF	652	—	
$\text{FB}(\text{OMe})_2$	15.6		307	—	
$[(2,6\text{-Ph}_2)\text{C}_6\text{H}_3]_2\text{BF}$	17.2		269	—	
$\text{Cl}_2\text{BOMe}$	31.9		107	—	
$\text{ClB}(\text{OMe})_2$	23.7		107	—	
	29.0 26.9	$\text{CDCl}_3$	188	$^{13}\text{C}$	188
X = Cl Br			204	—	
$\text{Br}_2\text{BOPh}$	27.3		204	—	
$\text{BrB}(\text{OEt})_2$	18.5		308	—	
$\text{Cl}_2\text{BSMe}$	51.8	—	127	—	
$\text{ClB}(\text{SMe})_2$	58.6	—	127	—	
	61.4	—	313	—	
	60.4	—	201	—	
$\text{Br}_2\text{BSH}$	49.8	$\text{CS}_2$	314	—	
$\text{BrB}(\text{SH})_2$	56.2	$\text{CS}_2$	314	—	
	58.9	—	313	—	
	51.5	$\text{CH}_2\text{Cl}_2$	200	$^{13}\text{C}$	200
	58.3	—	201	—	
$\text{I}_2\text{BSH}$	23.2	$\text{CS}_2$	314	—	
$\text{IB}(\text{SH})_2$	50.0	$\text{CS}_2$	314	—	

TABLE 19 (*cont.*)

$\delta^{11}\text{B}$  values of some trigonal boranes ( $\text{BX}_2\text{Y}$ ,  $\text{BXY}_2$ ,  $\text{BXYZ}$ ; X = H, halogen, O, S, Se, N, P, As, Sb) without B—C bonds.

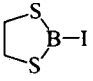
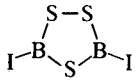
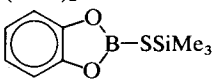
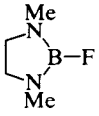
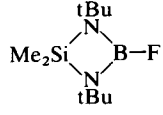
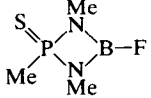
Compound	$\delta^{11}\text{B}$	Solvent	Ref.	Other nuclei	Ref.
	50.0	—	313	—	
	49.0	—	201	—	
$(\text{MeO})_2\text{BSMe}$	30.3	—	127	$^{17}\text{O}$	350
	29.7	$\text{CH}_2\text{Cl}_2$	199	$^{29}\text{Si}$	199
$\text{MeOB}(\text{SMe})_2$	45.8	—	127	$^{17}\text{O}$	350
$\text{Cl}_2\text{BSeH}$	56.7	$\text{CS}_2$	315	—	
$\text{Br}_2\text{BSeH}$	50.5	$\text{CS}_2$	315	—	
$\text{BrB}(\text{SeH})_2$	56.2	$\text{CS}_2$	315	—	
$\text{I}_2\text{BSeH}$	23.0	$\text{CS}_2$	315	—	
$\text{IB}(\text{SeH})_2$	50.0	$\text{CS}_2$	315	—	
$\text{F}_2\text{BNEt}_2$	17.2	—	127	$^{19}\text{F}$	526, 766
$\text{F}_2\text{BNHC}_6\text{H}_2(2,4,5\text{-tBu}_3)$	16.8	—	299	$^{19}\text{F}$	299
$\text{F}_2\text{BN}(\text{SCF}_3)_2$	18.0	—	5	—	
$(\text{F}_2\text{B})_3\text{N}$	17.7	$\text{C}_7\text{H}_8/\text{C}_6\text{D}_6$	310	$^{14}\text{N}$ , $^{19}\text{F}$	310
$\text{FB}(\text{NMe}_2)_2$	21.8	—	107	—	
	23.6	—	182	$^{19}\text{F}$	182
$\text{Cl}_2\text{BNMe}_2$	30.8	—	107	$\begin{cases} ^{13}\text{C} \\ ^{14}\text{N} \\ ^{35}\text{Cl} \end{cases}$	$\begin{matrix} 153 \\ 128 \\ 335 \end{matrix}$
$\text{Cl}_2\text{BNPh}_2$	33.5	$\text{CCl}_4$	129	—	
$(\text{Cl}_2\text{B})_2\text{NtBu}$	38.4	$\text{CH}_2\text{Cl}_2$	268	$^{14}\text{N}$	268
$(\text{Cl}_2\text{B})_2\text{NSiMe}_3$	39.2	$\text{CH}_2\text{Cl}_2$	268	$^{14}\text{N}$	268
$(\text{Cl}_2\text{B})_3\text{N}$	40.0	$\text{CH}_2\text{Cl}_2/\text{C}_6\text{D}_6$	310	$^{14}\text{N}$	310
	20.6	$\text{CH}_2\text{Cl}_2$	168	$^{14}\text{N}$	168
	20.1	$\text{CH}_2\text{Cl}_2$	168	$^{14}\text{N}$ , $^{31}\text{P}$	168

TABLE 19 (cont.)

$\delta^{11}\text{B}$  values of some trigonal boranes ( $\text{BX}_2\text{Y}$ ,  $\text{BXY}_2$ ,  $\text{BXYZ}$ ; X = H, halogen, O, S, Se, N, P, As, Sb) without B—C bonds.

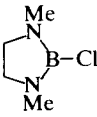
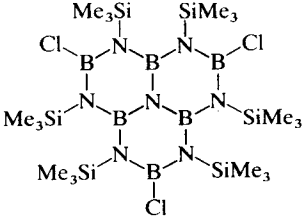
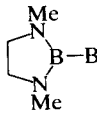
Compound	$\delta^{11}\text{B}$	Solvent	Ref.	Other nuclei	Ref.
$\text{ClB}(\text{NMe}_2)_2$	27.9	—	107	$\begin{cases} {}^{13}\text{C} \\ {}^{14}\text{N} \\ {}^{35}\text{Cl} \end{cases}$	$\begin{matrix} 10 \\ 128 \\ 335 \end{matrix}$
	27.0	—	209	$\begin{cases} {}^{13}\text{C} \\ {}^{14}\text{N} \\ {}^{35}\text{Cl} \end{cases}$	$\begin{matrix} 273 \\ 152 \\ 335 \end{matrix}$
$(\text{ClBNtBu})_4$ $(\text{XBNR})_3$ X       R	31.5	$\text{CH}_2\text{Cl}_2$	227	${}^{13}\text{C}, {}^{14}\text{N}$	227
F        Me	24.3	$\text{C}_6\text{H}_6$	249	$\begin{cases} {}^{13}\text{C} \\ {}^{14}\text{N} \end{cases}$	$\begin{matrix} 153 \\ 249 \end{matrix}$
Cl        Me	31.2	$\text{C}_6\text{H}_6$	249	$\begin{cases} {}^{13}\text{C} \\ {}^{14}\text{N} \end{cases}$	$\begin{matrix} 153 \\ 249 \end{matrix}$
Cl        OMe	31.7	$\text{CH}_2\text{Cl}_2$	230	${}^{13}\text{C}, {}^{14}\text{N}$	230
Br        Me	28.7	$\text{CH}_2\text{Cl}_2$	249	$\begin{cases} {}^{13}\text{C} \\ {}^{14}\text{N} \end{cases}$	$\begin{matrix} 153 \\ 249 \end{matrix}$
MeO    H	26.1	$\text{CH}_2\text{Cl}_2$	249	${}^{14}\text{N}$	249
MeO    MeO	24.4	$\text{CH}_2\text{Cl}_2$	230	${}^{13}\text{C}, {}^{14}\text{N}$	230
MeS    Me	37.3	$\text{CH}_2\text{Cl}_2$	249	$\begin{cases} {}^{13}\text{C} \\ {}^{14}\text{N} \end{cases}$	$\begin{matrix} 153 \\ 249 \end{matrix}$
	31.5	$\text{CH}_2\text{Cl}_2$	309	${}^{29}\text{Si}$	309
$\text{Br}_2\text{BNMe}_2$	25.7	—	107	$\begin{cases} {}^{13}\text{C} \\ {}^{14}\text{N} \end{cases}$	$\begin{matrix} 153 \\ 128 \end{matrix}$
$(\text{Br}_2\text{B})_2\text{NtBu}$	37.6	$\text{CH}_2\text{Cl}_2$	268	${}^{14}\text{N}$	268
$(\text{Br}_2\text{B})_3\text{N}$	37.1	$\text{CH}_2\text{Cl}_2/\text{C}_6\text{D}_6$	310	${}^{14}\text{N}$	268
$\text{BrB}(\text{NMe}_2)_2$	27.6	—	107	${}^{14}\text{N}$	128
	26.0	—	209	—	
$\text{I}_2\text{BNMe}_2$	4.9	—	107	$\begin{cases} {}^{13}\text{C} \\ {}^{14}\text{N} \end{cases}$	$\begin{matrix} 153 \\ 128 \end{matrix}$
$\text{IB}(\text{NMe}_2)_2$	26.4	—	128	${}^{14}\text{N}$	128

TABLE 19 (*cont.*)

$\delta^{11}\text{B}$  values of some trigonal boranes ( $\text{BX}_2\text{Y}$ ,  $\text{BXY}_2$ ,  $\text{BXYZ}$ ; X = H, halogen, O, S, Se, N, P, As, Sb) without B—C bonds.

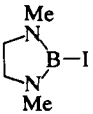
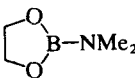
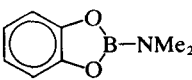
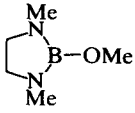
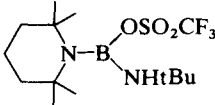
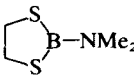
Compound	$\delta^{11}\text{B}$	Solvent	Ref.	Other nuclei	Ref.
	21.3	—	209	—	
$\text{ClB(OMe)NMe}_2$	24.9	—	107	—	
$\text{ClB} \left( \text{O}-\text{N} \left( \text{C}_6\text{H}_4 \right)_2 \right) \text{NMe}_2$	26.3	$\text{CH}_2\text{Cl}_2$	229	$^{13}\text{C}$ , $^{14}\text{N}$	229
$(\text{MeO})_2\text{BNMe}_2$	21.3	—	107	$\begin{cases} ^{13}\text{C} \\ ^{17}\text{O} \end{cases}$	$\begin{matrix} 153 \\ 350 \end{matrix}$
	24.7	—	152	$\begin{cases} ^{13}\text{C} \\ ^{14}\text{N} \\ ^{17}\text{O} \end{cases}$	$\begin{matrix} 153 \\ 152 \\ 350 \end{matrix}$
	25.6	$\text{CH}_2\text{Cl}_2$	188	$^{13}\text{C}$	188
$(\text{Me}_2\text{NBO})_3$	21.0	$\text{CH}_2\text{Cl}_2$	152	$\begin{cases} ^{13}\text{C} \\ ^{14}\text{N} \\ ^{17}\text{O} \end{cases}$	$\begin{matrix} 153 \\ 152 \\ 350 \end{matrix}$
$\left( \text{C}_6\text{H}_4\text{NBO} \right)_3$	21.9	—	438	$^{13}\text{C}$	438
$\text{MeOB(NMe}_2)_2$	25.1	—	107	$^{17}\text{O}$	350
	24.1	$\text{C}_6\text{H}_6$	152	$^{14}\text{N}$	152
	23.6	$\text{C}_6\text{D}_6$	170	$^{13}\text{C}$	170
$(\text{MeS})_2\text{BNMe}_2$	43.4	—	127	$^{13}\text{C}$	153
	46.3 45.9	$\text{CH}_2\text{Cl}_2$ $\text{CH}_2\text{Cl}_2$	152 311	$^{14}\text{N}$	152

TABLE 19 (*cont.*)

$\delta^{11}\text{B}$  values of some trigonal boranes ( $\text{BX}_2\text{Y}$ ,  $\text{BXY}_2$ ,  $\text{BXYZ}$ ;  $\text{X} = \text{H}$ , halogen,  $\text{O}$ ,  $\text{S}$ ,  $\text{Se}$ ,  $\text{N}$ ,  $\text{P}$ ,  $\text{As}$ ,  $\text{Sb}$ ) without  $\text{B}-\text{C}$  bonds.

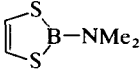
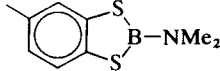
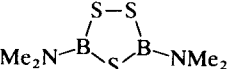
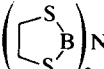
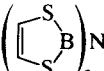
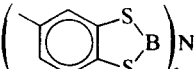
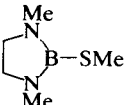
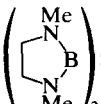
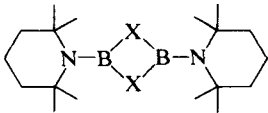
Compound	$\delta^{11}\text{B}$	Solvent	Ref.	Other nuclei	Ref.
	44.3	$\text{CH}_2\text{Cl}_2$	200, 311	$^{13}\text{C}$ , $^{14}\text{N}$	200
	43.0	$\text{CH}_2\text{Cl}_2$	188	$^{13}\text{C}$	188
	46.1	$\text{C}_6\text{D}_6$	154	—	
$(\text{Me}_2\text{NBS})_2$	36.4	—	258	$^{13}\text{C}$	258
$(\text{Me}_2\text{NBS})_3$	39.2	—	258	$^{13}\text{C}$	258
$[(\text{MeS})_2\text{B}]_3\text{N}$	54.4	$\text{C}_6\text{D}_6$	311	$^{14}\text{N}$	311
	56.3	$\text{CDCl}_3$	311	$^{13}\text{C}$ , $^{14}\text{N}$	311
	52.6	$\text{CH}_2\text{Cl}_2$	311	$^{13}\text{C}$ , $^{14}\text{N}$	311
	50.5	$\text{CDCl}_3$	311	$^{13}\text{C}$	311
$\text{MeSB}(\text{NMe}_2)_2$	34.6	—	127	—	
	31.2	—	152	$^{14}\text{N}$	152
	30.5		258	$^{13}\text{C}$ , $^{14}\text{N}$	258
					
X = O	28.2	$\text{C}_6\text{D}_6$	312	$^{13}\text{C}$	312
S	40.0	$\text{C}_6\text{D}_6$	312	$^{13}\text{C}$	312
Se	34.9	$\text{C}_6\text{D}_6$	312	$^{13}\text{C}$	312

TABLE 19 (cont.)

$\delta^{11}\text{B}$  values of some trigonal boranes ( $\text{BX}_2\text{Y}$ ,  $\text{BXY}_2$ ,  $\text{BXYZ}$ ;  $\text{X} = \text{H}$ , halogen,  $\text{O}$ ,  $\text{S}$ ,  $\text{Se}$ ,  $\text{N}$ ,  $\text{P}$ ,  $\text{As}$ ,  $\text{Sb}$ ) without  $\text{B}-\text{C}$  bonds.

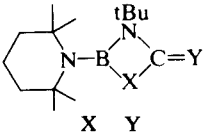
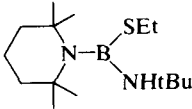
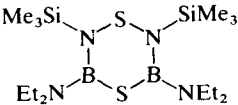
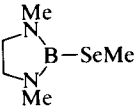
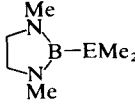
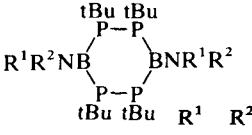
Compound	$\delta^{11}\text{B}$	Solvent	Ref.	Other nuclei	Ref.
 <div style="display: flex; justify-content: space-around; width: 100px;"> <span>X</span> <span>Y</span> </div>					
O O	27.9	$\text{C}_6\text{D}_6$	312	$^{13}\text{C}$	312
S O	43.4	Hexane	312	$^{13}\text{C}$	312
S S	44.8	$\text{C}_6\text{D}_6$	312	$^{13}\text{C}$	312
Se Se	44.2	$\text{C}_6\text{D}_6$	312	$^{13}\text{C}$	312
	37.5		297	$^{13}\text{C}$	297
	34.9	$\text{CCl}_4$	242	$^{13}\text{C}$ , $^{29}\text{Si}$	242
	31.7	$\text{C}_6\text{H}_6$	182	$^{77}\text{Se}$	182
$(\text{Me}_2\text{N})_2\text{B}-\text{PEt}_2$	36.4	$\text{C}_6\text{H}_6$	320	$^{31}\text{P}$	320
	36.1	$\text{C}_6\text{H}_6$	152		
$(\text{Me}_2\text{N})_2\text{B}-\text{PPh}_2$	41.3	$\text{C}_6\text{D}_6$	321, 374	—	
 <div style="display: flex; align-items: center;"> <div style="margin-right: 10px;"><math>\text{E} = \text{P}</math></div> <div><math>\text{As}</math></div> </div>	33.0	$\text{C}_6\text{H}_6$	182	$^{31}\text{P}$	182
	34.2	Hexane	322		
$\text{Et}_2\text{NB}(\text{PEt}_2)_2$	50.9	$\text{C}_6\text{H}_6$	320	$^{31}\text{P}$	320
 <div style="display: flex; justify-content: space-around; width: 100px;"> <span>R<sup>1</sup></span> <span>R<sup>2</sup></span> </div>					
Et Et	46.6	Pentane	323	$^{31}\text{P}$	323
Me Bu	48.2	Pentane	323	$^{31}\text{P}$	323
Me $\text{C}_6\text{H}_{11}$	48.6	Pentane	323	$^{31}\text{P}$	323

TABLE 19 (*cont.*)

$\delta^{11}\text{B}$  values of some trigonal boranes ( $\text{BX}_2\text{Y}$ ,  $\text{BXY}_2$ ,  $\text{BXYZ}$ ; X = H, halogen, O, S, Se, N, P, As, Sb) without B—C bonds.

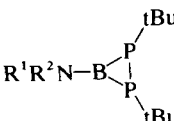
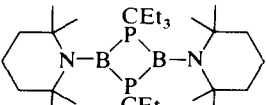
Compound	$\delta^{11}\text{B}$	Solvent	Ref.	Other nuclei	Ref.
					
<div style="display: flex; justify-content: space-around; width: 100%;"> <span>R¹</span> <span>R²</span> </div>					
Et Et	52.6	Hexane	323	$^{13}\text{C}$ , $^{31}\text{P}$	323
Me tBu	51.2	Hexane	323	$^{13}\text{C}$ , $^{31}\text{P}$	323
iPr iPr	50.7	Hexane	323	$^{13}\text{C}$ , $^{31}\text{P}$	323
Me Ph	60.6	Hexane	323	$^{31}\text{P}$	323
Ph Ph	59.5	Hexane	323	$^{31}\text{P}$	323
	66.1		341	$^{13}\text{C}$ , $^{31}\text{P}$	341
(Me₂N)₂B—AsEt₂	38.0	C₆H₆	320	—	
Et₂NB(AsEt₂)₂	55.5	C₆H₆	320	—	
(Me₂N)₂B—SbEt₂	39.3	C₆H₆	320	—	

TABLE 20

$\delta^{11}\text{B}$  values of some trigonal boranes (B—Si, B—Sn, B—Pb and B—Rh bonds, but *without* B—C bonds.

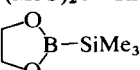
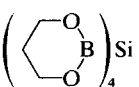
Compound	$\delta^{11}\text{B}$	Solvent	Ref.	Other nuclei	Ref.
F₂B—SiF₃	28.0		325	$^{19}\text{F}$	325
F₂B—Si₂F₅	23.4		326	$^{19}\text{F}$	325
F₂B—Si₃F₇	24.5		326	$^{19}\text{F}$	325
Cl₂B—SiCl₃	63.0		325	—	
(MeO)₂B—SiMe₃	34.5	C₆H₆	202, 329	—	
	34.4	C₆H₆	202, 329	—	
	37.1		327	—	

TABLE 20 (cont.)

 $\delta^{11}\text{B}$  values of some trigonal boranes (B—Si, B—Sn, B—Pb and B—Rh bonds, but *without* B—C bonds.

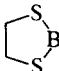
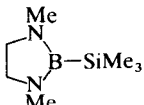
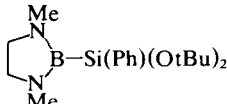
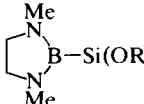
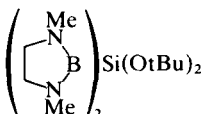
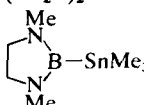
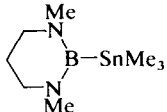
Compound	$\delta^{11}\text{B}$	Solvent	Ref.	Other nuclei	Ref.
$\text{MeOB}[\text{Si}(\text{SiMe}_3)_3]_2$	82.7		123, 329	—	
 $\text{B—SiMe}_3$	72.8	$\text{C}_6\text{H}_6$	202, 329	—	
$(\text{Me}_2\text{N})_2\text{B—SiMe}_3$	36.1		328	—	
$(\text{Me}_2\text{N})_2\text{B—SiPh}_3$	35.0		328	—	
$(\text{Me}_2\text{N})_2\text{B—Si}(\text{SiMe}_3)_3$	38.8		123, 329	—	
 $\text{B—SiMe}_3$	32.9	$\text{C}_6\text{H}_6$	182	$\begin{Bmatrix}^{13}\text{C} \\ ^{29}\text{Si}\end{Bmatrix}$	$\begin{matrix} 71 \\ 182 \end{matrix}$
$\text{Me}_2\text{N}(\text{Cl})\text{BSiMe}_3$	41.3	$\text{C}_6\text{H}_6$	202, 329	—	
$\text{Me}_2\text{N}(\text{MeO})\text{BSiMe}_3$	33.8	$\text{C}_6\text{H}_6$	202, 329	—	
$\text{Me}_2\text{N}(\text{MeS})\text{BSiMe}_3$	46.9	$\text{C}_6\text{H}_6$	202, 329	—	
 $\text{B—Si(Ph)(OtBu)}_2$	33.1	$\text{CDCl}_3$	330	—	
$(\text{Me}_2\text{N})_2\text{B—Si}(\text{OtBu})_3$	34.4	$\text{CDCl}_3$	330		
 $\text{B—Si(OR)}_3$ R = iPr tBu	31.2 30.9	$\text{CDCl}_3$ $\text{CDCl}_3$	330 330	$^{29}\text{Si}$ $^{29}\text{Si}$	$\begin{matrix} 330 \\ 330 \end{matrix}$
 $\text{Si}(\text{OtBu})_2$	32.4	$\text{CDCl}_3$	330	—	
$\text{Me}_2\text{N}(\text{iPrO})\text{BSi}(\text{OiPr})_3$	32.4	$\text{CDCl}_3$	330	$^{29}\text{Si}$	330
$\text{Me}_2\text{NB}(\text{SiMe}_3)_2$	58.4	$\text{C}_6\text{H}_6$	123, 329	$^{13}\text{C}, ^{14}\text{N}$	123
$\text{Me}_2\text{NB}[\text{Si}(\text{SiMe}_3)_3]_2$	61.0		123, 329	$^{13}\text{C}$	329
$(\text{Me}_2\text{N})_2\text{BSnMe}_3$	39.0	$\text{C}_6\text{H}_6$	331, 332	$^{13}\text{C}, ^{119}\text{Sn}$	133
 $\text{B—SnMe}_3$	39.3 36.5	$\text{C}_6\text{D}_6$ $\text{C}_6\text{D}_6$	133 133		
 $\text{B—SnMe}_3$	34.6		214	—	

TABLE 20 (cont.)

$\delta^{11}\text{B}$  values of some trigonal boranes (B—Si, B—Sn, B—Pb and B—Rh bonds, but *without* B—C bonds.

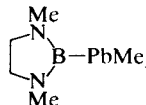
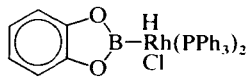
Compound	$\delta^{11}\text{B}$	Solvent	Ref.	Other nuclei	Ref.
$\text{Me}_2\text{N}(\text{Cl})\text{BSnMe}_3$	44.4	$\text{C}_6\text{H}_6$	332, 333	$^{119}\text{Sn}$	332
$\text{Et}_2\text{N}(\text{Cl})\text{BSnMe}_3$	45.2		333	—	
$\text{Me}_2\text{N}(\text{MeO})\text{BSnMe}_3$	37.4	$\text{C}_6\text{H}_6$	182	$^{119}\text{Sn}$	182
$\text{Me}_2\text{N}(\text{MeS})\text{BSnMe}_3$	58.5	$\text{C}_6\text{H}_6$	182	$^{119}\text{Sn}$	182
$\text{Me}_2\text{NB}(\text{SnMe}_3)_2$	63.9	$\text{C}_6\text{H}_6$	133, 182, 333	$^{13}\text{C}$ , $^{119}\text{Sn}$	133
$\text{Et}_2\text{NB}(\text{SnMe}_3)_2$	63.0	THF	333	—	
	41.7	$\text{C}_6\text{H}_6$	334	$^{207}\text{Pb}$	334
	37.7	$\text{CD}_2\text{Cl}_2$	367	—	

TABLE 21

$\delta^{11}\text{B}$  values of some compounds with B—B bonds. <sup>a, b, c</sup>

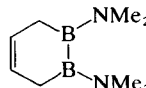
Compound	$\delta^{11}\text{B}$	Solvent	Ref.	Other nuclei	Ref.
$\text{Et}_4\text{B}_2$	105.5	Pentane	164		
$\text{iPr}_4\text{B}_2$	104.7	Pentane	164	$^{13}\text{C}$	164
$\text{tBu}_2\text{B—B}(\text{Me})\text{tBu}$	103.0	—	164	$^{13}\text{C}$	164
$[\text{tBu}(\text{neopent})\text{B}]_2$	104.0		165		
$[\text{Me}(\text{Cl})\text{B}]_2$	91.0		351	—	
$[\text{tBu}(\text{X})\text{B}]_2$ X = Cl	84.3	$\text{CDCl}_3$	166		
Br	88.0	$\text{CDCl}_3$	166		
I	89.4	$\text{CDCl}_3$	352		
$[\text{tBu}(\text{MeO})\text{B}]_2$	63.7	$\text{CDCl}_3$	166		
$[\text{tBu}(\text{MeS})\text{B}]_2$	87.5	$\text{CDCl}_3$	352		
$[\text{Me}(\text{Me}_2\text{N})\text{B}]_2$	51.1	—	107		
$[\text{tBu}(\text{Me}_2\text{N})\text{B}]_2$	54.8	$\text{CDCl}_3$	133	$^{13}\text{C}$	133
$[\text{Ph}(\text{Me}_2\text{N})\text{B}]_2$	49.1	$\text{CDCl}_3$	348	$^{13}\text{C}$	348
	51.0	$\text{CDCl}_3$	354	$^{13}\text{C}$	354

TABLE 21 (cont.)

 $\delta^{11}\text{B}$  values of some compounds with B—B bonds. <sup>a,b,c</sup>

Compound	$\delta^{11}\text{B}$	Solvent	Ref.	Other nuclei	Ref.
$2\text{Li}^+ \left( \text{C}_6\text{H}_4 \text{B}(\text{NMe}_2)_2 \right)^{2-}$	37.0	THF	354	$^{13}\text{C}$	354
	46.5		59	$^{13}\text{C}$	59
$\text{CH}_2 [\text{B}(\text{NMe}_2)\text{B}(\text{NMe}_2)_2\text{CH}_2]$	53.6		697	—	
$\text{tBu}_2\text{B—B}(\text{tBu})\text{SiMe}_3$	102.0(BC <sub>2</sub> ) 126.9(BSi)	$\text{C}_6\text{D}_6$	350		
$\text{tBu}_4\text{B}_4$	135.1		353		
$\text{Et}_2(\text{Cl}_2)\text{B}_4$	125.0(BEt) 94.9(BCl)		353		
$\text{Et}(\text{Cl}_3)\text{B}_4$	120.0(BEt) 89.6(BCl)		353	—	
$1\text{-BCl}_2\text{—B}_5\text{H}_8$	74.8(BCl <sub>2</sub> )		363	$^{11}\text{B}$	363
$2\text{-BCl}_2\text{—B}_5\text{H}_8$	75.7(BCl <sub>2</sub> )		364	$^{11}\text{B}$	364
$\text{B}_2\text{X}_4$ X = F	23.0		326		
	Cl		355	$^{35}\text{Cl}$	335
	Br	$\text{C}_7\text{H}_8$	356		
	I		349		
$(\text{MeO})_4\text{B}_2$	67.0 30.5	—	107	$^{17}\text{O}$	350
	31.5	$\text{CH}_2\text{Cl}_2$	357		
(corrected structure!)					
	30.4	$\text{CDCl}_3$	358	$^{13}\text{C}$	358
	30.7	$\text{CH}_2\text{Cl}_2$	357	—	
(corrected structure!)					
	30.8	$\text{CHCl}_3$	357	—	
	68.3	$\text{CH}_2\text{Cl}_2$	357	—	
(corrected structure!)					

TABLE 21 (*cont.*) $\delta^{11}\text{B}$  values of some compounds with B—B bonds. <sup>a, b, c</sup>

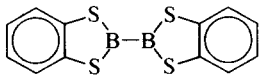
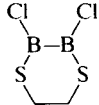
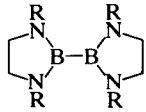
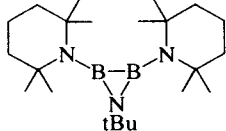
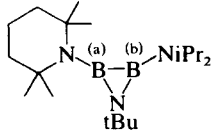
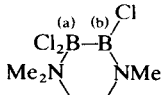
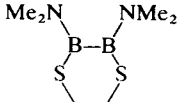
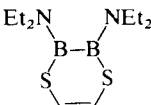
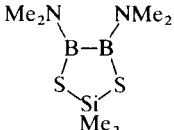
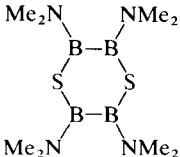
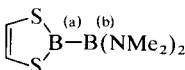
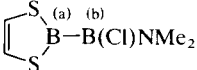
Compound	$\delta^{11}\text{B}$	Solvent	Ref.	Other nuclei	Ref.
	58.6	$\text{CH}_2\text{Cl}_2$	188	$^{13}\text{C}$	188
	67.8	Diglyme	357	—	
$(\text{Me}_2\text{N})_4\text{B}_2$	36.6	—	107	$^{13}\text{C}$ $^{14}\text{N}$	362 152
 <div style="display: inline-block; vertical-align: middle; margin-left: 10px;"> <math>\text{R} = \text{Me}</math>  <math>\text{iPr}</math> </div>	33.7 31.1	$\text{CH}_2\text{Cl}_2$ $\text{CD}_2\text{Cl}_2$	357 361	$^{13}\text{C}$ —	360
(corrected structure! <sup>359,361</sup> )					
	39.9	$\text{CD}_2\text{Cl}_2$	167	$^{13}\text{C}$	167
	36.0(a) 30.8(b)	$\text{C}_6\text{D}_6$	167	$^{13}\text{C}$	167
$[\text{Me}_2\text{N}(\text{Cl})\text{B}]_2$	37.5	$\text{CH}_2\text{Cl}_2$	362	$^{13}\text{C}$	362
	5.6(a) 41.6(b)		365	—	
$[\text{Me}_2\text{N}(\text{MeO})\text{B}]_2$	34.5	—	107	$^{14}\text{N}$ $^{17}\text{O}$ $^{13}\text{C}$	152 350
$[\text{Me}_2\text{N}(\text{MeS})\text{B}]_2$	47.7	$\text{CH}_2\text{Cl}_2$	362	$^{13}\text{C}$	362
	43.7 43.3	$\text{CH}_2\text{Cl}_2$ $\text{CDCl}_3$	357 362	$^{13}\text{C}$	362

TABLE 21 (cont.)

 $\delta^{11}\text{B}$  values of some compounds with B—B bonds. <sup>a,b,c</sup>

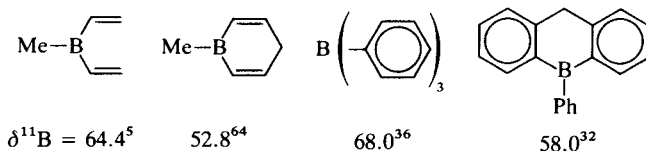
Compound	$\delta^{11}\text{B}$	Solvent	Ref.	Other nuclei	Ref.
	41.1	$\text{CH}_2\text{Cl}_2$	362	$^{13}\text{C}$	362
	45.1	$\text{CH}_2\text{Cl}_2$	366	—	
	44.3	$\text{CH}_2\text{Cl}_2$	366	—	
	60.1(a) 33.7(b)	$\text{CH}_2\text{Cl}_2$	362	$^{13}\text{C}$	362
	56.7(a) 38.7(b)	$\text{CH}_2\text{Cl}_2$	362	$^{13}\text{C}$	362
$[\text{Me}_2\text{N}(\text{Me}_3\text{Si})\text{B}]_2$	59.5	$\text{C}_6\text{D}_6$	133	$^{13}\text{C}, ^{14}\text{N}$	133
$(\text{Me}_2\text{N})_2\text{B—B}[\text{Si}(\text{OtBu})_3]\text{NMe}_2$	38.0(a) 56.1(b)	$\text{CH}_2\text{Cl}_2$	330	$^{13}\text{C}$	330
$[\text{Me}_2\text{N}(\text{Me}_3\text{Ge})\text{B}]_2$	59.8	$\text{C}_6\text{H}_6$	202	—	
$[\text{Me}_2\text{N}(\text{Me}_3\text{Sn})\text{B}]_2$	59.4	$\text{C}_7\text{D}_8$	133	$^{13}\text{C}, ^{14}\text{N}, ^{119}\text{Sn}$	133
$(\text{Me}_2\text{NB})_6$	65.0	$\text{C}_7\text{D}_8$	370	$^{13}\text{C}$	370
$\text{Me}_3\text{N—BH}_2\text{—BH}_2\text{—NMe}_3$	−3.5		706	—	
$\text{Me}_3\text{N—BH}_2\text{—BH}_2\text{—PMe}_3$	−2.9(BN) −37.0(BP)		706	—	

<sup>a</sup> For further  $^{11}\text{B}$  NMR data see Refs 5 and 7; for  $^{11}\text{B}$  NMR data of boron subhalides see Refs 724 and 758.

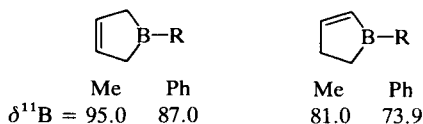
<sup>b</sup> For  $^{11}\text{B}$  NMR data of *closo*-halogenohydrohexaborates  $[\text{X}_n\text{B}_6\text{H}_{6-n}]^{2-}$  ( $n = 0, \dots, 6$ ;  $\text{X} = \text{Cl}, \text{Br}, \text{I}$ ) see Ref. 818.

<sup>c</sup> See Ref. 830 for  $^{11}\text{B}$ ,  $^{13}\text{C}$  NMR data of diaza-*nido*-hexaboranes and for tri-*tert*-butyl-azadiboridine:  $\delta^{11}\text{B}$ : 51.9 in  $\text{CDCl}_3$ .

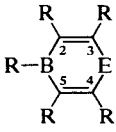
B—C  $\sigma$  orbitals and reduces the amount of  $B_0$ -induced mixing of the  $\sigma$  and  $\pi$  states; this reduces  $\sigma_p$  and therefore increases the shielding; (iii) contributions from the anisotropy of the  $C\equiv C$  triple bond may enhance the shielding effect observed for B-alkenyl groups. The arguments (i) and (ii) point in the same direction and emphasize that  $\sigma$  and  $\pi$  effects are difficult to separate. The influence of  $\pi$  effects is evident in particular when in cyclic systems the coplanarity of the boron  $p_z$  orbital and the  $C=C$   $\pi$  system is enforced; for example



The comparison of  $\delta^{11}\text{B}$  values for 3-borolenes and 2-borolenes is also very instructive in this respect:<sup>345</sup>

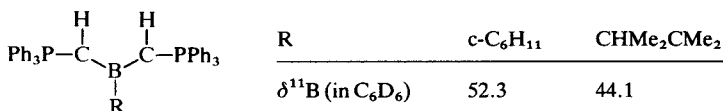


The  $\delta^{11}\text{B}$  values of bora-2,5-cyclohexadienes cover a remarkably large range for various substituents at the 1–6 positions and heteroatoms in the 4-position:

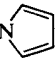
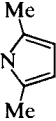
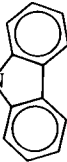
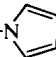
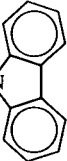
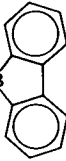
	$\delta^{11}\text{B}$	R—B	R(2)	R(3)	E	R(5)	R(6)
	52.8 <sup>64</sup>	Me	H	H	CH <sub>2</sub>	H	H
	58.3 <sup>60</sup>	Me	H	H	CMe <sub>2</sub>	H	H
	60.9 <sup>65, 66</sup>	Me	H	H	SnMe <sub>2</sub>	H	H
	61.0 <sup>65</sup>	Me	H	Me	SnMe <sub>2</sub>	Me	H
	61.9 <sup>65</sup>	tBu	H	Me	SnMe <sub>2</sub>	Me	H
	70.1 <sup>111</sup>	Et	Et	Me	SnMe <sub>2</sub>	Me	Et
	73.1 <sup>111</sup>	iPr	iPr	Me	SnMe <sub>2</sub>	Me	iPr
	57.2 <sup>112</sup>	tBu	H	Me	PPh	Me	H
	66.8 <sup>113</sup>	Bu	H	Ph	S	Ph	H

This range can be attributed to the structural flexibility of the six-membered ring system, which may adopt a planar, a twisted, a chair or a half-chair conformation, as has been found by dynamic  $^1\text{H}$  and  $^{13}\text{C}$  NMR.<sup>41</sup>

The variety of triorganylboranates with  $\text{BC}(\text{pp})\pi$  interactions has been enlarged by ylides with a  $\text{P}=\text{C}-\text{B}$  unit.<sup>519</sup>



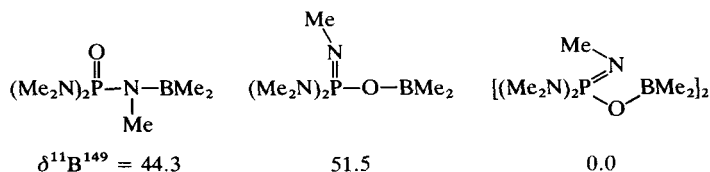
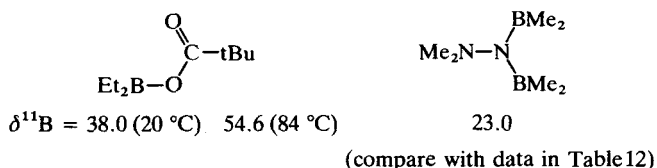
(b) *Diorganylboran*es,  $R_2BX$  ( $X = H$ , halogen,  $OR'$ ,  $SR'$ ,  $SeR'$ ,  $NR'_2$ ,  $PR'_2$ ,  $SiR'_3$ ) (Tables 8–12). The  $\delta^{11}B$  values of diorganoboranes are determined primarily by the nature of the third substituent  $X$ . Tables 8–12 list  $\delta^{11}B$  values of representative compounds. In general, different organyl groups  $R$  exert a similar influence on  $^{11}B$  nuclear shielding as in triorganoboranes. The following two exceptions are noteworthy: (i) If  $B-X(pp)\pi$  bonding is of importance (e.g.  $X = NR'_2$ ) then the steric requirements of  $R$  (and also of  $R'$ ) may be crucial; (ii) if  $X$  is a heavy halogen atom (I, Br) then the bulkiness of  $R$  appears to have a more significant effect than in triorganoboranes. On the other hand, various functionalities of the ligand  $X$  have a remarkable influence on  $^{11}B$  nuclear shielding. In many cases it is possible to prove the influence of steric or electronic effects. Both effects are of great importance if  $B-X(pp)\pi$  bonding is involved, and if there is a functionality in the ligand  $X$ , competing for the  $\pi$ -electron density. Instructive examples of these effects are found in *N*-azolyldiorganylboranes and in bis(diorganylboryl)amines:

$Me_2B-NMe_2$	$Me_2B-N$ 	$Me_2B-N$ 	$Me_2B-N$ 
$\delta^{11}B = 45.0^{107}$	56.2 <sup>152</sup>	60.3 <sup>152</sup>	58.5 <sup>152</sup>
49.9 <sup>143</sup>	67.0 <sup>143</sup>		73.6 <sup>143</sup>
$tBu_2B-NMe_2$	$tBu_2B-N$ 		$tBu_2B-N$ 
$Et_2B-N(Me)-BEt_2$	$Et_2B-N(Me)-BtBu_2$	$tBu_2B-(Me)N-B$ 	
$\delta^{11}B = 59.7^{134}$	45.7 <sup>137</sup> 72.7 <sup>137</sup>	72.8 <sup>259</sup> 38.6 <sup>259</sup>	

The bulky *t*Bu groups induce on average a nonplanar arrangement of the  $C_2B$  and the  $NC_2$  planes in the *N*-azolylboranes.<sup>143</sup> The reduced  $BN(pp)\pi$  bonding in azolylboranes is a function (i) of the electronic structure of the heteroaromatic  $\pi$  system and (ii) of the twisting of the azolyl group against the  $C_2BN$  plane.<sup>143,152</sup>

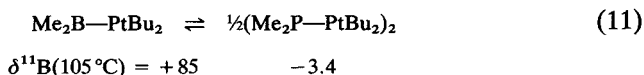
If the boryl groups in diborylamines do not prefer a distinct orientation then the nitrogen  $\pi$ -electron density is evenly spread between the two boron atoms, shown by the reduced  $^{11}\text{B}$ -nuclear shielding (see also Table 12) as compared with other aminodiorganylboranes. However, if the steric, requirements of the two boryl groups are sufficiently different then the  $\text{BC}_2$  plane of the more bulky group is twisted against the  $\text{C}_2\text{BN}$  plane of the remaining part of the molecule.<sup>259</sup> Thus there is efficient  $\text{BN}(\text{pp})\pi$  bonding in one part of the BNB system and negligible  $\text{BN}(\text{pp})\pi$  bonding in the other part, as indicated by the shift of the  $^{11}\text{B}$  resonances to lower and higher frequencies respectively.<sup>137,259</sup>

$^{11}\text{B}$  NMR is an extremely sensitive tool for studying association phenomena in solution. Examples are acyloxydiorganylboranes<sup>160</sup>, 1,1-bis(diorganylboryl)hydrazines<sup>161</sup> and phosphorylaminiorganylboranes.<sup>149,168</sup> In the latter case the presence of two signals in the typical range for three-coordinate boron suggests that there are two isomeric structures:



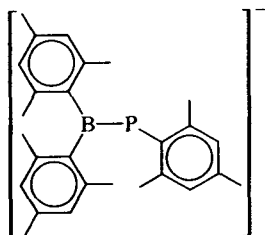
Most phosphino- or arsinodiorganyl boranes that have been studied by  $^{11}\text{B}$  NMR prove to be associated (dimer or trimer) rather than monomeric in solution.<sup>172,173</sup>

Bulky groups at phosphorus help to stabilize monomer species. At  $105^\circ\text{C}$  the equilibrium is shifted completely from the dimer to the monomer:<sup>171</sup>



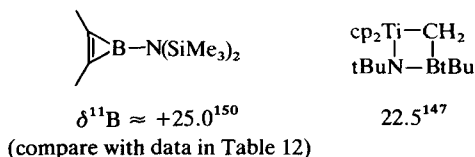
Bulky groups on the boron atom help to stabilize an anionic species for which both  $^{11}\text{B}$  NMR data and the results of the X-ray analysis indicate a

certain amount of PB(pp) $\pi$  interactions:<sup>346</sup>



$$\delta^{11}\text{B}^{346} = 64.0$$

In spite of the wealth of  $\delta^{11}\text{B}$  data available, in particular for trigonal boranes,<sup>5,7</sup> there remain numerous problems in the interpretation of  $\delta^{11}\text{B}$  data. The following three examples are given. Changes in the screening anisotropy due to the ring size and/or the electron delocalization in the heteroaromatic  $\pi$  system of borirenes are responsible for the increase in  $^{11}\text{B}$  nuclear shielding. There is also a highly shielded  $^{11}\text{B}$  nucleus in an 1-aza-2-bora-4-titanacyclobutane derivative,<sup>147</sup> indicating the influence of the spatial proximity between boron and titanium.



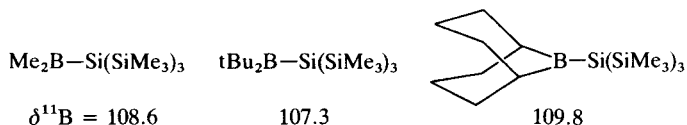
The  $\delta^{11}\text{B}$  values for products derived from 1,2-diboration of alkynes show a remarkably large range, depending on the other groups attached to the  $\text{C}=\text{C}$  double bond:<sup>163</sup>

	$\text{R}^1$	$\text{R}^2$	$\delta^{11}\text{B}$ (in $\text{CDCl}_3$ )
	H	H	68.0
	Me	Me	58.0
	Et	Et	60.0
	$\text{Me}_3\text{Si}$	H	71.0, 67.0

The influence of the alkyl substituents  $\text{R}_1$  and  $\text{R}_2$  on  $^{11}\text{B}$  is clearly not in accord with steric effects frequently found in the case of alkenylboranes (see Table 4).

Stable triphenylsilylorganyl boranes of the type  $\text{R}_n\text{B}(\text{SiPh}_3)_{3-n}$  ( $n = 0, 1$ ) have been reported.<sup>174</sup> However, no convincing proof for their structure has been given. In the light of the problems involved in the synthesis of

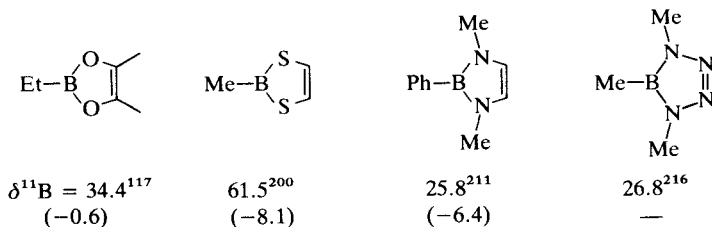
trialkylsilyldiorganylboranes,<sup>123</sup> their existence must be questioned, as is the case for various stannylboranes.<sup>176</sup> So far, only a few silyldiorganylboranes have been fully characterized, including those involving  $^{11}\text{B}$  NMR spectroscopy:<sup>123</sup>



The  $^{11}\text{B}$ -nuclear shielding is reduced by approx. 20 ppm with respect to trialkylboranes. This can be ascribed to the higher energy of the electrons in the  $\text{B}-\text{Si}$   $\sigma$  bond as compared with the  $\text{B}-\text{C}$   $\sigma$  bond. Similar arguments apply to other trigonal boranes with a  $\text{B}-\text{Si}$ ,  $\text{B}-\text{Sn}$ ,  $\text{B}-\text{Pb}$  or a  $\text{B}-\text{B}$  bond (see below).

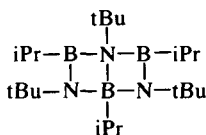
(c) *Monoorganyl boranes,  $\text{RBX}_2$  ( $X = \text{H}$ , halogen,  $\text{OR}'$ ,  $\text{SR}'$ ,  $\text{SeR}'$ ,  $\text{NR}'_2$ ,  $\text{PR}'_2$ ).* In general, all effects discussed for  $\delta^{11}\text{B}$  values of the diorganylboranes  $\text{R}_2\text{BX}$  (see above) are also found in the case of monoorganylboranes  $\text{RBX}_2$ . The heavy-atom effects<sup>176</sup> are amplified in the case of  $\text{RBX}_2$  ( $X = \text{Br}$ ,  $\text{I}$ ), whereas substituent-induced changes in the  $\pi$ -electron density at the boron atom are less evident in the presence of two ligands  $X$  suitable for  $\text{B}-\text{X}(\text{pp})\pi$  bonding. A great variety of cyclic and noncyclic compounds have been studied by  $^{11}\text{B}$  NMR.<sup>5,7</sup> This brief discussion is limited to  $\delta^{11}\text{B}$  values of some new compounds.  $\delta^{11}\text{B}$  data for representative compounds are listed in Tables 13–17.

With the exception of the oxygen derivative, there is a considerable increase in the  $^{11}\text{B}$  nuclear shielding of the five-membered heterocycles when a  $\text{C}=\text{C}$  double bond is in the 4,5-position ( $\Delta^{11}\text{B}$  values with respect to the saturated heterocycles in parentheses):

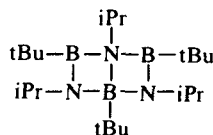


Therefore in the case of the sulphur<sup>200</sup> and nitrogen compounds this is in agreement with an increase in electron-density delocalization, as suggested for the nitrogen compounds on the basis of photoelectron spectroscopy and MO calculations.<sup>253</sup>

The development of the chemistry of iminoboranes<sup>49,52,53</sup> is related to the oligomerization of these reactive compounds. In the course of these studies, borazines with Dewar-benzene-like structures have been detected.<sup>228,248</sup>

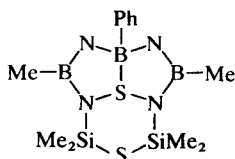


(structure by X-ray diffraction)  
(Two  $^{11}\text{B}$  resonances in the solid state)  
 $\delta^{11}\text{B} = 31.1$  ( $\text{CDCl}_3$ )



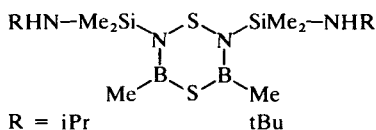
$\delta^{11}\text{B} = 29.9$  ( $20^\circ\text{C}$ )  
 $35.9$  (a),  $13.9$  (b)  
( $-50^\circ\text{C}$ ; ratio 2 : 1).

There is also an example for strong intramolecular S—B coordination as indicated by  $^{11}\text{B}$  NMR and X-ray analysis:<sup>347</sup>

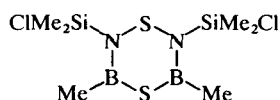


$\delta^{11}\text{B}$  ( $\text{CDCl}_3$ ) =  $35.7$ ,  $13.7$   
(ratio 2 : 1)

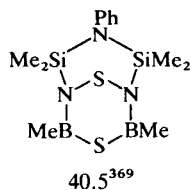
Weak intramolecular association appears to determine the  $\delta^{11}\text{B}$  values in some aminosilane derivatives, as is evident by comparison with the  $\delta^{11}\text{B}$  value of the corresponding chlorosilane derivative:



$\delta^{11}\text{B} = 33.9^{369}$   $34.5^{369}$



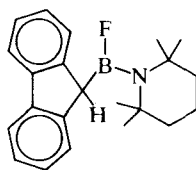
$54.9^{242}$



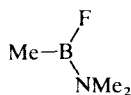
$40.5^{369}$

In the presence of a B—F bond the influence of steric strain on the  $\delta^{11}\text{B}$  values of aminoboranes is much reduced. This may be ascribed to the increased polarization of the  $\sigma$ -bonding framework. Typical examples have been reported for the tmp (tmp = 2,2,6,6-tetramethylpiperidino) and the

9-fluorenyl ligands.<sup>368</sup>

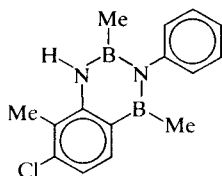


$$\delta^{11}\text{B} = 33.9^{368}$$



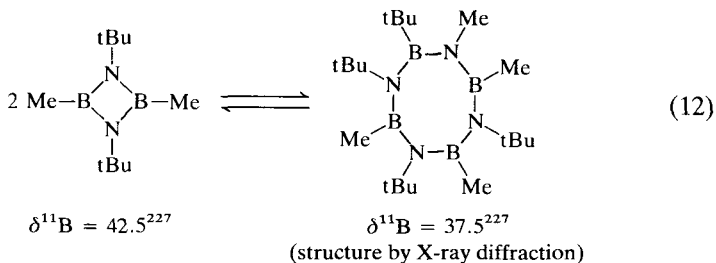
$$31.6^{127}$$

High-field  $^{11}\text{B}$  NMR is extremely useful, even in the study of trigonal boranes. Thus the resolution of broad overlapping resonances supports the structural assignment, as shown in the case of various heterocycles.<sup>373</sup>

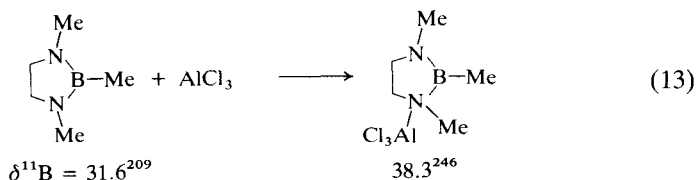


$$\delta^{11}\text{B} (\text{CS}_2) = 33.7 \text{ (a)}, 48.7 \text{ (b)}$$

The dimerization of the four-membered diazadiboretidines to the eight-membered octahydrotetrazatetraborocines is a reversible process and can be studied by  $^{11}\text{B}$  NMR:<sup>227,252</sup>

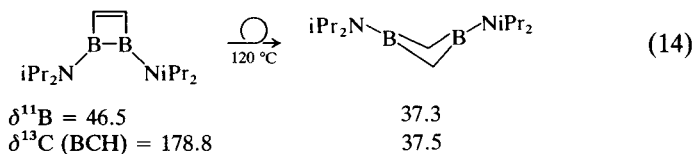


The addition of Lewis acids to bis(amino)boranes (cyclic and noncyclic) has been another interesting subject of recent  $^{11}\text{B}$  NMR studies:<sup>148,245,246,251</sup>

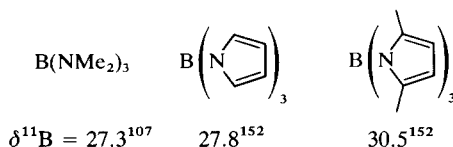


The rearrangement of a 1,2-dihydro-1,2-diborete into a 1,3-dihydro-1,3-diborete has been studied by  $^{11}\text{B}$  NMR. The increase in  $^{11}\text{B}$ -nuclear

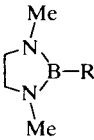
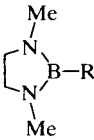
shielding is paralleled by the change in the  $\delta^{13}\text{C}$  value:<sup>59</sup>



(d) *Boranes,  $\text{BX}_3$ ,  $\text{BX}_2\text{Y}$ ,  $\text{BXY}_2$ ,  $\text{BXYZ}$  (Tables 18–20).* The influence of the substituents X, Y and Z on  $\delta^{11}\text{B}$  is analogous to that described for diorganyl- and monoorganyl boranes. The heavy-atom effect for  $\text{X} = \text{I}$ , e.g. in  $\text{BI}_3$  ( $\delta^{11}\text{B} = -7.1^{107}$ ) is more pronounced. The  $\delta^{11}\text{B}$  value for  $\text{BF}_3$  ( $\delta^{11}\text{B} = 10.0$ ) should not be taken as evidence for efficient  $\text{BF}(\text{pp})\pi$  bonding, but rather should be attributed to significant stabilization of  $\sigma$  versus  $\pi$  orbitals. Of course, the latter effect has to be considered for all trigonal boranes, but its influence on  $\delta^{11}\text{B}$  easily gets confused with  $\text{BX}(\text{pp})\pi$  bonding, in particular in the case of the compounds discussed in this section. Thus the comparison of the  $\delta^{11}\text{B}$  values for the following boron nitrogen compounds is very instructive. For electronic and for steric reasons,  $\text{BN}(\text{pp})\pi$  interactions should be negligible in the 2,5-dimethylpyrrole derivative. In spite of this, the  $\delta^{11}\text{B}$  value lies close to the “normal” range of  $\delta^{11}\text{B}$  values for tris(amino)boranes ( $\delta^{11}\text{B} = 22\text{--}30$  ppm):

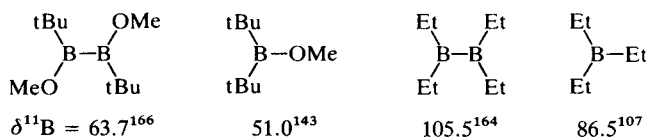


On the other hand, electropositive substituents should induce a destabilization of  $\sigma$  orbitals versus  $\pi$  orbitals, and therefore they cause a reduced magnetic shielding of the  $^{11}\text{B}$  nuclei. This is readily seen in the case of many silyl-, stannyl- or plumbylboranes (Table 20); for example

	R	tBu	$\text{Me}_3\text{Si}$	$\text{Me}_3\text{Sn}$	$\text{Me}_3\text{Pb}$
	$\delta^{11}\text{B}$	32.6	32.9 <sup>182</sup>	36.5 <sup>133</sup>	41.7 <sup>334</sup>
	R	tBu	$\text{Me}_3\text{Si}$	$\text{Me}_3\text{Sn}$	
	$\delta^{11}\text{B}$	49.9 <sup>143</sup>	58.4 <sup>329</sup>	63.9 <sup>133</sup>	

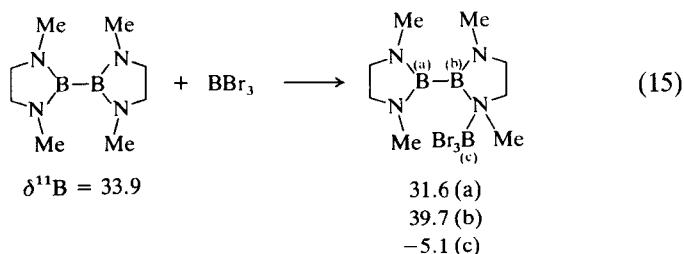
(e) *Diboranes(4) (Table 21).* The  $^{11}\text{B}$ -nuclear shielding in diborane(4) derivatives is controlled by the same effects as in other trigonal boranes. In

most diborane(4) compounds, the presence of the B—B bond is reflected by reduced  $^{11}\text{B}$ -shielding (approx. 5–20 ppm) with respect to that in the corresponding organylboranes; for example

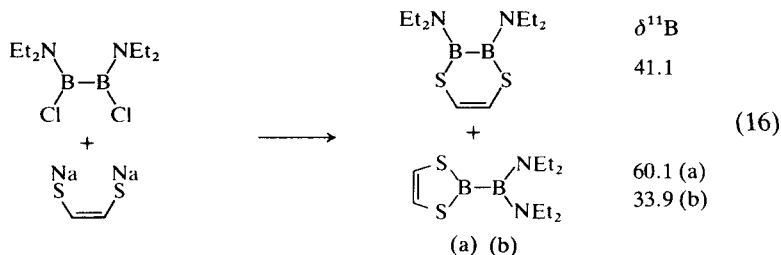


As in silyl-, stannyl- or plumbylboranes, this may be attributed to the electropositive character of the boryl group, which destabilizes the  $\sigma$ -bonding framework. Exceptions are  $\text{B}_2\text{F}_4$ ,  $\text{B}_2\text{Cl}_4$  and  $\text{B}_2(\text{OR})_4$  (in comparison with  $\text{RBF}_2$ ,  $\text{RBCl}_2$ ,  $\text{RB}(\text{OR})_2$ ;  $\text{R} = \text{alkyl}$ ), where electronegative ligands enhance the group electronegativity of the boryl group. In any case, a direct comparison of  $\delta^{11}\text{B}$  values of diborane(4) and borane(3) derivatives is somewhat hampered owing to the unknown magnitude of the mutual “ $\beta$ -effect” exerted by the substituents at the two boron atoms in diborane(4) compounds.

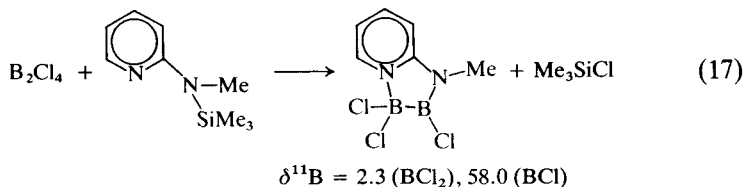
$^{11}\text{B}$  NMR is extremely useful in the investigation of the rich chemistry of diborane(4) compounds. Thus it proves that adduct formation takes place instead of exchange reactions:<sup>360</sup>



$^{11}\text{B}$  NMR shows the product distribution that arises from the following reaction:<sup>362</sup>



The existence of diborane(4) compounds with different coordination numbers is clearly demonstrated by  $^{11}\text{B}$  NMR.<sup>365</sup>



Similarly,  $^{11}\text{B}$  NMR is used to show the presence of unstable diborane(4) derivatives, like  $\text{B}_2\text{Et}_4$ .<sup>164</sup> Of course, it may also be used to study the decomposition of such species, and also other reactions that proceed via B—B bond cleavage.<sup>163</sup>

### 3. Tetracoordinate boron and boron with coordination number $\geq 4$

The increase in nuclear shielding observed for tetracoordinate boron atoms with respect to three-coordinate boron is predicted by theory. This finding is also in agreement with  $\delta^{13}\text{C}$  or  $\delta^{15}\text{N}$  data for tetracoordinate carbon or nitrogen atoms respectively. The  $\delta^{11}\text{B}$  values cover the range between approximately +40 and -130 ppm, and there is no relationship between  $\delta^{11}\text{B}$  values and the formal charge of the molecule (e.g. neutral in Lewis-base-borane adducts, cationic in boron(1+) compounds and anionic in borates). The  $\delta^{11}\text{B}$  values are determined by substituent effects in a similar way as known for  $\delta^{13}\text{C}$  values of substituted alkanes. Additional effects are observed in the case of transition-metal hydroborates, where the nature of the M—H—B bridge has to be taken into account. Finally, there are many borane-metal  $\pi$  complexes for which  $^{11}\text{B}$  NMR has been used to prove the presence of metal-boron bonding interactions.

(a) *Diboranes(6) and  $\mu$ -diboranes.* The  $^{11}\text{B}$  nuclear shielding in diboranes(6) depends greatly upon the nature and the number of substituents. There are extensive lists of data provided in Refs. 5, 7 (for  $\mu$ -diboranes see also Ref. 832), and discussions can be found in Ref. 662.

	(a) $\text{H}_2\text{BH}_2\text{BH}_2$	(b) $\text{Me(H)BH}_2\text{BH}_2$	$\text{Me(H)BH}_2\text{B(H)Me}$
$\delta^{11}\text{B(a)}$	17.7	26.7	21.9
$\delta^{11}\text{B(b)}$	17.7	8.8	21.9
	$\text{Me}_2\text{BH}_2\text{BH}_2$	$\text{Me}_2\text{BH}_2\text{B(H)Me}$	$\text{Me}_2\text{BH}_2\text{BMe}_2$
$\delta^{11}\text{B(a)}$	38.8	31.7	25.0
$\delta^{11}\text{B(b)}$	4.4	15.5	25.0

(Continued p. 148)

TABLE 22

 $\delta^{11}\text{B}$  values of some representative Lewis-base–organyborane adducts.<sup>a,b,c</sup>

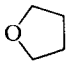
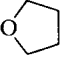
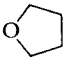
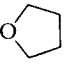
Compound		$\delta^{11}\text{B}$	Solvent	Ref.	Other nuclei	Ref.
<i>Base—BR<sub>3</sub></i>						
Base	R					
	Me	+18	THF, -50 °C	41	—	
NH <sub>3</sub>	Me	-8.7	CH <sub>2</sub> Cl <sub>2</sub>	474	<sup>14</sup> N	474
Pyridine	Me	0.0	CH <sub>2</sub> Cl <sub>2</sub>	474	<sup>14</sup> N	474
1-Me—imidazole	Me	-5.2	CH <sub>2</sub> Cl <sub>2</sub>	474	{ <sup>14</sup> N <sup>13</sup> C, <sup>15</sup> N <sup>31</sup> P	474
PMe <sub>3</sub>	Me	-12.3	—	478		478
	Et	+25.7	THF, -55 °C	475	—	
NH <sub>3</sub>	Et	-3.1	—	474	<sup>14</sup> N	474
Pyridine	Et	2.2	Et <sub>2</sub> O	474	<sup>14</sup> N	474
NH <sub>3</sub>	tBu	-2.5	CH <sub>2</sub> Cl <sub>2</sub>	477	<sup>13</sup> C	477
NH <sub>3</sub>	CH=CH <sub>2</sub>	-9.5		69	<sup>13</sup> C	69
NMe <sub>3</sub>	CH=CH <sub>2</sub>	-3.0		69	<sup>13</sup> C	69
PMe <sub>3</sub>	CH=CH <sub>2</sub>	-17.5		69	<sup>13</sup> C	69
(J(PB) = 47.0)						
<i>Base—1-boraadamantane</i>						
Base						
OEt <sub>2</sub>		15.6		480		
		-8.0		482		
Pyridine		-4.1		480	<sup>13</sup> C	479
PhC≡N		-9.1	CCl <sub>4</sub>	481		
<i>Base—C<sub>8</sub>H<sub>14</sub>B—R<sup>a</sup></i>						
Base	R					
Pyridine	Et	1.4	CDCl <sub>3</sub>	47	<sup>13</sup> C	47
	H	14.0	THF	483	—	
Me <sub>2</sub> S	H	3.9	Me <sub>2</sub> S	484	—	
Pyridine	H	-0.7	CDCl <sub>3</sub>	47	<sup>13</sup> C	47
Pyridine—BPh <sub>3</sub>		3.9		485	<sup>13</sup> C	486

TABLE 22 (cont.)

 $\delta^{11}\text{B}$  values of some representative Lewis-base-organylborane adducts.<sup>a,b,c</sup>

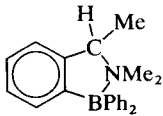
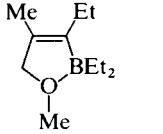
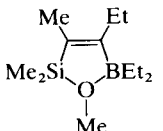
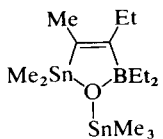
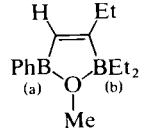
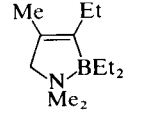
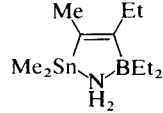
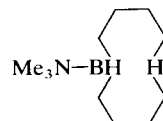
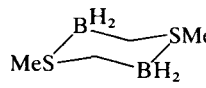
Compound	$\delta^{11}\text{B}$	Solvent	Ref.	Other nuclei	Ref.
	6.4	$\text{CDCl}_3$	489	—	
	25.0		487	—	
	21.2	Neohexane	5	—	
	9.6	$\text{C}_6\text{D}_6$	488	$^{13}\text{C}$ , $^{119}\text{Sn}$	488
	46.4(a) 25.3(b)	$\text{CH}_2\text{Cl}_2$	31	—	
	7.0	—	491		
	-0.7	$\text{C}_6\text{D}_6$	492	$^{13}\text{C}$ , $^{15}\text{N}$ , $^{119}\text{Sn}$	492
	2.0 (88.0)	1,4-Dioxane	494	—	
$[\text{H}_2\text{N}(\text{CH}_2)_2\text{NH}_2][(\text{c-C}_6\text{H}_{11})_2\text{BH}]_2$	-1.6		497		

TABLE 22 (cont.)

 $\delta^{11}\text{B}$  values of some representative Lewis-base-organylborane adducts.<sup>a,b,c</sup>

Compound	$\delta^{11}\text{B}$	Solvent	Ref.	Other nuclei	Ref.
					
Me(equatorial)	-13.6 (105)	$\text{CDCl}_3$	493	$^{13}\text{C}$	493
Me(axial)	-17.2 (105)	$\text{CDCl}_3$	493	$^{13}\text{C}$	
$\text{Me}_3\text{N}-\text{BH}_2\text{tBu}$	3.1		495	—	
$\text{Me}_3\text{N}-\text{BH}_2(\text{CH}_2)_4\text{BH}_2-\text{NMe}_3$	-1.1 (95.0)	$\text{C}_6\text{D}_6$	496	$^{13}\text{C}$	496
$[\text{Me}_2\text{N}(\text{CH}_2)_2\text{NMe}_2][\text{CHMe}_2\text{CMe}_2\text{BH}_2]_n$					
$n = 1$	-1.4	$\text{CDCl}_3$	498	—	
$n = 2$	-0.8	$\text{CDCl}_3$	498	—	
$\text{Me}_3\text{N}-\text{BH}_2\text{CH}_2\text{SMe}$	-3.9 (99.0)	$\text{CDCl}_3$	496	$^{13}\text{C}$	496
$\text{Me}_3\text{N}-\text{BH}_2\text{CN}$	-14.9 (108.0)		499		

<sup>a</sup>  $\text{C}_8\text{H}_{14}\text{B}$  = 9-borabicyclo[3.3.1]nonyl.<sup>b</sup>  $^{11}\text{B}$  NMR data for  $\text{Me}_n\text{NH}_{3-n}-\text{H}_2\text{B}-\text{C}(\text{O})\text{OR}$  are given in Ref. 819.<sup>c</sup>  $^1J(^{11}\text{B}^1\text{H})$  values in parentheses.

TABLE 23

 $\delta^{11}\text{B}$  values of some Lewis-base organylborane ( $\text{R}_2\text{BX}$  and  $\text{RBX}_2$ ) adducts.

Compound	$\delta^{11}\text{B}$	Solvent	Ref.	Other nuclei	Ref.
$\text{THF}-\text{ClBC}_8\text{H}_{14}$ <sup>a</sup>	17.8	THF	793	—	
$\text{Et}_2\text{O}-\text{CMe}_2\text{HCMe}_2\text{B}(\text{H})\text{Cl}$	17.7 ( $J(\text{BH}) = 145.0$ )		588	—	
$\text{Me}_2\text{S}-\text{XBC}_8\text{H}_{14}$ <sup>a</sup> X = Cl	18.5	$\text{CDCl}_3$	589	—	
Br	12.8	$\text{CDCl}_3$	589	—	
I	12.4	$\text{CDCl}_3$	589	—	
$\text{Me}_2\text{S}-2,6\text{-Cl}_2\text{-Cl-2,6-diboraadamantane}$	13.9		589	—	
$\text{Me}_2\text{S}-\text{BPhX}_2$ X = Cl	9.1		590	—	
Br	2.1		590	—	
I	-17.6		590	—	

TABLE 23 (*cont.*)

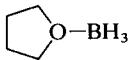
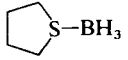
$\delta^{11}\text{B}$  values of some Lewis-base organylborane ( $\text{R}_2\text{BX}$  and  $\text{RBX}_2$ ) adducts.

Compound	$\delta^{11}\text{B}$	Solvent	Ref.	Other nuclei	Ref.
$\text{Me}_2\text{S}-\text{BRBr}_2$					
$\text{R} = (3Z)\text{-}3\text{-hexen-}3\text{-yl}$	-3.3	$\text{CDCl}_3$	591	—	
$(1E)\text{-}1\text{-hexen-}1\text{-yl}$	-0.9	$\text{CCl}_4$	591	—	
$(1E)\text{-}3,3\text{-dimethyl-}1\text{-buten-}1\text{-yl}$	0.3	$\text{CCl}_4$	591	—	
$(2Z)\text{-}4\text{-methyl-}2\text{-penten-}2\text{-yl}$	-3.6	$\text{CCl}_4$	591	—	
$(1E)\text{-}5\text{-chloro-}1\text{-penten-}1\text{-yl}$	-2.0	$\text{CCl}_4$	591	—	
$\text{Me}_2\text{S}-\text{CMe}_2\text{HCMe}_2\text{B(H)Cl}$	8.9 ( $J(\text{BH}) = 120.0$ )		588	—	
$\text{Me}_3\text{N}-\text{BEt}_2\text{F}$	10.1 ( $J(\text{FB}) = 67.0$ )		594	—	
$\text{Me}_3\text{N}-\text{BEtF}_2$	6.7 ( $J(\text{FB}) = 65.0$ )		107	—	
$\text{Me}_3\text{N}-\text{BEtCl}_2$	12.4	$\text{CHCl}_3$	107	—	
$\text{Pyridine}-\text{ClBC}_8\text{H}_{14}^a$	9.5	$\text{CDCl}_3$	47	$^{13}\text{C}$	47
$\text{Pyridine}-\text{BMe}_2\text{Br}$	6.5	$\text{C}_7\text{H}_8$	5	—	
$\text{Pyridine}-\text{BMeBr}_2$	2.8	$\text{C}_7\text{H}_8$	5	—	
$\text{Me}_3\text{P}-\text{BEt}_2\text{F}$	7.5	$\text{CH}_2\text{Cl}_2$	478	—	
$\text{Me}_3\text{P}-\text{BBuF}_2$	9.5	$\text{CH}_2\text{Cl}_2$	478	—	

<sup>a</sup>  $\text{C}_8\text{H}_{14}\text{B} = 9\text{-borabicyclo}[3.3.1]\text{nonyl}$ .

TABLE 24

$\delta^{11}\text{B}$  values of some Lewis-base-borane ( $\text{BH}_3$ ) adducts. <sup>b</sup>

Compound	$\delta^{11}\text{B}$	Solvent	Ref.	Other nuclei	Ref.
$\text{Me}_2\text{O}-\text{BH}_3$	2.5(106.0)	$\text{Me}_2\text{O}$	557	—	
 $\text{O}-\text{BH}_3$	-0.7(103.0)	THF	557	—	
$\text{Me}_2\text{S}-\text{BH}_3$	-20.1(104.0)	$\text{CH}_2\text{Cl}_2$	557	—	
 $\text{S}-\text{BH}_3$	-20.1(104.0)	$\text{CH}_2\text{Cl}_2$	557	—	
$\text{H}_3\text{N}-\text{BH}_3$	-22.3(98.2)	Monoglyme	474	$\begin{Bmatrix} ^{14}\text{N} \\ ^{15}\text{N} \end{Bmatrix}$	474
$\text{MeH}_2\text{N}-\text{BH}_3$	-19.1(92.0)	Monoglyme	474		556
				$^{14}\text{N}$	474

$\delta^{11}\text{B}$  values of some Lewis-base-borane ( $\text{BH}_3$ ) adducts.<sup>b</sup>

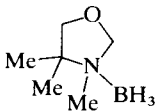
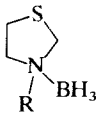
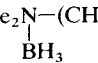
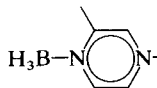
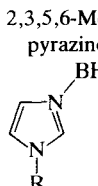
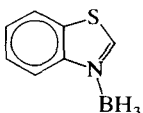
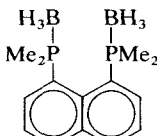
Compound	$\delta^{11}\text{B}$	Solvent	Ref.	Other nuclei	Ref.
$\text{Me}_2\text{HN}-\text{BH}_3$	-13.5(94.0)	Monoglyme	474	$^{14}\text{N}$	474
$\text{Me}_3\text{N}-\text{BH}_3$	-8.3(98.0)	Monoglyme	474	$^{14}\text{N}$	474
$\text{Et}_3\text{N}-\text{BH}_3$	-13.5(97.3)	—	474	$\begin{Bmatrix} ^{14}\text{N} \\ ^{15}\text{N} \end{Bmatrix}$	$\begin{Bmatrix} 474 \\ 556 \end{Bmatrix}$
	-16.0	$\text{CDCl}_3$	561	$^{13}\text{C}$	561, 562
	R = H Bu	THF THF	652 652	— —	
$\text{Me}_2\text{N}-(\text{CH}_2)_2-\text{O}-\text{C}(\text{O})\text{Me}$ 	-9.0(98.0)	$\text{CDCl}_3$	563	—	
Pyridine- $\text{BH}_3$	-11.8(98.0)	$\text{CH}_2\text{Cl}_2$	474	$^{14}\text{N}$	474
2- $\text{NH}_2$ -pyridine- $\text{BH}_3$	-17.0(90.0)	$\text{CHCl}_3$	558	—	
	-13.2(N(1)B) -11.7(N(4)B)	$\text{C}_6\text{D}_6$	559	—	
2,3,5,6- $\text{Me}_4$ - pyrazine- $(\text{BH}_3)_2$	-17.3	$\text{C}_6\text{D}_6$	560	—	
	R = H Me $\text{Me}_3\text{Si}$	$\text{CH}_2\text{Cl}_2$ Monoglyme $\text{CH}_2\text{Cl}_2$ $\text{CH}_2\text{Cl}_2$	474 564 474 474	$^{14}\text{N}$ — $^{14}\text{N}$ $^{14}\text{N}$	474  474 474
	-17.1(91.0)	THF	652	—	
$\text{H}_3\text{P}-\text{BH}_3$	-42.5(103.0) ( $J(\text{PB}) = 27.0$ )		565	$^{31}\text{P}$	566
$\text{Me}_3\text{P}-\text{BH}_3$	-36.8(94.6) ( $J(\text{PB}) = 64.3$ )	$\text{CH}_3\text{CN}$	568		
	-23.0(109.0) (exchange?)	$\text{CD}_2\text{Cl}_2$	569	—	

TABLE 24 (cont.)

 $\delta^{11}\text{B}$  values of some Lewis-base-borane ( $\text{BH}_3$ ) adducts.<sup>b</sup>

Compound	$\delta^{11}\text{B}$	Solvent	Ref.	Other nuclei	Ref.
$(\text{Ph}_2\text{P})_2(\text{CH}_2)_n \cdot 2\text{BH}_3$					
$n = 2$	-40.3	$\text{CDCl}_3$	570	—	
3	-39.8	$\text{CDCl}_3$	570	—	
4	-40.2	$\text{CDCl}_3$	570	—	
$\text{Ph}_2(\text{NHPh})\text{P}-\text{BH}_3^a$	-36.1	$\text{CD}_2\text{Cl}_2$	606	$^{31}\text{P}$	606
	$(J(\text{PB}) = 61.0)$				
$[\text{cpW}(\text{CO})_2(\text{PMe}_3)\text{PPh}_2-\text{BH}_3]$	-28.6	$\text{CD}_3\text{NO}_2$	592	$^{31}\text{P}$	592
	$(J(\text{PB}) = 48.0)$				
$[\text{cpMo}(\text{CO})_2\text{P}(\text{Ph})\text{N}(\text{SiMe}_3)_2-\text{BH}_3]$	-55.6	$\text{CD}_2\text{Cl}_2$	593	$^{13}\text{C}$ , $^{31}\text{P}$	593
$\text{F}_3\text{P}-\text{BH}_3$	-48.2(106.0)		567	$^{31}\text{P}$	567
	$(J(\text{PB}) = 39.0)$				
$\text{Me}_3\text{As}-\text{BH}_3$	-32.2(100.0)		571		
$\text{Me}_2\text{AsH}-\text{BH}_3$	-34.2(105.4)	THF	572		
$\text{Me}_2(\text{Et}_2\text{N})\text{As}-\text{BH}_3$	-36.6	THF	572	$^{13}\text{C}$	572
	-36.1(97.6)	THF	579	$^{13}\text{C}$	579
$\text{Me}_2(\text{NiPr}_2)\text{As}-\text{BH}_3$	-29.5(104.5)	THF	579	$^{13}\text{C}$	579
$[\text{cp}(\text{CO})_2(\text{Me}_3\text{P})\text{MAsMe}_2-\text{BH}_3]$					
$\text{M} = \text{Mo}$	-27.1(100.0)	$\text{CDCl}_3$	765	$^{31}\text{P}$	765
$\text{W}$	-28.0(104.0)	$\text{CDCl}_3$	765	$^{31}\text{P}$	765

<sup>a</sup> See Ref. 816 for  $^{11}\text{B}$ ,  $^{13}\text{C}$ ,  $^{29}\text{Si}$  and  $^{31}\text{P}$  NMR data of  $\text{BH}_3$  adducts of  $\text{Me}_2\text{P}-\text{NMe}_2$  (ratios 1 : 1 and 2 : 1) and  $\text{Me}_2\text{P}-\text{N}(\text{SiMe}_3)_2$ .

<sup>b</sup>  $J(^{11}\text{B}^1\text{H})$  values in parentheses.

TABLE 25

 $\delta^{11}\text{B}$  values of some Lewis-base-borane ( $\text{BH}_2\text{X}$ ,  $\text{BHX}_2$ ) adducts ( $\text{X} = \text{F}, \text{Cl}, \text{Br}, \text{I}$ ).<sup>a</sup>

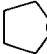
Compound	$\delta^{11}\text{B}$	Solvent	Ref.	Other nuclei	Ref.
$\text{Et}_2\text{O}-\text{BH}_2\text{Cl}$	4.3(131.0)	$\text{Et}_2\text{O}$	573	—	
	5.0(136.0)	$\text{Et}_2\text{O}$	580	—	
$\text{Et}_2\text{O}-\text{BHCl}_2$	7.9(152.0)	$\text{Et}_2\text{O}$	574	—	
	8.0(163.0)	$\text{Et}_2\text{O}$	582	—	
$\text{Et}_2\text{O}-\text{BH}_2\text{Br}$	2.6(137.0)	$\text{Et}_2\text{O}$	581	—	
$\text{Et}_2\text{O}-\text{BHBr}_2$	0.3(165.0)	$\text{Et}_2\text{O}$	581	—	
 - $\text{BH}_2\text{SPh}$	2.3	HF	575	—	

TABLE 25 (cont.)

 $\delta^{11}\text{B}$  values of some Lewis-base-borane ( $\text{BH}_2\text{X}$ ,  $\text{BHX}_2$ ) adducts ( $\text{X} = \text{F}, \text{Cl}, \text{Br}, \text{I}$ ).<sup>a</sup>

Compound	$\delta^{11}\text{B}$	Solvent	Ref.	Other nuclei	Ref.
$\text{Et}_2\text{O}-\text{BH}_2\text{NS}_7$	13.0(136.0)		576	—	
$\text{Me}_2\text{S}-\text{BH}_2\text{Cl}$	-6.7		578	—	
$\text{Me}_2\text{S}-\text{BH}_2\text{Br}$	-10.9(131.0)	$\text{CS}_2$	578	—	
	-10.5	$\text{Me}_2\text{S}$	578	—	
$\text{Me}_2\text{S}-\text{BH}_2\text{I}$	-19.9(136.0)	$\text{CS}_2$	577	—	
	-20.5	$\text{Me}_2\text{S}$	578	—	
$\text{Me}_2\text{S}-\text{BHBBr}_2$	-8.2(162.0)	$\text{CS}_2$	577		
$\text{Me}_2\text{S}-\text{BHI}_2$	-35.2(160.0)	$\text{CS}_2$	577	—	
$\text{H}_3\text{N}-\text{BHF}_2$	-3.6(140.0)		583	$^{19}\text{F}$	583
	( $J(\text{FB}) = 70.0$ )				
$\text{H}_3\text{N}-\text{BH}_2\text{Cl}$	-9.1(120.0)	$\text{Et}_2\text{O}$	581		
$\text{H}_3\text{N}-\text{BHCl}_2$	-1.3(141.0)	$\text{Et}_2\text{O}$	581		
$\text{H}_3\text{N}-\text{BH}_2\text{Br}$	-12.1(126.0)	$\text{Et}_2\text{O}$	581		
$\text{Me}_3\text{N}-\text{BH}_2\text{F}$	5.1(113.0)		584	$^{13}\text{C}$	586
	( $J(\text{FB}) = 88.5$ )				
$\text{Me}_3\text{N}-\text{BHF}_2$	4.1(146.0)		584	$^{13}\text{C}$	586
	( $J(\text{FB}) = 73.7$ )				
$\text{Me}_3\text{N}-\text{BH}_2\text{Cl}$	-0.5(121.0)	$\text{C}_6\text{H}_6$	585		
$\text{Me}_3\text{N}-\text{BH}_2\text{Br}$	-2.9(129.0)	$\text{C}_6\text{H}_6$	585		
$\text{Me}_3\text{N}-\text{HB} \begin{array}{c} \text{O} \\ \diagup \quad \diagdown \\ \text{O} \end{array}$	7.7(127.0)	$\text{CH}_2\text{Cl}_2$	557		
$\text{Me}_3\text{N}-\text{HB} \begin{array}{c} \text{S} \\ \diagup \quad \diagdown \\ \text{S} \end{array}$	5.9(128.0)	THF	557		
$\text{Me}_3\text{N}-\text{BH}_2\text{C}\equiv\text{N}$	-14.9(105.0)	$\text{CH}_2\text{Cl}_2$	587	—	
$\text{C}_5\text{H}_5\text{N}-\text{BH}_2\text{CN}$	-16.0(102.0)		649	—	
$2\text{-Me}-\text{C}_5\text{H}_5\text{N}-\text{BH}_2\text{CN}$	-18.0(105.0)		649	—	
$\text{Me}_3\text{N}-\text{BH}_2\text{N}\equiv\text{C}$	-7.5(115.0)	$\text{CH}_2\text{Cl}_2$	587	$^{13}\text{C}$	587
$\text{H}_3\text{P}-\text{BH}_2\text{Cl}$	-19.0(130.0)	$\text{MeI}$	595	$^{31}\text{P}$	595
	( $J(\text{PB}) = 41.0$ )				
$\text{H}_3\text{P}-\text{BHCl}_2$	-6.0(131.0)	$\text{MeI}$	595	$^{31}\text{P}$	595
	( $J(\text{PB}) = 131.0$ )				
$\text{H}_3\text{P}-\text{BH}_2\text{Br}$	-26.0(130.0)	$\text{MeI}$	595	$^{31}\text{P}$	595
	( $J(\text{PB}) = 55.0$ )				
$\text{Me}_3\text{P}-\text{BH}_2\text{Br}$	-24.1(92.0)	$\text{C}_6\text{H}_6$	585		
	( $J(\text{PB}) = 92.0$ )				
$\text{H}_3\text{P}-\text{BHBBr}_2$	-19.0(149.0)	$\text{MeI}$	595	$^{31}\text{P}$	595
	( $J(\text{PB}) = 91.0$ )				
$\text{H}_3\text{P}-\text{BH}_2\text{I}$	-39.0(130.0)	$\text{MeI}$	595	$^{31}\text{P}$	595
	( $J(\text{PB}) = 60.0$ )				
$\text{H}_3\text{P}-\text{BHI}_2$	-54.0(154.0)	$\text{MeI}$	595	$^{31}\text{P}$	595
	( $J(\text{PB}) = 91.0$ )				

TABLE 25 (cont.)

 $\delta^{11}\text{B}$  values of some Lewis-base-borane ( $\text{BH}_2\text{X}$ ,  $\text{BHX}_2$ ) adducts ( $\text{X} = \text{F}, \text{Cl}, \text{Br}, \text{I}$ ).<sup>a</sup>

Compound	$\delta^{11}\text{B}$	Solvent	Ref.	Other nuclei	Ref.
$\text{Me}_3\text{P}-\text{HB} \begin{array}{c} \diagup \text{S} \\ \diagdown \text{S} \end{array}$	-11.3(115.0) ( $J(\text{PB}) = 84.0$ )		557	$^{31}\text{P}$	557
$\text{Ph}_3\text{P}-\text{BH}_2\text{CN}$	-33.6(79.0) ( $J(\text{PB}) = 79.0$ )		649	—	
$(\text{MeO})_3\text{P}-\text{BH}_2\text{CN}$	-40.1(96.0) ( $J(\text{PB}) = 126.0$ )		649	—	

<sup>a</sup>  $^1J(^{11}\text{B}^1\text{H})$  values in parentheses.

TABLE 26

 $\delta^{11}\text{B}$  values of some Lewis-base-borane ( $\text{BX}_3$ ) adducts ( $\text{X} = \text{F}, \text{Cl}, \text{Br}, \text{I}$ ).<sup>a</sup>

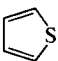
Compound	$\delta^{11}\text{B}$	Solvent	Ref.	Other nuclei	Ref.
$\text{Et}_2\text{O}-\text{BF}_3$	0	$\text{Et}_2\text{O}$	5	$^{19}\text{F}$	526
$\text{R}(\text{R}^1)\text{C}=\text{O}-\text{BF}_3$	+2.7 to -1		5	$^{13}\text{C}$	596
$\text{Et}_2\text{O}-\text{BCl}_3$	10.5	$\text{Et}_2\text{O}$	574	—	
$\text{Me}_3\text{Si}-\text{OS}(\text{CF}_3)\text{O}_2-\text{BCl}_3$	-2.6	$\text{SO}_2\text{ClF}$ , -35°C	608	$^{29}\text{Si}$	608
$\text{Et}_2\text{O}-\text{BBr}_3$	-6.1	$\text{Et}_2\text{O}$	308	—	
$\text{Me}_2\text{S}-\text{BF}_3$	3.1 ( $J(\text{FB}) = 24.0$ )		597	—	
$\text{Me}_2\text{S}-\text{BCl}_3$	7.1	$\text{CH}_2\text{Cl}_2$	597	—	
$\text{Me}_2\text{S}-\text{BBr}_3$	-11.2	$\text{CH}_2\text{Cl}_2$	597	—	
 $\text{S}-\text{BBr}_3$	-10.1	Thiophene	5	—	
$\text{Me}_2\text{S}-\text{BI}_3$	-68.7	$\text{CH}_2\text{Cl}_2$	597	—	
$\text{Me}_2\text{Se}-\text{BCl}_3$	4.5	$\text{CH}_2\text{Cl}_2$	182	$^{77}\text{Se}$	182
$\text{H}_3\text{N}-\text{BF}_3$	-0.9 ( $J(\text{FB}) = 13.9$ )	$\text{CH}_3\text{CN}$	568		
$\text{Me}_3\text{N}-\text{BF}_3^b$	0.8	$\text{CH}_3\text{CN}$	568	$^{13}\text{C}$ $^{15}\text{N}$ $^{19}\text{F}$	586 599 598
$\text{H}_3\text{N}-\text{BCl}_3$	4.2	$\text{Et}_2\text{O}$	581	—	
$\text{Me}_3\text{N}-\text{BCl}_3$	10.2	$\text{C}_6\text{H}_6$	107	$^{13}\text{C}$ $^{15}\text{N}$	586 599
$\text{Me}_3\text{N}-\text{BBr}_3$	-3.1	$\text{C}_6\text{H}_6$	107	$^{13}\text{C}$ $^{15}\text{N}$	586 599

TABLE 26 (cont.)

 $\delta^{11}\text{B}$  values of some Lewis-base-borane ( $\text{BX}_3$ ) adducts ( $\text{X} = \text{F}, \text{Cl}, \text{Br}, \text{I}$ ).<sup>a</sup>

Compound	$\delta^{11}\text{B}$	Solvent	Ref.	Other nuclei	Ref.
$\text{Me}_3\text{N}-\text{BI}_3$	-54.4	$\text{CHCl}_3$	107	$^{13}\text{C}$ $^{15}\text{N}$	586 599
Pyridine- $\text{BX}_3$					
$\text{X} = \text{F}$	-0.3		204	—	
Cl	8.0		204	—	
Br	-7.2	$\text{C}_7\text{H}_8$	474	$^{14}\text{N}$	474
I	-60		308	—	
$\text{Me}_3\text{P}-\text{BF}_3$	0.6 ( $J(\text{PB}) = 180.0$ ) ( $J(\text{FB}) = 50.0$ )		478	$^{19}\text{F}, ^{31}\text{P}$	600
$\text{H}_3\text{P}-\text{BCl}_3$	1.7	$\text{MeI}$	600	$^{31}\text{P}$	600
$\text{Me}_3\text{P}-\text{BCl}_3$	3.0 ( $J(\text{PB}) = 166.0$ )	Monoglyme	557	—	
$\text{H}_3\text{P}-\text{BBr}_3$	-22.7 ( $J(\text{PB}) = 134.0$ )	$\text{MeI}$	600	$^{31}\text{P}$	600
$\text{Me}_3\text{P}-\text{BBr}_3$	-15.5 ( $J(\text{PB}) = 165.0$ )	$\text{MeI}$	595	$^{31}\text{P}$	595
$\text{H}_3\text{P}-\text{BI}_3$	-89.4 ( $J(\text{PB}) = 127.0$ )	$\text{MeI}$	600	$^{31}\text{P}$	600
$\text{Me}_3\text{P}-\text{BI}_3$	-54.0 ( $J(\text{PB}) = 116.0$ )		601		
$\text{Ph}_3\text{As}-\text{BF}_3$	2.8	$\text{CH}_2\text{Cl}_2$	602	—	
$\text{Me}_3\text{As}-\text{BCl}_3$	4.5	$\text{CD}_2\text{Cl}_2$	603	—	
$\text{Me}_3\text{As}-\text{BBr}_3$	-14.7	$\text{CD}_2\text{Cl}_2$	603	—	
$\text{Me}_3\text{As}-\text{BI}_3$	-73.8	$\text{CD}_2\text{Cl}_2$	603	—	
$\text{Me}_3\text{Sb}-\text{BBr}_3$	-17.3	$\text{CDCl}_2$	604	—	
$\text{Me}_3\text{Sb}-\text{BI}_3$	-90.4	$\text{CDCl}_3$	604	—	

<sup>a</sup> See Ref. 5 for further data, as well as for data on  $\text{X} = \text{OR}, \text{SR}$ .<sup>b</sup> Ref. 791 lists some data for  $\text{Ph}(\text{Me})\text{NH}-\text{BF}_3$  ( $-0.6$ ,  $^1J(\text{FB}) = 14 \text{ Hz}$ ),  $-\text{BF}_2\text{Cl}$  ( $+3.3$ ,  $^1J(\text{FB}) = 42 \text{ Hz}$ ),  $-\text{BFCl}_2$  ( $+6.4$ ,  $^1J(\text{FB}) = 68 \text{ Hz}$ ),  $-\text{BCl}_3$  ( $+7.4$ ) and  $\text{Et}_3\text{N}-\text{BF}_3$  ( $-0.6$ ,  $^1J(\text{FB}) = 19 \text{ Hz}$ ),  $-\text{BF}_2\text{Cl}$  ( $+5.1$ ,  $^1J(\text{FB}) = 47 \text{ Hz}$ ).

TABLE 27

 $\delta^{11}\text{B}$  values of various dimeric and trimeric boranes.<sup>a</sup>

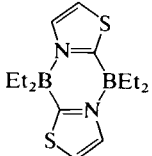
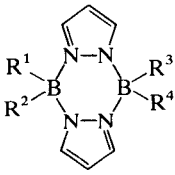
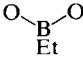
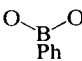
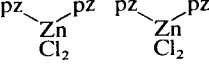
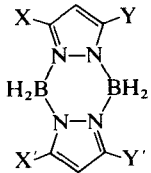
Compound	$\delta^{11}\text{B}$	Solvent	Ref.	Other nuclei	Ref.
$[\text{Me}_2\text{BNH}_2]_2$	-3.0	—	127	$^{15}\text{N}$	556
$[\text{H}_2\text{BN}(\text{H})\text{Me}]_3$	-5.4	Acetone- $\text{d}_6$	671	$^{13}\text{C}$	671
$[(\text{HC}\equiv\text{C})_2\text{BNMe}_2]_2$	-5.6	$\text{CH}_2\text{Cl}_2$	85	—	
$[\text{H}(\text{Me})\text{BNMe}_2]_2$	-6.0	—	627	—	
	$(J(\text{BH}) = 115.0)$				
$[\text{Me}(\text{F})\text{BNMe}_2]_2$	7.0		127	—	
$[\text{Me}(\text{Cl})\text{BNMe}_2]_2$	10.1		127	—	
$[\text{Me}(\text{Br})\text{BNMe}_2]_2$	10.5		127	$^{13}\text{C}$	7
$[\text{H}_2\text{BNH}_2]_2$	-10.9	MeOH	626	—	
$[\text{H}_2\text{BNMe}_2]_2$	5.3		627	—	
	$(J(\text{BH}) = 113.0)$				
$[\text{H}(\text{Cl})\text{BNMe}_2]_2$	6.2	$\text{CDCl}_3$	628	—	
	$(J(\text{BH}) = 137.0)$				
$[\text{H}(\text{Br})\text{BNMe}_2]_2$	8.5	$\text{CDCl}_3$	628	—	
	$(J(\text{BH}) = 139.0)$				
$[\text{F}_2\text{BOMe}]_3$	0.7	$\text{C}_6\text{D}_6$	776	$^{19}\text{F}$	776
$[\text{F}_2\text{BNMe}_2]_2$	0.9	$\text{C}_6\text{H}_6$	107	$^{19}\text{F}$	526, 766
$[\text{Cl}_2\text{BNMe}_2]_2$	10.4	$\text{C}_6\text{H}_6$	107	—	
$[\text{Br}_2\text{BNMe}_2]_2$	6.1	$\text{C}_6\text{H}_6$	107	—	
	-2.3	$\text{C}_6\text{D}_6$	41	$^{13}\text{C}, ^{14}\text{N}$	41
					
$\text{R}^1$	$\text{R}^2$	$\text{R}^3$	$\text{R}^4$		
Et	Et	Et	Et	2.2	631
Ph	Ph	Ph	Ph	1.8	637
Ph	Ph	H	H	-8.4( $\text{BH}_2$ ) 1.7( $\text{BPh}_2$ )	634
Et		Et		1.8	635
				31.5( $\text{BO}_2$ )	
Ph		Ph		1.5	635
				28.7( $\text{BO}_2$ )	

TABLE 27 (cont.)

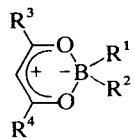
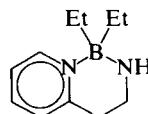
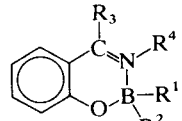
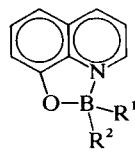
 $\delta^{11}\text{B}$  values of various dimeric and trimeric boranes.<sup>a</sup>

Compound				$\delta^{11}\text{B}$	Solvent	Ref.	Other nuclei	Ref.
H	H	H	H	-8.8 ( $J(\text{BH}) = 108.0$ )		629	$^{15}\text{N}$	630
Br	Br	Br	Br	-7.0	$\text{CDCl}_3$	633	—	
pz	pz	pz	pz	0.7	$\text{CD}_3\text{CN}$	635	$^{13}\text{C}$	630, 635
pz	pz	pz	pz	-0.4	$\text{CD}_3\text{CN}$	636	$^{13}\text{C}$	636
 <p>(pz = <i>N</i>-pyrazolyl)</p>								
								
X	X'	Y	Y'					
Me	Me	H	H	-12.2 ( $J(\text{BH}) = 105.0$ ) -9.0 ( $J(\text{BH}) = 105.0$ )	$\text{CDCl}_3$	638	—	
Me	H	H	Me	-10.5 ( $J(\text{BH}) = 105.0$ )	$\text{CDCl}_3$	638	—	
$(\text{H}_2\text{BPMe}_2)_3$				-32.4 ( $J(\text{BH}) = 100.0$ ) ( $J(\text{PB}) = 79.3$ )	$\text{C}_6\text{D}_6$	173	$^{13}\text{C}, ^{31}\text{P}$	173
$(\text{Cl}_2\text{BPEt}_2)_2$				-1.5 ( $J(\text{PB}) = 99.5$ )	$\text{C}_6\text{H}_6$	534	$^{13}\text{P}$	534
$(\text{H}_2\text{BAsMe}_2)_2$				-30.3 ( $J(\text{BH}) = 109.9$ )	$\text{C}_6\text{H}_6$	5	—	

<sup>a</sup> See Ref. 5 for more data.

TABLE 28

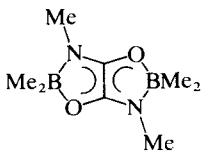
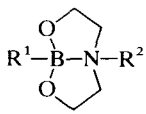
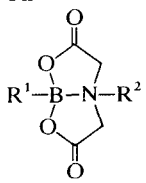
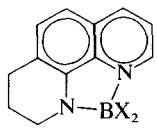
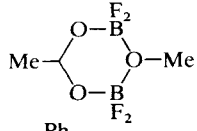
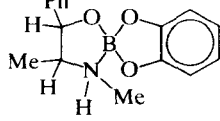
 $\delta^{11}\text{B}$  values of various chelate complexes.<sup>a</sup>

Compound	$\delta^{11}\text{B}$	Solvent	Ref.	Other nuclei	Ref.
 $\text{R}^1 \quad \text{R}^2 \quad \text{R}^3 \quad \text{R}^4$					
Me Me Me Me	13.0		621	—	
Et Et Me Me	14.7	$\text{C}_6\text{H}_6$	622		
Pr Pr Me Me	14.0	$\text{CHCl}_3$	618	$^{13}\text{C}$	618
Pr Cl Me Me	11.3	$\text{CHCl}_3$	618	$^{13}\text{C}$	618
Ph $\text{ClO}_4$ Ph Ph	8.1	$\text{CH}_2\text{Cl}_2$	623	$^{35}\text{Cl}$	623
Cl Cl Me Me	7.9	$\text{CHCl}_3$	618	$^{13}\text{C}$	618
Br Br Me Me	3.9	$\text{CHCl}_3$	618	$^{13}\text{C}$	618
	-2.5	$\text{CH}_2\text{Cl}_2$	613	$^{13}\text{C}, ^{14}\text{N}$	613
 $\text{R}^1 \quad \text{R}^2 \quad \text{R}^3 \quad \text{R}^4$					
Ph Ph H H	3.3	Dioxane	625	—	
Ph Ph Me OH	6.1	$\text{C}_6\text{H}_6$	614	$^{13}\text{C}$	614
Ph MeO H Pr	4.8	$\text{C}_6\text{H}_6$	614	$^{13}\text{C}$	614
 $\text{R}^1 \quad \text{R}^2$					
Et Et	14.4	$\text{C}_6\text{H}_6$	622	—	
$\text{C}_8\text{H}_{14}^b$	14.0		624	—	
H H	5.1	Monoglyme	612	—	

 $(J(\text{BH}) = 112.0)$

TABLE 28 (cont.)

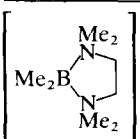
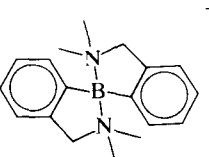
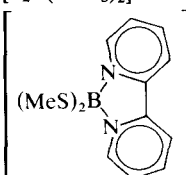
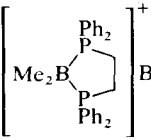
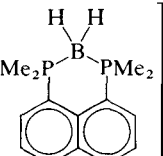
 $\delta^{11}\text{B}$  values of various chelate complexes.<sup>a</sup>

Compound	$\delta^{11}\text{B}$	Solvent	Ref.	Other nuclei	Ref.
	17.2	$\text{CDCl}_3$	620	—	
					
$\text{R}^{1c}$	$\text{R}^{2c}$				
$\text{CMe}_2\text{HCMe}_2$	H	14.0	THF	610	$^{13}\text{C}$ 610
Ph	H	10.7	$\text{DMSO-d}_6$	609	$^{15}\text{N}$ 611
Ph	Me	12.2	$\text{DMSO-d}_6$	609	$^{15}\text{N}$ 611
	$\text{R}^{1c}$ $\text{R}^{2c}$ Et H	11.8	DMF	616 617	— $^{13}\text{C}$ 617
	X = F 6.0 Br 8.5 I -25.6	$\text{CDCl}_3$ $\text{CDCl}_3$ $\text{CDCl}_3$	619 619 619	— — —	
	-0.9	$\text{CDCl}_3$	776	$^{19}\text{F}$	776
	11.8	$\text{CDCl}_3$	615	$^{13}\text{C}$	615

<sup>a</sup> Ref. 5, pp. 333–339 provides an extensive list of  $\delta^{11}\text{B}$  values for chelate complexes.<sup>b</sup>  $\text{C}_8\text{H}_{14}$  = carbon skeleton of the 9-borabicyclo[3.3.1]nonane system.<sup>c</sup> See Ref. 810 for further NMR data ( $^{11}\text{B}$ ,  $^{13}\text{C}$ ) of similar compounds.

TABLE 29

 $\delta^{11}\text{B}$  values of cationic tetracoordinate boron compounds.

Compound	$\delta^{11}\text{B}$	Solvent	Ref.	Other nuclei	Ref.
 $\text{Br}^-$	9.8	MeOH	5	—	
$[\text{Me}_2\text{B}(\text{pyridine})_2]^+ \text{Br}^-$	6.3	MeOH	5	—	
 $\text{Cl}^-$	10.1		763	$^{13}\text{C}$	763
$[\text{H}_2\text{B}(\text{NH}_3)_2]^+ \text{I}^-$	-14.1	$\text{D}_2\text{O}$	568	—	
$[\text{H}_2\text{B}(\text{pyridine})_2]^+$	2.1	$\text{CH}_2\text{Cl}_2$	641	—	
$[\text{F}_2\text{B}(\text{NMe}_3)_2]^+ \text{Br}^-$	1.9	$\text{CDCl}_3$	642	$^{19}\text{F}$	642
 $\text{Cl}^-$	11.5	$\text{CH}_2\text{Cl}_2$	644	—	
$[\text{Et}_2\text{B}(\mu\text{-pz})_2\text{B}(\mu\text{-pz})_2\text{BEt}_2]^{+a}$ $\text{PF}_6^-$	4.7( $\text{BEt}_2$ ) -2.2	$\text{DMSO-d}_6$	643		
$[\text{H}_2\text{B}(\mu\text{-pz})_2\text{B}(\mu\text{-pz})\text{BH}_2]^{+a}$ $\text{PF}_6^-$	-7.5( $\text{BH}_2$ ) -1.5	$\text{CD}_3\text{CN}$	643	$^{13}\text{C}$	643
 $\text{Br}^-$	-14.5		5		
$[\text{Me}_2\text{B}(\text{PMe}_3)_2]^+ \text{Br}^-$	-21.7		645	$^{13}\text{C}$ , $^{31}\text{P}$	645
 $\text{BH}_4^-$	-34.9 ( $J(\text{BH}) = 70.0$ ) -35.4( $\text{BH}_4^-$ ) ( $J(\text{BH}) = 85.5$ )		569	$^{13}\text{C}$ , $^{31}\text{P}$	569

<sup>a</sup> pz = N-pyrazolyl.

TABLE 30

 $\delta^{11}\text{B}$  values of some organylborates and zwitterionic adducts.<sup>a,b,c</sup>

Compound $[\text{RBH}_3]^-$	$\delta^{11}\text{B}$	Solvent	Ref.	Other nuclei	Ref.
R					
Me	-31.4(70.3) -30.9(73.0)	THF Et <sub>2</sub> O	500 501	—	
Et	-29.6(72.0)	Et <sub>2</sub> O	502	—	
iPr	-23.3(73.0)	THF	496	<sup>13</sup> C	406
Bu	-28.1(75.0) -29.0(74.0)	THF	501 500	—	
sBu	-25.4(77.0) -24.7(75.0)	THF	500 501	—	
tBu	-20.4(74.0) -21.2(77.7)	THF	501 500	<sup>13</sup> C	503
CHMe <sub>2</sub> CMe <sub>2</sub>	-29.0(73.0) <sup>d</sup>	Et <sub>2</sub> O	501	—	
c-C <sub>5</sub> H <sub>9</sub>	-26.3(75.0)	Et <sub>2</sub> O	501	—	
<i>trans</i> -2-Me—c-C <sub>5</sub> H <sub>8</sub>	-27.4(74.0)	Et <sub>2</sub> O	501	—	
c-C <sub>6</sub> H <sub>11</sub>	-24.5(73.0)	Et <sub>2</sub> O	501	—	
C <sub>6</sub> H <sub>5</sub>	-26.0(76.0)	Et <sub>2</sub> O	501	—	
[Me <sub>2</sub> (Ph)Si] <sub>3</sub> C			541	<sup>6</sup> Li	542
Me <sub>3</sub> SiCH <sub>2</sub>	-31.7(78.0)	THF	500		
PhCH <sub>2</sub>	-26.1(75.0)	C <sub>6</sub> D <sub>6</sub>	500	<sup>13</sup> C	496
Me <sub>2</sub> NCH <sub>2</sub>	-32.0(75.0)	C <sub>6</sub> D <sub>6</sub>	500	—	
CN	-43.9(90.0)		504	<sup>13</sup> C	505
C(O)OMe	-33.5		506		
[1-H <sub>3</sub> B—1,2-C <sub>2</sub> B <sub>10</sub> H <sub>11</sub> ] <sup>-</sup>	-20.4(88.0)		605	<sup>11</sup> B, <sup>13</sup> C	605
Me <sub>3</sub> P—CH <sub>2</sub> —BH <sub>3</sub>	-31.1(88.5)	CDCl <sub>2</sub>	764	<sup>13</sup> C, <sup>31</sup> P	764
Et <sub>3</sub> P—CH <sub>2</sub> —BH <sub>3</sub>	-32.0(88.5)	CD <sub>2</sub> Cl <sub>2</sub>	764	<sup>13</sup> C, <sup>31</sup> P	764
iPr <sub>3</sub> P—CH <sub>2</sub> —BH <sub>3</sub>	-33.7(87.0)	CDCl <sub>3</sub>	764	<sup>13</sup> C, <sup>31</sup> P	764
iPr <sub>3</sub> P—CH(Me)—BH <sub>3</sub>	-27.4(87.0)	CD <sub>2</sub> Cl <sub>2</sub>	764	<sup>13</sup> C, <sup>31</sup> P	764
tBu <sub>3</sub> P—CH <sub>2</sub> —BH <sub>3</sub>	-28.9(88.5)	C <sub>6</sub> D <sub>6</sub>	764	<sup>13</sup> C, <sup>31</sup> P	764
[R <sup>1</sup> R <sup>2</sup> BH <sub>2</sub> ] <sup>-</sup>					
R <sup>1</sup>	R <sup>2</sup>				
Me	Me	THF	500	—	
		Et <sub>2</sub> O	525	—	
Et	Et	Et <sub>2</sub> O	502	—	
		Et <sub>2</sub> O	825	—	
	—(CH <sub>2</sub> ) <sub>4</sub> —		507	—	
	—(CH <sub>2</sub> ) <sub>5</sub> —		507	—	
Pr	Pr	Et <sub>2</sub> O	825	—	
Bu	Bu		500	—	
iBu	iBu		507	—	
sBu	sBu		500	—	
tBu	tBu		500	—	
sBu	sBu		123	—	
sBu	tBu		123	—	

TABLE 30 (cont.)

 $\delta^{11}\text{B}$  values of some organylborates and zwitterionic adducts. <sup>a,b,c</sup>

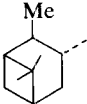
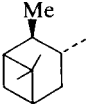
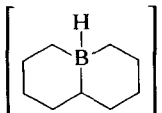
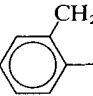


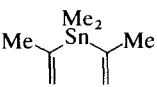

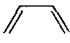
Compound $[\text{RBH}_3]^-$		$\delta^{11}\text{B}$	Solvent	Ref.	Other nuclei	Ref.
$\text{R}^1$	$\text{R}^2$					
$\text{C}_8\text{H}_{14}$		-17.8(70.0)		7	$^{13}\text{C}$	7
		-17.4(72.1)		509	—	
$\text{CHMe}_2\text{CHMe}$	$\text{CHMe}_2\text{CHMe}$	-12.3(68.0)		507	—	
$c\text{-C}_5\text{H}_9$	$c\text{-C}_5\text{H}_9$	-11.2(68.0)	$\text{Et}_2\text{O}$	825	—	
$c\text{-C}_6\text{H}_{11}$	$c\text{-C}_6\text{H}_{11}$	-9.3(67.0)		507	—	
		-4.8(69.0)	THF	509	—	
$\text{PhCH}_2$	$\text{PhCH}_2$	-12.9(72.0)	$\text{Et}_2\text{O}$	825	—	
Ph	Ph	-15.2		508	—	
CN	CN	-42.2(96.5)	1,4-Dioxane	7	$^{13}\text{C}$	7
$\text{Ph}_3\text{P}^+\text{CH}_2-\text{BH}_2\text{C}-\text{C}_6\text{H}_{11}$		-19.8	$\text{CDCl}_3$	519	$^{31}\text{P}$	519
$[\text{R}^1\text{R}^2\text{R}^3\text{BH}]^-$						
$\text{R}^1$	$\text{R}^2$	$\text{R}^3$				
Me	Me	Me	-21.0(66.6)	THF	500	—
Et	Et	Et	-12.9(70.0)	THF	510	—
			-12.8(70.0)	THF	511	—
Bu	Bu	Bu	-14.4(75.0)	THF	500	—
			-15.5(78.0)	THF	511	—
iBu	iBi	iBu	-18.4(68.0)	THF	511	—
sBu	sBu	sBu	-7.5(68.0)	THF	511	—
tBu	tBu	tBu	-2.3(83.0)	THF	500	—
$c\text{-C}_5\text{H}_9$	$c\text{-C}_5\text{H}_9$	$c\text{-C}_5\text{H}_9$	-10.7(65.0)	THF	511	—
$c\text{-C}_6\text{H}_{11}$	$c\text{-C}_6\text{H}_{11}$	$c\text{-C}_6\text{H}_{11}$	-8.0(70.0)	THF	511	—
Me	$c\text{-C}_6\text{H}_{11}$	$c\text{-C}_6\text{H}_{11}$	-12.0(60.0)	THF	512	—
Me		$\text{C}_8\text{H}_{14}$	-16.0(61.0)	THF	512	—
Ph		$\text{C}_8\text{H}_{14}$	-13.9(55.0)	THF	512	—
$\text{tBu}-\text{C}\equiv\text{C}$		$\text{C}_8\text{H}_{14}$	-20.0(66.0)	THF/hexane	7	—
Ph	Ph	Ph	-7.4(76.2)	$\text{Et}_2\text{O}$	496	—
			-11.8(70.0)	THF	511	—
			-12.2(68.0)	THF	511	—
(two isomers)						

TABLE 30 (cont.)

 $\delta^{11}\text{B}$  values of some organylborates and zwitterionic adducts.<sup>a, b, c</sup>

Compound $[\text{RBH}_3]^-$				$\delta^{11}\text{B}$	Solvent	Ref.	Other nuclei	Ref.
$[\text{R}^1\text{R}^2\text{R}^3\text{R}^4\text{B}]^-$	$\text{R}^1$	$\text{R}^2$	$\text{R}^3$	$\text{R}^4$				
Me	Me	Me	Me	-20.7	THF	500	$^{13}\text{C}$	513, 514
Et	Et	Et	Et	-16.6	THF	515	$^{13}\text{C}$	5
iPr	iPr	iPr	iPr	-15.4	THF	496	—	
Bu	Bu	Bu	Bu	-17.5	THF	500	$^{13}\text{C}$	516
	$\text{C}_8\text{H}_{14}$		$\text{C}_8\text{H}_{14}$	-19.8	THF	517	—	
	$\text{C}_8\text{H}_{14}$		Me	-19.2	THF	512	—	
	$\text{C}_8\text{H}_{14}$		Et	-17.8	THF	517	—	
c-C <sub>6</sub> H <sub>11</sub>	c-C <sub>6</sub> H <sub>11</sub>	Me	Me	-17.8	THF	512	—	
Et	Et	Et		-12.8	C <sub>6</sub> D <sub>6</sub>	490	$^{13}\text{C}$	490
	$\text{C}_8\text{H}_{14}$	Ph	Ph	-14.2	THF	512	—	
Et	Et	Et	$\text{C}\equiv\text{CH}$	-17.3	THF	518	—	
c-C <sub>6</sub> H <sub>11</sub>	tBu			-8.0	CD <sub>2</sub> Cl <sub>2</sub>	345	—	
c-C <sub>6</sub> H <sub>11</sub>	Ph			-9.5	Acetone-d <sub>6</sub>	345	—	
Bu	Bu			-16.9	C <sub>6</sub> D <sub>6</sub>	65	$^{13}\text{C}$ , $^{119}\text{Sn}$	65
Ph	Ph			-7.3	Acetone-d <sub>6</sub>	345	—	
	$\text{C}_8\text{H}_{14}$	$\text{C}\equiv\text{CtBu}$	$\text{C}\equiv\text{CtBu}$	-22.7	THF/hexane	7	—	
Ph	Ph	Ph	Ph	-6.3	CH <sub>3</sub> CN	107	$^{13}\text{C}$	513, 520, 521, 522
$\text{C}_6\text{H}_{13}\text{C}\equiv\text{C}$		$\text{C}_6\text{H}_{13}\text{C}\equiv\text{C}$		-33.6	THF	523	—	
	$\text{C}_6\text{H}_{13}\text{C}\equiv\text{C}$		$\text{C}_6\text{H}_{13}\text{C}\equiv\text{C}$					
Ph $\text{C}\equiv\text{C}$	Ph $\text{C}\equiv\text{C}$	Ph $\text{C}\equiv\text{C}$	Ph $\text{C}\equiv\text{C}$	-31.0	CDCl <sub>3</sub>	524	$^{13}\text{C}$	524
Et	Et	Et	CN	-17.0	THF	517	—	
Ph	$\text{C}\equiv\text{N}$			-15.3	Acetone-d <sub>6</sub>	378	—	
$[\text{B-Me-1-boraadamantane}]^-$				-20.3	Et <sub>2</sub> O/THF	525	—	

<sup>a</sup> The  $\delta^{11}\text{B}$  values vary with the cation and with the solvent; a range of approximately 1.5 ppm for each compound may be observed.

<sup>b</sup> For further data see Ref. 7.

<sup>c</sup>  $^1J(^{11}\text{B}^1\text{H})$  values in parentheses.

<sup>d</sup> Should be remeasured.

TABLE 31

 $\delta^{11}\text{B}$  values of borates with boron–element bonds.\*

Compound	$\delta^{11}\text{B}$	Solvent	Ref.	Other nuclei	Ref.
$[\text{BF}_4]^-$	0.1 to $-2.3^{b,c}$		5	$^{19}\text{F}$	526
$[\text{BCl}_4]^-$	4.5 to 8.0		5	—	
$[\text{BBr}_4]^-$	$-23.0$ to $-26.0$		5	—	
$[\text{BI}_4]^-$	$-128$		5	—	
$[\text{B(OR)}_4]^-$	1.1 to 3.5		5, 527, 528, 529, 530, 813	$^{13}\text{C}$	529, 531
$[\text{B(OP(O)F}_2)_4]^-$	$-4.4$	—	607	$^{19}\text{F}$ , $^{31}\text{P}$	607
$[\text{B(SPh)}_4]^-$	6.3		204	—	
$[\text{B(NHMe)}_4]^-$	0.2	THF	107	—	
$\left[ \text{B} \left( \text{N} \begin{array}{c} \diagup \text{X} \diagdown \\ \diagdown \diagup \end{array} \right)_4 \right]^-$ X = CH, N	1.0		5		
$[\text{B(NMe}_2\text{pz)}_3]^-$ , pz = <i>N</i> -pyrazolyl	2.7	DMSO- $d_6$	640	—	
$[\text{B(NO}_3)_4]^-$	5.3		5		
$[\text{B(NS(O)F}_2)_4]^-$	8.0	$\text{CD}_3\text{CN}$	533	$^{19}\text{F}$	533
$[\text{B(PEt}_2)_4]^-$	$-21.0$ ( $J(\text{PB}) = 32.2$ )	$\text{Et}_2\text{O}$	534	$^{31}\text{P}$	
$[\text{B(SiMe}_3)_4]^-$	$-53.4$ ( $J(\text{SiB}) = 48.0$ )	THF	535	$^{13}\text{C}$ , $^{29}\text{Si}$	535
$[\text{BuBF}_3]^-$	2.9, 0.4 ( $J(\text{FB}) = 65.0$ )	HMPA, $\text{Et}_2\text{O}$	540	$^7\text{Li}$	540
$[\text{PhBCl}_3]^-$	9.7		536		
$[\text{Ph}_2\text{BCl}_2]^-$	11.0		536		
$[\text{MeB(OMe)}_3]^-$	6.0	MeOH	123	—	
$[\text{Me}_2\text{B(OMe)}_2]^-$	14.4	MeOH	123	—	
$[\text{C}_8\text{H}_{14}\text{B(OH)}_2]^{-d}$	3.1	THF	7	—	
$[\text{C}_8\text{H}_{14}\text{B(OC(O)H)}_2]^{-d}$	8.0	THF	7	—	
$[\text{Me}_3\text{BOMe}]^-$	$-1.0$	MeOH	123	—	
$[\text{B-MeO-1-bora-adamantane}]^-$	$-3.1$	MeOH/THF	525	—	
$\left[ \text{C}_8\text{H}_{14}\text{B} \begin{array}{c} \text{H} \\ \diagup \quad \diagdown \\ \text{OCMe}_2\text{CHMe}_2 \end{array} \right]^-$	$-2.8$	THF	537	—	
$\left[ \text{Me(H)B} \begin{array}{c} \diagup \text{O} \diagdown \\ \diagdown \text{O} \diagup \end{array} \right]^-$	9.3	THF	650	—	
$\left[ \text{tBu(H)B} \begin{array}{c} \diagup \text{O} \diagdown \\ \diagdown \text{O} \diagup \end{array} \right]^-$	7.0 ( $J(\text{BH}) = 75$ )	THF	650	—	

TABLE 31 (*cont.*) $\delta^{11}\text{B}$  values of borates with boron—element bonds.<sup>a</sup>

Compound	$\delta^{11}\text{B}$	Solvent	Ref.	Other nuclei	Ref.
$[\text{Me}_3\text{BNHMe}]^-$	-9.5	$\text{Et}_2\text{O}/$ TMEDA	272	—	
$[\text{Et}_3\text{BNH}_2]^-$	-9.8	$\text{C}_7\text{H}_8$	7	—	
$[\text{C}_6\text{H}_{14}\text{BEtNH}_2]^-$	-10.6	$\text{C}_6\text{D}_6$	7	—	
$[\text{Ph}_3\text{BNH}_2]^-$	-6.0	THF	7	—	
$[\text{Et}_3\text{B}-\text{PPh}_2]^-$	-8.1	THF	7	—	
$[\text{MeB}(\text{SiMe}_3)_3]^-$	-45.3 ( $J(\text{SiB}) = 53.0$ )	$\text{C}_6\text{D}_6$	535, 538	$^{13}\text{C}$	535
$[\text{Me}_2\text{B}(\text{SiMe}_3)_2]^-$	-36.1 ( $J(\text{SiB}) = 63.0$ )	Hexane	538	$^{13}\text{C}$	535
$\left[ \begin{array}{c} \text{Cyclopentyl} \\ \text{B}(\text{SiMe}_3)_2 \end{array} \right]^-$	-31.2	$\text{C}_6\text{D}_6$	535	—	
$[\text{C}_8\text{H}_{14}\text{B}(\text{SiMe}_3)_2]^{-d}$	-25.0 ( $J(\text{SiB}) = 65.0$ )	THF	538	$^{13}\text{C}$	535
$[\text{Me}_3\text{BSiMe}_3]^-$	-28.5 ( $J(\text{SiB}) = 74.0$ )	$\text{C}_6\text{D}_6$	538	$^{13}\text{C}$	535
$[\text{Me}_3\text{BSi}(\text{SiMe}_3)_3]^-$	-17.9	$\text{C}_7\text{D}_8$	539	$^{13}\text{C}$	539
$[\text{C}_8\text{H}_{14}\text{B}(\text{Me})\text{SiMe}_3]^{-d}$	-23.0	$\text{C}_6\text{D}_6$	535	$^{13}\text{C}$	535
$[\text{H}_3\text{BOH}]^-$	-13.9(82.0)		543	—	
	-13.2(87.0)		639	—	
$[\text{H}_3\text{BSH}]^-$	-25.0(94)	THF	544	—	
$[\text{H}_2\text{B}(\text{SH})_2]$	-14.5(114)	THF	544	—	
$[\text{HB}(\text{SMe})_3]^-$	0.9(122)	Diglyme	5	—	
$[\text{H}_3\text{BNMe}_2]^-$	-14.7(87)	Monoglyme	545	—	
$\left[ \begin{array}{c} \text{N} \\ \text{H}_2\text{B}(\text{N} \text{---} \text{C}_4\text{H}_4) \end{array} \right]^-$	-7.4(96)	THF	546	—	
$\left[ \begin{array}{c} \text{N} \\ \text{HB}(\text{N} \text{---} \text{C}_4\text{H}_4)_3 \end{array} \right]^{-e}$	-1.5(105)		546	—	
$[\text{H}_3\text{B}-\text{PH}_2]^-$	-37.3(90) ( $J(\text{PB}) = 29$ )		547	$^{31}\text{P}$	547
$\begin{array}{c} \text{Me}_2 \\   \\ \text{Me}_2\text{Au} \text{---} \text{P} \text{---} \text{BH}_2 \\   \quad   \\ \text{P} \quad \text{P} \\   \quad   \\ \text{Me}_2 \end{array}$	-32.7 ( $J(\text{BH}) = 95$ ) ( $J(\text{PB}) = 95$ )	$\text{C}_6\text{D}_6$	761	$^{13}\text{C}, ^{31}\text{P}$	761
$\begin{array}{c} \text{Me}_2 \quad \text{Me}_2 \\   \quad   \\ \text{H}_2\text{B} \text{---} \text{P} \text{---} \text{Au} \text{---} \text{P} \text{---} \text{BH}_2 \\   \quad   \quad   \quad   \\ \text{Me}_2 \quad \text{P} \quad \text{P} \quad \text{P} \\   \quad   \quad   \\ \text{Me}_2 \end{array}$	-29.0 ( $J(\text{BH}) = 92.5$ ) ( $J(\text{PB}) = 96.8$ )	$\text{C}_6\text{D}_6$	761	$^{13}\text{C}, ^{31}\text{P}$	761

TABLE 31 (*cont.*)

 $\delta^{11}\text{B}$  values of borates with boron–element bonds.<sup>a</sup>

Compound	$\delta^{11}\text{B}$	Solvent	Ref.	Other nuclei	Ref.
$[\text{H}_3\text{B—SiMe}_3]^-$	–42.7(77.7) ( $J(\text{SiB}) = 74.0$ )	THF	133	$^{13}\text{C}$	133
$[\text{H}_3\text{B—SiF}_3]^{-f}$	–55.6(85.0)	$\text{CH}_2\text{Cl}_2$	548	$^{19}\text{F}$	548
$[\text{H}_2\text{B}(\text{SiF}_3)_2]^{-f}$	–46.9(86.0)	$\text{CH}_3\text{Cl}_2$	548	$^{19}\text{F}$	548
$[\text{H}_3\text{B—GeMe}_3]^-$	–40.5(81.3)	THF	133	—	—
$[\text{H}_3\text{B—SnMe}_3]^-$	–43.7(91.0)	THF	133	$^{13}\text{C}$ , $^{119}\text{Sn}$	133

<sup>a</sup> See Ref. 5 for further data.

<sup>b</sup> For  $[\{\text{U}(\eta\text{-C}_5\text{H}_3(\text{SiMe}_3)_2)_2(\mu\text{-BF}_4)(\mu\text{-F})\}_2]$  an equilibrium in solution between the dimer and the monomer has been observed by  $^{11}\text{B}$ ,  $^{19}\text{F}$  and  $^1\text{H}$  NMR; the paramagnetic species show  $^{11}\text{B}$  resonances at  $\delta^{11}\text{B} = -120.7$  (monomer) and  $-131.9$  (dimer).<sup>782</sup>
<sup>c</sup> Ref. 815 gives  $^{11}\text{B}$  and  $^{19}\text{F}$  NMR data for fluoroperoxide compounds of boron of the type  $[\text{BF}_{4-n}(\text{OOH})_n]^-$  with  $n = 1, 2, 3$ .

<sup>d</sup>  $\text{C}_8\text{H}_{14}\text{B} = 9\text{-borabicyclo}[3.3.1]\text{nonyl}$ .

<sup>e</sup> Ref. 822 lists  $^{11}\text{B}$  NMR data for hydrotris(3,5-dimethylpyrazolyl)borates of the type  $\text{MCl}_2(\text{cp})(\text{HBpz}_3)$  ( $\text{M} = \text{Th}(\text{IV})$ ,  $\text{U}(\text{IV})$ ,  $\text{MCl}_3(\text{HBpz}_3)\text{—THF}$ ,  $\text{MCl}_2(\text{NPh}_2)_3(\text{HBpz}_3)$  and  $\text{MCl}_2[\text{N}(\text{SiMe}_3)_2](\text{HBpz}_3)$ .

<sup>f</sup> Assignment in Ref. 548 has been corrected.

TABLE 32

 $\delta^{11}\text{B}$  values of some metal borates.<sup>a</sup>

Compound	$\delta^{11}\text{B}$	Solvent	Ref.	Other nuclei	Ref.
$\text{Li}[\text{BH}_4]$	–38 to –41.6		5		
$\text{Li}[\text{BD}_4]$	( $\Delta\delta^i - 0.558$ )		549		
$\text{Na}[\text{BH}_4]$	–38.7 to –43.6		5		
$[\text{Bu}_4\text{N}][\text{BH}_4]$	–34.8	$\text{CH}_2\text{Cl}_2$	548	—	
	–36.0 to –40.5		5		
$\text{Zr}(\text{BH}_4)_4$	–8.0(90)	$\text{C}_7\text{D}_8$	550	$^{91}\text{Zr}$	550
$[(\text{cp})_2\text{Zr}(\text{Me})\text{BH}_4]$	–3.4(86.0)	THF	762	—	
$[(\text{cp})_2\text{Zr}(\text{Me})\text{H}_3\text{BMe}]^b$	7.7(73.0)	THF	762	—	
$[(\text{cp})_2\text{Zr}(\text{H})\text{H}_2\text{BMe}_2]^b$	15.8(40.0)	THF	762	—	
$\text{Sc}(\text{NH}_4)_3$	–18.7(80)	$\text{C}_6\text{D}_6$	551	$^{45}\text{Sc}$	551
$\text{Y}(\text{BH}_4)_3$	–23.2(84)	$\text{C}_6\text{D}_6$	551	—	
$[\text{FeH}[\text{dmpe}]\text{BH}_4]$	–38.1(82)	$\text{C}_7\text{D}_8$	552	$^{31}\text{P}$	552
$[(\mu\text{-H})\text{Fe}_3(\text{CO})_9(\mu_3\text{-BH}_4)]^c$	1.8 (broad)	$\text{C}_6\text{D}_6$	654	—	

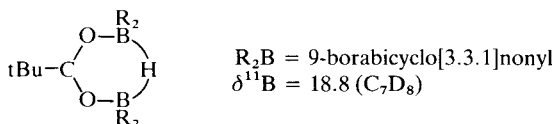
TABLE 32 (cont.)

 $\delta^{11}\text{B}$  values of some metal borates.<sup>a</sup>

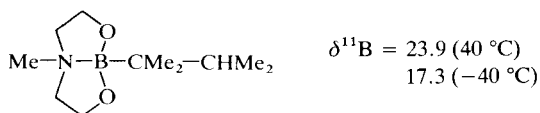
Compound	$\delta^{11}\text{B}$	Solvent	Ref.	Other nuclei	Ref.
$[(\mu\text{-H})\text{Fe}_3(\text{CO})_9(\mu_3\text{-BH}_3\text{Me})]^\text{c}$	22.1(40.0)	Hexane	656	—	
$[(\mu\text{-H})(\mu\text{-CO})\text{Fe}_3(\text{CO})_9\text{BH}_2]^\text{c}$	56.0(145, 50)	$\text{C}_6\text{D}_6$	655	—	
$[(\mu\text{-H})\text{Fe}_3(\text{CO})_9(\mu_2\text{-BH}_3)]^\text{c}$	6.2(96, 58)	Acetone- $\text{d}_6$	656	—	
$[(\mu\text{-H})\text{Fe}_3(\text{CO})_9(\mu_2\text{-BH}_2\text{Me})]^\text{c}$	29.3(53)	Acetone- $\text{d}_6$	656	—	
$[\text{Ru}(\text{CO})(\text{H})(\text{PiPr}_3)_2\text{BH}_4]$	8.9	$\text{C}_6\text{D}_6$	553	$^{31}\text{P}$	553
$[\text{Os}(\text{CO})(\text{H})(\text{PiPr}_3)_2\text{BH}_4]$	14.85	$\text{C}_6\text{D}_6$	553	$^{31}\text{P}$	553
$[\text{Co}(\text{terpy})\text{BH}_4]^\text{b}$	12.9(80)	Acetone- $\text{d}_6$	554	—	
$[\text{Th}(\text{MeBH}_3)_4\text{OEt}_2]^\text{d}$	-1.0	$\text{C}_7\text{D}_8$	555	$^{13}\text{C}$	555

<sup>a</sup> For an extensive list of  $\delta^{11}\text{B}$  values see Ref. 5.<sup>b</sup> Assumed structure.<sup>c</sup> See Ref. 824 for  $\text{Fe}_4(\text{CO})_{12}[\text{Au}(\text{PPh}_3)]_2\text{BH}$ ;  $\delta^{11}\text{B} = +141.3$ ;  $\delta^{31}\text{P} = 53.0$ .<sup>d</sup>  $^{11}\text{B}$  and  $^{13}\text{C}$  NMR data of  $\text{U}(\text{MeBH}_3)_4$ , Ref. 827.

A new type of  $\mu$ -diborane has been characterized by X-ray crystallography,  $^{11}\text{B}$  and  $^{13}\text{C}$  NMR, with a carboxyl group as a bridging ligand:<sup>282</sup>

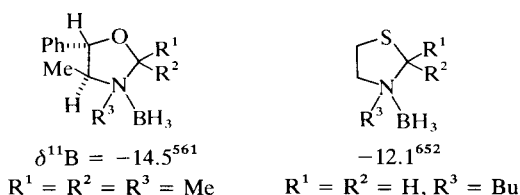


(b) *Lewis-base-borane adducts* (Tables 22–29). All trends in the  $\delta^{11}\text{B}$  values of Lewis-base-borane adducts have been stated in previous accounts.<sup>5,7</sup> It is noteworthy that the temperature dependence of  $^{11}\text{B}$  NMR signals is useful in the evaluation of the coordinative bond, for example in the case of the (*N-B*)-perhydro-2-thexyl-6-methyl-1,3-dioxo-6-aza-2-boracine<sup>610</sup>



Competition between various sites of coordination of a borane may be studied by  $^{11}\text{B}$  NMR. For a series of five-membered heterocycles, coordination occurs at the nitrogen atom and the attack of the borane takes

place preferably at the sterically less hindered position.<sup>561,562,652</sup>



(c) *Borates* (Tables 30–32). A large amount of  $\delta^{11}\text{B}$  data for organylborates has become available (see Table 30). Therefore a correlation between  $\delta^{13}\text{C}$  (alkanes) and  $\delta^{11}\text{B}$  (organylborates) can now be based on more data pairs:

$$\delta^{11}\text{B} = 0.52\delta^{13}\text{C} - 36.1 \quad (r = 0.988). \quad (18)$$

There are also a considerable number of new borates with boron–element bonds (Table 31), including B–Si, B–Ge and B–Sn bonds. In this context a comparison between the  $\text{Me}_3\text{Si}^-$ ,  $\text{F}_3\text{Si}^-$  anions and the  $\text{PMe}_3$ ,  $\text{PF}_3$  ligands is of interest:

	$[\text{H}_3\text{B}-\text{SiMe}_3]^-$	$\Delta^{11}\text{B}$	$[\text{H}_3\text{B}-\text{SiF}_3]^-$
$\delta^{11}\text{B} =$	$\begin{cases} -42.7 \\ -36.8 \end{cases}$	$\begin{matrix} 12.9 \\ 12.7 \end{matrix}$	$\begin{matrix} -55.6 \\ -49.5 \end{matrix}$
	$\text{H}_3\text{B}-\text{PMe}_3$		$\text{H}_3\text{B}-\text{PF}_3$

The extreme shielding effect of the  $\text{SiF}_3^-$  and  $\text{PF}_3$  groups on the  $^{11}\text{B}$  nucleus is not understood at present. The general interest in the influence of fluorine ligands on molecular properties should stimulate further work in this direction.

(d) *Organylboron  $\pi$  complexes* (Tables 33–38).  $^{11}\text{B}$  NMR has played an important role in the development of the chemistry of organylboron  $\pi$  complexes.<sup>377</sup> A large amount of data has been compiled in previous reviews.<sup>5,7</sup> Therefore this section deals only with some recent results, and Tables 33–38 list some data for representative compounds. The most common ligands are the borinato system<sup>16</sup> (Table 34), borole derivatives<sup>67,84,378–385</sup> (Table 36), heteroborole compounds<sup>15,158,219,386,409,455,460,817</sup> (Table 37), alkenylboranes<sup>410–419,461,817</sup> (Table 33) and a great number of various boron–oxygen,<sup>416,425</sup> –sulphur<sup>422–424</sup> and –nitrogen<sup>390,418–421</sup> compounds (Tables 37, 38). In addition to the transition-metal complexes, there is growing interest in  $\pi$  complexes of main-group elements.<sup>426–431</sup> For

TABLE 33

 $\delta^{11}\text{B}$  values of some alkenylborane-metal complexes.<sup>a</sup>

Compound		$\delta^{11}\text{B}$	Solvent	Ref.	Other nuclei	Ref.
$\text{M} \left[ (\text{CH}_2)_n \begin{array}{c} \diagup \quad \diagdown \\ \text{C} \quad \text{C} \\ \diagdown \quad \diagup \end{array} \text{B-Ph} \right]$						
M	n					
[Cr(CO) <sub>4</sub> ]	2	29.7	CDCl <sub>3</sub>	465	—	
[Mo(CO) <sub>4</sub> ]	2	28.3	CDCl <sub>3</sub>	465	—	
[W(CO) <sub>4</sub> ]	2	27.2	CDCl <sub>3</sub>	465	—	
[Mncp(CO)]	2	26.5	CDCl <sub>3</sub>	465	—	
[Fe(CO) <sub>3</sub> ]	1	23.0	C <sub>6</sub> D <sub>6</sub>	413	—	
[Cocp]	1	21.6	C <sub>2</sub> Cl <sub>4</sub>	450	—	
[Co(C <sub>5</sub> H <sub>5</sub> B—Ph)]	1	20.9	C <sub>6</sub> D <sub>6</sub>	450	—	
		(single resonance)				
[RhC <sub>5</sub> Me <sub>5</sub> ]	1	17.3	C <sub>2</sub> Cl <sub>4</sub>	450	—	
[NiL]	2	28.3	C <sub>6</sub> D <sub>6</sub>	415	<sup>13</sup> C	415
[PdL]	2	28.0	CDCl <sub>3</sub>	415	<sup>13</sup> C	415
[PtL]	2	27.0	CDCl <sub>3</sub>	415	<sup>13</sup> C	415
$\text{M} \left[ \begin{array}{c} \text{CH}_2=\text{CH} \\ \diagdown \quad \diagup \\ \text{CH}_2=\text{CH} \end{array} \text{B-X} \right]$						
M	X					
[RhC <sub>5</sub> Me <sub>5</sub> ]	Me	23.6	C <sub>6</sub> D <sub>6</sub>	414	—	
[RhC <sub>5</sub> Me <sub>5</sub> ]	Ph	21.3	C <sub>6</sub> D <sub>6</sub>	414	—	
[Ru(CO) <sub>3</sub> ]	Cl	27.7	C <sub>6</sub> D <sub>6</sub>	414	—	
[RhC <sub>5</sub> Me <sub>5</sub> ]	OMe	25.7	C <sub>6</sub> D <sub>6</sub>	414	—	
$\text{M} \left[ \begin{array}{c} \text{C} \quad \text{C} \\ \diagdown \quad \diagup \end{array} \text{B-Ph} \right]$						
M = [Co(CO) <sub>3</sub> ]		20.9	C <sub>6</sub> D <sub>6</sub>	413	<sup>13</sup> C	413
[Co(CO) <sub>2</sub> PMe <sub>3</sub> ]		19.6	C <sub>6</sub> D <sub>6</sub>	413	<sup>13</sup> C	413
[Ni(C <sub>5</sub> H <sub>5</sub> B—Ph)]		24.4	C <sub>6</sub> D <sub>6</sub>	413	<sup>13</sup> C	413
		(single resonance)				
$\text{M} \left[ \begin{array}{c} \text{C} \quad \text{C} \\ \diagdown \quad \diagup \end{array} \text{B-Ph} \right]$						
M = [Co(CO) <sub>3</sub> ]		38.6	C <sub>6</sub> D <sub>6</sub>	413	<sup>13</sup> C	413
[Co(CO) <sub>2</sub> PMe <sub>3</sub> ]		30.8	C <sub>6</sub> D <sub>6</sub>	413	<sup>13</sup> C	413

TABLE 33 (cont.)

 $\delta^{11}\text{B}$  values of some alkenylborane-metal complexes.<sup>a</sup>

Compound	$\delta^{11}\text{B}$	Solvent	Ref.	Other nuclei	Ref.
$[\text{Rh}(\text{COD})] \left[ \text{Cycloheptatriene-B-Ph} \right]$	35.0	$\text{C}_6\text{D}_6$	417	—	
$[\text{Cocp}] \left[ \begin{array}{c} \text{Et} \quad \text{Et} \\ \diagdown \quad \diagup \\ \text{R}^1\text{-B} \quad \text{B-R}^1 \\ \diagup \quad \diagdown \\ \text{R}^2 \quad \text{R}^3 \end{array} \right]$					
$\text{R}^1 \quad \text{R}^2 \quad \text{R}^3$					
Et    Me    H	27.5	$\text{C}_6\text{D}_6$	461	$^{13}\text{C}$	461
Me    H    H	27.3	$\text{C}_6\text{D}_6$	461	$^{13}\text{C}$	461
Et    Me    Me	42.0	$\text{C}_6\text{D}_6$	461	$^{13}\text{C}$	461
Me    Me    Me	41.6	$\text{C}_6\text{D}_6$	461	$^{13}\text{C}$	461
$\text{Me}_2\text{B} \begin{array}{c} \diagup \\ \text{C} \\ \diagdown \end{array} \text{Pt}(\text{PEt}_3)_2$ (b) Me BMe <sub>2</sub> (a)	40.0(a) 73.6(b)	$\text{C}_7\text{D}_8$	382	$^{13}\text{C}, ^{31}\text{P}$ $^{195}\text{Pt}$	382
$\begin{array}{c} \text{Et} \quad \text{BEt}_2 \\ \diagdown \quad \diagup \\ \text{H} \quad \text{C} \quad \text{Pt}(\text{depe}) \\ \diagup \quad \diagdown \\ \text{B} \quad \text{H} \\   \\ \text{Et} \end{array}$	46.0 (single resonance)	$\text{C}_7\text{D}_8$	382	$^{13}\text{C}, ^{31}\text{P}$ $^{195}\text{Pt}$	382
$[\text{Fe}(\text{CO})_3] \left[ \text{Cyclohexadiene-B-OMe} \right]$	38.8		445	—	
$[\text{Fe}(\text{CO})_3] \left[ \begin{array}{c} \text{Et} \quad \text{Me} \\ \diagdown \quad \diagup \\ \text{Et-B} \quad \text{SiMe}_2 \\   \\ \text{Me} \end{array} \right]$	18.2	$\text{C}_7\text{D}_8$	418	$^{13}\text{C}$	418
$[\text{Fe}(\text{CO})_3] \left[ \begin{array}{c} \text{CH}_2=\text{CH} \\ \diagdown \quad \diagup \\ \text{Me}_2\text{N} \quad \text{B-Br} \end{array} \right]$	27.2		466	—	

<sup>a</sup> L = borane as the ligand shown in the preceding formula.

TABLE 34

 $\delta^{11}\text{B}$  values of some borabenzene-metal complexes.<sup>a</sup>

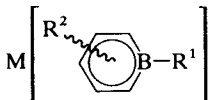
Compound		$\delta^{11}\text{B}$	Solvent	Ref.	Other nuclei	Ref.
						
M	R <sup>1</sup>	R <sup>2</sup>				
[HgCl]	Me	H	35.2	CD <sub>3</sub> CN, 50 °C	439	—
[HgCl]	Ph	H	33.0	CD <sub>3</sub> CN, 50 °C	439	—
[V(CO) <sub>4</sub> ]	Me	H	28.7	C <sub>6</sub> D <sub>6</sub>	439	—
[V(CO) <sub>4</sub> ]	Ph	H	26.0	Acetone-d <sub>6</sub>	439	—
Na[Cr(CO) <sub>3</sub> ] <sup>-</sup>	Me	H	24.6	D <sub>2</sub> O	452	—
Ph <sub>4</sub> P[Cr(CO) <sub>3</sub> ] <sup>-</sup>	Me	H	23.1	THF	452	—
Hg <sub>2</sub> [Cr(CO) <sub>3</sub> ] <sup>-</sup>	Me	H	26.7	THF	452	—
[Cr(CO) <sub>3</sub> ]	C <sub>5</sub> H <sub>5</sub> N	H	22.3	CD <sub>2</sub> Cl <sub>2</sub>	432	—
[Mo(CO) <sub>3</sub> ]	C <sub>5</sub> H <sub>5</sub> N	H	23.5	CD <sub>2</sub> Cl <sub>2</sub>	432	—
[W(CO) <sub>3</sub> ]	C <sub>5</sub> H <sub>5</sub> N	H	22.9	CD <sub>2</sub> Cl <sub>2</sub>	432	—
[Mn(CO) <sub>3</sub> ]	Me	H	26.8	Acetone-d <sub>6</sub>	440	—
[Mn(CO) <sub>3</sub> ]	Ph	H	24.6	Acetone-d <sub>6</sub>	441	—
[Mn(CO) <sub>3</sub> ]	Ph	4Me	22.7		442	—
[Mn(CO) <sub>3</sub> ]	Me	2-C(O)Me	30.0	CD <sub>2</sub> Cl <sub>2</sub>	440	—
[Re(CO) <sub>3</sub> ]	Ph	4-Me	22.4		442	—
[Fe <sub>2</sub> Cp]	Me	H	18.9		443	—
[Fe <sub>2</sub> Cp]	Ph	H	15.2		443	—
[LFe]	Me	H	20.5	CDCl <sub>3</sub>	444	—
[LFe]	tBu	H	24.6	CDCl <sub>3</sub>	444	—
[LFe]	Ph	H	14.4	CDCl <sub>3</sub>	444	—
[LFe]	Ph	4-Me	15.5		442	—
[LFe]	H	H	13.6		445	—
$J(^{11}\text{B}^1\text{H}) = 129.4$						
[Fe(toluene)] <sup>+</sup>	Ph	H	22.7		443	—
[Co(CO) <sub>2</sub> ]	Ph	H	20.4		446	—
[CoC <sub>4</sub> Me <sub>4</sub> ]	Me	H	23.1	CDCl <sub>3</sub>	451	—
[CoC <sub>4</sub> Me <sub>4</sub> ]	Me	2-C(O)H	26.4	C <sub>2</sub> Cl <sub>4</sub>	451	—
[CoC <sub>4</sub> Me <sub>4</sub> ]	Me	2-C(O)Me	23.7	C <sub>2</sub> Cl <sub>4</sub>	451	—
[Co(COD)]	Ph	H	20.9	C <sub>6</sub> D <sub>6</sub>	447	<sup>59</sup> Co 770
[Co <sub>2</sub> Cp] <sup>+</sup>	Ph	H	23.3	Acetone-d <sub>6</sub>	449	—
[LRu]	Me	H	12.4	CDCl <sub>3</sub>	448	—
[LRu]	Ph	H	14.4	C <sub>6</sub> D <sub>6</sub>	448	—
[RuC <sub>6</sub> H <sub>6</sub> ] <sup>+</sup>	Ph	H	18.2	Acetone-d <sub>6</sub>	450	—
[Rh(COD)]	Me	H	23.5	C <sub>6</sub> D <sub>6</sub>	448	—
[Rh(COD)]	Ph	H	20.9	C <sub>6</sub> D <sub>6</sub>	448	—

TABLE 34 (cont.)

 $\delta^{11}\text{B}$  values of some borabenzene-metal complexes.<sup>a</sup>

Compound			$\delta^{11}\text{B}$	Solvent	Ref.	Other nuclei	Ref.
$[\text{RhC}_5\text{Me}_5]^+$	Ph	H	21.3	$\text{CD}_3\text{CN}$	450	—	
$[\text{LOs}]$	Ph	H	19.8	$\text{CDCl}_3$	448	—	
$[\text{IrC}_5\text{Me}_5]^+$	Ph	H	17.7	$\text{CD}_3\text{CN}$	450	—	
$[\text{PtMe}_3]$	Ph	H	24.4	$\text{C}_6\text{D}_6$	448	—	
$[\text{LFe}]$	Ome	H	23.6		445	—	

<sup>a</sup> L = borane as the ligand shown in the preceding formula.

TABLE 35

 $\delta^{11}\text{B}$  values of some diborabenzene-metal complexes.<sup>a</sup>

Compound			$\delta^{11}\text{B}$	Solvent	Ref.	Other nuclei	Ref.
$\text{M} \left[ \begin{array}{c} \text{R}^2 \quad \text{R}^2 \\ \diagdown \quad \diagup \\ \text{R}^1 - \text{B} \quad \text{B} - \text{R}^1 \\ \diagup \quad \diagdown \\ \text{R}^2 \quad \text{R}^2 \end{array} \right]$							
M		R <sup>1</sup>	R <sup>2</sup>				
$[\text{Cocp}]$	Me	H	24.0	$\text{CS}_2$	433	—	
$[\text{Cocp}]$	Ph	H	22.0	$\text{CS}_2$	433	—	
$[\text{Cocp}]$	$\text{C}_5\text{H}_4\text{Fecp}$	H	21.0	$\text{CS}_2$	433	—	
$[\text{Cocp}]$	H	H	17.2	$\text{CS}_2$	433	—	
$(^1J(^{11}\text{B}^1\text{H}) = 125.0)$							
$[\text{Cocp}]$	Cl	H	24.0	$\text{CS}_2$	433	—	
$[\text{Cocp}]$	OMe	H	24.0	$\text{CS}_2$	433	—	
$[\text{Cocp}]$	$\text{NMe}_2$	H	22.0	$\text{CS}_2$	433	—	
$[\text{RhC}_5\text{Me}_5]$	Me	H	19.0	$\text{CS}_2$	433	—	
$[\text{RhC}_5\text{Me}_5]_2$	Me	H	8.0	$\text{CO}_3\text{NO}_3$	454	—	
$[\text{RhC}_5\text{Me}_5]$	H	H	14.0	$\text{CS}_2$	433	—	
$(J(^{11}\text{B}^1\text{H}) = 119)$							
$[\text{RhC}_5\text{Me}_5]$	OMe	H	24.0	$\text{CS}_2$	433	—	
$[\text{LNi}]$	Me	H	32.0	$\text{CS}_2$	433	—	
$[\text{LNi}]$	Ph	H	27.0	$\text{CS}_2$	433	—	
$[\text{Ni}(\text{CO})_2]$	$\text{C}_5\text{H}_4\text{Fecp}$	H	31.0	$\text{C}_7\text{D}_8$	84	—	
$[\text{Fe}(\text{CO})_3]$	F	Me	22.7	$\text{C}_6\text{H}_6$	453	$^{19}\text{F}$	453
$[\text{Cocp}]$	F	Me	23.1	$\text{C}_6\text{H}_6$	453	$^{19}\text{F}$	453
$[\text{Ni}(\text{CO})_2]$	F	Me	24.9	$\text{C}_6\text{H}_6$	453	$^{19}\text{F}$	453

TABLE 35 (cont.)

 $\delta^{11}\text{B}$  values of some diborabenzene-metal complexes.<sup>a</sup>

Compound			$\delta^{11}\text{B}$	Solvent	Ref.	Other nuclei	Ref.
[Ni(COD)]	F	Me	22.0	C <sub>6</sub> H <sub>6</sub>	453	<sup>19</sup> F	453
[LNi]	F	Me	21.7	C <sub>6</sub> H <sub>6</sub>	453	<sup>19</sup> F	453
$\text{M} \left[ \begin{array}{c} \text{iPr}_2\text{N} \\   \\ \text{B} \\   \quad   \\ \text{C}_6\text{H}_4 \\   \quad   \\ \text{B} - \text{NiPr}_2 \end{array} \right]$							
M = [Fe(CO) <sub>3</sub> ]			31.0	C <sub>6</sub> D <sub>6</sub>	434	<sup>13</sup> C	434
[Fe(CO) <sub>2</sub> PMe <sub>3</sub> ]			31.0	C <sub>6</sub> D <sub>6</sub>	434	—	
$\text{M} \left[ \begin{array}{c} \text{NMe}_2 \\   \\ \text{B} \\   \quad   \\ \text{C}_6\text{H}_4 \\   \quad   \\ \text{B} - \text{NMe}_2 \end{array} \right]$							
M = [RuC <sub>6</sub> Me <sub>6</sub> ]			30.4	CD <sub>2</sub> Cl <sub>2</sub>	354	<sup>13</sup> C	354
[Ru(COD)] <sub>2</sub>			19.0	CD <sub>2</sub> Cl <sub>2</sub>	354	<sup>13</sup> C	354

<sup>a</sup> L = borane as the ligand shown in the preceding formula.

TABLE 36

 $\delta^{11}\text{B}$  values of some borole-metal complexes.<sup>a</sup>

Compound						$\delta^{11}\text{B}$	Solvent	Ref.	Other nuclei	Ref.
$\text{M} \left[ \begin{array}{c} \text{R}^4 \quad \text{R}^3 \\ \diagup \quad \diagdown \\ \text{C} \\ \diagdown \quad \diagup \\ \text{B} \\   \\ \text{R}^1 \end{array} \right]$										
M	R <sup>1</sup>	R <sup>2</sup>	R <sup>3</sup>	R <sup>4</sup>	R <sup>5</sup>					
[LCr(CO) <sub>2</sub> ]	iPr <sub>2</sub> N	H	H	H	H	28.0	CDCl <sub>3</sub>	381	—	
[Mn(CO) <sub>3</sub> ] <sub>2</sub>	Ph	H	H	H	H	19.7	C <sub>2</sub> Cl <sub>4</sub>	379	<sup>13</sup> C	379
[Mn(CO) <sub>3</sub> ] <sub>2</sub>	Ph	Et	H	H	H	17.6	C <sub>6</sub> D <sub>6</sub>	383	—	
[Mn(CO) <sub>3</sub> ] <sub>2</sub>	MeO	H	H	H	H	25.2	CDCl <sub>3</sub>	379	—	
[LFe(CO)]	iPr <sub>2</sub> N	H	H	H	H	27.0	CDCl <sub>3</sub>	381	—	
[FeCp] <sub>2</sub>	Ph	Et	H	H	H	4.0	CDCl <sub>3</sub>	383	—	
[Fe(CO) <sub>3</sub> ]	Me	H	H	H	H	22.4	CD <sub>2</sub> Cl <sub>2</sub>	379	<sup>13</sup> C	379
[Fe(CO) <sub>3</sub> ]	Ph	H	H	H	H	20.2	CD <sub>2</sub> Cl <sub>2</sub>	379	<sup>13</sup> C	379

TABLE 36 (cont.)

 $\delta^{11}\text{B}$  values of some borole-metal complexes.\*

Compound						$\delta^{11}\text{B}$	Solvent	Ref.	Other nuclei	Ref.
M	R <sup>1</sup>	R <sup>2</sup>	R <sup>3</sup>	R <sup>4</sup>	R <sup>5</sup>					
[Fe(CO) <sub>3</sub> ]	MeO	H	H	H	H	27.6	C <sub>2</sub> Cl <sub>4</sub>	379	<sup>13</sup> C	379
{[Fecp][Cr(CO) <sub>3</sub> ]} <sup>-</sup>	Ph	H	H	H	H	9.4	Acetone-d <sub>6</sub>	380	—	
[cpFeLCo]	Ph	H	H	H	H	16.7	C <sub>6</sub> D <sub>6</sub>	648	—	
						7.3				
[Os(CO) <sub>3</sub> ]	Ph	H	H	H	H	19.5	CDCl <sub>2</sub>	653	—	
[Ru(C <sub>6</sub> Me <sub>6</sub> )]	Ph	H	H	H	H	14.0	CDCl <sub>3</sub>	653	—	
[Ru(PPh <sub>3</sub> ) <sub>2</sub> (Cl)H]	Ph	H	H	H	H	9.4	CD <sub>2</sub> Cl <sub>2</sub>	653	<sup>31</sup> P	
[Os(PPh <sub>3</sub> ) <sub>2</sub> (Cl)H]	Ph	H	H	H	H	9.0	CD <sub>2</sub> Cl <sub>2</sub>	653		
[Ru(CO) <sub>3</sub> ]	Me	H	H	H	H	22.8	CD <sub>2</sub> Cl <sub>2</sub>	653		
[Ru(CO) <sub>3</sub> ]	Ph	H	H	H	H	21.3	CD <sub>2</sub> Cl <sub>2</sub>	653		
[Ru(CO) <sub>3</sub> ]	Ph	H	Me	Me	H	18.0	Acetone-d <sub>6</sub>	653		
[Ru(CO) <sub>3</sub> ]	MeO	H	H	H	H	28.3	CD <sub>2</sub> Cl <sub>2</sub>	653		
[Ru(C <sub>6</sub> H <sub>6</sub> )]	Ph	H	H	H	H	13.5	Acetone-d <sub>6</sub>	653		
[cpFe(CO)(μ-CO)-Co(CO)]	Ph	H	H	H	H	28.1	CDCl <sub>3</sub>	648	—	
[Co(CO) <sub>2</sub> I]	Me	H	H	H	H	27.9	CDCl <sub>3</sub>	648	—	
[Co(CO) <sub>2</sub> I]	Ph	H	H	H	H	24.5	CD <sub>2</sub> Cl <sub>2</sub>	648	—	
[Co(CO) <sub>2</sub> Br]	Ph	H	H	H	H	25.1	CD <sub>2</sub> Cl <sub>2</sub>	648	—	
[LCo <sub>2</sub> (CO) <sub>4</sub> ]	Me	H	H	H	H	27.9	CDCl <sub>3</sub>	379	—	
[LCo <sub>2</sub> (CO) <sub>4</sub> ]	Ph	H	H	H	H	25.5	CD <sub>2</sub> Cl <sub>2</sub>	379	—	
[Cocp]	Me	H	H	H	H	21.9	CDCl <sub>3</sub>	648	—	
[Cocp]	Ph	H	H	H	H	18.0	CD <sub>2</sub> Cl <sub>2</sub>	648	—	
[LCo] <sub>2</sub>	Me	H	H	H	H	22.8	CDCl <sub>3</sub>	648	—	
						12.3				
[LCo] <sup>-</sup> [NMe <sub>4</sub> ] <sup>+</sup>	Me	H	H	H	H	14.1	Acetone-d <sub>6</sub>	648	—	
[LCo] <sub>2</sub> Ru	Ph	H	H	H	H	19.6	CD <sub>2</sub> Cl <sub>2</sub>	648	—	
						8.2				
[CODRhLCo]	Ph	H	H	H	H	18.2	Acetone-d <sub>6</sub>	648	—	
						12.9				
[Cocp]	H	Ph	Ph	Ph	Ph	17.0		385	—	
[Rhcp]	Me	H	H	H	H	19.6	C <sub>2</sub> Cl <sub>4</sub>	378	—	
[Rhcp]	Ph	H	H	H	H	16.4	C <sub>2</sub> Cl <sub>4</sub>	378	—	
[RhC <sub>5</sub> Me <sub>5</sub> ]	iPr <sub>2</sub> N	H	H	H	H	22.0	CDCl <sub>3</sub>	381	—	
[LRh] <sup>-</sup>	Me	H	H	H	H	13.5	Acetone-d <sub>6</sub>	378	—	
[LRhH]	Me	H	H	H	H	16.0	CDCl <sub>3</sub>	378	—	
[RhPMe <sub>3</sub> ] <sup>+</sup>	Ph	H	H	H	H	23.7	CD <sub>2</sub> Cl <sub>2</sub>	378	—	
[Rh(PMe <sub>3</sub> ) <sub>3</sub> ] <sup>+</sup>	Ph	H	H	H	H	25.2	CD <sub>2</sub> Cl <sub>2</sub>	653	<sup>31</sup> P	
[Rh(PPh <sub>3</sub> ) <sub>2</sub> Cl]	Ph	H	H	H	H	32.0	CD <sub>2</sub> Cl <sub>2</sub>	653	<sup>31</sup> P	
[Rh(CN) <sub>3</sub> ] <sup>2-</sup>	Ph	H	H	H	H	23.6	CD <sub>2</sub> Cl <sub>2</sub>	378	—	
[LRh] <sub>2</sub>	Me	H	H	H	H	22.3	CD <sub>2</sub> Cl <sub>2</sub>	378	<sup>13</sup> C	378
						10.8				
						(bridge)				

TABLE 36 (*cont.*) $\delta^{11}\text{B}$  values of some borole-metal complexes.<sup>a</sup>

Compound						$\delta^{11}\text{B}$	Solvent	Ref.	Other nuclei	Ref.
M	R <sup>1</sup>	R <sup>2</sup>	R <sup>3</sup>	R <sup>4</sup>	R <sup>5</sup>					
[Rh(COD)]	iPr <sub>2</sub> N	H	H	H	H	15.0	C <sub>2</sub> Cl <sub>4</sub>	381	—	
[Rh(C <sub>2</sub> H <sub>4</sub> ) <sub>2</sub> ] <sub>2</sub>	iPr <sub>2</sub> N	H	H	H	H	14.0	C <sub>6</sub> D <sub>6</sub>	381	—	
[LNi]	iPr <sub>2</sub> N	H	H	H	H	26.0	CDCl <sub>3</sub>	381	—	
[Nicp] <sub>2</sub>	iPr <sub>2</sub> N	H	H	H	H	10.0	C <sub>2</sub> Cl <sub>4</sub>	381	—	
[Pt(PEt <sub>3</sub> ) <sub>2</sub> ]	Me	Me	H	H	Me	19.1	CD <sub>2</sub> Cl <sub>2</sub>	382	<sup>13</sup> C, <sup>31</sup> P, <sup>195</sup> Pt	382
[Pt(dppe)]	Me	H	Me	Me	H	18.0	C <sub>7</sub> D <sub>8</sub>	382	<sup>13</sup> C, <sup>31</sup> P, <sup>195</sup> Pt	382
[Pt(COD)]	Ph	Ph	Ph	Ph	Ph	16.0	CD <sub>2</sub> Cl <sub>2</sub>	67	—	

<sup>a</sup> L = borane as the ligand shown in the preceding formula; see Ref. 826 for further NMR data of borole-metal complexes.

TABLE 37

 $\delta^{11}\text{B}$  values of some 1,3-diborole-, 1,2,5-thiadiborole- and 1,2-azaborole-metal complexes.<sup>a</sup>

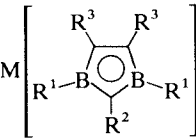
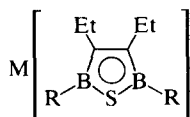
Compound				$\delta^{11}\text{B}$	Solvent	Ref.	Other nuclei	Ref.
M	R <sup>1</sup>	R <sup>2</sup>	R <sup>3</sup>					
								
[Sn(Cocp) <sub>2</sub> ]	Et	Me	Et	13.0	C <sub>6</sub> D <sub>6</sub>	455	—	
[TiCocp]	Me	H	Me	20.4	C <sub>6</sub> D <sub>6</sub>	426	—	
[(Fecp)(Cocp)]	Et	Me	Et	19.6	CS <sub>2</sub>	460	—	
[(Fecp) <sub>2</sub> Pt]	Et	Me	Et	15.0	C <sub>6</sub> D <sub>6</sub>	404	<sup>13</sup> C	404
[Co(CO) <sub>3</sub> ]	Et	Me	Et	30.0	C <sub>6</sub> D <sub>6</sub>	406	—	
[(Cocp) <sub>2</sub> ] <sup>+</sup>	Me	H	Et	18.3	CD <sub>2</sub> Cl <sub>2</sub>	458	—	
(Cocp) <sub>2</sub> [Ni(CO)] <sub>2</sub>	Et	Me	Et	14.8	C <sub>6</sub> D <sub>6</sub>	459	—	
[(Cocp)NiC <sub>3</sub> H <sub>5</sub> ]	Me	H	Et	7.6	C <sub>6</sub> D <sub>6</sub>	403	—	
[(Cocp)Ni <sub>3</sub> ]	Me	Et	Et	34.0	C <sub>6</sub> D <sub>6</sub>	403	—	
[Nicp]	Et	Me	Et	35.3	C <sub>6</sub> D <sub>6</sub>	457	—	
[Nicp] <sub>2</sub> <sup>-</sup>	Et	Me	Et	7.0	THF	405	<sup>13</sup> C	405
[(Cocp)Pt]	Et	Me	Et	38.0	C <sub>6</sub> D <sub>6</sub>	404	—	
				15.0				
				(bridge)				

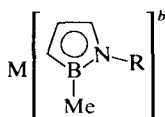
TABLE 37 (cont.)

 $\delta^{11}\text{B}$  values of some 1,3-diborole-, 1,2,5-thiadiborole- and 1,2-azaborole-metal complexes.\*

Compound				$\delta^{11}\text{B}$	Solvent	Ref.	Other nuclei	Ref.
M	R <sup>1</sup>	R <sup>2</sup>	R <sup>3</sup>					
[(Ntcp) <sub>2</sub> Pt]	Et	Me	Et	13.0	C <sub>6</sub> D <sub>6</sub>	404	<sup>13</sup> C	404
[(NiC <sub>3</sub> H <sub>5</sub> )Ni]	Et	Me	Et	20.7	C <sub>6</sub> D <sub>6</sub>	407	—	
[Ni(C <sub>3</sub> H <sub>5</sub> )Ni(C <sub>3</sub> H <sub>5</sub> ) <sub>2</sub> ]	Me	H	Me	21.6	C <sub>6</sub> D <sub>6</sub>	408	—	
[Pdcp]	Et	Me	Et	37.0	C <sub>6</sub> D <sub>6</sub>	409	<sup>13</sup> C	409
[LPt]	Et	Me	Et	48.0	C <sub>6</sub> D <sub>6</sub>	409	<sup>13</sup> C	409
[LPt] <sup>2-</sup>	Et	Me	Et	23.0	THF	409	<sup>13</sup> C	409



M	R
[Cr(CO) <sub>4</sub> ]	Me
[Mo(CO) <sub>4</sub> ]	Me
{[Mn(CO) <sub>3</sub> ][Fecp]}	Me
[Fe(CO) <sub>3</sub> ]	Me
[Fe(CO) <sub>3</sub> ]	Cl
[Fe(CO) <sub>3</sub> ]	SMc
[Cocp]	Me
[Ni(CO) <sub>2</sub> ]	Me
[LCo] <sub>2</sub>	Me

 14.0  
(bridge)


M	R
[Sn]	tBu
[LTiCl <sub>2</sub> ]	SiMe <sub>3</sub>
[LVCl]	SiMe <sub>3</sub>
[Cr(CO) <sub>3</sub> ] <sup>-</sup>	tBu
[Cr(CO) <sub>3</sub> SnMe <sub>3</sub> ]	tBu
[Mo(CO) <sub>3</sub> ] <sup>-</sup>	tBu
[Mo(CO) <sub>3</sub> GeMe <sub>3</sub> ]	tBu
[Mo(CO) <sub>3</sub> PbMe <sub>3</sub> ]	tBu
[W(CO) <sub>3</sub> ] <sup>-</sup>	tBu
[Mn(CO) <sub>3</sub> ]	tBu

31.5	C <sub>7</sub> D <sub>8</sub>	427	<sup>13</sup> C	427
40.9	C <sub>6</sub> D <sub>6</sub>	390	—	
56.8	THF	390	—	
19.5	DMSO-d <sub>6</sub>	387	—	
19.4	C <sub>6</sub> D <sub>6</sub>	387	<sup>13</sup> C, <sup>119</sup> Sn	387
22.2	Acetone-d <sub>6</sub>	387	—	
22.9	C <sub>6</sub> D <sub>6</sub>	387	<sup>13</sup> C	387
22.4	C <sub>6</sub> D <sub>6</sub>	387	<sup>13</sup> C, <sup>207</sup> Pb	387
22.1	DMSO-d <sub>6</sub>	387	—	
19.0	C <sub>6</sub> D <sub>6</sub>	392	—	

TABLE 37 (*cont.*) $\delta^{11}\text{B}$  values of some 1,3-diborole-, 1,2,5-thiadiborole- and 1,2-azaborole-metal complexes.<sup>a</sup>

Compound		$\delta^{11}\text{B}$	Solvent	Ref.	Other nuclei	Ref.
M	R					
[LFe]	Et	13.0	$\text{C}_7\text{D}_8$	396	—	
[FeC <sub>6</sub> H <sub>6</sub> ] <sup>+</sup>	tBu	19.0	Acetone-d <sub>6</sub>	389	<sup>13</sup> C	389
[LRu]	tBu	16.2	$\text{C}_6\text{D}_6$	386	—	
		14.2				
[LRu]	SiMe <sub>3</sub>	16.0	$\text{C}_6\text{D}_6$	386	—	
		17.8				
[Co(CO) <sub>2</sub> ]	tBu	21.0	$\text{C}_6\text{D}_6$	394	<sup>13</sup> C	394
[Co(COD)]	tBu	18.0	$\text{C}_6\text{D}_6$	394	<sup>13</sup> C	394

<sup>a</sup> L = borane as the ligand shown in the preceding formula.<sup>b</sup> See Refs 811, 829 for NMR data (<sup>11</sup>B, <sup>13</sup>C, <sup>31</sup>P) of other azaborole complexes and Ref. 833 for other 1,3-diborole complexes.

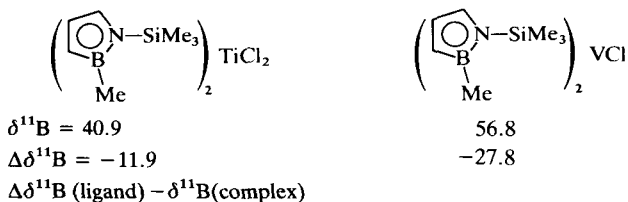
TABLE 38

 $\delta^{11}\text{B}$  values of some boron-element(sulphur, nitrogen)-metal complexes.

Compound	$\delta^{11}\text{B}$	Solvent	Ref.	Other nuclei	Ref.
[Cr(CO) <sub>3</sub> ][MeSBMe <sub>2</sub> ]	72.9	$\text{C}_6\text{H}_6$	424	—	
[Fe(CO) <sub>3</sub> ][(MeS) <sub>2</sub> BMe]	34.2	$\text{C}_6\text{H}_6$	422	—	
[Cr(CO) <sub>3</sub> ][(MeS) <sub>3</sub> B]	20.0		467	—	
[NiC <sub>3</sub> H <sub>5</sub> ][Me <sub>2</sub> NBMe <sub>2</sub> ]	32.5		466	—	
[Fe(CO) <sub>3</sub> ][(Me <sub>2</sub> N) <sub>2</sub> BMe]	20.0		466	—	
[W(CO) <sub>3</sub> ][(Me <sub>2</sub> N) <sub>3</sub> B]	21.2		468	—	
[Cr(CO) <sub>3</sub> ] <div style="display: inline-block; vertical-align: middle; text-align: center;"> <math>\left[ \begin{array}{c} \text{tBu} \\ \diagup \quad \diagdown \\ \text{N} \quad \text{N} \\   \quad   \\ \text{B}-\text{Me} \\ \diagdown \quad \diagup \\ \text{N} \quad \text{N} \\ \diagup \quad \diagdown \\ \text{tBu} \end{array} \right]</math> </div>	18.3	$\text{CDCl}_3$	219	—	
[Cr(CO) <sub>3</sub> ][(MeBNMe) <sub>3</sub> ]	24.3	$\text{C}_6\text{D}_6$	469	<sup>14</sup> N	469
[Co <sub>2</sub> (CO) <sub>6</sub> ][tBu≡NBu]	18.8	$\text{CDCl}_3$	421	<sup>13</sup> C	421
[Cr(CO) <sub>4</sub> ][(BuB≡NBu) <sub>2</sub> ]	16.7	$\text{CDCl}_3$	420	<sup>13</sup> C, <sup>14</sup> N	420
[W(CO) <sub>4</sub> ][(BuB≡NBu) <sub>2</sub> ]	19.5	$\text{CDCl}_3$	420	—	

various reasons not discussed here, the ligating ability of organylboron compounds may be superior to that of their well-known carbon analogues. Several new developments have been reported for borabenzene derivatives. Metal derivatives of the 2-boranaphthalene anion have been prepared.<sup>142</sup> The neutral adducts pyridine–borabenzene and pyridine–2-boranaphthalene are coordinated to metal fragments  $M(CO)_3$  ( $M = Cr, Mo, W$ ).<sup>432</sup> Following work on 1,4-diborabenzene complexes,<sup>433</sup> transition-metal derivatives of 1,3-diborabenzene<sup>434</sup> and 1,2-diborabenzene have been prepared (Table 35).<sup>354</sup>

The most interesting information from  $^{11}B$  NMR concerns the metal–boron bond in  $\pi$  complexes. In general, an increase in  $^{11}B$ -nuclear shielding with respect to that of the “free” ligand (or a comparable trigonal borane) has been assumed as evidence for metal–boron bonding interactions. So far, all direct structural information from X-ray analysis in the solid state corroborates this assumption, with very few exceptions. However, a caveat is necessary: the magnitude of the shift differences  $\Delta\delta^{11}B$  (with respect to the “free” ligand) *should not* be viewed as a measure of the metal–boron bond strength. The  $\Delta\delta^{11}B$  values depend (i) on the electronic structure of the “free” ligand, (ii) on the electronic structure of the  $\pi$  complex and therefore on the nature of all other ligands and on the oxidation state of the metal, (iii) on the changes in the chemical-shielding anisotropy,  $\Delta\sigma$ . The first argument (i) is readily recognized by comparing, for example, the  $\delta^{11}B$  values of the borabenzene anion and its metal complexes ( $\Delta\delta^{11}B \approx 2$ –13 ppm, cf. Table 34) with those of alkenylboranes and their metal complexes ( $\Delta\delta^{11}B \approx 30$ –40 ppm, cf. Table 33). In the case of the second argument (ii), it is appropriate to cite at least two noteworthy exceptions to the “rule” of the low-frequency shift of the borane ligand upon complexation. In the titanium- and vanadium-chloride complexes with the 1,2-azaborolinylligand the shielding of the  $^{11}B$  nuclei is reduced with respect to the “free” ligand.<sup>390</sup>



This high-frequency shift has been attributed to negligible metal–boron bonding interactions. However, it seems more likely, considering the electronic structure of such complexes,<sup>470</sup> that  $B_0$ -induced paramagnetic circulations, involving the formally empty metal 3d orbitals, are responsible.

Thus the changes in the  $\delta^{11}\text{B}$  values in these complexes remind one of analogous changes in the  $\delta^{13}\text{C}$  values of corresponding cyclopentadienyl complexes.<sup>471</sup>

Finally, the third argument (iii) has been studied by  $^{13}\text{C}$  NMR of  $\pi$  complexes in the solid state,<sup>100</sup> and the results may also apply to  $^{11}\text{B}$  NMR of  $\pi$  complexes. Since values of the principal components of the  $^{11}\text{B}$ -shielding tensor are not available, the interpretation of the isotropic  $\sigma$  values is not straightforward—in particular if a change in the coordination number is involved in addition to other factors.

$^{11}\text{B}$  resonances in the case of bridging and nonbridging borane ligands in  $\pi$  complexes can be assigned without difficulty. In all cases studied the  $^{11}\text{B}$  resonance of the bridging ligand is shifted to lower frequency. This increase in  $^{11}\text{B}$ -nuclear shielding may be related to an increase in the coordination number.

### C. Indirect nuclear spin–spin couplings $^nJ(^{11}\text{BX})$

Although most of the values  $^nJ(\text{BX})$  are obtained from the X NMR spectra, a brief discussion of general effects is presented in this section.

#### 1. General theory<sup>657–661</sup>

The spin–spin-coupling interaction  $J_{\text{AB}}$  between nuclei A and B is mediated by valence electrons and is a scalar quantity. According to Ramsey's formulation,<sup>657</sup> it is described by more than one mechanism. It is assumed that the contact term dominates the coupling mechanism and that the spin–orbital and spin–dipole terms are of minor importance. In the case of boron, this assumption appears to be justified for spin–spin coupling to  $^1\text{H}$ ,  $^{11}\text{B}$ ,  $^{13}\text{C}$ ,  $^{29}\text{Si}$  and  $^{31}\text{P}(\text{v})$ , whereas the treatment of spin–spin coupling to  $^{15}\text{N}$ ,  $^{19}\text{F}$  and  $^{31}\text{P}(\text{III})$  is less simple. For spin–spin coupling to the heavier nucleides like  $^{77}\text{Se}$ ,  $^{103}\text{Rh}$ ,  $^{119}\text{Sn}$ ,  $^{195}\text{Pt}$ ,  $^{205}\text{Tl}$ ,  $^{207}\text{Pb}$  relativistic effects<sup>658</sup> may have to be considered in order to get more than a rough qualitative picture. The present account will be limited to a purely qualitative discussion, and for this purpose the formulation of the contact term in the original approach of Pople and Santry<sup>659</sup> is useful:

$$K_{\text{AB}} = \frac{4}{9} \mu_0^2 \mu_{\text{B}}^2 \psi_{\text{A}}(\text{O})^2 \psi_{\text{B}}(\text{O})^2 \pi_{\text{AB}}, \quad (19)$$

where  $K$  is the reduced coupling constant ( $K_{\text{AB}} = (4\pi^2/h) J_{\text{AB}}(\gamma_{\text{A}}\gamma_{\text{B}})^{-1}$ ),  $\psi_{\text{A}}(\text{O})^2$  and  $\psi_{\text{B}}(\text{O})^2$  are the respective valence-s-electron densities at nuclei A and B,  $\pi_{\text{AB}}$  is the mutual polarizability of the A and B s orbitals and the other symbols have their usual meaning. The term  $\pi_{\text{AB}}$  represents the difference of one-electron energies and controls both the sign and

magnitude of  $K_{AB}$ . The introduction of an average excitation energy  $\Delta E$  leads to the replacement of the term  $\pi_{AB}$  in (19):

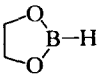
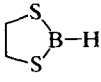
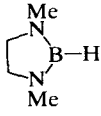
$$\pi_{AB} = \Delta E^{-1} P_{S(A)S(B)}^2 \quad (20)$$

This requires that  $K_{AB}$  is always  $>0$ , and that there is a linear correlation between  $K_{AB}$  and the "s character" ( $P_{S(A)S(B)}^2$ ) of the A—B bond. Clearly, this is a very crude picture, and its careful application should be restricted to the discussion of *changes* in the magnitudes of couplings rather than to discussing their absolute values. Furthermore, it should be limited to spin-spin coupling between  $^{11}\text{B}$  and nuclei such as  $^1\text{H}$ ,  $^{11}\text{B}$ ,  $^{13}\text{C}$ ,  $^{29}\text{Si}$  that possess an open s-shell electron configuration.

## 2. Patterns of couplings $^nJ(^{11}\text{B}X)$

(a)  $J(^{11}\text{B}^1\text{H})$  (Table 39). Many values  $^1J(^{11}\text{B}^1\text{H})$  can be found in the tables for chemical shifts. For a brief survey a few representative data are listed in Table 39 in order to get an impression of the whole range.

TABLE 39  
Some selected couplings  $^1J(^{11}\text{B}^1\text{H})$ .<sup>a</sup>

Compound	$^1J(^{11}\text{B}^1\text{H})(\text{Hz})$	Ref.
$[\text{C}(\text{H})\text{Me}_2\text{CMe}_2]_2\text{BH}$	114	114
$\text{F}_2\text{BH}$	211	5
	173	302
	140	302
	130	182
$\text{Et}_2\text{NBH}_2$	120	127
$[\text{BH}_4]^-$	$81.5 \pm 1.0$	5
$\text{H}_3\text{N}-\text{BH}_3$	$98.2 \pm 1$	556
$\text{B}_2\text{H}_6$	$133.5 \pm 1.0$ (terminal) $46.3 \pm 0.5$ (bridge)	668
$[(\text{H}_3\text{N})_2\text{BH}_2]^+$	110	5
$[(\text{Me}_3\text{P})_2\text{BH}_2]^+$	90	5

<sup>a</sup> For further data see the relevant Tables and Refs 5-9.

MO calculations have shown that the magnitude of  $^1J(^{11}\text{B}^1\text{H})$  is roughly linearly related to the "s character" of the B—H bond.<sup>662,663</sup> This includes the  $^{11}\text{B}$ — $^1\text{H}$  coupling in electron deficient B—H—B or B—H—metal bridges. As similar observations apply to  $^1J(^{13}\text{C}^1\text{H})$ , correlations between  $^1J(^{11}\text{B}^1\text{H})$  and  $^1J(^{13}\text{C}^1\text{H})$  exist,<sup>663</sup> and they include rather extreme values from carbaboranes.<sup>10,663</sup>

For the tetrahedral compounds the model of "rehybridization"<sup>664</sup> can be used. In borates or borane adducts, the greater polarity of B—H, or B—element bonds in comparison with C—H or C—element bonds, is expected to induce greater changes in the values of  $^1J(^{11}\text{B}^1\text{H})$ :

	$\text{BH}_4^-$	$\text{CH}_3\text{—BH}_3^-$	$(\text{CH}_3)_2\text{BH}_2$	$(\text{CH}_3)_3\text{BH}$
$^1J(^{11}\text{B}^1\text{H})$ (Hz) =	81.5	70.3	66.6	66.6
$^1J(^{13}\text{C}^1\text{H})$ (Hz) =	125.0	124.9	125.4	125.0
	$\text{CH}_4$	$\text{CH}_3\text{—CH}_3$	$(\text{CH}_3)_2\text{CH}_2$	$(\text{CH}_3)_3\text{CH}$

(b)  $J(^{11}\text{B}^{11}\text{B})$ ,  $J(^{205}\text{Tl}^{11}\text{B})$  (Table 40). As for the values of  $^1J(^{11}\text{B}^1\text{H})$ , the magnitude of  $^1J(^{11}\text{B}^{11}\text{B})$  corresponding to two-electron two-centre B—B bonds is significantly increased when compared with those for electron deficient multicentre B—B bonds. There are strong indications that changes in  $^1J(^{11}\text{B}^{11}\text{B})$  are related to the "s character" of the two-centre or the multicentre bond.<sup>662</sup> A positive sign has been determined for  $^1J(^{11}\text{B}^{11}\text{B})$  in 1-methylpentaborane(9).<sup>513</sup> In general,  $^{11}\text{B}$ — $^{11}\text{B}$  coupling is small between boron atoms bridged by hydrogens. This helps to analyse the B—B connectivity of polyhedral boranes by two-dimensional  $^{11}\text{B}$ — $^{11}\text{B}$  COSY NMR, based on scalar  $^{11}\text{B}$ — $^{11}\text{B}$  coupling.<sup>665,666</sup>

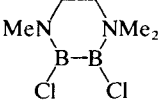
The shortcomings of this method may be compensated by the use of  $^1\text{H}$ — $^1\text{H}$  COSY NMR, with  $^{11}\text{B}$  decoupling.<sup>667</sup> Experimentally, it has been shown that  $^1J(^{11}\text{B}^{11}\text{B})$  in diborane(6) is  $3.8 \pm 0.2$  Hz.<sup>668</sup> In *nido*[ $\text{Me}_2\text{TlB}_{10}\text{H}_{12}$ ] $^-$  the magnitudes and relative signs of  $^nJ(^{205}\text{Tl}^{11}\text{B})$  have been determined, using one-dimensional and two-dimensional ( $^{11}\text{B}$ — $^{11}\text{B}$  COSY) experiments.<sup>670</sup>

(c)  $^1J(^{13}\text{C}^{11}\text{B})$  (Table 41). A large number of values of  $^1J(^{13}\text{C}^{11}\text{B})$  have become available in the last decade. In most cases, changes in the magnitude of  $^1J(^{13}\text{C}^{11}\text{B})$  are related to the "s character" of the B—C bond.<sup>505</sup> As discussed for  $^1J(^{11}\text{B}^1\text{H})$ , the polarizability of the B—C bond is much greater than for the C—C bond. This leads to a greater range of  $^1J(^{13}\text{C}^{11}\text{B})$  values for similar compounds.

$^1J(^{13}\text{C}^{11}\text{B}) =$	$\frac{[(\text{CH}_3)_4\text{B}]^-}{39.5 \text{ Hz}}$	$\frac{[(\text{CH}_3)_3\text{C—BH}_3]}{50.0 \text{ Hz}}$	$\frac{(\text{CH}_3)_4\text{C}}{^1J(^{13}\text{C}^{13}\text{C}) = 36.0 \text{ Hz}}$
-------------------------------------	---	--	---

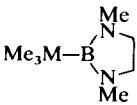
TABLE 40

Some representative couplings  $J(^{11}\text{B}^1\text{B})$ .<sup>a</sup>

Compound	$^1J(^{11}\text{B}^1\text{B})$ (Hz)	Ref.
$\text{B}_2\text{Br}_4$	110	356
$\text{B}_2(\text{NMe}_2)_4$	75	679
	120	365
$\text{B}_4\text{Cl}_4$	<20	41
$\text{B}_2\text{H}_6$	3.8	668
$1\text{-(Cl}_2\text{B)B}_5\text{H}_8$	124	363
$2\text{-(Cl}_2\text{B)B}_5\text{H}_8$	106	364
$1:1'\text{-[B}_5\text{H}_8]_2$	149	680
$1:2'\text{-[B}_5\text{H}_8]_2$	115	680
$2:2'\text{-[B}_5\text{H}_8]_2$	79	680
$1:2'\text{-[B}_{10}\text{H}_{13}]_2$	105	681
$2:2'\text{-[1,5-C}_2\text{B}_3\text{H}_4]_2$	137	680
$3:3'\text{-[2,4-C}_2\text{B}_5\text{H}_6]_2$	151	680
$\text{B}_4\text{H}_{10}$	$20.4[\text{B}(1)\text{B}(3)]$	663
	$\geq 25$	684
$\text{B}_5\text{H}_9$	19.2	682
$1\text{-ClB}_5\text{H}_9$	23.9	683
$2,3\text{-C}_2\text{B}_4\text{H}_8$	$26.6[\text{B}(1)\text{B}(5)]$	685
	$\geq 12.0[\text{B}(1)\text{B}(4)]$	663
$2\text{-CB}_5\text{H}_9$	$18.0[\text{B}(1)\text{B}(4)]$	663
	$< 9.0[\text{B}(1)\text{B}(3)]$	663
$2,4\text{-C}_2\text{B}_5\text{H}_7$	$< 15.0[\text{B}(1)\text{B}(5)]$	663
	$< 5.0[\text{B}(1)\text{B}(3)]$	663

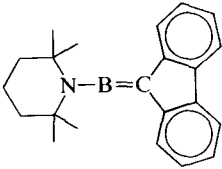
<sup>a</sup> In the case of equivalent boron atoms the coupling  $^1J(^{11}\text{B}^{10}\text{B})$  has been determined:  $J(^{11}\text{B}^{11}\text{B}) = 3J(^{10}\text{B}^{10}\text{B})$ .

(d)  $^1J(^{29}\text{Si}^{11}\text{B})$ ,  $^1J(^{119}\text{Sn}^{11}\text{B})$ ,  $^1J(^{207}\text{Pb}^{11}\text{B})$  (Table 42). The sign and magnitude of the couplings  $^1J(\text{M}^{11}\text{B})$  ( $\text{M} = ^{29}\text{Si}$ ,  $^{182} \text{ } ^{119}\text{Sn}$ ,  $^{332} \text{ } ^{207}\text{Pb}$  <sup>334</sup>) have been determined for the 1,3,2-diazaborolidine derivatives

	$^1J(\text{M}^{11}\text{B})$ (Hz) =	-97.0	-930	+1330
	M	$^{29}\text{Si}$	$^{119}\text{Sn}$	$^{207}\text{Pb}$
	$K(\text{M}^{11}\text{B})$ (nm <sup>-3</sup> ) =	+12.7	+64.8	+165.0

The ratios of the reduced couplings are close to the respective ratios of the calculated valence-s-electron densities, as expected if (19) is valid. <sup>332,334</sup>

TABLE 41  
Some representative couplings  $J(^{13}\text{C}^{11}\text{B})$ .<sup>a</sup>

Compound	$^1J(^{13}\text{C}^{11}\text{B})$ (Hz)	Ref.
	$102 \pm 5^b$	686
$\text{Me}_3\text{B}$	+45–52	10
$\text{Me}_2\text{B}-\text{CH}=\text{CH}_2$	$\geq 75$ (B—C=)	687
$\text{Me}_2\text{B}-\text{C}\equiv\text{C}-\text{Me}$	$\geq 110$ (B—C $\equiv$ )	524 <sup>c</sup>
$\text{Me}_2\text{BF}$	$\geq 70$	41
$\text{Me}_2\text{BOMe}$	$\geq 64$	205
$\text{MeBF}_2$	$\geq 95$	41
$(\text{MeBO})_3$	$\geq 78$	41
$\text{MeB}(\text{NMe}_2)_2$	$\geq 59$	204
$\text{MeC}\equiv\text{C}-\text{B}(\text{NMe}_2)_2$	$\geq 135$	10
$\text{CF}_3-\text{B}(\text{NMe}_2)_2$	99	218
$[\text{Me}_4\text{B}]^-$	+39.5	513
$[\text{Ph}_4\text{B}]^-$	49.5	10
$[(\text{PhC}\equiv\text{C})_4\text{B}]^-$	70.0	524
$[\text{C}_8\text{H}_{14}\text{BH}_2]^-$	41.0	41
$[\text{BuBH}_2]^-$	48.0	496
$[\text{tBuBH}_2]^-$	50.0	503
$[\text{C}_6\text{H}_5\text{CH}_2\text{BH}_2]^-$	43.3	496
$[\text{PhBH}_2]^-$	56.6	496
$[\text{N}\equiv\text{C}-\text{BH}_2]^-$	53.0	505
1-MeB <sub>5</sub> H <sub>8</sub>	+73.1	513
1,5-C <sub>2</sub> B <sub>3</sub> H <sub>5</sub>	18.0	688
1,3,4,6-Me <sub>4</sub> -2,3,4,5-C <sub>4</sub> B <sub>2</sub> H <sub>2</sub>	$\geq 81$ [BN(1)CH <sub>3</sub> ] $\geq 76$ [B(6)CH <sub>3</sub> ] $\geq 59$ [B(6)C(2,5)] $< 5$ [B(1)C(2,3,4,5)]	689

<sup>a</sup> For more data see Refs 7 and 10.

<sup>b</sup> Calculated from  $T^{\text{Q}}(^{11}\text{B})$  and the  $^{13}\text{C}$  linewidth.

<sup>c</sup> J. D. Odom, personal communication, cited in Ref. 524.

In particular, for  $\text{M} = ^{207}\text{Pb}$  more data are required for further discussions. In the case of  $\text{M} = \text{Si}$  the comparison between  $^1J(^{29}\text{Si}^{11}\text{B})$  and  $^1J(^{29}\text{Si}^{13}\text{C})$  reveals analogous trends:

	$[\text{B}(\text{SiMe}_3)_4]^-$	$[\text{MeB}(\text{SiMe}_3)_3]^-$	$[\text{Me}_3\text{BSiMe}_3]^-$	$[\text{H}_3\text{BSiMe}_3]^-$
$^1J(^{29}\text{Si}^{11}\text{B})$ (Hz) =	48.0 <sup>535</sup>	53.0 <sup>538</sup>	74.0 <sup>538</sup>	74.0 <sup>133</sup>
$^1J(^{29}\text{Si}^{13}\text{C})$ (Hz) =	30.9 <sup>672</sup>	38.0 <sup>123</sup>	57.0 <sup>672</sup>	51.0 <sup>672</sup>
	$\text{C}(\text{SiMe}_3)_4$	$\text{MeC}(\text{SiMe}_3)_3$	$\text{Me}_3\text{CSiMe}_3$	$\text{H}_3\text{C}-\text{SiMe}_3$

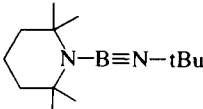
TABLE 42

Some representative couplings  $^1J(M^{11}B)$  ( $M = {}^{29}\text{Si}, {}^{119}\text{Sn}, {}^{207}\text{Pb}$ ).<sup>a</sup>

Compound	$^1J(M^{11}B)$ (Hz)	Ref.
$\text{Me}_3\text{Si}-\text{B}[\text{N}(\text{Me})\text{CH}_2]_2$	97	182
$[\text{Me}_3\text{Si}-\text{BH}_3]^-$	74	133
$[(\text{Me}_3\text{Si})_3\text{Si}-\text{BH}_3]^-$	52.5	123
$[(\text{Me}_3\text{Si})_4\text{B}]^-$	48	535
$\text{Me}_3\text{Sn}-\text{B}(\text{NMe}_2)_2$	953	332
$\text{Me}_3\text{Sn}-\text{B}[\text{N}(\text{Me})\text{CH}_2]_2$	930	334
$(\text{Me}_3\text{Sn})_2\text{B}-\text{NMe}_2$	657	133
$[\text{Me}_3\text{Sn}-\text{BH}_3]^-$	554	133
$[\text{Et}_3\text{Sn}-\text{BH}_3]^-$	520	123
$\text{Me}_3\text{Pb}-\text{B}[\text{N}(\text{Me})\text{CH}_2]_2$	1330	334

TABLE 43

Some representative couplings  $^1J({}^{15}\text{N}^{11}\text{B})$ .<sup>a</sup>

Compound	$^1J({}^{15}\text{N}^{11}\text{B})$ (Hz)	Ref.
	$70 \pm 4^b$ ( $\text{B}\equiv\text{N}$ )	41
$\text{Me}_2\text{BNH}_2$	$>30$	7
$\text{MeB}(\text{NHMe})_2$	$>33$	7
$\text{B}(\text{NHMe})_3$	$>45$	690
$\text{H}_3\text{N}-\text{BH}_3$	$<3$	556
$\text{Et}_3\text{N}-\text{BH}_3$	$>6$	556
$\text{Me}_3\text{N}-\text{BF}_3^c$	18.7	599
$\text{Me}_3\text{N}-\text{BCl}_3^c$	16.5	599
$\text{Me}_3\text{N}-\text{BBBr}_3^c$	15.2	599
$\text{Me}_3\text{N}-\text{BI}_3^c$	12.1	599

<sup>a</sup> For more data see Ref. 7.<sup>b</sup> From  ${}^{14}\text{N}$  NMR spectra at 90 °C in toluene.<sup>c</sup>  ${}^{15}\text{N}$ -enriched samples.

(e)  $^1J({}^{15}\text{N}^{11}\text{B})$  (Table 43). There are very few examples where  ${}^{14}\text{N}-{}^{11}\text{B}$  spin-spin coupling is resolved (see Table 43). Values of  $^1J({}^{15}\text{N}^{11}\text{B})$  have been determined either from the measurement of  ${}^{15}\text{N}$ -enriched samples,<sup>599</sup> or at natural abundance, using polarization-transfer techniques.<sup>22,476</sup> A linear correlation has been found between  $^1J({}^{15}\text{N}^{11}\text{B})$  and  $^1J({}^{31}\text{P}^{11}\text{B})$

for the corresponding amine- and phosphine-boranes,<sup>556</sup> indicating that  $^1K(^{15}\text{N}^{11}\text{B}) > 0$ , as shown for  $^1K(^{31}\text{P}^{11}\text{B})$ .<sup>566</sup>

(f)  $^1J(^{31}\text{P}^{11}\text{B})$  (Table 44). The P—B bond is readily recognized in both the  $^{11}\text{B}$  and the  $^{31}\text{P}$  NMR spectra by the splitting due to  $^1J(^{31}\text{P}^{11}\text{B})$ . The values cover a range of approximately 200 Hz, and so far all experimental evidence shows that  $^1J(^{31}\text{P}^{11}\text{B}) > 0$ .<sup>182,566</sup>

The linear correlation between  $^1J(^{31}\text{P}^{11}\text{B})$  and  $^1J(^{15}\text{N}^{11}\text{B})$  for borane adducts<sup>566</sup> indicates that d-orbital participation in the phosphine-borane has a negligible influence on the coupling mechanism. The analogous behaviour of  $^1J(^{31}\text{P}^{11}\text{B})$  and  $^1J(^{15}\text{N}^{11}\text{B})$  is no longer observed in the case of trigonal boranes. This is in accord with the different natures of the lone electron pairs on phosphorus and nitrogen respectively.

(g)  $^1J(^{17}\text{O}^{11}\text{B})$ ,  $^1J(^{77}\text{Se}^{11}\text{B})$ . So far, no values of  $^1J(^{17}\text{O}^{11}\text{B})$  have been reported, although a great number of boron-oxygen compounds have been studied.<sup>117,236,350,436</sup> Attempts at the measurement of the coupling  $^1J(^{77}\text{Se}^{11}\text{B})$  have shown that its magnitude is small, at least for the compounds studied.<sup>182</sup>

(h)  $^1J(^{19}\text{F}^{11}\text{B})$  (Table 45). Comparison between  $^1J(^{19}\text{F}^{11}\text{B})$  and  $^1J(^{19}\text{F}^{13}\text{C})$  shows that  $^1J(^{19}\text{F}^{11}\text{B}) > 0$  in most compounds;  $^1J(^{19}\text{F}^{11}\text{B})$  may be of either sign in  $\text{BF}_3$  and  $\text{BF}_4^-$ , and it may be  $> 0$  in  $\text{BuBF}_3^-$ , considering the

TABLE 44  
Some representative couplings  $^1J(^{31}\text{P}^{11}\text{B})$ .<sup>a</sup>

Compound	$^1J(^{31}\text{P}^{11}\text{B})$ (Hz)	Ref.
$\text{Me}_2\text{P—B}[\text{N}(\text{Me})\text{CH}_2]_2$	44.5 <sup>b</sup>	182
$[(\text{Et}_2\text{P})_4\text{B}]^-$	32.2 <sup>c</sup>	534
$[\text{H}_2\text{P—BH}_3]^-$	29.2	691
$\text{H}_3\text{P—BH}_3$	27.0	566
$\text{Me}_3\text{P—BH}_3$	59.8 <sup>b</sup>	566
$\text{F}_3\text{P—BH}_3$	39.0	566
$(\text{MeO})_3\text{P—BH}_3$	97.2 <sup>b</sup>	566
$\text{Me}_3\text{P—BF}_3$	180.0	478
$\text{Me}_3\text{P—BCl}_3$	166.0	557
$(\text{Me}_2\text{P—BH}_2)_3$	79.3	692
$(\text{Et}_2\text{P—BCl}_2)_2$	99.5	534

<sup>a</sup> For an extensive list of data see Ref. 5.

<sup>b</sup>  $^1J(^{31}\text{P}^{11}\text{B}) > 0$ .

<sup>c</sup>  $^1J(^{31}\text{P}^{11}\text{B}) = 23.5$  Hz, in diglyme.<sup>534</sup>

TABLE 45

Some representative couplings  $^1J(^{19}\text{F}^{11}\text{B})$ .<sup>a</sup>

Compound	$^1J(^{19}\text{F}^{11}\text{B})$ (Hz)	Ref.
$\text{Me}_2\text{BF}$	119	
$\text{MeBF}_2$	76	180
$\text{PhBF}_2$	62	178
$\text{CH}_2(\text{BF}_2)_2$	69	693
$\text{BF}_3$	14.5	5
$\text{Et}_2\text{NBF}_2$	15	5
$(\text{Me}_2\text{N})_2\text{BF}$	23	182
$[\text{BF}_4]^-$	1	5
$\text{Me}_2\text{S}-\text{BF}_3$	24	5
$\text{H}_3\text{N}-\text{BF}_3$	13.9	5
$\text{Me}_3\text{N}-\text{BF}_3$	14-15	5
$\text{Me}_3\text{N}-\text{BH}_2\text{F}$	88.5	5
$\text{Me}_3\text{N}-\text{BHF}_2$	71	5
$\text{Me}_3\text{P}-\text{BF}_3$	50	478

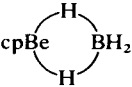
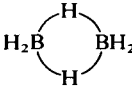
<sup>a</sup> For further data see Ref. 5.

change of  $^1J(^{19}\text{F}^{13}\text{C})$  from  $\text{CF}_4$  ( $-259.2$  Hz) to  $\text{R}-\text{CF}_3$  ( $-163.3$  Hz). In the trigonal boranes the trend in the changes in  $^1J(^{19}\text{F}^{11}\text{B})$  corresponds to that found for comparable carbocations; for example

	$\text{Me}_2\text{BF}$	$\text{Et}_2\text{BF}$	$\text{PhBF}_2$
$^1J(^{19}\text{F}^{11}\text{B})$ (Hz) =	122.0	125.0	58.0
$^1J(^{19}\text{F}^{13}\text{C})$ (Hz) =	420.0	429.1	178.2
	$\text{Me}_2\text{CF}^+$	$\text{Et}_2\text{CF}^+$	$\text{PhCF}_2^+$

(i)  $^1J(\text{M}^{11}\text{B})$  ( $\text{M} = \text{transition metal}$ ). There are very few examples for  $\text{M}-^{11}\text{B}$  spin-spin couplings when  $\text{M}$  is a transition metal (e.g.  $\text{M} = ^{103}\text{Rh}^{673,674}$ ). For  $\text{M} = ^{195}\text{Pt}$ , values of  $^nJ(^{195}\text{Pt}^{11}\text{B})$  have been observed for various complexes in which platinum is connected to a polyhedral borane cluster or is part of the cluster.<sup>675-678</sup>

(j)  $^2J(\text{M}^{11}\text{B})$  (through  $\text{M}-\text{H}-\text{B}$  bridges). Spin-spin coupling  $\text{M}(\text{M}^{11}\text{B})$  through an  $\text{M}-\text{H}-\text{B}$  bridge has been observed for various metals  $\text{M}$ :

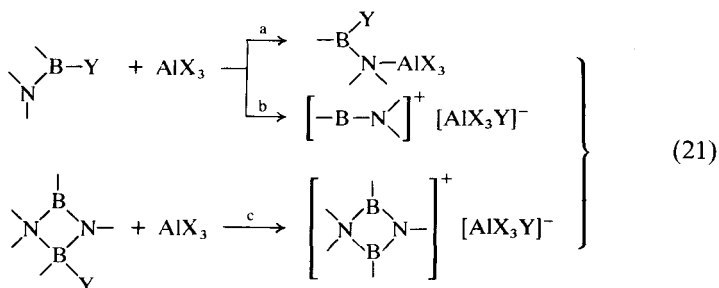
		$\text{Al}(\text{BH}_4)_3$	$\text{Sc}(\text{BH}_4)_3$	$\text{Zr}(\text{BH}_4)_4$
$^2J(\text{M}^{11}\text{B})$ (Hz) = $3.6^{696}$	$3.8^{668}$	$9.0^{698}$	$15.0^{551}$	$18.0^{550}$



arguments from  $^{11}\text{B}$  NMR); (ii) measurement of  $^{10}\text{B}$ – $^{11}\text{B}$  spin–spin coupling if the  $^{11}\text{B}$  nuclei are isochronous.<sup>668,679</sup>

## 2. $^{27}\text{Al}$ NMR

An important application of  $^{27}\text{Al}$  NMR concerns the question whether the reaction of aluminum halides with boranes(3) leads to adduct formation (equation (21a))<sup>148,246,360,711</sup> or to abstraction of an appropriate leaving group (equations (21b,c)):<sup>42, 55, 56, 108, 144, 256, 743</sup>



The former process gives rise to broad resonances (efficient quadrupolar relaxation of the  $^{27}\text{Al}$  nucleus), whereas the latter process leads to sharp  $^{27}\text{Al}$  resonances of  $[\text{AlX}_3\text{Y}]^-$  and—possibly, if  $\text{X} \neq \text{Y}$ —there may be up to five different signals ( $\text{AlX}_4^-$ ,  $\text{AlX}_3\text{Y}^-$ ,  $\text{AlX}_2\text{Y}_2^-$ ,  $\text{AlXY}_3^-$ ,  $\text{AlY}_4^-$ ).

There are only a few other applications of  $^{27}\text{Al}$  NMR; for example monitoring exchange reactions between boronic or borinic esters and  $\text{LiAlH}_4$  or  $\text{Li}(\text{EtOAlH}_3)$  respectively,<sup>501,507</sup> or recording  $^{27}\text{Al}$  NMR spectra if the aluminum is part of the borane structure.<sup>265,266</sup>

## 3. $^{71}\text{Ga}$ NMR

In principle,  $^{71}\text{Ga}$  NMR can be used for the same purpose as  $^{27}\text{Al}$  NMR (although the  $^{71}\text{Ga}$  resonances are much broader) according to (21).<sup>108</sup>

## D. $^{13}\text{C}$ NMR<sup>18,471</sup>

Nowadays,  $^{13}\text{C}$  NMR is routinely used to characterize boranes whenever possible, and there is no need to stress the general advantage of  $^{13}\text{C}$  NMR for structural assignments. A survey of the literature cited in this review shows that more than 200 boron NMR references contain  $^{13}\text{C}$  NMR data. Examples are novel neutral, anionic and cationic boranes(3),<sup>60,68,70,75–77, 84, 110, 139, 147, 151, 162, 163, 167, 227, 248, 256, 257, 276, 304, 305, 312, 319, 323, 345, 646, 705, 715, 716, 720, 721, 783, 784, 787, 790, 792, 795, 796, 798, 799, 801, 821, 823</sup> many  $\pi$ -complexes of boranes<sup>43, 59, 86, 142,</sup>

378,379,382,387,389,394,405,409,413,421,427,440,646 and a great number of borane adducts and borates.<sup>47,141,173,347,476,492,493,515,522,561,572,579,610,614,615,618,632-637,643,719,760,761,763,764,785,786,788,795,797,802,803,820</sup>

Of course, only a fraction of these data are crucial for unambiguous structural assignments. Thus this account concentrates on some features which are characteristic for boron compounds.

### 1. Boron-bonded carbon atoms<sup>7,10</sup>

One aspect is the broadening of  $^{13}\text{C}$  resonances of carbon atoms linked to boron as a result of scalar relaxation of the second kind (see Section II.B and Fig. 1 above). There are still numerous publications in which it is simply stated that these resonances were not detected. This is a negligent attitude, since in general very slight modifications (for example lowering the temperature by approx. 30 °C) are sufficient to observe these signals. In our experience, it may just be necessary to point out that the expected resonance is broad in order to stimulate the operator into taking a closer look at the

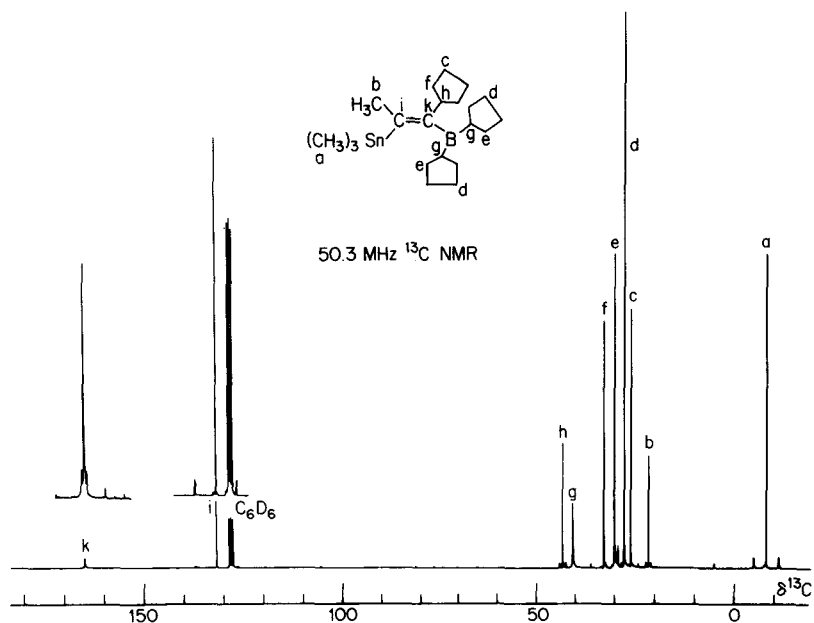


FIG. 2. 50.3 MHz  $^{13}\text{C}\{-^1\text{H}\}$  NMR of the organoborane product from  $\text{B}(\text{c-C}_5\text{H}_9)_3 + \text{Me}_3\text{Sn}-\text{C}\equiv\text{C}-\text{Me}$ , 1:1 ratio. This is a typical  $^{13}\text{C}$  NMR spectrum of a medium-sized organoborane; the broadened  $^{13}\text{C}(\text{BC})$  resonances (g,k) are clearly distinguished and, in this case,  $^{117/119}\text{Sn}$  satellites (a,b,h,i,k) also support structural assignments.

spectrum. In any case, these data are slowly accumulating and there are a growing number of studies where the broad resonances of boron-bonded carbon atoms serve as an excellent tool for structural assignment. Figure 2 shows a typical example.

It was realized in early  $^{13}\text{C}$  NMR studies of methylboranes<sup>205</sup> that there is a relation between  $^{11}\text{B}$  nuclear shielding and the  $\delta^{13}\text{C}$ -values of boron-bonded carbon atoms.

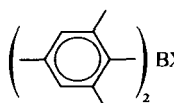
	$\text{Me}_3\text{B}$	$\text{Me}_2\text{BF}$	$\text{Me}_2\text{BOMe}$	$\text{Me}_2\text{BNMe}_2$
$\delta^{13}\text{C}^{205} =$	14.8	7.0 <sup>41</sup>	6.3	44.6
$\delta^{11}\text{B}^5 =$	86	59.0	53.0	4.0
	$\text{MeBF}_2$	$(\text{MeBO})_3$	$\text{MeB}(\text{NMe}_2)_2$	
$\delta^{13}\text{C}^{205} =$	-4.0 <sup>41</sup>	-1.2 <sup>41</sup>	-1.0	
$\delta^{11}\text{B}^5 =$	28.2	29.5	34.0	

Of course, these  $\delta^{13}\text{C}$  values change according to substituent effects exerted by other groups in the  $\alpha$ ,  $\beta$ ,  $\gamma$  and  $\delta$  positions<sup>133,143,151,206</sup>. The increase in  $^{13}\text{C}$  nuclear shielding with increasing electronegativity of the boryl group indicates that changes in the B—C  $\sigma$  bond are responsible for the change in the  $\delta^{13}\text{C}$  values. Therefore this observation corroborates the argument that the energy of the  $\sigma$ -bonding framework is of prime importance in the discussion of the  $\delta^{11}\text{B}$  values of trigonal boranes (see Section III.A.2 and III.B.2 above).

A large number of phenylboranes have been studied by  $^{13}\text{C}$  NMR<sup>10,36,273,707</sup>. The  $\delta^{13}\text{C}(1)$  values of the *ipso*-carbon atoms are affected by influences similar to alkyl carbon atoms. In addition, changes in the electron-density distribution of the whole phenyl ring may have a marked influence.<sup>36,707</sup> With the exception of amino ligands, the changes in  $\delta^{13}\text{C}(1)$  are analogous to those in  $\delta^{13}\text{C}(\text{alkyl})$ :

	$\text{PhB}(\text{CH}_2)_5$	$\text{PhBF}_2$	$\text{PhB}(\text{OMe})_2$	$\text{PhB}(\text{NHMe})_2$
$\delta^{13}\text{C}(1)^{36} =$	140.7	124.0	131.7	140.0 <sup>10</sup>
$\delta^{11}\text{B}^5 =$	77.5	25.1	28.6	30.0

It is conceivable that BN(pp) $\pi$  interactions contribute to the deshielding of the C(1) nucleus. In the case of the mesitylboranes ( $\text{mes}_2\text{BX}$ ), where a coplanar arrangement of the mesityl rings with the  $\text{C}_2\text{BX}$  plane is unlikely, the change in the  $\delta^{13}\text{C}(1)$  value is more regular:

	X = alkyl	Ph	F	OMe	NMe <sub>2</sub>
$\delta^{13}\text{C}(1) = 142.4^{708}$	141.7 <sup>708</sup>	134.3 <sup>709</sup>	136.2 <sup>709</sup>	138.8 <sup>156</sup>	
$\delta^{11}\text{B} = 84.4$	79.3	53.0	51.0	44.5	

In borane adducts or organyl borates changes in the  $^{13}\text{C}(\text{BC})$  resonances remind one closely of the effects observed in the corresponding hydrocarbons or other isostructural compounds (e.g. ammonium or phosphonium salts).<sup>18</sup>

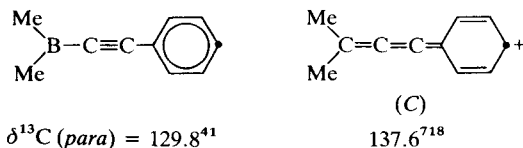
Most  $^{13}\text{C}$  resonances of carbaboranes are also severely broadened by scalar  $^{13}\text{C}$ – $^{11}\text{B}$  spin–spin interactions.<sup>10,43,59,162,429–431,605,689,700–702,723,726,748</sup> The range of the  $\delta^{13}\text{C}$  values is fairly large (approximately 80 ppm) and, similarly to the  $^{11}\text{B}$ -nuclear shielding, prediction of the  $\delta^{13}\text{C}$  values is difficult.

## 2. Carbon atoms removed from boron by two or more bonds

A specific influence of the boron atom upon  $^{13}\text{C}$  resonances of other than B–C carbon atoms has been noted especially for alkenylboranes,<sup>65,69,710,711,714</sup> alkynylboranes<sup>10,524</sup> and phenylboranes<sup>10,36,273,707,712</sup>. In the first two classes of compounds an increase in the shielding of boron is connected with the shielding of the  $\beta$ -carbon atom. Although it is tempting to relate this behaviour to significant contributions of VB structures of the types (A) and (B), it is more appropriate to consider the influence of the boryl group upon the energy of  $\sigma$  and  $\pi$  orbitals:<sup>717</sup>

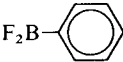
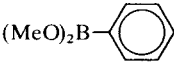
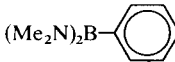


In the case of phenylethynylboranes, it is clearly shown that the deshielding influence of the boryl group is confined mainly to the  $\beta$ -alkynyl carbon atom,<sup>524</sup> whereas in the corresponding carbocations<sup>718</sup> a VB-structure like (C) is more reasonable, and this effect is felt also by the  $^{13}\text{C}$  resonance of the respective *para*- $^{13}\text{C}$  nucleus:

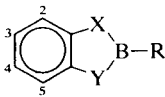
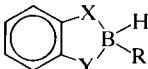


Assuming that strong deshielding of the  $^{13}\text{C}(\text{para})$  resonances in phenyl carbocations is the result of  $\text{CPh}(\text{pp})\pi$  bonding, the weak  $\text{BPh}(\text{pp})\pi$  interactions are indicated by the parallel changes in  $\delta^{13}\text{C}(\text{para})$  for isoelectronic compounds.<sup>36</sup> Again it should be emphasized that boryl groups are weak  $\pi$  acceptors. Interestingly, the  $^{13}\text{C}(\text{para})$  resonances appear to be a

better indicator for the  $\pi$ -acceptor strength of the boryl group than the  $^{11}\text{B}$  resonances. Thus the  $\text{F}_2\text{B}$  group is a stronger  $\pi$  acceptor compared with the  $(\text{MeO})_2\text{B}$  or  $(\text{Me}_2\text{N})_2\text{B}$  groups, although the  $\delta^{11}\text{B}$  values suggest the opposite trend:<sup>36</sup>

		
$\delta^{13}\text{C}(\text{para})$ 136.3	131.1	127.2
$\delta^{11}\text{B} =$ 25.1	28.6	32.4

Another way to demonstrate the relative  $\pi$ -acceptor strength of boron is provided by the measurement of the aromatic  $^{13}\text{C}$  resonances of benzanelated heteroborolenes. This shows that the benzene  $\pi$  system competes successfully for the  $\pi$ -electron density of the heteroatoms (O, N), whereas the  $^{11}\text{B}$  resonances deceptively reflect electronic saturation of the boron atoms.<sup>188</sup>

	X	Y	R	$^{13}\text{C}(2)$	$^{13}\text{C}(3)$	$^{11}\text{B}$
	O	O	alkyl	113.2	123.3	35.5
	O	NH	Me	112.0	119.8	34.4
				110.0(5)	121.9(4)	
	NH	NH	Me	110.7	119.1	30.7
	O	O	NMe <sub>3</sub>	109.4	119.2	10.0

Two-dimensional NMR methods are increasingly used for structural assignment. They have also proved useful in organoboron chemistry.<sup>142,725,727,728,732</sup>

### 3. Dynamical $^{13}\text{C}$ NMR spectroscopy<sup>729</sup>

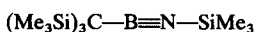
The simplicity of  $^1\text{H}$ -decoupled  $^{13}\text{C}$  NMR spectra frequently permits the study of complex dynamical processes in solution. The selection of the following references show that there are applications in many areas of boron chemistry. This comprises conformational equilibria and exchange processes,<sup>45,291,323,490,596,615,722,731,733,734</sup> rotation about  $\sigma$  bonds<sup>730,735,742</sup> or about B—X bonds with assumed  $\text{BX}(\text{pp})\pi$  interactions,<sup>22,76,126,133,144,156,229,323,707,709,721,735–740,742</sup> rotation of metal fragments about the axis through the plane of the  $\pi$  ligand,<sup>378,382,415</sup> as well as all kinds of intramolecular rearrangements.<sup>77,99,281,296a,579</sup>

## E. $^{29}\text{Si}$ , $^{119}\text{Sn}$ and $^{207}\text{Pb}$ NMR

### 1. $^{29}\text{Si}$ NMR

The first  $^{29}\text{Si}$  resonances of *B*-trimethylsilylboranes have been determined by  $^1\text{H}\{-^{29}\text{Si}\}$  heteronuclear double resonance.<sup>182</sup> Later on, the introduction of polarization-transfer techniques such as INEPT and DEPT<sup>19-21</sup> has made  $^{29}\text{Si}$  NMR more popular. These pulse sequences are easy to apply if the magnitude of a given coupling  $^nJ(^{29}\text{Si}^1\text{H})$  is known.  $^{29}\text{Si}$  NMR spectra, even from diluted reaction solutions, can be obtained in less than 5 min, which means that  $^{29}\text{Si}$  NMR is extremely useful for the determination of the product distribution. There are many examples in the literature where  $^{29}\text{Si}$  NMR has contributed to the structural characterization of boron compounds.

*N*-silyl- and *B*-silyliminoboranes have been studied by  $^{29}\text{Si}$  NMR.<sup>57</sup> The observation of  $^1J(^{29}\text{Si}^{14}\text{N})$  indicates the peculiar bonding situation that results in a symmetrical charge distribution at the nitrogen atom similar to that in isonitriles or isonitrile complexes.



$$\delta^{29}\text{Si} = 0.12 \quad -12.2$$

$$J(^{29}\text{Si}^{14}\text{N}) = 15 \text{ Hz}$$

The shielding of the  $^{29}\text{Si}(\text{NSi})$  nucleus is reminiscent of the trend observed for monoalkynyltrimethylsilanes ( $\delta^{29}\text{Si} = -17$  to  $-20$ ). Most of the  $^{29}\text{Si}$  NMR data for trigonal boranes have been reported for  $\text{B}-\text{Si}$ ,<sup>133,182,330,342</sup>  $\text{S}-\text{Si}$ ,<sup>199</sup>  $\text{N}-\text{Si}$ ,<sup>150,206,228,230,239,241,271,292,309,342,347,369,437,711,730</sup>  $\text{C}-\text{Si}$ ,<sup>70,71,151,342,646,744,745</sup>. Few  $\delta^{29}\text{Si}$  data are available for borane adducts ( $\text{N}-\text{Si}$ ,<sup>476</sup>  $\text{B}-\text{OSi}$ ,<sup>608</sup> and carbaboranes ( $\text{C}-\text{Si}$ ,<sup>429-431,835</sup> and a cage- $^{29}\text{Si}^{430}$ ,  $\delta^{29}\text{Si} = -137.9$ ).

### 2. $^{119}\text{Sn}$ NMR<sup>746</sup>

Except for the significantly broadened resonances found for  $\text{Sn}-\text{B}$  moieties,<sup>182,133,332,334</sup>  $^{119}\text{Sn}$  NMR measurements of tin-containing boron compounds are readily performed.  $^{119}\text{Sn}$  NMR data for various *N*-stannylaminoboranes have been reported.<sup>268,274,492,748</sup> The majority of  $^{119}\text{Sn}$  NMR data concern the products from the organoboration of alkynylstannanes.<sup>66,71,77,111,492,727,728,730,735,744,745,749-757,809</sup> The  $\delta^{119}\text{Sn}$  values, together with the linewidths of the  $^{119}\text{Sn}$  resonances,<sup>71</sup> are extremely useful for studying the mechanism<sup>750,754,755</sup> of the organoboration reaction, as well as in the final characterization of the products. Figure 3 shows an example where the structures of different isomers can be assigned on the basis of the  $^{119}\text{Sn}$  linewidths and the  $\delta^{119}\text{Sn}$  values.

Few  $^{119}\text{Sn}$  NMR data are available for stannacarbaboranes.<sup>429,781</sup>

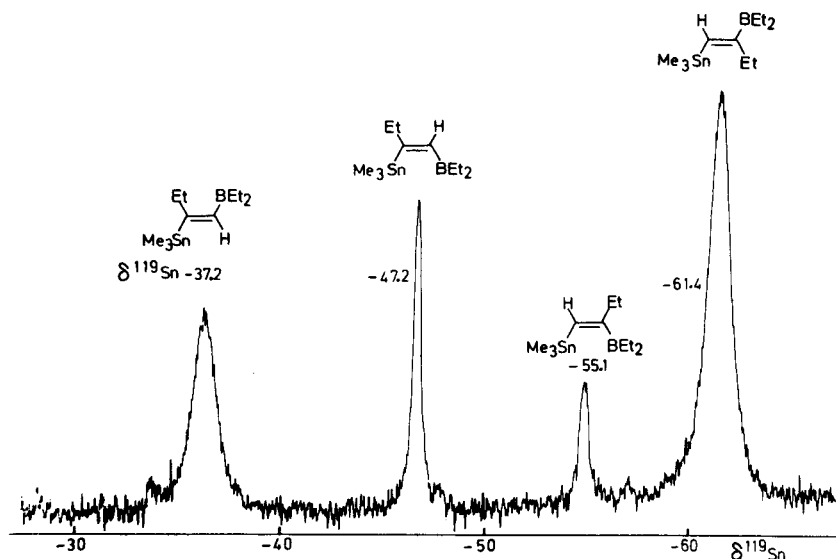


FIG 3. 74.6 MHz  $^{119}\text{Sn}$  NMR of a mixture of isomers obtained after UV-irradiation of the pure product ( $\delta^{119}\text{Sn} = -55.1$ ). Assignments are based on the  $\delta^{119}\text{Sn}$  values and, in particular, on the different linewidth due to partially relaxed scalar coupling  $^3J(^{119}\text{Sn}^{11}\text{B})$  (with  $|^3J(^{119}\text{Sn}^{11}\text{B})_{\text{trans}}| > |^3J(^{119}\text{Sn}^{11}\text{B})_{\text{cis}}|$ ). This is supported by evidence from  $^{13}\text{C}$  and  $^1\text{H}$  NMR.<sup>71</sup>

### 3. $^{207}\text{Pb}$ NMR

Only a single compound with a  $\text{Pb}-\text{B}$  bond has been studied by  $^1\text{H}-\{^{207}\text{Pb}\}$  heteronuclear double resonance.<sup>334</sup> ( $\text{Me}_3\text{PbB}[\text{N}(\text{Me})\text{CH}_2]_2$ ,  $\delta^{207}\text{Pb} = -362.0$ ). However, direct measurement of  $^{207}\text{Pb}$  NMR provides no problem. A number of organoboration products of alkynylplumbanes has been studied by  $^{207}\text{Pb}$  NMR.<sup>41</sup>

### F. $^{14}\text{N}$ and $^{15}\text{N}$ NMR<sup>692</sup>

Nitrogen NMR has been used much more for the discussion of the bonding situation rather than for characterizing a particular boron compound. This is due to (i) the existence of fairly broad  $^{14}\text{N}$  resonances that, in general, do not allow the resolution of several overlapping resonances, and (ii) the low natural abundance of the  $^{15}\text{N}$  isotope. Furthermore, the  $^{15}\text{N}$  resonances may be severely broadened owing to  $^{15}\text{N}-^{11}\text{B}$  scalar spin-spin interactions which significantly reduce the signal-to-noise ratio.

### 1. $^{14}\text{N}$ NMR

In most cases,  $\delta^{14}\text{N}$  values of boron–nitrogen compounds containing a single nitrogen atom per molecule or chemically equivalent nitrogen atoms are readily determined.<sup>5,7,57,85,128,132,143,152,248,249,268,298</sup> The linewidth of the  $^{14}\text{N}$  resonance reflects, among other variables (some of which may be kept constant), the symmetry of the charge distribution at the quadrupolar  $^{14}\text{N}$  nucleus (see equation (2)). In the case of trigonal boranes or amine–borane adducts, this parameter is of some interest. Figure 4 shows the  $^{14}\text{N}$  NMR spectrum of 1,2-dimethylimidazole–borane. In addition to the  $\delta^{14}\text{N}$  values, the different linewidths of the  $^{14}\text{N}$  resonances contain important information on the charge distribution (see also the  $^{14}\text{N}$  NMR spectrum in Fig. 5).

In the case of iminoboranes (see Table 2) the small linewidths are significant.<sup>57</sup> They prove the relationship between the electronic structure of iminoboranes and the isoelectronic nitrilium cations:



The  $\delta^{14}\text{N}$  values of boron–nitrogen compounds reflect the influence of symmetry (as for  $\delta^{11}\text{B}$  values, see Section III.A.2 above) BN(pp) $\pi$  interactions<sup>7,128,152</sup> and steric effects (as for  $\delta^{13}\text{C}$  of alkanes).

### 2. $^{15}\text{N}$ NMR

The few applications of  $^{15}\text{N}$  NMR to boron chemistry are promising for future work. Of the polarization-transfer techniques,<sup>19–21</sup> the basic INEPT

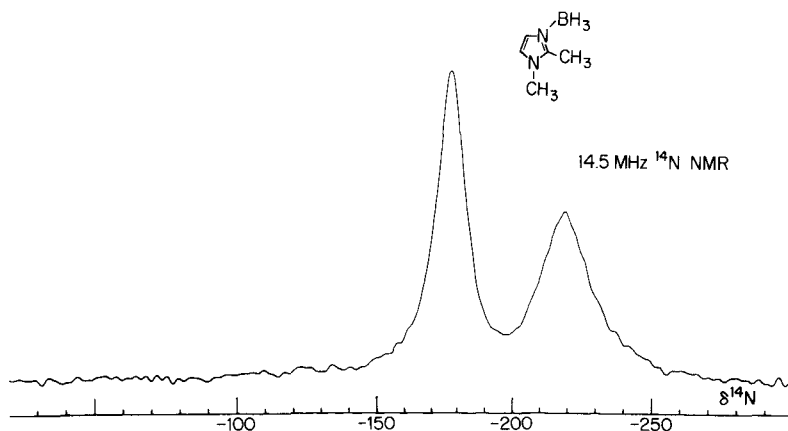


FIG. 4. 14.4 MHz  $^{14}\text{N}$  NMR of 1,2-dimethylimidazole–borane adduct in  $\text{C}_6\text{D}_6$  (10%). The different  $^{14}\text{N}$  linewidths of the two resonances provide information on the charge distribution at the two  $^{14}\text{N}$  nuclei in the ground state.

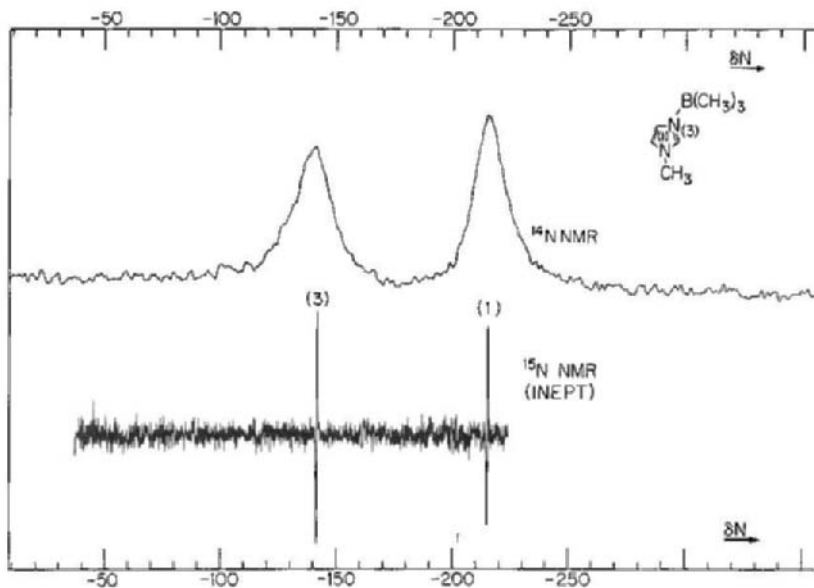


FIG. 5. 14.4 MHz  $^{14}\text{N}$  and 20.8 MHz  $^{15}\text{N}$  NMR spectra of 1-methylimidazole-trimethylborane adduct in  $\text{C}_6\text{D}_6$  (10%). The  $^{14}\text{N}$  NMR signals are still well resolved and fairly accurate;  $\delta\text{N}$  values can be measured. However, it takes only approximately 1 h to obtain the  $^{15}\text{N}$  NMR spectrum at natural abundance using the basic INEPT sequence.<sup>19</sup> The  $^{15}\text{N}(3)$  signal is not significantly broadened, which means that the magnitude of  $|^1J(^{15}\text{N}^{11}\text{B})|$  is very small ( $<5\text{ Hz}$ ).<sup>476,556</sup>

sequence<sup>19a</sup> has proved most useful.<sup>22,476,556</sup> Figure 5 shows an example of this together with the corresponding  $^{14}\text{N}$  NMR spectrum. It is expected that reverse two-dimensional  $^1\text{H}\{-^{15}\text{N}\}$  measurements<sup>669</sup> will be of great use for studying boron compounds containing one or more N—H units.

The broadening of  $^{15}\text{N}(\text{NB})$  resonances together with the magnitude of  $^1J(^{15}\text{N}^1\text{H})$  has already been used to distinguish between the following isomers:<sup>711</sup>

$\delta^{15}\text{N}(\text{NH}) = -297.0$	$-234.0$	$-317.0$
$^1J(^{15}\text{N}^1\text{H}) (\text{Hz}) = 79.3$	$89.5$	$68.0$
$\delta^{11}\text{B} = 44.8$	$38.6$	$38.6$
$\delta^{29}\text{Si} = 10.1$	$-2.7$	$-6.4$

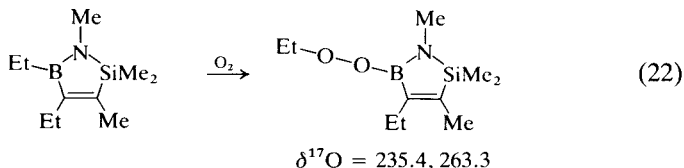
### G. $^{31}\text{P}$ NMR<sup>780</sup>

$^{31}\text{P}$  NMR is routinely measured for boron compounds containing phosphorus. Of course, the wide scope of application of  $^{31}\text{P}$  NMR does not depend on the presence of the boron. However, there are numerous examples that demonstrate that  $^{31}\text{P}$ ,  $^{11}\text{B}$  and other NMR data are complementary<sup>7,61,112,149,168,275,323,346,382,519,592,606,607,759,761,764,765,801-803,814</sup> to name just a few references. The presence of a P—B bond is indicated either by the splitting of the  $^{31}\text{P}$  resonance according to  $^1J(^{31}\text{P}^{11}\text{B})$  or by a distinct broadening due to the efficient relaxation of the  $^{11}\text{B}$  nucleus. The absence of broadening may indicate rapid exchange or the absence of any P—B bonding interaction. The  $\delta^{31}\text{P}$  data fit into the general pattern of  $\delta^{31}\text{P}$  values.<sup>780</sup> A large range is observed for  $\delta^{31}\text{P}$  values of monomer phosphinoboranes. Thus the  $^{31}\text{P}$  resonance of the monomer  $\text{tBu}_2\text{P—BMe}_2$  (105°C) is found at  $\delta^{31}\text{P} = 51.2$ ,<sup>171</sup> in contrast with the  $\delta^{31}\text{P}$  value of  $\text{Me}_2\text{P—B[N(Me)CH}_2\text{]}_2$  ( $\delta^{31}\text{P} = -129.8$ ).<sup>182</sup> This reminds one of the analogous trend of  $\delta^{77}\text{Se}$  for  $\text{MeB(SeMe)}_2$  and  $\text{MeSe—B[N(Me)CH}_2\text{]}_2$  ( $\delta^{77}\text{Se} = 153.5$  and  $-242.0$ ).<sup>182</sup> Since it is unlikely that  $\text{BP(pp)}\pi$  bonding plays an important role, it is again the  $\sigma\text{P—B}$  bond that appears to be of importance.

### H. $^{17}\text{O}$ and $^{77}\text{Se}$ NMR

#### 1. $^{17}\text{O}$ NMR

Following the first natural-abundance  $^{17}\text{O}$  NMR measurements of boron-oxygen compounds,<sup>117,350</sup> the use of  $^{17}\text{O}$ -enriched compounds has led to the study of complex reactions of boroxines<sup>264,265</sup> and diboroxanes.<sup>264,266</sup> There appears to be a great potential for the elucidation of reaction mechanisms with the help of  $^{17}\text{O}$  NMR and compounds selectively labelled with  $^{17}\text{O}$ . Thus it has been shown that a cyclic aminoborane reacts with oxygen to give selectively a stable peroxide:<sup>236</sup>



The  $^{17}\text{O}$ -nuclear shielding of oxoboranes(3)<sup>117,350</sup> decreases with decreasing  $^{11}\text{B}$ -nuclear shielding. In the case of boroxines or tetraalkyldiboroxanes, which show  $\delta^{11}\text{B}$  values close to the corresponding

boroxanes, the  $^{17}\text{O}$ -nuclear shielding is further reduced. This may be interpreted as a result of the extended  $\pi$  system. In any case,  $\sigma$  effects are not negligible, as have been demonstrated for  $\delta^{13}\text{C}(\text{BC})$  values of alkylboranes (see Section IV.D.1 above):

	$\text{B}(\text{OMe})_3$	$\text{EtB}(\text{OMe})_2$	$\text{Et}_2\text{B}-\text{OMe}$	$(\text{EtBO})_3$	$\text{Et}_2\text{B}-\text{O}-\text{BEt}_2$
$\delta^{17}\text{O}^{350}$	11.0	50.0	94.0 <sup>41</sup>	145.0 <sup>117</sup>	223.0
$\delta^{11}\text{B}^5$	18.3	31.5	53.6	33.5 <sup>117</sup>	53.0

Figure 6 shows that  $^{17}\text{O}$  NMR may reveal important information on the bonding situation in oxoboranes:<sup>117</sup> exchange between the two oxygens at the carboxyl group is slow on the NMR timescale (in contrast with monocyclic compounds). Clearly this information is difficult to obtain by other methods.

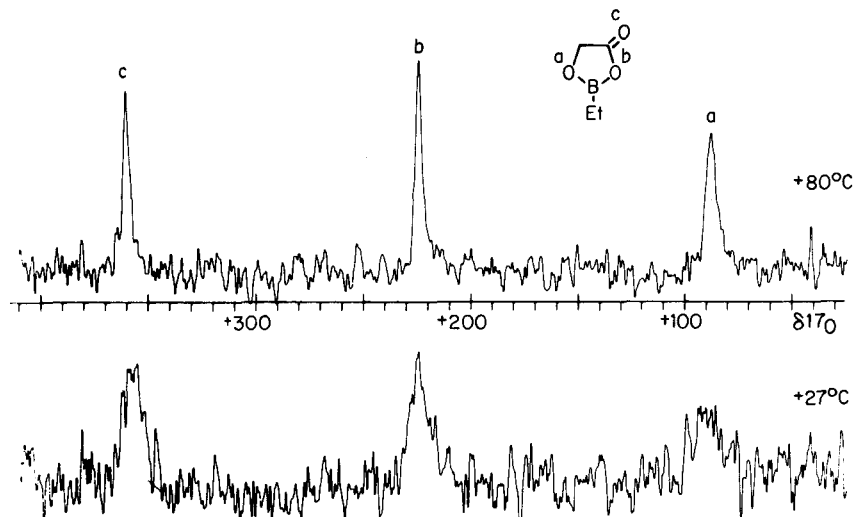


FIG. 6. 27.13 MHz  $^{17}\text{O}$  NMR spectra of 2-ethyl-4-oxo-1,3,2-dioxaborolane ( $\sim 60\%$  in  $\text{C}_7\text{D}_8$ ); spectrometer time 10 min for each spectrum (acquisition time  $\approx 0.06$  s, pulse width  $\approx 40 \mu\text{s} = 90^\circ$  pulse). The influence of increasing temperature on the quadrupolar relaxation rate is obvious. The spectra prove that the exchange of the oxygen sites b and c is slow when compared with the NMR timescale.

## 2. $^{77}\text{Se}$ NMR

After the first indirect observation of  $^{77}\text{Se}$  resonances of boron-selenium compounds by  $^1\text{H}-\{^{77}\text{Se}\}$  heteronuclear double-resonance experiments<sup>182,205</sup> several direct measurements have been carried out.<sup>41,206,270</sup> The large range of  $\delta^{77}\text{Se}$  values is certainly useful for distinguishing between various selenium-boron compounds.

## I. $^{19}\text{F}$ , $^{35}\text{Cl}$ and $^{37}\text{Cl}$ NMR

### 1. $^{19}\text{F}$ NMR<sup>526,766</sup>

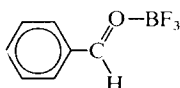
Measurements of  $^{19}\text{F}$  NMR are a matter of routine. Compilations of  $\delta^{19}\text{F}$  values and couplings  $J(^{19}\text{F}^{11}\text{B})$  characterize boron-fluorine compounds.<sup>526,766</sup> Frequently,  $^{19}\text{F}$ – $^{11}\text{B}$  spin-spin coupling serves to establish the presence of the F–B bond. The following references are cited to give some examples of the application of  $^{19}\text{F}$  NMR to boron chemistry.<sup>108,218,275,283,298,342,453,548,598,600,607,642,758,767–769</sup> Further references can be found in

Refs. 5 and 7.

The origin of changes in the  $\delta^{19}\text{F}$  values is poorly understood. There is an increase in  $^{19}\text{F}$ -nuclear shielding as the  $^{11}\text{B}$ -nuclear shielding increases. Since this seems to be a general phenomenon for many nuclei linked to boron, irrespective of possible (pp) $\pi$  interactions, a significant influence of the nature of the  $\sigma\text{F}$ –B bond on  $\delta^{19}\text{F}$  is indicated:

	$\text{Me}_2\text{B}-\text{F}$	$\text{MeBF}_2$	$\text{BF}_3$	$(\text{Me}_2\text{N})_2\text{B}-\text{F}$	$[\text{CH}_2(\text{Me})\text{N}]_2\text{B}-\text{F}$
$\delta^{19}\text{F}^{182} =$	–21.0	–73.0	–131.0	–134.0	–168.0
$\delta^{11}\text{B}^5 =$	59.0	28.1	11.6	21.8	23.4

NOE measurements are of importance for structural assignments as shown in the case of  $^1\text{H}$ – $\{^{19}\text{F}\}$  for the benzaldehyde– $\text{BF}_3$  adduct, indicating that the  $\text{BF}_3$  is complexed *anti* to the phenyl group. This is confirmed by X-ray crystallography and MNDO calculations:<sup>767</sup>



$$\delta^{19}\text{F} = -150.5 \text{ in } \text{CD}_2\text{Cl}_2$$

### 2. $^{35}\text{Cl}$ and $^{37}\text{Cl}$ NMR

Chlorine NMR of fairly small molecules of covalent boron-chlorine compounds gives very broad resonances.<sup>335</sup> In contrast with  $\delta^{19}\text{F}$  values (for the corresponding fluorides), the  $^{35}\text{Cl}$ -nuclear shielding increases slightly from  $\text{BCl}_3$  to  $\text{Me}_2\text{BCl}$  and, similarly to  $\delta^{19}\text{F}$ , a marked increase is noted for bis(amino)chloroboranes:

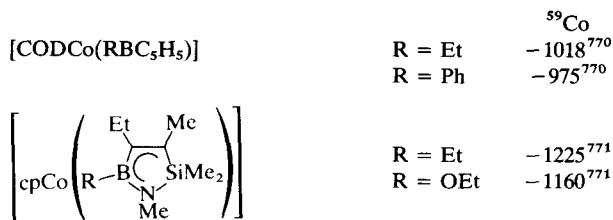
	$\text{Me}_2\text{B}-\text{Cl}$	$\text{MeBCl}_2$	$\text{BCl}_3$	$(\text{Me}_2\text{N})_2\text{B}-\text{Cl}$	$[\text{CH}_2(\text{Me})\text{N}]_2\text{B}-\text{Cl}$
$\delta^{35}\text{Cl}^{335} =$	244.0	288.0	300.0	162.0	71.0
$\delta^{11}\text{B}^5 =$	77.2	62.3	46.5	27.9	26.7

## J. NMR of transition-metal nuclei<sup>725</sup>

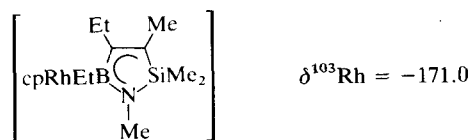
There are a few applications of the NMR of transition-metal nuclei to boron chemistry. For the early transition metals, <sup>45</sup>Sc<sup>551</sup> and <sup>93</sup>Zr resonances<sup>550</sup> have been observed in Sc(BH<sub>4</sub>)<sub>3</sub> and Zr(BH<sub>4</sub>)<sub>4</sub> respectively.

The  $\delta^{183}\text{W}$  value has been determined for a borane adduct as part of the series of [cp(CO)<sub>3</sub>W—PPh<sub>2</sub>—X] compounds with a decrease in <sup>183</sup>W-nuclear shielding for the sequence (X = lone pair, BX<sub>3</sub>, Me, S, Se).<sup>592</sup>

Three studies report  $\delta^{59}\text{Co}$  values; one deals with dicobalt hexacarbonyl- $\eta^2$ -alkyne complexes with organometallic ligands, including boryl groups.<sup>86</sup> All of the  $\delta^{59}\text{Co}$  values are found in a range of approximately 100 ppm (−2450 ± 50). The others are concerned with  $\pi$  complexes of boranes to the CODCo and the cpCo fragments respectively:<sup>770,771</sup>



For the  $\pi$  complex of the 1,2,5-azasilaborole ligand with the cpRh fragment, the <sup>103</sup>Rh resonance has been determined by <sup>1</sup>H-<sup>103</sup>Rh heteronuclear double resonance:<sup>771</sup>



A number of <sup>195</sup>Pt resonances have been measured for various platinum-containing boron compounds,<sup>382,772,773</sup> including borole complexes.<sup>382</sup> In the latter case the  $\delta^{195}\text{Pt}$  data support the arguments of <sup>1</sup>H and <sup>13</sup>C NMR that boroles may be linked as  $\eta^5$  or  $\eta^3$  ligands to platinum depending on the substituents of the borole ring.

## ACKNOWLEDGMENTS

I am grateful to the Deutsche Forschungsgemeinschaft and to the Fonds der Chemischen Industrie for supporting our research. I should also like to thank my wife for her patience and for the careful typing of the manuscript.

## REFERENCES

1. R. Köster (ed.), *Organobor-Verbindungen I-III*, Vol. 13/3a-c, *Houben-Weyl, Methoden der Organischen Chemie*, Thieme, Stuttgart, 1982-1984.
2. H. C. Brown, *Organic Synthesis via Boranes*, Wiley, New York, 1975.
3. (a) W. N. Lipscomb, *Acc. Chem. Res.*, 1973, **6**, 257.  
(b) R. W. Rudolph, *Acc. Chem. Res.*, 1976, **9**, 446.  
(c) W. N. Lipscomb, *Angew. Chem.*, 1977, **89**, 685.
4. G. R. Eaton and W. N. Lipscomb, *NMR Studies of Boron Hydrides and Related Compounds*, Benjamin, New York, 1969.
5. H. Nöth and B. Wrackmeyer, Nuclear magnetic resonance of boron compounds, in *NMR—Basic Principles and Progress* (P. Diehl, E. Fluck and R. Kosfeld, eds), Vol. 14, Springer-Verlag, Berlin, 1978.
6. L. J. Todd and A. R. Siedle, *Prog. NMR Spectrosc.*, 1979, **13**, 87.
7. B. Wrackmeyer and R. Köster, in *Houben-Weyl, Methoden der Organischen Chemie* (R. Köster, ed.), Vol. 13/3c, Thieme, Stuttgart, 1984, pp. 377-611.
8. J. D. Kennedy, in *Multinuclear NMR (NMR in Inorganic and Organometallic Chemistry)* (J. Mason, ed.), Plenum Press, New York, 1987, Chapter 8, 221.
9. A. R. Siedle, *Ann. Rep. NMR Spectrosc.* 1982, **12**, 177.
10. B. Wrackmeyer, *Prog. NMR Spectrosc.*, 1979, **12**, 227.
11. H. Nöth and P. Kölle, *Chem. Rev.*, 1985, **85**, 399.
12. T. Davan and J. A. Morrison, *Inorg. Chem.*, 1986, **25**, 2366.
13. R. N. Grimes, *Adv. Inorg. Chem. Radiochem.*, 1983, **26**, 55.
14. (a) R. N. Grimes, *Acc. Chem. Res.*, 1983, **16**, 22.  
(b) N. N. Greenwood, *Nova Acta Leopold.*, 1985, **59**, 264, 291.
15. W. Siebert, *Angew. Chem.*, 1985, **97**, 924; *Angew. Chem. Int. Ed. Engl.*, 1985, **24**, 943.
16. G. E. Herberich and H. Ohst, *Adv. Organomet. Chem.*, 1986, **25**, 199.
17. (a) A. Allerhand, A. O. Clouse, R. R. Rietz, T. Roseberry and R. Schaeffer, *J. Am. Chem. Soc.*, 1972, **94**, 2445.  
(b) R. R. Rietz and R. Schaeffer, *J. Am. Chem. Soc.*, 1973, **95**, 4580.  
(c) E. J. Stampf, A. R. Garber, J. D. Odom and P. D. Ellis, *Inorg. Chem.*, 1975, **14**, 2446.  
(d) J. D. Kennedy and N. N. Greenwood, *Inorg. Chim. Acta*, 1980, **38**, 93.
18. (a) J. B. Stothers, *Carbon-13 NMR*, Academic Press, New York, 1972.  
(b) H.-O. Kalinowski, S. Berger and S. Braun, *NMR Spektroskopie*, Thieme, Stuttgart, 1984.
19. (a) G. A. Morris and R. Freeman, *J. Am. Chem. Soc.*, 1979, **101**, 760.  
(b) D. P. Burum and R. R. Ernst, *J. Magn. Reson.*, 1980, **39**, 163.  
(c) G. A. Morris, *J. Magn. Reson.*, 1980, **41**, 185.
20. (a) D. T. Pegg, D. M. Doddrell, W. M. Brooks and M. R. Bendall, *J. Magn. Reson.*, 1981, **44**, 32.  
(b) O. W. Sørensen and R. R. Ernst, *J. Magn. Reson.*, 1983, **51**, 477.
21. D. T. Pegg, D. M. Doddrell and M. R. Bendall, *J. Chem. Phys.*, 1982, **77**, 2745.
22. B. Wrackmeyer, *Z. Naturforsch.*, 1986, **41b**, 59.
23. D. Shaw, *Fourier Transform N.M.R. Spectroscopy*, Elsevier, Amsterdam, 1984.
24. R. K. Harris and B. E. Mann (eds), *NMR and the Periodic Table*, Academic Press, New York, 1978.
25. A. Abragam, *The Principles of Nuclear Magnetism*, Oxford University Press, 1961.
26. V. Mlynarik, *Prog. NMR Spectrosc.*, 1986, **18**, 277.
27. R. Köster, H. J. Horstschäfer and P. Binger, *Liebigs Ann. Chem.*, 1986, **717**, 1.
28. R. Goetze and H. Nöth, *J. Organomet. Chem.*, 1978, **145**, 151.

29. T. Renk, W. Ruf and W. Siebert, *J. Organomet. Chem.*, 1976, **120**, 1.
30. G. E. Herberich, E. Bauer, J. Hengesbach, U. Kölle, G. Huttner and H. Lorenz, *Chem. Ber.*, 1977, **110**, 760.
31. G. Menz and B. Wrackmeyer, *Z. Naturforsch.*, 1977, **32b**, 1400.
32. P. Jutzi, *Angew. Chem.*, 1972, **84**, 28; *Angew. Chem. Int. Ed. Engl.*, 1972, **11**, 53.
33. N. M. D. Brown, F. Davidson and J. W. Wilson, *J. Organomet. Chem.*, 1980, **185**, 277.
34. A. T. Jeffries and A. T. Parkanyi, *J. Phys. Chem.*, 1976, **80**, 287.
35. B. Wrackmeyer and H. Nöth, *Chem. Ber.*, 1976, **109**, 1075.
36. J. D. Odom, T. F. Moore, R. Goetze, H. Nöth and B. Wrackmeyer, *J. Organomet. Chem.*, 1979, **173**, 15.
37. E. J. Stampf and J. D. Odom, *J. Organomet. Chem.*, 1977, **131**, 171.
38. B. Wrackmeyer, *Z. Naturforsch.*, 1980, **35b**, 439.
39. B. M. Mikhailov, T. A. Shchegoleva, E. M. Shashkova and V. G. Kiselev, *Izvest. Akad. Nauk SSSR Ser. Khim.*, 1977, 894.
40. B. M. Mikhailov and V. A. Dorokhov, *Izvest. Akad. Nauk SSSR Ser. Khim.*, 1973, 2165.
41. B. Wrackmeyer, Unpublished results.
42. H. Nöth, R. Staudigl and H.-U. Wagner, *Inorg. Chem.*, 1982, **21**, 706.
43. M. Hildenbrand, H. Pritzkow, U. Zenneck and W. Siebert, *Angew. Chem.*, 1984, **96**, 371; *Angew. Chem. Int. Ed. Engl.*, 1984, **23**, 371.
44. J.-P. Costes, G. Cros and J.-P. Laurent, *Org. Magn. Reson.*, 1977, **9**, 703.
45. M. E. Gursky, A. S. Shashkov and B. M. Mikhailov, *J. Organomet. Chem.*, 1980, **199**, 171.
46. R. Contreras and B. Wrackmeyer, *Z. Naturforsch.*, 1980, **35b**, 1236.
47. H. C. Brown and J. A. Soderquist, *J. Org. Chem.*, 1980, **45**, 846.
48. R. Contreras and B. Wrackmeyer, *J. Organomet. Chem.*, 1981, **205**, 15.
49. P. Paetzold and C. von Platho, *Chem. Ber.*, 1982, **115**, 2819.
50. H. Nöth and S. Weber, *Z. Naturforsch.*, 1983, **38b**, 1460.
51. H. C. Brown, D. Basavalah and N. G. Bhat, *Organometallics*, 1983, **2**, 1468.
52. P. Paetzold, A. Richter, T. Thijsen and S. Württemberg, *Chem. Ber.*, 1979, **112**, 3811.
53. P. Paetzold, C. von Platho, G. Schmid, R. Boese, B. Schrader, D. Bougeard, U. Pfeiffer, R. Gleiter and W. Schäfer, *Chem. Ber.*, 1984, **117**, 1089.
54. P. v. R. Schleyer, P. H. M. Budzelaar, D. Kremer and E. Kraka, *Angew. Chem.*, 1984, **96**, 374; *Angew. Chem. Int. Ed. Engl.*, 1984, **23**, 374.
55. H. Nöth, B. Rasthofer and S. Weber, *Z. Naturforsch.*, 1984, **39b**, 1058.
56. R. Staudigl, Dissertation, Universität München, 1981.
57. M. Haase and U. Klingebiel, *Angew. Chem.*, 1985, **97**, 335; *Angew. Chem. Int. Ed. Engl.*, 1985, **24**, 324.
58. B. Glaser and H. Nöth, *Angew. Chem.*, 1985, **97**, 424; *Angew. Chem. Int. Ed. Engl.*, 1985, **24**, 416.
59. M. Hildenbrand, H. Pritzkow and W. Siebert, *Angew. Chem.*, 1985, **97**, 769; *Angew. Chem. Int. Ed. Engl.*, 1985, **24**, 759.
60. A. J. Ashe, S. T. Abu-Orabi, O. Eisenstein and H. F. Sandford, *J. Org. Chem.*, 1983, **48**, 901.
61. H. J. Bestmann and T. Arenz, *Angew. Chem.*, 1984, **96**, 363; *Angew. Chem. Int. Ed. Engl.*, 1984, **24**, 381.
62. C. Eaborn, M. N. A. El-Kheli, P. B. Hitchcock and J. D. Smith, *J. Organomet. Chem.*, 1984, **272**, 1.
63. J. J. Eisch, J. E. Galle and S. Kozima, *J. Am. Chem. Soc.*, 1986, **108**, 379.
64. A. J. Ashe, E. Meyers, P. Shu and T. von Lehman, *J. Am. Chem. Soc.*, 1975, **97**, 6865.
65. H.-O. Berger, H. Nöth and B. Wrackmeyer, *Chem. Ber.*, 1979, **112**, 2866.

66. B. Wrackmeyer, *Rev. Silicon, Germanium, Tin, Lead Compds*, 1982, **6**, 75.
67. G. E. Herberich, B. Buller, B. Hessner and W. Oschmann, *J. Organomet. Chem.*, 1980, **195**, 253.
68. C. Pues and A. Berndt, *Angew. Chem.*, 1984, **96**, 306; *Angew. Chem. Int. Ed. Engl.*, 1984, **23**, 313.
69. L. W. Hall, J. D. Odom and P. D. Ellis, *J. Am. Chem. Soc.*, 1975, **97**, 4527.
70. N. S. Hosmane, N. N. Sirmokadam and M. N. Mollenhauer, *J. Organomet. Chem.*, 1985, **279**, 359.
71. B. Wrackmeyer, *Polyhedron*, 1986, **5**, 1709.
72. R. Köster, H. J. Horstschäfer, P. Binger and P. K. Mattschei, *Liebigs Ann. Chem.*, 1975, 1339.
73. M. P. Brown, A. K. Holliday and G. Way, *J. Chem. Soc. Dalton Trans.*, 1975, 148.
74. R. Köster, G. Seidel and B. Wrackmeyer, *Angew. Chem.*, 1985, **97**, 317; *Angew. Chem. Int. Ed. Engl.*, 1985, **24**, 326.
75. R. Wehrmann, H. Klusik and A. Berndt, *Angew. Chem.*, 1984, **96**, 369; *Angew. Chem. Int. Ed. Engl.*, 1984, **23**, 369.
76. M. V. Garad and J. W. Wilson, *J. Chem. Res. (S)*, 1982, 132.
77. B. Wrackmeyer, *Organometallics*, 1984, **3**, 1.
78. P. Jutzi and A. Seufert, *J. Organomet. Chem.*, 1979, **169**, 373.
79. M. V. Garad, A. Pelter, B. Singaram and J. W. Wilson, *Tetrahedron Lett.*, 1983, 637.
80. A. J. Ashe and P. Shu, *J. Am. Chem. Soc.*, 1971, **93**, 1804.
81. G. E. Herberich, H. J. Becker and C. Engelke, *J. Organomet. Chem.*, 1978, **153**, 265.
82. G. E. Herberich, B. Hessner and D. Söhnen, *J. Organomet. Chem.*, 1982, **233**, C35.
83. G. E. Herberich, B. Hessner and D. Söhnen, *J. Organomet. Chem.*, 1983, **256**, C23.
84. G. E. Herberich and B. Hessner, *J. Organomet. Chem.*, 1978, **161**, C36.
85. B. Wrackmeyer and H. Nöth, *Chem. Ber.*, 1977, **110**, 1086.
86. P. Galow, A. Sebald and B. Wrackmeyer, *J. Organomet. Chem.*, 1983, **259**, 253.
87. H. C. Brown and J. A. Sinclair, *J. Organomet. Chem.*, 1977, **131**, 163.
88. N. F. Ramsey, *Phys. Rev.*, 1950, **78**, 689.
89. (a) J. A. Pople, *Discuss. Faraday Soc.*, 1962, **34**, 7.  
(b) J. A. Pople, *J. Chem. Phys.*, 1962, **37**, 60.  
(c) J. A. Pople, *Mol. Phys.*, 1964, **7**, 301.
90. M. Mehring, *High Resolution NMR in Solids*, Springer-Verlag, Berlin, 1983.
91. A. J. Beeler, P. Cutts, A. Orendt, D. M. Grant, J. Michl, K. W. Zilm, J. W. Downing, J. C. Facelli, M. Schindler and W. J. Kutzelnigg, *J. Am. Chem. Soc.*, 1984, **106**, 7672.
92. K. W. Zilm, R. T. Conlin, D. M. Grant and J. Michl, *J. Am. Chem. Soc.*, 1980, **102**, 6672.
93. K. A. K. Ebraheem and G. A. Webb, *Org. Magn. Reson.*, 1977, **10**, 258.
94. J. L. Hubbard and G. W. Kramer, *J. Organomet. Chem.*, 1978, **156**, 81.
95. S. Hermanek, V. Gregov, B. Stibr, J. Plesek, Z. Janousek and V. A. Antonovich, *Collect. Czech. Chem. Commun.*, 1976, **41**, 1492.
96. R. E. Williams, *Progress in Boron Chemistry* (R. J. Brotherton and H. Steinberg, eds), Vol. 2, Pergamon, Oxford, 1970.
97. S. Hermanek and J. Plesek, *Z. Anorg. Allg. Chem.*, 1974, **409**, 115.
98. F. Teixidor, C. Vinas and R. W. Rudolph, *Inorg. Chem.*, 1986, **25**, 3339.
99. H. Klusik and A. Berndt, *Angew. Chem.*, 1983, **95**, 895; *Angew. Chem. Int. Ed. Engl.*, 1983, **22**, 877.
100. (a) M. M. Maricq, J. S. Waugh, J. L. Fletcher and M. J. M. McGlinchey, *J. Am. Chem. Soc.*, 1978, **100**, 6902.  
(b) D. E. Wemmer and A. Pines, *J. Am. Chem. Soc.*, 1981, **103**, 34.
101. W. Siebert and W. Rothmel, *Ang. Chem.*, 1977, **89**, 346; *Angew. Chem. Int. Ed. Engl.*, 1977, **16**, 333.

102. A. Berndt and B. Wrackmeyer, Unpublished results, 1985.
103. P. H. M. Budzelaar, P. von R. Schleyer and K. Krogh-Jespersen, *Angew. Chem.*, 1984, **96**, 809; *Angew. Chem. Int. Ed. Engl.*, 1984, **23**, 825.
104. T. Vladimiroff and E. R. Malinowski, *J. Chem. Phys.*, 1967, **46**, 1830.
105. B. F. Spielvogel, W. R. Nutt and R. A. Izydore, *J. Am. Chem. Soc.*, 1975, **97**, 1609.
106. (a) J. Kroner, D. Nölle and H. Nöth, *Z. Naturforsch.*, 1973, **28b**, 416.  
(b) J. Kroner, D. Nölle, H. Nöth and W. Winterstein, *Z. Naturforsch.*, 1974, **29b**, 476.
107. H. Nöth and H. Vahrenkamp, *Chem. Ber.*, 1966, **99**, 1049.
108. H. Nöth and B. Rasthofer, *Chem. Ber.*, 1986, **119**, 2075.
109. M. Armbrecht and A. Meller, *J. Organomet. Chem.*, 1986, **311**, 1.
110. G. Schmidt, G. Baum, W. Massa and A. Berndt, *Angew. Chem.*, 1986, **98**, 1123; *Angew. Chem. Int. Ed. Engl.*, 1986, **25**, 1111.
111. L. Killian and B. Wrackmeyer, *J. Organomet. Chem.*, 1977, **132**, 213.
112. H.-O. Berger and H. Nöth, *J. Organomet. Chem.*, 1983, **250**, 33.
113. C. Habben, W. Maringgele and A. Meller, *Z. Naturforsch.*, 1982, **37b**, 43.
114. R. Contreras and B. Wrackmeyer, *Spectrochim. Acta*, 1982, **A38**, 941.
115. I. Kronawitter and H. Nöth, *Chem. Ber.*, 1972, **105**, 242.
116. W. Tenzl and R. Köster, *Inorg. Synth.*, 1983, **22**, 188.
117. B. Wrackmeyer and R. Köster, *Chem. Ber.*, 1982, **115**, 2022.
118. H. Prigge, Dissertation, Universität München, 1983.
119. C. S. Cundy and H. Nöth, *J. Organomet. Chem.*, 1971, **30**, 135.
120. J. D. Odom, A. J. Zozulin, S. A. Johnston, J. R. Durig, S. Riethmiller and E. J. Stampf, *J. Organomet. Chem.*, 1980, **201**, 351.
121. H. Vahrenkamp, *J. Organomet. Chem.*, 1971, **28**, 167.
122. V. A. Dorokhov, O. G. Boldyreva and B. M. Mikhailov, *Izv. Akad. Nauk SSSR*, 1971, 191.
123. W. Biffar, Dissertation, Universität München, 1981.
124. U. Schuchardt, Dissertation, Universität München, 1973.
125. F. Davidson and J. W. Wilson, *J. Organomet. Chem.*, 1981, **204**, 147.
126. R. I. Baxter, R. J. M. Sands and J. W. Wilson, *J. Chem. Res. (S)*, 1983, 94.
127. H. Nöth and H. Vahrenkamp, *Chem. Ber.*, 1967, **100**, 3353.
128. W. Becker, W. Beck, H. Nöth and B. Wrackmeyer, *Chem. Ber.*, 1972, **105**, 2883.
129. J. Casanova and M. Geisel, *Inorg. Chem.*, 1974, **13**, 2783.
130. H. Nöth, *Chem. Ber.*, 1971, **104**, 558.
131. H. Nöth and W. Storch, *Chem. Ber.*, 1977, **110**, 2607.
132. H. Nöth, W. Tinhof and B. Wrackmeyer, *Chem. Ber.*, 1974, **107**, 518.
133. W. Biffar, H. Nöth, H. Pommerening, R. Schwerthöffer, W. Storch and B. Wrackmeyer, *Chem. Ber.*, 1981, **114**, 49.
134. H. Nöth and H. Vahrenkamp, *J. Organomet. Chem.*, 1969, **16**, 357.
135. W. Storch and H. Nöth, *Chem. Ber.*, 1977, **110**, 1636.
136. H. Fußstetter, R. Kroll and H. Nöth, *Chem. Ber.*, 1977, **110**, 3829.
137. H. Nöth, H. Prigge and A.-R. Rotsch, *Chem. Ber.*, 1986, **119**, 1361.
138. C. K. Narula and H. Nöth, *J. Organomet. Chem.*, 1985, **281**, 131.
139. R. Boese, N. Finke, J. Henkelmann, G. Maier, P. Paetzold, H. P. Reisenauer and G. Schmid, *Chem. Ber.*, 1985, **118**, 1644.
140. H. C. Brown, D. Basavaiah and N. G. Bhat, *Organometallics*, 1983, **2**, 1309.
141. H. E. Katz, *J. Org. Chem.*, 1985, **50**, 5027.
142. P. Paetzold, N. Finke, P. Wennek, G. Schmid and R. Boese, *Z. Naturforsch.*, 1986, **41b**, 167.
143. H. Nöth and H. Prigge, *Chem. Ber.*, 1986, **119**, 338.
144. P. Kölle and H. Nöth, *Chem. Ber.*, 1986, **119**, 313.

145. U. Höbel, H. Nöth and H. Prigge, *Chem. Ber.*, 1986, **119**, 325.
146. P. J. Domaille, J. D. Druliner, L. W. Gosser, J. M. Read, E. R. Schmelzer and W. R. Stevens, *J. Org. Chem.*, 1985, **50**, 189.
147. P. Paetzold, K. Delpy, R. P. Hughes and W. A. Herrmann, *Chem. Ber.*, 1985, **118**, 1724.
148. K. Anton, P. Konrad and H. Nöth, *Chem. Ber.*, 1984, **117**, 863.
149. H. Nöth and W. Storch, *Chem. Ber.*, 1984, **117**, 2140.
150. C. Habben and A. Meller, *Chem. Ber.*, 1984, **117**, 2531.
151. R. Wehrmann, H. Meyer and A. Berndt, *Angew. Chem.*, 1985, **97**, 779; *Angew. Chem. Int. Ed. Engl.*, 1985, **24**, 788.
152. H. Nöth and B. Wrackmeyer, *Chem. Ber.*, 1973, **106**, 1145.
153. H. Nöth and B. Wrackmeyer, *Chem. Ber.*, 1981, **114**, 1150.
154. H. Nöth and R. Staudigl, *Z. Anorg. Allg. Chem.*, 1981, **481**, 41.
155. R. Köster and G. Seidel, *Liebigs Ann. Chem.*, 1977, 1837.
156. N. M. D. Brown, F. Davidson and J. W. Wilson, *J. Organomet. Chem.*, 1980, **192**, 133.
157. F. A. Davis, M. J. S. Dewar, R. Jones and S. D. Worley, *J. Am. Chem. Soc.*, 1969, **91**, 2094.
158. S. Amirkhalili, R. Boese, U. Höhner, D. Kampmann, G. Schmid and P. Rademacher, *Chem. Ber.*, 1982, **115**, 732.
159. H. Fußstetter and H. Nöth, *Liebigs Ann. Chem.*, 1981, 633.
160. R. Köster and G. Seidel, *Inorg. Synth.*, 1983, **22**, 185.
161. G. W. Herberich and H. Ohst, *Z. Naturforsch.*, 1983, **38b**, 1388.
162. G. E. Herberich, H. Ohst and H. Mayer, *Angew. Chem.*, 1984, **96**, 975; *Angew. Chem. Int. Ed. Engl.*, 1984, **23**, 969.
163. H. Klusik, C. Pues and A. Berndt, *Z. Naturforsch.*, 1984, **39b**, 1042.
164. H. Nöth and H. Pommerening, *Chem. Ber.*, 1981, **114**, 3044.
165. K. Schlüter and A. Berndt, *Angew. Chem.*, 1980, **92**, 64; *Angew. Chem. Int. Ed. Engl.*, 1980, **19**, 57.
166. W. Biffar, H. Nöth and H. Pommerening, *Angew. Chem.*, 1980, **92**, 63; *Angew. Chem. Int. Ed. Engl.*, 1980, **19**, 56.
167. F. Dirschl, E. Hanecker, H. Nöth, W. Rattay and W. Wagner, *Z. Naturforsch.*, 1986, **41b**, 32.
168. W. Jacksties, H. Nöth and W. Storch, *Chem. Ber.*, 1985, **118**, 2030.
169. H. Nöth and S. Weber, *Chem. Ber.*, 1986, **118**, 2554.
170. H. Nöth and S. Weber, *Chem. Ber.*, 1984, **116**, 2144.
171. E. Sattler, Personal communication, 1985.
172. R. Goetze and H. Nöth, *Z. Naturforsch.*, 1975, **30b**, 875.
173. M. A. Sens, J. D. Odom and M. H. Goodrow, *Inorg. Chem.*, 1976, **15**, 2825.
174. B. Pachaly and R. West, *Angew. Chem.*, 1984, **96**, 444; *Angew. Chem. Int. Ed. Engl.*, 1984, **23**, 454.
175. H. Nöth, H. Schäfer and G. Schmid, *Z. Naturforsch.*, 1971, **26b**, 497.
176. A. A. Cheremisin and P. V. Schastnev, *J. Magn. Reson.*, 1980, **40**, 459.
177. A. H. Cowley and T. A. Furtch, *J. Am. Chem. Soc.*, 1969, **91**, 39.
178. S. S. Krishnamurthy, M. F. Lappert and J. B. Pedley, *J. Chem. Soc. Dalton Trans.*, 1975, 1214.
179. C. D. Good und D. M. Ritter, *J. Am. Chem. Soc.*, 1962, **84**, 1162.
180. H. Nöth and H. Vahrenkamp, *J. Organomet. Chem.*, 1968, **11**, 399.
181. W. Haubold und J. Weidlein, *Z. Anorg. Allg. Chem.*, 1976, **420**, 251.
182. H. Fußstetter, H. Nöth, B. Wrackmeyer and W. McFarlane, *Chem. Ber.*, 1977, **110**, 3172.
183. W. G. Woods and P. L. Strong, *J. Organomet. Chem.*, 1967, **7**, 371.

184. C. Eaborn, M. N. El-Kheli, N. Retta and J. D. Smith, *J. Organomet. Chem.*, 1983, **249**, 23.
185. W. V. Dahlhoff and R. Köster, *Liebigs Ann. Chem.*, 1975, 1625.
186. L. Barton and J. M. Cramp, *Inorg. Chem.*, 1973, **12**, 2252.
187. R. H. Cragg and J. C. Lockhart, *J. Organomet. Chem.*, 1969, **31**, 2282.
188. R. Goetze, H. Nöth, H. Pommerening, D. Sedlak and B. Wrackmeyer, *Chem. Ber.*, 1981, **114**, 1884.
189. F. A. Davis, M. J. S. Dewar and R. Jones, *J. Am. Chem. Soc.*, 1968, **90**, 706.
190. H. C. Brown and T. E. Coole, *Organometallics*, 1985, **4**, 816.
191. H. Vahrenkamp, Dissertation, Universität München, 1967.
192. P. Paetzold, Unpublished results, 1975.
193. H. C. Brown and T. E. Coole, *Organometallics*, 1983, **2**, 1316.
194. W. Siebert, U. Ender and R. Schütze, *Z. Naturforsch.*, 1985, **40b**, 996.
195. G. W. Kabalka, U. Sastry, K. A. R. Sastry, F. F. Knapp and P. C. Srivastava, *J. Organomet. Chem.*, 1983, **259**, 269.
196. H. C. Brown, N. G. Bhat and V. Somayaji, *Organometallics*, 1983, **2**, 1311.
197. H. Nöth and U. Schuchardt, *Chem. Ber.*, 1974, **107**, 3104.
198. A. Haas and M. Häberlein, *Z. Anorg. Allg. Chem.*, 1976, **427**, 97.
199. K. Hennemuth, A. Meller and M. Wojnowska, *Z. Anorg. Allg. Chem.*, 1982, **489**, 47.
200. R. Goetze and H. Nöth, *Z. Naturforsch.*, 1980, **35b**, 1212.
201. M. Schmidt and W. Siebert, *Chem. Ber.*, 1969, **102**, 2752.
202. R. Schwerthöffer, Dissertation, Universität München, 1974.
203. W. Haubold and U. Kraatz, *Chem. Ber.*, 1979, **112**, 1083.
204. E. F. Mooney and M. G. Anderson, *Ann. Rep. NMR Spectrosc.*, 1969, **2**, 219.
205. W. McFarlane, B. Wrackmeyer and H. Nöth, *Chem. Ber.*, 1975, **105**, 3831.
206. C. Habben and A. Meller, *Chem. Ber.*, 1986, **119**, 9.
207. (a) C. Habben, W. Maringele and A. Meller, *Z. Naturforsch.*, 1982, **37b**, 43.  
(b) M. Noltemeyer, G. M. Sheldrick, C. Habben and A. Meller, *Z. Naturforsch.*, 1983, **38b**, 1182.
208. W. Storch, Dissertation, Universität München, 1974.
209. E. F. Rothgery, P. J. Busse and K. Niedenzu, *Inorg. Chem.*, 1971, **10**, 2243.
210. L. Weber and G. Schmid, *Angew. Chem.*, 1974, **86**, 519; *Angew. Chem. Int. Ed. Engl.*, 1974, **13**, 467.
211. K. Niedenzu and J. S. Merriam, *Z. Anorg. Allg. Chem.*, 1974, **406**, 251.
212. H. Fußstetter, Dissertation, Universität München, 1977.
213. H. Nöth and W. Storch, *Chem. Ber.*, 1976, **109**, 884.
214. E. B. Bradley, R. H. Herber, P. J. Busse and K. Niedenzu, *J. Organomet. Chem.*, 1973, **52**, 297.
215. F. A. Davis, I. J. Turchi, B. E. Maryanoff and R. O. Hutchins, *J. Org. Chem.*, 1972, **37**, 1583.
216. J. B. Leach and J. H. Morris, *J. Organomet. Chem.*, 1969, **13**, 313.
217. P. Paetzold and R. Truppat, *Chem. Ber.*, 1983, **116**, 1531.
218. H. Bürger, M. Grunwald and G. Pawelke, *J. Fluor. Chem.*, 1986, **31**, 89.
219. G. Schmid and J. Schulze, *Angew. Chem.*, 1977, **89**, 258; *Angew. Chem. Int. Ed. Engl.*, 1977, **16**, 249.
220. K. Nölle, H. Nöth and W. Winterstein, *Z. Anorg. Allg. Chem.*, 1974, **406**, 235.
221. D. Nölle and H. Nöth, *Chem. Ber.*, 1978, **111**, 469.
222. H. Nöth, W. Winterstein, W. Kaim and H. Bock, *Chem. Ber.*, 1979, **112**, 2494.
223. K. Barlos and H. Nöth, *Z. Naturforsch.*, 1980, **35b**, 407.
224. P. Paetzold, C. von Plotho, E. Niecke and R. Rüger, *Chem. Ber.*, 1983, **116**, 1678.

225. P. Paetzold and T. von Bennigsen-Mackiewicz, *Chem. Ber.*, 1981, **114**, 298.
226. W. Storch, W. Jackstiess, H. Nöth and G. Winter, *Angew. Chem.*, 1977, **89**, 494; *Angew. Chem. Int. Ed. Engl.*, 1977, **16**, 478.
227. T. Franz, E. Hanecker, H. Nöth, W. Stöcker, W. Storch and G. Winter, *Chem. Ber.*, 1986, **119**, 900.
228. H.-A. Steuer, A. Meller and G. Elter, *J. Organomet. Chem.*, 1985, **295**, 1.
229. M. Armbrrecht, W. Maringgele, A. Meller, M. Noltemeyer and G. M. Sheldrick, *Z. Naturforsch.*, 1985, **40b**, 1113.
230. A. Meller and M. Armbrrecht, *Chem. Ber.*, 1986, **119**, 1.
231. F. Kumpfmüller, D. Nölle, H. Nöth, H. Pommerening and R. Staudigl, *Chem. Ber.*, 1985, **118**, 483.
232. W. Maringgele, *J. Organomet. Chem.*, 1981, **222**, 17.
233. J. Bielawski, K. Niedenzu and J. S. Stewart, *Z. Naturforsch.*, 1985, **40b**, 389.
234. P. Paetzold, C. von Plotho, H. Schwan and H.-U. Meier, *Z. Naturforsch.*, 1984, **39b**, 610.
235. B. M. Mikhailov, V. A. Dorokhov, N. V. Mostovi, O. G. Boldyreva and M. N. Bochkareva, *Zh. Obshch. Chim.*, 1970, **40**, 1817.
236. R. Köster and G. Seidel, *Angew. Chem.*, 1984, **96**, 146; *Angew. Chem. Int. Ed. Engl.*, 1984, **23**, 155.
237. D. Nölle and H. Nöth, *Z. Naturforsch.*, 1972, **27b**, 1425.
238. K. Barlos, D. Nölle and H. Nöth, *Z. Naturforsch.*, 1977, **32b**, 1005.
239. R. Oesterle, W. Maringgele and A. Meller, *J. Organomet. Chem.*, 1985, **284**, 281.
240. J. Bielawski and K. Niedenzu, *Synth. React. Inorg. Met.-Org. Chem.*, 1980, **10**, 479.
241. C. Habben, A. Meller, M. Noltemeyer and G. M. Sheldrick, *J. Organomet. Chem.*, 1985, **288**, 1.
242. C. Habben and A. Meller, *Z. Naturforsch.*, 1984, **39b**, 1022.
243. W. Siebert, R. Full, J. Edwin and K. Kinberger, *Chem. Ber.*, 1978, **111**, 823.
244. H. Nöth and R. Staudigl, *Chem. Ber.*, 1982, **115**, 1555.
245. K. Anton, H. Nöth and H. Pommerening, *Chem. Ber.*, 1984, **117**, 2479.
246. K. Anton, C. Euringer and H. Nöth, *Chem. Ber.*, 1984, **117**, 1222.
247. M. F. Hawthorne, *J. Am. Chem. Soc.*, 1961, **83**, 833.
248. P. Paetzold, C. von Plotho, G. Schmid and R. Boese, *Z. Naturforsch.*, 1984, **39b**, 1069.
249. B. Wrackmeyer and H. Nöth, *Chem. Ber.*, 1976, **109**, 3480.
250. P. Fritz, K. Niedenzu and J. W. Dawson, *Inorg. Chem.*, 1964, **3**, 626.
251. K. Anton, H. Fußstetter and H. Nöth, *Chem. Ber.*, 1981, **114**, 2723.
252. K. Delpy, H.-U. Meier, P. Paetzold and C. von Plotho, *Z. Naturforsch.*, 1984, **39b**, 1696.
253. J. Kroner, H. Nöth and K. Niedenzu, *J. Organomet. Chem.*, 1974, **71**, 165.
254. M. F. Lappert, M. R. Litzow, J. B. Pedley and A. Tweedale, *J. Chem. Soc. (A)*, 1971, 2426.
255. G. Walzl, Dissertation, Universität München, 1982.
256. C. K. Narula and H. Nöth, *Inorg. Chem.*, 1985, **24**, 2532.
257. J. A. Soderquist and M. R. Najafi, *J. Org. Chem.*, 1986, **51**, 1330.
258. H. Nöth and W. Rattay, *J. Organomet. Chem.*, 1986, **312**, 139.
259. D. Männig, H. Nöth, H. Prigge, A.-R. Rotsch, S. Gopinathan and J. W. Wilson, *J. Organomet. Chem.*, 1986, **310**, 1.
260. H. C. Brown and S. M. Singh, *Organometallics*, 1986, **5**, 998.
261. H. C. Brown and S. M. Singh, *Organometallics*, 1986, **5**, 994.
262. H. C. Brown, M. Srebnik and T. E. Cole, *Organometallics*, 1986, **5**, 2300.
263. H. E. Katz, *Organometallics*, 1986, **5**, 2308.
264. R. Köster, K. Angermund, A. Sporzynski and J. Serwatowski, *Chem. Ber.*, 1986, **119**, 1931.

265. R. Köster, K. Angermund, J. Serwatowski and A. Sporzynski, *Chem. Ber.*, 1986, **119**, 1301.
266. R. Köster, Y.-H. Tsay, C. Krüger and J. Serwatowski, *Chem. Ber.*, 1986, **119**, 1174.
267. S. Alloud and B. Frange, *Inorg. Chem.*, 1985, **24**, 2520.
268. H. Nöth, P. Otto and W. Storch, *Chem. Ber.*, 1986, **119**, 2517.
269. W. Maringgele, A. Meller, M. Noltemeyer and G. M. Sheldrick, *Z. Anorg. Allg. Chem.*, 1986, **536**, 24.
270. C. Habben and A. Meller, *Chem. Ber.*, 1986, **119**, 1189.
271. C. Habben, A. Meller, M. Noltemeyer and G. M. Sheldrick, *Z. Naturforsch.*, 1986, **41b**, 799.
272. H. Fußstetter and H. Nöth, *Chem. Ber.*, 1978, **111**, 3596.
273. K. Niedenzu, K.-D. Müller, W. J. Layton and L. Komorowski, *Z. Anorg. Allg. Chem.*, 1978, **439**, 112.
274. H. Fußstetter and H. Nöth, *Chem. Ber.*, 1979, **112**, 3672.
275. J. D. Odom, Z. Szafran, S. A. Johnston, Y. S. Li and J. R. Durig, *J. Am. Chem. Soc.*, 1980, **102**, 7173.
276. J. A. Soderquist and H. C. Brown, *J. Org. Chem.*, 1980, **45**, 3571.
277. B. Pachaly and R. West, *J. Am. Chem. Soc.*, 1985, **107**, 2987.
278. H. C. Brown, R. G. Naik, B. Singaram and C. Pyun, *Organometallics*, 1985, **4**, 1925.
279. W. Maringgele and A. Meller, *J. Organomet. Chem.*, 1980, **188**, 401.
280. J. W. Wilson, *J. Organomet. Chem.*, 1980, **186**, 297.
281. P. Jutzi and A. Seufert, *J. Organomet. Chem.*, 1979, **169**, 327.
282. R. Köster, P. Idelmann, G. Müller, W. R. Scheidt, W. Schübler and K. Seevogel, *Angew. Chem.*, 1984, **96**, 145; *Angew. Chem. Int. Ed. Engl.*, 1984, **23**, 153.
283. P. Jutzi and A. Seufert, *J. Organomet. Chem.*, 1979, **169**, 357.
284. P. Jutzi and A. Seufert, *J. Organomet. Chem.*, 1978, **161**, C5.
285. A. Meller, W. Maringgele and H. Fetzer, *Chem. Ber.*, 1980, **113**, 1950.
286. H. Nöth and T. Taeger, *Z. Naturforsch.*, 1979, **34b**, 135.
287. W. Kliegel, *J. Organomet. Chem.*, 1983, **253**, 9.
288. R. Goetze and H. Nöth, *Chem. Ber.*, 1976, **109**, 3249.
289. K. N. Scott and W. S. Brey, *Inorg. Chem.*, 1969, **8**, 1414.
290. C. K. Narula and H. Nöth, *J. Chem. Soc. Chem. Commun.*, 1984, 1023.
291. F. Dirschl, H. Nöth and W. Wagner, *J. Chem. Soc. Chem. Commun.*, 1984, 1533.
292. (a) U. Klingebiel, *Angew. Chem.*, 1984, **96**, 807; *Angew. Chem. Int. Ed. Engl.*, 1984, **23**, 815.  
(b) R. Boese and U. Klingebiel, *J. Organomet. Chem.*, 1986, **306**, 295.
293. A. Haas and M. Wilbert-Porada, *Chem. Ber.*, 1985, **118**, 1463.
294. H. Nöth, M. Schwartz and S. Weber, *Chem. Ber.*, 1985, **118**, 4716.
295. W. Pieper, D. Schmitz and P. Paetzold, *Chem. Ber.*, 1981, **114**, 3801.
296. (a) W. Weber and K. Niedenzu, *J. Organomet. Chem.*, 1981, **205**, 147.  
(b) T. G. Hodgkins, K. Niedenzu, K. S. Niedenzu and S. S. Seelig, *Inorg. Chem.*, 1981, **20**, 2097.
297. A. Brandl and H. Nöth, *Chem. Ber.*, 1985, **118**, 3759.
298. K. Anton, H. Fußstetter and H. Nöth, *Chem. Ber.*, 1984, **117**, 2542.
299. P. B. Hitchcock, H. A. Jasim, M. F. Lappert and H. D. Williams, *J. Chem. Soc. Chem. Commun.*, 1984, 662.
300. K. Niedenzu and B. K. Christmas, *Z. Anorg. Allg. Chem.*, 1978, **439**, 103.
301. P. C. Bharara and H. Nöth, *Z. Naturforsch.*, 1979, **34b**, 1352.
302. G. E. McAchran and S. G. Shore, *Inorg. Chem.*, 1966, **5**, 2044.

303. P. Wisian-Neilson and D. R. Martin, *J. Inorg. Nucl. Chem.*, 1979, **41**, 1545.
304. H. Nöth and S. Weber, *Chem. Ber.*, 1984, **117**, 2504.
305. D. Männig, H. Nöth, M. Schwarz, S. Weber and U. Wietelmann, *Angew. Chem.*, 1985, **97**, 979; *Angew. Chem. Int. Ed. Engl.*, 1985, **24**, 998.
306. W. Haubold and R. Schaeffer, *Chem. Ber.*, 1971, **104**, 513.
307. J. E. de Moor and G. P. van der Kelen, *J. Organomet. Chem.*, 1966, **6**, 235.
308. H. Landesmann and R. E. Williams, *J. Am. Chem. Soc.*, 1961, **83**, 2663.
309. T. Gasparis-Ebeling and H. Nöth, *Angew. Chem.*, 1984, **96**, 301; *Angew. Chem. Int. Ed. Engl.*, 1984, **23**, 303.
310. R. Lang, H. Nöth, P. Otto and W. Storch, *Chem. Ber.*, 1985, **118**, 86.
311. H. Nöth, R. Staudigl and W. Storch, *Chem. Ber.*, 1981, **114**, 3024.
312. D. Männig, C. K. Narula, H. Nöth and U. Wietelmann, *Chem. Ber.*, 1985, **118**, 3748.
313. S. G. Shore, J. L. Christ and D. R. Long, *J. Chem. Soc. Dalton Trans.*, 1972, 1123.
314. J. Bouix and R. Hillel, *Can. J. Chem.*, 1973, **51**, 292.
315. R. Hillel and J. Bouix, *C.R. Acad. Sci. Paris*, 1972, **C275**, 829.
316. J. H. Morris and P. G. Perkins, *J. Chem. Soc. (A)*, 1966, 580.
317. O. T. Beachley, *Inorg. Chem.*, 1969, **8**, 981.
318. D. Nölle, H. Nöth and W. Winterstein, *Z. Anorg. Allg. Chem.*, 1974, **406**, 235.
319. J. Komorowski and K. Niedenzu, *J. Organomet. Chem.*, 1978, **149**, 141.
320. W. Becker and H. Nöth, *Chem. Ber.*, 1972, **105**, 1962.
321. S. N. Sze, Dissertation, Universität München, 1975.
322. R. Goetze and H. Nöth, *Z. Naturforsch.*, 1975, **30b**, 875.
323. M. Baudler and A. Marx, *Z. Anorg. Allg. Chem.*, 1981, **474**, 18.
324. M. Feher, R. Fröhlich and K.-F. Tebbe, *Z. Anorg. Allg. Chem.*, 1981, **474**, 81.
325. R. W. Kirk, D. L. Smith, W. Airley and P. L. Timms, *J. Chem. Soc. Dalton Trans.*, 1972, 1392.
326. P. L. Timms, T. C. Ehlert, J. L. Margrave, F. E. Brinckman, T. C. Farrar and T. D. Coyle, *J. Am. Chem. Soc.*, 1965, **87**, 3819.
327. R. J. Wilcsek, D. S. Matteson and J. D. Douglas, *J. Chem. Soc. Chem. Commun.*, 1976, 401.
328. H. Nöth and G. Höllerer, *Chem. Ber.*, 1966, **99**, 2197.
329. W. Biffar, H. Nöth and R. Schwerthöffer, *Liebigs Ann. Chem.*, 1981, 2067.
330. J. Pfeiffer, W. Maringele and A. Meller, *Z. Anorg. Allg. Chem.*, 1984, **511**, 185.
331. H. Nöth and G. Schmid, *J. Organomet. Chem.*, 1966, **5**, 109.
332. J. D. Kennedy, W. McFarlane, G. S. Pyne and B. Wrackmeyer, *J. Chem. Soc. Dalton Trans.*, 1975, 386.
333. H. Nöth and R. Schwerthöffer, *Chem. Ber.*, 1981, **114**, 3056.
334. J. D. Kennedy, W. McFarlane and B. Wrackmeyer, *Inorg. Chem.*, 1976, **15**, 1299.
335. K. Barlos, J. Kroner, H. Nöth and B. Wrackmeyer, *Chem. Ber.*, 1977, **110**, 2774.
336. P. Paetzold and H.-J. Hansen, *Z. Anorg. Allg. Chem.*, 1966, **345**, 79.
337. H. Nöth and H. Vahrenkamp, *J. Organomet. Chem.*, 1968, **12**, 23.
338. H. C. Brown and S. U. Kulkarni, *J. Organomet. Chem.*, 1979, **168**, 281.
339. W. Siebert, M. Schmidt and E. Gast, *J. Organomet. Chem.*, 1969, **20**, 29.
340. G. E. Herberich and B. Hessner, *J. Organomet. Chem.*, 1978, **161**, C36.
341. P. Kölle, H. Nöth and R. T. Paine, *Chem. Ber.*, 1986, **119**, 2681.
342. M. Haase, U. Klingebiel, R. Boese and M. Polk, *Chem. Ber.*, 1986, **119**, 1117.
343. W. Haubold, J. Herdtle, W. Gollinger and W. Einholz, *J. Organomet. Chem.*, 1986, **315**, 1.
344. W. Einholz and W. Haubold, *Z. Naturforsch.*, 1986, **41b**, 1367.
345. G. E. Herberich, W. Boveleth, B. Heßner, M. Hostalek, D. P. J. Köffer, H. Ohst and D. Söhnen, *Chem. Ber.* 1986, **119**, 420.

346. R. A. Bartlett, X. Feng and P. P. Power, *J. Am. Chem. Soc.*, 1986, **108**, 6817.
347. C. Habben, A. Meller, M. Noltemeyer and G. M. Sheldrick, *Angew. Chem.*, 1986, **98**, 717; *Angew. Chem. Int. Ed. Engl.*, 1986, **25**, 741.
348. H. Nöth and F. Dirschl, Universität München, unpublished, 1982.
349. W. Haubold, Cited in Ref. 133.
350. W. Biffar, H. Nöth, H. Pommerening and B. Wrackmeyer, *Chem. Ber.*, 1980, **113**, 333.
351. P. L. Timms, *J. Chem. Soc. Chem. Commun.*, 1968, 1525.
352. H. Pommerening, Dissertation, Universität München, 1979.
353. T. Davan and J. A. Morrison, *J. Chem. Soc. Chem. Commun.*, 1981, 250.
354. G. E. Herberich, B. Heßner and M. Hostalek, *Angew. Chem.*, 1986, **98**, 637; *Angew. Chem. Int. Ed. Engl.*, 1986, **25**, 642.
355. W. Haubold, Habilitationsschrift, Universität Stuttgart, 1975.
356. H. Nöth and H. Pommerening, *Chem. Ber.*, 1981, **114**, 398.
357. G. N. Welch and S. G. Shore, *Inorg. Chem.*, 1968, **7**, 225.
358. H. Nöth, *Z. Naturforsch.*, 1984, **39b**, 1463.
359. H. Fußstetter, J. C. Huffman, H. Nöth and R. Schaeffer, *Z. Naturforsch.*, 1976, **31b**, 1441.
360. K. Anton, H. Nöth and H. Pommerening, *Chem. Ber.*, 1984, **117**, 2495.
361. G. Ferguson, M. Parvez, R. P. Brint, D. C. M. Power, T. R. Spalding and D. R. Lloyd, *J. Chem. Soc. Dalton Trans.*, 1986, 2283.
362. H. Nöth and H. Pommerening, *Chem. Ber.*, 1986, **119**, 2261.
363. D. F. Gaines, J. A. Heppert, D.E. Coons and M. W. Jorgensen, *Inorg. Chem.*, 1982, **21**, 3662.
364. S. A. Snow and G. Kodama, *Inorg. Chem.*, 1985, **24**, 3339.
365. W. Haubold, J. Hrebicek and G. Sawitzki, *Z. Naturforsch.*, 1984, **39b**, 1027.
366. H. Nöth, H. Fußstetter, H. Pommerening and T. Taeger, *Chem. Ber.*, 1980, **113**, 342.
367. D. Männig and H. Nöth, *Angew. Chem.*, 1985, **97**, 854; *Angew. Chem. Int. Ed. Engl.*, 1985, **24**, 878.
368. B. Glaser and H. Nöth, *Chem. Ber.*, 1986, **119**, 3253.
369. D. Fest, C. Habben and A. Meller, *Chem. Ber.*, 1986, **119**, 3121.
370. H. Nöth and H. Pommerening, *Angew. Chem.*, 1980, **92**, 481; *Angew. Chem. Int. Ed. Engl.*, 1980, **19**, 482.
371. T. E. Cole, R. K. Bakshi, M. Srebnik, B. Singaram and H. C. Brown, *Organometallics*, 1986, **5**, 2303.
372. H. C. Brown, P. V. Ramachandran and J. Chandrasekhavan, *Organometallics*, 1986, **5**, 2138.
373. S. Alaoud, M. ElMouhtadi and B. Frangle, *Nouv. J. Chim.*, 1985, **9**, 499.
374. H. Nöth and S. N. Sze, *Z. Naturforsch.*, 1978, **33b**, 1313.
375. H. C. Brown, J. S. Cha, B. Nazer and C. A. Brown, *J. Org. Chem.*, 1985, **50**, 549.
376. H. C. Brown and J. A. Sikorski, *Organometallics*, 1982, **1**, 28.
377. G. E. Herberich, in *Comprehensive Organometallic Chemistry*, (G. Wilkinson, F. G. A. Stone and E. W. Abel, eds), Vol. 1, Pergamon, Oxford, 1982, p. 381.
378. G. E. Herberich, K. Büschges, B. Heßner and H. Lütke, *J. Organomet. Chem.*, 1986, **312**, 13.
379. G. E. Herberich, W. Boveleth, B. Heßner, D. P. J. Köffer, M. Negele and R. Saive, *J. Organomet. Chem.*, 1986, **308**, 153.
380. G. E. Herberich, B. Heßner, J. A. K. Howard, D. P. J. Köffer and R. Saive, *Angew. Chem.*, 1986, **98**, 177; *Angew. Chem. Int. Ed. Engl.*, 1986, **25**, 165.
381. G. E. Herberich and H. Ohst, *Chem. Ber.*, 1985, **118**, 4303.
382. A. Sebald and B. Wrackmeyer, *J. Organomet. Chem.*, 1986, **304**, 271.

383. G. E. Herberich, J. Hengesbach, G. Huttner, A. Frank and U. Schubert, *J. Organomet. Chem.*, 1983, **246**, 141.
384. G. E. Herberich, B. Heßner, W. Boveleth, H. Lütke, R. Saive and L. Zelenka, *Angew. Chem.*, 1983, **95**, 1024; *Angew. Chem. Int. Ed. Engl.*, 1983, **22**, 996; *Angew. Chem. Suppl.*, 1983, 1503.
385. D. B. Palladino and T. P. Fehlner, *Organometallics*, 1983, **2**, 1692.
386. G. Schmid, O. Boltsch, D. Bläser and R. Boese, *Z. Naturforsch.*, 1984, **39b**, 1082.
387. G. Schmid, F. Schmidt and R. Boese, *Chem. Ber.*, 1986, **118**, 1949.
388. G. Schmid, *Comments Inorg. Chem.*, 1985, **4**, 17.
389. G. Schmid, G. Barbenheim and R. Boese, *Z. Naturforsch.*, 1985, **40b**, 787.
390. G. Schmid, D. Kampmann, W. Meyer, R. Boese, P. Paetzold and K. Delpy, *Chem. Ber.*, 1985, **118**, 2418.
391. G. Schmid, U. Höhner, D. Kampmann, D. Zaika and R. Boese, *J. Organomet. Chem.*, 1983, **256**, 225.
392. G. Schmid, D. Kampmann, U. Höhner, D. Bläser and R. Boese, *Chem. Ber.*, 1984, **117**, 1052.
393. G. Schmid, U. Höhner, D. Kampmann, F. Schmidt, D. Bläser and R. Boese, *Chem. Ber.*, 1984, **117**, 672.
394. G. Schmid and F. Schmidt, *Chem. Ber.*, 1986, **119**, 1766.
395. G. Schmid and R. Boese, *Z. Naturforsch.*, 1983, **38b**, 485.
396. G. Schmid, U. Höhner, D. Kampmann, D. Zaika and R. Boese, *Chem. Ber.*, 1983, **116**, 951.
397. G. Schmid, S. Amirkhalili, U. Höhner, D. Kampmann and R. Boese, *Chem. Ber.*, 1982, **115**, 3830.
398. G. Schmid, U. Höhner and D. Kampmann, *Z. Naturforsch.*, 1983, **38b**, 1094.
399. W. Siebert, *Adv. Organomet. Chem.*, 1980, **18**, 301.
400. W. Siebert, M. E.-D. M. El-Essavi, R. Full and J. Heck, *Z. Naturforsch.*, 1985, **40b**, 458.
401. K. Kinberger and W. Siebert, *Chem. Ber.*, 1978, **111**, 356.
402. W. Siebert, C. Böhle, C. Krüger and Y.-H. Tsay, *Angew. Chem.*, 1978, **90**, 558; *Angew. Chem. Int. Ed. Engl.*, 1978, **17**, 527.
403. T. Kuhlmann and W. Siebert, *Z. Naturforsch.*, 1985, **40b**, 167.
404. H. Wadepohl, H. Pritzkow and W. Siebert, *Chem. Ber.*, 1985, **118**, 729.
405. F. H. Köhler, U. Zenneck, J. Edwin and W. Siebert, *J. Organomet. Chem.*, 1981, **208**, 137.
406. M. Bochmann, K. Geilich and W. Siebert, *Chem. Ber.*, 1985, **118**, 401.
407. T. Kuhlmann and W. Siebert, *Z. Naturforsch.*, 1984, **39b**, 1046.
408. T. Kuhlmann, S. Roth, J. Rozière and W. Siebert, *Angew. Chem.*, 1986, **98**, 87; *Angew. Chem. Int. Ed. Engl.*, 1986, **25**, 105.
409. H. Wadepohl and W. Siebert, *Z. Naturforsch.*, 1984, **39b**, 50.
410. G. E. Herberich and H. Müller, *Angew. Chem.*, 1971, **83**, 1020; *Angew. Chem. Int. Ed. Engl.*, 1971, **10**, 937.
411. G. E. Herberich and M. Thönnessen, *J. Organomet. Chem.*, 1979, **177**, 357.
412. G. E. Herberich, E. A. Mintz and H. Müller, *J. Organomet. Chem.*, 1980, **187**, 17.
413. G. E. Herberich and E. Raabe, *J. Organomet. Chem.*, 1986, **309**, 143.
414. G. E. Herberich and G. Pampaloni, *J. Organomet. Chem.*, 1982, **240**, 121.
415. G. E. Herberich, M. Thönnessen and D. Schmitz, *J. Organomet. Chem.*, 1980, **191**, 27.
416. J. Edwin, W. Siebert and C. Krüger, *J. Organomet. Chem.*, 1981, **215**, 255.
417. G. E. Herberich, J. Hengesbach and U. Kölle, *Chem. Ber.*, 1977, **110**, 1171.
418. R. Köster, G. Seidel, S. Amirkhalili, R. Boese and G. Schmid, *Chem. Ber.*, 1982, **115**, 738.

419. R. Köster and G. Seidel, *Angew. Chem.*, 1982, **94**, 225; *Angew. Chem. Int. Ed. Engl.*, 1982, **21**, 207.
420. K. Delpy, D. Schmitz and P. Paetzold, *Chem. Ber.*, 1983, **116**, 2994.
421. P. Paetzold and K. Delpy, *Chem. Ber.*, 1985, **118**, 2552.
422. H. Nöth and U. Schuchardt, *Z. Anorg. Allg. Chem.*, 1975, **418**, 97.
423. W. Siebert, G. Augustin, R. Full, C. Krüger and Y.-H. Tsay, *Angew. Chem.*, 1975, **87**, 286; *Angew. Chem. Int. Ed. Engl.*, 1975, **14**, 262.
424. W. Ehrl and H. Vahrenkamp, *Chem. Ber.*, 1970, **103**, 3563.
425. A. J. Ashe, W. Butler and H. F. Sandford, *J. Am. Chem. Soc.*, 1979, **101**, 7066.
426. K. Stumpf, H. Pritzkow and W. Siebert, *Angew. Chem.*, 1985, **97**, 64; *Angew. Chem. Int. Ed. Engl.*, 1985, **24**, 71.
427. G. Schmid, D. Zaika and R. Boese, *Angew. Chem.*, 1985, **97**, 581; *Angew. Chem. Int. Ed. Engl.*, 1985, **24**, 602.
428. N. S. Hosmane, N. N. Sirmokadam and R. H. Herber, *Organometallics*, 1984, **3**, 1665.
429. N. S. Hosmane, P. de Meester, N. N. Maldar, S. B. Potts, S. S. C. Chu and R. H. Herber, *Organometallics*, 1986, **5**, 772.
430. N. S. Hosmane, P. de Meester, U. Siriwardane, M. S. Islam and S. S. C. Chu, *J. Chem. Soc. Chem. Commun.*, 1986, 1421.
431. N. S. Hosmane, P. de Meester, U. Siriwardane, M. S. Islam and S. S. C. Chu, *J. Am. Chem. Soc.*, 1986, **108**, 6050.
432. R. Boese, W. Finke, T. Keil, P. Paetzold and G. Schmid, *Z. Naturforsch.*, 1985, **40b**, 1327.
433. G. E. Herberich and B. Heßner, *Chem. Ber.*, 1982, **115**, 3115.
434. G. E. Herberich and H. Ohst, *J. Organomet. Chem.*, 1986, **307**, C16.
435. J. Schulze and G. Schmid, *Angew. Chem.*, 1980, **92**, 61; *Angew. Chem. Int. Ed. Engl.*, 1980, **19**, 54.
436. K. von Werner and B. Wrackmeyer, *J. Fluor. Chem.*, 1986, **31**, 183.
437. P. Kölle and H. Nöth, *Chem. Ber.*, 1986, **119**, 3849.
438. B. Glaser and H. Nöth, *Chem. Ber.*, 1986, **119**, 3856.
439. G. E. Herberich, W. Boveleth, B. Heßner, W. Koch, E. Raabe and D. Schmitz, *J. Organomet. Chem.*, 1984, **265**, 225.
440. G. E. Herberich, B. Heßner and T. T. Kho, *J. Organomet. Chem.*, 1980, **197**, 1.
441. G. E. Herberich and H. J. Becker, *Angew. Chem.*, 1973, **85**, 817; *Angew. Chem. Int. Ed. Engl.*, 1973, **12**, 764.
442. G. E. Herberich and E. Bauer, *Chem. Ber.*, 1977, **110**, 1167.
443. G. E. Herberich and K. Carsten, *J. Organomet. Chem.*, 1978, **144**, C1.
444. A. J. Ashe, E. Meyer, P. Shu, T. von Lehmann and J. Bastide, *J. Am. Chem. Soc.*, 1975, **97**, 6865.
445. A. J. Ashe, W. Butler and H. F. Sandford, *J. Am. Chem. Soc.*, 1979, **101**, 7066.
446. G. E. Herberich and H. J. Becker, *Z. Naturforsch.*, 1974, **29b**, 439.
447. G. E. Herberich, W. Koch and H. Lueken, *J. Organomet. Chem.*, 1978, **160**, 17.
448. G. E. Herberich, H. J. Becker, K. Carsten, C. Engelke and W. Koch, *Chem. Ber.*, 1976, **109**, 2382.
449. G. E. Herberich and G. Greiss, *Chem. Ber.*, 1972, **105**, 3413.
450. G. E. Herberich, C. Engelke and W. Pahlmann, *Chem. Ber.*, 1979, **112**, 607.
451. G. E. Herberich and A. K. Naithani, *J. Organomet. Chem.*, 1983, **241**, 1.
452. G. E. Herberich and D. Söhnen, *J. Organomet. Chem.*, 1983, **254**, 143.
453. P. S. Madren, A. Modinos, P. L. Timms and P. Woodward, *J. Chem. Soc. Dalton Trans.*, 1975, 1272.

454. G. E. Herberich, B. Heßner, G. Huttner and L. Zsolnai, *Angew. Chem.*, 1981, **93**, 471; *Angew. Chem. Int. Ed. Engl.*, 1981, **20**, 472.
455. H. Wadepohl, H. Pritzkow and W. Siebert, *Organometallics*, 1983, **2**, 1899.
456. J. Edwin, M. Bochmann, M. C. Böhm, D. E. Brennan, W. E. Geiger, C. Krüger, J. Pebler, H. Pritzkow, W. Siebert, W. Swiridoff, H. Wadepohl, J. Weiss and U. Zenneck, *J. Am. Chem. Soc.*, 1983, **105**, 2582.
457. W. Siebert and M. Bochmann, *Angew. Chem.*, 1977, **89**, 483; *Angew. Chem. Int. Ed. Engl.*, 1977, **16**, 468.
458. W. Siebert, J. Edwin, H. Wadepohl and H. Pritzkow, *Angew. Chem.*, 1982, **94**, 148; *Angew. Chem. Int. Ed. Engl.*, 1982, **21**, 149.
459. M. W. Whiteley, H. Pritzkow, U. Zenneck and W. Siebert, *Angew. Chem.*, 1982, **94**, 464; *Angew. Chem. Int. Ed. Engl.*, 1982, **21**, 453.
460. W. Siebert and M. Bochmann, *Angew. Chem.*, 1977, **89**, 895; *Angew. Chem. Int. Ed. Engl.*, 1977, **16**, 857.
461. J. Edwin, M. C. Böhm, N. Chester, D. M. Hoffman, R. Hoffmann, H. Pritzkow, W. Siebert, K. Stumpf and H. Wadepohl, *Organometallics*, 1983, **2**, 1666.
462. W. Siebert, R. Full, J. Edwin and K. Kinberger, *J. Organomet. Chem.*, 1977, **131**, 1.
463. W. Siebert, R. Full, C. Krüger and Y.-H. Tsay, *Z. Naturforsch.*, 1976, **31b**, 203.
464. W. Siebert and W. Rothermel, *Angew. Chem.*, 1977, **89**, 346; *Angew. Chem. Int. Ed. Engl.*, 1977, **16**, 333.
465. U. Kölle, W.-D. H. Beiersdorf and G. E. Herberich, *J. Organomet. Chem.*, 1978, **152**, 7.
466. G. Schmid, *Chem. Ber.*, 1970, **103**, 528.
467. H. Nöth and U. Schuchardt, *J. Organomet. Chem.*, 1970, **24**, 435.
468. G. Schmid, H. Nöth and J. Deberitz, *Angew. Chem.*, 1968, **80**, 282; *Angew. Chem. Int. Ed. Engl.*, 1968, **7**, 293.
469. H. Werner, R. Prinz and E. Deckelmann, *Chem. Ber.*, 1969, **102**, 95.
470. J. W. Lauher and R. Hoffmann, *J. Am. Chem. Soc.*, 1976, **98**, 1729.
471. B. E. Mann and B. F. Taylor, *<sup>13</sup>C NMR Data for Organometallic Compounds*, Academic Press, London, 1981.
472. R. Balz, U. Brändle, E. Kammerer, D. Köhnlein, O. Lutz, A. Nolle, R. Schafitel, and E. Veil, *Z. Naturforsch.*, 1986, **41a**, 737.
473. H. C. Brown and S.-C. Kim, *J. Org. Chem.*, 1984, **49**, 1064.
474. H. Nöth and B. Wrackmeyer, *Chem. Ber.*, 1974, **107**, 3070.
475. B. Wrackmeyer, *J. Organomet. Chem.*, 1976, **117**, 313.
476. H. Nöth and B. Wrackmeyer, *J. Magn. Reson.*, 1986, **69**, 492.
477. H. Nöth and T. Taeger, *J. Organomet. Chem.*, 1977, **142**, 281.
478. J. P. Tuchagues and J. P. Laurent, *Bull. Soc. Chim. France*, 1971, 4246.
479. B. M. Mikhailov and K. L. Cherkasova, *J. Organomet. Chem.*, 1983, **246**, 9.
480. B. M. Mikhailov, *Sov. Sci. Rev., Sect. B, Chem. Rev.*, 1980, **2**, 283; *CA*, 1981, **94**, 47381.
481. B. M. Mikhailov and T. K. Baryshnikova, *J. Organomet. Chem.*, 1984, **260**, 25.
482. B. M. Mikhailov, V. N. Smirnov and V. A. Kasparov, *Izv. Akad. Nauk SSSR Ser. Khim.*, 1976, 2303.
483. R. Contreras and B. Wrackmeyer, *Z. Naturforsch.*, 1980, **35b**, 1236.
484. J. A. Soderquist and H. C. Brown, *J. Org. Chem.*, 1981, **46**, 4599.
485. T. Wizeman, H. Mueller, D. Seybold and K. Dehnicke, *J. Organomet. Chem.*, 1969, **20**, 211.
486. B. R. Gragg, W. J. Layton and K. Niedenzu, *J. Organomet. Chem.*, 1977, **132**, 29.
487. P. Binger and R. Köster, *Synthesis*, 1974, 350.
488. S. Kersch, B. Wrackmeyer, D. Männig, H. Nöth and R. Staudigl, *Z. Naturforsch.*, 1987, **42b**, 387.

489. L. Horner, U. Kaps and G. Simons, *J. Organomet. Chem.*, 1985, **287**, 1.  
490. E. Kalbarczyk and S. Pasynkiewicz, *J. Organomet. Chem.*, 1985, **292**, 119.  
491. P. Binger and R. Köster, *Chem. Ber.*, 1975, **108**, 395.  
492. S. Kersch and B. Wrackmeyer, *Z. Naturforsch.*, 1985, **40b**, 845.  
493. H. Nöth and D. Sedlak, *Chem. Ber.*, 1983, **116**, 1479.  
494. D. E. Young and S. G. Shore, *J. Am. Chem. Soc.*, 1969, **91**, 3497.  
495. D. E. Walmsley, W. L. Budde and M. F. Hawthorne, *J. Am. Chem. Soc.*, 1971, **93**, 3150.  
496. D. Sedlak, Dissertation, Universität München, 1982.  
497. H. C. Brown and B. Singaram, *Inorg. Chem.*, 1979, **18**, 53.  
498. H. C. Brown, B. Singaram and J. R. Schwier, *Inorg. Chem.*, 1979, **18**, 51.  
499. C. Weidig, S. S. Uppal, and H. C. Kelly, *Inorg. Chem.*, 1974, **13**, 1763.  
500. W. Biffar, H. Nöth and D. Sedlak, *Organometallics*, 1983, **2**, 579.  
501. B. Singaram, T. E. Cole and H. C. Brown, *Organometallics*, 1984, **3**, 774.  
502. J. Ewerling and H. Nöth, *Z. Naturforsch.*, 1970, **25b**, 780.  
503. B. Wrackmeyer, *Spectrosc. Int. J.*, 1982, **1**, 201.  
504. R. C. Wade, E. A. Sullivan, J. R. Berscheid and K. F. Purcell, *Inorg. Chem.*, 1970, **9**, 2146.  
505. L. W. Hall, D. W. Lowman, P. D. Ellis and J. D. Odom, *Inorg. Chem.*, 1975, **14**, 580.  
506. B. F. Spielvogel, A. T. McPhail, J. A. Knight, C. G. Moreland, C. L. Gatchell and K. W. Morse, *Polyhedron*, 1983, **2**, 1345.  
507. B. Singaram, T. E. Cole and H. C. Brown, *Organometallics*, 1984, **3**, 1520.  
508. G. W. Kabalka, U. Sastry, K. A. R. Sastry, F. F. Knapp and P. C. Srivastava, *J. Organomet. Chem.*, 1983, **259**, 269.  
509. H. C. Brown, B. Singaram and C. P. Mathew, *J. Org. Chem.*, 1981, **46**, 2712.  
510. H. C. Brown and J. L. Hubbard, *J. Org. Chem.*, 1979, **44**, 467.  
511. C. A. Brown and S. Krishnamurthy, *J. Organomet. Chem.*, 1978, **156**, 111.  
512. J. L. Hubbard and G. W. Kramer, *J. Organomet. Chem.*, 1978, **156**, 81.  
513. A. J. Zozulin, H. J. Jakobsen, T. F. Morre, A. R. Garber and J. D. Odom, *J. Magn. Reson.*, 1980, **41**, 458.  
514. M. Yanagisawa and O. Yamamoto, *Org. Magn. Reson.*, 1980, **14**, 76.  
515. H. C. Brown and U. S. Rocherla, *Organometallics*, 1986, **5**, 391.  
516. D. J. Hart and W. T. Ford, *J. Org. Chem.*, 1974, **39**, 363.  
517. R. Köster, Private communication.  
518. M. M. Midland, J. A. Sinclair and H. C. Brown, *J. Org. Chem.*, 1974, **39**, 731.  
519. H. J. Bestmann and T. Arenz, *Angew. Chem.*, 1986, **98**, 571; *Angew. Chem. Int. Ed. Engl.*, 1986, **25**, 559.  
520. F. J. Weigert and J. D. Roberts, *J. Am. Chem. Soc.*, 1969, **91**, 4940.  
521. J. D. Odom, L. W. Hall and P. D. Ellis, *Org. Magn. Reson.*, 1980, **41**, 458.  
522. E. Negishi, M. J. Idacavage, K.-W. Chiu, T. Yoshida, A. Abramovitch, M. E. Goettel, A. Silveira and H. D. Bretherick, *J. Chem. Soc. Perkin Trans. II*, 1978, 1225.  
523. H. C. Brown, K. S. Racherla and S. M. Singh, *Tetrahedron Lett.*, 1984, 2411.  
524. B. Wrackmeyer, *Z. Naturforsch.*, 1982, **37b**, 788.  
525. B. M. Mikhailov, M. E. Gurskii and D. G. Pershin, *J. Organomet. Chem.*, 1983, **246**, 19.  
526. J. W. Emsley and L. Phillips, *Prog. NMR Spectrosc.*, 1971, **7**, 1.  
527. M. van Duin, J. A. Peters, A. P. G. Kieboom and H. van Bakkum, *Tetrahedron*, 1984, **40**, 2901.  
528. M. van Duin, J. A. Peters, A. P. G. Kieboom and H. van Bakkum, *Tetrahedron*, 1985, **41**, 3411.  
529. M. Makkee, A. P. G. Kieboom and H. van Bakkum, *Recl. Trav. Chim.*, 1985, **104**, 230.  
530. C. F. Bell, R. D. Beauchamp and E. L. Short, *Carbohydr. Res.*, 1986, **147**, 191.

531. M. van Duin, J. A. Peters, A. P. G. Kieboom and H. van Bekkum, *Recl. Trav. Chim.*, 1986, **105**, 488.
532. B. D. James, R. K. Nanda, M. G. H. Wallbridge, *J. Chem. Soc. (A)*, 1966, 182.
533. R. Eisenbarth and W. Sundermeyer, *Angew. Chem.*, 1978, **90**, 226; *Angew. Chem. Int. Ed. Engl.*, 1978, **17**, 212.
534. G. Fritz and E. Sattler, *Z. Anorg. Allg. Chem.*, 1975, **413**, 195.
535. W. Biffar and H. Nöth, *Chem. Ber.*, 1982, **115**, 934.
536. J. R. Blackborow and J. C. Lockhart, *J. Chem. Soc. (A)*, 1971, 1343.
537. H. C. Brown, J. S. Cha and B. Nazer, *J. Org. Chem.*, 1984, **49**, 2073.
538. W. Biffar and H. Nöth, *Angew. Chem.*, 1980, **92**, 65; *Angew. Chem. Int. Ed. Engl.*, 1980, **19**, 58.
539. W. Biffar and H. Nöth, *Z. Naturforsch.*, 1981, **36b**, 1509.
540. D. Barr, K. B. Hutton, J. H. Morris, R. E. Mulvey, D. Reed and R. Snaith, *J. Chem. Soc. Chem. Commun.*, 1986, 127.
541. C. Eaborn, M. N. A. El-Kheli, P. B. Hitchcock and J. D. Smith, *J. Chem. Soc. Chem. Commun.*, 1984, 1673.
542. A. G. Avent, C. Eaborn, M. N. A. El-Kheli, M. E. Molla, J. D. Smith and A. C. Sullivan, *J. Am. Chem. Soc.*, 1986, **108**, 3854.
543. J. A. Gardiner and J. W. Collat, *J. Am. Chem. Soc.*, 1964, **86**, 3165.
544. B. F. Spielvogel and E. F. Rothgery, *J. Chem. Soc. Chem. Commun.*, 1966, 765.
545. P. C. Keller, *J. Am. Chem. Soc.*, 1969, **91**, 1231.
546. S. Trofimenko, *J. Am. Chem. Soc.*, 1967, **89**, 3170.
547. E. A. Dietz, K. W. Morse and R. W. Parry, *Inorg. Chem.*, 1976, **15**, 1.
548. S. Brownstein, *J. Chem. Soc. Chem. Commun.*, 1980, 149.
549. B. E. Smith, B. D. James and R. M. Peachey, *Inorg. Chem.*, 1977, **16**, 2057.
550. B. G. Sayer, J. I. A. Thompson, T. Birchall, D. R. Eaton and M. J. McGlinchey, *Inorg. Chem.*, 1981, **20**, 3748.
551. M. Mancini, P. Bougeard, R. C. Burns, M. Mlekuz, B. G. Sayer, J. I. A. Thompson and M. J. McGlinchey, *Inorg. Chem.*, 1984, **23**, 1072.
552. M. V. Baker and L. D. Field, *J. Chem. Soc. Chem. Commun.*, 1984, 996.
553. H. Werner, M. A. Esteruelas, U. Meyer and B. Wrackmeyer, *Chem. Ber.*, 1987, **120**, 11.
554. D. J. Wink and N. J. Cooper, *J. Chem. Soc. Dalton Trans.*, 1984, 1257.
555. R. Shinomoto, J. G. Brennan, N. N. Edelstein and A. Zalkin, *Inorg. Chem.*, 1985, **24**, 2896.
556. B. Wrackmeyer, *J. Magn. Reson.*, 1986, **66**, 172.
557. D. E. Young, G. E. McAchran and S. G. Shore, *J. Am. Chem. Soc.*, 1966, **88**, 4390.
558. C. J. Forget, M. A. Chiusano, J. D. O'Brien and D. R. Martin, *J. Inorg. Nucl. Chem.*, 1980, **42**, 165.
559. D. R. Martin, C. M. Merkel, J. U. Mondal and C. R. Rushing, *Inorg. Chim. Acta*, 1985, **99**, 81.
560. C. M. Merkel and D. R. Martin, *Inorg. Chim. Acta*, 1985, **96**, L59.
561. R. Contreras, F. Santiesteban, M. A. Paz-Sandoval and B. Wrackmeyer, *Tetrahedron*, 1984, **40**, 3829.
562. M. A. Paz-Sandoval, F. Santiesteban and R. Contreras, *Magn. Reson. Chem.*, 1985, **23**, 428.
563. B. F. Spielvogel, F. U. Ahmed and A. T. McPhail, *Inorg. Chem.*, 1986, **25**, 4395.
564. P. C. Keller, K. K. Knapp and J. V. Rund, *Inorg. Chem.*, 1985, **24**, 2382.
565. R. W. Rudolph, R. W. Parry and C. F. Farran, *Inorg. Chem.*, 1966, **5**, 723.
566. R. W. Rudolph and C. W. Shultz, *J. Am. Chem. Soc.*, 1971, **93**, 6821.
567. A. H. Cowley and M. C. Damasco, *J. Am. Chem. Soc.*, 1971, **93**, 6815.

568. C. W. Heitsch, *Inorg. Chem.*, 1965, **4**, 1019.  
569. T. Costa and H. Schmidbaur, *Chem. Ber.*, 1982, **115**, 1374.  
570. D. R. Martin, C. M. Merkel, J. P. Ruiz and J. U. Mondal, *Inorg. Chim. Acta*, 1985, **100**, 293.  
571. J. R. Durig, B. A. Hudgens and J. D. Odom, *Inorg. Chem.*, 1974, **13**, 2306.  
572. R. K. Kanjolia, L. K. Krannich and C. L. Watkins, *Inorg. Chem.*, 1985, **24**, 445.  
573. D. J. Pasto and P. Balasubramanian, *J. Am. Chem. Soc.*, 1967, **89**, 295.  
574. T. P. Onak, H. Landesmann, R. E. Williams and I. Shapiro, *J. Phys. Chem.*, 1959, **63**, 1533.  
575. B. M. Mikhailov, M. N. Bochkareva, T. A. Shchegoleva and L. I. Lavrinovich, *Izv. Akad. Nauk SSSR Ser. Khim.*, 1968, 1876.  
576. M. H. Mendelsohn and W. L. Jolly, *Inorg. Chem.*, 1971, **11**, 1944.  
577. K. Kinberger and W. Siebert, *Z. Naturforsch.*, 1975, **30b**, 55.  
578. H. C. Brown and S. U. Kulkarni, *J. Org. Chem.*, 1979, **44**, 2422.  
579. R. K. Kanjolia, L. K. Krannich and C. L. Watkins, *J. Chem. Soc. Dalton Trans.*, 1986, 2345.  
580. H. C. Brown and N. Ravindran, *J. Am. Chem. Soc.*, 1976, **98**, 1785.  
581. M. G. Hu and R. A. Geanangel, *Inorg. Chem.*, 1979, **18**, 3297.  
582. H. C. Brown and N. Ravindran, *J. Am. Chem. Soc.*, 1976, **98**, 1798.  
583. J. P. Tuchagues, J. P. Laurent, H. Mongeot, J. Dazord and J. Cuellerson, *J. Organomet. Chem.*, 1973, **54**, 69.  
584. J. M. van Paaschen and M. A. Geanangel, *J. Am. Chem. Soc.*, 1972, **94**, 2680.  
585. M. L. Denniston, D. A. Chiusano and D. R. Martin, *J. Inorg. Nucl. Chem.*, 1976, **38**, 979.  
586. R. A. Geanangel, *Inorg. Chem.*, 1975, **14**, 696.  
587. J. L. Vidal and G. E. Ryschkewitsch, *Inorg. Chem.*, 1977, **16**, 1898.  
588. H. C. Brown and J. A. Sikorski, *Organometallics*, 1982, **1**, 28.  
589. S. U. Kulkarni and H. C. Brown, *J. Org. Chem.*, 1979, **44**, 1747.  
590. M. Schmidt and F. R. Rittig, *Chem. Ber.*, 1970, **103**, 3343.  
591. H. C. Brown, N. Ravindran and S. U. Kulkarni, *J. Org. Chem.*, 1980, **45**, 384.  
592. R. Maisch, E. Ott, W. Buchner, W. Malisch, I. Colquhoun and W. McFarlane, *J. Organomet. Chem.*, 1985, **286**, C31.  
593. W. F. McNamara, E. N. Duester, R. T. Paine, J. V. Ortiz, P. Kölle and H. Nöth, *Organometallics*, 1986, **5**, 380.  
594. J. P. Tuchagues and J. P. Laurent, *Bull. Soc. Chim. France*, 1969, 385.  
595. B. Rapp and J. R. Drake, *Inorg. Chem.*, 1973, **12**, 2868.  
596. J. Torri, *Magn. Reson. Chem.*, 1986, **24**, 279.  
597. M. J. Bula and J. S. Hartman, *J. Chem. Soc. Dalton Trans.*, 1973, 1047.  
598. A. Fox, J. S. Hartman and R. E. Humphries, *J. Chem. Soc. Dalton Trans.*, 1982, 1275.  
599. J. M. Miller, *Inorg. Chem.*, 1983, **22**, 2384.  
600. J. E. Drake and B. Rapp, *J. Inorg. Nucl. Chem.*, 1974, **36**, 2613.  
601. M. L. Denniston and D. R. Martin, *J. Inorg. Nucl. Chem.*, 1974, **36**, 1461.  
602. E. Muylle, G. P. van der Keelen and E. G. Claeys, *Spectrochim. Acta*, 1976, **A32**, 1149.  
603. J. M. Chehayber and J. E. Drake, *Inorg. Chim. Acta*, 1986, **112**, 209.  
604. M. L. Denniston and D. R. Martin, *J. Inorg. Nucl. Chem.*, 1974, **36**, 2175.  
605. J. Plešek, T. Jelinek, S. Heřmanek and B. Štibr, *Coll. Czech. Chem. Commun.*, 1986, **51**, 81.  
606. G. Süß-Fink, *Chem. Ber.*, 1986, **119**, 2393.  
607. M. F. A. Dove, R. C. Hibbert and N. Logan, *J. Chem. Soc. Dalton Trans.*, 1984, 2719.  
608. G. A. Olah, K. Laali and O. Farooq, *Organometallics*, 1984, **3**, 1337.  
609. R. Csuk, H. Hönig and C. Romanin, *Monatsh. Chem.*, 1982, **113**, 1025.

610. R. Contreras, C. Garcia, T. Mancilla and B. Wrackmeyer, *J. Organomet. Chem.*, 1983, **246**, 213.
611. R. Csuk, N. Müller and H. Sterk, *Z. Naturforsch.*, 1985, **40b**, 987.
612. P. C. Keller, R. L. Marks and J. V. Rund, *Polyhedron*, 1983, **2**, 595.
613. K. Niedenzu and R. B. Read, *Z. Anorg. Allg. Chem.*, 1981, **473**, 139.
614. E. Hohaus, *Z. Anorg. Allg. Chem.*, 1982, **484**, 41.
615. F. Santiesteban, M. A. Campos, H. Morales, R. Contreras and B. Wrackmeyer, *Polyhedron*, 1984, **3**, 589.
616. B. Garigues, M. Mulliez and Raharinirina, *J. Organomet. Chem.*, 1986, **302**, 153.
617. T. Mancilla, R. Contreras and B. Wrackmeyer, *J. Organomet. Chem.*, 1986, **307**, 1.
618. J.-P. Costes, G. Cros and J.-P. Laurent, *Synth. React. Inorg. Met.-Org. Chem.*, 1981, **11**, 383.
619. G. Klebe and D. Tranqui, *Inorg. Chim. Acta*, 1984, **81**, 1.
620. W. Maringele, G. M. Sheldrick, A. Meller and M. Noltemeyer, *Chem. Ber.*, 1984, **117**, 2112.
621. S. L. Ioffe, L. M. Leont'eva, L. M. Makarenkova, A. L. Blumenfel'd, V. F. Tsyatrikov and V. V. Tartakowski, *Izv. Akad. Nauk SSSR Ser. Khim.*, 1975, 1146.
622. C. H. Toporcer, R. E. Dessey and S. I. E. Green, *Inorg. Chem.*, 1965, **4**, 1649.
623. C. K. Narula and H. Nöth, *Z. Naturforsch.*, 1983, **38b**, 1161.
624. N. Farfan and R. Contreras, *Nouv. J. Chim.*, 1982, **6**, 269.
625. E. Hohaus and W. Riepe, *Z. Naturforsch.*, 1974, **29b**, 663.
626. K. W. Bøddeker, S. G. Shore and R. K. Bunting, *J. Am. Chem. Soc.*, 1966, **88**, 4396.
627. W. Haubold and R. Schaeffer, *Chem. Ber.*, 1971, **104**, 513.
628. O. T. Beachley and B. Washburn, *Inorg. Chem.*, 1976, **15**, 284.
629. S. Trofimenko, *J. Am. Chem. Soc.*, 1966, **88**, 1842.
630. W. J. Layton, K. Niedenzu and S. L. Smith, *Z. Anorg. Allg. Chem.*, 1982, **495**, 52.
631. S. Trofimenko, *J. Am. Chem. Soc.*, 1967, **89**, 3165.
632. C. E. May, K. Niedenzu and S. Trofimenko, *Z. Naturforsch.*, 1977, **33b**, 220.
633. K. Niedenzu and H. Nöth, *Chem. Ber.*, 1983, **116**, 1132.
634. W. J. Layton, K. Niedenzu, P. M. Niedenzu and S. Trofimenko, *Inorg. Chem.*, 1985, **24**, 1454.
635. J. Bielawski and K. Niedenzu, *Inorg. Chem.*, 1986, **25**, 85.
636. J. Bielawski, T. G. Hodgkins, W. J. Layton, K. Niedenzu, P. M. Niedenzu and S. Trofimenko, *Inorg. Chem.*, 1986, **25**, 87.
637. J. Bielawski and K. Niedenzu, *Inorg. Chem.*, 1986, **25**, 1771.
638. K. Niedenzu, P. M. Niedenzu, and K. R. Warner, *Inorg. Chem.*, 1985, **24**, 1604.
639. A. Ouassas and B. Frange, *Bull. Soc. Chim. France*, 1984, 1-336.
640. K. Niedenzu and S. Trofimenko, *Inorg. Chem.*, 1985, **24**, 4222.
641. G. E. Ryschkewitsch, *J. Am. Chem. Soc.*, 1967, **89**, 3145.
642. M. J. Farquharson and J. S. Hartman, *J. Chem. Soc. Chem. Commun.*, 1984, 256.
643. C. M. Clarke, K. Niedenzu, P. M. Niedenzu and S. Trofimenko, *Inorg. Chem.*, 1985, **24**, 2648.
644. H. Nöth und U. Schuchardt, *Chem. Ber.*, 1974, **107**, 3104.
645. G. Müller, Dissertation, Technische Universität, München, 1980.
646. P. Hornbach, M. Hildenbrand, H. Pritzkow and W. Siebert, *Angew. Chem.*, 1986, **98**, 1121; *Angew. Chem. Int. Ed. Engl.*, 1986, **25**, 1112.
647. C. Camacho, M. A. Paz-Sandoval and R. Contreras, *Polyhedron*, 1986, **5**, 1723.
648. G. E. Herberich, B. Hessner and R. Saive, *J. Organomet. Chem.*, 1987, **319**, 9.
649. D. R. Martin, M. A. Chinsana, M. L. Denniston, D. J. Pye, E. D. Martin and B. T. Pennington, *J. Inorg. Nucl. Chem.*, 1978, **40**, 9.

650. H. C. Brown, W. S. Park, J. S. Cha, B. T. Cho and C. A. Brown, *J. Org. Chem.*, 1986, **51**, 337.
651. H. C. Brown and U. S. Racherla, *J. Org. Chem.*, 1986, **51**, 427.
652. R. Contreras, H. R. Morales, M. de L. Mendoza and C. Dominguez, *Spectrochim. Acta*, 1987, **A43**, 43.
653. G. E. Herberich, W. Boveleth, B. Hessner, M. Hostalek, D. P. J. Köffer and M. Negele, *J. Organomet. Chem.*, 1987, **319**, 311.
654. J. C. Vites, C. Eigenbrot and T. P. Fehlner, *J. Am. Chem. Soc.*, 1984, **106**, 4633.
655. J. C. Vites, C. E. Housecroft, G. B. Jacobsen and T. P. Fehlner, *Organometallics*, 1984, **3**, 1591.
656. J. Vites, C. E. Housecroft, C. Eigenbrot, M. L. Buhl, G. J. Long and T. P. Fehlner, *J. Am. Chem. Soc.*, 1986, **108**, 3304.
657. N. F. Ramsey, *Phys. Rev.*, 1953, **91**, 303.
658. P. Pykkö, *Chem. Phys.*, 1977, **22**, 289.
659. J. A. Pople and D. P. Santry, *Mol. Phys.*, 1964, **8**, 1.
660. J. Kowalewski, *Ann. Rep. NMR Spectrosc.*, 1982, **12**, 81.
661. I. Ando and G. A. Webb, *Theory of NMR Parameters*, Academic Press, London, 1983.
662. J. Kroner and B. Wrackmeyer, *J. Chem. Soc. Faraday Trans. II*, 1976, **72**, 2283.
663. T. Onak, J. B. Leach, S. Anderson, M. J. Frisch and D. Marynick, *J. Magn. Reson.*, 1976, **23**, 237.
664. H. A. Bent, *Chem. Rev.*, 1961, **61**, 275.
665. T. L. Venable and R. N. Grimes, *J. Am. Chem. Soc.*, 1984, **106**, 29.
666. D. Reed, *J. Chem. Res. (S)*, 1984, 198.
667. X. L. R. Fontaine and J. D. Kennedy, *J. Chem. Soc. Chem. Commun.*, 1986, 779.
668. T. C. Farrar and G. R. Quating, *Inorg. Chem.*, 1985, **24**, 1941.
669. (a) G. Bodenhausen and D. J. Ruben, *Chem. Phys. Lett.*, 1980, **69**, 185.  
(b) A. G. Redfield, *Chem. Phys. Lett.*, 1983, **96**, 537  
(c) A. Bax, R. H. Griffey and B. L. Hawkins, *J. Am. Chem. Soc.*, 1983, **105**, 7188.
670. M. A. Beckett, J. D. Kennedy and O. W. Howarth, *J. Chem. Soc. Chem. Commun.*, 1985, 855.
671. C. K. Narula, J. F. Janik, E. N. Duesler, R. T. Paine and R. Schaeffer, *Inorg. Chem.*, 1986, **25**, 3346.
672. B. Wrackmeyer and W. Biffar, *Z. Naturforsch.*, 1979, **34b**, 1270.
673. D. D. Lehman and D. F. Shriver, *Inorg. Chem.*, 1974, **13**, 2203.
674. P. Powell and H. Nöth, *J. Chem. Soc. Chem. Commun.*, 1966, 637.
675. D. A. Thompson, T. K. Hilty and R. W. Rudolph, *J. Am. Chem. Soc.*, 1977, **99**, 6774.
676. J. D. Kennedy and J. Staves, *Z. Naturforsch.*, 1979, **34b**, 808.
677. J. D. Kennedy and B. Wrackmeyer, *J. Magn. Reson.*, 1980, **38**, 529.
678. N. N. Greenwood, M. J. Hails, J. D. Kennedy and W. S. McDonald, *J. Chem. Soc. Dalton Trans.*, 1985, 953.
679. F. Bachmann, H. Nöth, H. Pommerening, B. Wrackmeyer and T. Wirthlin, *J. Magn. Reson.*, 1979, **34**, 237.
680. J. A. Anderson, R. J. Astheimer, J. D. Odom and L. G. Sneddon, *J. Am. Chem. Soc.*, 1984, **106**, 2275.
681. S. K. Boocock, Y. Cheek, N. N. Greenwood and J. D. Kennedy, *J. Chem. Soc. Dalton Trans.*, 1981, 1430.
682. J. D. Odom, P. D. Ellis and H. C. Walsh, *J. Am. Chem. Soc.*, 1971, **93**, 3529.
683. D. W. Lowman, P. D. Ellis and J. D. Odom, *Inorg. Chem.*, 1973, **12**, 682.
684. E. J. Stampf, A. R. Garber, J. D. Odom and P. D. Ellis, *J. Am. Chem. Soc.*, 1976, **98**, 6550.

685. J. W. Akitt and C. G. Savory, *J. Magn. Reson.*, 1975, **17**, 122.
686. B. Glaser, Dissertation, Universität München, 1985.
687. J. D. Odom, T. F. Moore, S. A. Johnston and J. P. Durig, *J. Mol. Struct.*, 1979, **54**, 49.
688. T. Onak and E. Wan, *J. Chem. Soc. Dalton Trans.*, 1974, 665.
689. H.-O. Berger, H. Nöth and B. Wrackmeyer, *Chem. Ber.*, 1979, **112**, 2884.
690. B. Wrackmeyer, *J. Magn. Reson.*, 1983, **43**, 174.
691. E. A. Dietz, Jr., K. W. Morse and R. W. Parry, *Inorg. Chem.*, 1976, **15**, 1.
692. (a) G. J. Martin, M. L. Martin and J. P. Gouesnard, in *NMR—Basic Principles and Progress* (P. Diehl, E. Fluck and R. Kosfeld, eds), Vol. 18, Springer-Verlag, Berlin, 1981.  
(b) M. Wilanowski, L. Stefaniak and G. A. Webb, *Ann. Rep. NMR Spectrosc.*, 1981, **11B**, 1.
693. N. J. Maraschin and R. J. Lagow, *Inorg. Chem.*, 1975, **14**, 1855.
694. R. J. Hogan, P. A. Scherr, A. T. Weibel and J. P. Oliver, *J. Organomet. Chem.*, 1975, **85**, 265.
695. F. W. Wehrli, *J. Magn. Reson.*, 1978, **30**, 193.
696. D. F. Gaines, K. M. Coleson and D. F. Hillenbrand, *J. Magn. Reson.*, 1981, **44**, 265.
697. H. Fisch, H. Pritzkow and W. Siebert, *Angew. Chem.*, 1984, **96**, 595; *Angew. Chem. Int. Ed. Engl.*, 1984, **23**, 608.
698. P. C. Lauterbur, R. C. Hopkins, R. W. King, D. V. Ziebarth and C. W. Heitsch, *Inorg. Chem.*, 1968, **7**, 1025.
699. K. Hensen and K. P. Messer, *Theor. Chim. Acta*, 1967, **9**, 17.
700. R. Köster and B. Wrackmeyer, *Z. Naturforsch.*, 1981, **36b**, 704.
701. B. Wrackmeyer, *Z. Naturforsch.*, 1982, **37b**, 412.
702. R. Köster, G. Seidel and B. Wrackmeyer, *Angew. Chem.*, 1984, **96**, 520; *Angew. Chem. Int. Ed. Engl.*, 1984, **23**, 512.
703. T. L. Venable, C. T. Brewer and R. N. Grimes, *Inorg. Chem.*, 1985, **24**, 4751.
704. (a) P. Laszlo (ed.), *NMR of Newly Accessible Nuclei*, Vols 1 and 2, Academic Press, London, 1983.  
(b) J. B. Lambert and F. G. Riddell (eds), *The Multinuclear Approach to NMR Spectroscopy*, Reidel, Dordrecht, 1983.
705. R. Wehrmann, H. Klusik and A. Berndt, *Angew. Chem.*, 1984, **96**, 810; *Angew. Chem. Int. Ed. Engl.*, 1984, **23**, 826.
706. R. E. DePoy and G. Kodama, *Inorg. Chem.*, 1985, **24**, 2871.
707. R. H. Cragg and T. J. Miller, *J. Organomet., Chem.*, 1983, **241**, 289, and references cited therein.
708. N. M. D. Brown, F. Davidson and J. W. Wilson, *J. Organomet. Chem.*, 1981, **209**, 1.
709. N. M. D. Brown, F. Davidson, R. McMullan and J. W. Wilson, *J. Organomet. Chem.*, 1980, **193**, 271.
710. Y. Yamamoto and I. Moritani, *J. Org. Chem.*, 1975, **40**, 3434.
711. R. Köster, G. Seidel and B. Wrackmeyer, *Chem. Ber.*, 1987, **120**, 669.
712. B. G. Ramsey and K. Longmuir, *J. Org. Chem.*, 1980, **45**, 1322.
713. C. D. Blue and D. J. Nelson, *J. Org. Chem.*, 1983, **48**, 4538.
714. J. R. Durig, S. A. Johnston, T. F. Moore and J. D. Odom, *J. Mol. Struct.*, 1981, **72**, 85.
715. R. Köster, P. Idelmann and W. V. Dahlhoff, *Synthesis*, 1982, 650.
716. M. E. Gurskii, S. V. Baranin, A. S. Shashkov, A. I. Lutsenko and B. M. Mikhailov, *J. Organomet. Chem.*, 1983, **246**, 129.
717. J. Mason, *J. Chem. Soc. Faraday Trans. II*, 1979, **75**, 607.
718. G. A. Olah, R. J. Spear, P. W. Westerman and J. M. Denis, *J. Am. Chem. Soc.*, 1974, **96**, 5855.
719. J. E. Richman, N.-C. Yang and L. L. Andersen, *J. Am. Chem. Soc.*, 1980, **102**, 5790.
720. B.-L. Li and R. H. Neilson, *Inorg. Chem.*, 1986, **25**, 361.
721. B.-L. Li, M. A. Goodman and R. H. Neilson, *Inorg. Chem.*, 1984, **23**, 1368.

722. M. E. Gurskii, A. S. Shashkov and B. M. Mikhailov, *Izv. Akad. Nauk SSSR Ser. Khim.*, 1981, 341.
723. L. J. Todd, *Pure Appl. Chem.*, 1972, **30**, 587.
724. N. A. Kutz and J. A. Morrison, *Inorg. Chem.*, 1980, **19**, 3295.
725. R. Benn and A. Rufinska, *Angew. Chem.*, 1986, **98**, 851; *Angew. Chem. Int. Ed. Engl.*, 1986, **25**, 861.
726. R. Wehrmann, C. Poes, H. Klusik and A. Berndt, *Angew. Chem.*, 1984, **96**, 372; *Angew. Chem. Int. Ed. Engl.*, 1984, **23**, 372.
727. C. Bihlmayer, S. T. Abu-Orabi and B. Wrackmeyer, *J. Organomet. Chem.*, 1987, **322**, 25.
728. S. Kersch and B. Wrackmeyer, *J. Organomet. Chem.*, 1987, **332**, 25.
729. M. Oki, *Application of Dynamic NMR Spectroscopy to Organic Chemistry*, VCH, Weinheim, 1985.
730. R. Köster, G. Seidel, S. Kersch and B. Wrackmeyer, *Z. Naturforsch.*, 1987, **42b**, 191.
731. H. Kessler, G. Zimmermann, H. Fietze and H. Möhrle, *Chem. Ber.*, **111**, 2605.
732. H. C. Brown, G. G. Pai and R. G. Naik, *J. Org. Chem.*, 1984, **49**, 1972.
733. G. Hunter, W. S. Wadsworth and K. Mislow, *Organometallics*, 1982, **1**, 968.
734. T. Burgemeister, R. Grobe-Einsler, R. Grotstollen, A. Mannschreck and G. Wulff, *Chem. Ber.*, 1981, **114**, 3403.
735. S. Kersch and B. Wrackmeyer, *J. Chem. Soc. Chem. Commun.*, 1986, 403.
736. R. H. Cragg and T. J. Miller, *J. Organomet. Chem.*, 1981, **217**, 283.
737. C. Brown, R. H. Cragg, T. J. Miller and D. O'N. Smith, *J. Organomet. Chem.*, 1983, **244**, 209.
738. C. Brown, R. H. Cragg, T. J. Miller and D. O'N. Smith, *J. Organomet. Chem.* 1985, **296**, C17.
739. R. H. Cragg, T. J. Miller and D. O'N. Smith, *J. Organomet. Chem.*, **291**, 273.
740. N. M. D. Brown, F. Davidson and J. W. Wilson, *J. Organomet. Chem.*, 1981, **210**, 1.
741. R. J. Spear, D. A. Forsyth and G. A. Olah, *J. Am. Chem. Soc.*, 1976, **98**, 2493.
742. K. K. Curry and J. W. Gilje, *J. Am. Chem. Soc.*, 1978, **100**, 1442.
743. H. Nöth and S. Weber, *Angew. Chem.*, 1984, **96**, 998; *Angew. Chem. Int. Ed. Engl.*, 1984, **23**, 994.
744. B. Wrackmeyer, *J. Organomet. Chem.*, 1986, **310**, 151.
745. B. Wrackmeyer, C. Bihlmayer and M. Schilling, *Chem. Ber.*, 1983, **116**, 3182.
746. B. Wrackmeyer, *Ann. Rep. NMR Spectrosc.*, 1985, **16**, 73.
747. W. Biffar, T. Gasparis-Ebeling, H. Nöth, W. Storch and B. Wrackmeyer, *J. Magn. Reson.*, 1981, **44**, 54.
748. R. Schlögl and B. Wrackmeyer, *Polyhedron*, 1985, **4**, 885.
749. S. Kersch and B. Wrackmeyer, *J. Chem. Soc. Chem. Commun.*, 1985, 1199.
750. A. Sebal, P. Seiberlich and B. Wrackmeyer, *J. Organomet. Chem.*, 1986, **303**, 73.
751. A. Sebal and B. Wrackmeyer, *J. Organomet. Chem.*, 1986, **307**, 157.
752. S. Kersch and B. Wrackmeyer, *Z. Naturforsch.*, 1986, **41b**, 890.
753. S. Kersch, B. Wrackmeyer, A. Willhalm and A. Schmidpeter, *J. Organomet. Chem.*, 1987, **319**, 49.
754. S. Kersch and B. Wrackmeyer, *Z. Naturforsch.*, 1984, **39b**, 1037.
755. C. Bihlmayer and B. Wrackmeyer, *Z. Naturforsch.*, 1981, **36b**, 1265.
756. C. Bihlmayer, S. Kersch and B. Wrackmeyer, *Z. Naturforsch.*, 1987, **42b**, 715.
757. B. Wrackmeyer, *J. Organomet. Chem.*, 1981, **205**, 1.
758. A. G. Massay, *Adv. Inorg. Radiochem.*, 1983, **26**, 1.
759. H. Schmidbauer and E. Weiß, *Angew. Chem.*, 1981, **93**, 300; *Angew. Chem. Int. Ed. Engl.*, 1981, **20**, 283.
760. A. N. Esaulenko, Yu. N. Shevchenko, M. A. Porai-Koshits, S. I. Tyukhtenko, G. A. Kukina and V. V. Trachevskii, *Dokl. Akad. Nauk SSSR*, 1986, **286**, 381.

761. H. Schmidbaur, G. Müller, K. C. Dask and B. Milewski-Mahrle, *Chem. Ber.*, 1981, **114**, 441.
762. J. A. Marsella and K. G. Caulton, *J. Am. Chem. Soc.*, 1982, **104**, 2361.
763. M. Lauer and G. Wulff, *J. Organomet. Chem.*, 1983, **256**, 1.
764. H. Schmidbaur, G. Müller and G. Blaschke, *Chem. Ber.*, 1980, **113**, 1480.
765. R. Janta, R. Maisch, W. Malisch and E. Schmid, *Chem. Ber.*, 1983, **116**, 3951.
766. (a) J. W. Emsley, L. Phillips and V. Wray, *Prog. NMR Spectrosc.*, 1976, **10**, 83.  
(b) V. Wray, *Ann. Rep. NMR Spectrosc.*, 1980, **10B**, 1.  
(c) V. Wray, *Ann. Rep. NMR Spectrosc.*, 1983, **14**, 1.
767. M. T. Reetz, M. Hüllmann, W. Massa, S. Berger, P. Rademacher and P. Heymanns, *J. Am. Chem. Soc.*, 1986, **108**, 2405.
768. J. S. Hartman, B. D. McGarvey and C. V. Raman, *Inorg. Chim. Acta*, 1981, **49**, 63.
769. H. Bürger, M. Grunwald and G. Pawelke, *J. Fluor. Chem.*, 1985, **28**, 183.
770. H. Bönnemann, *Angew. Chem.*, 1985, **97**, 264; *Angew. Chem. Int. Ed. Engl.*, 1985, **24**, 248.
771. R. Köster, G. Seidel and B. Wrackmeyer, Unpublished results.
772. A. Sebald and B. Wrackmeyer, *J. Chem. Soc. Chem. Commun.*, 1983, 309.
773. A. Sebald and B. Wrackmeyer, *J. Chem. Soc. Chem. Commun.*, 1983, 1293.
774. H. Nöth, *Nachr. Chem. Techn. Lab.*, 1984, **32**, 956.
775. P. Kölle, Dissertation, Universität München, 1987.
776. H. Binder, W. Matheis, H.-J. Deiseroth and H. Fu-San, *Z. Naturforsch.*, 1983, **38b**, 554.
777. B. M. Mikhailov, V. V. Negrebetskii, V. S. Bogdanov, A. V. Kessenikh, Yu. N. Bubnov, T. K. Baryshnikova and V. N. Smirnov, *Zh. Obshch. Khim.*, 1974, **44**, 1878.
778. L. Zetta and G. Gatti, *Org. Magn. Reson.*, 1972, **4**, 585.
779. B. Wrackmeyer, *J. Organomet. Chem.*, 1985, **297**, 265.
780. (a) M. M. Crutchfield, C. H. Dungan, J. H. Letcher, V. Mark and J. R. van Wazer, *Top. Phosphorus Chem.*, 1967, **5**.  
(b) G. Mavel, *Ann. Rep. NMR Spectrosc.*, 1973, **513**, 1.  
(c) D. G. Gorenstein (ed.), *Phosphorus-31 NMR, Principles and Application*, Academic Press, New York, 1984.
781. P. Jutzi and P. Galow, *J. Organomet. Chem.*, 1987, **319**, 139.
782. P. B. Hitchcock, M. F. Lappert and R. G. Taylor, *J. Chem. Soc. Chem. Commun.*, 1984, 1082.
783. C. J. Cardin, H. E. Parge and J. W. Wilson, *J. Chem. Res. (S)*, 1983, 93; (M), 1983, 0801.
784. R.-J. Binnewirtz, H. Klingenberg, R. Welte and P. Paetzold, *Chem. Ber.*, 1983, **116**, 1271.
785. M. K. Das and P. Mukherjee, *J. Chem. Res. (S)*, 1985, 66.
786. E. Kalbarczyk and S. Pasynkiewicz, *J. Organomet. Chem.*, 1984, **262**, 11.
787. Y. F. Beswick, P. Wisian-Neilson and R. H. Neilson, *J. Inorg. Nucl. Chem.*, 1981, **43**, 2639.
788. E. Hohaas, *Z. Anorg. Allg. Chem.*, 1983, **506**, 185.
789. H.-U. Hürter, B. Krebs, H. Eckert and W. Müller-Warmuth, *Inorg. Chem.*, 1985, **24**, 1288.
790. P. Zanirato, *J. Organomet. Chem.*, 1985, **293**, 285.
791. K. Sasakura, Y. Terui and T. Sugawara, *Chem. Pharm. Bull.*, 1985, **33**, 1836.
792. H. Yatagai, Y. Yamamoto and K. Maruyama, *J. Am. Chem. Soc.*, 1980, **102**, 4548.
793. H. C. Brown and J. C. Chen, *J. Org. Chem.*, 1981, **46**, 3978.
794. F. Alam and K. Niedenzu, *J. Organomet. Chem.*, 1982, **240**, 107.
795. Y. Yamamoto, H. Yatagai and K. Maruyama, *J. Am. Chem. Soc.*, 1981, **103**, 1969.
796. R. W. Hoffman and H.-J. Zeiß, *J. Org. Chem.*, 1981, **46**, 1309.
797. L. Bhal, R. V. Singh and J. P. Tandon, *Acta Chim. Hung.*, 1984, **115**, 251.
798. P. G. M. Wuts and P. A. Thompson, *J. Organomet. Chem.*, 1982, **234**, 137.

799. S. Allaoud, H. Bitar, M. El Mouhtadi and B. Frange, *J. Organomet. Chem.*, 1983, **248**, 123.
800. R. Ahmad, J. E. Crook, N. N. Greenwood and J. D. Kennedy, *J. Chem. Soc. Dalton Trans.*, 1986, 2433.
801. A. H. Cowley, J. E. Kilduff and J. C. Wilburn, *J. Am. Chem. Soc.*, 1981, **103**, 1575.
802. H. Schmidbaur, E. Weiß and G. Müller, *Synth. React. Inorg. Met.-Org. Chem.*, 1985, **15**, 401.
803. H. Schmidbaur, E. Weiß and G. Müller, *Synth. React. Inorg. Met.-Org. Chem.*, 1985, **15**, 415.
804. S. Schramm and E. Oldfield, *J. Chem. Soc. Chem. Commun.*, 1982, 980.
805. I. A. Harris and P. J. Bray, *Phys. Chem. Glasses*, 1984, **25**, 69.
806. T. M. Duncan, *J. Am. Chem. Soc.*, 1984, **106**, 2270.
807. C. Conard, M. Bouchacourt, F. Thevenot and G. Hermann, *J. Less-Common Met.*, 1986, **117**, 51.
808. E. C. Reynhardt, *J. Magn. Reson.*, 1986, **69**, 337.
809. C. Bihlmayer, S. T. Abu-Orabi and B. Wrackmeyer, *J. Organomet. Chem.*, 1987, **322**, 25.
810. T. Mancilla and R. Contreras, *J. Organomet. Chem.*, 1987, **321**, 191.
811. G. Schmid and G. Barbenheim, *Chem. Ber.*, 1987, **120**, 401.
812. B. Glaser and H. Nöth, *Chem. Ber.*, 1987, **120**, 345.
813. J. G. Dawber and S. I. E. Green, *J. Chem. Soc. Faraday Trans. I*, 1986, **82**, 3407.
814. B. A. Arbuzov, G. N. Nikonov and O. A. Erastov, *Izv. Akad. Nauk. SSSR Ser. Khim.*, 1986, 171.
815. E. G. Ippolitov, B. N. Chernyshov, G. P. Shchetinina, O. V. Brovkina, Yu. L. Martynyuk and Yu. V. Gorin, *Ukr. Khim. Zh.*, 1986, **52**, 818; *CA*, 1987, **106**, 42927v.
816. R. K. Kanjolia, C. L. Watkins and L. K. Krannich, *Inorg. Chem.*, 1987, **26**, 222.
817. K. Stumpf, W. Siebert, R. Köster and G. Seidel, *Z. Naturforsch.*, 1987, **42b**, 186.
818. J. Fritze, W. Preetz and H. C. Marsmann, *Z. Naturforsch.*, 1987, **42b**, 287.
819. B. F. Spielvogel, F. U. Ahmed and A. T. McPhail, *Synthesis*, 1986, 833.
820. B. M. Mikhailov, M. E. Gurskii, S. V. Baranin, Yu. N. Bubnov, M. V. Sergeeva, A. I. Yanowskii, K. A. Potekhina, A. V. Maleev and Yu. T. Truchkov, *Izv. Akad. Nauk SSSR Ser. Khim.*, 1986, 1645.
821. M. T. Reetz, F. Kunisch and P. Heitmann, *Tetrahedron Lett.*, 1986, 4721.
822. J. Marcalo, N. Marques, A. Pires de Matos and K. W. Bagnall, *J. Less-Common Met.*, 1986, **122**, 219.
823. R. Köster and M. Yalpani, *J. Org. Chem.*, 1986, **51**, 3054.
824. C. E. Housecroft and A. L. Rheingold, *J. Am. Chem. Soc.*, 1986, **108**, 6420.
825. H. C. Brown, M. V. Rangaishenvi and U. S. Racherla, *J. Org. Chem.*, 1987, **52**, 728.
826. G. E. Herberich, B. Heßner, M. Negele and J. A. K. Howard, *J. Organomet. Chem.*, 1987, **336**, 29.
827. E. Gamp, R. Shinomoto, N. Edelstein and B. R. McGarvey, *Inorg. Chem.*, 1987, **26**, 2177.
828. M. M. Olmstead, P. P. Power and K. J. Weese, *J. Am. Chem. Soc.*, 1987, **109**, 2541.
829. G. Schmid, O. Boltsch and R. Boese, *Organometallics*, 1987, **6**, 435.
830. R. Boese, B. Kröckert and P. Paetzold, *Chem. Ber.*, 1987, **120**, 1913.
831. R. Boese, P. Paetzold and A. Tapper, *Chem. Ber.*, 1987, **120**, 1069.
832. H. Binder, A. Ziegler, R. Ahlrichs and H. Schiffer, *Chem. Ber.*, 1987, **120**, 1545.
833. K. Geilich, K. Stumpf, H. Pritzkow and W. Siebert, *Chem. Ber.*, 1987, **120**, 911.
834. M. Yalpani, R. Boese and R. Köster, *Chem. Ber.*, 1987, **120**, 607.
835. U. Siwardane, M. S. Islam, T. A. West, N. S. Hosmane, J. A. Maguire and A. H. Cowley, *J. Am. Chem. Soc.*, 1987, **109**, 4600.

This Page Intentionally Left Blank

# $^{11}\text{B}$ NMR Spectroscopy

A. R. SIEDLE

*3M Corporate Research Laboratories,  
St Paul, Minnesota 55144, USA*

I. Introduction . . . . .	205
II. Spectroscopic techniques and general results . . . . .	206
III. Analytical applications . . . . .	208
IV. One-boron compounds . . . . .	209
A. Analogues of pharmacologically active compounds . . . . .	209
B. Cationic boron compounds . . . . .	209
C. Compounds with multiple bonds to boron and small-ring boron compounds . . . . .	212
D. Pyrazaboles . . . . .	217
E. Boron-containing heterocycles . . . . .	219
F. Alkylboranes and related compounds . . . . .	225
G. Other one-boron compounds . . . . .	229
V. Polyboranes and carboranes . . . . .	233
A. $\text{B}_{2,3}$ boranes and carboranes . . . . .	233
B. $\text{B}_4$ boranes and carboranes . . . . .	235
C. $\text{B}_5$ boranes and carboranes . . . . .	237
D. $\text{B}_{6,8,9}$ boranes and carboranes . . . . .	240
E. $\text{B}_{10,11,12}$ boranes and carboranes . . . . .	251
VI. Metalloboranes and metallocarboranes . . . . .	254
A. $\text{B}_1$ metalloboranes and metallocarboranes . . . . .	254
B. $\text{B}_{2,3,4}$ metalloboranes and metallocarboranes . . . . .	259
C. $\text{B}_{5,7,8}$ metalloboranes and metallocarboranes . . . . .	263
D. $\text{B}_9$ metalloboranes and metallocarboranes . . . . .	275
E. $\text{B}_{10}$ and larger metalloboranes and metallocarboranes . . . . .	285
VII. Coupled boranes and carboranes . . . . .	294
VIII. Transition-metal complexes of boron-containing heterocycles . . . . .	299
IX. $^{11}\text{B}$ NMR studies of solids . . . . .	302
Acknowledgments . . . . .	305
References . . . . .	306

## I. INTRODUCTION

This chapter covers developments in  $^{11}\text{B}$  NMR spectroscopy subsequent to a previous review in this series.<sup>1</sup> In addition, it serves to complement the preceding chapter. As in previous years, a major use of  $^{11}\text{B}$  has been archival—that is, use for routine characterization of new compounds—

although considerable efforts to elucidate correlations between structure and NMR parameters continue. However, some significant trends may be noted. First, availability of high-field spectrometers with multinuclear capability as well as software for sophisticated data manipulation is increasingly common, and, with these instruments, lack of chemical-shift dispersion in the face of relatively large linewidths presents much less of a problem than previously when complex polyboron compounds are to be characterized. Coupled with this, potent separation techniques, exemplified by thin-layer, high-pressure and ion-exchange chromatography, are able to unravel complex mixtures and make pure compounds available for study. Use of X-ray crystallographic facilities with which to structurally characterize compounds whose spectra are reported is today almost routine. Less routine is an appreciation of the fact that one crystal teased from a reaction mixture is not necessarily representative of the system from which it was extracted; use of X-ray powder-diffraction analysis to test this hypothesis is to be encouraged. Thus inability to separate mixtures, to secure high-resolution spectra and structural data are of decreasing importance in boron chemistry, leaving, perhaps, as the rate-limiting factors, creativity and the propensity to select for detailed study systems that offer new, significant and fundamental insights into the chemistry of boron and of the elements to which it bonds.

The chemical-shift convention used here has positive shifts to high frequency of the reference, external  $\text{BF}_3 \cdot \text{Et}_2\text{O}$ . It is questionable, at least in some cases, whether chemical shifts can be measured with a precision of  $\pm 0.01$  ppm and so values reported are rounded off to within 0.1 ppm. Couplings are given in Hz and rounded off to the nearest Hz; symbols for peak multiplicities are s (singlet), d (doublet), t (triplet) and q (quartet). Relative intensities are represented by *n*B. Chemical shifts are followed by, in parentheses, multiplicity,  $J_{\text{BH}}$  (unless otherwise specified), additional coupling, and peak assignment or relative intensity.

## II. SPECTROSCOPIC TECHNIQUES AND GENERAL RESULTS

There is little doubt that the most significant developments in technique are those related to two-dimensional or COSY  $^{11}\text{B}$  NMR spectroscopy.<sup>2,3</sup> Boron-boron connectives may be directly determined by *J*-correlated two-dimensional NMR spectroscopy, and this is of great value in interpretation of spectra of complex molecules. A detailed description of the method has been presented and results obtained for 1,2- and 1,7- $\text{B}_{10}\text{C}_2\text{H}_{12}$ , 2,3- $\text{Et}_2\text{B}_4\text{C}_2\text{H}_5^-$ ,  $\text{Et}_2\text{B}_4\text{C}_2\text{H}_6$ ,  $(\text{B}_5\text{H}_8)_2\text{Hg}$ ,  $\mu$ -4,5- $\text{ClHg}[\text{Me}_5\text{CpCo}(\text{Me}_2\text{B}_3\text{C}_2\text{H}_4)]$ ,  $(\text{Me}_6\text{C}_6)\text{Fe}(\text{Et}_2\text{B}_3\text{C}_2\text{H}_5)$ ,  $\text{CpCoB}_4\text{H}_8$  and

$\text{Me}_4\text{B}_7\text{C}_4\text{H}_9$ . The 2D spectrum of  $5\text{-Me}_5\text{CpCoB}_8\text{H}_{13}$  (Fig. 1) is an example of what has been achieved.

Cross-peaks appear when four conditions are met: (1) there is sufficient electron density between  $^{11}\text{B}$  nuclei to permit scalar coupling so that  $\text{B-H-B}$  borons usually do not cross-couple; (2) the two nuclei are not decoupled by a longitudinal relaxation time  $T_1$  that is short relative to the reciprocal of the coupling, i.e.  $2\pi JT_1 \ll 1$ ; (3) transverse relaxation times,  $T_2$ , are long enough to permit loss of cross-peak signals through signal decay;

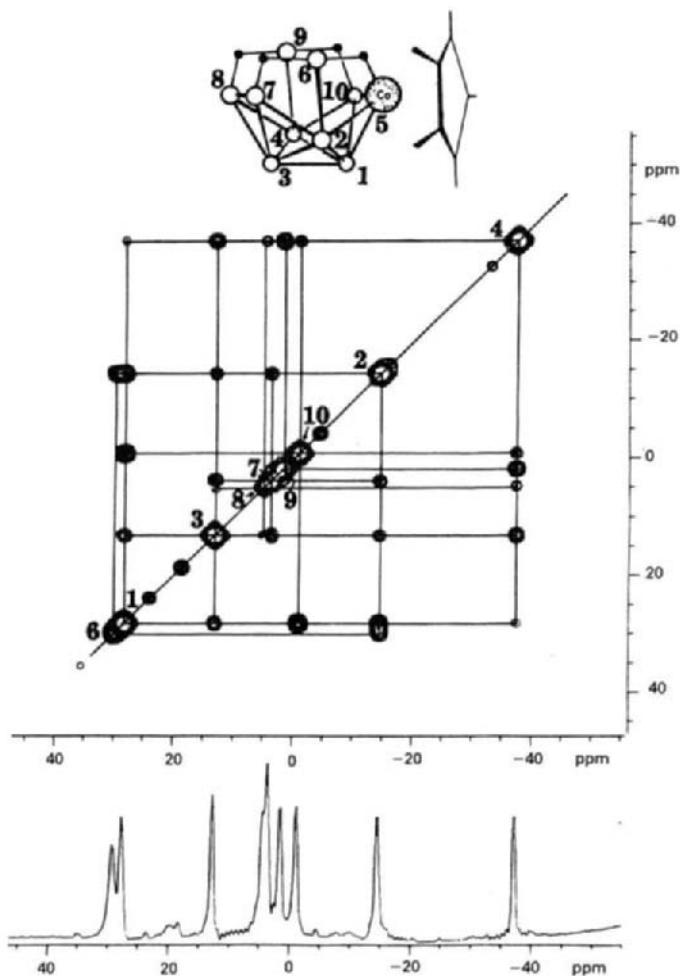


FIG. 1. Spectrum of  $5\text{-[C}_5\text{Me}_5\text{]CoB}_9\text{H}_{13}$  in  $n$ -hexane.

(4) the individual resonances are resolved in the 1D spectrum. This last requirement makes the use of high-field spectrometers important. Because scalar coupling propagates through bonding electrons, 2D NMR provides a qualitative picture of bonding-electron density in a molecule.

Two-dimensional  $^1\text{H}$ - $^1\text{H}$  NMR (with broadband  $^{11}\text{B}$  decoupling) has also been applied to  $\text{Me}_5\text{CpRhB}_9\text{H}_{13}$ . The advantages of this technique are (i) observation of  $^3J(\text{H-B-B-H})$  when the corresponding  $^2J(\text{B-B})$  correlation is unapparent; (ii) larger chemical-shift dispersion in the  $^1\text{H}$  spectrum; and (iii) bridging protons show correlations.<sup>4</sup>

Reports of relaxation times are becoming increasingly common. For  $\text{B}_{10}\text{H}_{14}$  in toluene- $d_8$ ,  $T_1$  depends only on the rotational correlation time,  $\tau_R$ , when isotropic tumbling occurs. With increasing temperature,  $T_1$  increases and  $\tau_R$  decreases.<sup>5</sup>

The effect of solvent on  $^{11}\text{B}$  NMR parameters for  $\text{B}_{10}\text{H}_{14}$  has been reported. In low-polarity solvents, such as n-pentane, an 18 Hz coupling between B(2, 4) and B(6, 0) may be resolved with the use of line narrowing. The coupling is obscured in higher-molecular-weight solvents such as n-octane and  $\text{C}_6\text{F}_6$ , probably because of the effect of viscosity on the correlation times.<sup>6</sup>

The magnitude of  $J(\text{BH})$  in an extensive series of carboranes has been correlated with structural features:

$$J(\text{BH}) = \frac{-2.08(13.4)^c \theta}{449^c} + \frac{394(1.69)^c}{3.87^c},$$

where  $c$  is the number of contiguous cage carbon atoms and  $\theta$ , the "umbrella angle", is the average interior angle of a conical-shaped figure having the BH unit at the apex.<sup>7</sup>

### III. ANALYTICAL APPLICATIONS

$^{11}\text{B}$  NMR spectroscopy has been used as an analytical tool to monitor reactions of various boron-containing compounds. Examples include  $\text{BH}_{4-x}\text{R}_x^-$  derivatives obtained from  $\text{RLi}$  and  $\text{BH}_3 \cdot \text{L}$  ( $\text{L} = \text{THF}$ ,  $\text{Me}_2\text{S}$ ,  $\text{Me}_3\text{N}$ ),<sup>8</sup> and from Grignard reagents.<sup>9</sup> Considerable work has been done on the cleavage of  $\mu\text{-Me}_2\text{NB}_2\text{H}_5$ ,  $\text{B}_4\text{H}_{10}$  and  $\text{B}_3\text{H}_7 \cdot \text{THF}$  with tetramethylphenylenediamine.<sup>10,11</sup> Also studied have been reactions of  $\text{B}_5\text{H}_{11}$  with  $\text{B}_2\text{H}_4 \cdot (\text{PMe}_3)_2$ ,<sup>12</sup> of  $\text{B}_3\text{H}_6(\text{PMe}_3)_2^+ \text{B}_3\text{H}_8^-$  with Lewis bases,<sup>13</sup>  $\text{B}_6\text{H}_{10}$  and  $\text{B}_4\text{H}_{10}$  with  $\text{Me}_3\text{P}$ ,<sup>14,15</sup> as well as the thiocyanation of  $\text{B}_{10}\text{H}_{10}^{2-}$ .<sup>16</sup>

## IV. ONE-BORON COMPOUNDS

## A. Analogues of pharmacologically active compounds

Boron analogues of amino acids have been prepared. Chemical shifts of some examples are given in Table 1.<sup>17,18</sup> Data are also included for metal complexes of  $\text{Me}_3\text{N}\cdot\text{BH}_2\text{CO}_2^-$  in which the carboxylate moiety functions as a bidentate ligand.<sup>19</sup>

Boron analogues of uracils, 1,3,5-triaza-2-phenyl-2-boracyclohexan-4,6-diones, have been prepared. Their  $^{11}\text{B}$  spectra comprise broad (half-width 425–600 Hz) singlets at 32–36 ppm.<sup>20</sup>  $\text{CH}_3\text{CO}_2\text{C}_2\text{H}_4\text{NMe}_2\cdot\text{BH}_3$ ,  $\delta^{11}\text{B} = -9.4$  (q, 98) was also synthesized.<sup>21</sup> Shifts for  $\text{Na}[\text{BH}_2(\text{CN})_2]$  and  $\text{Bu}_4\text{N}[\text{BH}_2(\text{CN})_2]$  are  $-36.4$  (t, 93, DMSO) and  $-41.4$  ( $\text{CDCl}_3$  solvent) ppm respectively; the difference may be an effect of ion pairing.<sup>22</sup>

TABLE 1

 $^{11}\text{B}$  Chemical shifts of boron analogues of amino acids.

Compound	$\delta^{11}\text{B}$ ( $J(\text{B}-\text{H})$ )
$\text{Me}_3\text{N}\cdot\text{BH}_2\text{CO}_2\text{Et}$	$-9.2$ (98)
$\text{Me}_3\text{N}\cdot\text{BH}_2\text{CO}_2\text{Me}$	$-9.1$ (99)
$\text{Me}_2\text{NH}\cdot\text{BH}_2\text{CO}_2\text{Me}$	$-12.6$ (95)
$\text{MeNH}_2\cdot\text{BH}_2\text{CO}_2\text{Me}$	$-16.2$ (98)
$\text{Me}_3\text{N}\cdot\text{BH}_2\text{CO}_2\text{C}_2\text{H}_4\text{Cl}$	$-8.8$ (97)
$\text{NH}_3\cdot\text{BH}_2\text{CO}_2\text{Me}$	$-20.5$ (94)
$\text{Me}_3\text{N}\cdot\text{BH}_2\text{CONHEt}$	$-7.4$
$\text{Me}_2\text{NH}\cdot\text{BH}_2\text{CONHEt}$	$-11.6$
$\text{MeNH}_2\cdot\text{BH}_2\text{CONHEt}$	$-15.4$
$\text{NH}_3\cdot\text{BH}_2\text{CONHEt}$	$-19.6$
$\text{Me}_3\text{N}\cdot\text{BH}_2\text{CO}_2\text{H}$	$-10.2$ (98)
$\text{Na}[\text{Me}_3\text{N}\cdot\text{BH}_2\text{CO}_2]$	$-8.8$ (93)
<i>cis</i> - $\text{Co}(\text{en})_2(\text{Me}_3\cdot\text{BH}_2\text{CO}_2)_2$	$-9.4$ (95)
$\text{Co}(\text{Me}_3\text{N}\cdot\text{BH}_2\text{CO}_2)(\text{NO}_3)\cdot\text{MeCN}\cdot 3\text{MeOH}$	$-11.0$ (103)
$\text{Ca}(\text{Me}_3\text{N}\cdot\text{BH}_2\text{CO}_2)(\text{NO}_3)\cdot\text{Me}_2\text{CO}\cdot 0.5\text{H}_2\text{O}$	$-9.0$ (95)
$\text{Zn}(\text{Me}_3\text{N}\cdot\text{BH}_2\text{CO}_2)(\text{NO}_3)\cdot\text{EtOH}$	$-9.7$ (98)

## B. Cationic boron compounds

Recent developments in the chemistry and  $^{11}\text{B}$  NMR spectroscopy of borinium,  $(\text{R}_2\text{N})_2\text{B}^+$ , and borenium,  $\text{R}_2\text{B}(\text{donor})^+$ , cations have been extensively reviewed.<sup>23–25</sup>

Halide abstraction from  $(\text{R}_2\text{N})_2\text{BX}$  yields  $(\text{R}_2\text{N})_2\text{B}^+$ , which have  $^{11}\text{B}$  chemical shifts of about 5–8 ppm to high frequency of their precursors.

Typical shielding values are in the 35–38 ppm range, but the linewidths increase greatly to 400–800 Hz owing to more rapid relaxation associated with the increase in nuclear field gradient. Trialkylsilyl substitution at nitrogen further deshields the boron nucleus, but replacement of one  $R_2N$  group by  $t\text{-Bu}_3\text{SiO-}$  has the opposite effect.

The  $^{11}\text{B}$  chemical shifts of  $R_2\text{B(donor)}^+$  salts are in the 24–32 ppm range with large linewidths. Alkyl substitution produces low-frequency shifts, e.g.  $[\text{Bu}_2\text{B(2,6-lutidine)}]\text{CF}_3\text{SO}_3$ ,  $\delta^{11}\text{B} = 54.7$ , and  $[\text{9-borobicycloborenum(2,6-lutidine)}]\text{CF}_3\text{SO}_3$ ,  $\delta^{11}\text{B} = 59.2$ . In solution, these compounds are in equilibrium with  $R_2\text{BOSO}_2\text{CF}_3$  and free 2,6-lutidine. In contrast,  $[\text{Ph}_2\text{B(2,6-lutidine)}]\text{CF}_3\text{SO}_3$  is in equilibrium with four-coordinate  $\text{Ph}_2\text{BOSO}_2\text{CF}_3 \cdot 2,6\text{-lutidine}$ .

A wide variety of trimethylsilylaminoboranes have been found to react with  $\text{BBr}_3$  to give (silylamino)boronium  $\text{BBr}_4^-$  salts.  $^{11}\text{B}$  data for these and the precursors are given in Table 2.

A series of *N*-substituted haloboranes of the type  $(\text{TMP})\text{B}(\text{NEt}_2)\text{X}$  (TMP is 2,2,6,6-tetramethylpiperidiny) has been prepared. For  $\text{X} = \text{F}$ ,  $\text{Cl}$ ,  $\text{Br}$  and  $\text{I}$ ,  $\delta^{11}\text{B}$  (halfwidth) values are 25.9 (201), 31.0 (189), 29.9 (164) and

TABLE 2

 $^{11}\text{B}$  Chemical shifts for some boronium salts.

	$\delta^{11}\text{B}$		$\delta^{11}\text{B}$
$\left(\text{Me}_3\text{C} \begin{array}{c} \diagup \\ \text{N} \\ \diagdown \end{array} \text{Me}_3\text{Si} \right)_2 \text{BF}$	27.1	$\begin{array}{c} \diagup \\ \text{N}=\text{N} \\ \diagdown \end{array}$	5.4
$\left(\text{Me}_3\text{C} \begin{array}{c} \diagup \\ \text{N} \\ \diagdown \end{array} \text{Me}_3\text{Si} \right)_2 \text{B}^+ \text{BBr}_4^-$	35.2 -24.5	$\begin{array}{c} \diagup \\ \text{N}=\text{B}-\text{N} \begin{array}{c} \diagup \\ \text{SiMe}_3 \\ \diagdown \end{array} \\ \diagdown \end{array} + \text{I}^-$	36.1
$\text{Me}_3\text{C} \begin{array}{c} \diagup \\ \text{N}-\text{B} \begin{array}{c} \diagup \\ \text{F} \\ \diagdown \end{array} \\ \diagdown \end{array} \text{N}(\text{SiMe}_3)_2$	26.9	$\begin{array}{c} \diagup \\ \text{N}-\text{B} \begin{array}{c} \diagup \\ \text{F} \\ \diagdown \end{array} \\ \diagdown \end{array} \text{Me}_3\text{Si} \begin{array}{c} \diagup \\ \text{N} \\ \diagdown \end{array}$	26.9
$\text{Me}_3\text{C} \begin{array}{c} \diagup \\ \text{N}=\text{B}-\text{N} \begin{array}{c} \diagup \\ \text{SiMe}_3 \\ \diagdown \end{array} \\ \diagdown \end{array} \text{SiMe}_3 + \text{BBr}_4^-$	32.8 -24.5	$\begin{array}{c} \diagup \\ \text{N}-\text{B}=\text{N} \begin{array}{c} \diagup \\ \text{SiMe}_3 \\ \diagdown \end{array} \\ \diagdown \end{array} + \text{BBr}_4^-$	35.8 -24.5
$\text{Me}_3\text{C} \begin{array}{c} \diagup \\ \text{N}-\text{B} \begin{array}{c} \diagup \\ \text{F} \\ \diagdown \end{array} \\ \diagdown \end{array} \text{Si} \begin{array}{c} \diagup \\ \text{N} \\ \diagdown \end{array} \text{N}(\text{SiMe}_3)_2$	26.9	$\text{Me}_3\text{C} \begin{array}{c} \diagup \\ \text{N}-\text{B} \equiv \text{N}-\text{CMe}_3 \\ \diagdown \end{array} \text{Me}_3\text{Si}$	7.0
$\text{Me}_3\text{C} \begin{array}{c} \diagup \\ \text{N}=\text{B}-\text{N} \begin{array}{c} \diagup \\ \text{SiMe}_3 \\ \diagdown \end{array} \\ \diagdown \end{array} \text{Si} \begin{array}{c} \diagup \\ \text{N} \\ \diagdown \end{array} \text{N}(\text{SiMe}_3)_2 + \text{BBr}_4^-$	33.3 -24.5	$\left(\text{Me}_3\text{C} \begin{array}{c} \diagup \\ \text{N} \\ \diagdown \end{array} \text{Me}_3\text{Si} \right)_2 \text{B}^+ \text{I}^-$	36.1
$[(\text{Me}_3\text{Si})_2\text{N}]_2\text{BF}$	27.1		
$[(\text{Me}_3\text{Si})_2\text{N}]_2\text{B}^+ \text{BBr}_4^-$	32.8 -24.5		

TABLE 3

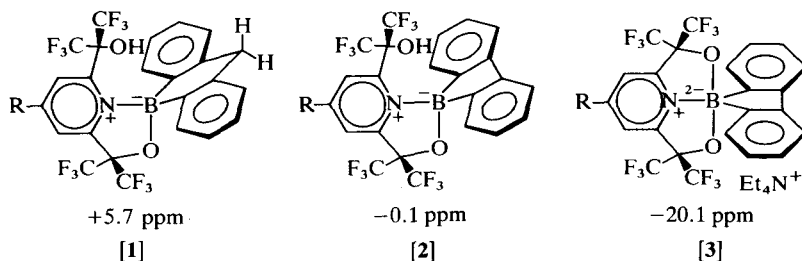
 $^{11}\text{B}$  NMR data for (amine) $_2\text{BF}_2^+$  cations.

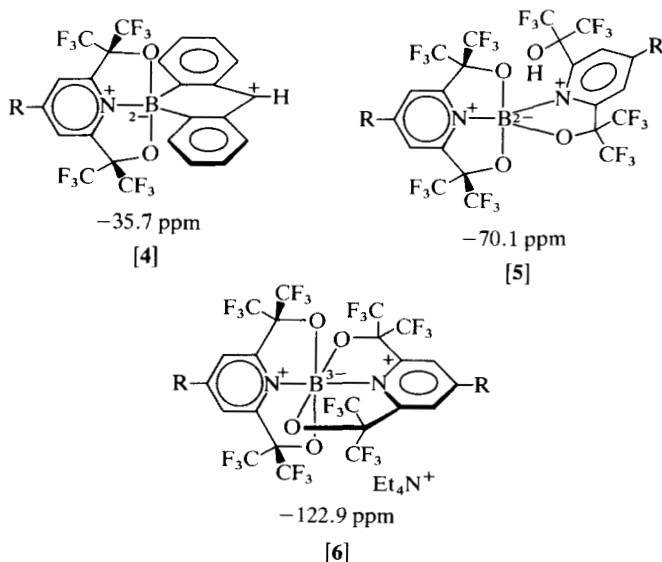
D = D'		$\delta^{19}\text{F}$	$J(^{19}\text{F}-^{11}\text{B})$	$\delta^{11}\text{B}$
Pyridine		-155.6	22.9	1.8
Q		-161.5	39.5	1.4
$\text{Me}_3\text{N}$		-165.4	36.2	1.9
$\text{Me}_2\text{NEt}$		-158.9	39.3	2.3
$\text{MeNEt}_2$				
$\text{Et}_3\text{N}$				
Pyridine	Q	-161.3	28.6	1.6
$\text{Me}_3\text{N}$	Q	-163.7	38.1	1.5
$\text{Me}_2\text{NEt}$	Q	-159.9	38.8	1.8
$\text{MeNEt}_2$	Q	-155.2	40.5	1.9
$\text{Et}_3\text{N}$	Q	-148.4	43.0	2.2

Q = 1-azabicyclo[2.2.2]octane.

26.0 (214) respectively. These compounds undergo halide abstraction to form  $[(\text{TMP})\text{BNEt}_2]\text{Y}$ , whose  $^{11}\text{B}$  shifts range from 35.4 ( $\text{Y} = \text{TaBr}_6^-$ ) to 38.6 ( $\text{Y} = \text{AlBr}_4^-$ ). Similarly,  $\delta^{11}\text{B}$  in  $[(\text{TMP})_2\text{B}]\text{Y}$  ranges from 35.0 ( $\text{Y} = \text{BF}_4^-$ ) to 36.1 ( $\text{Y} = \text{CF}_3\text{SO}_3^-$ ).<sup>24</sup>  $^{11}\text{B}$  spectra of compounds previously considered to be 1,3,2-dioxaborinium salts reveal the presence of covalent four-coordinate boron.<sup>27</sup> Tertiary amines, D, having low steric hindrance, displace  $\text{Br}^-$  from  $\text{D}'\text{BrBF}_2$  to form bis(amine)difluoroboron  $\text{DD}'\text{BF}_2^+$  salts, whose  $^{11}\text{B}$  shifts are given in Table 3.

Borinium salts may be considered to contain formal two-coordinate boron. Five- and six-coordinate boron compounds, connected by fractional bonds in clusters, are well known, but such coordination in "simple"  $\text{B}_1$  compounds is a recent development. Materials proposed to have these bonding features, i.e. hypervalent boron, have  $^{11}\text{B}$  shieldings greater than those of compounds containing normal, four-coordinate boron, for example  $\text{Bu}_4\text{B}^-$ ,  $\delta^{11}\text{B} = -17.5$ . This is illustrated by structures [1]–[6] and the corresponding chemical shifts:<sup>29</sup>

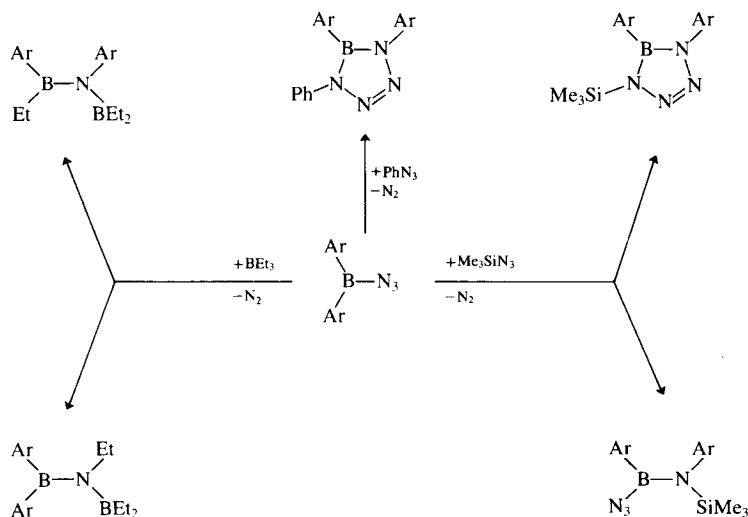




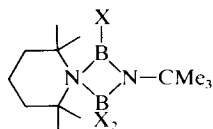
### C. Compounds with multiple bonds to boron and small-ring boron compounds

Research in this area has progressed with a renaissance of interest in multiply bonded nonmetallic elements. Pyrolysis of  $\text{Ar}_2\text{BN}_3$  (Ar is a general aryl group) presumably generates the nitrene  $\text{Ar}_2\text{BN}$  as a transient species, but this rearranges to the iminoborane  $\text{ArB}=\text{NAr}$ , which is not isolated but has a prolific chemistry as shown in Fig. 2.<sup>30</sup>

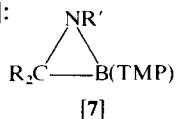
The chemistry of iminoboranes is also well developed.<sup>31-34</sup> Gas-phase pyrolysis of  $\text{t-Bu}(\text{Cl})\text{B}-\text{N}(\text{t-Bu})\text{SiMe}_3$  yields the iminoborane  $\text{t-BuB}=\text{N-t-Bu}$ , whose  $^{11}\text{B}$  chemical shift, 2.4 ppm, reveals boron in a greatly shielded environment; the chemical shift of its cyclic dimer is 41.0 ppm. This highly reactive iminoborane adds  $\text{Et}_3\text{B}$  to form  $\text{t-Bu}(\text{Et})\text{B}=\text{N}(\text{t-Bu})\text{BET}_2$ , in which the shifts of the four- and three-coordinate boron are 44.8 and 76.8 ppm respectively, i.e. the  $\text{B}=\text{N}$  bond is localized. Addition of  $\text{Me}_3\text{SiN}_3$  gives  $\text{t-Bu}(\text{N}_3)\text{B}-\text{N}(\text{t-Bu})\text{SiMe}_3$ ,  $\delta^{11}\text{B} = 50.8$ , but cyclic 1,2-di-*t*-butyl-5-phenyl-1-boratetrazole,  $\delta^{11}\text{B} = 28.1$ , is formed from  $\text{PhN}_3$ . Similarly, elimination at high temperature of  $\text{Me}_3\text{SiF}$  from  $(\text{Me}_3\text{Si})_3\text{SiB}(\text{F})-\text{N}(\text{SiMe}_3)_2$ ,  $\delta^{11}\text{B} = 44.6$ , produces the iminoborane  $(\text{Me}_3\text{Si})_3\text{B}=\text{NSiMe}_3$ ,  $\delta^{11}\text{B} = 21.9$ , whose stability is probably due to steric factors.<sup>34</sup> The iminoborane  $\text{i-PrB}=\text{N-t-Bu}$  cyclotrimerizes to form  $(\text{i-PrB}-\text{N-t-Bu})_3$ , whose X-ray structure discloses a significant (1.75 Å) 1,4 B—N contact; it is thus a Dewar borazine. How-

FIG. 2. Reactions of  $(\text{aryl})_2\text{BN}_3$ .

ever, the  $^{11}\text{B}$  NMR spectrum comprises a singlet at 31.1 ppm, indicative of a dynamical process within the ring.<sup>35</sup> An aminoiminoborane has been prepared by converting  $(\text{TMP})\text{BCl}_2$  ( $\delta^{11}\text{B} = 33.0$ , halfwidth 50) to  $(\text{TMP})\text{B}(\text{Cl})\text{NH}-t\text{-Bu}$  ( $\delta^{11}\text{B} = 30.4$ , halfwidth 126). This, on loss of  $\text{HCl}$ , forms  $(\text{TMP})\text{B}=\text{N}-t\text{-Bu}$  ( $\delta^{11}\text{B} = 4.1$ , halfwidth 102). It forms 1:1 complexes with  $\text{BX}_3$  ( $\text{X} = \text{Cl}$ , 27.5 ppm (halfwidth 25);  $\text{X} = \text{Br}$ , 25.9 ppm, (halfwidth 35)), which contain a  $\text{B}_2\text{N}_2$  ring resulting from formal addition of  $\text{BX}_2$  and  $\text{X}$  across the  $\text{B}=\text{N}$  bond:<sup>36</sup>



Likewise, dehydrohalogenation of 9-fluorenyltetramethylpiperidino-boranes of the type  $(\text{TMP})\text{B}(\text{X})\text{CHR}$  ( $\text{R} = 9\text{-fluorenyl}$ ) ( $\text{X} = \text{F}$ ,  $\delta^{11}\text{B} = 33.9$ ;  $\text{X} = \text{Cl}$ , 42.3 ppm;  $\text{X} = \text{OMe}$ , 34.3;  $\text{X} = \text{NMe}_2$ , 37.9) yields the allene analogue  $(\text{TMP})\text{B}=\text{C}=\text{CR}$ ,  $\delta^{11}\text{B} = 59.2$ . This compound is highly reactive and is the precursor of a wide variety of new materials. Reaction with  $\text{Ph}_2\text{CO}$  yields  $(\text{TMP})\text{B}(\text{O})\text{C}(\text{R})\text{CPh}_2$ ,  $\delta^{11}\text{B} = 36.9$ , which contains a four membered  $\text{B}-\text{C}-\text{C}-\text{O}$  ring. Reaction with  $\text{R}'\text{N}_3$  yields the three membered ring compound [7]:



( $R' = \text{Ph}$ ,  $\delta^{11}\text{B} = 21.3$ ;  $R' = \text{Me}_3\text{Si}$ , 24.0). In these cyclic species, boron is deshielded relative to the precursors and the shift is in the range appropriate for three-coordinate boron.<sup>37</sup>

Protic reagents readily add to the formal  $\text{B}\equiv\text{N}$  bonds in iminoboranes to yield adducts of the type  $\text{RB}(\text{X})=\text{NHR}'$ . Some  $^{11}\text{B}$  chemical-shift data are collected in Table 4.<sup>38</sup>  $^{11}\text{B}$  data for some addition products of aminoiminoboranes have been published, e.g.  $(\text{TMP})\text{B}(\text{OSO}_2\text{CF}_3)-[\text{N}(\text{Me})\text{t-Bu}]$ ,<sup>38</sup>  $\delta^{11}\text{B} = 23.9$ , and  $[(\text{TMP})\text{B}=\text{N}(\text{SiMe}_3)\text{t-Bu}]\text{I}$ ,  $\delta^{11}\text{B} = 35.9$ .<sup>39</sup>  $^{11}\text{B}$  chemical shifts for adducts of the type  $(\text{TMP})\text{B}(\text{X})-\text{N}(\text{H})\text{t-Bu}$  ( $\text{X} = \text{OH}$ ,  $\text{OR}$ ,  $\text{OCOR}$ ,  $\text{NH}_2$ ,  $\text{NHR}$ ) are in the range  $25 \pm 2$  ppm except for  $\text{X} = \text{SEt}$  (37.5 ppm) and  $\text{S-t-Bu}$  (34.7 ppm).<sup>40</sup> Addition of bromine to  $\text{RB}\equiv\text{N-t-Bu}$  affords  $\text{R}(\text{Br})\text{B}=\text{N}(\text{Br})\text{t-Bu}$ .  $^{11}\text{B}$  chemical shifts for these adducts are in the range 41.5–45.5 ppm for  $\text{R} = \text{alkyl}$ , 29.9 ppm for  $\text{R} = \text{Me}_3\text{Si}(\text{t-Bu})\text{N}$  and 35.3 for  $\text{R} = \text{C}_6\text{F}_5$ . Bromine attached to nitrogen exchanges with hydrogen in the alkyl group to give, e.g.  $\text{BrCH}_2-\text{CMe}_2\text{B}(\text{Br})=\text{N}(\text{t-Bu})\text{H}$ ,  $\delta^{11}\text{B} = 39.6$ . This compound loses  $\text{C}_4\text{H}_8$  to form  $\text{Br}_2\text{B}=\text{N}(\text{t-Bu})\text{H}$ ,  $\delta^{11}\text{B} = 24.6$ .<sup>335</sup> The dimeric aldiminoborane  $(\text{PhCH}=\text{NBMe}_2)_2$  has  $\delta^{11}\text{B} = 5.3$ , which is appropriate for four-coordinate boron. The tris(ketiminoborane)  $(\text{t-Bu}_2\text{C}=\text{N})_3\text{B}$ ,  $\delta^{11}\text{B} = 22.8$ , formally contains three-coordinate boron, but  $d(\text{B-N})$  is quite short,  $1.39(1) \text{ \AA}$ .<sup>41</sup>

Boron-phosphorus multiple bonds with  $d(\text{B-P}) = 1.83 \text{ \AA}$  and planar boron and phosphorus are found in  $[\text{Li}(\text{Et}_2\text{O})_2]\text{RP}=\text{B}(\text{mes})_2$  (mes is 2,4,6-mesityl) ( $\text{R} = \text{Ph}$ ,  $\delta^{11}\text{B} = 65.4$ ;  $\text{R} = \text{c-C}_6\text{H}_{11}$ , 65.6;  $\text{R} = \text{mes}$ , 63.7).<sup>42</sup> Likewise,  $\text{Ph}_2\text{P}=\text{B}(\text{mes})_2$ ,  $\delta^{11}\text{B} = 51.7$ , has a short ( $1.859(3) \text{ \AA}$ )  $\text{B-P}$  separation, supporting the  $\text{B}=\text{P}$  formulation.  $^{11}\text{B}$ – $^{31}\text{P}$  coupling is apparently not observed.<sup>43</sup> Zwitterionic dilakylboryl-substituted triphenylphosphonium ylides of the type  $\text{RC}(\text{PPh}_3)=\text{BR}'_2$  ( $\text{R} = \text{Me}$ ,  $\text{Et}$ ,  $\text{Ph}$ ;  $\text{R}' = \text{c-C}_5\text{H}_{11}$ ,  $\text{c-C}_6\text{H}_{11}$ ) have  $\delta^{11}\text{B}$  in the 51–58 ppm range.<sup>44</sup>

Novel routes to  $\text{B}_2\text{N}$  and  $\text{BN}_2$  ring systems have been developed. Reaction of  $(\text{TMP})\text{B}\equiv\text{N-t-Bu}$  and  $(\text{TMP})\text{BCl}_2$  yields  $[(\text{TMP})\text{BCl}_2]_2\text{N-}$

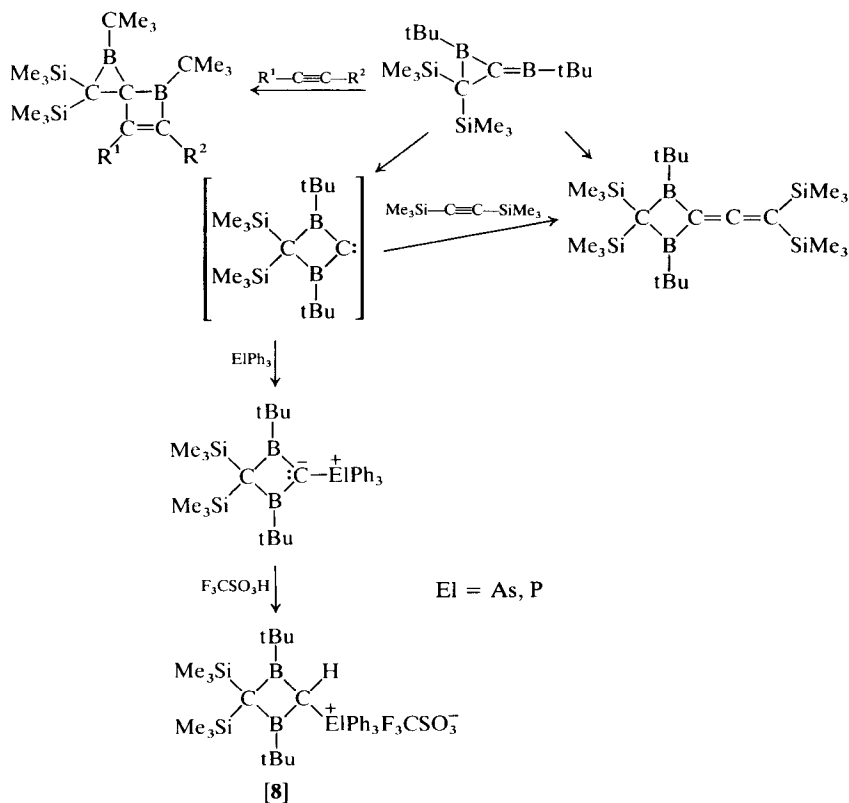
TABLE 4

$^{11}\text{B}$  chemical shifts for adducts of iminoboranes  $\text{R}(\text{X})\text{B}=\text{N}(\text{H})\text{R}'$ .

X	$\delta^{11}\text{B}$ , $\text{R} = \text{R}' = \text{i-Pr}$	$\delta^{11}\text{B}$ , $\text{R} = \text{Bu}$ , $\text{R} = \text{t-Bu}$
Cl	42.3	40.4
t-BuO	31.4	31.6
t-BuNH	32.9	31.8
$\text{Et}_2\text{N}$	32.8	31.9
i-Pr <sub>2</sub> N	32.8	31.8
$(\text{Me}_3\text{Si})_2\text{N}$	40.8	43.3

*t*-Bu,  $\delta^{11}\text{B} = 31.2$ , which cyclizes on treatment with Na-K to yield 1,2-(TMP)<sub>2</sub>-3-*t*-Bu-1,2,3-B<sub>2</sub>N. This compound possesses a two  $\pi$ -electron system and has  $\delta^{11}\text{B} = 39.9$ . Reaction of (TMP)BCl<sub>2</sub> with Li[(*i*-PrN(H)—N-*i*-Pr)] affords (TMP)B(Cl)—N(*i*-Pr)-*i*-Pr,  $\delta^{11}\text{B} = 33.3$ , which can be cyclized to 1-(TMP)-2,3-(*i*-Pr)<sub>2</sub>-1,2,3-BN<sub>2</sub>,  $\delta^{11}\text{B} = 26.5$ .<sup>45</sup>

The small-ring compound 1-*t*-Bu-2,2-(Me<sub>3</sub>Si)<sub>2</sub>-2-*t*-Bu-borandiylborirane, which contains an exocyclic B=C double bond, has been prepared [8].

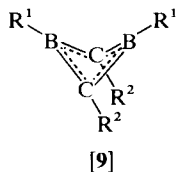


It has  $\delta^{11}\text{B} = 52$  ( $\underline{\text{B}}_2\text{C}$ ) and 18 ( $\underline{\text{B}}=\text{C}$ ) at  $-30^\circ\text{C}$ , but a methylenecyclopropane topomerization interconverts the two types of boron at higher temperatures.<sup>46</sup> It undergoes cycloaddition with 2-butyne to form the corresponding 1,2-dihydroborate. In this, the  $^{11}\text{B}$  chemical shifts for boron in the  $\underline{\text{BC}}_2$  and  $\underline{\text{BC}}_3$  rings are 83 and 34.5 ppm respectively. Because boron in the four-membered ring is so strongly deshielded, there may be a significant transannular B—C interaction.<sup>47</sup> The borandiylborirane also exhibits

carbene character and is converted to an allene analogue,  $\delta^{11}\text{B} = 78$ , on treatment with  $(\text{Me}_3\text{Si})_2\text{C}_2$ . This is also reflected in reactions with  $\text{Ph}_3\text{El}$ , which lead to ylides ( $\text{El} = \text{P}$ ,  $\delta^{11}\text{B} = 63$ ;  $\text{El} = \text{As}$ ,  $\delta^{11}\text{B} = 59$ ). The protonated ylides give rise to such broad (halfwidth 1600 Hz)  $^{11}\text{B}$  signals that chemical shifts are not measured.<sup>48</sup>

1-Borirines are related to cyclopropenes by replacement of the  $\text{CH}_2$  moiety by  $\text{RB}$  and are isoelectronic with cyclopropenium ions. In 1-*t*-Bu-2-B(*t*-Bu)Cl-3-Me<sub>3</sub>Si-1,2,3-BC<sub>2</sub>, boron in the BC<sub>2</sub> ring has  $\delta^{11}\text{B} = 43$  and that in the exocyclic B(*t*-Bu)Cl group has  $\delta^{11}\text{B} = 72$ . Shifts in the 1:1 pyridine adduct are 47 and 9 ppm, indicating that this potentially bifunctional donor complexes with the B(*t*-Bu)Cl portion of the molecule.<sup>49</sup> Desulphurization and ring contraction of 3-(Me<sub>3</sub>Si)<sub>2</sub>N-4,5-R<sub>2</sub>-1,2,3-S<sub>2</sub>BC<sub>2</sub> (R = alkyl;  $\delta^{11}\text{B} = 50$ –55) yields 1-(Me<sub>3</sub>Si)<sub>2</sub>N-substituted borirines. For R = H or a variety of alkyl substituents,  $\delta^{11}\text{B} = 27 \pm 0.5$ .<sup>50</sup>

The first 1,3-dihydro-1,3-diborete has been characterized. *Cis*-1,2-(BCl<sub>2</sub>)<sub>2</sub>-1,2-(*t*-Bu)<sub>2</sub>C<sub>2</sub>H<sub>2</sub>,  $\delta^{11}\text{B} = 56.8$ , may be converted to *cis*-1,2-(Me<sub>2</sub>NBCl)<sub>2</sub>-1,2-(*t*-Bu)<sub>2</sub>C<sub>2</sub>H<sub>2</sub>,  $\delta^{11}\text{B} = 34.8$ . Ring closure with potassium affords the diborete 1,3-(Me<sub>2</sub>N)<sub>2</sub>-2,4-(*t*-Bu)<sub>2</sub>-1,3-B<sub>2</sub>C<sub>2</sub>, which has the predicted puckered ring structure [9]:<sup>51</sup>



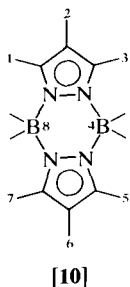
Its  $^{11}\text{B}$  chemical shift, 33.0 ppm, suggests partial  $\pi$  character in the B—N and B—C bonds, cf. 41.2 ppm for 1,3-(*t*-Bu)<sub>2</sub>-2,3-Me<sub>2</sub>-1,3-B<sub>2</sub>C<sub>2</sub>. These compounds may be reduced to form stable anion radicals, and the value of  $a_{\text{N}}^{\text{B}}$  in *c*-(*t*-BuB)<sub>2</sub>(CMe)<sub>2</sub><sup>•−</sup> is 0.95 mT. Spin density is considered to reside largely on the carbon; the large  $^{11}\text{B}$  hyperfine coupling is thought to arise from spin polarization.<sup>52–54</sup>

The 1,3-dioxa-2,4-diboretanes [(mes)BO]<sub>2</sub> and (2,4-*t*-Bu<sub>2</sub>BO)<sub>2</sub> have  $\delta^{11}\text{B} = 32.4$  and 33.0 respectively. Deshielding of boron in these compounds is consistent with a strained ring structure, cf. 1-(mes)-3,3,6,6-Me<sub>4</sub>-1-bora-3,6-disila-2,7-dioxacycloheptane,  $\delta^{11}\text{B} = 30.5$ .<sup>55</sup> In the related cyclo-B<sub>4</sub> compound *t*-Bu<sub>4</sub>B<sub>4</sub>, the  $^{11}\text{B}$  chemical shift is 135.7 ppm;  $a_{\text{B}}^{\text{B}}$  in the anion radical is rather small, 0.12 mT.<sup>56</sup> Dehydrohalogenation of (TMP)B(Cl)—PH—CEt<sub>3</sub> produces a cyclic dimer [(TMP)B—PCet<sub>3</sub>]<sub>2</sub>,  $\delta^{11}\text{B} = 66.1$  (halfwidth 320), which features a four-membered B<sub>2</sub>P<sub>2</sub> ring. Lack of observed B—P coupling may be associated with the long (1.925 Å av.) B—P bonds and the large  $^{11}\text{B}$  linewidth.<sup>57</sup> The tetraborinane 1,2,4,5-(Me<sub>2</sub>N)<sub>4</sub>-

1,2,4,5- $\text{B}_4\text{C}_2\text{H}_4$  has  $\delta^{11}\text{B} = 53.7$ , which is typical of diborane(4) derivatives.<sup>58</sup>

#### D. Pyrazaboles

Pyrazaboles are heterocycles containing a  $\text{B}_2\text{N}_4$  ring; boron occupies the 1,4 positions and each pair of vicinal nitrogen atoms is contributed by a pyrazole (PZ) ring. The numbering scheme adopted for these compounds is shown in [10]. Considerable effort has been invested in developing new pyrazabole chemistry.



$^{11}\text{B}$  NMR data have been reported for 1,5- and 3,5-dimethylpyrazabole. The former has  $\delta^{11}\text{B} = -10.5$  and the latter displays two resonances at  $-9.0$  and  $-12.2$  ( $J(\text{BH}) = 105$ ). The low-frequency peak is assigned to the boron atom closer to the  $\text{C}-\text{Me}$  groups. A mixture of the two isomers reacts with 3-methylpyrazole to form the tetrakis(3-methylpyrazolyl)pyrazabole derivative,  $\delta^{11}\text{B} = -0.6$ , which yields a single spectroscopically detectable isomer,  $\delta^{11}\text{B} = -7.4$ , upon bromination. The salts  $\text{K}[(3\text{-methylpyrazol-1-yl})_3\text{BH}]$  and  $\text{K}[(3\text{-methylpyrazol-1-yl})_4\text{B}]$  have  $\delta^{11}\text{B} = -1.3$  (d, 105) and  $0.9$  respectively.<sup>59</sup>

Cationic spiropyrazaboles of the type  $\text{R}_2\text{B}(\mu\text{-PZ})_2\text{B}(\mu\text{-PZ})_2\text{BR}'_2^+$  have been reported. For  $\text{R} = \text{R}' = \text{H}$ ,  $\delta^{11}\text{B} = -7.7$  (2B) and  $-1.3$  (1B). Thus the spiro boron appears at higher frequency. For  $\text{R} = \text{H}$ ,  $\text{R}' = \text{Et}$ , shifts are  $-7.5$  (2B),  $-1.5$  (1B) and  $5.2$  (1B); and for  $\text{R} = \text{R}' = \text{Et}$ ,  $-1.8$  (1B) and  $5.1$  (2B). In the more elaborate spiro compounds  $\text{R}_2\text{B}(\mu\text{-PZ})_2\text{-B}(\mu\text{-PZ})_2\text{B}(\mu\text{-PZ})_2\text{BR}_2$ ,  $\delta^{11}\text{B}$  is  $-7.5$ ,  $-1.5$  for  $\text{R} = \text{H}$  and  $-1.5$ ,  $6.5$  for  $\text{R} = \text{Et}$ .<sup>60</sup>

Pyrazaboles with  $\text{RBO}_2$  bridging the two boron atoms,<sup>61</sup>  $\mu$ -amido- $\mu$ -pyrazolatoboranes,<sup>62</sup>  $B$ -pyrazolyl-substituted pyrazaboles<sup>63</sup> and pyrazabole complexes containing allylpalladium moieties<sup>64</sup> have been reported.  $^{11}\text{B}$  NMR data for these materials and for other pyrazaboles<sup>65,66</sup> are collected in Table 5.

$^{11}\text{B}$  NMR has been used to detect intermediates in the electrophilic halogenation of pyrazaboles with  $^{10}\text{BBr}_3$ .<sup>67</sup> Boroxins,  $(\text{RBO})_3$ , form 1 : 1

TABLE 5

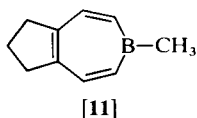
<sup>11</sup>B NMR data for pyrazaboles and related compounds.

Compound	$\delta^{11}\text{B}$
$\text{EtB}(\mu\text{-PZ})_2(\mu\text{-EtBO}_2)\text{BEt}$	31.5 (1B, halfwidth 600), 1.8 (2B, halfwidth 140)
$\text{PhB}(\mu\text{-PZ})_2(\mu\text{-PhBO}_2)\text{BEt}$	28.7 (1B, halfwidth 800), 1.5 (2B, halfwidth 290)
$[\text{Et}(\mu\text{-PZ})_3\text{BEt}]\text{PF}_6$	0.2 (halfwidth 100)
$[\text{HB}(\mu\text{-MePZ})_3\text{BEt}]\text{PF}_6$	-8.4 (d, 127), 0.2 (halfwidth 95)
$[\text{HB}(\mu\text{-Me}_2\text{PZ})_3\text{BH}]\text{CF}_3\text{SO}_3$	-4.1 (d, 127)
$\text{Et}_2\text{B}(\mu\text{-PZ})_2\text{B}(\text{PZ})_2$	0.3 (1B), 3.9 (1B, br)
$(\text{PZ})_2\text{B}(\mu\text{-PZ})_2\text{B}(\text{PZ})_2$	0.7
$\text{R}(\text{PZ})\text{B}(\mu\text{-NHR}')(\mu\text{-PZ})\text{B}(\text{PZ})\text{BR}$	2.1-3.0 (halfwidth 135-250)
$\text{Et}(\text{PZ})\text{B}(\mu\text{-PZ})_2\text{B}(\text{PZ})\text{Et}$	2.2 (halfwidth 190)
$4,8\text{-(3,5-Me}_2\text{PZ)}_2[\text{HB}(\mu\text{-Me}_2\text{PZ})_2\text{BH}]$	-4.9 (d, 105)
$(3,5\text{-Me}_2\text{PZ})_4[\text{B}(\mu\text{-Me}_2\text{PZ})_2\text{B}]$	-0.7 (halfwidth 50)
$(\text{PZ})_2\text{B}(\mu\text{-PZ})_2\text{Pd}(\text{RC}_3\text{H}_4)$	1.3
$([\text{C}_3\text{H}_5]\text{Pd})_2(\mu\text{-PZ})_2\text{B}(\mu\text{-PZ})_2\text{PF}_6$	0.5
$[\text{Et}_2\text{B}(\mu\text{-PZ})_2\text{B}(\mu\text{-PZ})_2\text{Pd}(\text{MeC}_3\text{H}_4)]\text{PF}_6$	0.4, 5.0 (br)
$([\text{MeC}_3\text{H}_4]\text{Pd})_2(\mu\text{-PZ})_2\text{B}(\mu\text{-PZ})_2\text{B}(\mu\text{-PZ})_2\text{PF}_6$	-0.4
$\text{H}_2\text{B}(\mu\text{-PZ})_2\text{B}(\mu\text{-PZ})_2\text{ZnCl}_2$	-8.6 (br), -0.1 ( $\text{CDCl}_3$ ) 5.3, -3.2 (br) ( $\text{CD}_3\text{CN}$ )
$(\text{ZnCl}_2)_2(\mu\text{-PZ})_2\text{B}(\mu\text{-PZ})_2\text{B}(\mu\text{-PZ})_2$	-0.4
$\text{Br}(\text{H})\text{B}(\mu\text{-PZ})_2\text{BH}_2$	-6.5 (d), -7.5 (t)
$\text{Br}(\text{H})\text{B}(\mu\text{-PZ})_2\text{B}(\text{H})\text{Br}$	-0.8 (d, 143), -1.7 (d, 143) ( $\text{CD}_3\text{CN}$ )
(mixture of <i>cis</i> and <i>trans</i> isomers)	0.3 (THF)
$\text{Br}_2\text{B}(\mu\text{-PZ})_2\text{B}(\text{H})\text{Br}$	-6.6 (d, 139), -7.1 (s) ( $\text{CH}_2\text{Cl}_2$ )
$\text{Br}_2\text{B}(\mu\text{-PZ})_2\text{BBr}_2$	-2.6 (THF)
$\text{K}[(\text{PZ})_2\text{BPh}_2]$	0.5
$\text{Ph}_2\text{B}(\mu\text{-PZ})_2\text{BH}_2$	1.7 (s), -8.4 (d)
$\text{Ph}_2\text{B}(\mu\text{-PZ})_2\text{BPh}_2$	1.7
$\text{Ph}_2\text{B}(\mu\text{-PZ})_2\text{BBr}_2$	1.9 ( <u>B</u> Ph), -6.6 ( <u>B</u> Br)
$\text{Et}_2\text{B}(\mu\text{-Me}_2\text{PZ})_2\text{BBr}_2$	4.8 ( <u>B</u> Et), -6.7 ( <u>B</u> Br)
$\text{Et}_2\text{B}(\mu\text{-Me}_2\text{PZ})_2\text{BEt}_2$	4.4
$\text{Br}(\text{H})\text{B}(\mu\text{-Me}_2\text{PZ})_2\text{B}(\text{H})\text{Br}$	-8.3, -10.3
$\text{Br}_2\text{B}(\mu\text{-Me}_2\text{PZ})_2\text{BBr}_2$	-7.5
$(\text{PZ})_2\text{B}(\mu\text{-Me}_2\text{PZ})_2\text{B}(\text{PZ})_2$	-0.2
$\text{Ph}_2\text{B}(\mu\text{-PZ})_2\text{BPh}_2$	1.8 (halfwidth 300)
$[(\text{Me}_2\text{N})\text{PhB}]_2\text{O}$	29.4 (halfwidth 300)
$[(\text{PZ})\text{PhB}(\mu\text{-PZ})_2\text{BPh}]_2\text{O}$	1.8 (halfwidth 600)
$(\text{PhBO})_3\cdot\text{HPZ}$	29.6 (1B, halfwidth 140), 20.9 (2B, halfwidth 400)
$(\text{PhBO})_3\cdot\text{Me}_2\text{PZH}$	20.5 (halfwidth 750)
$(\text{PhBO})_3\cdot\text{imidazole}$	19.5
$(\text{EtBO})_3\cdot\text{Me}_2\text{PZH}$	24.0 (halfwidth 670)

complexes with amines. These have only one four-coordinate boron atom in the solid state.  $^{11}\text{B}$  NMR indicates that, in solution, dissociation occurs because one signal is observed at ambient temperature but two appear on cooling. Pyrazole behaves differently. The 1 : 1 complex of  $(\text{PhBO})_3$  with pyrazole shows signals at 29.4 ppm (1B) and 20.9 ppm (2B), implying that both nitrogens are coordinated to boron. Addition of two more equivalents of pyrazole gives rise to new peaks at 18.8 ppm (major) and 2.5 ppm (minor). The former is due to a 3 : 1 complex in which all three borons are thought to be coordinated.<sup>68</sup>

### E. Boron-containing heterocycles

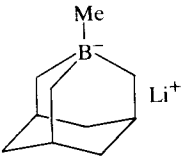
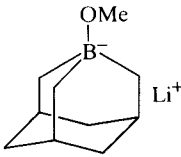
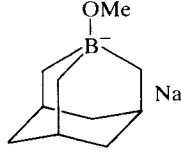
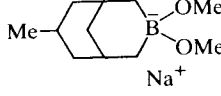
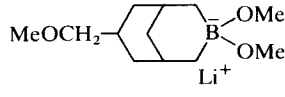
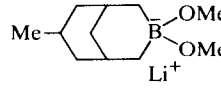
A novel  $\text{B}_4\text{C}_2$  ring compound 1,2,4,5-( $\text{Me}_2\text{N}$ )<sub>4</sub>-1,2,4,5- $\text{B}_4\text{C}_2\text{H}_4$  is stabilized by  $\text{Me}_2\text{N}$  groups. It has  $\delta^{11}\text{B} = 53.7$ , which is typical of a diborane(4) derivative substituted by carbon and nitrogen.<sup>69</sup>  $^{11}\text{B}$  NMR data for a series of 1-boraadamantane and 3-borabicyclo[3.3.1] nonane complexes have been published, cf. Table 6. In the latter compounds, ion pairing may strongly influence the chemical shift.<sup>70,71</sup> The reaction of  $\text{CH}_2(\text{BI}_2)_2$  with alkynes  $\text{R}_2\text{C}_2$  yields 4,5-diaklyl-1,3-diiodo-2,3-dihydro-1,3-boroles, from which iodide may be displaced by nucleophiles.  $^{11}\text{B}$  shift data for a very extensive series of such compounds are in the range 67–72 ppm. Substitution of EtO or  $\text{Me}_2\text{N}$  on boron leads to shielding increases (52.7, 44.2 ppm) but for MeS,  $\delta^{11}\text{B} = 69.0$ .<sup>72</sup> The heterocycle 2,5-( $\text{Me}_3\text{Sn}$ )<sub>2</sub>-1,2,5-Et<sub>3</sub>-3,4- $\text{Me}_2$ -3-borolene has  $\delta^{11}\text{B} = 64.0$  (halfwidth  $400 \pm 20$  Hz at 40 °C and  $1200 \pm 100$  Hz at –30 °C). Both  $\text{Me}_3\text{Sn}$  groups participate in intramolecular ring shifts.<sup>73</sup> 1,4,4-Trimethyl-1-boracyclohexa-2,5-diene has  $\delta^{11}\text{B} = 58.3$ . This changes to 56.5 ppm when the geminal Me groups are connected to form a cyclopropane ring. Absence of large chemical-shift differences has been interpreted as meaning that there is little conjugation between boron and the spiro cyclopropyl group, but  $^{11}\text{B}$  shifts may not be a sufficiently sensitive probe.<sup>74</sup> 1-Methyl-4,5-cyclopentenoborepin [11], a neutral analogue of the tropylium cation, has recently been reported.



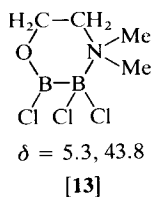
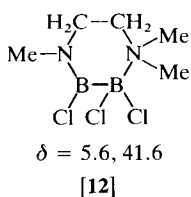
It has  $\delta^{11}\text{B} = 53.6$ , which changes to 49.2 in the  $\text{Cr}(\text{CO})_3$  complex. Weak conjugation involving boron probably obtains in this compound for the  $^{11}\text{B}$  shifts of 1-phenyl-1-boracycloheptadiene and its  $\text{Cr}(\text{CO})_4$  complex are at 54.6 and 29.7 ppm respectively.<sup>75</sup>

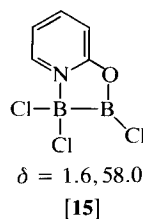
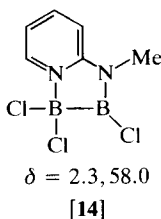
TABLE 6

<sup>11</sup>B NMR chemical shifts of ate complexes of 1-boraadamantane and 7-substituted 3-methoxy-3-borabicyclo[3.3.1]nonanes.

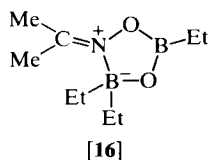
Compound	Solvent	$\delta^{11}\text{B}$
	Et <sub>2</sub> O/THF (1/1)	-20.3
	MeOH/THF (2/3)	-3.1
	THF	-3.0
	THF	6.0
	MeOH/THF (2/3)	14.3
	MeOH/THF (2/3)	15.5

Heterocycles [12]–[15] containing two centre B—B bonds may be prepared from B<sub>2</sub>Cl<sub>4</sub> and suitable organic ligands. In these, the high-frequency <sup>11</sup>B resonance is due to the Cl<sub>2</sub>B group, and in the C<sub>2</sub>B<sub>2</sub>N<sub>2</sub> heterocycle [12] a B—B coupling of 120 Hz is observed.<sup>76</sup>

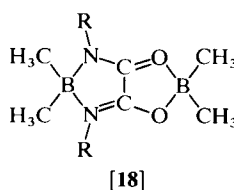
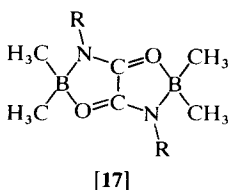


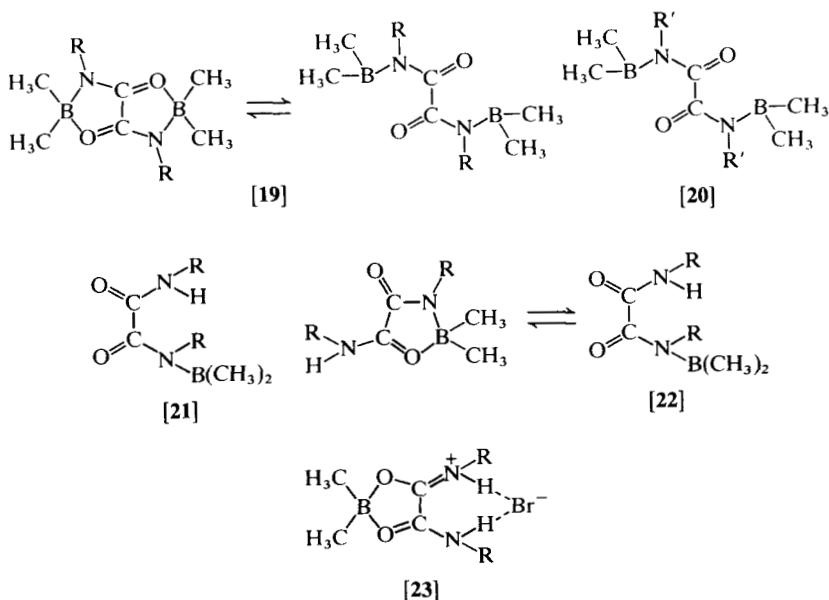


A transannular B—N bond in  $[o\text{-C}_6\text{H}_4(\text{CH}_2\text{N}(\text{H})\text{Me})_2\text{B}^+\text{Cl}^-]$  is suggested by its  $^{11}\text{B}$  chemical shift, 10.1 ppm.<sup>77</sup> Condensation of  $\text{PhB}(\text{OH})_2$ , *N*-alkylhydroxylamines and  $\text{H}_2\text{CO}$  yields bis(phenylboronates) of *N,N'*-methylenebis(*N*-alkylhydroxylamines)s, which have  $\delta^{11}\text{B} \approx 22$ , indicating the presence of a transannular B—N bond.<sup>78</sup>  $^{11}\text{B}$  NMR data have been collected for adducts and condensation products of  $\text{BCl}_3$  with N-, P- and As-oxo compounds.<sup>79</sup> Chemical-shift data have been reported for a series of esters formed from *t*-hexylboronic acid and  $\text{RN}(\text{C}_2\text{H}_4\text{OH})_2$ : R = H, 14.0 ppm; R = Ph, 30.0 ppm. The chemical shift of the N—Me ester changes from 23.9 to 17.3 ppm on cooling from 40 to  $-40^\circ\text{C}$ , indicating that there is an equilibrium between two conformations, one having three coordinate boron and the other having four coordinate boron and a 1,8-transannular B—N bond.<sup>80</sup> Shift data have been published for a series of heterocycles derived from  $\text{Ph}_2\text{BOH}$  and *N*-hydroxyalkylsalicylaldehydes, 4.4–7.0 ppm.<sup>81</sup> Chiral B—N heterocycles, azoborata-benz[*e*]indenes and -indans have been prepared. Their  $^{11}\text{B}$  chemical shifts, 6.4, 7.0 and 6.7 ppm, are indicative of four-coordinate boron and thus a B—N dative bond.<sup>82</sup> The  $^{11}\text{B}$  NMR spectrum of a  $\text{B}_2\text{NO}_2$  heterocycle [16] shows two singlets at  $-12.8$  and 32 ppm due to the three- and four-coordinate boron sites:<sup>83</sup>

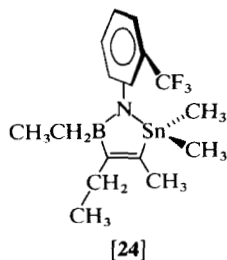


Reaction of  $\text{Me}_2\text{BBr}$  with symmetrically substituted oxamides yields a rich variety of heterocycles [17]–[23]:



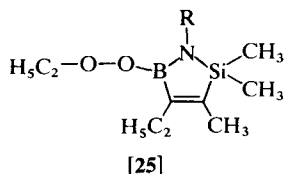


The  $^{11}\text{B}$  shifts for compounds [17] are in the range 16.8–17.7 ppm except for  $\text{R} = i\text{-Pr}$  (15.4 ppm) and  $\text{R} = m\text{-CF}_3\text{Ph}$  (10.6 ppm). Resonances for  $\text{BO}_2$  and  $\text{BN}_2$  in the heterocycles [18] fall in the ranges 22.7–25.7 and 6–10.6 ppm respectively. Compounds of the type [19] exist in solution as an equilibrium mixture of two conformers having  $\delta^{11}\text{B} = 54.1\text{--}54.7$  and  $12.2\text{--}18.5$ . The same obtains for compounds of type [22], but these exhibit separate  $^{11}\text{B}$  signals, at 54 and 10.3–16.8 ppm. Chemical shifts for heterocycles of types [21] and [23] are  $54.6 \pm 0.2$  and 19.7–22.4 ppm respectively.<sup>84</sup>  $^{11}\text{B}$  NMR has been used to analyse products of the reaction of diborane with 8-hydroxyquinoline and *N*-methyldihydrophenidine.<sup>85</sup> The heterocycle 4,5-Et<sub>2</sub>-2,3,3-Me<sub>3</sub>-1-(*o*-CF<sub>3</sub>Ph)-2,5-dihydro-1*H*-1,2,5-azastannaborole [24],  $\delta^{11}\text{B} = 45.3$  (47.8 in the Si analogue), exhibits atropomerism due to hindered rotation about the  $\text{N}\text{--CF}_3\text{Ph}$  bond:<sup>86</sup>

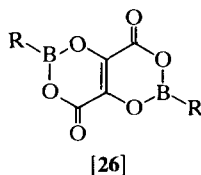


Chemical-shift data for a large series of 1,2,4,6-tetrasubstituted 1-phospha-4-boracyclohexa-2,5-dienes have been published. Many of these have Ph, Me or Et groups on phosphorus,  $\text{Et}_2\text{N}$  or MeO on boron and Me or H substituents in the 2,6 positions and have  $\delta^{11}\text{B} = 30.1\text{--}37.9$ . Conversion to the  $\text{P}=\text{O}$ ,  $\text{P}=\text{S}$  or  $\text{P}=\text{Se}$  derivatives has hardly any effect on boron shielding, nor does replacement of P by As.<sup>87</sup>

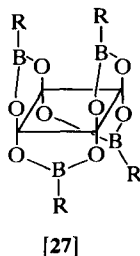
Autooxidation of 4,5- $\text{Et}_2$ -1,2,2,3- $\text{Me}_4$ -2,5-dihydro-1*H*-1,2,5-azasilaborole,  $\delta^{11}\text{B} = 44.8$ , produces the unusually stable *B*-peroxyethyl derivative [25],  $\delta^{11}\text{B} = 30.0$ :



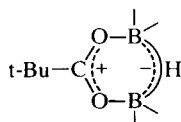
This can transfer one oxygen atom to  $\text{Et}_3\text{B}$ , forming the *B*-ethoxy heterocycle,  $\delta^{11}\text{B} = 60.1$ .<sup>88</sup> The interesting cycloboratrissiloxane  $\text{Me}_2\text{Si}[\text{OSi}(\text{t-Bu})_2\text{O}]_2\text{BF}$  has  $\delta^{11}\text{B} = 12.3$ ,<sup>89</sup> and the chemical shift for  $\text{B}(\text{OCH}_2\text{-1,2-}c\text{-C}_3\text{H}_4\text{-CH}_2\text{O})_3$  is 47 ppm.<sup>90</sup> Octahydroxycyclobutane reacts with the activated borane  $\text{Me}_3\text{CCO}_2\text{BEt}_2$  to give the thermochromic heterocycle [26]:



This compound has  $\delta^{11}\text{B} = 7.6$  in DMSO, but it may coordinate solvent. Structures of the high- and low-temperature forms have been determined.<sup>91,92</sup> Novel heterocycles of the type  $(\text{RB})_4\text{O}_8\text{C}_4$  [27] are obtained from  $c\text{-C}_4(\text{OH})_8$  and  $\text{R}_3\text{B}$ :

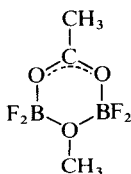


The RB groups form five-membered rings by bridging alternate edges of the oxocarbon. For R = alkyl,  $\delta^{11}\text{B} = 37.1\text{--}38.3$ ,  $30.0$  for R = Ph, and  $29.1$  for the bis(pyridine) complex of the B—Et compound.<sup>93</sup> 1,3,2-Dioxaborolane, formed from  $\text{B}_2\text{Cl}_4$  and  $\text{Me}_2\text{C}(\text{OH})\text{—C}(\text{OH})\text{Me}_2$ , has  $\delta^{11}\text{B} = 30.4$  (halfwidth 445).<sup>94</sup> A series of spiroborates, derived from catechol borane and ephidrine-type aminoalcohols, has been reported. The  $^{11}\text{B}$  chemical shifts,  $12 \pm 0.2$  ppm, are significantly lower than  $\text{C}_6\text{H}_4\text{O}_2\text{BOR}$  compounds owing to the intramolecular B—N dative bond.<sup>95</sup> A dipolar  $\text{HB}_2\text{O}_2\text{C}$  heterocycle [28]  $\delta^{11}\text{B} = 18.8$ , is formed from borabicyclononane and pivalic acid:<sup>96</sup>

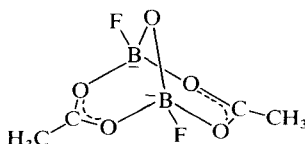


[28]

Monocyclic acyloxyfluoroboranes, 2,2,6,6- $\text{F}_4$ -1,4- $\text{R}_2$ -1,3,5-trioxa-2,6-diboracyclohexenes [29], are formed from  $(\text{RCO})_2$  and  $(\text{F}_2\text{BOMe})_3$ . They exhibit  $^{11}\text{B}$  singlets at  $0.7 \pm 0.1$  ppm and  $J(\text{F—B})$  is not observed. Two conformational isomers occur in the solid state and may also exist in solution, giving rise to averaged chemical shifts. Bicyclic acyloxyfluoroboranes [30], 1,5- $\text{F}_2$ -3,7- $\text{R}_2$ -2,4,6,8,9-pentaoxa-1,5-diborabicyclo[3.3.1]-nonadienes, are synthesized from the monocyclic compounds and additional  $(\text{RCO})_2\text{O}$ .  $^{11}\text{B}$  shifts are  $2.0 \pm 0.4$  ppm and again  $J(\text{F—B})$  is not observed.<sup>97</sup>



[29]

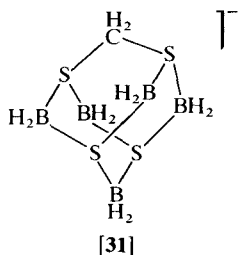


[30]

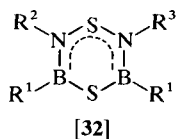
Chemical-shift data for an extensive series of amine complexes with  $(\text{EtBO})_3$  and  $(\text{PhBO})_3$  have been published. The increase in  $^{11}\text{B}$  shielding roughly parallels the amine  $\text{p}K_a$  values. Observation of only one  $^{11}\text{B}$  resonance suggests that dissociation of the complexes occurs in solution. The solid-state structures of  $2(\text{PhBO})_3 \cdot 3[1,4\text{-C}_6\text{H}_4(\text{NH}_2)_2]$  and  $2(\text{PhBO})_3 \cdot (\text{diazabicyclooctane})$  reveal that only one boron atom in each boroxin ring is bonded to nitrogen.<sup>98</sup>

Reactions of 1,2,4-trithia-3,5-diborolanes with alkynes unexpectedly produces 1,2,3-dithiaboroles in which the sulphur atoms are found by

*B*-arylamino derivatives are as follows: 3-Et<sub>2</sub>N-4,5-Ph<sub>2</sub>-1,2,3-BS<sub>2</sub>C<sub>2</sub>, 43.8 ppm; 3-(2,6-Me<sub>2</sub>PhNH)-4,5-Et<sub>2</sub>-1,2,3-BS<sub>2</sub>C<sub>2</sub>, 44.7 ppm. Structure-chemical-shift correlations can be made in these and related heterocycles: for the RBS<sub>2</sub>, RBSN and RBSC moieties,  $^{11}\text{B}$  shift ranges are 59–72, 39–55 and 66–80 ppm respectively.<sup>99</sup> 3-(2,6-Me<sub>2</sub>PhNH)-4,5-Et<sub>2</sub>-1,2,3-BSe<sub>2</sub>C<sub>2</sub> has  $\delta^{11}\text{B} = 44.7$ ; the change on replacing S by Se is remarkably small.<sup>100</sup> The BCS cluster compound Na[CH<sub>2</sub>(BH<sub>2</sub>)<sub>5</sub>S<sub>4</sub>] has been prepared from NaB<sub>3</sub>H<sub>8</sub> and CS<sub>2</sub>. Its  $^{11}\text{B}$  NMR spectrum discloses two 116 Hz triplets at –13.7 (4B) and –15.8 (1B) ppm, in agreement with its crystallographically determined adamantane-like structure [31]:<sup>101</sup>



Both 1 : 1 and 2 : 1 condensation products have been prepared from 2-isopropoxy-1,3,2-benzodioxaborole and salicylaldehyde-2-mercaptoanil. These have  $^{11}\text{B}$  resonances at 6.1 and at 8.8, 23.1 ppm respectively. The deshielded peak is assigned to tricoordinate boron.<sup>102</sup> 1,4-Dithia-2,6-diaza-3,5-diborinanes [32] are formed from 1,2,4-trithia-3,5-diborolanes and 1,3-disubstituted sulphur diimides:



$^{11}\text{B}$  chemical shifts are typically 50–55 ppm (52.6 ppm for  $\text{R}^1 = \text{Me}$ ,  $\text{R}^2 = \text{R}^3 = \text{Me}_3\text{Si}$ ). Lower values occur for analogues in which  $\text{R}^1 = \text{Et}_2\text{N}$  (34.9 ppm) and  $(\text{Me}_3\text{Si})_2\text{N}$  (44.9 ppm).<sup>103</sup>

## F. Alkylboranes and related compounds

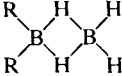
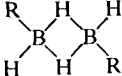
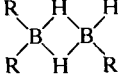
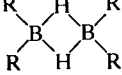
A large series of amino- and alkenylboranes has been prepared in a search for long-range couplings between  $^{11}\text{B}$  and  $^{13}\text{C}$ ,  $^{29}\text{Si}$  or  $^{119}\text{Sn}$ , cf. Table 7.<sup>104</sup> Boron-carbon couplings in  $\text{Li}[(\text{PhC}\equiv\text{C})_4\text{B}]$  have been extracted from  $^{13}\text{C}\{^1\text{H}, ^{11}\text{B}\}$  NMR experiments:  $^1J(\text{C-B}) = 70.0$  Hz and  $^2J(\text{C-B}) = 14.0$  Hz,

TABLE 7

Compound	$\delta^{11}\text{B}$			
$\begin{array}{c} \text{R}^1 \quad \text{R}^2 \\ \diagdown \quad \diagup \\ \text{C}=\text{C} \\ \diagup \quad \diagdown \\ \text{Br}_2\text{B} \quad \text{Br} \end{array}$	$\text{R}^1$	$\text{R}^2$		
	H	$\text{C}_4\text{H}_9$	(a)	52.7
	$\text{C}_2\text{H}_5$	$\text{C}_2\text{H}_5$	(b)	55.7
	$\text{C}_3\text{H}_7$	$\text{C}_3\text{H}_7$	(c)	55.8
	$\text{C}_4\text{H}_9$	$\text{C}_4\text{H}_9$	(d)	55.6
$\begin{array}{c} \text{R}^1 \quad \text{Br} \\ \diagdown \quad \diagup \\ \text{C}=\text{C} \\ \diagup \quad \diagdown \\ \text{Br}_2\text{B} \quad \text{R}^2 \end{array}$	$\text{R}^1$	$\text{R}^2$		
	H	$\text{C}_4\text{H}_9$	(a)	50.1
	$\text{C}_2\text{H}_5$	$\text{C}_2\text{H}_5$	(b)	58.0
	$\text{C}_3\text{H}_7$	$\text{C}_3\text{H}_7$	(c)	57.8
	$\text{C}_4\text{H}_9$	$\text{C}_4\text{H}_9$	(d)	58.1
$\begin{array}{c} \text{R}^1 \quad \text{CH}_3 \\ \diagdown \quad \diagup \\ \text{N}-\text{B} \\ \diagup \quad \diagdown \\ \text{R}^2 \quad \text{X} \end{array}$	X	$\text{R}^1$	$\text{R}^2$	
	$\text{CH}_3\text{O}$	$\text{CH}_3$	$\text{CH}_3$	(a) 31.8
	$\text{CH}_3\text{S}$	$\text{CH}_3$	$\text{CH}_3$	(b) 43.6
	Br	$\text{C}_2\text{H}_5$	$\text{C}_2\text{H}_5$	(c) 37.8
$\begin{array}{c} \text{CH}_3 \\ \diagup \\ \text{N} \\ \diagdown \quad \diagup \\ \text{B}-\text{X} \\ \diagup \quad \diagdown \\ \text{N} \\ \diagdown \\ \text{CH}_3 \end{array}$	X			
	$\text{CH}_3$	(a)		32.4
	$(\text{CH}_3)_3\text{Si}$	(b)		32.9
	$\begin{array}{c} \text{CH}_3 \\ \diagdown \\ \text{N} \end{array}$	(c)		25.5
	H			
	$\text{CH}_3\text{Se}$	(d)		31.7
	Cl	(e)		27.0
$\begin{array}{c} \text{R}^1 \quad \text{R}^2 \\ \diagdown \quad \diagup \\ \text{C}=\text{C} \\ \diagup \quad \diagdown \\ \text{B}(\text{H})_3 \end{array}$	$\text{R}^1 = \text{R}^2$			
	$\text{C}_2\text{H}_5$			68.6
	$(\text{CH}_3)_3\text{Si}$			70.0
$\begin{array}{c} \text{R}^1 \quad \text{R}^2 \\ \diagdown \quad \diagup \\ \text{C}=\text{C} \\ \diagup \quad \diagdown \\ \text{C}_8\text{H}_{14}\text{B} \quad \text{H} \end{array}$	$\text{R}^1$	$\text{R}^2$		
	$\text{C}_2\text{H}_5$	$\text{C}_2\text{H}_5$		
	H	$(\text{CH}_3)_3\text{Si}$		78.6

TABLE 8

 $\delta^{11}$  data (ppm) of diborane(6) compounds, organylborane adducts and triorganylboranes.

Compound		Me(a)	Et(b)	Pr <sup>n</sup> (c)	Pr <sup>i</sup> (d)	Bu <sup>n</sup> (e)	Bu <sup>i</sup> (f)	Bu <sup>q</sup> (b)	Bu <sup>i</sup> (h)	C <sub>6</sub> H <sub>11</sub> (i)	Thex(j)	Ph(k)
	(1)	38.8	41.4	40.3	44.2	40.6	39.3	43.6	44.1	42.4	—	—
	(2)	4.4	3.6	4.5	3.2	3.7	5.2	3.5	4.8	3.8	—	—
	(1, 2)	21.9	23.0	23.0	23.9	22.8	23.0	23.9	24.3	23.0	24.3	—
	(1)	31.7	34.5	33.6	37.2	33.7	33.0	37.0	—	35.0	—	—
	(2)	15.5	16.9	17.2	17.8	16.8	17.9	18.0	—	17.0	—	—
	(12)	25.0	28.4	28.5	30.2	28.0	28.2	30.8	—	30.6	—	—
R <sub>2</sub> BH—THF		—	—	—	—	—	—	—	29.5	19.4	—	12.3
R <sub>2</sub> BH—DMS		—	3.6	2.0	4.0	1.7	1.0	—	—	7.7	—	1.4
RBH <sub>2</sub> —THF		—	—	—	—	9.7	9.9	11.0	12.0	9.7	12.6	8.4
RBH <sub>2</sub> —DMS		-10.4	-6.6	-8.0	-3.6	-7.7	-8.8	-4.6	-1.0	-4.6	-1.5	-8.1
R <sub>3</sub> B		86.0	86.5	86.6	86.0	86.5	87.5	86.0	83.0	87.0	—	68.0

cf. 46.7 Hz in  $\text{Me}_3\text{B}$ .<sup>105</sup>  $^{11}\text{B}$  chemical-shift data have been published for a huge variety of organosubstituted  $\text{B}_2\text{H}_6$  derivatives obtained from exchange reactions between  $\text{R}_3\text{B}$  and  $\text{BH}_3\cdot\text{THF}$  or  $\text{BH}_3\cdot\text{Me}_2\text{S}$ , cf. Table 8.<sup>106</sup> The chiral borane *B*-allyldiisopinocampheylborane has  $\delta^{11}\text{B} = 78$ .<sup>107</sup>

A series of 1,1-diborylalkenes has been described. Compounds of the type  $\text{R}(\text{Me}_3\text{Si})\text{C}=\text{C}[\text{B}(\text{t-Bu})\text{Cl}]_2$  and  $\text{R}(\text{Me}_3\text{Si})\text{C}=\text{C}[\text{B}(\text{NMe}_2)\text{Cl}]_2$  exhibit  $\delta^{11}\text{B}$  values of  $74 \pm 1$  and 35 respectively. The shift range for 1,2-diborylalkenes  $[\text{t-BuB}(\text{Cl})]\text{CR}^1=\text{CR}^2[\text{B}(\text{Cl})\text{t-Bu}]$  is larger: 68 and 58 ppm for  $\text{R}^1 = \text{R}^2 = \text{H}$  and Me respectively; and 71 ppm for  $\text{R}^1 = \text{SiMe}_3$ ,  $\text{R}^2 = \text{H}$ .<sup>108</sup> Tin-containing alkenylboranes  $\text{R}_3\text{Sn}(\text{R}')\text{C}=\text{C}(\text{R}'')\text{BR}_2''$  and allenylboranes  $\text{R}_3\text{Sn}(\text{R}')\text{-C}=\text{C}=\text{C}(\text{R}'')\text{BR}_2''$  have  $^{11}\text{B}$  chemical shifts of 82–85 and 77 ppm respectively.<sup>109</sup>  $\delta^{11}\text{B}$  for (t-hexyl) (1-octenyl) (1-hexynyl) borane is 63; structural variations affect this value by  $\pm 2$  ppm.<sup>110</sup> Chemical-shift data for an extensive collection of alkenylboranes, produced by the addition of halo-boranes to acetylenes, have been tabulated.<sup>111</sup> The silicon-substituted vinylboranes  $[\text{R}(\text{H})\text{C}=\text{C}(\text{SiMe}_3)]_3\text{B}$  have  $\delta^{11}\text{B} = 68.7, 69.9$  and  $74.4$  for  $\text{R} = \text{Me}_3\text{Si}, \text{Me}$  and  $\text{H}$  respectively.<sup>112</sup> Table 9 presents data for bis(chloroboryl)alkanes and some of their cyclic condensation products.

The 5 ppm shift difference between the 1,3,2- $\text{B}_2\text{OC}_2$  and 1,3,2- $\text{B}_2\text{OC}_3$  rings may be attributable to ring-strain effects. Curiously,  $\text{Cl}(\text{Me})\text{-BC}_2\text{H}_4\text{B}(\text{Me})\text{OMe}$  shows only one  $^{11}\text{B}$  resonance, but the chemical shift is temperature-dependent so this compound may have a Cl or OMe bridge; or these two groups may be interchanging.<sup>113</sup> Chemical shifts for

TABLE 9

$^{11}\text{B}$  NMR data for bis(chloroboryl)alkanes and derivatives.

Compound	$\delta^{11}\text{B}$
1,2- $(\text{Cl}_2\text{B})_2\text{C}_2\text{H}_4$	63
1,2- $[\text{Cl}(\text{Me})\text{B}]_2\text{C}_2\text{H}_4$	75
$\text{Cl}(\text{Me})\text{BC}_2\text{H}_4\text{B}(\text{Me})\text{OMe}$	41
1,3- $(\text{Cl}_2\text{B})_2\text{C}_3\text{H}_6$	60.7
1,3- $(\text{Me}_2\text{B})_2\text{C}_3\text{H}_6$	84.5
1,3- $[\text{Me}(\text{OMe})\text{B}]_2\text{C}_3\text{H}_6$	50.9
$(\text{Et}_2\text{B})_2\text{NMe}$	59.7
$[\text{Me}(\text{Br})\text{B}]_2\text{NMe}$	52.0
$(\text{Me}_2\text{B})_2\text{O}$	52.0
1,2,3- $\text{Me}_3\text{-1,3,2-B}_2\text{NC}_2\text{H}_4$	62
1,3- $\text{Cl}_2\text{-2-Me-1,3,2-B}_2\text{NC}_2\text{H}_4$	54
1,2,3- $\text{Me}_3\text{-1,3,2-B}_2\text{NC}_3\text{H}_6$	63.2
1,3- $\text{Cl}_2\text{-2-Me-1,3,2-B}_2\text{NC}_3\text{H}_6$	55
1,3- $\text{Me}_2\text{-1,3,2-B}_2\text{OC}_3\text{H}_6$	56.6
1,3- $\text{Me}_2\text{-1,3,2-B}_2\text{OC}_2\text{H}_4$	61.6

(i-PrO) $_2$ BR range from 27.7 to 30.7 ppm, except for R = CHCl $_2$  for which  $\delta^{11}\text{B}$  = 23.5.<sup>114</sup> Trimethylamine complexes of CF $_2$ XBF $_2$  have  $\delta^{11}\text{B}$  = -0.6, -0.4 and -0.2 for X = F, Cl and Br respectively;  $^1J(\text{F-B})$  and  $^2J(\text{F-B})$  are 52-48 and 24-33 Hz respectively.<sup>115</sup> The  $^{11}\text{B}$  shifts for the thioalkylboranes Li[MeSCH $_2$ BH $_3$ ], MeSCH $_2$ BH $_2$ ·Me $_3$ N and [Me $_2$ SCH $_2$ BH $_2$ ·Me $_3$ N]I are -30.5, -3.9 and -7.2 ppm. The dimer (MeSCH $_2$ BH $_2$ ) $_2$  exhibits two signals at -13.6 and -17.2 ppm, probably due to compounds with different ring conformations. In the solid state the ring adopts a chair conformation with equatorial methyl groups.<sup>116</sup>  $^{11}\text{B}$  NMR chemical shifts of a series of 25  $\eta^1$ -pentamethylcyclopentadienyl-substituted boron compounds have been published, e.g. crystallographically characterized (Me $_5$ Cp) $_2$ BF,  $\delta^{11}\text{B}$  = 53.0 ( $J(\text{F-B})$  = 106). Many of these compounds are fluxional and undergo 1,2 boron shifts.<sup>336</sup> Gas-phase pyrolysis of the borabicyclo[3.3.1]-nonane dimer yields 1-borabicyclo[4.3.0]nonane,  $\delta^{11}\text{B}$  = 90.5, and 8-borabicyclo[4.3.0]nonane,  $\delta^{11}\text{B}$  = 27.0. Further heating of the latter, as the solid, provides 1,2:1,2-bis(biphenyl-2,2'-diyl)diborane(6),  $\delta^{11}\text{B}$  = 27.0.<sup>337</sup>

### G. Other one-boron compounds

Data have been presented for an extensive series of amine complexes of mixed boron halides. The  $^{11}\text{B}$  and ( $^{19}\text{F}$ ) chemical shifts (Table 10) depend primarily on the number and type of heavy halogen(s) present, the amine substituents having a relatively small effect. The  $^{19}\text{F}$ - $^{11}\text{B}$  couplings appear to increase with increasing steric size of the amine. Line-widths are too large to permit resolution of signals for diastereomeric PhCH $_2$ (Et) (Me)N·BFCIBr.<sup>117</sup>

Similarly, substituent groups have very little effect on the  $^{11}\text{B}$  chemical shifts of 3-RC $_5$ H $_4$ N·BX $_3$  complexes (R = F, Cl, Br, CN), which have  $\delta^{11}\text{B}$  = 17.8  $\pm$  0.1 for X = F and 25.9  $\pm$  0.1 for X = Br.<sup>118</sup> Complexes of mixed boron halides with Me $_3^{15}\text{N}$  have been studied, cf. Table 11, and values of  $J(\text{N-B})$  and  $J(\text{F-B})$  correlated.<sup>119</sup>

NMR data for a series of aminoboron halides have been reported. For (TMP)BRF (R = alkyl),  $\delta^{11}\text{B}$  ranges from 35.1 to 36.7 and  $J(\text{F-B})$  from 81 to 89 Hz. For (TMP)B(X)C(Y)Ph $_2$   $\delta^{11}\text{B}$  = 33.6, 41.8 and 41.8 for Y = H and X = F, Cl, Br respectively, and 36.3 ppm for X = F, Y = SiMe $_3$ .<sup>120</sup>

Cyclenphosphorane forms a bis(borane) adduct,  $\delta^{11}\text{B}$  = -15.7 (q, 100), in which phosphorus retains its five-coordination.<sup>120</sup> A series of phosphorylaminoboranes X $_2$ P(O)—NR'—BR $_2$  has been prepared, cf. Table 12. The borotropic isomers X $_2$ P(NR')—OBR $_2$  have been detected by NMR and evidently arise from intramolecular rearrangements in dimers.<sup>122</sup>

TABLE 10

<sup>11</sup>B chemical shifts for some mixed boron halides and their amine complexes.

		Donor				
		Quinuclidine	NEtPr <sup>i</sup> <sub>2</sub>	NMe <sub>2</sub> Ph	NMeEtPh	PhCH <sub>2</sub> NMeEt
Acceptor						
BF <sub>3</sub>	10.0	−0.5	0.2	−0.1	0.1	−0.1
BF <sub>2</sub> Cl	19.8	4.1	4.9	4.3	4.3	4.6
BFCl <sub>2</sub>	32.3	7.7	8.8	8.0	8.0	8.3
BCl <sub>3</sub>	46.5	9.2		10.0	10.1	9.8
BF <sub>2</sub> Br	19.5	3.6	3.3	3.6	3.9	3.8
BFBBr <sub>2</sub>	29.0	3.1		3.0	3.3	3.2
BBr <sub>3</sub>	38.7	−3.9		−3.5	−3.4	−3.7
BF <sub>2</sub> I					2.3	1.3
BFI <sub>2</sub>				−17.3	−16.9	−16.0
BI <sub>3</sub>	−7.9	−53.1		−54.0	−54.0	−53.3
BCl <sub>2</sub> Br	44.7	5.8		6.4	6.7	6.3
BClBr <sub>2</sub>	42.3	1.4		1.8	2.3	1.8

TABLE 11

NMR data for boron-halide complexes of  $\text{Me}_3^{15}\text{N}$ .

Boron halide	$J(\text{F-B})$	$J(\text{N-B})$	$\delta^{11}\text{B}$
$\text{BF}_3$	15.3	-18.7	0.6
$\text{BF}_2\text{Cl}$		-18.6	5.2
$\text{BF}_2\text{Br}$	54.2	-18.5	4.4
$\text{BFCl}_2$	60.1	-17.5	8.2
$\text{BFBBr}_2$	91.9	-17.4	3.7
$\text{BCl}_3$		-16.5	10.2
$\text{BFCl}_2$		-14.3	-19.0
$\text{BCl}_2\text{Br}$		-16.1	6.7
$\text{BCl}_2\text{I}$		-15.4	-3.2
$\text{BClBr}_2$		-15.7	2.2
$\text{BClBrI}$		-14.7	-9.8
$\text{BBr}_3$		-15.2	-3.3
$\text{BClI}_2$		-13.4	-24.8
$\text{BBr}_2\text{I}$		-14.3	-17.0
$\text{BBrI}_2$		-13.2	-33.9
$\text{BI}_3$		-12.1	-54.2

TABLE 12

 $\delta^{11}\text{B}$  NMR data for phosphorylaminoboranes.

Compound	$\delta^{11}\text{B}$
$\text{Me}_2\text{P}(\text{O})\text{—NMe—BMe}_2$	10.5
$(\text{Me}_2\text{N})_2\text{P}(\text{O})\text{—NMe—BMe}_2$	51.5, 44.3, 0
$(\text{Me}_2\text{N})_2\text{P}(\text{O})\text{—NMe—B}(\text{NMe}_2)_2$	27.3
$\text{Me}_2\text{N}(\text{Cl})\text{P}(\text{O})\text{—NMe—B}(\text{Cl})\text{NMe}_2$	7.0, 28.5
$\text{Cl}_2\text{P}(\text{O})\text{—NMeOBMe}_2$	54.8
$[\text{Cl}_2\text{P}(\text{O})\text{—NMe—BCl}_2]_2$	6.0
$[\text{Cl}_2\text{P}(\text{O})\text{—NMe—BBr}_2]_2$	6.8

$^{11}\text{B}$  NMR spectroscopy has been used to study monomer–dimer equilibria in  $\text{Ph}_2\text{P}(\text{O})\text{OBt}_2$  and related compounds.<sup>123</sup>

Use of very bulky silicon-containing substituents has led to structurally novel boron compounds, e.g. the alkylborohydride  $(\text{THF})_3\text{Li}(\mu\text{-H})_3\text{-BC}(\text{SiMe}_3)_3$ ,  $\delta^{11}\text{B} = -30.2$  ( $J(\text{B-H}) = 80$ ).<sup>124</sup> The compound  $[(\text{Me}_2\text{PhSi})_3\text{C}]\text{BF}(\text{OH})$  is a rare example of a crystallographically characterized organofluorohydroxyborane. It has  $\delta^{11}\text{B} = 29.3$ , but the  $^{11}\text{B}$  (and  $^{19}\text{F}$ ) signal in  $\text{CDCl}_3$  is too broad to observe B–F coupling.<sup>125</sup> Other

materials obtained with bulky silicon substituents include  $(\text{Me}_3\text{Si})_3\text{-CB}(1,2\text{-C}_6\text{H}_4\text{O}_2)$ ,  $\delta^{11}\text{B} = 34$ ;  $(\text{Me}_3\text{Si})_3\text{CB}(\text{OH})\text{OC}_4\text{H}_8\text{C}(\text{SiMe}_3)_3$ , 29.6;  $(\text{Me}_3\text{Si})_3\text{CB}(\text{OMe})$ , 31.0;<sup>126</sup>  $(\text{Me}_3\text{Si})_3\text{CB}(\text{F})\text{OC}_4\text{H}_8\text{C}(\text{SiMe}_3)_3$ , 30.0;  $(\text{Me}_3\text{Si})_3\text{CB}(\text{Ph})\text{OC}_4\text{H}_8\text{C}(\text{SiMe}_3)_3$ , -10 (halfwidth 3900 Hz);<sup>127</sup> and  $(\text{Me}_3\text{Si})_3\text{CBPh}_2$ , 77.5.<sup>128</sup> The very bulky 2,4,6-(*t*-Bu)<sub>3</sub>PhNH group has also been found to be useful in the synthesis of interesting boranes such as (*t*-Bu)<sub>3</sub>PhNHBCl<sub>2</sub>,  $\delta^{11}\text{B} = 32.8$ , and (*t*-Bu)<sub>3</sub>PhNHB(NH<sub>2</sub>)<sub>2</sub>, 24.6, and (*t*-Bu)<sub>3</sub>PhNHBFB<sub>2</sub>, 16.8. In the latter compound <sup>2</sup>*J*(F-F) and <sup>3</sup>*J*(F-H) be measured because there is a high barrier to rotation about the B-N bond.<sup>129</sup> The compounds R(Et)B-C(Et)=C(Me)SnMe<sub>3</sub> (R = *N*-indolyl,  $\delta^{11}\text{B} = 53.5$ ; R = *N*-pyrazolyl, 53.2) exhibit chirality owing to restricted rotation about the B-N bond.<sup>130</sup> The "hydridge sponge" 1,8-bis(dimethylboryl)naphthalene,  $\delta^{11}\text{B} = 79$ , is a strong hydride acceptor analogous to the "proton sponge", 1,8-(Me<sub>2</sub>N)<sub>2</sub>C<sub>10</sub>H<sub>6</sub>. It reacts with KH to form K[H-1,8-(Me<sub>2</sub>B)<sub>2</sub>C<sub>10</sub>H<sub>6</sub>] in which the hydride unsymmetrically bridges the two boron atoms (*d*(BH) = 1.20(5), 1.49(5) Å), but in etheral solutions, a single <sup>11</sup>B resonance at 4 ppm is observed, indicative of a symmetrical or rapidly tautomerizing structure.<sup>131</sup>

The <sup>11</sup>B chemical shifts of Ph<sub>4</sub>B<sup>-</sup> salts are nearly independent of solvent and concentration; this is probably because of the effective shielding of boron by the four phenyl groups.<sup>132</sup> The PPN<sup>+</sup> (PPN is (Ph<sub>3</sub>P)<sub>2</sub>N<sup>+</sup>) salts of BH<sub>3</sub>Cl<sup>-</sup>,  $\delta^{11}\text{B} = -14.6$  (*J*(B-H) = 104) and BH<sub>2</sub>Cl<sub>2</sub><sup>-</sup>, 3.4 (131), have been characterized. Disproportionation of the former into BH<sub>2</sub>Cl<sub>2</sub><sup>-</sup>, B<sub>2</sub>H<sub>7</sub><sup>-</sup> and Cl<sup>-</sup> has been followed by <sup>11</sup>B NMR spectroscopy.<sup>133</sup>

Reaction of BCl<sub>3</sub> with CF<sub>3</sub>SO<sub>3</sub>H yields (CF<sub>3</sub>SO<sub>3</sub>)<sub>3</sub>B,  $\delta^{11}\text{B} = -1.1$ , which is converted by additional CF<sub>3</sub>SO<sub>3</sub>H to the superacid [(CF<sub>3</sub>SO<sub>3</sub>)<sub>4</sub>B]-CF<sub>3</sub>SO<sub>3</sub>H<sub>2</sub>,  $\delta^{11}\text{B} = -3.6$  (halfwidth 198). An intermediate, (CF<sub>3</sub>SO<sub>3</sub>)<sub>2</sub>BCl, has  $\delta^{11}\text{B} = -3.3$  (halfwidth 470).<sup>134</sup> The methoxytetrafluorotellurate esters (*cis*-MeOTeF<sub>4</sub>O)<sub>3</sub>B and (*trans*-MeOTeF<sub>4</sub>O)<sub>3</sub>B have recently been reported. In CFCl<sub>3</sub> they have  $\delta^{11}\text{B} = -2.2$  and  $-4.8$  respectively. These values change to  $-21.3$  and  $-22.2$  in CH<sub>3</sub>CN as solvent, indicating the formation of adducts.<sup>135</sup>

Complex formation between aqueous NaB(OH)<sub>4</sub> and polyhydroxy compounds such as propane-1,2- and -1,3-diol, glycerol, mannitol and sorbitol have been examined by <sup>11</sup>B NMR. The mixture obtained with, for example, ethylene glycol contains free B(OH)<sub>4</sub><sup>-</sup>,  $\delta^{11}\text{B} = -17.3$ , (C<sub>2</sub>H<sub>4</sub>O<sub>2</sub>)-B(OH)<sub>2</sub><sup>-</sup>, -13.4, and (C<sub>2</sub>H<sub>4</sub>O<sub>2</sub>)<sub>2</sub>B<sup>-</sup>, -9.7 (br, probably owing to relaxation effects).<sup>136</sup> Variable temperature <sup>11</sup>NMR data, obtained at 127 and 160 MHz, have been reported for aqueous KB<sub>5</sub>O<sub>8</sub>·4H<sub>2</sub>O, K<sub>2</sub>B<sub>5</sub>O<sub>8</sub>(OH)·2H<sub>2</sub>O and K<sub>2</sub>B<sub>4</sub>O<sub>7</sub>·4H<sub>2</sub>O, and these shed much light on polyborate equilibria in water. Species recognized by this technique are B(OH)<sub>3</sub>/B(OH)<sub>4</sub><sup>-</sup>,  $\delta^{11}\text{B} = 18$ , B<sub>3</sub>O<sub>3</sub>(OH)<sub>4</sub><sup>-</sup>, 13, and B<sub>5</sub>O<sub>6</sub>(OH)<sub>4</sub><sup>-</sup>, 1.<sup>137</sup> Organoboron monosaccharides also have  $\delta^{11}\text{B} = -0.1 \pm 0.1$ .<sup>138</sup>

## V. POLYBORANES AND CARBORANES

Qualitative methods have been cited for estimating trends in  $^{11}\text{B}$  chemical shifts in *closo*-boranes and -carboranes as well as heteroatom boranes. In a  $\text{B}_n\text{H}_n^{2-}$  ion the lower the coordination number of boron, the smaller the shielding. Shifts in heteroatom boranes, i.e. ones in which some other element such as C or S replaces boron (or BH) can be estimated relative to  $\text{B}_n\text{H}_n^{2-}$  by taking into account several factors:

- (1) antipodal effects (AE) of a heteroatom on a diametrically opposite or antipodal  $^{11}\text{B}$  nucleus;
- (2) rhomboidal effects (RE) produced by an atom on one at the opposite vertex of a rhombus in the cluster;
- (3) butterfly effects (BE) caused by one atom on another two bonds away; each of these occupies an unshared vertex of two edge-shared triangular faces;
- (4) neighbour effects (NE).

In general, if the heteroatom is four-coordinate then  $\text{AE} > \text{NE} > \text{BE}$ , but if it is five-coordinate then  $\text{AE} > \text{RE} > \text{BE} > \text{NE}$ . An example of what can be achieved using these guidelines is shown in Fig. 3, which displays trends in the  $^{11}\text{B}$  chemical shifts of  $\text{B}_{10}\text{H}_{10}^{2-}$ ,  $\text{B}_2\text{CH}_{10}^-$  and  $1,2\text{-B}_8\text{C}_2\text{H}_{10}$ .<sup>138</sup>

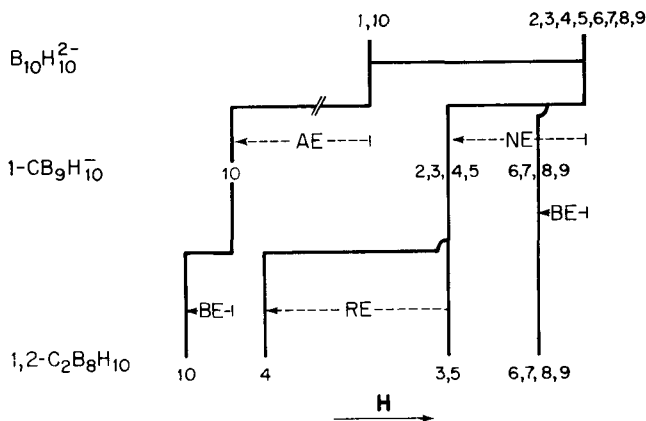
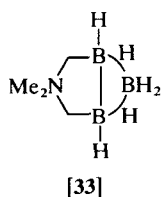


FIG. 3. Schematic representation of the  $^{11}\text{B}$  NMR spectra of  $\text{B}_{10}\text{H}_{10}^{2-}$ ,  $1\text{-CB}_9\text{H}_{10}^-$ , and  $1,2\text{-C}_2\text{B}_8\text{H}_{10}$ .

A.  $\text{B}_{2,3}$  boranes and carboranes

The diborane(4) derivative  $\text{B}_2\text{H}_4(\text{Me}_3\text{N})_2$ ,  $\delta^{11}\text{B} = -3.5$ , has recently been prepared. It reacts with  $\text{B}_2\text{H}_6$  to form  $\text{B}_3\text{H}_6(\text{Me}_3\text{N})_2^+$ ,  $\delta^{11}\text{B} = -9.7$  ( $\underline{\text{B}}\text{H}_2$ ) and  $-15.8$  ( $\underline{\text{B}}\text{—N}$ ), which is degraded by additional base to provide

$\text{BH}_2(\text{Me}_3\text{N})\text{—BH}(\text{Me}_3\text{N})^+$ . The  $^{11}\text{B}$  spectrum of this cation displays two very broad signals at 12.5 and  $-3.9$  ppm.<sup>139</sup>  $^{11}\text{B}$  chemical-shift data for  $\text{B}_2\text{X}_4$  have been compared; for  $\text{X} = \text{F}, \text{Cl}, \text{Br}$  and  $\text{I}$ ,  $\delta^{11}\text{B} = 23, 62, 67$  and  $67.5$  respectively.<sup>140</sup> A diborane derivative,  $\text{Me}_2\text{P}(\text{CH}_2\text{BH}_2)_2\text{H}$ ,  $\delta^{11}\text{B} = -13.1$  (t, 109), in which a  $\text{Me}_2\text{P}(\text{CH}_2)_2$  unit replaces a bridging hydrogen, has been prepared. A similar triborane compound [33],  $\text{Me}_2\text{N}(\text{CH}_2\text{BH}_2)_2\text{BH}_2$ , shows  $^{11}\text{B}$  signals at 2.6 (1B) and  $-27.5$  (2B) ppm. The most shielded resonance is a poorly resolved heptet having  $J(\text{B—H}) \approx 30$  Hz.<sup>141</sup>



$^{11}\text{B}$  (and  $^{13}\text{C}$ ) NMR data have been reported for a series of peralkylated 1,6- $\text{B}_2\text{C}_4\text{H}_6$  derivatives. The  $\text{B}_2\text{C}_4\text{R}_6$  carboranes ( $\text{R} = \text{Me}, \text{Et}, i\text{-Pr}$ ) are thought to have a pentagonal pyramidal geometry with one apical and one basal boron atom. The chemical shift of the apical boron ranges from  $-44.2$  to  $-46.2$  ppm and that of the basal boron from 17.8 to 19.3 ppm. The  $T_1$  values for the apical basal boron nuclei in 1,2,3,4,5- $\text{Me}_5$ -6- $\text{EtB}_2\text{C}_4$  are 16.2 and 4 ms respectively; and 7.5 and 1.9 ms in  $\text{Et}_6\text{B}_2\text{C}_4$ . The  $T_1(^{10}\text{B})/T_1(^{11}\text{B})$  ratios agree well with the theoretical value of 1.53.<sup>142,143</sup>

Two-dimensional  $^{11}\text{B}$ – $^{11}\text{B}$  correlated spectra have been obtained for a series of triborane derivatives of the types  $\text{B}_3\text{H}_7\text{X}^-$  and  $\text{B}_3\text{H}_6\text{ClX}^-$ , cf. Tables 13 and 14 and Fig. 4, which displays their topological representations. In the  $\text{B}_3\text{H}_7^-$  series two COSY correlations between the substituted (B(1)) and unsubstituted (B(2,3)) boron nuclei occur. However, in  $\text{B}_3\text{H}_6\text{ClX}^-$  only correlations between substituted boron atoms are found.

TABLE 13

Chemical shifts, COSY correlations and structural types of disubstituted triborane anions  $[\text{B}_3\text{H}_6(\text{Cl})(\text{X})]^-$ .

Disubstituted anion	$\delta(1)$ ( $\text{B—Cl}$ )	$\delta(2)$ ( $\text{B—X}$ )	$\delta(3)$ ( $\text{B—H}$ )	COSY correlation	Structure type
$[\text{B}_3\text{H}_6(\text{Cl})_2]^-$	$-11.9$	$-11.9$	$-4.3$	(1,2)–3	c
$[\text{B}_3\text{H}_6(\text{Cl})(\text{NCS})]^-$	$-8.3$	$-25.1$	$-4.2$	1–2	c
$[\text{B}_3\text{H}_6(\text{Cl})(\text{NC})\text{BH}_2\text{Cl}]^-$	$0.6$	$-30.9$	$-4.1$	1–2	
$[\text{B}_3\text{H}_6(\text{Cl})(\text{NC})\text{B}_3\text{H}_7]^-$	$-0.2$	$-31.0$	$-3.8$	1–2	

TABLE 14

Chemical shifts, COSY correlations and structural types of monosubstituted triborane anions  $[\text{B}_3\text{H}_7(\text{X})]^-$ .

Monosubstituted anion	$\delta(1)$ (B—X)	$\delta(2, 3)$ ( $\text{B}_2$ )	COSY correlation	Structure type
$[\text{B}_3\text{H}_7(\text{Cl})]^-$	-21.0	-14.5	1-(2, 3)	
$[\text{B}_3\text{H}_7(\text{NCS})]^-$	-32.5	-13.0	1-(2, 3)	d
$[\text{B}_3\text{H}_7(\text{NCSe})]^-$	-33.3	-10.0	1-(2, 3)	d
$[\text{B}_3\text{H}_7(\text{NC})\text{BH}_3]^-$	-36.1	-9.9	1-(2, 3)	b
$[\text{B}_3\text{H}_7(\text{NC})\text{BH}_2\text{Cl}]^-$	-34.8	-8.9	1-(2, 3)	
$[\text{B}_3\text{H}_7(\text{NC})\text{BPh}_3]^-$	-34.8	-9.2	1-(2, 3)	
$[\text{B}_3\text{H}_7(\text{NC})\text{BH}_2(\text{CN})]^-$	-34.8	-8.9	1-(2, 3)	
$[\text{B}_3\text{H}_7(\text{NC})\text{B}_3\text{H}_7]^-$ (i)	-34.9	-9.5	1-(2, 3)	b
(ii)	-49.5	-12.4	1-(2, 3)	b
$[\text{B}_3\text{H}_7(\text{CN})\text{B}_3\text{H}_6\text{Cl}]^-$	-49.8	-11.9	1-(2, 3)	

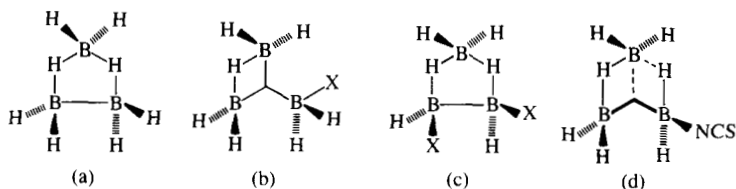


FIG. 4. Topological representations of crystallographically identified structures of substituted octahydrotriborate anions.

In this latter series observation of only one correlation does not necessarily provide evidence for a two centre B—B bond. Apparent lack of coupling between boron nuclei giving rise to wide resonances may be due to fast relaxation, which results in broad, low-intensity signals whose FIDs decay significantly on the time scale of the COSY pulse sequence.<sup>144</sup> Additional  $^{11}\text{B}$  NMR data have been reported for  $\text{B}_3\text{H}_7\text{X}^-$  anions, which have  $\delta^{11}\text{B}$  (BX and B(2,3)): X = NCO (-21.0, -21.3); X = Br (-28.4, -12.2; X = F (-15.4, -17.6); and  $\text{Ag}[\text{B}_3\text{H}_7(\text{NC})_2]^-$  (-36.8, -10.2).<sup>145</sup>

## B. $\text{B}_4$ boranes and carboranes

$^{11}\text{B}$  NMR spectra for two  $\text{B}_4\text{H}_8$  complexes have been published:  $\text{B}_4\text{H}_8 \cdot \text{PMe}_3$ ,  $\delta^{11}\text{B} = -51.5$  (dd, 110,  $J(\text{P}-\text{B}) = 115$ , B1) -7.0 (d, 122, B2, 4), -1.8 (d,  $J(\text{B}-\text{B})$  12, B3); and  $\text{B}_4\text{H}_8 \cdot \text{P}(\text{NMe}_2)_3$ ,  $\delta^{11}\text{B} = -52.7$  (dd, 110,  $J(\text{P}-\text{B}) = 180$ , B1), -7.8 (d, 120, B2, 4), -0.7 (d, 120, B3). The spectrum of the former compound also contains a weak feature at 5.1 ppm attributed to

B(3) in a stereoisomer. The spectrum of the mixed complex  $B_4H_8 \cdot P(NMe_2)_3$  has three peaks at  $-8.2$ ,  $-16.2$  and  $-46.5$  in a 1:2:1 ratio, which are assigned to  $\underline{B}-N$ , two unligated boron atoms and  $\underline{B}-P$  respectively. On cooling, the  $\underline{B}-P$  resonance is resolved into two peaks at  $-39.3$  and  $-48.9$  ppm. This is thought to be due to an isomerization [34], which interconverts  $\underline{B}-P$  and  $\underline{B}-N$ :<sup>146</sup>

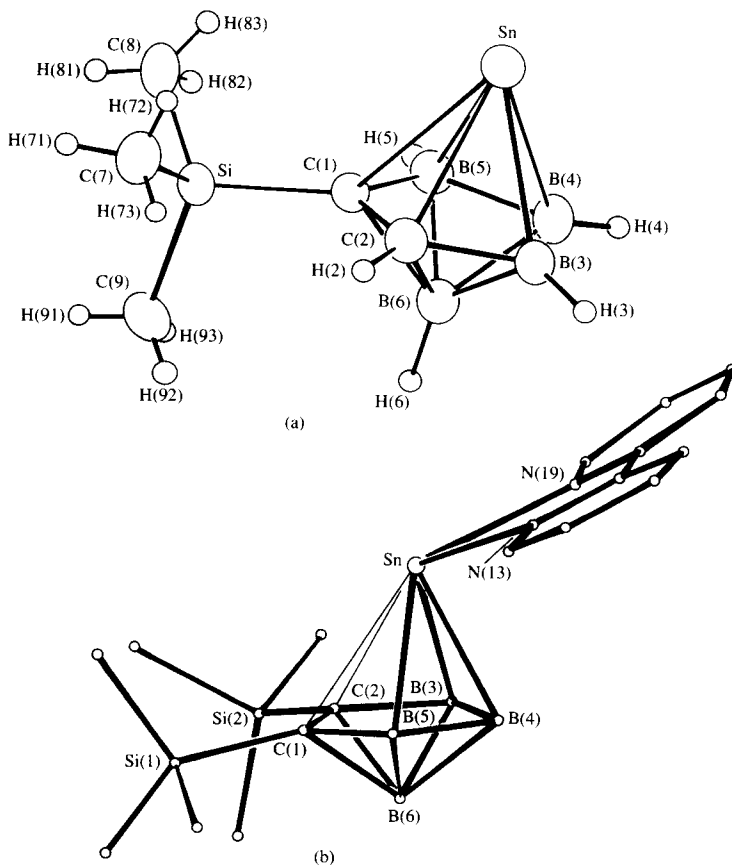
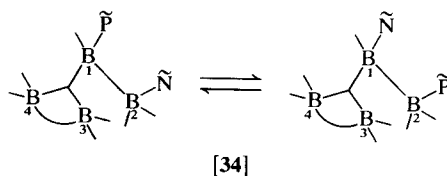


FIG. 5. Structures of  $(Me_3Si)B_4C_2SnH_5$  (a) and its complex with bipyridyl (b).

Three silicon-substituted  $\text{B}_4\text{C}_2\text{H}_8$  carboranes have been synthesized: 2,3-( $\text{Me}_3\text{Si}$ )<sub>2</sub>-2,3- $\text{B}_4\text{C}_2\text{H}_6$ ,  $\delta^{11}\text{B} = 1.9, 1.6$  (3B)  $-50.1$  (d, 173, 1B); 2- $\text{Me}_3\text{Si}$ -3- $\text{B}_4\text{C}_2\text{H}_6$ ,  $\delta^{11}\text{B} = 0.1$  (d, 153, 1B),  $-0.7$  (dd, 153, 47, 1B),  $-1.5$  (dd, 153, 47, 1B),  $-48.3$  (d, 176, 1B); and 2- $\text{Me}_3\text{Si}$ -2,3- $\text{B}_4\text{C}_2\text{H}_7$ ,  $\delta^{11}\text{B} = 0.5, -0.1$  (3B),  $-51.2$  (d, 176, 1B).<sup>112</sup> Stannacarboranes, which incorporate tin in the polyhedral framework, have been characterized.<sup>147</sup> Lewis acidity is, surprisingly, associated with the Sn(II) centre in these materials. Complexation with 2,2'-bipyridyl leads to a distortion from  $\eta^5$  towards  $\eta^3$  carborane-tin bonding as shown in Fig. 5.

Chemical-shift data for these stannacarboranes and their derivatives are collected in Table 15. The most-shielded doublet, having unit area, is assigned to B(6), the apical boron. Complexation with bipyridyl or THF is associated with a reduction in  $J(\text{B-H})$  for B(3,5) and also a significant shielding of B(6), which may represent an antipodal effect.<sup>148</sup>

TABLE 15

 $\delta^{11}\text{B}$  chemical-shift data for stannacarboranes.

Compound	$\delta^{11}\text{B}$
( $\text{Me}_3\text{Si}$ ) <sub>2</sub> $\text{B}_4\text{C}_2\text{SnH}_4$	24.5 (d, 146, 3 basal B), 20.3 (d, 168, 1B), $-4.7$ (d, 168, 1B)
( $\text{Me}_3\text{Si}$ ) $\text{MeB}_4\text{C}_2\text{SnH}_4$	22.3 (d, 140, 1B), 20.3 (d, 140, 2B), $-6.7$ (d, 167, 1B)
$\text{Me}_3\text{SiB}_4\text{C}_2\text{SnH}_5$	23.7 (d, 152, 1B), 19.7 (d, 136, 1B), 18.6 (d, 134, 1B), $-6.7$ (d, 171, 1B)
( $\text{Me}_3\text{Si}$ ) <sub>2</sub> $\text{B}_4\text{C}_2\text{SnH}_4 \cdot \text{bipy}$	22.3 (d, 110, 1B), 19.8 (d, 82, 2B), $-21.1$ (d, 162, 1B)
( $\text{Me}_3\text{Si}$ ) $\text{MeB}_4\text{C}_2\text{SnH}_4 \cdot \text{bipy}$	20.0 (d, 131, 1B), 15.1 (d, 108, 2B), $-20.2$ (d, 164, 1B)
$\text{Me}_3\text{SiB}_4\text{C}_2\text{SnH}_5 \cdot \text{bipy}$	21.1 (d, 146, 1B), 15.1 (d, 101, 2B), $-23.1$ (d, 166, 1B)
( $\text{Me}_3\text{Si}$ ) <sub>2</sub> $\text{B}_4\text{C}_2\text{SnH}_4 \cdot 2\text{THF}$	22.5 (d, 106, 3B), $-11.0$ (d, 145, 1B)
( $\text{Me}_3\text{Si}$ ) $\text{MeB}_4\text{C}_2\text{SnH}_4 \cdot 2\text{THF}$	22.8 (d, 150, 1B), 18.0 (d, 134, 2B), $-9.3$ (d, 161, 1B)
$\text{Me}_3\text{SiB}_4\text{C}_2\text{SnH}_5 \cdot 2\text{THF}$	22.2 (d, 140, 1B), 16.6 (d, 118, 2B), $-9.9$ (d, 161, 1B)

### C. $\text{B}_5$ boranes and carboranes

The chemistry of pentaborane(9) has continued to attract interest. Two pathways for intramolecular deuterium exchange in labelled pentaborane derivatives,  $\text{Me}_3\text{SiB}_5\text{H}_8$  and  $\text{ClB}_5\text{H}_8$ , have been elucidated by  $^{11}\text{B}$  and  $^2\text{H}$  NMR. One leads to bridge-basal terminal migration and the other, which is at higher energy, results in basal terminal-apical exchange.<sup>149</sup> New insights into the movement of framework boron atoms in  $\text{B}_5\text{H}_9$  have resulted from  $^{10}\text{B}$  and  $^{11}\text{B}$  studies of  $^{10}\text{B}$ -labelled derivatives.<sup>150</sup> Aluminum chloride catalyses the exchange between  $\text{C}_6\text{D}_6$  and  $\text{B}_5\text{H}_9$ .<sup>150</sup>  $^{11}\text{B}$  NMR spectroscopy indicates that incorporation of D occurs at B(1). An unusual uncatalysed

reaction introduces D into all terminal positions at 45°C and into all positions at 120°C.<sup>151</sup> Deuterium-labelled B<sub>5</sub>H<sub>9</sub> derivatives may also be obtained by reduction of the halogenated analogues with Bu<sub>3</sub>SnD.<sup>152</sup>

Dichloroborylpentaborane derivatives have been obtained using BCl<sub>3</sub>—AlCl<sub>3</sub> in an analogue of a Friedel–Crafts reaction. Chemical shifts for these and other B<sub>5</sub> compounds discussed in this section are collected in Table 16. The  $\sigma$ -BCl<sub>2</sub> group may be recognized by a high-frequency signal at approx. 75 ppm, closer to B<sub>2</sub>Cl<sub>4</sub> than to RBCl<sub>2</sub>. It exhibits an approx. 120 Hz coupling to the adjacent B(1). However, the B(1) resonance is too broad to reveal *J*(B–B) fine structure.<sup>153</sup> An isomer in which the Cl<sub>2</sub>B group bridges two basal boron atoms,  $\mu$ -Cl<sub>2</sub>BB<sub>5</sub>H<sub>8</sub>, has also been reported.<sup>154</sup>

Palladium bromide catalyses the coupling reactions of olefins and B<sub>5</sub>H<sub>9</sub> to

TABLE 16

<sup>11</sup>B NMR data for B<sub>5</sub>H<sub>9</sub> derivatives and related compounds.

Compound	$\delta^{11}\text{B}$
1-Cl <sub>2</sub> B <sub>5</sub> H <sub>8</sub>	75.8 (q, <i>J</i> (B–B) $\approx$ 124, Cl <sub>2</sub> B), –13.1 (d, 161, B2–5), –51.8 (br s, B1)
1-Cl <sub>2</sub> B-2-ClB <sub>5</sub> H <sub>7</sub>	73.0 (q, <i>J</i> (B–B) $\approx$ 122, Cl <sub>2</sub> B), –1.6 (s, B2), –14.0 (d, 164, B3, 5), –23.6 (d, 174, B4), –51.5 (br s, B1)
$\mu$ -Cl <sub>2</sub> BB <sub>5</sub> H <sub>8</sub>	74.8 (s, Cl <sub>2</sub> B), –4.5 (d, 160, B2–5), –34.2 (d, 185, B1)
(1- <i>trans</i> -propenyl)B <sub>5</sub> H <sub>8</sub>	–13.8 (d, 161, <i>J</i> (B–B) = 19, B2–5), –43.3 (s, B1)
(1- <i>cis</i> -propenyl)B <sub>5</sub> H <sub>8</sub>	–13.1 (d, 162, <i>J</i> (B–B) = 19.7, B2–5), –45.9 (s, B1)
(2- <i>trans</i> -1-but-1-enyl)B <sub>5</sub> H <sub>8</sub>	1.2 (s, B2), –13.5 (d, 153, B3, 5), –18.2 (d, 161, B4), –51.6 (d, 165, B1)
(1- <i>trans</i> -1-but-1-enyl)B <sub>5</sub> H <sub>8</sub>	–12.8 (d, 166, <i>J</i> (B–B) = 20, B2–5), –45.2 (s, B1)
2,4,6-Et <sub>3</sub> B <sub>5</sub> H <sub>6</sub>	2.0 (s, B3), –2.5 (s, B2, 4), –19.5 (d, 151, B5), –49.6 (d, 156, B1)
2-( <i>s</i> -Bu)B <sub>5</sub> H <sub>8</sub>	3.9 (s, B2), –15.0 (d, 167, B3, 5), –19.4 (d, 163, B4), –53.3 (d, 175, B1)
$\mu$ -(Me <sub>2</sub> NCH <sub>2</sub> )B <sub>5</sub> H <sub>8</sub>	16.3 (d, 112), 0.9 (d, 156), –0.7 (d, 117), –4.0 (d, 146), –47.4 (d, 117, B1)
1-Et- $\mu$ -(Me <sub>2</sub> NCH <sub>2</sub> )B <sub>5</sub> H <sub>7</sub>	14.3 (d, 88), 4.0 (d, 151), –0.8 (d, 112), –3.5 (d, 154), –36.3 (s, B1)
1-Br- $\mu$ -(Me <sub>2</sub> NCH <sub>2</sub> )B <sub>5</sub> H <sub>7</sub>	14.9 (d, 93), 3.7, 1.6, –3.0 (d, 151), –31.8 (s, B1)
2-[HO(CF <sub>3</sub> ) <sub>2</sub> C]B <sub>5</sub> H <sub>8</sub>	–8.4 (s, B2), –13.3 (d, 165, B3, 5), –15.0 (d, 165, B4), –52.1 (d, 178, B1)
1-[HO(CF <sub>3</sub> ) <sub>2</sub> C]B <sub>5</sub> H <sub>8</sub>	–12.9 (d, 168, <i>J</i> (B–B) = 21, B2–5), –41.6 (s, B1)
1-[HO(C(CF <sub>3</sub> ) <sub>2</sub> O)]B <sub>5</sub> H <sub>8</sub>	–14.2 (d, 165, B2–5), –19.9 (s, B1)
5-[HO(CF <sub>3</sub> ) <sub>2</sub> C]-2,4-B <sub>5</sub> C <sub>2</sub> H <sub>6</sub>	15.9 (s, B5), 2.8 (d, 184, B3), –3.6 (d, 182, B6), –20.2 (d, 182, B1, 7)
5-[HO(C(CF <sub>3</sub> ) <sub>2</sub> O)]-2,4-B <sub>5</sub> C <sub>2</sub> H <sub>6</sub>	15.9 (s, B5), 2.8 (d, 184, B3), –3.3 (d, 170, B6), –20.3 (d, 186, B1, 7)

TABLE 17

<sup>11</sup>B NMR data for 2,4-B<sub>5</sub>C<sub>2</sub>H<sub>7</sub> derivatives.

Compound	$\delta^{11}\text{B}$ (J(B-H))				
	B1	B3	B5	B6	B7
1,3-Cl <sub>2</sub> -2,4-B <sub>5</sub> C <sub>2</sub> H <sub>5</sub>	-13.4 (s)	15.1 (s)	3.0 (173)	3.0 (173)	-29.6 (186)
1,5-Cl <sub>2</sub> -2,4-B <sub>5</sub> C <sub>2</sub> H <sub>5</sub>	-14.8 (s)	6.5 (190)	12.9 (s)	0.7 (170)	-31.3 (192)
1,7-Cl <sub>2</sub> -2,4-B <sub>5</sub> C <sub>2</sub> H <sub>5</sub>	-22.5 (185)	7.8 (184)	3.2 (172)	3.2 (172)	-22.5 (s)
3,5-Cl <sub>2</sub> -2,4-B <sub>5</sub> C <sub>2</sub> H <sub>5</sub>	-17.1 (185)	12.6 (s)	12.3 (s)	-0.2 (170)	-17.1 (185)
5,6-Cl <sub>2</sub> -2,4-B <sub>5</sub> C <sub>2</sub> H <sub>5</sub>	-18.7 (190)	1.8 (193)	10.2 (s)	10.2 (s)	-18.7 (190)
5-Br-2,4-B <sub>5</sub> C <sub>2</sub> H <sub>6</sub>	-20.1 (185)	5.9 (189)	7.7 (s)	2.2 (173)	-20.1 (185)
5-Br-2,4-B <sub>5</sub> C <sub>2</sub> H <sub>6</sub> -Me <sub>3</sub> N	-19.9 (186)	6.1 (ca. 180)	16.9 (s)	0.8 (176)	-19.9 (186)
1-Cl-2,4-B <sub>5</sub> C <sub>2</sub> H <sub>6</sub>	-15.8 (s)	8.8 (167)	3.5 (173)	3.5 (173)	-32.8 (190)
5-Cl-6-Me-2,4-B <sub>5</sub> C <sub>2</sub> H <sub>5</sub>	-19.0 (180)	4.3 (180)	12.0 (s)	9.8 (s)	-19.0 (180)
[5-Me <sub>3</sub> N-6-Me-2,4-B <sub>5</sub> C <sub>2</sub> H <sub>5</sub> ]BCl <sub>4</sub>	-18.0 (189)	5.8 (200)	14.0 (s)	9.9 (s)	-18.0 (189)
[3-Me <sub>3</sub> N-2,4-B <sub>5</sub> C <sub>2</sub> H <sub>6</sub> ]BCl <sub>4</sub>	-17.8 (184)	17.1 (s)	3.9 (s)	3.9 (s)	-17.8 (184)
[5-Me <sub>3</sub> N-2,4-B <sub>5</sub> C <sub>2</sub> H <sub>6</sub> ]BCl <sub>4</sub>	-19.3 (190)	6.3 (183)	16.8 (s)	1.7 (156)	-19.3 (190)
5-Cl-2,4-B <sub>5</sub> C <sub>2</sub> H <sub>6</sub> -Me <sub>3</sub> N	-19.4 (179)	6.3 (157)	17.4 (s)	2.3 (130)	-19.4 (190)

yield alkenylpentaboranes.<sup>155</sup> Pentaborane is trialkylated by  $\text{LiHBEt}_3$  to form 2,4,6- $\text{Et}_3\text{B}_5\text{H}_6$ , but  $\text{LiHB(s-Bu)}_3$  produces only 2-(s-Bu) $\text{B}_5\text{H}_8$ .<sup>156</sup> Pentaborane derivatives proposed to contain a  $\text{Me}_2\text{NCH}_2$  group bridging a basal edge on the  $\text{B}_5$  cage have recently been prepared.<sup>157</sup> Hydroxy-perfluoropropyl and -pinacolyl substituted boranes and carboranes are produced by the photolysis of  $(\text{CF}_3)_2\text{CO}$  and  $\text{B}_5\text{H}_9$ . In the carborane derivatives both substituents produce a similar deshielding, but in the 1-substituted pentaborane compounds,  $\text{HO}(\text{CF}_3)_2\text{C}-\underline{\text{B}}$  is more deshielded than  $\text{HO}[\text{C}(\text{CF}_3)_2]_2\text{O}-\underline{\text{B}}$ , cf. Table 16.<sup>158</sup>

$^{11}\text{B}$  NMR spectra obtained at 160 MHz indicate that 2- and 3- $\text{MeB}_5\text{H}_{10}$ , previously believed to be pure substances, are actually identical equilibrium mixtures of the two isomers.<sup>159</sup>

$^{11}\text{B}$  NMR spectroscopy has been used to study rearrangements of various isomers of  $\text{Cl}_2$ -2,4- $\text{B}_5\text{C}_2\text{H}_5$ . These have been separated and their  $^{11}\text{B}$  spectra obtained, cf. Table 17. Antipodal shielding effects are indicated by a 7–9 ppm shielding increase of B(7) in the 1,3- and 1,5-dichloro isomers.<sup>160</sup>

B-halogen-substituted  $\text{B}_5\text{C}_2$  carboranes form dipolar complexes with  $\text{Me}_3\text{N}$ . Thus  $\text{Me}_3\text{N}$  and 5-Br-2,4- $\text{B}_5\text{C}_2\text{H}_6$  yield a 1 : 1 crystalline adduct. The amine is probably attached to B5, as this boron nucleus experiences the greatest relative chemical-shift change on complex formation. Interestingly, only this complex reacts with  $\text{CH}_2\text{Cl}_2$  (a solvent frequently employed in  $^{11}\text{B}$  NMR spectroscopy) to form 5-Cl-2,4- $\text{B}_5\text{C}_2\text{H}_6$  and  $(\text{Me}_3\text{NCH}_2\text{Cl})\text{Br}$ .<sup>161</sup> Reactions of these complexes with  $\text{BCl}_3$  leads to  $\text{BCl}_4^-$  salts in which  $\text{Cl}^-$  is replaced by  $\text{Me}_3\text{N}$ , e.g.  $[\text{5-Me}_3\text{N-2,4-B}_5\text{C}_2\text{H}_6]\text{BCl}_4$ . The anion is recognized by its characteristic  $^{11}\text{B}$  shift of 7.7 ppm.<sup>162</sup>

Halogenation of  $\text{B}_6\text{H}_6^{2-}$  has been reinvestigated and the numerous products separated by ion exchange chromatography. The  $^{11}\text{B}$  chemical shifts of the various halogen-substituted clusters, which display significant antipodal shielding effects, are shown in Table 18.<sup>163,164</sup>

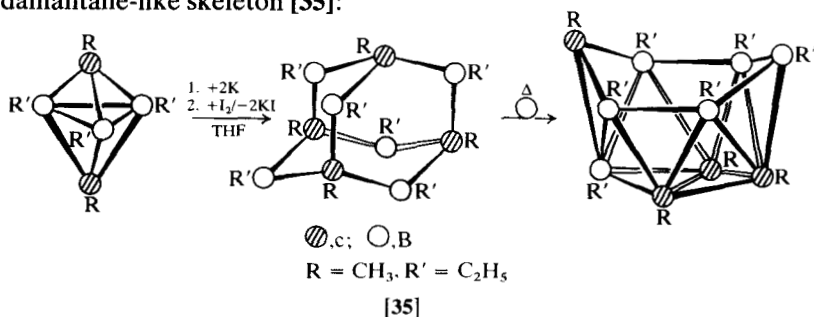
#### D. $\text{B}_{6,8,9}$ boranes and carboranes

The controlled reduction, with potassium in THF, of  $\text{Et}_5$ -1,3- $\text{B}_3\text{C}_2$  affords the dianion,  $\delta^{11}\text{B} = -14$  (2B),  $-37$  (1B). Reoxidation with iodine provides the perethylated carbon-rich carborane  $\text{Et}_{10}\text{B}_6\text{C}_4$ . Connectivities established by 2D  $^{11}\text{B}$  NMR have led to the proposal that this compound has a *nido*- $\text{B}_6\text{C}_4$  structure, similar to that of  $\text{B}_{10}\text{H}_{14}$ , with carbon atoms in the 1,2,3 and 9 positions. Using this numbering scheme, the  $^{11}\text{B}$  NMR spectrum can be assigned:  $\delta^{11}\text{B} = 50.3$  (B4), 6.7 (B5,7),  $-6.3$  (B6),  $-20.7$  B(8,10).<sup>165</sup> Similar reduction of 1,5- $\text{Me}_2$ -2,3,4- $\text{Et}_3$ -1,5- $\text{B}_3\text{C}_2$  leads to a small amount of the dianion,  $\delta^{11}\text{B} = -10$ ,  $-24$ ,  $-37$ , and a strong, unassigned signal at 6.5 ppm (halfwidth 900). Subsequent oxidation produces  $\text{Et}_6\text{Me}_4\text{B}_6\text{C}_4$ ,

TABLE 18  
<sup>11</sup>B NMR data for derivatives of B<sub>6</sub>H<sub>6</sub><sup>2-</sup>.

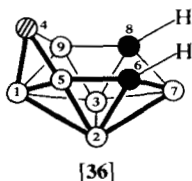
Compound	$\delta^{11}\text{B}$		
	X = Cl	X = Br	X = I
1-XB <sub>6</sub> H <sub>5</sub> <sup>2-</sup>	-1.0 (s, B1) -14.5 (d, 147, B2-5) -30.4 (d, 157, B6)	-7.6 (s, B1) -14.0 (d, 147, B2-5) -27.3 (d, 160, B6)	-23.2 (s, B1) -13.1 (d, 150, B2-5) -21.6 (B6)
1,2-X <sub>2</sub> B <sub>6</sub> H <sub>4</sub> <sup>2-</sup>	-2.4 (s, B1, 2) -15.4 (B3, 5) -30.3 (d, 159, B4, 6)	-8.4 (B1, 2) -26.9 (d, 162, B4, 6)	
1,6-X <sub>2</sub> B <sub>6</sub> H <sub>4</sub> <sup>2-</sup>	-10.4 (B1, 6) -13.6 (B2-5)	-15.0 (B1, 6) -12.6 (d, 159, B2-5)	-25.2 (B1, 6) -13.1 (d, 150, B2-5)
1,2,3-X <sub>3</sub> B <sub>6</sub> H <sub>3</sub> <sup>2-</sup>	-8.8 (B1-3) -26.7 (B4-6)	-14.0 (B1-3) -23.6 (B4-6)	
1,2,6-X <sub>3</sub> B <sub>6</sub> H <sub>3</sub> <sup>2-</sup>	-8.6 (B2) -11.9 (B1, 6) -16.0 (d, 136, B3, 5) -26.7 (d, 140, B4)	-14.0 (B2) -15.4 (B1, 3, 5, 6) -23.6 (d, 137, B4) —	-24.2 (B2)  -26.2 (B1, 6) -12.7 (d, 141, B3, 5) -17.7 (d, 136, B4)
1,2,3,4-X <sub>4</sub> B <sub>6</sub> H <sub>2</sub> <sup>2-</sup>	-11.1 (B1, 3) -13.7 (B2, 4) -27.3 (d, 126, B5, 6)	-14.5 (B1, 3) -16.4 (B2, 4) -27.3 (d, 140, B5, 6)	
1,2,4,6-X <sub>4</sub> B <sub>6</sub> H <sub>2</sub> <sup>2-</sup>	-13.8 (B1, 2, 4, 6) -18.3 (d, 128, B3, 5)	-16.0 (B1, 2, 4, 6) -15.9 (B3, 5)	-26.1 (B1, 2, 4, 6)
X <sub>5</sub> B <sub>6</sub> H <sup>2-</sup>	-13.9, -15.7 (B1-5) -27.4 (d, 128, B6)	-15.8, -17.6 (B1-5) -23.4 (d, 150, B6)	-22.0 (B1) -25.6 (B2-5) -15.7 (d, 160, B6)
X <sub>6</sub> B <sub>6</sub> <sup>2-</sup>	-17.4	-18.5	-27.4

whose  $^{11}\text{B}$  NMR spectrum comprises a singlet at 65 ppm. It is proposed, and confirmed by X-ray crystallography, that this compound has an adamantane-like skeleton [35]:



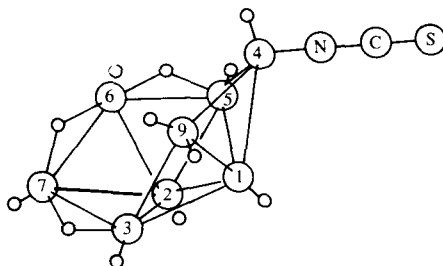
It rearranges on heating to an isomer having the  $\text{B}_{10}\text{H}_{14}$ -like structure and whose  $^{11}\text{B}$  NMR spectrum resembles that of the decaethyl analogue:  $\delta^{11}\text{B} = 51$  (1B), 6.4 (2B),  $-7.9$  (1B),  $-21.2$  (2B). However, this material exhibits dynamic behaviour in solution, and above  $100^\circ\text{C}$  the three lowest-frequency resonances coalesce while that at 51 ppm becomes very broad.<sup>166</sup> These compounds merit further investigation. The compound described as *nido*-2,5- $\text{B}_7\text{C}_2\text{H}_{11}$  has been misformulated for 15 years and recently shown to be *arachno*-4,5- $\text{B}_7\text{C}_2\text{H}_{13}$ ,  $\delta^{11}\text{B}$  9.7 (brd), 3.7 (brd),  $-4.1$ ,  $-4.8$ ,  $-6.3$ ,  $-30.1$  (t),  $-56.8$ .<sup>338</sup>

The thiacarborane 4,6,8- $\text{B}_6\text{SC}_2\text{H}_{10}$  [36] has been obtained from 7,9- $\text{B}_8\text{C}_2\text{H}_{12}^-$  and  $\text{Na}_2\text{SO}_3$  in dilute acid:



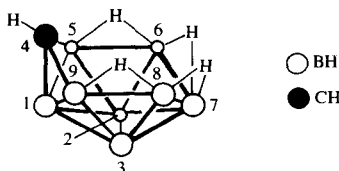
It has  $^{11}\text{B}$  resonances at 7.6 (d, 156, 1B), 5.7 (d, 168, 2B),  $-21.7$  (d, 160, 2B) and  $-35.6$  (d, 175, 1B) ppm. Placement of the sulphur atom at the 4 position is indicated, but not proved, by the mirror-plane symmetry indicated by the  $^{11}\text{B}$  NMR spectrum; and by the empirical rule that boron on an open face between two heteroatoms (carbon) gives rise to a relatively narrow resonance. For the 7.6 and  $-35.6$  ppm signals, the halfwidths are 26 and 65 Hz respectively.<sup>167</sup>

Chemical-shift data and assignments have been reported for a rare example of an octaborane derivative,  $\text{B}_8\text{H}_{12}\text{NCS}^-$ : 0.3 (d, 155, B1), 0.98 (d, 140, B6,7),  $-10.4$  (d, 140, B5),  $-23.6$  (d, 93, B4)  $-27.8$  (t, 90, B9),  $-52.0$  (d, 146, B2). The numbering scheme and proposed structure are

FIG. 6. Proposed structure of  $[\text{B}_8\text{H}_{12}(\text{NCS})]^-$ .

shown in Fig. 6. For comparison,  $\text{B}_8\text{H}_{10}\text{NEt}_3$  has  $\delta^{11}\text{B} = 6.5$  (2B), 1.9 (d, 3B, 148),  $-21.9$  (d, 2B, 136) and  $-30.5$  (d, 1B, 136).<sup>169</sup>

Incisive use of 2D COSY and  $^1\text{H}$  decoupling techniques has led to an unambiguous assignment of the  $^{11}\text{B}$  NMR spectra of  $\text{B}_8\text{CH}_{14}$  and its conjugate base  $\text{B}_8\text{CH}_{13}^-$ , cf. Fig. 7. In  $\text{B}_8\text{CH}_{14}$  assignments are 17.0 (B7),  $-3.7$  (B1),  $-6.3$  (B5,9),  $-34.9$  B(6, 8),  $-41.1$  (B2, 3) ppm. Coupling between B(6, 8) and B(7) was noted, even though, in general, boron atoms connected by bridging hydrogen atoms do not give rise to cross-correlated peaks. In contrast, B(6, 8) and B(5, 9), also connected by bridging hydrogens, do not observably couple. The absence of scalar B–B coupling is thought to be associated with low electron density along the B–B vector in the B–H–B unit; however, if the hydrogen bridge is sufficiently asymmetrical, this restriction may not apply. Assignments for  $\text{Li}(\text{B}_8\text{CH}_{13})$  are 4.0 (B5, 9),  $-3.9$  (B7),  $-21.5$  (B1),  $-30.4$  (B2, 3),  $-35.2$  (B6, 8) ppm. In this anion there is considered to be a unique hydrogen atom that bridges B(6, 7, 8). Now, strong coupling appears between B(5, 9) and B(6, 8), indicating the presence of an unsymmetrical hydrogen bridge; B(6, 8) and B(9, 7) are weakly coupled. There is a reduction in  $J(\text{B}(1)\text{--}\text{B}(5, 9))$  on deprotonation, attributed to a shift in electron density on the open face of the carborane cluster away from positions adjacent to the carbon atom and towards B(6, 8). Thus B(5, 9) has a greater shielding on removal of a proton. Reduction in B(7) coordination number probably accounts for its large low-frequency shift in the conjugate base. Interestingly, saturation-transfer experiments demonstrate that the *endo-C*—H and all three bridging

FIG. 7. Proposed structure of  $\text{CB}_8\text{H}_{14}$ .

hydrogen atoms interchange at room temperature in the anion but not in the neutral carborane.<sup>170</sup> One hopes that, eventually, absolute values of  $^1J(\text{B}-\text{B})$  may be obtained and correlated with calculated B—B bond orders.

Use of labelled derivatives has led to an assignment of the 64 MHz  $^{11}\text{B}$  NMR spectrum of 5,6- $\text{B}_8\text{C}_2\text{H}_{12}$ , cf. Table 19.<sup>171</sup>

The  $^{11}\text{B}$  NMR spectrum of *arachno*-6- $\text{Me}_3\text{Si}$ -6,9- $\text{B}_8\text{C}_2\text{H}_{13}$ , which is iso-electronic with and similar in structure to  $\text{B}_{10}\text{H}_{14}^{2-}$  (cf. Fig. 8), has been assigned with the use of 160.4 MHz and COSY data:  $\delta^{11}\text{B} = 5.7$  (B2), 4.8 (B4),  $-15.0$  (B8, 10),  $-16.2$  (B5, 7),  $-35.6$  B(1, 3).<sup>172</sup> Reaction of  $\text{Na}_2(6,9\text{-B}_8\text{C}_2\text{H}_{10})$  with HX yields 5-X-6,9- $\text{B}_8\text{C}_2\text{H}_{13}$  and  $^{11}\text{B}$  NMR data for a series of X = halogen derivatives are presented in Table 20.

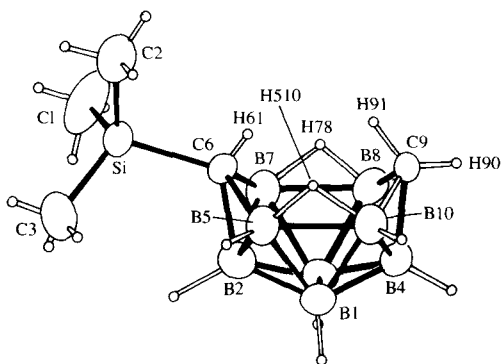


FIG. 8. Molecular structure of *arachno*-6-( $\text{SiMe}_3$ )-6,9- $\text{B}_8\text{C}_2\text{H}_{13}$  showing the atom-numbering scheme.

The tetracarbon carborane  $\text{Me}_4\text{B}_8\text{C}_4\text{H}_8$  exists in solution as two readily interconvertible isomers: A ( $\delta^{11}\text{B} = 10.6$  (d, 171, 2B), 8.7 (d, 216, 2B),  $-22.3$  (d, 159, 2B) and  $-29.0$  (d, 147, 2B)) and B ( $\delta^{11}\text{B} = -1.5$  (d, 127, 2B),  $-2.3$  (d, 129, 4B),  $-10.7$  (d, 144, 2B)), cf. Fig. 9. One of the  $^1J(\text{B}-\text{H})$  values, 216 Hz, appears to be anomalously large. In the solid state the tetramethyl

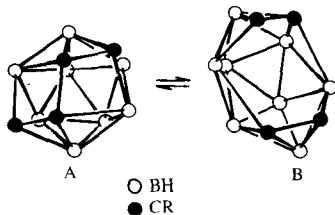


FIG. 9. Interconversion of A and B isomers of  $\text{R}_4\text{C}_4\text{B}_8\text{H}_8$ .

TABLE 19

<sup>11</sup>B NMR data for 5,6-B<sub>8</sub>C<sub>2</sub>H<sub>12</sub> derivatives.

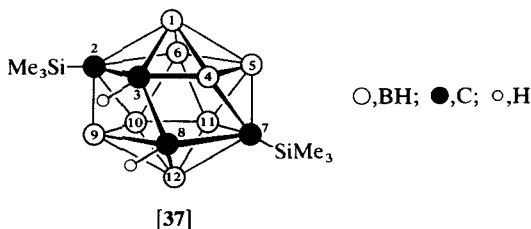
Compound	$\delta^{11}\text{B}$							
	B7	B1	B8	B3	B9	B10	B2	B4
$\mu\text{-D}_2\text{-B}_8\text{C}_2\text{H}_{10}$	6.8	5.2	3.6	-2.1	-4.2	-9.1	-27.0	-38.8
4-ClB <sub>8</sub> C <sub>2</sub> H <sub>11</sub>	7.2	6.4	4.0	-0.8	-3.2	-10.0	-26.9	-21.8 (s)
8-ClB <sub>8</sub> C <sub>2</sub> H <sub>11</sub>	9.3	5.3	11.7 (s)	-2.4	-6.2	-15.5	-27.2	-37.5
10-ClB <sub>8</sub> C <sub>2</sub> H <sub>11</sub>	7.6	6.7	-0.2	-0.2	-6.7	-10.0	-27.1	-38.0
3,4,8,9-B <sub>8</sub> C <sub>2</sub> D <sub>4</sub> H <sub>8</sub>	6.5	5.0	3.3 (s)	-2.6 (s)	3.7 (s)	-0.2 (s)	-27.2	-39.1 (s)
7-BrB <sub>8</sub> C <sub>2</sub> H <sub>11</sub>	9.6 (s)	7.4	5.7	-1.0	-2.5	-10.0	-26.3	-39.2
7-IB <sub>8</sub> C <sub>2</sub> H <sub>11</sub>	-4.5 (s)	6.8	6.7	0.0	-2.8	-8.8	-26.0	-38.3
3,4,7-B <sub>8</sub> C <sub>2</sub> D <sub>3</sub> H <sub>9</sub>	6.5 (s)	5.0	3.3	-2.6 (s)	-3.7	-10.0	-27.2	-39.1 (s)

TABLE 20

<sup>11</sup>B NMR data for 5-XB<sub>8</sub>C<sub>2</sub>H<sub>13</sub> derivatives.

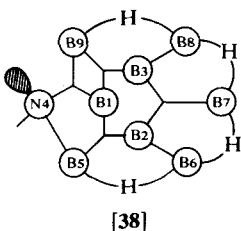
	$\delta^{11}\text{B } (J(\text{B-H}))$							
	B2	B4	B5	B10	B8	B7	B1	B3
F	3.3 (145)	0.7 (156)	4.6	-19.4 (135, 51)	-21.5 (145, 51)	-23.7 (140, 49)	-39.3 (154)	-39.3 (154)
Cl	5.9 (164)	1.9 (162)	-5.5 (57)	-17.2 (158, 55)	-18.2 (161, 54)	-20.6 (152, 49)	-37.5 (150)	-37.9 (151)
Br	6.6 (166)	2.5 (164)	-13.0 (61)	-16.3 (157, 54)	-17.3 (157, 51)	-19.6 (150, 50)	-35.0 (154)	-37.4 (154)
I	7.2 (175)	3.4 (173)	-30.0 (50)	15.8 (160)	15.8 (160)	18.1 (140, 50)	-34.3 (157)	-36.7 (157)
OB <sub>8</sub> C <sub>2</sub> H <sub>13</sub>	2.0 (179)	0.8 (173)	3.3	-20.4 (154, 43)	-21.2 (157, 59)	-23.8 (173, 35)	-38.8 (155)	-40.0 (144)

derivative adopts structure A, whereas the tetraethyl compound crystallizes in structure B.  $^{11}\text{B}$  NMR spectroscopy has been used to determine thermodynamic parameters for the solution-phase rearrangements.  $^1\text{H}$  NMR data suggest that B undergoes additional rearrangement processes that are not manifest in the  $^{11}\text{B}$  spectra.<sup>174</sup> Pyrolysis of 2,3-( $\text{Me}_3\text{Si}$ )<sub>2</sub>-2,3- $\text{B}_4\text{C}_2\text{H}_6$  yields directly the four-carbon carborane ( $\text{Me}_3\text{Si}$ )<sub>2</sub> $\text{B}_8\text{C}_4\text{H}_{10}$  [37]:



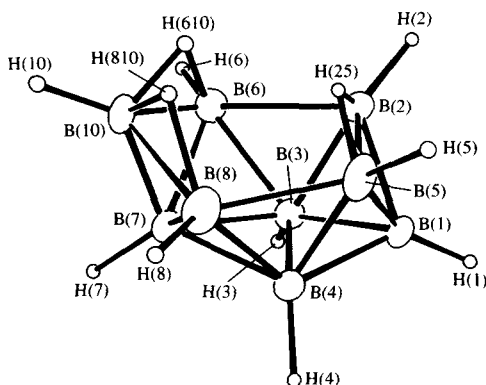
The  $^{11}\text{B}$  NMR spectrum has been assigned: 10.0 (d, 152, B4), 8.9 (d, 156, B9), 6.2 (d, 158, B6,11),  $-17.3$  (d, 178, B5,10) and  $-20.9$  (d, 181, B1, 12) ppm. Unlike the alkyl derivatives  $\text{R}_4\text{B}_8\text{C}_4\text{H}_8$ , this compound has a static structure in solution.<sup>175</sup>

Hydrolysis of  $\text{B}_9\text{H}_{12}\text{N}$  yields  $\text{B}_8\text{H}_{13}\text{N}$ . The structure of this azaborane may be derived from  $\text{B}_{10}\text{H}_{14}$  by replacing B6 by N and deleting B9; four B—H—B bridges span the B—B bonds on the open face of the molecule [38]:



An assignment of the 32 MHz  $^{11}\text{B}$  NMR spectrum has been proposed: 7.8 (B7),  $-7.1$  (B5, 9),  $-25.4$  (B1),  $-46.0$  (B2, 3),  $-47.7$  (B6, 7) ppm. An NMR study of its conjugate base would be of interest, since the anion should exhibit bridge-proton mobility. The sulphur analogue  $\text{B}_8\text{H}_{12}\text{S}$  has been obtained from  $\text{B}_{10}\text{H}_{14}$  and aqueous  $\text{KHSO}_3$ . The proposed assignment of the 32 MHz  $^{11}\text{B}$  NMR spectrum is:  $\delta^{11}\text{B} = 13.8$  (B7),  $-3.8$  (B5, 9),  $-12.3$  (B1),  $-41.3$  (B2, 3, 6, 8).<sup>176</sup>

The boron subhalide  $\text{B}_9\text{Cl}_8\text{H}$ , prepared by pyrolysis of  $(\text{H}_3\text{O})_2\text{B}_{10}\text{Cl}_{10} \cdot x\text{H}_2\text{O}$ , was originally reported to exhibit four  $^{11}\text{B}$  resonances. This reaction has been reinvestigated and found to afford numerous clusters, containing nine and thirteen to twenty boron atoms,

FIG. 10. Structure of  $\text{B}_9\text{H}_{12}^-$  showing numbering scheme.

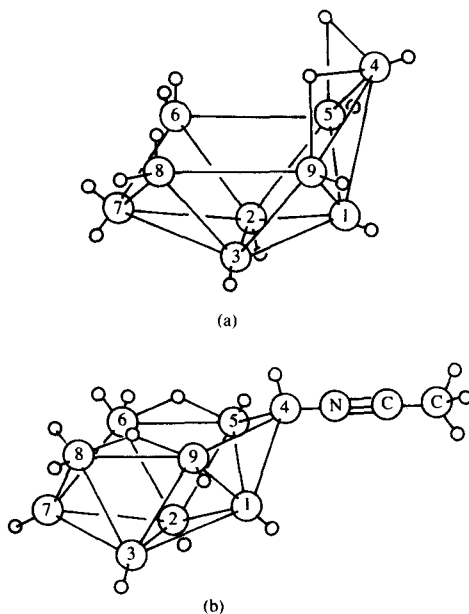
that are exceedingly difficult to separate. Pure compounds for which  $^{11}\text{B}$  NMR data are obtained are:  $\text{B}_9\text{Cl}_7\text{H}_2$ ,  $\delta^{11}\text{B} = 69.8$ ; and  $\text{B}_9\text{Cl}_8\text{H}$ ,  $\delta^{11}\text{B} = 63.2, 29.8$  (d, 165). Thus  $\text{B}_9\text{Cl}_8\text{H}$  presumably has a tricapped trigonal prismatic geometry.<sup>177</sup>

$^{11}\text{B}$  NMR data for  $\text{B}_9\text{H}_{12}^-$  may now be interpreted in terms of the recently determined structure shown in Fig. 10. The assignments are  $-9.9$  (B1, 6, 8),  $-13.9$  (B3, 4),  $-14.5$  (B10),  $-34.1$  (B(2), 5),  $-51.9$  (B7) ppm. At room temperature, the two types of B—H—B protons rapidly interconvert.<sup>178</sup>  $^{11}\text{B}$  NMR data, including relaxation times, for  $\text{B}_9\text{H}_{14}$  and a series of derivatives have been published (Table 21). Line-narrowed spectra indicate

TABLE 21

 $^{11}\text{B}$  NMR data for  $\text{B}_9\text{H}_{14}^-$  and some derivatives.

Compound	$\delta^{11}\text{B}$
$\text{Me}_4\text{N}(\text{B}_9\text{H}_{14})$	$-6.8$ (d, 137, B5, 7, 9), $-19.2$ (d, 136, B4, 6, 8), $-22.4$ (d, 138, B1, 2, 3)
$\text{PPN}[\text{B}_9\text{H}_{13}(\text{NCS})]$	$14.8$ (d, 134, B7), $4.2$ (d, 140, B1), $-16.4$ (d, 146, B5, 9), $-18.0$ (d, 143, B6, 8), $-22.0$ (s, B4), $-38.3$ (d, 146, B2, 3)
$\text{PPN}[\text{B}_9\text{H}_{13}(\text{NCBH}_3)]$	$16.2$ (d, 130, B7), $4.8$ (d, 137, B1), $-15.5$ (d, 141, B5, 9), $-19.4$ (d, 124, B6, 8), $-25.5$ (s, B4), $-38.6$ (d, 146, B2, 3), $-43.0$ (NCBH <sub>3</sub> )
$\text{B}_9\text{H}_{13}(\text{SMe}_2)$	$18.8$ (d, 152, B7), $5.1$ (d, 134, B1), $-15.8$ (d, 144, B5, 9), $-20.8$ (d, 150, B6, 8), $-23.0$ (d, 131, B4), $-38.6$ (d, 149, B2, 3)
$\text{B}_9\text{H}_{13}(\text{CH}_3\text{CN})$	$17.7$ (d, 155, B7), $5.6$ (d, 137, B1), $-14.0$ (d, 145, B5, 9), $-20.2$ (d, 150, B6, 8), $-27.0$ (d, 134, B4), $-38.3$ (d, 149, B2, 3)
$\text{B}_9\text{H}_{13}(\text{PMe}_2\text{Ph})$	$18.4$ (d, 160, B7; $T_1 = 1.9$ ms), $3.4$ (d, 135, B1, 8.2 ms), $-15.1$ (d, 145, B5, 9, 8.5 ms), $-21.8$ (d, 140, B6, 8, 4.0 ms), $-36.3$ (B4, 13.0 ms), $-38.5$ (d, 145, B2, 3, 18.0 ms)

FIG. 11. Structures of  $[B_9H_{14}]^-$  (a) and  $B_9H_{13}(MeCN)$  (b).

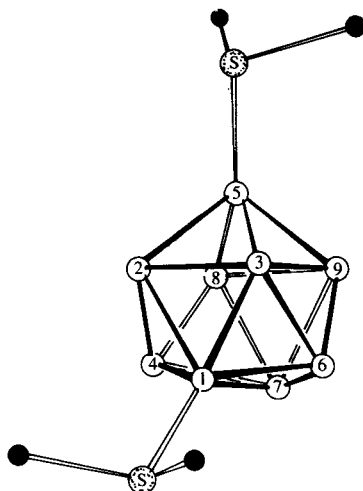
that the  $B(6,8) H_2$  resonances are in fact doublets of doublets with coupling to the nonequivalent bridge hydrogens,  $J(B-H(exo))$  and  $J(B-H(endo))$ , being 150 and 60 Hz respectively. Note that the numbering system employed (Fig. 11) differs from that used above for  $B_9H_{12}^{179}$ .

The 2D COSY  $^{11}B$  spectrum of  $B_9H_{13}(SMe_2)$  has been reported. Table 22 summarizes the B-B couplings observed. Note that B1 and B2, 3 are coupled to all adjacent  $^{11}B$  nuclei; and B5, 9 do not couple to their hydrogen-bridged neighbours, B6, 8. The 2D spectra of  $B_9H_{13}(NCS)^-$  and  $B_9H_{13}^-$

TABLE 22

2D  $^{11}B$  NMR data for  $B_9H_{13}(SMe_2)$ .

$^{11}B$ nucleus	Couplings detected
7	B(2, 3)
1	B(5, 9), B(4), B(2, 3)
5, 9	B(1), B(4), B(2, 3)
6, 8	B(2, 3)
4	B(1), B(5, 9)
2, 3	B(7), B(1), B(5, 9), B(6, 8)

FIG. 12. Molecular structure of  $1,5\text{-B}_9\text{H}_7(\text{SMe}_2)_2$ .

(NSCe) $^-$  are stated to be similar.<sup>180</sup> The  $^{11}\text{B}$  NMR spectrum of crystallographically characterized  $1,5\text{-B}_9\text{H}_7(\text{SMe}_2)_2$  (Fig. 12) shows peaks at  $\delta^{11}\text{B} = 6.3$  (B5),  $-0.2$  (d, 148, B(4, 6)),  $-9.5$  (B1),  $-12.9$  (d, 143, B7),  $-15.9$  (d, B2, 3) and  $-17.5$  (d, B8, 9). Above  $25^\circ\text{C}$  rearrangement to, probably, the 4,5- and 1,8-isomers occurs.<sup>181</sup>

Decaborane reacts with  $\text{NaNO}_2$  in THF to give, after addition of aqueous acid,  $\text{B}_9\text{H}_{12}\text{NH}^-$ . This undergoes protonation and loss of  $\text{H}_2$  thus forming the acidic  $\text{B}_9\text{H}_{11}\text{NH}$ .  $^{11}\text{B}$  NMR data are available for these materials and a series of Lewis-base complexes of  $\text{B}_9\text{H}_{11}\text{NH}$ , cf. Table 23 and Fig. 13, which shows the structure of  $\text{B}_9\text{H}_{11}\text{NH}(\text{c-C}_6\text{H}_{11}\text{NC})$  and the numbering scheme employed. Chemical-shift trends in  $\text{B}_9\text{H}_{12}\text{E}$  ( $\text{E} = \text{NH}, \text{S}, \text{Se}$ ) are similar, but B8,10 and the distal B9 are most affected by variation in the heteroatom. The  $^{11}\text{B}$  spectrum of  $\text{B}_9\text{H}_{12}\text{S}^-$  is assigned with the use of specifically labelled derivatives, which are unavailable for  $\text{E} = \text{NH}$  and Se. Two-dimensional  $^{11}\text{B}$  studies would therefore be of interest. Pyrolysis of  $\text{B}_9\text{H}_{11}\text{NH}$  yields  $\text{B}_9\text{H}_9\text{NH}$ , which has a bicapped square antiprismatic structure with the NH group at one of the two four-coordinate vertices. Assignment of the equatorial  $^{11}\text{B}$  resonances cannot be made on symmetry grounds, and 2D spectra might be helpful in distinguishing the B(2–5) and B(6–9) sets.<sup>182</sup> The thiaboranes  $\text{B}_9\text{H}_{11}\text{S}(\text{t-BuNC})$  and  $\text{Me}_4\text{N}[\text{B}_9\text{H}_{11}\text{S}(\text{CN})]$  have  $\delta^{11}\text{B} = 9.2$  (d, 147, 1B),  $-4.2$  (d, 153, 1B),  $-9.1$  (d, 152, 2B),  $-29.9$  (d, 149, 2B),  $-34.0$  (d, 126, 1B) and  $-36.0$  (d, 147, 2B); and  $9.2$  (d, 137, 1B),  $-6.1$  (3B),  $-18.7$  (d, 117, 1B),  $-29.9$  (d, 147, 2B) and  $33.3$  (d, 142, 2B) respectively.<sup>183</sup>

TABLE 23

<sup>11</sup>B NMR data for B<sub>9</sub>H<sub>11</sub>NH and related derivatives.

Compound (area ratio)	$\delta^{11}\text{B}$ ( $J(\text{B-H})$ )
PPN[B <sub>9</sub> H <sub>12</sub> NH] (1 : 2 : 1 : 1 : 4)	-1.2 (127), -12.6 (156), -20.4, -22.3 (119), -42
B <sub>9</sub> H <sub>11</sub> NH (1 : 2 : 2 : 2 : 1 : 1)	15.2 (162), 11.8 (160), -1.5 (140), -14.5 (149), -27.4 (156), -33.0 (176)
B <sub>9</sub> H <sub>11</sub> NH·CN( <i>t</i> -C <sub>4</sub> H <sub>9</sub> ) (1 : 3 : 2 : 1 : 2)	4.6 (136), -12.7 (142), -36.1 (137), -38, -40.5 (144)
B <sub>9</sub> H <sub>11</sub> NH·CN(C <sub>6</sub> H <sub>11</sub> ) (1 : 3 : 3 : 2)	5.1 (131), -11.8, -36.0 (151), -39.7 (143)
B <sub>9</sub> H <sub>11</sub> NH·py (1 : 3 : 1 : 2 : 2)	2.4 (127), -11.4 (121), -19.5 (143), -38.1 (121), -40.8 (140)

Proposed assignments for <sup>11</sup>B NMR resonances of selected B<sub>9</sub>H<sub>11</sub>E·L compounds (E = NH, S, Se).

Compound	$\delta^{11}\text{B}$					
	B(4)	B(5, 7)	B(2)	B(9)	B(8, 10)	B(1, 3)
CsB <sub>9</sub> H <sub>12</sub> S	-4.0	-7.9	-11.6	-15.0	-33.4	-36.6
PPN(B <sub>9</sub> H <sub>12</sub> NH)	-1.2	-12.6	-20.4	-22.3	-42	-42
B <sub>9</sub> H <sub>11</sub> Se·N(C <sub>2</sub> H <sub>5</sub> ) <sub>3</sub>	2.6	-8.8	-8.8	-4.0	-29.8	-38.1

<sup>11</sup>B NMR data for B<sub>9</sub>H<sub>9</sub>NH and its derivatives.

Compound	$\delta^{11}\text{B}$ ( $J(\text{B-H})$ )		
	B(10)	B(2, 3, 4, 5)	B(6, 7, 8, 9)
B <sub>9</sub> H <sub>9</sub> NH	61 (165)	-6.1 (175)	-21.5 (153)
(CH <sub>3</sub> ) <sub>4</sub> N[B <sub>9</sub> H <sub>9</sub> N]	50 (149)	-8.3 (161)	-18.3 (140)
B <sub>9</sub> H <sub>9</sub> NCH <sub>3</sub>	59.1 (168)	-1.5 (175)	-20.8 (150)

Base degradation of 1,2-(HS)<sub>2</sub>-1,2-B<sub>10</sub>C<sub>2</sub>H<sub>10</sub> yields Me<sub>4</sub>N-[(B<sub>9</sub>C<sub>2</sub>H<sub>10</sub>(SH)<sub>2</sub>],  $\delta^{11}\text{B}$  = -5.9 (d, 2B, 140), -7.5 (d, 165, 1B), -16.2 (d, 142, 4B), -33.0 (d, 124, 1B) and -34.2 (d, 127, 1B). This compound, on oxidative coupling, forms the S—S linked carborane anion (B<sub>9</sub>C<sub>2</sub>H<sub>11</sub>) ( $\mu$ -S<sub>2</sub>)<sub>2</sub>(B<sub>9</sub>C<sub>2</sub>H<sub>11</sub>)<sup>2-</sup>,  $\delta^{11}\text{B}$  = -4.2 (B9,11), -9.4 (B3), -15.0, -17.1 (B2, 4, 5, 6), -32.5 (B10) and -34.6 (B1).<sup>184</sup> The complexing agent 18-crown-6 promotes reaction of 1,12-B<sub>10</sub>C<sub>2</sub>H<sub>12</sub> with potassium hydroxide to give K[2,9-B<sub>9</sub>C<sub>2</sub>H<sub>12</sub>], which has one carbon in each of the two 5-atom

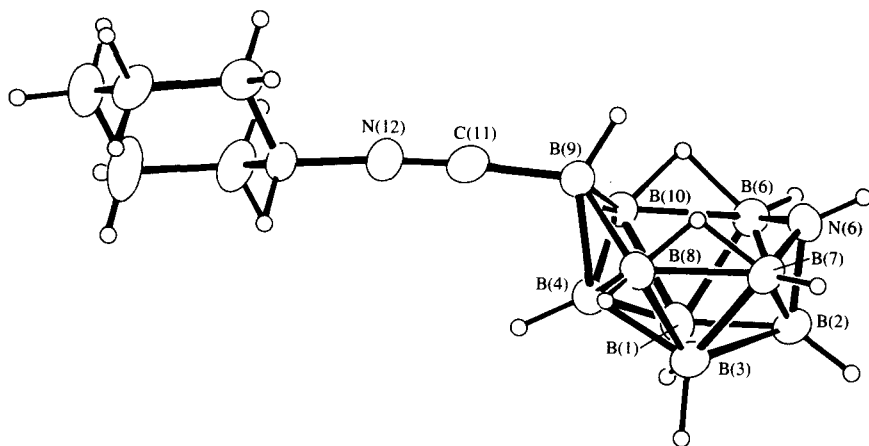


FIG. 13. ORTEP diagram of 9-[(C<sub>6</sub>H<sub>11</sub>)NC]-6-NHB<sub>9</sub>H<sub>11</sub>.

equatorial belts and  $\delta^{11}\text{B} = -13.1$  (d, 140, 2B),  $-19.2$  (d, 148, 2B),  $-21.6$  (d, 148, 2B),  $-28.5$  (d, 139, 2B) and  $-42.9$  (d, 156, 1B).<sup>185</sup>

#### E. B<sub>10,11,12</sub> boranes and carboranes

Electrophilic halogenation of B<sub>10</sub>H<sub>10</sub><sup>2-</sup> has been reinvestigated. Use of advanced chromatographic techniques permits the separation and independent characterization of 1- and 2-XB<sub>10</sub>H<sub>9</sub><sup>2-</sup>; and 1,6- and 1,10-X<sub>2</sub>B<sub>10</sub>H<sub>8</sub><sup>2-</sup> (X = Cl, Br, I).  $^{11}\text{B}$  NMR data for these ions are given in Table 24.<sup>186</sup>

The diazoketone 1-N<sub>2</sub>CH-CO-CH<sub>2</sub>-1,2-B<sub>10</sub>C<sub>2</sub>H<sub>10</sub> has been converted via a carbene intermediate to the cyclic ketone 1,6-(2-C<sub>3</sub>H<sub>4</sub>O)-1,2-B<sub>10</sub>C<sub>2</sub>H<sub>10</sub> in which the C<sub>3</sub> ring connects C1 and B6. It has  $\delta^{11}\text{B} = -2.9$  (1B),  $-4.9$  (s, 1B),  $-7.0$  (d, 1B),  $-10.5$  (br d, 4B),  $-14.1$  (d, 2B),  $-16.0$  (d, 1B), and for the analogous 1,6-(2-C<sub>4</sub>H<sub>6</sub>O)-1,2-B<sub>10</sub>C<sub>2</sub>H<sub>10</sub>,  $\delta^{11}\text{B} = -2.4$  (d, 1B)  $-5.3$  (s, 1B),  $-7.7$  (d, 1B),  $-10.0$  (d, 2B),  $-12.7$  (d, 2B),  $-13.7$  (d, 2B) and  $-17.1$  (d, 1B). The location of the B-terminus of the C<sub>3</sub> bridge is determined by a  $^1\text{H}$  NOE experiment. The C<sub>3</sub> ketone is transformed into the cyclopentene analogue 1,6-(C<sub>3</sub>H<sub>4</sub>O)-1,2-B<sub>10</sub>C<sub>2</sub>H<sub>10</sub>,  $\delta^{11}\text{B} = -0.1$  (s, 1B),  $-4.2$  (d, 1B),  $-7.9$  (d, 2B),  $-9.7$  (d, 2B),  $-11.9$  (d, 1B),  $-13.0$  (d, 2B),  $-17.6$  (d, 1B). The relative shielding decrease of the vinyl-substituted boron may be due to a combination of electronic and ring-strain effects, partitioning of which may be possible when a larger series of compounds is studied.<sup>187</sup>  $^{11}\text{B}$  NMR spectra of a series of bis(mercapto)-1,2-carboranes have been published (Table 25).<sup>188</sup>

TABLE 24

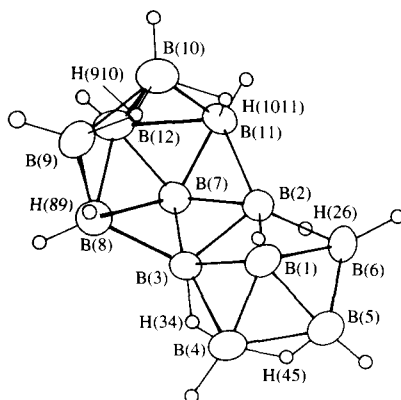
<sup>11</sup>B NMR data for halogenated B<sub>10</sub>H<sub>10</sub><sup>2-</sup>-derivatives.

Compound	δ <sup>11</sup> B		
	X = Cl	X = Br	X = I
2-XB <sub>10</sub> H <sub>9</sub> <sup>2-</sup>	-2.0 (d, 141, B1, 10) -9.2 (B2)  -24.4 (B3, 5, 6, 9)  -27.6 (d, 133, B7, 8) -30.8 (d, 126, B4)	-1.6 (d, 145, B1, 10) -13.2 (B2)  -24.6, -25.6 (B3, 5, 6, 9) -27.3 (d, 134, B7, 8) -30.1 (d, 137, B4)	-0.6 (d, 144, B1, 10) -25.6, -26.5 (B2, 3, 5, 7, 8, 9) -28.8 (B4)
1-XB <sub>10</sub> H <sub>9</sub> <sup>2-</sup>			0.0 (d, 168, B10) -8.9 (B1) -25.2 (d, 132, B2-5) -25.8 (d, 127, B6-9)
1,6-X <sub>2</sub> B <sub>10</sub> H <sub>8</sub> <sup>2-</sup>			-0.1 (d, 149, B10) -8.9 (B1) -22.0, -23.1 (B2, 3, 7, 9) -26.5, -28.7 (B4, 5, 6, 8)
1,10-X <sub>2</sub> B <sub>10</sub> H <sub>8</sub> <sup>2-</sup>			-5.9 (B1, 10) -24.8 (d, 133, B2-9)

TABLE 25

<sup>11</sup>B NMR data for 1,2-(HS)<sub>2</sub>-1,2-B<sub>10</sub>C<sub>2</sub>H<sub>10</sub> derivatives.

Compound	δ <sup>11</sup> B
1,2-(HS) <sub>2</sub> -1,2-B <sub>10</sub> C <sub>2</sub> H <sub>10</sub>	-4.0 (d, 152, 2B), -8.1 (d, 171, 6B), -10.0 (d, 171, 2B)
1,1',2,2'-(S <sub>2</sub> B <sub>10</sub> C <sub>2</sub> H <sub>10</sub> ) <sub>2</sub>	-3.6 (d, 141, 2B), -7.3 (d, 161, 8B)
(NH <sub>4</sub> ) <sub>2</sub> (1,2-S <sub>2</sub> B <sub>10</sub> C <sub>2</sub> H <sub>10</sub> )	-2.4 (d, 171, 2B), -9.0 (d, 156, 6B), -11.4 (d, 137, 2B)
(Me <sub>4</sub> N) <sub>2</sub> [(CH <sub>2</sub> S) <sub>2</sub> B <sub>9</sub> C <sub>2</sub> H <sub>10</sub> ]	-7.8 (d, 140, 2B), -10.6 (d, 168, 1B), -17.9 (d, 130, 2B), -18.8 (d, 143, 2B), -33.1 (d, 122, 1B), -36.6 (d, 140, 1B)
(Me <sub>4</sub> N) <sub>2</sub> (-CH <sub>2</sub> SB <sub>9</sub> C <sub>2</sub> H <sub>10</sub> CS-)	-11.4 (d, 134, 2B), -15.2 (d, 159, 1B), -17.3 (d, 159, 2B), -18.8 (d, 146, 2B), -31.2 (d, 130, 1B), -35.6 (d, 134, 1B)
(1,2-B <sub>10</sub> C <sub>2</sub> H <sub>10</sub> SC <sub>2</sub> H <sub>4</sub> ) <sub>2</sub>	-3.6 (d, 170, 2B), -7.3 (d, 149, 8B)

FIG. 14. Structure of  $\text{B}_{12}\text{H}_{16}$ .

The  $^{11}\text{B}$  NMR spectrum of  $\text{PPN}(4\text{-Me}_2\text{SB}_{11}\text{H}_{10})$ , in which the  $\text{Me}_2\text{S}$  ligand is attached to five-coordinate boron, shows peaks at  $-10.2$  (s, 1B) and  $-16.9$  (d, 134, 10B). The spectrum is invariant to temperatures as low as  $-140^\circ\text{C}$  at 126.7 MHz, indicating that the  $\text{B}_{11}$  cluster has a very low barrier to polytopal rearrangement.<sup>189</sup>

$\text{B}_{12}\text{H}_{16}$ , the first neutral  $\text{B}_{12}$  hydride, has been synthesized by oxidative

TABLE 26

$^{11}\text{B}$  NMR data for halogenated  $\text{B}_{12}\text{H}_{12}^{2-}$ -derivatives.

Compound	$\delta^{11}\text{B}$		
	X = Cl	X = Br	X = I
$1\text{-XB}_{12}\text{H}_{11}^{2-}$	$-2.5$ (B1) $-14.2$ (d, 135, B2-6) $-15.9$ (d, 134, B7-11) $-19.5$ (d, 134, B12)	$-7.6$ (B1) $-13.7$ (d, 122, B2-6) $-15.1$ (d, 120, B7-11) $-18.2$ (d, 115, B12)	$-21.5$ (B1) $-13.3$ (d, 123, B2-6) $-14.7$ (d, 124, B7-11) $-16.5$ (d, 152, B12)
$1,2\text{-X}_2\text{B}_{12}\text{H}_{10}^{2-}$	$-3.4$ (B1, 2) $-13.5$ (d, 130, B3, 6) $-15.0$ (d, 137, B4, 5, 7, 11) $-17.1$ (d, 160, B8, 10) $-18.8$ (d, 137, B9, 12)	$-8.5$ (B1, 2) $-12.7$ (d, 120, B3, 6) $-14.1$ (d, 129, B4, 5, 7, 11) $-16.0$ (d, 128, B8, 10) $-17.2$ (d, 120, B9, 12)	
$1,2,3\text{-X}_3\text{B}_{12}\text{H}_9^{2-}$	$-4.3$ (B1, 2, 3) $-14.1$ (d, 141, B4, 6, 7) $-16.0$ (d, 166, B5, 8, 11) $-18.7$ (d, 165, B9, 10, 12)		

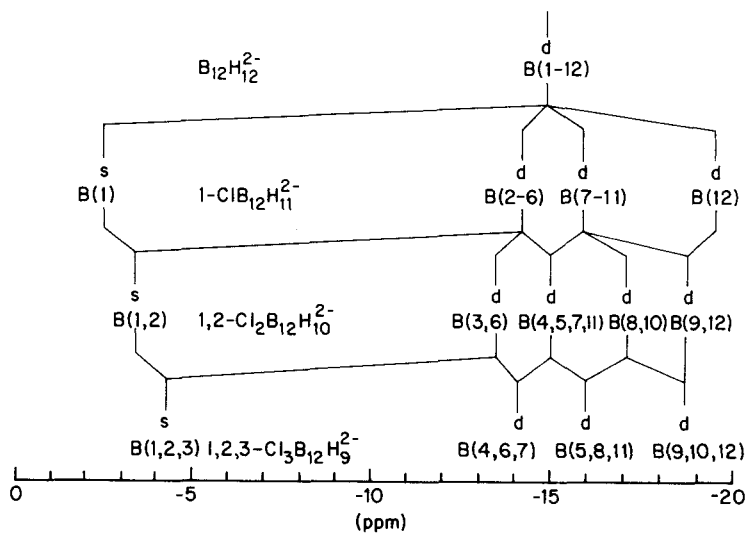


FIG. 15. Trends in the  $^{11}\text{B}$  chemical shifts of chlorinated  $\text{B}_{12}\text{H}_{12}^{2-}$  derivatives.

coupling of  $\text{B}_6\text{H}_9^-$  with  $\text{FeCl}_2/\text{FeCl}_3$ . Its structure has been determined (Fig. 14) and its  $^{11}\text{B}$  NMR spectrum assigned with the use of 2D data: 15.4 (d, 193, B7), 13.4 (d, 203, B4,6), 11.4 (d, 213, B5), 4.5 (B2, 3, 9, 10), -18.4 (d, 150, B8,11), -40.8 (d, 156, B1) and -43.1 (d, 159, B12).<sup>190</sup>

Halogenation of  $\text{B}_{12}\text{H}_{12}^{2-}$  has been reinvestigated, and ion-exchange chromatography used to separate  $1\text{-XB}_{12}\text{H}_{11}^{2-}$ ,  $1,2\text{-X}_2\text{B}_{12}\text{H}_{10}^{2-}$  and  $1,2,3\text{-X}_3\text{B}_{12}\text{H}_9^{2-}$  ( $\text{X} = \text{Cl}, \text{Br}, \text{I}$ ).  $^{11}\text{B}$  NMR data for these compounds are presented in Table 26, and Fig. 15 displays trends in chemical shifts for  $\text{X} = \text{Cl}$ .<sup>191</sup>

## VI. METALLOBORANES AND METALLOCARBORANES

Borane and carborane compounds containing transition metals continue to be the subject of intense study. Structural and bonding principles pertaining to metalloboranes have been thoroughly reviewed.<sup>192,193</sup>

### A. $\text{B}_1$ metalloboranes and metallocarboranes

Metal-boron couplings have been compared for  $\text{NaBH}_4$ ,  $\text{Al}(\text{BH}_4)_3$ ,  $\text{Sc}(\text{BH}_4)_3$ ,  $\text{Y}(\text{BH}_4)_3$  and  $\text{Zr}(\text{BH}_4)_4$ , 0.9, 15.5, <2 and 18 Hz respectively;  $\delta^{11}\text{B}$  values are -40, -37, -18.7, -23.2 and -8.0 respectively. However,

it has been pointed out that a comparison of observed  $J(A-B)$  values may be misleading and that one must refer to reduced couplings  $K(A-B)$ , which are given by

$$J(A-B) = K(A-B) \gamma_A \gamma_B h/4\pi^2,$$

where  $\gamma_{A,B}$  are the gyromagnetic ratios of the nuclei involved. Thus  $K(A-B)$  values for  $Al(BH_4)_3$ ,  $Sc(BH_4)_3$  and  $Zr(BH_4)_4$  are 0.90, 1.61 and  $5.02 \times 10^{20} \text{ N A}^{-2} \text{ m}^{-3}$ .  $K$  values usually increase with atomic number, but the  $^{89}\text{Y}-^{11}\text{B}$  coupling in  $Y(BH_4)_3$  is unobserved, probably because the bonding is more ionic than in the Sc analogue.  $^{45}\text{Sc}$  NMR data have been obtained for  $Sc(BH_4)_3$ ; there is a small  $^{10}\text{B}$  isotope effect, 6 Hz to high frequency.  $\delta^{11}\text{B}$  for  $\text{Cp}_2\text{ScBH}_4$  is  $-17.7$ , with  $J(^{45}\text{Sc}-^{11}\text{B}) = 15.5 \text{ Hz}$ .<sup>194</sup>

An unusual example of a B—H—Fe three-centre bond is found in  $\text{FeH}(\text{Me}_2\text{PC}_2\text{H}_4\text{PMe}_2)\text{HBH}_3$ , which has  $\delta^{11}\text{B} = -38.1$ . The  $^{11}\text{B}$  resonance is an 82 Hz quintet resulting from coupling with four dynamically equivalent protons.<sup>195</sup> A similar situation prevails in  $(\text{terpyridyl})\text{CoH}_2\text{BH}_2$ ,  $\delta^{11}\text{B} = 12.9$ ,  $^1J(\text{B}-\text{H}) \approx 80 \text{ Hz}$ , which features a  $\text{Co}(\mu\text{-H})_2\text{BH}_2$  unit. B—H coupling is not observed in the  $^1\text{H}$  NMR spectrum owing to rapid quadrupolar decoupling.<sup>196</sup> The lanthanide borohydrides  $[(\text{Me}_3\text{Si})_2\text{Cp}]_2\text{-ScH}_2\text{BH}_2$ ,  $[(\text{Me}_3\text{Si})_2\text{Cp}]_2\text{Y}(\text{THF})\text{H}_2\text{BH}_2$ ,  $[(\text{Me}_3\text{Si})_2\text{Cp}]\text{La}(\text{THF})\text{H}_3\text{BH}$  and  $[(\text{Me}_3\text{Si})_2\text{Cp}]_2\text{Sm}(\text{THF})\text{H}_3\text{BH}$  have been studied.  $\delta^{11}\text{B}$  values for the latter three compounds are  $-22.0$ ,  $-26.7$  and  $-43.1$  respectively. Only for the Sc compound is the  $\text{BH}_4$  ligand bidentate and nonfluxional, as revealed by a broad signal in the  $^{11}\text{B}$  NMR spectrum that transforms into a quintet at  $100^\circ\text{C}$ . The Y, La and Sm borohydrides are fluxional, and the latter two contain tridentate  $\text{BH}_4$ .<sup>197</sup> The compound  $\text{Yb}[\text{HB}(\text{PZ})_3]_3$  exhibits in its  $^{11}\text{B}$  NMR spectrum peaks at 57.7 (B1),  $-69.1$  (B2) and 16.3 (B3) ppm; B1, 2 are each contained in an  $\eta^3 \text{HB}(\text{PZ})_3$  ligand and are strongly influenced by the paramagnetic metal whereas B3 is contained in an  $\eta^2 (\text{PZ})\text{BH}(\text{PZ})_2$  moiety, as shown in Fig. 16. Reference to the solid-state structure, which appears to persist in solution, and the McConnell–Robertson expression for dipolar shifts indicates that the  $^{11}\text{B}$  chemical shifts are affected primarily by a dipolar mechanism and that contact shifts are less important.<sup>198</sup> Dimeric  $[\text{Th}(\text{BH}_3\text{Me})_4]_2 \cdot \text{Et}_2\text{O}$  has  $\delta^{11}\text{B} = 19.3$ , but the aggregation is thought not to persist in hydrocarbon solutions.<sup>199</sup> The  $^{11}\text{B}$  NMR spectrum of  $\text{U}(\text{BH}_4)_4$  in THF has been interpreted as indicating that dissociation to  $\text{U}(\text{BH}_4)_6^{2-}$  and  $\text{U}(\text{BH}_4)_3^+$  occurs. Similarly,  $\text{U}(\text{BH}_4)_3$  is considered to dissociate in THF to form  $\text{U}(\text{BH}_4)_5^{2-}$  and  $\text{U}(\text{BH}_4)_2^+$ .<sup>200</sup>

Reaction of  $(\text{Me}_5\text{Cp})_2(\mu\text{-H})_3\text{Ir}_2^+$  with  $\text{LiBH}_4$  gives  $(\text{Me}_5\text{Cp})_2(\mu\text{-H})(\mu\text{-BH}_4)\text{H}_2\text{Ir}_2$ ,  $\delta^{11}\text{B} = 5.5$  (br s,  $-50^\circ\text{C}$  in toluene). In this compound, a bidentate  $\text{BH}_4$  ligand bridges two iridium atoms. Hydrolysis yields  $(\text{Me}_5\text{CpIrH}_3)_2$ .<sup>201</sup> This borohydride is interesting in that it may serve as a

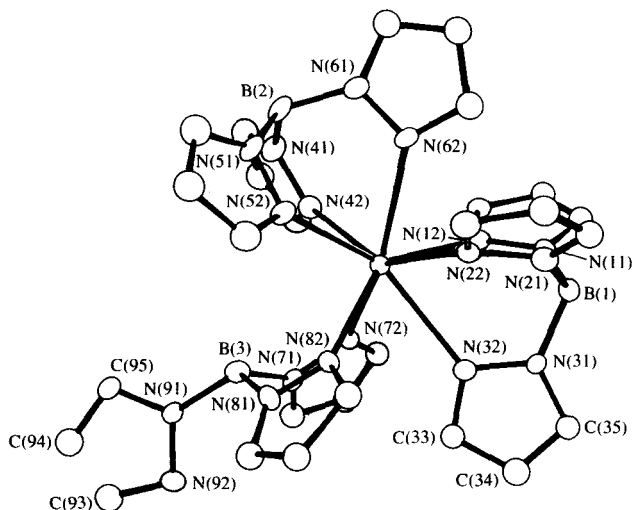


FIG. 16. Perspective view of the solid-state structure of  $\text{Yb}(\text{HBPz}_3)_3$  perpendicular to the approximate molecular mirror plane. The atom-numbering scheme is also shown.

model for intermediates in the reduction of coordination compounds by  $\text{BH}_4^-$ . Another example of such a material is  $\text{V}_2\text{Zn}_2\text{H}_4(\text{BH}_4)_2(\text{PMePh}_2)_4$ . It has a  $\text{P}_4\text{V}_2[(\mu\text{-H})_2\text{ZN}]_2$  core with a bidentate  $\text{BH}_4$  ligand attached to each zinc atom. The  $^{11}\text{B}$  chemical shift,  $-30.6$  ppm, is quite different from that of the above Ir borohydride.<sup>202</sup>

Reaction of  $\text{Na}[\text{Fe}(\text{CO})_4\text{COMe}]$ ,  $\text{BH}_3 \cdot \text{THF}$  and  $\text{Fe}(\text{CO})_5$  yields, after acidification, numerous products including  $\text{HFe}_3(\text{CO})_{10}\text{BH}_2$ . The proposed structure of the former is shown in Fig. 17. Its  $^{11}\text{B}$  NMR spectrum comprises a single resonance at 56 ppm with 145 and 50 Hz coupling to the terminal and bridge protons respectively. These values appear to be typical for boron bonded to a  $\text{Fe}_3$  triangle. Deprotonation removes one of the  $\text{B-H-Fe}$  bridges and in  $\text{PPN}[\text{Fe}_3(\text{CO})_{10}\text{BH}_2]$  the  $^{11}\text{B}$  parameters,  $\delta^{11}\text{B} = 57.4$  (dd, 130, approx. 50), are little changed.<sup>203</sup> The cluster ferraboranes

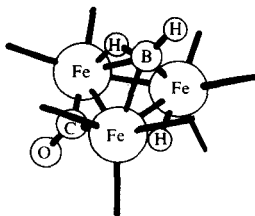


FIG. 17. Proposed structure of  $\text{HFe}_3(\text{CO})_{10}\text{BH}_2$ .

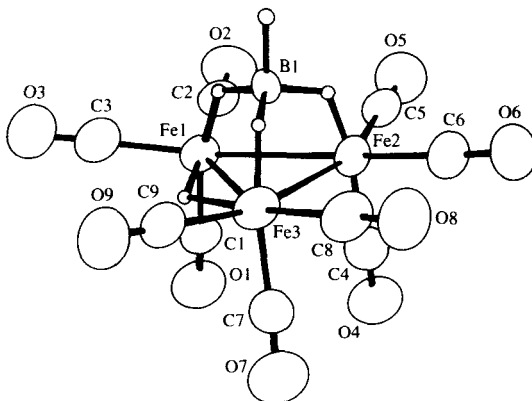
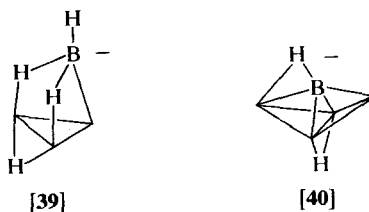


FIG. 18. Structure of  $\text{HFe}_3(\text{CO})_9\text{BH}_4$ . Hydrogen-atom locations are based on spectroscopic data.

$\text{HFe}_3(\text{CO})_9\text{BH}_3\text{R}$  ( $\text{R} = \text{H}$ ,  $\delta^{11}\text{B} = 1.8$ , halfwidth 230 Hz;  $\text{R} = \text{Me}$ ,  $\delta^{11}\text{B} = 22.1$ , quintet,  $^1J(\text{B-H}) = 40$ ) have been prepared, and the structure of the former is shown in Fig. 18. In this compound, the  $\text{B-H-Fe}$  protons become equivalent at approx.  $-50^\circ\text{C}$  and at  $80^\circ\text{C}$ , the  $\text{B-H-Fe}$  and  $\text{Fe-H-Fe}$  protons interconvert, but the terminal  $\text{B-H}$  proton remains uninvolved. Chemical shifts for the conjugate bases  $\text{PPN}[\text{HFe}_3(\text{CO})_9\text{BH}_2\text{R}]$  ( $\text{R} = \text{H}$ ,  $\delta^{11}\text{B} = 6.2$ , br dq;  $\text{R} = \text{Me}$ ,  $\delta^{11}\text{B} = 29.3$ , br q, 53), which are also at the low end of the range expected for four-coordinate boron, reflect a small relative deshielding and a small increase in  $J(\text{B-H})$ . The  $^{11}\text{B}$  spectra of these anions show that boron is coupled to three equivalent  $\text{B-H-Fe}$  protons, and therefore the  $\text{Fe-H-Fe}$  and  $\text{B-H-Fe}$  protons must be rapidly interconverting at room temperature. This process, rapid on the  $^{11}\text{B}$  NMR timescale, also averages Fe environments, but two types of iron can be detected by Mössbauer spectroscopy, which has a shorter timescale. A linear correlation between  $J(\text{B-H}(\text{terminal}))$  and the number of  $\text{B-H-Fe}$  interactions in  $\text{Fe}_3\text{B}$  clusters has been noted (Fig. 19).<sup>204</sup>

A cluster-expansion reaction using  $\text{Fe}_2(\text{CO})_9$  converts  $\text{HFe}_3(\text{CO})_9\text{BH}_3^-$  [39] to  $\text{HFe}_4(\text{CO})_{12}\text{BH}^-$  [40]:



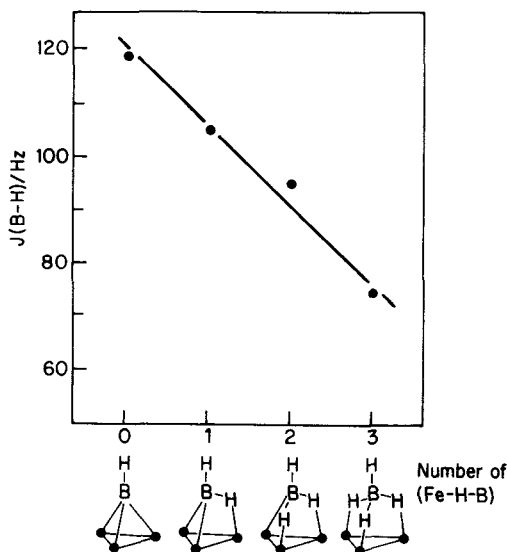
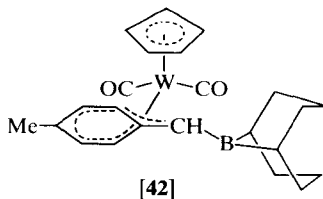
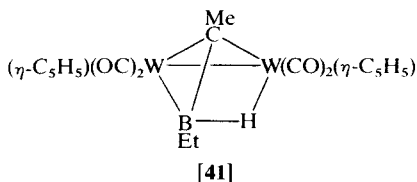


FIG. 19. Plot of  $J(\text{B-H})$  (terminal) versus number of Fe-H-B interactions.

In the structures of these two anions Fe atoms are displayed as vertices. The  $^{11}\text{B}$  shift of the  $\text{Fe}_4\text{B}$  cluster is 150.0 ppm, reflecting a gross perturbation in boron chemical environment on passing from an apical boron bearing a terminal hydrogen to a boron, surrounded by four iron atoms, with a B—H—Fe bridge.<sup>205</sup> The  $^{11}\text{B}$  chemical shift of the conjugate acid  $\text{HFe}_4(\text{CO})_{12}\text{BH}_2$  is 116 ppm (s); this is consistent with the crystallographically confirmed proton addition to a B—Fe edge.<sup>206</sup>

The borane complex  $\text{CpMo}(\text{CO})_2[\text{PhP}[\text{N}(\text{SiMe}_3)_2]](\mu\text{-H—BH}_2)$  features a  $\text{BH}_2$  group bonded to phosphorus; and a B—H—Mo bridge. It has a single  $^{11}\text{B}$  resonance at  $-55.6$  ppm with  $J(\text{P-B}) = 52$  Hz. No B—H coupling is observed, so hydrogen migration may be occurring.<sup>207</sup>

The carbyne complex  $\text{W}(\equiv\text{CMe})(\text{CO})_2\text{Cp}$  reacts with  $\text{BH}_3 \cdot \text{THF}$  to form  $\text{W}_2[\mu\text{-MeCB}(\text{H})\text{Et}](\text{CO})_4\text{Cp}_2$ , [41],  $\delta^{11}\text{B} = -30.0$  (br). This compound contains a W—W bond bridged by an  $\text{EtB—CMe}$  group; and a hydride bridging B and W. A similar reaction of 9-borabicyclo[3.3.1]nonane with  $\text{W}(\equiv\text{C-}p\text{-tolyl})(\text{CO})_2\text{Cp}$  leads to  $\text{W}[\text{CH}(\text{BC}_8\text{H}_{14})(p\text{-tolyl})](\text{CO})_2\text{Cp}$ , [42],  $\delta^{11}\text{B} = -3.0$  (br), in which a BH unit has added to the carbyne ligand.<sup>208</sup>



The carbon-rich metallocarborane  $\text{CpCoBHC}_4\text{Ph}_4$ ,  $\delta^{11}\text{B} = 17$ , is formed from  $(\text{Ph}_4\text{C}_4)\text{CoCpPPh}_3$ . It is considered to have a pentagonal pyramidal geometry with an apical  $\text{CpCo}$  moiety; and four contiguous  $\text{PhC}$  units, plus a  $\text{BH}$  group in the base.<sup>209</sup>

### B. $\text{B}_{2,3,4}$ metalloboranes and metallocarboranes

The two boron atoms in  $(\text{CpCo})_4(\mu_3\text{-H})_2\text{B}_2\text{H}_2$  give rise to a doublet at rather high frequency: 114 ppm ( $J(\text{B-H}) = 170$ ). This is consistent with the solid-state structure (Fig. 20), which discloses that two hydrides bridge  $\text{Co}_3$  triangular faces.<sup>210</sup> A 1:1 complex in which a  $\text{ZnCl}_2$  moiety is bonded to  $\text{B}_2\text{H}_4\text{P}(\text{Me}_3)_2$  by two  $\text{B-H-Zn}$  bonds been obtained. It has  $\delta^{11}\text{B} = -43.1$  ( $J(\text{P-B}) = 71$ ), and thus has a static structure in solution.<sup>211</sup> The  $\text{Ph}_3\text{PCuI}$ ,  $\text{Ph}_3\text{PCuCl}$  and  $\text{Ni}(\text{CO})_2$  complexes have similar  $^{11}\text{B}$  chemical shifts.<sup>212</sup>

A dicobalt thiaborane complex  $4,6\text{-(CpCo)}_2\text{-}3,5\text{-B}_2\text{S}_2\text{H}_2$ ,  $\delta^{11}\text{B} = 17.6$  (d, 169), has been prepared from  $\text{Co}$  vapour,  $\text{C}_5\text{H}_6$ ,  $\text{B}_5\text{H}_9$  and  $\text{COS}$  or  $\text{H}_2\text{S}$ . The  $\text{Co}_2\text{B}_2\text{S}_2$  cage can be viewed as a pentagonal bipyramid with one equatorial vertex missing. Cobalt atoms are at the apices; two boron atoms comprise an equatorial edge and the two sulphur atoms are not directly bonded.<sup>213</sup>

The metalloboranes  $(\text{B}_3\text{H}_8)\text{OsH}(\text{CO})(\text{PPh}_3)_2$  and  $(\text{B}_3\text{H}_8)\text{IrH}_2(\text{PPh}_3)_2$  have  $\delta^{11}\text{B} = 1.0$  (B1),  $-39.5$ ,  $-40.5$  (B1,3); and  $1.2$  (B1),  $39.4$  (B2,3) respectively, this is consistent with the solid-state structures (Fig. 21).<sup>214</sup>  $(\text{B}_4\text{H}_8)\text{Os}(\text{CO})(\text{PPh}_3)_2$  is considered to have a square pyramidal  $\text{B}_4\text{Os}$  framework with an apical (B1) boron atom based on the pattern of  $^{11}\text{B}$  resonances:  $8.9$  (B1),  $-7.5$ ,  $-14.2$  (B3,5) and  $-34.4$  B(4) ppm.<sup>214</sup> Structurally novel  $\text{B}_4$  metalloboranes have been synthesized from  $\text{B}_4\text{H}_5^-$ . The structure of  $(\text{B}_4\text{H}_9)\text{Ir}(\text{CO})(\text{PhPMe}_2)_2$  (Fig. 22a) is rather like that of  $\text{B}_5\text{H}_{11}$ . In solution, NMR data reveal a site-exchange process that interconverts B(2, 5) and also B(3, 4); it is fast on the NMR timescale at  $87^\circ\text{C}$  and  $28.87\text{ MHz}$  but slow at  $25^\circ\text{C}$  and  $96.28\text{ MHz}$ . In the latter case  $^{11}\text{B}$

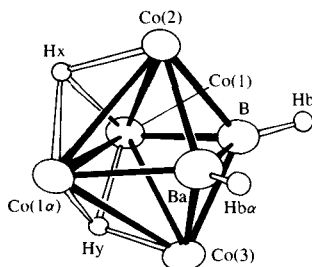
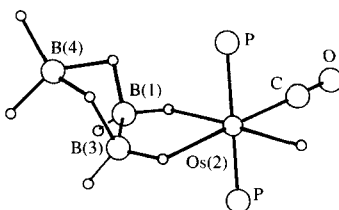


FIG. 20.  $\text{Co}_4(\text{BH})_2(\mu_3\text{-H})_2$  core.

FIG. 21. Structure of  $(B_3H_8)Os(H)(Ph_3P)_2$ .

chemical shifts are 3.4,  $-1.0$  (B3, 4) and  $-14.5$  (B5), which reflects the asymmetry found by X-ray crystallography. A more compact structure is thought to be adopted by  $(B_4H_8)Rh(H)(PPh_3)_2$  (Fig. 22b), which has  $\delta^{11}B = -4.2$  (B4),  $-12.4$  (B3, 5) and  $-18.4$  (B1). The corresponding shifts in  $(B_4H_8)Ni(\text{diphos})$  (diphos is  $Ph_2PC_2H_4PPh_2$ ) are 10.2,  $-6.4$  and  $-22.8$  ppm. The structure of  $(B_4H_8)Cu(PPh_3)_2$  is not established, but one possibility is shown in Fig. 22(c). At  $-20^\circ C$  the 96 MHz  $^{11}B$  NMR spectrum contains resonances at 1.6 (1B),  $-6.5$  (2B) and  $-55.8$  (1B) ppm. Low-temperature  $^1H\{-^{11}B\}$  spectra show that, unlike  $K[B_4H_9]$ , rapid bridge-terminal proton exchange does not occur.<sup>215</sup>

The osmacarborane  $1-(CO)_3Os-2,3-(Me_3Si)_2-2,3-B_4C_2H_4$ , formed from  $Os_3(CO)_{12}$  and  $(Me_3Si)_2B_4C_2SnH_4$  or  $(Me_3Si)_2B_4C_2H_6$ , has  $\delta^{11}B = 15.8$  (d, 168, B5), 2.7 (d, 156, B7) and 11.1 (d, 158, B4,6).<sup>216</sup> The arene complex

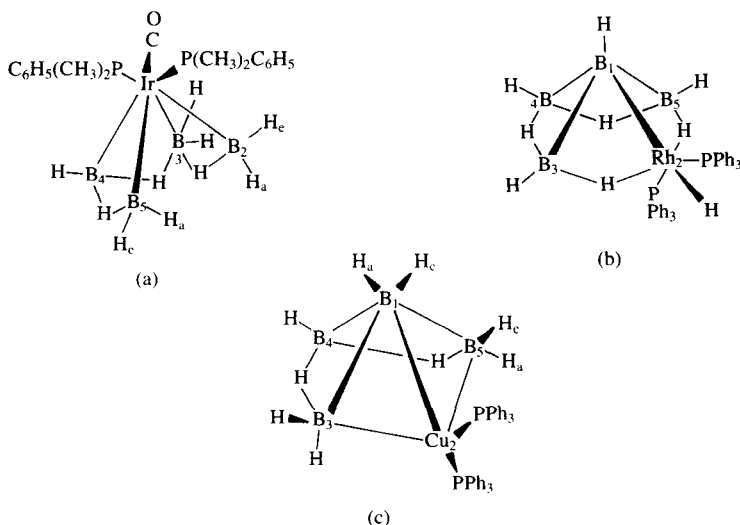


FIG. 22. Established structure of  $(B_4H_8)Ir(CO)(PhPMe_2)_2$  (a) and proposed structure of  $(B_4H_8)Rh(H)(Ph_3P)_2$  (b) and  $(B_4H_8)Cu(Ph_3P)_2$  (c).

(MePh)Fe(Et<sub>2</sub>-2,3-B<sub>4</sub>C<sub>2</sub>H<sub>4</sub>) is formed from iron vapour, toluene and Et<sub>2</sub>B<sub>4</sub>C<sub>2</sub>H<sub>6</sub>. The  $^{11}\text{B}$  NMR spectrum shows peaks at 8.1 (d, 147, 1B), 5.7 (d, 164, 1B) and 2.0 (d, 147, 2B) ppm, implying the presence of a mirror plane. The X-ray structure shows no such symmetry element and therefore, in solution, the carborane cage and toluene ring are likely to be rotating relative to one another.<sup>217</sup>

$^{11}\text{B}$  NMR data for recently reported B<sub>4</sub>C<sub>2</sub> metallocarboranes are collected in Table 27. These include (C<sub>8</sub>H<sub>8</sub>)Ti<sup>218</sup> and (olefin)Fe derivatives of Et<sub>2</sub>B<sub>4</sub>C<sub>2</sub>H<sub>5</sub>.<sup>219,220</sup> Copper-containing metallocarboranes, exemplified by (B<sub>4</sub>C<sub>2</sub>H<sub>7</sub>)Cu(PPh<sub>3</sub>)<sub>2</sub>, have been prepared, and it is considered that a (Ph<sub>3</sub>P)<sub>2</sub>Cu unit replaces one of the bridging hydrogens in 2,3-B<sub>4</sub>C<sub>2</sub>H<sub>8</sub>.<sup>221</sup> Their  $^{11}\text{B}$  spectra should be interpreted with care, since  $^{31}\text{P}$  NMR studies indicate that, even at low temperatures, rapid ligand-exchange processes occur.

A class of hybrid metallocarboranes, which eludes the taxonomy used in this review, contains Co(III) and both borane and carborane ligands, as exemplified by (Et<sub>2</sub>B<sub>4</sub>C<sub>2</sub>H<sub>4</sub>)Co(B<sub>5</sub>H<sub>10</sub>). Structures and numbering schemes are shown in Fig. 23, and  $^{11}\text{B}$  NMR data are presented in Table 28. Generally, the  $^{11}\text{B}$  spectra are composites in that the borane ligand has only a minor effect on the shifts of the 2,3-Et<sub>2</sub>B<sub>4</sub>C<sub>2</sub>H<sub>4</sub> group. Replacement of hydride by THF in B<sub>9</sub>H<sub>13</sub> leads to a large deshielding.<sup>222,223</sup>

TABLE 27

 $^{11}\text{B}$  NMR data for B<sub>4</sub>C<sub>2</sub> metallocarboranes.

Compound	$\delta^{11}\text{B}$
(C <sub>8</sub> H <sub>8</sub> )Ti(Et <sub>2</sub> B <sub>4</sub> C <sub>2</sub> H <sub>4</sub> )	22.1 (d, 125, B4, 6), 16.2 (d, 139, B3), -21.2 (d, 159, B1)
(C <sub>8</sub> H <sub>8</sub> )Ti(5-I-Et <sub>2</sub> B <sub>4</sub> C <sub>2</sub> H <sub>3</sub> )	17.7 (d, 124, B4, 6), 9.4 (s, B5), -21.3 (d, 167, B1)
(C <sub>8</sub> H <sub>8</sub> )Ti(4,5-I <sub>2</sub> -Et <sub>2</sub> B <sub>4</sub> C <sub>2</sub> H <sub>2</sub> )	17.2 (d, 145, 1B), 10.8 (s, 1B), 8.6 (s, 1B), -20.6 (d, 171, B1)
(C <sub>8</sub> H <sub>10</sub> )Fe(Et <sub>2</sub> B <sub>4</sub> C <sub>2</sub> H <sub>4</sub> )	10.7 (d, 141, 1B), 6.2 (d, 160, 1B), 3.1 (d, 149, 2B)
(C <sub>6</sub> H <sub>6</sub> )Fe(Et <sub>2</sub> B <sub>4</sub> C <sub>2</sub> H <sub>4</sub> )	2.5 (1B), 6.6 (d, 140, 1B), 3.5 (2B)
(C <sub>16</sub> H <sub>18</sub> )Fe(Et <sub>2</sub> B <sub>4</sub> C <sub>2</sub> H <sub>4</sub> )	12.5 (1B), 6.6 (1B), 3.2 (2B)
(C <sub>8</sub> H <sub>10</sub> )Fe(Et <sub>2</sub> B <sub>3</sub> C <sub>2</sub> H <sub>5</sub> )	3.5 (d, 130)
(C <sub>6</sub> H <sub>6</sub> )Fe(Et <sub>2</sub> B <sub>4</sub> C <sub>2</sub> H <sub>4</sub> )	12.5 (1B), 6.6 (d, 140, 1B), 3.5 (2B) (C <sub>6</sub> D <sub>6</sub> ); 6.2 (d, 158, 1B), 4.6 (d, 158, 1B), 1.1 (d, 134, 2B) (acetone)
(Me <sub>3</sub> Ph)Fe(Et <sub>2</sub> B <sub>4</sub> C <sub>2</sub> H <sub>4</sub> )	6.9 (d, 134, 1B), 3.0 (d, 152, 1B), 1.7 (d, 146, 2B)
(Me <sub>6</sub> C <sub>6</sub> )Fe(Et <sub>2</sub> B <sub>4</sub> C <sub>2</sub> H <sub>4</sub> )	8.7 (d, 135, 1B), 2.4 (d, 158, 2B), 0.8 (d, 179, 1B)
(Ph <sub>3</sub> P) <sub>2</sub> Cu(2,3-B <sub>4</sub> C <sub>2</sub> H <sub>7</sub> )	-0.4 (3B), -50.5 (d, 165, B1)
(Ph <sub>3</sub> P) <sub>2</sub> Cu(2,3-Me <sub>2</sub> B <sub>4</sub> C <sub>2</sub> H <sub>5</sub> )	-3.5, -0.9, -46.5 (d, 191, B1)
(diphos)Cu(2,3-B <sub>4</sub> C <sub>2</sub> H <sub>7</sub> )	2.4 (br, B4, 5), -5.7 (d, 180, B6), -56.4 (d, 173, B1)
(diphos)Cu(2,3-Me <sub>2</sub> B <sub>4</sub> C <sub>2</sub> H <sub>5</sub> )	3.2, -0.2 (B4, 5), -7.8 (d, 133, B6), -46.8 (d, 145, B1)

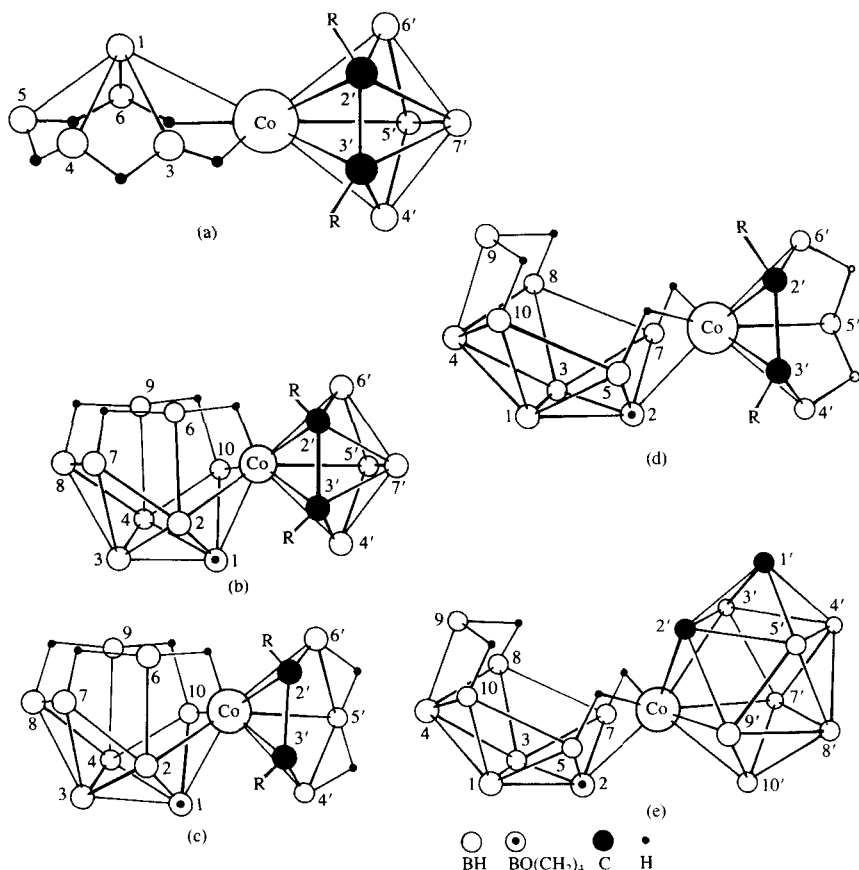


FIG. 23. (a) Proposed structure of  $[2,3\text{-Et}_2\text{C}_2\text{B}_4\text{H}_4]\text{-2-Co[B}_5\text{H}_{10}]$ ; (b) established structure of  $[2,3\text{-Et}_2\text{C}_2\text{B}_4\text{H}_4]\text{-5-Co[B}_9\text{H}_{12}\text{-1-O(CH}_2)_4]$ ; (c) established structure of  $[2,3\text{-Et}_2\text{C}_2\text{B}_3\text{H}_5]\text{-Co[B}_9\text{H}_{12}\text{-1-O(CH}_2)_4]$ ; (d) proposed structure of  $[2,3\text{-Et}_2\text{C}_2\text{B}_3\text{H}_5]\text{-6-Co[B}_9\text{H}_{12}\text{-2-O(CH}_2)_4]$ ; (e) established structure of  $[1,2\text{-Et}_2\text{C}_2\text{B}_7\text{H}_7]\text{-6-Co[B}_9\text{H}_{12}\text{-2-O(CH}_2)_4]$ .

Cobaltacarborane clusters containing the 4,6- or 4,5- $(\text{Me}_3\text{Si})_2\text{B}_6\text{C}_2\text{H}_6$  ligand have been prepared from Co atoms,  $\text{C}_5\text{H}_6$ ,  $\text{B}_6\text{H}_{10}$  and  $(\text{Me}_3\text{Si})_2\text{C}_2$ . One of the products,  $5:1',2'\text{-CpCo-2,3-(Me}_3\text{Si})_2\text{B}_4\text{C}_2\text{H}_3(\text{B}_2\text{H}_5)$  (cf. Table 28), is unusual in that it contains a  $\text{B}_2\text{H}_5$  unit linked to B5 in the  $\text{B}_4\text{C}_2$  cage by means of a  $\text{B-B-B}$  three-centre bond as shown in Fig. 24. Boron nuclei in this environment give rise to a poorly resolved signal at  $-7.0$  ppm.<sup>224</sup> Carbon-rich metalloboranes, e.g.  $1\text{-(Me}_6\text{C}_6)\text{Fe-4,5,7,8-Me}_4\text{B}_3\text{C}_4\text{H}_3$ , have been reported. In this example the cluster represents a  $2n+4$  skeletal electron system that adopts an *arachno* rather than a *nido* geometry.<sup>225</sup>

TABLE 28

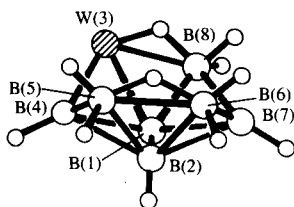
 $^{11}\text{B}$  NMR data for hybrid metallocarboranes.

Compound	$\delta^{11}\text{B}$
(Et <sub>2</sub> B <sub>4</sub> C <sub>2</sub> H <sub>4</sub> )-2-Co(B <sub>5</sub> H <sub>10</sub> )	34.1 (d, 112, B3, 6), 13.1 (d, 151, B4, 5, 5'), 5.5 (d, 139, B4', 6'), 2.2 (d, 161, B7'), -47.7 (d, 148, B1)
(Et <sub>2</sub> B <sub>4</sub> C <sub>2</sub> H <sub>4</sub> )-5-Co(B <sub>9</sub> H <sub>12</sub> -1-THF)	36.6 (s, 1B), 20.6 (d, 110, 1B), 14.2 (d, 128, 1B), 7.5 (d, 139, 2B), 5.3 (d, 133, 2B), -0.4 (d, 105, 2B), -3.5 (d, 151, 1B), -11.5 (d, 128, 1B), -27.1 (d, 139, 1B), -39.2 (d, 151, 1B)
(Et <sub>2</sub> B <sub>3</sub> C <sub>2</sub> H <sub>5</sub> )-5-Co(B <sub>9</sub> H <sub>12</sub> -1-THF)	36.7 (s, 1B), 19.2 (d, 110, 1B), 7.0 (d, 128, 1B), 3.2 (2B), 1.4 (1B), -0.7 (1B), -2.2 (d, 116, 1B), -3.2 (1B), -12.8 (d, 103, 1B), -26.4 (d, 116, 1B), -38.8 (d, 140, 1B)
(Et <sub>2</sub> B <sub>3</sub> C <sub>2</sub> H <sub>5</sub> )-6-Co-(B <sub>9</sub> H <sub>12</sub> -2-THF)	10.7 (d, 124, 2B), 8.3 (d, 140, 2B), 4.4 (3B), 1.7 (1B), -3.1 (d, 130, 2B), -6.5 (d, 147, 1B), -38.4 (d, 154, 1B)
(Et <sub>2</sub> B <sub>7</sub> C <sub>2</sub> H <sub>7</sub> )-6-Co(B <sub>9</sub> H <sub>12</sub> -2-THF)	78.8 (d, 165, 1B), 10.7 (d, 141, 1B), 8.5 (d, 126, 2B), 7.3 (1B), 3.0 (2B), -2.1 (d, 130, 2B), -3.9 (d, 124, 2B), -9.3 (d, 156, 1B), -18.8 (d, 137, 1B), -22.9 (d, 151, 1B), -24.8 (d, 140, 1B), -34.9 (d, 148, 1B)
1-CpCo-4,6-(Me <sub>3</sub> Si) <sub>2</sub> B <sub>6</sub> C <sub>2</sub> H <sub>6</sub>	27.4 (d, 154, 1B), 10.6 (d, 138, 2B), -2.2 (d, 154, 2B), -10.3 (d, 154, 1B)
1-CpCo-4,5-(Me <sub>3</sub> Si) <sub>2</sub> B <sub>6</sub> C <sub>2</sub> H <sub>6</sub>	72.0 (d, 144, 1B), 7.1 (d, 173, 1B), -1.6 (d, 183, 1B), -4.7 (d, 183, 1B), -13.4 (d, 164, 1B), -18.0 (d, 161, 1B)
5:1', 2'-CpCo-2,3-(Me <sub>3</sub> Si) <sub>2</sub> B <sub>4</sub> C <sub>2</sub> H <sub>3</sub> (B <sub>2</sub> H <sub>5</sub> )	13.8 (d, 186, 2B), 4.5 (d, 164, 1B), -7.0 (m, 3B)
1-(Me <sub>6</sub> C <sub>6</sub> )Fe-2,3-Me <sub>2</sub> B <sub>4</sub> C <sub>2</sub> H <sub>4</sub>	9.8 (d, 134, 1B), 4.3 (d, 141, 2B), 3.7 (d, 128, 1B)
1-(Me <sub>6</sub> C <sub>6</sub> )Fe-4,5,7,8-Me <sub>4</sub> B <sub>3</sub> C <sub>4</sub> H <sub>3</sub>	14.8 (d, 156, 1B), -12.2 (d, 129, 2B)
1-(MePh)Fe-4,5,7,8-Me <sub>4</sub> B <sub>3</sub> C <sub>4</sub> H <sub>3</sub>	16.1 (d, 156, 1B), -12.7 (d, 125, 2B)
2-(MePh)Fe-6,7,9,10-Me <sub>4</sub> B <sub>5</sub> C <sub>4</sub> H <sub>5</sub>	14.1 (d, 156, 1B), 6.2 (d, 141, 1B), 1.6 (d, 166, 1B)

**C. B<sub>5,7,8</sub> metalloboranes and metallocarboranes**

Two metal-substituted pentaborane compounds have been prepared: 2-CpFe(CO)<sub>2</sub>B<sub>5</sub>H<sub>8</sub> has  $\delta^{11}\text{B}$  = 7.6 (s, B2), -11.0 (d, 159, B3,5), -14.8 (d, 164, B4) and -48.6 (d, 169, B1); while the corresponding shifts for 2-(CO)<sub>4</sub>CoB<sub>5</sub>H<sub>8</sub> are -4.5(s), -11.0 (d, 133), -14.5 (d, 171) and -49.0



FIG. 25. Structure of  $(\text{CO})_4\text{WB}_7\text{H}_{12}^-$ .

From  $\text{B}_9\text{H}_{12}^-$  and *trans*-( $\text{Me}_3\text{P}$ ) $_2\text{Ir}(\text{CO})\text{Cl}$  a number of  $\text{B}_8$  iridaboranes have been obtained a plethora of  $\text{B}_8$  iridaboranes, exemplified by  $\text{B}_8\text{H}_{12}\text{IrH}(\text{CO})(\text{PMe}_3)_2$ . Non-equivalence of B5, 9, B6, 8 and B2, 3 in this compound is attributed to asymmetry associated with disposition of ligands about the six-coordinate iridium atom, cf. Fig. 26.<sup>231</sup> Thermal elimination of hydrogen from  $\text{B}_8\text{H}_{12}\text{IrH}(\text{CO})(\text{PMe}_3)_2$  (and related compounds) produces  $\text{B}_8\text{H}_{11}\text{Ir}(\text{CO})-(\text{PMe}_3)_2$ , a *nido* nine-vertex metalloborane (Fig. 26a).<sup>232</sup>  $^{11}\text{B}$  chemical-shift data are given in Table 29. Assignment of B5 follows from observation of its coupling to the  $-14.5$  ppm  $\text{B}-\text{H}-\text{Ir}$  proton. Deprotonation of  $\text{B}_8\text{H}_{12}\text{IrH}(\text{CO})(\text{PMe}_3)_2$  and condensation with  $\text{Cl}_2\text{Pt}(\text{PMe}_3)_2$  affords the mixed bimetalloborane  $\text{B}_8\text{H}_{10}[\text{IrH}(\text{CO})-(\text{PMe}_3)_2][\text{Pt}(\text{PMe}_3)_2]$  (Fig. 26b). Its  $^{11}\text{B}$  NMR parameters are similar to those of  $\text{B}_8\text{H}_{10}[\text{Pt}(\text{PMe}_2\text{Ph})_2]_2$ .<sup>233</sup> Two gold-containing  $\text{B}_8$  metalloboranes  $4-(\text{S}_2\text{CNet}_2)\text{AuB}_8\text{H}_{12}$  and  $6,9-[(\text{S}_2\text{CNet}_2)\text{Au}]_2\text{B}_8\text{H}_{10}$  have been reported.<sup>234</sup>

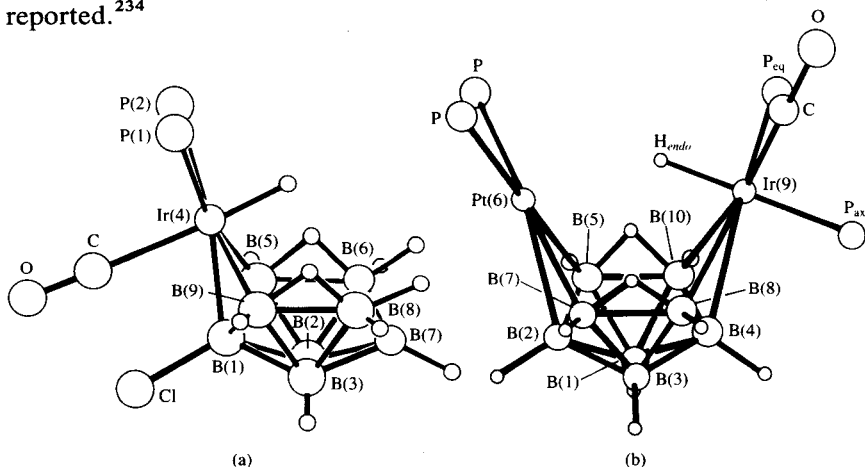


FIG. 26. (a) Schematic view of the molecular structure of  $[(\text{HIrB}_8\text{H}_{11}\text{Cl})(\text{CO})(\text{PMe}_3)_2]$ , with cluster hydrogen atoms (evident from NMR spectroscopy) drawn in but with *P*-methyl groups omitted. (b) Representation of the proposed molecular structure of *arachno*- $[(\text{PMe}_3)_2\text{PtB}_8\text{H}_{10}\text{IrH}(\text{PMe}_3)_2(\text{CO})]$ .

TABLE 29

<sup>11</sup>B NMR data for B<sub>8</sub> metalloboranes.

Compound	δ <sup>11</sup> B
B <sub>8</sub> H <sub>11</sub> Ir(CO)(PMe <sub>3</sub> ) <sub>2</sub>	23.1, 8.8, -5.3, -13.6, -14.5, -15.3, -39.9 (B5), -52.5
B <sub>8</sub> H <sub>10</sub> ClIr(CO)(PMe <sub>3</sub> ) <sub>2</sub>	22.6, 13.5, 1.1 (B—Cl), -3.5, -9.0, -14.2, -47.4
B <sub>8</sub> H <sub>11</sub> Ir(PMe <sub>3</sub> ) <sub>3</sub>	26.9, 10.1, -3.4, -15.0, -16.2, -40.5, -49.8
B <sub>8</sub> H <sub>12</sub> [IrH(CO)(PMe <sub>3</sub> ) <sub>2</sub> ] [Pt(PMe <sub>3</sub> ) <sub>2</sub> ]	25.2 (B2, J(Pt—B) = 280), 15.9 B(4), -4.0, -5.0 (B5, 7), -9.5, -12.3 (B8, 10), -27.1, -28.9 (B1, 3)
B <sub>8</sub> H <sub>12</sub> IrH(CO)(PMe <sub>3</sub> ) <sub>2</sub>	17.7 (B7), 10.0 (B1), -13.3, -12.0 (B5, 9), -22.1, -26.9 (B6, 8), -32.8, -40.5 (B2, 3)
B <sub>8</sub> H <sub>11</sub> ClIrH(CO)(PMe <sub>3</sub> ) <sub>2</sub>	18.1 (B7), 24.1 (B—Cl), -11.9 (B5, 9), -24.0 (B6, 8), -32.8 (B2, 3)
B <sub>8</sub> H <sub>12</sub> IrH(PMe <sub>3</sub> ) <sub>3</sub>	18.3 (B7), 12.0 (B1), -12.7 (B5, 9), -24.3 (B6, 8), -35.7 (B2, 3)
B <sub>8</sub> H <sub>12</sub> Pt(PPh <sub>3</sub> ) <sub>2</sub>	22.0 (B1), 18.0 (B7), 2.0 B(5, 9), -24.4 (B6, 8), -30.6 (B2, 3)
B <sub>8</sub> H <sub>12</sub> Pd(PPh <sub>3</sub> ) <sub>2</sub>	22.5 (B1), 15.4 (B7), 5.5 (B5, 9), -22.3 (B6, 8), -29.4 (B2, 3)
B <sub>8</sub> H <sub>10</sub> [Pt(PMe <sub>2</sub> Ph) <sub>2</sub> ] <sub>2</sub>	28.1 (B2, 4, J(Pt—B) = 300), 0.7 (B5, 7, 8, 10, J(Pt—B) = 280), -19.3 (B1, 3)
B <sub>8</sub> H <sub>10</sub> PdPt(PMe <sub>2</sub> Ph) <sub>4</sub>	32 (B2), 30 (B4), 8.5 (B5, 7), 2 (B8, 10), -1.6 (B1, 3)
4-(S <sub>2</sub> CNEt <sub>2</sub> )AuB <sub>8</sub> H <sub>12</sub>	18.8 (d, 130, B1), 9.5 (d, 130, B7), -15.9 (d, 130, B5, 6, 8, 9), -35.7 (d, 150, B2, 3)
6,9-[(S <sub>2</sub> CNEt <sub>2</sub> )Au] <sub>2</sub> B <sub>8</sub> H <sub>10</sub>	34.5 (d, 120, B2, 4), 8.7 (d, 100, B5, 7, 8, 10), -16.9 (d, 130, B1, 3)
5,8-(CpCo) <sub>2</sub> B <sub>8</sub> H <sub>12</sub>	33.2 (d, 130, 2B), 26.1 (d, 102, 2B), 11.0 (d, 132, 2B), -11.3 (d, 134, 2B)
2,4-(CpCo) <sub>2</sub> B <sub>8</sub> H <sub>12</sub>	21.5 (d, 128, 2B), 12.3 (d, 146, 2B), 3.5 (d, 140, 4B)

TABLE 30

<sup>11</sup>B NMR data for some arene metallocarboranes.

Compound (MHz, solvent)	Relative areas	δ <sup>11</sup> B (J(B—H))
2,5,6-(η-C <sub>6</sub> H <sub>6</sub> )RuC <sub>2</sub> B <sub>7</sub> H <sub>11</sub> (115.8, C <sub>6</sub> D <sub>6</sub> )	1 : 1 : 1 : 1 : 1 : 1 : 1	12.5 (142), 9.8 (140), 5.3, 3.8, -2.4 (135), -5.7 (146), -38.5 (149)
1,2,4-(η-C <sub>6</sub> H <sub>6</sub> )RuC <sub>2</sub> B <sub>8</sub> H <sub>10</sub> (115.8, CH <sub>2</sub> Cl <sub>2</sub> )	1 : 1 : 1 : 1 : 1 : 1 : 1 : 1	62.5 (152), 11.7 (142), -0.8 (152), -2.0 (126), -14.0 (154), -20.7, -26.3 (146), -43.2 (149)
3,1,2-(η-C <sub>6</sub> H <sub>6</sub> )OsC <sub>2</sub> B <sub>9</sub> H <sub>11</sub> (70.6, CD <sub>3</sub> CN)	1 : 1 : 2 : 2 : 2 : 1	-0.2 (142), -6.8 (138), -11.4 (127), -13.3 (144), -21.5 (151), -25.8 (164)
3,1,2-[endo-H-η <sup>5</sup> -(CH <sub>3</sub> ) <sub>6</sub> H]- CoC <sub>2</sub> B <sub>9</sub> H <sub>11</sub> (115.8, CDCl <sub>3</sub> )	1 : 1 : 4 : 2 : 1	7.8 (139), -3.5 (142), -6.7 (136), -18.4 (154), -23.4 (167)

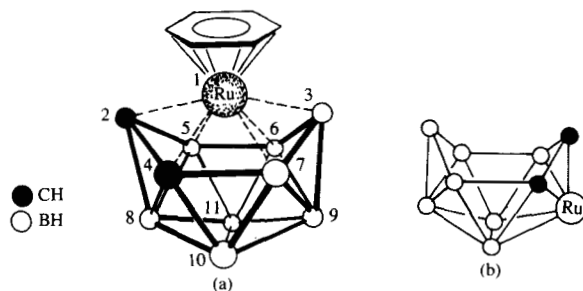


FIG. 27. (a) Proposed structure of  $1,2,4-(\eta\text{-C}_6\text{H}_6)\text{RuC}_2\text{B}_8\text{H}_{10}$ . (b) Heavy-atom skeleton of  $1,2,4-(\text{C}_6\text{H}_6)\text{RuB}_7\text{C}_2\text{H}_{11}$ , with arene ring omitted.

Oxidative fusion of  $\text{CpCoB}_4\text{H}_7$  yields  $(\text{CpCo})_2\text{B}_8\text{H}_{12}$ . The 5,8 and 2,4, isomers are characterized by  $^{11}\text{B}$  NMR; the 1,5 and 1,7 isomers have been isolated but are not differentiated.<sup>235</sup>

Degradation of  $(\text{C}_6\text{H}_6)\text{RuB}_9\text{C}_2\text{H}_{11}$  with ethanolic KOH produces  $1,2,4-(\text{C}_6\text{H}_6)\text{RuB}_8\text{C}_2\text{H}_{10}$  and  $2,5,6-(\text{C}_6\text{H}_6)\text{RuB}_7\text{C}_2\text{H}_{11}$ . The proposed structure of the former and the established structure of the latter are shown in Fig. 27, and the  $^{11}\text{B}$  NMR data are given in Table 30.<sup>236</sup>

A series of  $\text{B}_7\text{C}_2$  metalloboranes has been synthesized by condensation of metal atoms (Fe, Co, Ni) with  $2,6\text{-B}_7\text{C}_2\text{H}_{11}$  and a hydrocarbon ligand. The  $^{11}\text{B}$  data are collected in Table 31. A new isomer of  $\text{CpCoB}_7\text{C}_2\text{H}_9$  has been isolated. A 1 : 2 : 2 : 2 pattern of  $^{11}\text{B}$  resonances (at 64 MHz) is indicative of

TABLE 31

 $^{11}\text{B}$  NMR data for  $\text{B}_7\text{C}_2$  metalloboranes.

Compound	$\delta^{11}\text{B}$
2-CpCo-1,4- $\text{B}_7\text{C}_2\text{H}_9$	27.5 (d, 110, 1B), 9.3 (d, 169, 2B), 5.6 (d, 173, 2B), -13.6 (d, 177, 2B)
4-CpCo-2,3- $\text{B}_7\text{C}_2\text{H}_{13}$	13.1 (d, 141), 0.2 (d, 148), -7.9 (d, 148), -10.1 (d, 148), -12.3 (d, 133, 54), -18.7 (d, 134), -32.5 (d, 154)
2-(PhMe)Fe-6,9- $\text{B}_7\text{C}_2\text{H}_9$	81.3 (d, 148, 1B), -2.9 (d, 155, 1B), -10.6 (d, 146, 2B), -22.9 (d, 167, 1B), -30.2 (d, 148, 2B)
2-(PhMe)Fe-1,6- $\text{B}_7\text{C}_2\text{H}_9$	20.4 (d, 180), -3.9 (d, 143), -8.2 (d, 153), -19.8 (d, 153), -26.2 (d, 107), -26.9 (d, 156), -33.7 (d, 153)
2-(Me <sub>3</sub> Ph)Fe-1,6- $\text{B}_7\text{C}_2\text{H}_9$	20.2 (d, 155), -4.5 (d, 118), -7.8 (d, 150), -19.5 (d, 131), -25.1 (d, 168), -26.6 (d, 156), -33.1 (d, 171)
6-(Me <sub>3</sub> Ph)Fe-9,10- $\text{B}_7\text{C}_2\text{H}_{11}$	24.7 (d, 141), 10.2 (d, 150), 8.8 (d, 147), 4.3 (d, 137), 1.9 (m), -16.4 (d, 110), -17.6 (d, 146)
(Me <sub>4</sub> C <sub>4</sub> H)Ni-5,7,8-Me <sub>3</sub> B <sub>7</sub> C <sub>3</sub> H <sub>7</sub>	8.1 (d, 158), -1.2 (d, 150), -5.0, -5.9 (d, 184), -7.3 (d, 161), -13.9 (d, 167), -15.3 (d, 159)

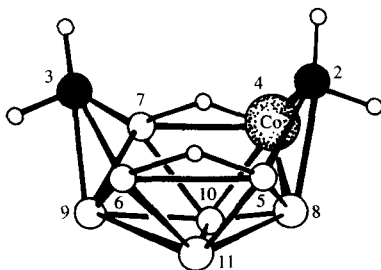
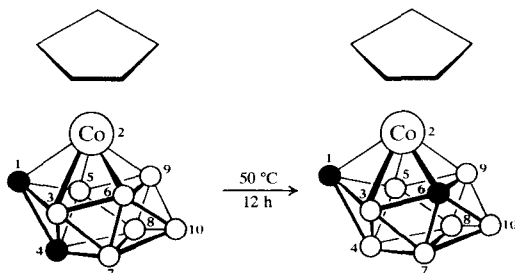


FIG. 28. Proposed structure of  $(4-\eta\text{-C}_5\text{H}_5)\text{Co}-2,3\text{-C}_2\text{B}_7\text{H}_{13}$ . Terminal B—H hydrogens and the  $\eta^5\text{-C}_5\text{H}_5$  group are not shown.

a mirror plane of symmetry; and the absence of very high frequency peaks implies that one carbon atom occupies the four-coordinate position adjacent to cobalt; see Fig. 28 for the numbering scheme. The remaining carbon atom must therefore lie on the mirror plane, i.e. the compound contains either a 1,10- or 1,4- $\text{B}_7\text{C}_2\text{H}_9$  ligand. Because the former has been reported, it is concluded that 2-CpCo-1,4- $\text{B}_7\text{C}_2\text{H}_9$  has been obtained. It is not rigorously excluded that identification of the two isomers could be interchanged. A proposed structure of 4-CpCo-2,3- $\text{B}_7\text{C}_2\text{H}_{13}$  (Fig. 28) is advanced on the basis of a partial crystal structure and of a 2D  $^{11}\text{B}$  NMR spectrum. In the latter the expected B7–B10 and B10–B11 cross peaks are not observed. This occasionally happens and serves as a reminder that caution must be used in the interpretation of 2D spectra. As an additional cautionary note, putative 2-CpCo-1,4- $\text{B}_7\text{C}_2\text{H}_9$  rearranges to the 2,1,6 isomer on standing at room temperature:



In some cases, it is possible that such isomerizations may occur during TLC separation or, worse, during crystal-growth procedures. The structure 2-(MePh)Fe-1,6- $\text{B}_7\text{C}_2\text{H}_9$  has been determined. Gross similarity of its  $^{11}\text{B}$  chemical shifts to those of other (arene)Fe and CpCoB $_7$ C $_2$  metallocarboranes supports the NMR identification of 2-CpCo-1,6- $\text{B}_7\text{C}_2\text{H}_9$ . A quite unusual C $_3$  metallocarborane  $(\text{Me}_4\text{C}_4\text{H})\text{Ni}-5,7,8\text{-Me}_3\text{B}_7\text{C}_3\text{H}_7$  has

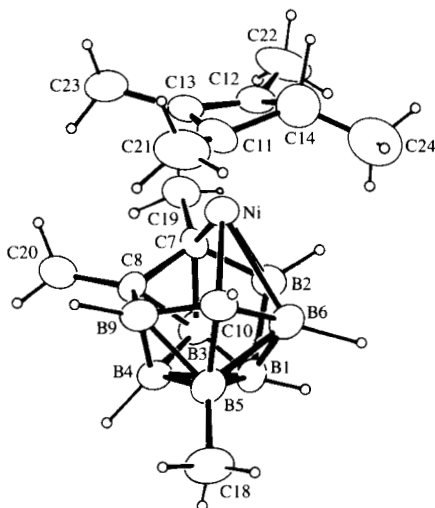
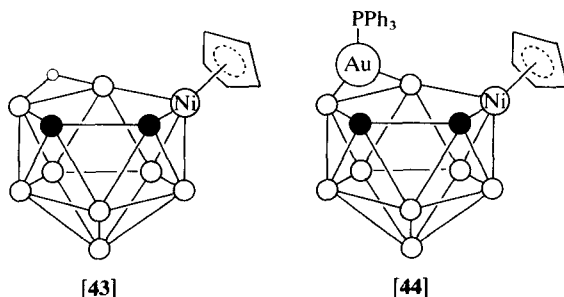


FIG. 29. ORTEP drawing of 5,7,8-Me<sub>3</sub>-11,7,8,10-[7<sup>3</sup>-C<sub>4</sub>Me<sub>4</sub>H]NiC<sub>3</sub>B<sub>7</sub>H<sub>7</sub>.

been obtained from Ni atoms, 2-butyne and 2,6-B<sub>7</sub>C<sub>2</sub>H<sub>11</sub>. Its structure is shown in Fig. 29.<sup>237</sup>

The reaction of Li[Me<sub>5</sub>Cp], CoCl<sub>2</sub> and B<sub>5</sub>H<sub>8</sub><sup>-</sup> or B<sub>9</sub>H<sub>14</sub><sup>-</sup> generates, like the C<sub>5</sub>H<sub>5</sub><sup>-</sup> systems, an enormous number and variety of metalloboranes. <sup>11</sup>B NMR data for these compounds are collected in Table 32, even though it is organizationally untidy to lump them all together. Among these a 5,7-(Me<sub>5</sub>CpCo)<sub>2</sub>B<sub>8</sub>H<sub>12</sub>, a structural analogue of B<sub>10</sub>H<sub>14</sub>, exhibits a signal of unit area at 57.3 ppm that is assigned to B6, the unique boron atom between the two cobalt atoms. This assignment is supported by the presence of a 49.9 ppm singlet in the <sup>11</sup>B NMR spectrum of the 6-chloro derivative. Deshielding is less pronounced when B6 is adjacent to only one cobalt atom as in 5-Me<sub>5</sub>CpCoB<sub>9</sub>H<sub>13</sub>. The structures of these materials, where they have been determined, are similar to those of the cyclopentadienyl counterparts.<sup>238-240</sup> B<sub>8</sub>C metalloboranes have been prepared by metal-insertion reactions of 4-B<sub>8</sub>CH<sub>12</sub> (see Table 32).<sup>241</sup>

Metallocarboranes have been prepared by successive replacement of B—H—B bridges in 5,6-B<sub>8</sub>C<sub>2</sub>H<sub>12</sub> with transition-metal fragments. Thus this carborane reacts with Cp<sub>2</sub>Ni to form 7,8,9-CpNiB<sub>8</sub>C<sub>2</sub>H<sub>11</sub>, [43],  $\delta^{11}\text{B} = 19.3$  (d, 142), 13.7 (d, 156), 3.4 (d, 156), -2.7 (br d, 151), -7.9 (dd, 149, 46), -17.5 (br d, 117), -19.7 (br d, 161 and -22.2 (Br d, 156). Subsequent gold insertion using Ph<sub>3</sub>PAuMe yields (CpNi)(Ph<sub>3</sub>PAu)-B<sub>8</sub>C<sub>2</sub>H<sub>10</sub>, [44],  $\delta^{11}\text{B} = 13.2$  (1B), 7.0 (1B), 3.0 (1B), 1.1 (1B), -13.3 (1B), -16.4 (1B) and -20.8 (2B).<sup>242</sup>



Platinum insertion into 5,6-B<sub>8</sub>C<sub>2</sub>H<sub>12</sub> produces (Et<sub>3</sub>P)<sub>2</sub>Pt(H)B<sub>8</sub>C<sub>2</sub>H<sub>11</sub>,  $\delta^{11}\text{B} = 8.9$  (2B),  $-11.9$  (2B),  $-26.8$  (4B). On heating, this compound eliminates hydrogen and undergoes a rearrangement that transfers one Et<sub>3</sub>P ligand from platinum to the adjacent B9 position, thus forming (Et<sub>3</sub>P)Pt(H)(9-Et<sub>3</sub>PB<sub>8</sub>C<sub>2</sub>H<sub>9</sub>),  $\delta^{11}\text{B} = 9.4$  ( $J(\text{Pt}-\text{B}) = 275$ ),  $8.9$ ,  $4.8$  ( $J(\text{Pt}-\text{B}) = 261$ ),  $-0.5$ ,  $-14.2$  ( $J(\text{Pt}-\text{B}) = 387$ ),  $-14.9$  ( $J(\text{P}-\text{B}) = 122$ ),  $-21.8$ ,  $-24.4$  ( $J(\text{Pt}-\text{B}) = 326$ ). The B9 resonance may be recognized by the <sup>31</sup>P-<sup>11</sup>B coupling. It is interesting that <sup>195</sup>Pt-<sup>11</sup>B coupling is observed in one compound but not the other.<sup>243</sup>

TABLE 32

<sup>11</sup>B NMR data for metalloboranes.

Compound	$\delta^{11}\text{B}$
Me <sub>5</sub> CoCpB <sub>9</sub> H <sub>13</sub>	20.5 (d, 107, 2B), 15.4 (d, 136, 2B), 5.2 (d, 143, 1B), -1.2 (d, 143, 2B), -12.4 (d, 139, 1B), -29.8 (d, 148, 1B)
(Me <sub>5</sub> CpCo) <sub>2</sub> B <sub>8</sub> H <sub>12</sub>	20.8 (d, 116, 6B), 2.3 (d, 134, 2B)
5,7-(Me <sub>5</sub> CpCo) <sub>2</sub> B <sub>8</sub> H <sub>12</sub>	57.3 (1B), 24.4 (3B), 6.0 (2B), 7.4 (1B), -40.3 (d, 139, 1B)
6-Cl-5,7-(Me <sub>5</sub> CpCo) <sub>2</sub> B <sub>8</sub> H <sub>11</sub>	49.9 (s, 1B), 23.1 (d, 124, 2B), 19.4 (d, 94, 1B), 7.1 (2B), -7.1 (1B), -40.7 (d, 141, 1B)
2-Me <sub>5</sub> CpCoB <sub>4</sub> H <sub>8</sub>	2.7 (d, 137, 1B), -13.6 (d, 135, 3B)
1,2-(Me <sub>5</sub> CpCo) <sub>2</sub> B <sub>4</sub> H <sub>6</sub>	63.8 (d, 140, B4, 6), 17.4 (d, 127, B3, 5)
1,2,3-(Me <sub>5</sub> CpCo) <sub>3</sub> B <sub>4</sub> H <sub>4</sub>	154.1 (B7), 91.0 (d, 140, B4, 5, 6)
1,2-(Me <sub>5</sub> CpCo) <sub>2</sub> B <sub>5</sub> H <sub>7</sub>	31.5 (d, 102, B4, 5), 26.3 (d, 89, B3, 6?), 17.5 (d, 122, B7)
(Me <sub>5</sub> CpCo) <sub>3</sub> B <sub>5</sub> H <sub>6</sub>	62.5 (d, 137, B2, 4, 5), 23.8 (B6), 18.4 (d, 112, B7)
5,9-(Me <sub>5</sub> CpCo) <sub>2</sub> B <sub>8</sub> H <sub>12</sub>	32.7 (d, 140), 30.3, 27.9, 24.6, 16.3 (d, 128), 8.6 (d, 93)
1-Me <sub>5</sub> CpCoB <sub>4</sub> H <sub>8</sub>	-2.9 (d, 158)
1,2-(Me <sub>5</sub> CpCo) <sub>2</sub> B <sub>5</sub> H <sub>5</sub>	135.6 (d, <i>ca.</i> 174, B7), 96.3 (d, 140, B5), 76.6 (d, 140, B4, 6), 2.9 (d, 128, B3)
6-CpNi-1-B <sub>8</sub> CH <sub>9</sub>	76.5 (d, 1B), 2.0 (d, 2B), -1.4 (d, 1B), -17.0 (d, 2B), -19.1 (d, 2B)
10-CpNi-1-B <sub>8</sub> CH <sub>9</sub>	2.4 (d, 160, 4B), 26.9 (d, 145, 4B)
Me <sub>4</sub> N-[2-CpCo-1-B <sub>8</sub> CH <sub>9</sub> ]	34.2 (d, 148, 1B), 2.3 (d, 142, 1B), 0.4 (d, 136, 2B), -21.3 (d, 140, 2B), -25.5 (d, 136, 2B)

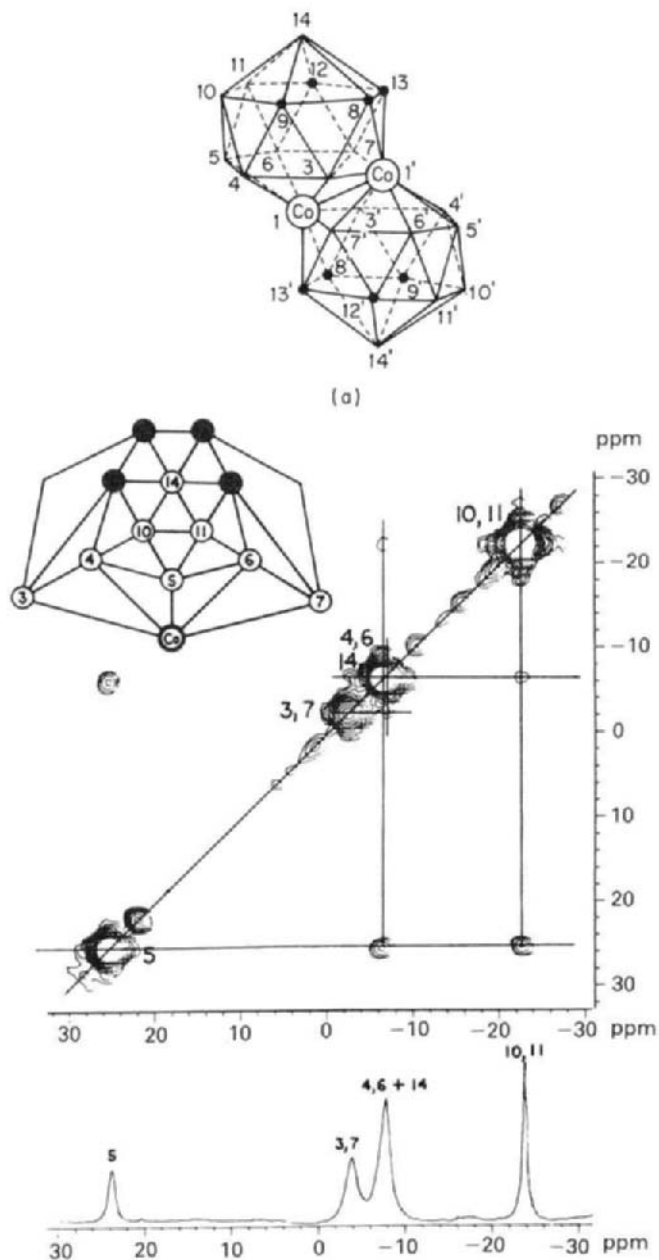


FIG. 30. (a) Proposed structure of  $(\text{Et}_4\text{B}_8\text{C}_4\text{H}_8)_2\text{Co}_2$ . (b) 115.8 MHz 2D  $^{11}\text{B}$  NMR spectrum of  $(\text{Et}_4\text{B}_8\text{C}_4\text{H}_8)_2\text{Co}_2$ . The connectivity diagram is shown as an inset and the normal 1D spectrum is at the bottom.

Research in the area of tetracarbon carboranes has continued to produce novel boron compounds.  $^{11}\text{B}$  NMR data for some of these are collected in Table 33. From  $\text{Et}_4\text{B}_8\text{C}_4\text{H}_8^{2-}$  and  $\text{CoCl}_2$  is obtained, *inter alia*,  $(\text{Et}_4\text{B}_8\text{C}_4\text{H}_8)_2\text{Co}_2$ , which is considered to contain two  $\text{B}_8\text{C}_4\text{Co}$  cages edge-fused so that a Co—Co vector forms the common edge (Fig. 30a). This structure is supported by the 2D  $^{11}\text{B}$  NMR spectrum (see Fig. 30b) in that all of the expected off-diagonal peaks are found within the limits of resolution. Also formed in the same reaction is a paramagnetic isomer of  $(\text{Et}_4\text{B}_8\text{C}_4\text{H}_7)_2\text{Co}_2$ . When  $\text{B}_5\text{H}_8^-$  is included in the reaction mixture, a diamagnetic isomer I of  $(\text{Et}_4\text{B}_8\text{C}_4\text{H}_7)_2\text{Co}_2$  is obtained. Its  $^{11}\text{B}$  NMR spectrum contains two singlets associated with a B—B bond between two nonequivalent boron cage positions; diamagnetism presumably arises from spin pairing between two cobalt atoms in close proximity. In solution rearrangement to the diamagnetic isomer II occurs. Also formed in these very complicated reactions are  $(\text{Et}_4\text{B}_8\text{C}_4\text{H}_7)_2\text{CoH}$  and  $(\text{Et}_4\text{B}_8\text{C}_4\text{H}_8)\text{CoH}(\text{Et}_4\text{B}_4\text{C}_5\text{H}_6)$ . The former exhibits in its  $^{11}\text{B}$  NMR spectrum eight peaks of unit area, including one singlet. Iodine in acetone reacts with  $(\text{Et}_4\text{B}_8\text{C}_4\text{H}_8)_2\text{Co}_2$  to yield a variety of products, including three hydroxyl-substituted derivatives. Also formed is  $(\text{Et}_4\text{B}_8\text{C}_4\text{H}_7)_2(\text{Me}_2\text{CO})_2\text{CoH}$ , whose structure (Fig. 31) reveals terminal and bridging acetone ligands.<sup>244</sup>

Condensation of  $\text{Et}_4\text{B}_8\text{C}_4\text{H}_8^{2-}$ ,  $\text{Et}_2\text{B}_4\text{C}_2\text{H}_5^-$  and  $\text{CoCl}_2$  produces numerous metallocarboranes (see Table 33), whose structural schematics are depicted in Fig. 32. These include  $(\text{Et}_4\text{B}_8\text{C}_4\text{H}_8)_2(\text{THF})\text{CoH}$ , whose  $^{11}\text{B}$  NMR spectrum matches that of  $(\text{Et}_4\text{B}_8\text{C}_4\text{H}_7)_2\text{CoH}$  except that the B(12, 13) and B(10, 13) cross-peaks in the 2D spectrum of the former are absent in that of the latter. The data are accommodated by the proposed structures (Fig. 33a,b). The two missing cross-peaks indicate the presence of

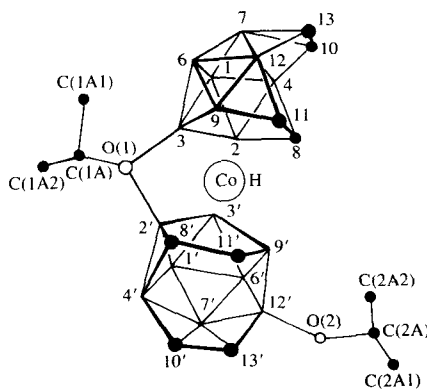


FIG. 31. Structure of  $(\text{Et}_4\text{B}_8\text{C}_4\text{H}_7)_2(\text{Me}_2\text{CO})_2\text{CoH}$ .

TABLE 33

 $^{11}\text{B}$  NMR data for metallocarboranes derived from  $\text{B}_5\text{C}_4\text{H}_6^{2-}$ .

Compound	$\delta^{11}\text{B}$
$(\text{Et}_4\text{B}_8\text{C}_4\text{H}_8)_2\text{Co}_2$	23.7 (d, 125, 1B), -3.9 (d, 65, 2B), -7.8 (d, 115, 3B), -23.9 (d, 136, 2B)
$(\text{Et}_4\text{B}_8\text{C}_4\text{H}_7)_2\text{Co}_2$ (I)	28.5 (s, 1B), 18.8 (d, 123, 1B), 6.9 (s, 1B), -3.8, -8.1, -7.7 (9B), -21.0 (d, 163, 1B), -25.1 (d, 138, 1B), -27.6 (d, 137, 1B), -30.2 (d, 146, 1B)
$(\text{Et}_4\text{B}_8\text{C}_4\text{H}_7)_2\text{Co}_2$ (II)	19.8 (d, 124, 1B), 6.1 (s, 3B), -1.0 (d, 140, 1B), -4.5 (2B), -13.2 (d, 131, 2B), -15.4 (d, 146, 1B), -18.1 (d, 136, 1B), -23.3 (1B), -24.5 (d, 143, 2B), -28.9 (d, 143, 2B)
$(\text{Et}_4\text{B}_8\text{C}_4\text{H}_7)_2(\text{Me}_2\text{CO})_2\text{CoH}$	27.1 (s, 1B), 16.2 (d, 132, 1B), 6.6 (s, 1B), 3.8 (s, 1B), -4.1 (d, 172, 2B), -6.5 (d, 139, 1B), -7.7 (d, 126, 1B), -8.7 (d, 145, 1B), -12.2 (d, 112, 1B), -13.0 (d, 129, 1B), -14.3 (d, 132, 1B), -20.3 (d, 136, 1B), -26.0 (d, 144, 1B), -28.1 (d, 129, 1B), -29.1 (d, 104, 1B)
$(\text{Et}_4\text{B}_8\text{C}_4\text{H}_7)_2(\text{OH})\text{Co}$ (I)	28.6 (s, 1B), 18.9 (s, 1B), -4.1 (d, 137), -11.2, -15.4, -16.8, -19.8 (2B), -28.3 (d, 141, 3B)
$(\text{Et}_4\text{B}_8\text{C}_4\text{H}_7)_2(\text{OH})\text{Co}$ (II)	12.9 (s, 1B), 5.5 (s, 1B), 1.7 (d, 146, 1B), -3.0 (d, 130, 1B), -14.7 (d, 149, 2B), -16.5 (d, 186, 2B), -17.9 (d, 150, 2B)
$(\text{Et}_4\text{B}_8\text{C}_4\text{H}_7)_2\text{CoH}$ (I)	35.6 (s, 2B), 9.3 (d, 160, 2B), 1.8 (d, 169, 2B), -7.0 (d, 146, 2B), -8.3 (d, 163, 2B), -15.7 (d, 159, 2B), -26.1 (d, 159, 2B), -43.7 (d, 148, 2B)
$(\text{Et}_4\text{B}_8\text{C}_4\text{H}_8)\text{Co}(\text{Et}_4\text{B}_4\text{C}_2\text{H}_6)$	32.7 (s, 1B), 19.0 (d, 148, 1B), -10.3 (6B), -23.7 (d, 145, 2B), -25.9 (d, 133, 2B)
$(\text{Et}_4\text{B}_8\text{C}_4\text{H}_8)_2(\text{THF})\text{CoH}$	35.6 (s), 8.9 (d, 126), 1.9 (d, 168), -6.7 (d, 149), 8.5, -15.6 (d, 152), -25.5 (d, 159), -43.7 (d, 149)
$(\text{Et}_4\text{B}_8\text{C}_4\text{H}_7)_2\text{CoH}$ (second isomer)	33.6 (s, 1B), 19.8 (d, 107, 1B), 8.8 (d, 144, 1B), 1.7 (d, 165, 1B), -6.9 (d, 150), -8.8 (7B), -15.7 (d, 157, 1B), -23.6, -25.4 (3B), -43.9 (d, 147, 1B)
$(\text{Et}_4\text{B}_8\text{C}_4\text{H}_7, \text{THF})\text{Co}(\text{Et}_2\text{B}_4\text{C}_2\text{H}_4)$	11.8 (1B), 9.2 (s, 2B), 6.1 (2B), 1.4 (d, 131, 1B), -3.8 (d, 126, 1B), -12.0 (1B), -17.8 (d, 130, 1B), -23.1 (d, 163, 1B), -24.5 (d, 137, 1B), -32.3 (d, 128, 1B)
$(\text{Et}_4\text{B}_8\text{C}_4\text{H}_6, \text{THF})\text{Co}(\text{Et}_2\text{B}_4\text{C}_2\text{H}_3)$	-2.9, -7.6 (9B), -22.5 (d, 133, 3B)
$(\text{Et}_4\text{B}_8\text{C}_4\text{H}_8, \text{THF})\text{Fe}(\text{Et}_2\text{B}_4\text{C}_2\text{H}_4)$ (paramagnetic)	63.0, ca. -3, -194.3

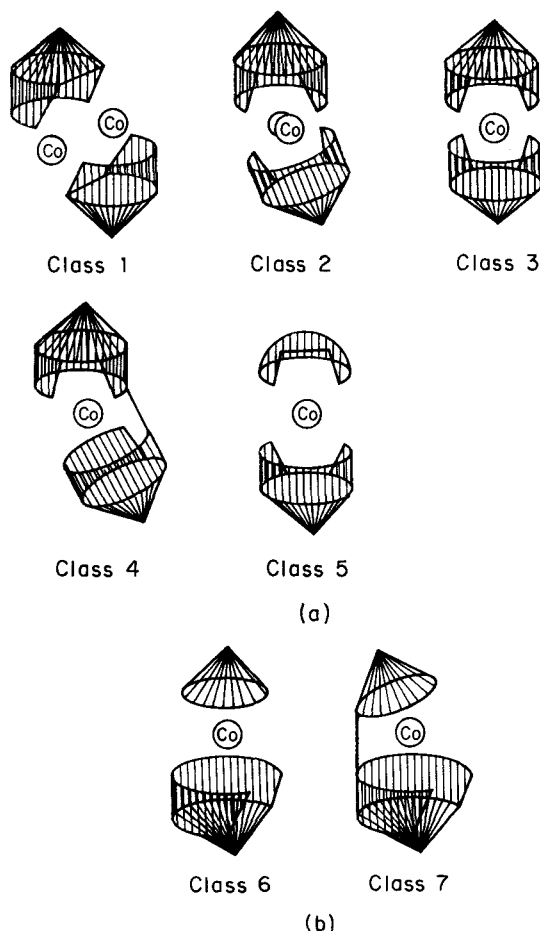


FIG. 32. (a) Schematic drawings of geometrical modes (established or proposed) exhibited by  $(C_4B_8)_2Co_2$ ,  $(C_4B_8)_2Co$ , and  $(C_4B_8)Co(C_4B_4)$  complexes. Connections between cobalt and ligands are omitted for clarity, an artistic device having no bonding significance. Ligands represented are  $Et_4C_4B_8H_8^{2-}$  or  $(Et_4C_4B_8H_7)H_2^{4-}$ , except for the small ligand in class 5, which is  $Et_4C_4B_4H_6^{2-}$ . (b) Schematic representations of structure types of  $(C_2B_4)Co(C_4B_8)$  complexes. The small ligand is  $Et_2C_2B_4H_4^{2-}$ ; the large ligand is  $Et_4C_4B_8H_8^{2-}$ .

B—H—B bridges between B10–B13 and B10'–B13'; these may undergo a tautomeric shift to the B12–B13 and B12'–B13' edges. Because the shifts of B8 in both compounds are the same, the THF substituent may be mobile as well. The mixed cage compound  $[Et_4B_8C_4H_7(THF)]Co(Et_2B_4C_2H_4)$  has been crystallographically characterized, and the cluster geometry is shown schematically in Fig. 33(c); the THF is attached to B11.<sup>245</sup>

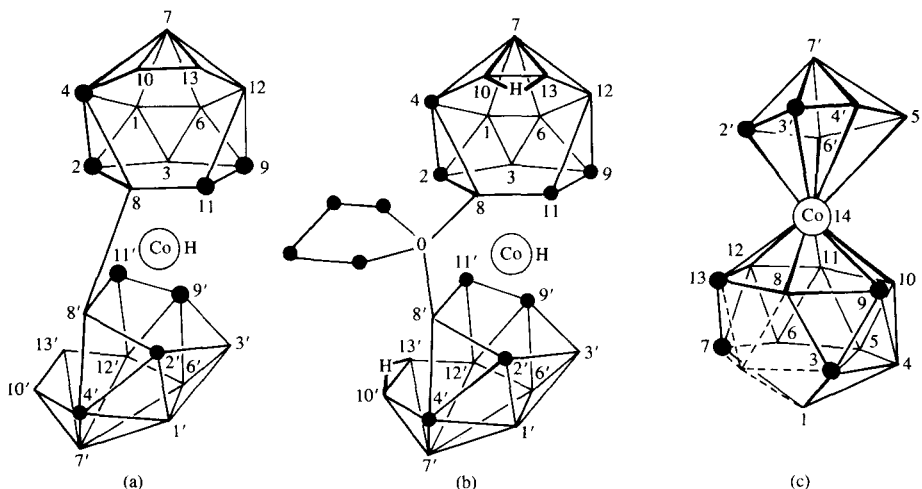


FIG. 33. (a, b) Proposed structures of  $(\text{Et}_4\text{B}_8\text{C}_4\text{H}_7)_2\text{CoH}$  (a) and  $(\text{Et}_4\text{B}_8\text{C}_4\text{H}_8)_2(\text{THF})\text{CoH}$  (b). Skeletal and THF carbon atoms are shown as solid circles. (c) Cage geometry of  $(\text{Et}_4\text{B}_8\text{C}_4\text{H}_7 \cdot \text{THF})\text{Co}(\text{Et}_2\text{B}_4\text{C}_2\text{H}_4)$  depicting the 13-vertex unit as a fragment of a bicapped hexagonal antiprism. The missing vertex (2) is shown by dashed lines. Framework carbon atoms are shown as solid circles.

#### D. $\text{B}_9$ metalloboranes and metallocarboranes

An extensive series of copper-containing metalloboranes of the type  $(\text{B}_9\text{H}_{13}\text{X})\text{Cu}(\text{PPh}_3)_2$  has been obtained by metathetical reactions of  $\text{B}_9\text{H}_{13}\text{X}^-$  with  $(\text{PPh}_3)_2\text{CuBH}_4$ . The numbering scheme is shown in Fig. 34(a), and 115.5 MHz  $^{11}\text{B}$  NMR data are collected in Table 34. The compounds in which  $\text{X} = \text{H}$ ,  $\text{NCSe}$ ,  $\text{NCS}$  and  $\text{NCBPh}_3$  are fluxional at room temperature, so that the borane ligand contains a plane of symmetry. A structure is proposed in which two of the three *endo*-hydrogen atoms at B4, 6, 8 participate in  $\text{B}-\text{H}-\text{Cu}$  bridging, as shown in Fig. 34(b). The resonances due to B7, B6, 8 and B4 are singlets; broadening is attributed to quadrupolar relaxation induced by the  $(\text{Ph}_3\text{P})_2\text{Cu}$  moiety. The compounds in which  $\text{X} = \text{NCBH}_3$  and  $\text{NCBH}_2\text{NCBH}_3$  are viewed as static  $(\text{Ph}_3\text{P})_2\text{CuBH}_4$  complexes (see Fig. 34).<sup>246</sup>

Metalloboranes of the  $\text{B}_9\text{Re}$  class, e.g.  $(\text{B}_9\text{H}_{13})\text{ReH}(\text{PMe}_2\text{Ph})_3$ , have been obtained from  $\text{ReCl}_3(\text{PMe}_2\text{Ph})_3$  and  $\text{B}_9\text{H}_{14}^-$  (cf. Table 35). The  $\text{HRe}(\text{PMe}_2\text{Ph})_3$  unit exhibits a dual pseudo-rotational fluxionality that leads to time-averaged structures of effective  $\text{C}_s$  mirror-plane symmetry. The  $^{11}\text{B}$  resonances are so broadened by efficient quadrupolar relaxation that low-temperature spectra do not resolve enantiomeric forms. Interestingly, the slope of the line relating  $\delta^{11}\text{B}$  and  $\delta^1\text{H}$  is about 12.5 rather than the more frequently observed value of 16. This may reflect an anomalous shielding of B2,

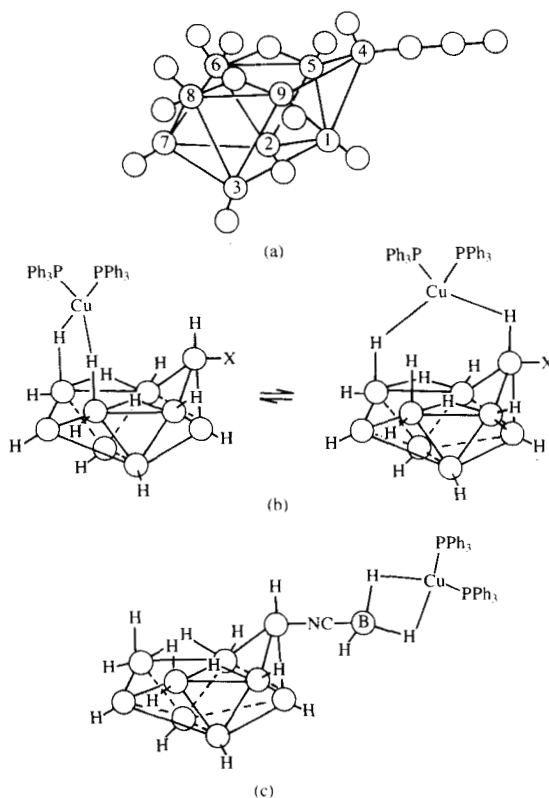


FIG. 34. (a) Numbering scheme for  $B_9H_{13}X^-$ . (b) Dynamic structure of  $B_9H_{13}Cu(Ph_3P)_2$ . (c) Static structure of  $B_9H_{13}NCBH_3Cu(Ph_3P)_2$ .

which is adjacent to rhenium.<sup>247</sup> The osmium- and tungsten-containing metalloboranes  $(B_9H_{13})WH_2(PMe_2Ph)_3$  and  $(B_9H_{13})Os(PMe_2Ph)_3$  have recently been reported (see Table 35). A comparison of the  $^{11}B$  NMR chemical shifts of these compounds, together with those of  $(B_9H_{13})ReH(PMe_2)_3$ ,  $(B_9H_{13})Ru(PMe_2)_3$ ,  $(B_9H_{13})IrH(PMe_3)_3$  and  $B_{10}H_{14}$ , is shown in Fig. 35. The shifts of B1, 3, 4, 8, distant from the metal centre, vary by only 5 ppm and B9 by 7 ppm. B2 in the  $WB_9$  and B5, 7 in the Rh and Os metalloboranes are significantly more deshielded (10–14 ppm).<sup>248</sup> The  $^{11}B$  NMR spectrum of  $(B_9H_{13})RhMe_5Cp$ , whose structure is shown in Fig. 36, has been assigned with the use of 2D techniques: 19.4 (dd, 149, 54, B5, 7), 12.7 (d, 138, B1, 3), 4.7 (d, 158, B9), -0.9 (d, 152, B8, 10), -10.8 (d, 141, B2) and -30.6 (d, 150, B4) ppm. For comparison,  $^{11}B$  chemical shifts in the analogous  $(B_9H_{13})CoMe_5Cp$  are 20.5, 15.4, 5.2, -1.2, -12.4 and -29.8 ppm.<sup>249</sup>

TABLE 34

Comparison of the correlated  $^{11}\text{B}$  and  $^1\text{H}$ - $\{^{11}\text{B}$ , continuous wave $\}$  spectra of the  $[\text{B}_9\text{H}_{13}\text{X}]^-$  anions and the  $\text{Cu}(\text{PPh}_3)_2(\text{B}_9\text{H}_{13}\text{X})$  complexes in  $\text{CDCl}_3$ .

Compound anion	Atom position	Free anion		Copper complex	
		$\delta^{11}\text{B}$	$\delta^1\text{H}$	$\delta^{11}\text{B}$	$\delta^1\text{H}$
(1) $[\text{B}_9\text{H}_{14}]^-$	5, 7, 9	-6.8	2.10	-5.3	2.70
	4, 6, 8	-19.2	1.60	-22.5	1.26
	1, 2, 3	-22.4	1.10	-25.4	1.62
	bridge		-1.50 (5)		-1.61 (3)
	$\text{PPh}_3$				7.4 (30)
	$\text{CuHB}$				0.42 (2)
(2) $[\text{B}_9\text{H}_{13}(\text{NCS})]^-$	7	14.8	3.68	15.46	3.91
	1	4.2	2.85	4.49	3.0
	5, 9	-16.4	1.53	-15.6	1.68
	6, 8	-18.0	1.86	-19.1	1.99
			-0.41		
	4	-22.0	0.60	-24	—
	2, 3	-38.3	0.25	-38.4	0.4
	bridge		-1.4 (5)		-1.3 (3)
	$\text{PPh}_3$				7.4 (30)
(3) $[\text{B}_9\text{H}_{13}(\text{NCSe})]^-$	7	15.8	3.73	16.7	3.9
	1	5.2	2.86	5.21	3.05
	5, 9	-15.6	1.58	-15.14	1.73
	6, 8	-17.8	1.89	-19.4	1.91
	4	-22.7	—	-25.7	—
	2, 3	-37.8	0.22	-38.4	0.38
	bridge		-1.42 (5)		-1.3 (3)
	$\text{PPh}_3$				7.4 (30)
(4) $[\text{B}_9\text{H}_{13}(\text{NCBPh}_3)]^-$	7	16.6		16.93	4.0
	1	5.2		5.20	3.16
	$\text{NCBPh}_3$	-10.7		-10.67	
	5, 9	14.9		-15.11	1.83
	6, 8	-19.5		-19.40	2.0
	4	-25.7		-26.03	—
	2, 3	-38.4		-38.41	0.5
(5) $[\text{B}_9\text{H}_{13}(\text{NCBH}_3)]^-$	7	16.2		17.5	3.97
	1	4.8		4.9	2.97
	5, 9	-15.5		-14.8	1.70
	bridge				-3.55 (2)
	6, 8	-19.4		-20.0	
	<i>exo</i>				1.94
	<i>endo</i>				-0.25
	4	-25.5		-26.6	0.24
	2, 3	-38.6		-38.6	0.41
	$\text{BH}_3$	-43.0		-36.5	1.73

TABLE 34 (*cont.*)

Comparison of the correlated  $^{11}\text{B}$  and  $^1\text{H}$ - $\{^{11}\text{B}$ , continuous wave $\}$  spectra of the  $[\text{B}_9\text{H}_{13}\text{X}]^-$  anions and the  $\text{Cu}(\text{PPh}_3)_2(\text{B}_9\text{H}_{13}\text{X})$  complexes in  $\text{CDCl}_3$ .

Compound anion	Atom position	Free anion		Copper complex	
		$\delta^{11}\text{B}$	$\delta^1\text{H}$	$\delta^{11}\text{B}$	$\delta^1\text{H}$
(6) $[\text{B}_9\text{H}_{13}(\text{NCBH}_2\text{NCBH}_3)]^-$	7	17.1	3.9	17.97	4.08
	1	5.07	3.03	5.3	3.21
	5, 9	-14.7	1.79	-14.4	1.99
	bridge		-3.53 (2)		-3.37 (2)
	6, 8	-20.2		-20.2	
	<i>exo</i>		1.88		2.07
	<i>endo</i>		-0.27		-0.12
	4		0.43		0.55
		-27.3		-26.9	
	$\text{BH}_2$		2.09		2.07
	2, 3	-38.6	0.37	-38.44	0.59
	$\text{BH}_3$	-43.3	0.57	-37	1.83
	$\text{PPh}_3$				7.45 (30)

Metalloboranes of the  $\text{B}_9\text{Fe}$  class have been prepared from iron atoms,  $\text{B}_{10}\text{H}_{14}$  and mesitylene.  $^{11}\text{B}$  chemical-shift data are given in Table 36. The very high-frequency  $^{11}\text{B}$  resonance of (mesitylene) $\text{FeB}_9\text{H}_9$  is characteristic of low-coordination-number boron atoms that are bonded to a transition metal (Fig. 37).<sup>250</sup> The nickelaborane  $2,4\text{-Cl}_2\text{-B}_9\text{H}_7\text{Ni}(\text{PMe}_2\text{Ph})_2$  features a bicapped Archimedean square-antiprismatic geometry with nickel at the apical, i.e. 1, position.<sup>251</sup>

Archival  $^{11}\text{B}$  NMR spectra have been obtained for a wide variety of transition-metal complexes of various isomers of the  $\text{B}_9\text{C}_2\text{H}_{11}^{2-}$  ligand, and the chemical shifts are summarized in Table 37.  $^{11}\text{B}$  NMR data have been reported for a series of tertiary-phosphine complexes of  $\text{B}_9\text{C}_2\text{H}_{11}$  metallocarboranes containing rhodium and ruthenium; these compounds are of interest on account of the catalytic activity exhibited by the metal centres. Some of the spectra are not well resolved, e.g.  $3\text{-Ph}_3\text{P-3,1,2-RhB}_9\text{C}_2\text{H}_{11}$ , as is often the case when bulky phosphine ligands are present. An X-ray study of  $(7,9\text{-B}_9\text{C}_2\text{H}_{11})\text{RhCl}(\text{PPh}_3)$  has shown that, notwithstanding the formalisms of electron counting, there is negligible movement of the metal from the  $\text{B}_3\text{C}_2$  bonding face of the carborane ligand. The electron deficiency is thus proposed to be metal-centered.<sup>252-255</sup> The C-aryliridacarborane  $[(\text{Ph}_3\text{P})_2\text{IrH}]\text{-8-Ph-1,8-B}_9\text{C}_2\text{H}_{10}$ ,  $\delta^{11}\text{B} = -0.1, 6.3, 9.4$  and  $20.5$ , rearranges under relatively mild conditions, at  $110^\circ\text{C}$ , to form an isomer having the phenyl group on the lower equatorial belt.<sup>256</sup>

TABLE 35

<sup>11</sup>B NMR data for B<sub>9</sub> metalloboranes.

Compound	$\delta^{11}\text{B}$					
	B1, 3	B5, 7	B9	B8, 10	B2	B4
(B <sub>9</sub> H <sub>13</sub> )ReH(PMe <sub>2</sub> Ph) <sub>3</sub>	10.2	12.2	5.5	-1.5	-29.8	-29
(9-EtOB <sub>9</sub> H <sub>12</sub> )ReH(PMe <sub>2</sub> Ph) <sub>3</sub>	3.8	14.8	23.0	-14.9	33.8	-26
(8-EtOB <sub>9</sub> H <sub>12</sub> )ReH(PMe <sub>2</sub> Ph) <sub>3</sub>	13.9, 1.8	20.4, 1.7	-6.2	23.0, -16.3	-32.2	-31
[2-(PMe <sub>2</sub> Ph)B <sub>9</sub> H <sub>12</sub> ]ReHCl(PMe <sub>2</sub> Ph) <sub>2</sub>	5.9	12.7	0.7	-0.7	-41.8	-32
(2-ClB <sub>9</sub> H <sub>12</sub> )ReH(PMe <sub>2</sub> Ph) <sub>3</sub>	11.2	10.4	0.2	2.1	-15.8	-32
(B <sub>9</sub> H <sub>13</sub> )WH <sub>2</sub> (PMe <sub>2</sub> Ph) <sub>3</sub>	7.2	12.3	2.5	-3.0	-23.1	-33
(B <sub>9</sub> H <sub>13</sub> )Os(PMe <sub>2</sub> Ph) <sub>3</sub>	11.4	8.8	3.0	-1.6	-29.2	-31

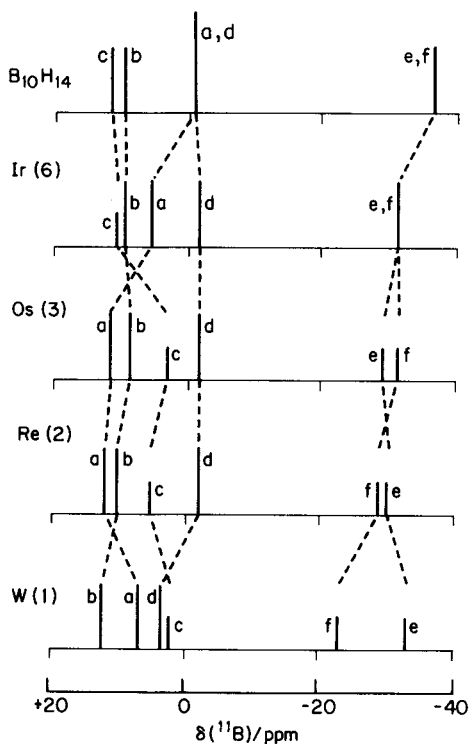


FIG. 35. Stick diagram of the  $^{11}\text{B}$  NMR positions for  $[(\text{PMe}_2\text{Ph})_3\text{H}_2\text{WB}_9\text{H}_{13}]$  (1),  $[(\text{PMe}_2\text{Ph})_3\text{HReB}_9\text{H}_{13}]$  (2),  $[(\text{PMe}_2\text{Ph})_3\text{OsB}_9\text{H}_{13}]$  (3),  $[(\text{PMe}_3)_2\text{HIrB}_9\text{H}_{13}]$  (6) and  $\text{B}_{10}\text{H}_{14}$ . Mean resonance positions have been plotted for the asymmetric species  $[(\text{PMe}_3)_2\text{HIrB}_9\text{H}_{13}]$  (6), and it should also be noted that the  $^{11}\text{B}(2)$  and  $^{11}\text{B}(4)$  resonances are accidentally coincident for this compound. Assignments are  $^{11}\text{B}(5, 7)$  a,  $^{11}\text{B}(1, 3)$  b,  $^{11}\text{B}(9)$  c,  $^{11}\text{B}(8, 10)$  d,  $^{11}\text{B}(2)$  e, and  $^{11}\text{B}(4)$  f. Resonances e and f are assigned on the basis of  $^1\text{H}$ -shielding behaviour.

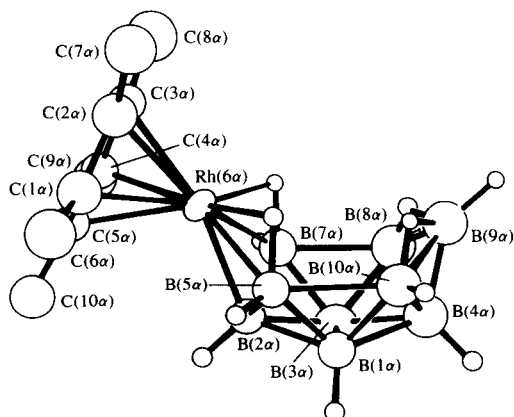


FIG. 36. Crystallographically determined molecular structure of  $[6-(\eta^5\text{-C}_5\text{Me}_5)\text{RhB}_9\text{H}_{13}]$ .

TABLE 36

 $^{11}\text{B}$  NMR data for  $\text{B}_9\text{Fe}$ -type metalloboranes.

Compound	$\delta^{11}\text{B}$
$(\text{Me}_3\text{Ph})\text{FeB}_9\text{H}_{13}$	30.1 (d, 144, 1B), 22.5 (d, 126, 1B), 12.6 (d, 126, 1B), 4.3 (d, 133, 2B), 0.1 (d, 155, 1B), -3.0 (d, 133, 1B), -18.6 (d, 150, 1B), -37.8 (d, 162, 1B)
$(\text{Me}_3\text{Ph})\text{FeB}_9\text{H}_9$	106.5 (d, 178, 3B), 27.7 (d, 144, 3B), -11.4 (d, 148, 3B)
$2,4\text{-Cl}_2\text{-B}_9\text{H}_7\text{Ni}(\text{PMe}_2\text{Ph})_2$	47.4 (s, B2, 4), 26.6 (d, 140, B3, 5), 3.8 (d, 150, B6, 7, 8, 9), 88.6 (d, 130, B10)

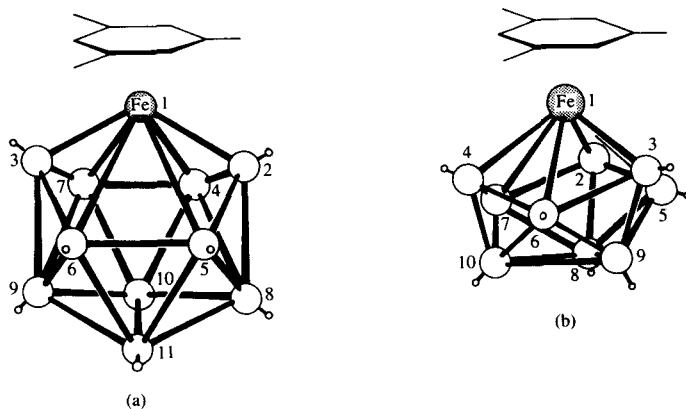
Fig. 37. Proposed structures for  $1\text{-}[\eta^6\text{C}_6\text{Me}_3\text{H}_3]\text{FeB}_{10}\text{H}_{10}$  (a) and  $1\text{-}[\eta^6\text{-C}_6\text{Me}_3\text{H}_3]\text{FeB}_9\text{H}_9$  (b).

TABLE 37

 $^{11}\text{B}$  NMR data for  $\text{B}_9\text{C}_2$  metallocarboranes.

Compound	$\delta^{11}\text{B}$
$(7,9\text{-B}_9\text{C}_2\text{H}_{11})\text{RhH}(\text{PhPMe}_2)_2$	-1.8 (1B), -4.4 (1B), -8.5 (2B), -10.0 (2B), -21.3 (3B)
$(7,9\text{-B}_9\text{C}_2\text{H}_{11})\text{RhCl}(\text{PhPMe}_2)_2$	6.9 (1B), -2.6 (1B), -3.7 (2B), -6.0 (2B), -18.1 (3B)
$(7,9\text{-B}_9\text{C}_2\text{H}_{11})\text{RhCl}(\text{PPh}_3)_2$	11.9 (1B), 8.0 (2B), 4.6 (1B), -7.8 (1B), -9.1 (1B), -13.6 (2B), -17.2 (1B)
$[(\text{CH}_3\text{CN})_2(\text{Ph}_3\text{P})\text{-}3,1,2\text{-RhB}_9\text{C}_2\text{H}_{11}]\text{HSO}_4$	-23.4, -7.6, -3.9, 11.0, 13.1

TABLE 37 (cont.)

<sup>11</sup>B NMR data for B<sub>9</sub>C<sub>2</sub> metallocarboranes.

Compound	δ <sup>11</sup> B
3-Ph <sub>3</sub> P-3,1,2-RhB <sub>9</sub> C <sub>2</sub> H <sub>11</sub>	-25.7, -9.2, -3.1, 11.8
[Ph <sub>3</sub> P(μ-CN)-3,1,2-B <sub>9</sub> C <sub>2</sub> H <sub>11</sub> ] <sub>4</sub>	8.5, -1.6, -5.3, -8.8
3,3-(PhPMe <sub>2</sub> ) <sub>2</sub> -3-NO <sub>3</sub> -3,1,2-RhB <sub>9</sub> C <sub>2</sub> H <sub>11</sub>	-19.6, -15.5, -2.4, 8.0
[Ph <sub>3</sub> PH][(Ph <sub>3</sub> P)Br <sub>2</sub> -3,1,2-RhB <sub>9</sub> C <sub>2</sub> H <sub>11</sub> ]	16.3 (2B), 3.8 (1B), 1.4 (3B), -3.8 (2B), 17.1 (1B)
[Bu <sub>4</sub> N][(Ph <sub>3</sub> P)I <sub>2</sub> -3,1,2-RhB <sub>9</sub> C <sub>2</sub> H <sub>11</sub> ]	8.1 (1B), 5.9 (2B), -4.9 (2B), -7.0 (2B), -13.8 (1B), -24.9 (1B)
[K(18-crown-6)-[(CO) <sub>2</sub> Ru(H)B <sub>9</sub> C <sub>2</sub> H <sub>11</sub> ]]	-22.0 (d, 148, 3B), -12.6 (d, 140, 2B), -9.5 (d, 127, 2B), -6.8 (d, 129, 1B), -4.9 (d, 142, 1B)
[K(18-crown-6)] <sub>2</sub> -[(CO)(μ-CO)RuB <sub>9</sub> C <sub>2</sub> H <sub>11</sub> ]	-21.0 (d, 148, 3B), -10.8 (d, 139, 2B), -8.8 (d, 139, 3B), -0.8 (d, 132, 1B)
(Me <sub>4</sub> N)[(CO) <sub>2</sub> Ru(COMe)B <sub>9</sub> C <sub>2</sub> H <sub>11</sub> ]	-21.3 (d, 148, 3B), -11.6 (d, 140, 2B), -7.9 (d, 137, 3B), -4.8 (d, 145, 1B)
(Me <sub>4</sub> N)[(CO) <sub>2</sub> Ru(CO <sub>2</sub> CF <sub>3</sub> )B <sub>9</sub> C <sub>2</sub> H <sub>11</sub> ]	-21.5 (d, 155, 2B), -17.6 (d, 172, 1B), -10.1 (d, 151, 1B), -7.8 (d, 143, 4B), 1.4 (d, 135, 1B)
3,3-(Ph <sub>3</sub> P) <sub>2</sub> Ni(3,1,2-B <sub>9</sub> C <sub>2</sub> H <sub>11</sub> )	-19.4 (2B), -12.7 (2B), -9.1 (5B)
3,3-(Et <sub>3</sub> P) <sub>2</sub> Ni(3,1,2-B <sub>9</sub> C <sub>2</sub> H <sub>11</sub> )	-19.8 (2B), -13.1 (2B), -9.1 (4B), -4.7 (1B)
3,3-(PhPMe <sub>2</sub> ) <sub>2</sub> Ni(3,1,2-B <sub>9</sub> C <sub>2</sub> H <sub>11</sub> )	-19.0 (2B), -12.3 (2B), -8.7 (3B), -6.3 (1B), -2.8 (1B)
2,2-(Ph <sub>3</sub> P) <sub>2</sub> Ni(2,1,7-B <sub>9</sub> C <sub>2</sub> H <sub>11</sub> )	-19.8 (3B), -15.7 (1B), -10.7 (4B), -2.8 (1B)
2,2-(Ph <sub>3</sub> P) <sub>2</sub> Ni(2,1,12-B <sub>9</sub> C <sub>2</sub> H <sub>11</sub> )	-20.0 (4B), -14.9 (2B), -10.1 (2B), -8.1 (1B)
3,8-(Ph <sub>3</sub> P) <sub>2</sub> NiH(3,1,2-B <sub>9</sub> C <sub>2</sub> H <sub>11</sub> )	-23 (7B), -15 (2B)
3-Ph <sub>3</sub> P-3-(CO)Ni(3,1,2-B <sub>9</sub> C <sub>2</sub> H <sub>11</sub> )	-22.6 (3B), -13.5 (2B), -10.3 (2B), -6.3 (2B)
3-Cl-3,8-(Ph <sub>3</sub> P) <sub>2</sub> Ni(3,1,2-B <sub>9</sub> C <sub>2</sub> H <sub>11</sub> )	-19.8, -10.7, -2.0 (d, 128, 1B)
[3-μ-(CO)-8-Ph <sub>3</sub> P]Ni(3,1,2-B <sub>9</sub> C <sub>2</sub> H <sub>11</sub> )	-19.1 (2B), -15.3 (4B), -10.7 (2B), -7.0 (d, 132, 1B)
(MePh)Fe(2,4-Me <sub>2</sub> B <sub>9</sub> C <sub>2</sub> H <sub>9</sub> )	-1.1 (1B), -4.1 (2B), -7.4 (1B), -12.9 (2B), -15.2 (1B), -16.3 (2B)
(C <sub>10</sub> H <sub>8</sub> )Fe(2,4-Me <sub>2</sub> B <sub>9</sub> C <sub>2</sub> H <sub>11</sub> )	-2.1 (1B), -3.6 (2B), -6.0 (1B), -13.9 (2B), -16.9 (3B)
RuW(μ-CC <sub>6</sub> H <sub>4</sub> Me)(CO) <sub>3</sub> Cp-(Me <sub>2</sub> B <sub>9</sub> H <sub>11</sub> )	19.5 (s, 1B), -7.6 (br, 8B)
RuW[μ-σ-CH(C <sub>6</sub> H <sub>4</sub> Me)-(CO) <sub>3</sub> Cp(Me <sub>2</sub> B <sub>9</sub> C <sub>2</sub> H <sub>11</sub> )]	65.4 (s, 1B, B—C—Ru), 20.3 (1B), 6.0 (1B), -4.5 (4B), -14.8 (2B)

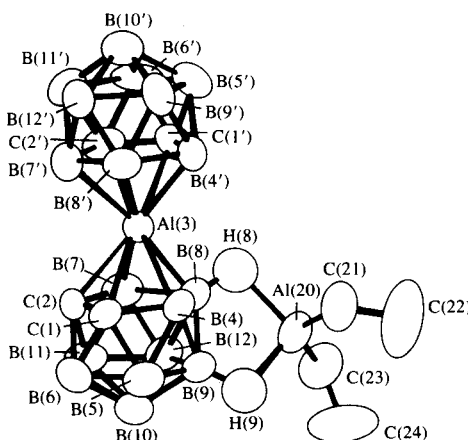


FIG. 38. Structure of  $[8,9\text{-Et}_2\text{Al}(\mu\text{-H})_2\text{-}1,2\text{-B}_9\text{C}_2\text{H}_9]\text{Al}(1,2\text{-B}_9\text{C}_2\text{H}_{11})$ .

Bis(phosphine)-substituted  $\text{B}_9\text{C}_2\text{H}_{11}$  nickel complexes rearrange on heating so that the phosphine migrates to a terminal boron position on the open face of the carborane ligand, and, in such compounds  $J(\text{P-B}) \approx 130 \text{ Hz}$ .<sup>257</sup> The reaction of  $(\text{C}_8\text{H}_{12})\text{Fe}(\text{C}_5\text{H}_5)$  with  $2,3\text{-Me}_2\text{B}_9\text{C}_2\text{H}_9$  in the presence of arenes provides a versatile route to compounds of the type (arene)- $\text{Fe}(\text{Me}_2\text{B}_9\text{C}_2\text{H}_9)$ .<sup>258</sup> The  $^{11}\text{B}$  NMR spectrum of the indenyl complex  $(\text{C}_9\text{H}_7)\text{Co}(1,2\text{-B}_9\text{C}_2\text{H}_{11})$  shows peaks at 7.6 (1B), 1.7 (1B), -3.6 (2B), -4.0 (2B), -15.9 (2B) and -22.4 (1B). Interestingly, it exists in two different crystal forms.<sup>259</sup>

The compound  $[8,9\text{-Et}_2\text{Al}(\mu\text{-H})_2\text{-}1,2\text{-B}_9\text{C}_2\text{H}_9]\text{Al}(1,2\text{-B}_9\text{C}_2\text{H}_{11})$ , prepared by the catalytic action of CO on  $\text{EtAlB}_9\text{C}_2\text{H}_{11}$ , may, in a formal sense, be regarded as a zwitterion containing a  $[(\text{B}_9\text{C}_2\text{H}_{11})_2\text{Al}]^-$  sandwich bonded through two B—H units at B8,9 to an  $\text{Et}_2\text{Al}^+$  ion (Fig. 38). It has  $\delta^{11}\text{B} = -12.3$  (d, 3B), -16.8 (d, 4B), -21.6 (d, 1B), -31.7 (d, 1B) in  $\text{C}_6\text{D}_6$ . The lowest frequency resonance, which does not exhibit B—H coupling, is assigned to the B8, 9 bridge sites.<sup>260</sup>

The novel silicon sandwich compound  $(1,2\text{-B}_9\text{C}_2\text{H}_{11})_2\text{Si}$  has  $\delta^{11}\text{B} = -8.5$  (2B), -11.2 (1B), -12.9 (4B), -20.4 (1B) and -24.7 (1B).<sup>261</sup>

Reactions of  $[\text{M}(\text{CO})_2(\text{CH}_3\text{CN})(\eta^5\text{-C}_9\text{H}_7)]\text{BF}_4$  ( $\text{M} = \text{Mo}, \text{W}$ ) and  $\text{PPN}[\text{W}(\equiv\text{CC}_6\text{H}_4\text{Me})(\text{CO})_2(7,8\text{-B}_9\text{R}_2\text{C}_2\text{H}_9)]$  ( $\text{R} = \text{H}, \text{Me}$ ) yield the bimetallic carborane compounds  $\text{MW}(\mu\text{-CC}_6\text{H}_4\text{Me})(\text{CO})_3(\eta^5\text{-C}_9\text{H}_7)(7,8\text{-B}_9\text{R}_2\text{C}_2\text{H}_9)$ . These materials feature a B—H—M bond (see Fig. 39a), which is manifested in their  $^{11}\text{B}$  NMR spectra by a peak at 9.2–16.2 ppm (1B) that is quite distinct from the other, poorly resolved B—H peaks at -8.3 to -12.6 ppm (8B);  $J(\text{B-H}) \approx 82 \text{ Hz}$  is less than the usual value

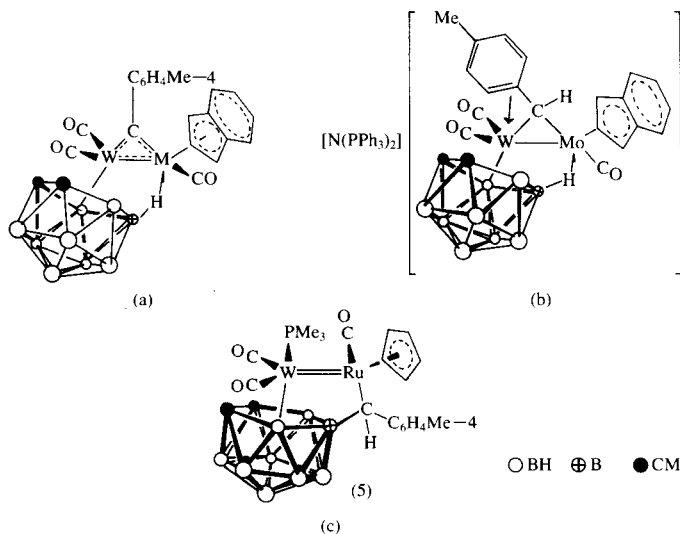


FIG. 39. Schematic structures of  $MW(\mu\text{-CC}_6\text{H}_4\text{Me})(\text{CO})_3(\text{C}_9\text{H}_7)(\text{B}_9\text{R}_2\text{C}_2\text{H}_9)$  (a),  $\text{PPN}[\text{MoW}(\mu\text{-CHC}_6\text{H}_4\text{Me})(\text{CO})_3(\text{C}_9\text{H}_7)(\text{B}_9\text{C}_2\text{Me}_2\text{H}_9)]$ , (b) and  $\text{RuW}(\mu\text{-CHC}_6\text{H}_4\text{Me})(\text{CO})_3(\text{Me}_3\text{P})\text{Cp}$  (c).

of approx. 130 Hz for two-centre B—H units, which further indicates participation of B—H in agnostic bonding. This interaction is maintained in the 7,9- $\text{B}_9\text{R}_2\text{C}_2\text{H}_9$  isomers, which are formed on heating, and in the hydride-addition product  $\text{PPN}[\text{MoW}(\mu\text{-CHC}_6\text{H}_4\text{Me})(\text{CO})_3(\eta^5\text{-C}_9\text{H}_7)(7,8\text{-B}_9\text{R}_2\text{C}_2\text{H}_9)]$  (Fig. 39b). Replacement by  $\text{PMe}_3$  of one CO molecule on

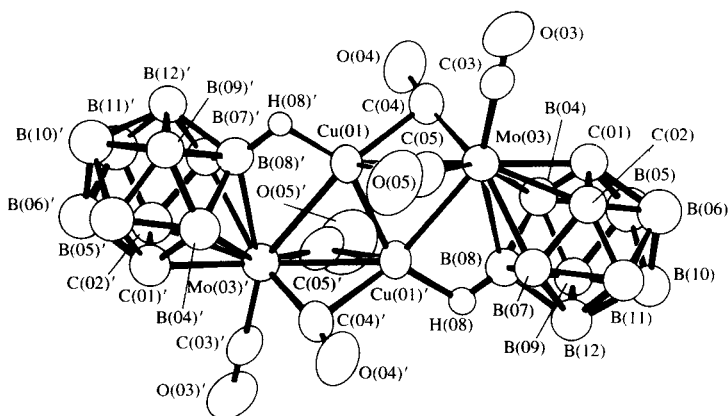
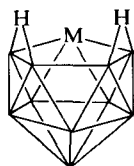


FIG. 40. Structure of  $[\text{Mo}_2\text{Cu}_2(\mu\text{-CO})_4(\text{CO})_2(\mu\text{-H})_2(\text{C}_2\text{B}_9\text{H}_{10})_2]^{2-}$ .

the tungsten atom bonded to the carborane cage preserves the B—H—M bond; but it is ruptured upon like displacement of CO at the distal metal atom.<sup>262</sup> Structurally analogous compounds such as  $\text{RuW}(\mu\text{-CC}_6\text{H}_4\text{Me})\text{-(CO)}_3\text{Cp(B}_9\text{Me}_2\text{C}_2\text{H}_9\text{)}$  have also been prepared. These too exhibit high frequency (approx. 19 ppm) signals for the B—H—Ru group. Treatment with base removes the bridging proton and generates  $[\text{RuW}(\mu\text{-CC}_6\text{H}_4\text{Me})\text{-(CO)}_3\text{(B}_9\text{Me}_2\text{C}_2\text{H}_9\text{)}]^-$ , in which the unique boron atom, now directly bonded to Ru, appears at 45.9 ppm. Reaction of the alkylidyne complex with  $\text{PMe}_3$  yields  $\text{RuW}[\mu,\sigma,\eta\text{-CH(C}_6\text{H}_4\text{Me)(B}_9\text{Me}_2\text{C}_2\text{H}_8\text{)(CO)}_3\text{(PMe}_3\text{)-Cp}](\text{PMe}_3\text{)Cp}$  (Fig. 39c), in which the boron atom substituted by ruthenium has  $\delta^{11}\text{B} = 65.4$ .<sup>263</sup> A novel heterotetranuclear metallocarborane anion  $(\text{B}_9\text{C}_2\text{H}_{10})_2\text{Mo}_2\text{Cu}_2(\mu\text{-CO)}_4(\text{CO})_2(\mu\text{-H})_2^{2-}$  has recently been reported (Fig. 40). It has  $\delta^{11}\text{B} = -9.8, -11.2, -14.1, -18.5$  and  $-21.9$ .<sup>264</sup>

### E. $\text{B}_{10}$ and larger metalloboranes and metallocarboranes

The  $\text{B}_{10}\text{H}_{12}\text{M}$  class of metalloboranes is densely populated, there being over 100 examples, incorporating some 20 different metals.<sup>265,266</sup> All but two have the structure [45] with bridging hydrogen atoms on the B8–B9 and B10–B11 edges. The exceptions,  $7\text{-Me}_5\text{CpRhB}_{10}\text{H}_{11}\text{Cl(PhPMe}_2\text{)}$  and  $(\text{Me}_6\text{C}_6)\text{RuB}_{10}\text{H}_{13}$ , have two B—H—M and one B—H—B bridge [46].



[45]



[46]

Reaction of  $\text{B}_{10}\text{H}_{12}(\text{SMe}_2)_2$  and *cis*-( $\text{PhPMe}_2$ )<sub>2</sub> $\text{PtCl}_2$  produces, *inter alia*,  $8\text{-ClB}_{10}\text{H}_{11}\text{Pt(PhPMe}_2\text{)}_2$  and  $8\text{-Me}_2\text{SB}_{10}\text{H}_{11}\text{Pt(Cl)(PhPMe}_2\text{)}$ , the chlorine in the former compound being derived from the  $\text{CH}_2\text{Cl}_2$  solvent. X-ray crystallography has shown that the halogen is attached to B8 in  $8\text{-ClB}_{10}\text{H}_{11}\text{Pt(PhPMe}_2\text{)}_2$  (Fig.41), which has  $\delta^{11}\text{B} = 22.1$  (B2), 19.5 ( $J(\text{Pt-B}) = 310 \pm 60$ , B8), 12.9 (B5), 5.0 (B3), 4.4 (B11), 1.2 (B1),  $-0.8$  (B10),  $-7.4$  (B9),  $-21.2$  (B4), and  $-30.7$  (B6). Chemical shifts in the  $\text{Me}_2\text{S}$  compound are 16.0 (B2), 14.9 (B5), 4.6 (s,  $J(\text{Pt-B}) \approx 260$ , B8), 7.2, 7.0 (B3, 11),  $-4.4$  (B10),  $-5.7$  (B1),  $-9.1$  (B9),  $-27.5$  (B4) and  $-32.0$  (B6) ppm. Its structure is deduced from the similarity of its  $^{11}\text{B}$  NMR spectrum to that of  $8\text{-ClB}_{10}\text{H}_{11}\text{Pt(PhPMe}_2\text{)}_2$ ; shifts for the  $\text{Me}_3\text{P}$  analogue are the same to within 1 ppm. The 4.6 ppm singlet has approx. 260 Hz satellites due to splitting by  $^{195}\text{Pt}$ . Therefore the  $\text{Me}_2\text{S}$  ligand must

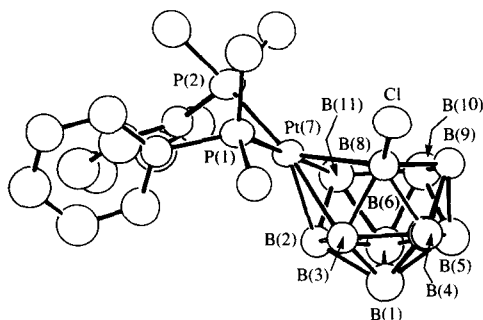


FIG. 41. ORTEP drawing of the molecular structure of  $[8\text{-Cl-}7,7\text{-(PMe}_2\text{Ph)}_2\text{-}7\text{-PtB}_{10}\text{H}_{11}]$ . Hydrogen atoms were not located, but the presence of terminal hydrogen atoms on all boron atoms except B(8), and the presence of bridging hydrogen atoms at B(8)/B(9) and B(10)/B(11), are reasonably inferred from NMR spectroscopy.

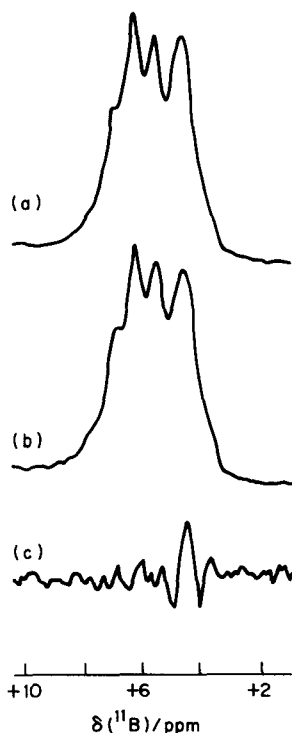


FIG. 42.  $^{11}\text{B}$  spectra (128 MHz) of the B(1)B(8)B(10) region for the trimethylphosphine compound  $[8\text{-(SMe}_2\text{)-}7\text{-(PMe}_3\text{)-}7\text{-Cl-}7\text{-PtB}_{10}\text{H}_{11}]$  in  $\text{CDCl}_3$  solution at  $+20^\circ\text{C}$ : (a) spectrum with simultaneous  $\{^1\text{H}\}$  selective-decoupling irradiation at  $\nu[^1\text{H}(\text{bridge})]$ ; (b) straightforward unperturbed spectrum; (c) difference between (a) and (b), showing that selective sharpening of the singlet resonance (plus its  $^{195}\text{Pt}$  satellites) occurs in the  $^{11}\text{B}\text{-}\{^1\text{H}\}$  experiment which therefore assigns this resonance and the site of  $\text{SMe}_2$  substitution to B(8).

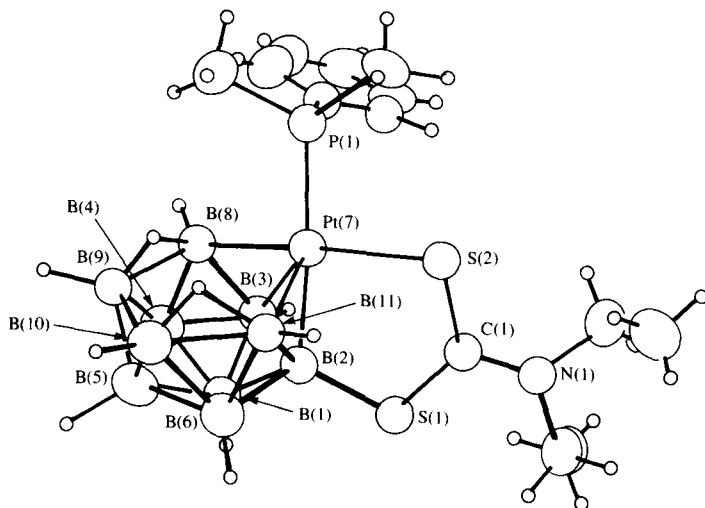


FIG. 43. ORTEP drawing of  $[\mu\text{-}2,7\text{-(SCSNET}_2\text{)}\text{-}7\text{-(PMe}_2\text{Ph)}\text{-nido-}7\text{-PtB}_{10}\text{H}_{11}]$ , showing numbering scheme.

be attached to either B3 or B8. The latter is the case, since decoupling of the bridge protons results in sharpening of this singlet because B8 is located on the “open face” of the molecule and participates in B—H—B bridging. This sharpening, which is unobvious in the normal FT spectrum, is revealed by difference spectra (Fig. 42).<sup>267</sup> In  $\text{B}_{10}\text{H}_{11}\text{Pt(PhPMe}_2\text{)}(\mu\text{-}2,7\text{-S}_2\text{CNET}_2)$ , a dithiocarbamate ligand bridges platinum and B2 (Fig. 43). The 32 MHz  $^{11}\text{B}$  NMR spectrum is well resolved and shows peaks at 27.8, 15.6, 14.3, 9.1, 0.3, -6.2, -9.1, -22.9 and -28.3 ppm; that at 9.1 ppm is a singlet attributable to B2. A linear correlation in this compound between the  $^{11}\text{B}$  and  $^1\text{H}$  chemical shifts with a slope of 16 is noted; this is a value similar to that found in other  $\text{B}_{6,8,10}$  metalloboranes.<sup>268</sup>

The compounds  $2,5\text{-(EtO)}_2\text{-}1,1\text{-(PhPMe}_2\text{)}_2\text{MB}_{10}\text{H}_8$  have been obtained for  $\text{M} = \text{Ru}$  and  $\text{Os}$ , and they have very similar  $^{11}\text{B}$  NMR spectra, both exhibiting a very high-frequency resonance (approx. 87 ppm) for B2, 5 and a cluster of peaks near 5 ppm (see Table 38). Proposed spectral assignments are based on  $^{11}\text{B}\text{-}^{11}\text{B}$  COSY NMR data for  $(\text{PhPMe}_2)_2\text{RuB}_{10}\text{H}_8\text{(OMe)}_2$  and  $(\text{PhPMe}_2)_2\text{RhHB}_{10}\text{H}_8\text{(OMe)}_2$ . If  $(\text{Ph}_3\text{P})_3\text{OsCl}_2$  is used as the source of osmium instead of  $(\text{PhPMe}_2)_3\text{OsCl}_3$ , the *ortho*-cycloboronated osmaborane  $(\text{Ph}_3\text{P})(\text{Ph}_2\text{PC}_6\text{H}_4)\text{OsB}_{10}\text{H}_7\text{(OEt)}_2$  is obtained, in which a bond between one of the phenyl carbon atoms and B3 is established. In this compound B3 is slightly deshielded and gives rise to a singlet at 14.1 ppm (Fig. 44 and Table 39).<sup>269</sup>

TABLE 38

Measured NMR parameters for  $[(\text{PMe}_2\text{Ph})_2\text{MB}_{10}\text{H}_8(\text{OEt})_2]$  ( $\text{M} = \text{Os}$  or  $\text{Ru}$ ) in  $\text{CD}_2\text{Cl}_2$  solution at  $+21^\circ\text{C}$ .

Tentative assignment	M = Os		M = Ru	
	$\delta^{11}\text{B}$	$\delta^1\text{H}$	$\delta^{11}\text{B}$	$\delta^1\text{H}$
(2, 5)	85.5 (2B)		88.3 (2B)	
(8, 10)	10.8 (2B)	4.04 (2H)	7.8 (2B)	3.63 (2H)
(9, 11)	5.5 (2B)	2.55 (2H)	3.0 (2B)	2.37 (2H)
(3, 4, 6, 7)	4.8 (4B)	1.96 (4H)	6.8 (4B)	2.24 (4H)

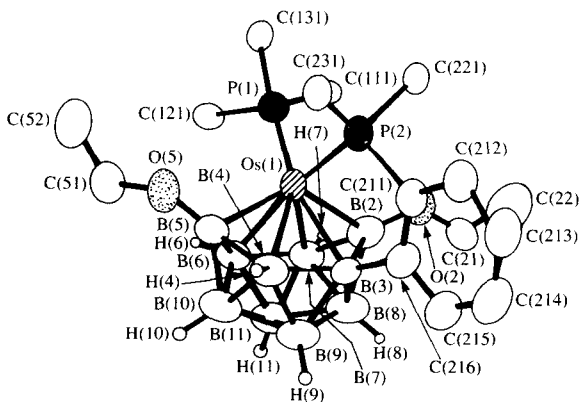


FIG. 44. ORTEP drawing of the molecular structure of  $[(\text{PPh}_3)(\text{Ph}_2\text{PC}_6\text{H}_4)\text{OsB}_{10}\text{H}_7(\text{OEt})_2]$ , with selected organyl group atoms omitted for clarity.

The rhodaborane  $(\text{PhPMe}_2)_2\text{RhHB}_{10}\text{H}_8(\text{OMe})_2$  is obtained from  $(\text{Et}_3\text{NH})_2\text{B}_{10}\text{H}_{10}$  and  $(\text{PhPMe}_2)_3\text{RhCl}_3$ . It has  $\delta^{11}\text{B} = 99.9$  (B5, B—OEt), 70.7 (B2), 0.7 (B9, 11),  $-2.0$ ,  $-3.1$  (B3, 4; B6, 7),  $-4.7$ ,  $-5.8$  (B8, 10). Assignments are made by analogy with  $(\text{PhPMe}_2)_2\text{RuB}_{10}\text{H}_8(\text{OMe})_2$ . The B—H coupling in the B(2)—H—Rh unit is estimated to be  $55 \pm 15$  Hz.<sup>270</sup>

Two-dimensional  $^{11}\text{B}$ — $^{11}\text{B}$  NMR has been applied to  $\text{Me}_2\text{TiB}_{10}\text{H}_{12}$  (Fig. 45) and has yielded an assignment of the spectrum together with magnitudes and relative signs of  $^{205}\text{Tl}$ — $^{11}\text{B}$  couplings (Table 40). Because each component of a particular  $^{11}\text{B}$  doublet corresponds to a particular  $^{205}\text{Tl}$  spin state, only one component of a particular doublet arising from  $^{205}\text{Tl}$  splitting correlates with a particular component of another such doublet. Thus only two off-diagonal correlations link a given pair of doublets; and the sense of these two pairwise correlations gives the relative

TABLE 39

Measured NMR parameters for  $[(PPh_3)(Ph_2PC_6H_4)OsB_{10}H_7(OEt)_2]$  in  $CD_2Cl_2$  solution at +21 °C.

$\delta^{11}B$	$\delta^1H$	Tentative assignment
84.5 } 78.9 }		2, 5
14.1		3
7.9 } 6.1 }	3.99 } 3.92 }	8, 10
5.1	1.69	One of 4, 6, 7; probably 4
2.9 } 1.7 }	2.33 } 2.42 }	9, 11
-0.7 } 1.1 }	1.53 } 1.20 }	Two of 4, 6, 7; probably 6, 7

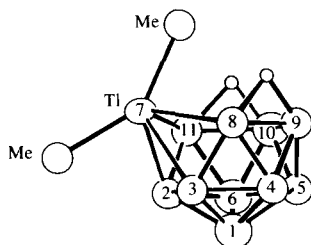

FIG. 45. Numbering scheme for  $Me_2TiB_{10}H_{12}^-$ .

TABLE 40

Selected <sup>11</sup>B NMR parameters for a saturated solution of  $[TiMe_2]^+[Me_2TiB_{10}H_{12}]^-$  in  $(CD_3)_2CO$  at +21 °C.

Assignment	$\delta^{11}B$	Relative intensity	$^nJ(^{205}Ti-^{11}B)$	<i>n</i>	Approx. $T_1(^{11}B)$ (ms)
(8, 11)	8.2	2B	173	1	2.9
(1)	3.0	1B	84	2	15.5
(2, 3)	-3.1	2B	258	1	9.7
(5)	-2.8	1B	<30	2	17.3
(9, 10)	-4.7	2B	<30	2	9.0
(4, 6)	-31.7	2B	77	2	23.1

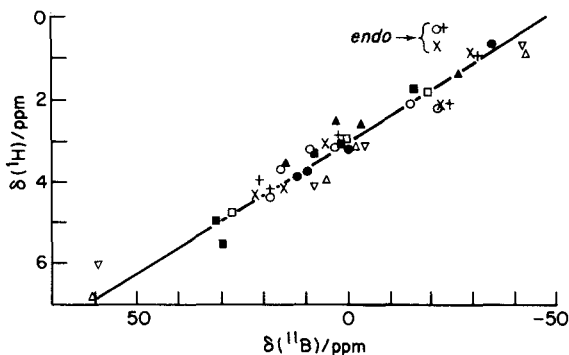


FIG. 46.  $^1\text{H}$ - $^{11}\text{B}$  nuclear-shielding correlation plot (with bridging protons omitted) for the compounds  $[(\text{PhMe}_2\text{P})_2\text{PdB}_8\text{H}_{12}]$  (X),  $\text{B}_{10}\text{H}_{14}$  (●),  $\text{PhMe}_2\text{P} \cdot \text{B}_9\text{H}_{13}$  (○),  $[(\text{PhMe}_2\text{P})_4\text{PtB}_8\text{H}_{10}]$  (■),  $[(\text{PhMe}_2\text{P})_4\text{Pt}_2\text{B}_8\text{H}_{10}]$  (□),  $(\text{PhMe}_2\text{P})_2\text{PtB}_{10}\text{H}_{12}$  (▲),  $[(\text{PhMe}_2\text{P})_2\text{PtB}_8\text{H}_{12}]$  (+),  $[(\text{PhMe}_2\text{P})_2\text{Pt}_2(\text{B}_6\text{H}_9)_2]$  (Δ), and  $[(\text{Ph}_3\text{P})_2\text{Pt}_2(\text{B}_6\text{H}_9)_2]$  (▽). The line drawn represents the ratio  $\delta(^{11}\text{B}) : \delta(^1\text{H}) = 16 : 1$ .

signs of  $^nJ(^{205}\text{Tl}-^{11}\text{B})$ .<sup>271</sup> A linear correlation between  $^1\text{H}$  and  $^{11}\text{B}$  chemical shifts in a coherent series of  $\text{B}_6$ ,  $\text{B}_8$  and  $\text{B}_{10}$  metalloboranes containing Pd and Pt has been noted (Fig. 46).<sup>272</sup> Such welcome data will be of assistance in assigning spectra by spin-decoupling techniques.

A metalloborane, *nido*-( $\text{Me}_5\text{Cp}$ ) $\text{RhB}_{10}\text{H}_{11}\text{Cl}(\text{PhPMe}_2)$ , that is an exception to the  $\text{B}_{10}\text{H}_{12}\text{M}$  structural pattern, and which may be viewed as an analogue of  $\text{B}_{11}\text{H}_{14}$ , has recently been reported (Fig. 47). The  $\text{B}-\text{H}-\text{Rh}$

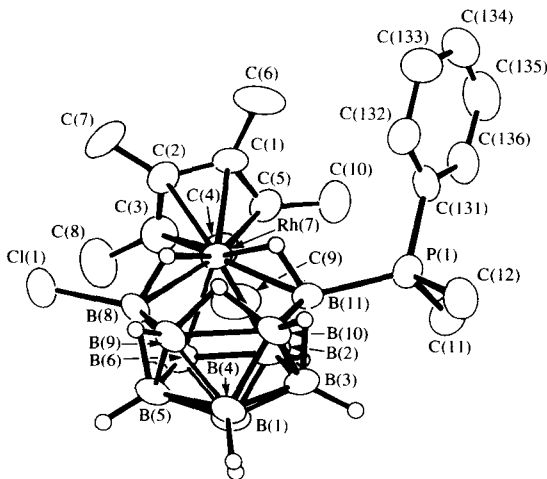


FIG. 47. Drawing of the molecular structure of  $[(\text{C}_5\text{Me}_5)\text{Rh}_{10}\text{H}_{11}\text{Cl}(\text{PMe}_2\text{Ph})]$ , with organyl hydrogen atoms omitted for clarity.

and B—H—B bridges are located, but they readily interconvert in solution as is the case with  $\text{B}_{11}\text{H}_{14}^-$ .  $^{11}\text{B}$  NMR assignments are made with the use of 2D NMR spectroscopy: 14.2 (B3), 2.5 (B2), 1.7 B(4), -5.6 (B8), -9.5 (B6), -13.3 (B9), -16.9 (B10), -17.0 (B1), -18.5 (B5), and -29.2 (B11) ppm. The shielding values are grossly different from those for 8-Cl(PhPMe<sub>2</sub>)<sub>2</sub>PtB<sub>10</sub>H<sub>11</sub>, and it is probable that the fundamental structures of these two types of metalloboranes are also dissimilar.<sup>273</sup> A second example of this uncommon structural type is [Ru(NCMe)<sub>6</sub>]-[7-Me<sub>6</sub>C<sub>6</sub>-*nido*-7-RuB<sub>10</sub>H<sub>13</sub>]<sub>2</sub>. It has  $\delta^{11}\text{B}$  = -0.8 B(2,3), -7.2 (B4,6), -17.2 (B1), -17.7 (B9,10), -22.8 (B5), and -23.8 (B8,11).<sup>274</sup>

The novel double-cluster metalloborane [(Me<sub>6</sub>C<sub>6</sub>)<sub>2</sub>Ru<sub>2</sub>H<sub>4</sub>] $\text{RuB}_{10}\text{H}_8(\text{OEt})_2$  has been obtained from (Me<sub>6</sub>C<sub>6</sub>)RuCl(B<sub>3</sub>H<sub>8</sub>) and B<sub>10</sub>H<sub>10</sub><sup>2-</sup>; the two ethoxy groups are derived from the ethanol solvent. Its structure, shown in Fig. 48, features an (arene)<sub>2</sub>Ru<sub>2</sub>( $\mu$ -H<sub>2</sub>) unit linked by two bridging hydrogen atoms to a B<sub>10</sub>Ru cluster. Its  $^{11}\text{B}$  NMR spectrum has been assigned: 88.1 (B—OEt), 1.6 (B4, 5, 6, 7), 3.6 (B8, 9), -0.1 (B10, 11) ppm. Note that the numbering scheme adopts the latest recommended artifices and so is inconsistent with that used in earlier publications.<sup>275</sup> In an elaboration of the isolobal relationship between the R<sub>3</sub>PAu and  $\mu$ -H ligands it has been discovered that B<sub>10</sub>H<sub>14</sub> and Et<sub>3</sub>PAuMe react to form (B<sub>10</sub>H<sub>12</sub>Au)-(AuPEt<sub>3</sub>)<sub>4</sub>(AuB<sub>10</sub>H<sub>12</sub>). In this triple-cluster compound two AuB<sub>10</sub>H<sub>12</sub> cages are connected by an Au—Au bond (Fig. 49a). It has  $\delta^{11}\text{B}$  = 119.9

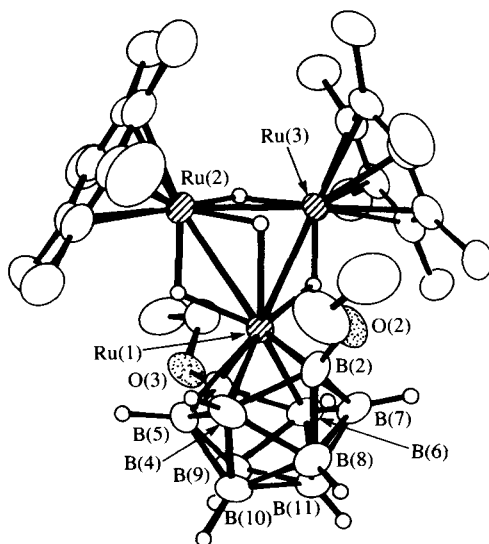


FIG. 48. Structure of [(Me<sub>6</sub>C<sub>6</sub>)<sub>2</sub>Ru<sub>2</sub>H<sub>4</sub>] $\text{RuB}_{10}\text{H}_8(\text{OEt})_2$ .

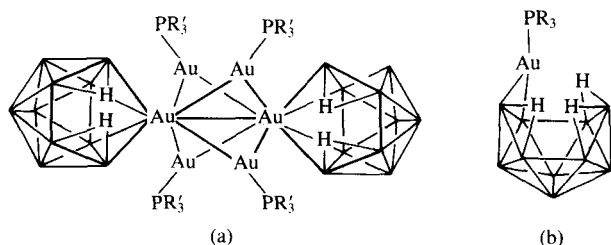


FIG. 49. Structures of  $(B_{10}H_{12})(AuPEt_3)_4(AuB_{10}H_{12})$  (a) and  $R_3PAuB_{10}H_{13}$  (b).

(br, 4B), 0.7 (2B),  $-4.9$  (2B) and  $-24.5$  (2B). However, use of more bulky phosphines permits isolation of smaller clusters, e.g.  $(c-C_6H_{11})_3PAuB_{10}H_{13}$ ,  $\delta^{11}B = 16.1$  (1B),  $9.3$  (1B),  $8.4$  (1B),  $2.8$  (1B),  $1.4$  (1B),  $-0.6$  (2B),  $-1.0$  (1B),  $-29.5$  (1B) and  $-35.6$  (1B), whose structure is essentially like that of  $B_{10}H_{14}$  with one bridging hydrogen atom replaced by a  $R_3PAu$  unit (Fig. 49b).<sup>276</sup>

Platinum insertion into  $B_{11}SeH_{11}$  yields  $(Ph_3Pt)_2PtB_{10}H_{10}$ . The  $^{11}B$  NMR spectrum exhibits resonances at  $18.5$  (1B),  $6.7$  (m, 3B,  $J(Pt-B) = 226$ ),  $-2.1$  (2B),  $-12.2$  (2B) and  $-20.9$  (2B) ppm.<sup>277</sup>

Reaction of  $(PhPMe_2)_3RuCl_3$  with  $Na_2B_{12}H_{12}$  yields  $(PhPMe_2)_3RuB_{12}H_{12}$ , a novel  $RuB_{12}$  metalloborane in which a  $P_3Ru$  fragment is linked via three  $B-H-Ru$  bonds to one triangular face of the  $B_{12}$  cage (Fig. 50). Its  $^{11}B$  NMR spectrum shows four doublets of unit area at  $-8.0$ ,  $-10.2$ ,  $-16.4$  and  $-24.6$  ppm (cf.  $-16$  ppm for  $B_{12}H_{12}^{2-}$ ). Similarly,  $[(Ph_3P)_2ClRu]B_{12}H_{11}-7-NEt_3$ , in which the  $P_2ClRu$  fragment is similarly bonded and in which  $Et_3N$  substitutes for  $H^-$  on B7, adjacent to the ligating  $B_3$  triangle, has  $\delta^{11}B = 1.9$  (s, 1B),  $-13.2$  (2B),  $-14.5$  and approx.  $15$  (4B),  $-16.1$  (1B),  $-17.4$  (1B) and  $-21.9$  (2B). The tridentate  $B-H-Ru$  interaction is associated with approx.  $9$  ppm shielding of the three  $B-H-Ru$  positions in the cage and a reduction to about  $100$  Hz of  $^1J(B-H)$ .<sup>278</sup>

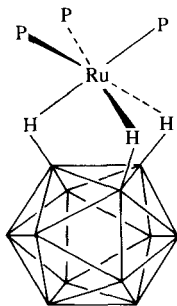


FIG. 50. Structure of  $(PhPMe_2)_3RuB_{12}H_{12}$ .

In a paper that is a cornucopia of new results, Greenwood and coworkers describe the reaction of  $\text{B}_{10}\text{H}_{12}(\text{SMe}_2)_2$  with concentrated  $\text{H}_2\text{SO}_4$  to provide  $(6\text{-B}_{10}\text{H}_{13})_2\text{O}$  and  $6\text{-HOB}_{10}\text{H}_{13}$ . The  $^{11}\text{B}$  NMR spectra of both are assigned with the use of partially relaxed Fourier-transform (PRFT) techniques.  $6\text{-HOB}_{10}\text{H}_{13}$  has  $\delta^{11}\text{B} = 26.1$  (B6), 6.5 (B1, 3), 5.0 (B9), 4.3 (B8, 10),  $-13.7$  (B5),  $-31.7$  (B6), and  $-43.7$  (B7); in  $(6,6'\text{-B}_{10}\text{H}_{13})_2\text{O}$ , the analogous peaks occur at 21.8, 5.6, 7.2, 3.0,  $-10.7$ ,  $-33.2$  and  $-42.5$  ppm.  $T_1$  data are obtained for  $6\text{-HOB}_{10}\text{H}_{13}$  as a function of temperature; values for the hydroxy compound are somewhat longer on account of the smaller molecular size (Fig. 51). Both oxygenated decaborane derivatives are provenders of a wide variety of metalloboranes. Reaction with *cis*- $\text{PtCl}_2\text{L}_2$  ( $\text{L} = \text{PhPMe}_2$  or  $\text{Ph}_3\text{P}$ ) yields *arachno*- $\text{B}_8\text{H}_{12}\text{PtL}_2$  (see above) and *nido*- $\text{B}_{10}\text{H}_{12}\text{PtL}_2$ . Also formed is  $\text{Pt}_2(\mu\text{-}\eta^3\text{-B}_6\text{H}_9)_2\text{L}_2$ . This unusual compound has a  $\text{P}\text{---}\text{Pt}\text{---}\text{Pt}\text{---}\text{P}$  unit bonded to two tridentate  $\text{B}_6\text{H}_9$  ligands (Fig. 52). The  $^{11}\text{B}$  chemical shifts are  $-42.0$  (d, 140, B1),  $-3.6$  (d, 135, B2,4), 8.3 (d, 130, B5,6) and 59.7 (d, 135, B3);  $T_1$  values are 7.7, approx. 0.9, approx. 1.0 and 2.5 ms respectively. The unusual high-frequency shift of B3 may be related to the  $\text{Pt}_2\text{B}$  feature in this molecule, and in the  $\text{Ph}_3\text{P}$  analogue it occurs at 60.5 ppm. Spin coupling between B2, 3, and B3, and  $^{195}\text{Pt}$  is quite large, approx. 300 Hz. Additional structural features, not apparent in the electron-density maps but revealed by NMR studies are

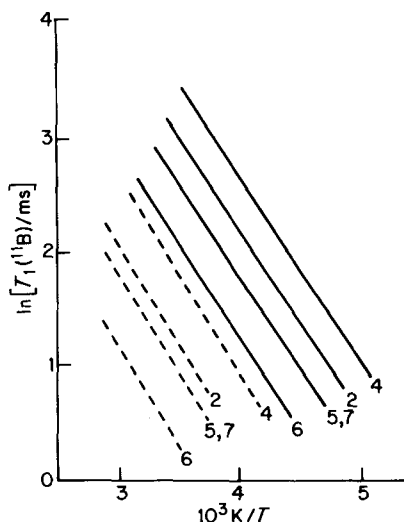
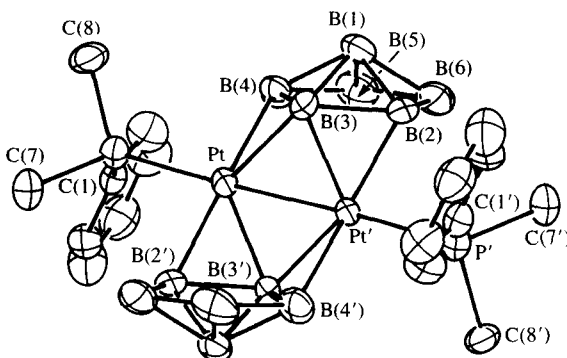
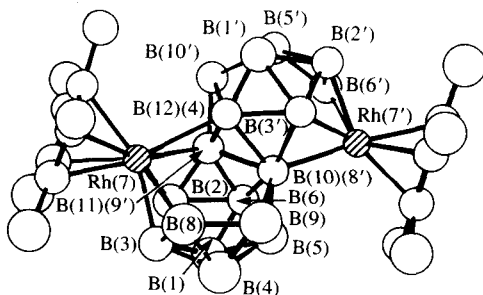


FIG. 51. Gross variation with temperature of the longitudinal relaxation times  $T_1(^{11}\text{B})$  of selected  $^{11}\text{B}$  resonances of  $\text{B}_{10}\text{H}_{13}\text{OH}$  in  $\text{CDCl}_3$  (—) and  $(\text{B}_{10}\text{H}_{13})_2\text{O}$  in  $^{11}\text{B}$   $\text{CD}_3\text{C}_6\text{D}_5$  (---).

FIG. 52. Structure of  $\text{Pt}_2(\text{B}_6\text{H}_9)_2(\text{PhPMe}_2)_2$ .

bridging hydrogen atoms between B4—B5 and B2—B6, and a B5—H—B6 bridge.<sup>233</sup>

A unique example of a  $\text{B}_{17}$  metalloborane,  $(\text{Me}_5\text{CpRh})_2\text{B}_{17}\text{H}_{19}$ , arises from *anti*- $\text{B}_{18}\text{H}_{20}^{2-}$  and  $(\text{Me}_5\text{CpRhCl}_2)_2$ . Its structure is shown in Fig. 53, and an assignment of the  $^{11}\text{B}$  NMR spectrum proposed: 28.0 (B6'), 19.2 (B6), 15.3 (B11), 13.8 (B3), 12.8 (B3'), 8.8 (B1'), 3.8 (B5), 3.1 (B2), 1.6 (B1), 1.3 (B8), 1.0 (B5'), -2.2 (B9), -5.6 (B10), -10.8 (B10'), -17.8 (B2'), -28.2 (B4), and -44.1 (B12) ppm.<sup>279</sup>

FIG. 53. Molecular structure of  $(\text{C}_5\text{Me}_5)_2\text{Rh}_2\text{B}_{17}\text{H}_{19}$ .

## VII. COUPLED BORANES AND CARBORANES

Chloro and bromo derivatives of 2,2'-( $\text{B}_5\text{H}_8$ )<sub>2</sub> have been prepared by Lewis-base-catalysed halogenation.  $^{11}\text{B}$  NMR data for these compounds are in Table 41.<sup>280</sup> Boranes and carboranes coupled by B—B two-centre

TABLE 41

 $^{11}\text{B}$  NMR data for coupled boranes.

Compound	$\delta^{11}\text{B}$
1-Cl-2,2'-( $\text{B}_5\text{H}_7$ )( $\text{B}_5\text{H}_8$ )	-11.4 (B2-5), -12.4 (B2'-5'), -28.6 (B1), -51.3 (d, 171, B1')
1-Br-2,2'-( $\text{B}_5\text{H}_7$ )( $\text{B}_5\text{H}_8$ )	-10.9 (B2-5), -12.0, -13.0 (B2'-5'), -35.6 (B1), -51.1 (d, 182, B1')
1,1'-Cl <sub>2</sub> -2,2'-( $\text{B}_5\text{H}_7$ ) <sub>2</sub>	-10.6, -12.1, -28.7 (B1)
1,1'-Br <sub>2</sub> -2,2'-( $\text{B}_5\text{H}_7$ ) <sub>2</sub>	-9.1, -10.9, -12.2, -35.7 (B1)
1'-Cl-1,2'-( $\text{B}_5\text{H}_8$ )( $\text{B}_5\text{H}_7$ )	-3.4 (B2'), -13.3 (d, 156, B2-5 and B3'-5'), -27 (B1'), -56.8 (B1)
1:2'-[2-MeB <sub>5</sub> H <sub>7</sub> ][3'-MeB <sub>5</sub> H <sub>7</sub> ]	2.0 (s, B2, 3'), -4.0 (s, B2', J(B-B) = 112), -12.9 (d, 162, B3, 5, 4'), -17.8 (d, 162, B4, 5'), -49.1 (d, 177, B1'), -55.0 (s, B1, J(B-B) $\approx$ 115)
1:1'[B <sub>4</sub> H <sub>9</sub> ] <sub>2</sub>	-5.7 (t, 131, B2, 2', 4, 4'), -38.1 (s, B1, 1'), -39.5 (d, 174, B3, 3')
1:2'-[B <sub>4</sub> H <sub>9</sub> ][B <sub>5</sub> H <sub>8</sub> ]	-5.9 (t, 126, B2, 4), -5.9 (s, B2'), -11.6 (d, 159, B3', 5'), -13.1 (d, 157, J(B-B) $\approx$ 21, B4'), -39.2 (d, 170, B3), -41.5 (s, J(B-B) = 103, B1), -50.9 (d, 168, B1)
1:2'-[B <sub>4</sub> H <sub>9</sub> ][1'-MeB <sub>5</sub> H <sub>7</sub> ]	-7.1 (t, 124, B2, 4), -7.1 (s, B2'), -12.3 (d, 157, B3', 5'), -13.7 (d, 171, J(B-B) = 25, B4'), -40.3 (d, 153, B3), -41.8 (s, B1), -43.3 (s, B1')
2:2'-[1,6-B <sub>4</sub> C <sub>2</sub> H <sub>5</sub> ] <sub>2</sub>	-13.8 (d, 202, B4, 4'), -15.3 (s, B2, 2'), -15.6 (d, 196, B3, 3', 5, 5')

bonds have been prepared by PtBr<sub>2</sub>-catalysed fusion reactions. Structural assignments are derived from  $^{11}\text{B}$  NMR data (Table 42). Values of approx. 100 Hz for  $J(\text{B-B})$  are typical in materials such as 1:1'-( $\text{B}_4\text{H}_9$ )<sub>2</sub>.<sup>281</sup> High-resolution 128.4 MHz  $^{11}\text{B}$  NMR spectra of a series of coupled boranes and carboranes have been published (see Table 42). The B-B coupling for two-centre bonds ranges from 149 Hz in 1:1'-( $\text{B}_5\text{H}_8$ )<sub>2</sub> to approx. 105 Hz in 1:2'-( $\text{B}_{10}\text{H}_{13}$ )<sub>2</sub>, but is substantially lower, 75 Hz, in ( $\text{Me}_2\text{N}$ )<sub>4</sub>B<sub>2</sub>. Spin coupling between boron nuclei within a cluster are an order of magnitude smaller. In cases where two  $^{11}\text{B}$  nuclei are chemically equivalent, B-B couplings may be obtained from the  $^{10}\text{B}$  NMR spectra. Application of relationships between  $J(\text{B-B})$  and s-orbital content<sup>282</sup> are used to calculate the fractional s character of exopolyhedral B-B bonds.<sup>283</sup>

Platinum bromide also catalyses the dehydrogenative coupling of small boranes and carboranes. Thus 1,5-B<sub>3</sub>C<sub>2</sub>H<sub>5</sub> and B<sub>2</sub>H<sub>6</sub> give the new carborane 5,6-B<sub>6</sub>C<sub>2</sub>H<sub>12</sub> (Fig. 54a), which has  $\delta^{11}\text{B} = -10.6$  (d, 160, B3), -17.6 (td, 134, 28, B2,4) and -29.5 (dd, 160, 39, B8,10). The spectrum indicates the presence of a mirror plane of symmetry and of two

TABLE 42

Spin-spin couplings in two-centre two-electron BB bonds.

Compound	$J(^{11}\text{B}-^{11}\text{B})$
3:3'-[2,4-C <sub>2</sub> B <sub>5</sub> H <sub>6</sub> ] <sub>2</sub>	151
1:1'-[B <sub>5</sub> H <sub>8</sub> ] <sub>2</sub>	149
2:2'-[1,5-C <sub>2</sub> B <sub>3</sub> H <sub>4</sub> ] <sub>2</sub>	137
2:2',3':1''-[1,5-C <sub>2</sub> B <sub>3</sub> H <sub>4</sub> ][1',5'-C <sub>2</sub> B <sub>3</sub> H <sub>3</sub> ][1'',5''-C <sub>2</sub> B <sub>3</sub> H <sub>4</sub> ]	135 B' <sub>2</sub>
2':2-[1',5'-C <sub>2</sub> B <sub>3</sub> H <sub>4</sub> ][1,6-C <sub>2</sub> B <sub>4</sub> H <sub>5</sub> ]	131, 126
1-(Cl <sub>2</sub> B)B <sub>5</sub> H <sub>8</sub>	≈124
1:3'-[2,4-C <sub>2</sub> B <sub>5</sub> H <sub>6</sub> ] <sub>2</sub>	124 B' <sub>3</sub> (120 B <sub>1</sub> )
1-(Cl <sub>2</sub> B)-2-ClB <sub>5</sub> H <sub>7</sub>	≈122
1:5'-[2,4-C <sub>2</sub> B <sub>5</sub> H <sub>6</sub> ] <sub>2</sub>	119
1:2'-[B <sub>5</sub> H <sub>8</sub> ] <sub>2</sub>	115 B <sub>1</sub> (110 B <sub>2</sub> ) 106
2:1'-[1-(CH <sub>3</sub> )B <sub>5</sub> H <sub>7</sub> ][B <sub>5</sub> H <sub>8</sub> ]	121 B' <sub>1</sub> (103 B <sub>2</sub> )
1:2'-[B <sub>10</sub> H <sub>13</sub> ] <sub>2</sub>	≈105
3:5'-[2,4-C <sub>2</sub> B <sub>5</sub> H <sub>6</sub> ] <sub>2</sub>	≥100
2:2'-[B <sub>5</sub> H <sub>8</sub> ] <sub>2</sub>	≥79
B <sub>2</sub> [N(CH <sub>3</sub> ) <sub>2</sub> ] <sub>4</sub>	75

<sup>11</sup>B NMR parameters for the dimers of B<sub>5</sub>H<sub>9</sub>.

Compound	$J(^{11}\text{B}-^{11}\text{B})$		$\delta^{11}\text{B}$	
	Base-to-apex	Exopolyhedral	Base	Apex
1:1'-[B <sub>5</sub> H <sub>8</sub> ] <sub>2</sub>	17.7 ± 0.6	149.3 ± 3.7 (B1-B1')	-13.2	-55.4
1:2'-[B <sub>5</sub> H <sub>8</sub> ] <sub>2</sub>	17.6 ± 2.4 (B2, 3, 4, 5; B(3', 5'))	109.6 ± 2.4 (B2'-B1)	-3.6 (B2')	-50.7 (B1')
		115.0 ± 2.4 (B1-B2')	-12.6 (B2, 3, 4, 5; B3', 5')	-56.2 (B1)
	19.4 ± 2.4 (B4')		-13.4 (B4')	
2:2'-[B <sub>5</sub> H <sub>8</sub> ] <sub>2</sub>	20.5 ± 2.0 (B3, 3', 5, 5')	79.4 ± 1.4 (B2-B2')	-11.0 (B2, 2') -11.6 (B4, 4')	-51.2
	21.3 ± 2.0 (B4, 4')		-12.6 (B3, 5, 3', 5')	

TABLE 42 (*cont.*) $^{11}\text{B}$  NMR parameters for  $2,4\text{-C}_2\text{B}_5\text{H}_7$  and selected coupled dimers.

Compound	$J(^{11}\text{B}\text{--}^{11}\text{B})$		$\delta^{11}\text{B}$	
	Base-to-apex	Exopolyhedral	Base	Apex
$2,4\text{-C}_2\text{B}_5\text{H}_7$	$9.2 \pm 0.5$ (B1–B5)		6.7 (B3)	–22.1 (B1, 7)
	$9.7 \pm 0.5$ (B5–B1)		3.6 (B5, 6)	
$1:3'\text{-}[2,4\text{-C}_2\text{B}_5\text{H}_6]_2$		$119.9 \pm 2.9$ (B3'–B1)	8.0 (B3)	–17.1 (B1)
		$123.7 \pm 2.9$ (B1–B3')	7.1 (B3')	–18.5 (B7)
			5.3 (B5, 6)	–21.4 (B1', 7')
			4.6 (B5', 6')	
$3:3'\text{-}[2,4\text{-C}_2\text{B}_5\text{H}_6]_2$	$9.8 \pm 0.6$ (B1–B5)	$151.4 \pm 3.6$	9.5 (B3, 3')	–21.1 (B1, 7, 1', 7')
	$9.3 \pm 0.6$ (B5–B1)		5.0 (B5, 6, 5', 6')	
$3:5'\text{-}[2,4\text{-C}_2\text{B}_5\text{H}_6]_2$		$\geq 100$	$\sim 10.8$ (B3)	–21.0 (B1, 7, 1', 7')
			8.0 (B3')	
			$\sim 6.2$ (B5')	
			5.5 (B6')	
			4.9 (B5, 6)	

B—H—BH<sub>2</sub> groups that appear as a triplet of doublets. Spin coupling between B3 and B9 is unobserved in the 2D NMR spectrum. This may be a general phenomenon when one of the boron atoms is situated between two carbon atoms and on an “open face”. The coupling product of  $1,6\text{-B}_4\text{C}_2\text{H}_6$  and B<sub>2</sub>H<sub>6</sub> is  $2:1',2'\text{-}[1,6\text{-B}_4\text{C}_2\text{H}_5][\text{B}_2\text{H}_5]$  (Fig. 54b), which is considered to feature a  $1,6\text{-B}_4\text{C}_2\text{H}_5$  cage linked at B2 to an exopolyhedral B<sub>2</sub>H<sub>5</sub> unit by means of a B—B—B three-centre bond. Its  $^{11}\text{B}$  NMR spectrum contains peaks at –3.9 (t, 154, B1',2',  $J(\text{B—B}) = 23$  Hz), –12.6 (d, 202, B3,5), –16.0 (d, 128, B4) and –23.7 (s, B2) ppm. The –3.9 ppm triplet is assigned to the ligating BH<sub>2</sub> moiety. Spin coupling to B2, however,

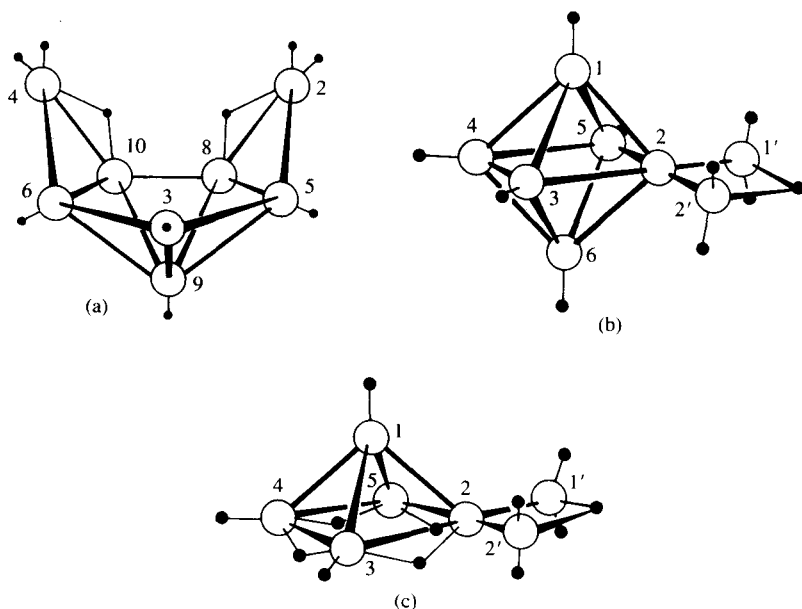
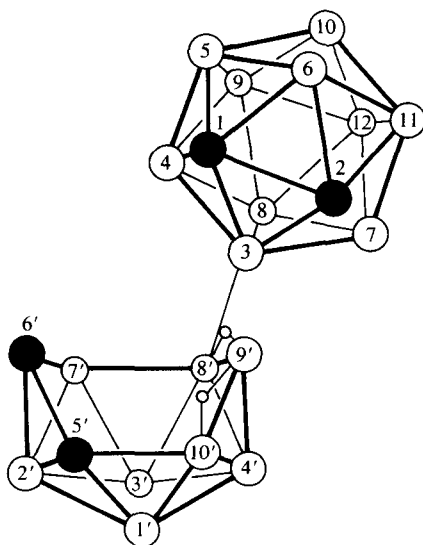


FIG. 54. Proposed structures for 5,6- $\text{C}_2\text{B}_6\text{H}_{12}$  (a), 2:1',2'-[1,6- $\text{C}_2\text{B}_4\text{H}_5$ ][ $\text{B}_2\text{H}_5$ ] (b) and 2:1',2'-[ $\text{B}_5\text{H}_8$ ][ $\text{B}_2\text{H}_5$ ] (c).

is unobserved. The  $^{11}\text{B}$  NMR spectrum of 2:1',2'-[ $\text{B}_5\text{H}_8$ ]-[ $\text{B}_2\text{H}_5$ ] (Fig. 54c),  $-1.5$  (t, 128,  $J(\text{B}-\text{B}) = 26$  Hz,  $\text{B}1'2'$ ),  $-10.9$  (d, 161,  $J(\text{B}-\text{B}) = 18$  Hz,  $\text{B}3, 5$ ), approx. 11 (s,  $\text{B}2$ ),  $-12.0$  (d, 161,  $J(\text{B}-\text{B}) = 19$  Hz,  $\text{B}4$ ), and  $-50.5$  (d, 193,  $\text{B}1$ ) ppm, may be similarly interpreted.<sup>284</sup>

$^{11}\text{B}$  and  $^{11}\text{B}(\text{COSY})$  data for  $[\text{Bu}_4\text{N}][\text{anti-}\text{B}_{18}\text{H}_{21}]$  have been published: 11.5 (s, 1B), 14.1 (1B), 10.2 (1B), 5.7 (1B), 4.0 (1B), 0.9 (s, 1B),  $-0.4$  (1B),  $-3.7$  (2B),  $-7.1$  (1B),  $-9.9$  (2B),  $-12.7$  (2B),  $-23.3$  (1B),  $-28.5$  (1B),  $-38.4$  (1B) and  $-40.4$  (1B) ppm.<sup>178</sup>

Iso- $\text{B}_{18}\text{C}_4\text{H}_{22}$ , formed in the pyrolysis of 7,8- $\text{B}_9\text{C}_2\text{H}_{13}$ , has been reported to be 3-(8'-nido-5,6- $\text{B}_8\text{C}_2\text{H}_{11}$ )-1,2- $\text{B}_{10}\text{C}_2\text{H}_{11}$ , i.e. a two-centre bond connects  $\text{B}3$  and  $\text{B}8$  in the two cages (Fig. 55). This conclusion is indicated by the  $^{11}\text{B}$  NMR spectrum, which is approximately a composite due to the two independent clusters.  $B$ -substitution generally leads to a  $7 \pm 1$  ppm shift for the substituted boron atom and a  $-2 \pm 1$  ppm shift for adjacent atoms. Chemical-shift data and assignments are: 8.5 (br,  $\text{B}8'$ ), 6.9 ( $\text{B}7'$ ), 5.3 ( $\text{B}1'$ ),  $-2.4$  ( $\text{B}9'$ ),  $-2.7$  ( $\text{B}3', 9, 12$ ),  $-7.9$  ( $\text{B}10'$ ),  $-8.8$  ( $\text{B}8, 10$ ),  $-11.6$  ( $\text{B}3$ ),  $-13.1$  ( $\text{B}4, 11$ ),  $-13.6$  ( $\text{B}5, 7$ ),  $-14.6$  ( $\text{B}6$ ),  $-27.0$  ( $\text{B}2'$ ) and  $-37.4 \pm 0.3$  ( $\text{B}4'$ ) ppm.<sup>285</sup>

FIG. 55. Structure of  $i\text{-B}_{18}\text{C}_4\text{H}_{22}$ .

### VIII. TRANSITION-METAL COMPLEXES OF BORON-CONTAINING HETEROCYCLES

Transition metals can bond to both planar faces of certain boron-containing heterocycles. This structural feature, uncommonly encountered with carbocyclic ligands, permits synthesis of linear, aggregated or "multiple-decker" compounds and even polymers.<sup>286-288</sup> Even less aggregated structures display common and interesting bonding features, which distinguish this class of compounds.

The sandwich compound  $(1\text{-Me-2-}t\text{-Bu-1,2-BNC}_3\text{H}_6)_2\text{Ru}$  forms two isomers, which have a clockwise and anticlockwise conformation of the two 1,2-azaborolanyl rings. The  $^{11}\text{B}$  shifts for the undifferentiated isomers are  $16.2$  and  $14.2 \pm 0.5$  ppm; and  $16.0$ ,  $17.8$  ppm for the  $\text{B-SiMe}_3$  analogue.<sup>289</sup> A series of cationic  $\pi$ -azaborolanyl complexes, illustrated by  $(1,2\text{-Me}_2\text{-1,2-BNC}_3\text{H}_6)_2\text{Co}^+$ , have  $\delta^{11}\text{B} = 23 \pm 1$  ppm.<sup>290</sup> The chemical shifts of  $\text{Li}[1\text{-Me-2-}t\text{-Bu-1,2-BNC}_3\text{H}_6]$  and the complex  $(1\text{-Me-2-}t\text{-Bu-1,2-BNC}_3\text{H}_6)_2\text{Ni}$  are both  $27$  ppm,<sup>291</sup> and that of  $(1,3\text{-Me}_2\text{-4,5-Et}_2\text{-1,3,2-B}_2\text{SC}_2)\text{NiCp}$  is  $26.8$  ppm.<sup>292</sup>

The  $^{11}\text{B}$  chemical shift for pentaphenylborole, which contains a  $\text{C}_4\text{B}$  ring, is  $55$  ppm. It undergoes a large shielding increase to  $5$  ppm upon complexation with pyridine.<sup>293</sup> Transition-metal compounds catalyze the

isomerization of 3-borolenes to 2-borolenes.<sup>294</sup> A huge variety of transition-metal  $\pi$ -borole complexes has been prepared and studied.<sup>295–302</sup> Chemical shifts of representative examples are given in Table 43. Variation in the metal identity appears to produce little change in  $\delta^{11}\text{B}$  on proceeding down a column in the periodic table (e.g. Ru to Os), but there is a significant shielding increase on proceeding across a row (e.g. Rh to Ru). Thus the  $^{11}\text{B}$  chemical shifts of  $(\text{PhBC}_4\text{H}_4)\text{Ru}(\text{CO})_3$ ,  $(\text{PhBC}_4\text{H}_4)\text{Os}(\text{CO})_3$ ,  $(\text{PhBC}_4\text{H}_4)\text{-RhHCl}(\text{PPh}_3)_2$  and  $(\text{PhBC}_4\text{H}_4)\text{RuHCl}(\text{PPh}_3)_2$  are 21.4, 19.5, 32 and 9.4 ppm respectively.<sup>295</sup> The triple-decker complex  $(\text{MeBC}_4\text{H}_4)\text{Co}(\text{MeBC}_4\text{H}_4)\text{Co}(\text{MeBC}_4\text{H}_4)$  has  $\delta^{11}\text{B} = 12.3$  (1B) and 22.8 (2B). These data reflect the general trend that boron in the centre  $\text{RBC}_4\text{H}_4$  ring, to which two metals are bonded, is more shielded than that in the end or capping  $\text{RBC}_4\text{H}_4$  rings to which only one metal atom is bonded.<sup>296,298</sup>

TABLE 43

<sup>11</sup>B NMR data for boron-heterocycle–metal complexes.

Compound	$\delta^{11}\text{B}$
Ph-3-borolene	86.2
Mesityl-3-borolene	95.0
$\text{Me}_2\text{N}$ -3-borolene	51.1
$\text{Et}_2\text{N}$ -3-borolene	52.3
Ph-2-borolene	73.9
$\text{Me}_2\text{N}$ -2-borolene	48.3
Me-2-borolene	81.0
Cl-2-borolene	71.4
MeO-2-borolene	54.8
$(\text{MeOBC}_4\text{H}_4)\text{Ru}(\text{CO})_3$	28.3
$(\text{MeBC}_4\text{H}_4)\text{Ru}(\text{CO})_3$	22.8
$(1,3,5\text{-Me}_3\text{BC}_4\text{H}_2)\text{Ru}(\text{CO})_3$	18
$(\text{PhBC}_4\text{H}_4)\text{OsHCl}(\text{PPh}_3)_2$	9.0
$[(\text{PhBC}_4\text{H}_4)\text{Rh}(\text{PMe}_3)_3]\text{Cl}$	25.2
$(\text{PhBC}_4\text{H}_4)\text{Ru}(\text{C}_6\text{H}_6)$	13.5
$(\text{MeBC}_4\text{H}_4)\text{Co}(\text{CO})_2\text{I}$	27.9
$(\text{MeBC}_4\text{H}_4)\text{CoCp}$	21.9
$(\text{PhBC}_4\text{H}_4)\text{Co}(\text{PhBC}_4\text{H}_4)\text{Co}(\text{PhBC}_4\text{H}_4)$	19.2 (2B), 11.9 (1B)
$\text{CpFe}(\text{PhBC}_4\text{H}_4)\text{Co}(\text{PhBC}_4\text{H}_4)$	16.7 (2B), 7.3 (2B)
$(\text{MeBC}_4\text{H}_4)\text{Co}(\text{MeBC}_4\text{H}_4)\text{Mn}(\text{CO})_3$	24.7 (2B), 15.7 (1B)
$\text{Me}_4\text{N}[(\text{MeBC}_4\text{H}_4)_2\text{Co}]$	13.9
$(\text{PhBC}_4\text{H}_4)\text{Co}(\text{PhBC}_4\text{H}_4)\text{Rh}(\text{C}_8\text{H}_{12})$	18.2 (2B), 11.6 (1B)
$[(\text{PhBC}_4\text{H}_4)\text{Co}(\text{PhBC}_4\text{H}_4)\text{Cr}(\text{CO})_3]^-$	16.2 (2B), 12.9 (1B)
$(\text{CO})_3\text{Mn}(\text{PhBC}_4\text{H}_4)\text{Mn}(\text{CO})_3$	19.7
$(\text{MeBC}_4\text{H}_4)\text{Fe}(\text{CO})_3$	22.4
$(\text{MeBC}_4\text{H}_4)_2\text{Co}_2(\text{CO})_4$	27.9
$\text{Li}_2[\text{i-Pr}_2\text{NBC}_4\text{H}_4]$	22

TABLE 43 (*cont.*) $^{11}\text{B}$  NMR data for boron-heterocycle-metal complexes.

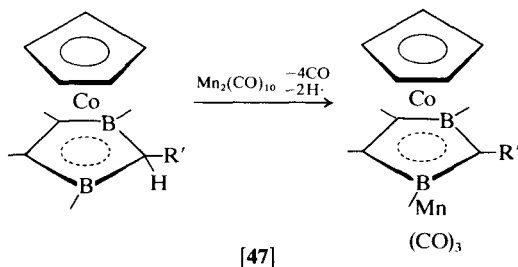
Compound	$\delta^{11}\text{B}$
( <i>i</i> -Pr <sub>2</sub> NBC <sub>4</sub> H <sub>4</sub> )Ru(Me <sub>6</sub> C <sub>6</sub> )	22
( <i>i</i> -Pr <sub>2</sub> NBC <sub>4</sub> H <sub>4</sub> )Rh( <i>i</i> -Pr <sub>2</sub> NBC <sub>4</sub> H <sub>4</sub> )Rh( <i>i</i> -Pr <sub>2</sub> NBC <sub>4</sub> H <sub>4</sub> )	22 (2B), 11 (1B)
( <i>i</i> -Pr <sub>2</sub> NBC <sub>4</sub> H <sub>4</sub> ) <sub>2</sub> Rh <sub>2</sub> (CO) <sub>4</sub>	29
<i>i</i> -Pr <sub>2</sub> NBC <sub>4</sub> H <sub>4</sub> (NiCp) <sub>2</sub>	10
( <i>i</i> -Pr <sub>2</sub> NBC <sub>4</sub> H <sub>4</sub> ) <sub>2</sub> Ni	26
(MeBC <sub>4</sub> H <sub>4</sub> )Rh(MeBC <sub>4</sub> H <sub>4</sub> )Rh(MeBC <sub>4</sub> H <sub>4</sub> )	22.3 (2B), 10.8 (1B)
(MeBC <sub>4</sub> H <sub>4</sub> ) <sub>2</sub> RhH	16.0
Ph <sub>4</sub> P[(PhBC <sub>4</sub> H <sub>4</sub> )Rh(CN) <sub>3</sub> ]	23.6
CpFe(PhBC <sub>4</sub> H <sub>4</sub> )Cr(CO) <sub>3</sub>	9.4
(CpFe) <sub>2</sub> -1-Ph-2-EtBC <sub>4</sub> H <sub>3</sub>	4
1-( <i>i</i> -Pr <sub>2</sub> N)-2,3-(Me <sub>3</sub> Si) <sub>2</sub> -1-BC <sub>4</sub> H <sub>2</sub>	22
(MeBC <sub>5</sub> H <sub>5</sub> )Co(C <sub>8</sub> H <sub>12</sub> )	24.3
(2-MeCOPhBC <sub>5</sub> H <sub>5</sub> )Co(Me <sub>4</sub> C <sub>4</sub> )	23.7
(MeBC <sub>5</sub> H <sub>5</sub> )V(CO) <sub>4</sub>	28.7
(MeBC <sub>5</sub> H <sub>5</sub> )HgCl	35.2
[(MeBC <sub>5</sub> H <sub>5</sub> )Cr(CO) <sub>3</sub> ] <sub>2</sub> Hg	26.7
PPN[(MeBC <sub>5</sub> H <sub>5</sub> )Cr(CO) <sub>3</sub> ]	23.1
[(PhBC <sub>5</sub> H <sub>5</sub> )Ni(CO)] <sub>2</sub>	27
CpCo(1,3,4,5-Et <sub>4</sub> -2-Me-1,3-B <sub>2</sub> C <sub>3</sub> )CoCp <sup>+</sup>	19.5
CpCo(1,3,4,5-Et <sub>4</sub> -2-Me-1,3-B <sub>2</sub> C <sub>3</sub> ) <sub>2</sub> Pt	38, 15
[CpFe(1,3,4,5-Et <sub>4</sub> -2-Me-1,3-B <sub>2</sub> C <sub>3</sub> )] <sub>2</sub> Pt	15
(1,3,4,5-Et <sub>4</sub> -2-Me-1,3-B <sub>2</sub> C <sub>3</sub> )PdCp	37
(1,3,4,5-Et <sub>4</sub> -2-Me-1,3-B <sub>2</sub> C <sub>3</sub> ) <sub>2</sub> Pt	48
[(1,3,4,5-Et <sub>4</sub> -2-Me-1,3-B <sub>2</sub> C <sub>3</sub> ) <sub>2</sub> Pt] <sup>2-</sup>	23

Treatment of 1-MeO-6-Me<sub>3</sub>Si-1-bora-2,4-cyclohexadiene,  $\delta^{11}\text{B} = 47.1$ , with pyridine yields the borabenzene complex Py—BC<sub>5</sub>H<sub>5</sub>,  $\delta^{11}\text{B} = 33.9$ .<sup>303</sup> This compound forms a wide variety of complexes in which a transition metal is  $\pi$ -bonded to the BC<sub>5</sub>H<sub>5</sub> ring such as (Py—BC<sub>5</sub>H<sub>5</sub>)M(CO)<sub>3</sub> (M = Cr, Mo, W),  $\delta^{11}\text{B} = 22.3$ –23.5.<sup>304</sup> Other exemplary borabenzene complexes include (PhBC<sub>5</sub>H<sub>5</sub>)Co(Ph<sub>4</sub>C<sub>4</sub>),  $\delta^{11}\text{B} = 23$ , (MeBC<sub>5</sub>H<sub>5</sub>)<sub>2</sub>Co<sub>2</sub>-(Me<sub>4</sub>C<sub>4</sub>)<sub>2</sub>, 26.9,<sup>305</sup> (PhBC<sub>5</sub>H<sub>5</sub>)V(CO)<sub>4</sub>, 26.0, (PhBC<sub>5</sub>H<sub>5</sub>)HgCl, 33.0,<sup>306</sup> [(MeBC<sub>5</sub>H<sub>5</sub>)Cr(CO)<sub>3</sub>]<sub>2</sub>Hg, 26.7,<sup>307</sup> and [(PhBC<sub>5</sub>H<sub>5</sub>)Ni(CO)]<sub>2</sub>, 27.<sup>308</sup> Structure and bonding in this class of complexes have been thoroughly reviewed.<sup>286</sup>

2,3-Dihydro-1,3-diboroles can act as three- or four-electron donors. Formal cleavage of a hydrogen atom from the methylene bridge leads to an intermediate radical, which can bind transition metals on one or both faces of the ring to form mono- or binuclear complexes.<sup>287</sup> Thus reaction of

$\text{CpCo}(\text{C}_2\text{H}_4)_2$  with 1,3,4,5-Et<sub>4</sub>-2-Me-1,3-diborolene affords (1-Me-2,3,4,5-Et<sub>4</sub>-1,3-B<sub>2</sub>C<sub>3</sub>H)CoCp,  $\delta^{11}\text{B} = 27.5$ . The position of the proton on C1 is not well established, but it is considered that cobalt attains an 18-electron configuration by means of a three-centre two-electron Co—C—H or B—C—H interaction. In any event, the axial C—H proton is acidic, and methylation at C1 affords 1,1-Me<sub>2</sub>-2,3,4,5-Et<sub>4</sub>-1,3-B<sub>2</sub>C<sub>3</sub>)CoCp, whose  $^{11}\text{B}$  chemical shift, 42.0 ppm, is greatly and unexpectedly different. It is thought that, owing to steric effects, the Me<sub>2</sub>C(1) group may pivot so that the other methyl group comes into contact with the CpCo group. As a result, bonding between Co and C(1) is weakened and the Cp—B<sub>2</sub>C<sub>3</sub> dihedral angle opens, and there arises a decreased shielding of the boron nuclei.

Diborolene complexes of CoCp may be converted to higher-nuclearity metal compounds. Reaction of (1,2,5-Me-3,4-Et<sub>2</sub>-1,3-B<sub>2</sub>C<sub>3</sub>H)CoCp with  $\text{Mn}_2(\text{CO})_{10}$  affords  $(\text{CO})_3\text{Mn}(1,2,5\text{-Me}_3\text{-3,4-Et}_2\text{-1,3-B}_2\text{C}_3)\text{CoCp}$ , [47],  $\delta^{11}\text{B} = 18.3$ .<sup>309,310</sup>



Other examples of polymetallic diborolene complexes include  $\text{CpNi}(1,3,4,5\text{-Et}_4\text{-2-Me-1,3-B}_2\text{C}_3)\text{NiCp}$ ,  $\delta^{11}\text{B} = 7$ , the cation radical formed by one-electron oxidation,  $\delta^{11}\text{B} = 1874$ ,<sup>311</sup> and  $[\text{CpCo}(1,3\text{-Me}_2\text{-4,5-Et}_2\text{B}_2\text{C}_3\text{H})_2\text{Sn}]$ ,  $\delta^{11}\text{B} = 13$ .<sup>312</sup> Diborolene complexes containing cobalt,<sup>313</sup> and palladium and platinum<sup>314,315</sup> have also been reported (see Table 43). The tetradeccker compound  $[(\text{C}_3\text{H}_5)\text{Ni}(1,3,4,5\text{-Et}_4\text{-2-Me-1,3-B}_2\text{C}_3)]_2\text{Ni}$  has  $\delta^{11}\text{B} = 20.7$ .<sup>316</sup> Synthesis of molecular (as opposed to polymeric) polymetallic diborolene derivatives has culminated with the hexadecker compound  $[\text{CpCo}(1,3\text{-Me}_2\text{-4,5-Et}_2\text{-1,3-B}_2\text{C}_3\text{H})\text{Ni}(1,3\text{-Me}_2\text{-4,5-Et}_2\text{-1,3-B}_2\text{C}_3\text{H})_2\text{Ni}]$ ,  $\delta^{11}\text{B} = 34$  (Fig. 56)<sup>317</sup> Introduction of additional heteroatoms, however, opens up possibilities for additional complexity, an example of which is  $(3,4\text{-Et}_2\text{-2,5-Me}_2\text{-1,2,5-SB}_2\text{C}_2)_2\text{Fe}(\text{CO})$ ,  $\delta^{11}\text{B} = 32.8$ .<sup>318</sup>

## IX. $^{11}\text{B}$ NMR STUDIES OF SOLIDS

It is generally recognized that NMR spectra of solids are becoming increasingly easy to obtain, and application of this technique to solids is,

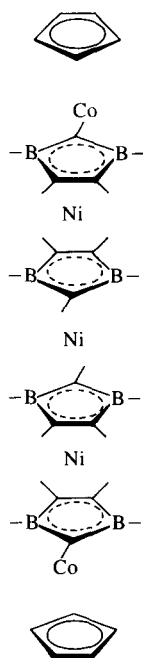


FIG. 56. Structure of a hexadecker metalloboron sandwich compound.

albeit slowly, gaining well-deserved attention. A principle application has been to the study of amorphous solids and materials lacking long-range order. In glasses  $^{11}\text{B}$  NMR is sensitive only to nearest-neighbour boron-bonding arrangements. On the other hand,  $^{10}\text{B}$  NMR is more sensitive to differences in quadrupole parameters that may reveal the presence of longer range structural order.  $^{11}\text{B}$  NMR experiments have shown that boron atoms having one or two nonbridging oxygens form in  $\text{Na}_2\text{O}-\text{B}_2\text{O}_3-\text{SiO}_2$  glasses when the  $\text{Na}_2\text{O}$  content is increased. However, this effect is also a function of the  $\text{SiO}_2$  content, a phenomenon that has been used to develop new models for local glass structure.<sup>319</sup> The amount of three-coordinate boron in  $\text{BaO}-\text{B}_2\text{O}_3-\text{SiO}_2$  glasses is very sensitive to added  $\text{Ti}^{3+}$  according to  $^{11}\text{B}$  (and  $^{137}\text{Ba}$ ) NMR results. It is suggested that microheterogeneities may arise from interaction of clustered titanium centres with nonbridging oxygen atoms in these glasses.<sup>320</sup>  $^{11}\text{B}$  NMR measurements on the glassy ionic conductors  $(\text{Ag}_2\text{O})_x(\text{Li}_2\text{O})_{1-x}\cdot 2\text{B}_2\text{O}_3$  have demonstrated the presence of both  $\text{BO}_3$  and  $\text{BO}_4$  units.<sup>321</sup> Glasses of compositions  $(\text{ZnO})_x(\text{B}_2\text{O}_3)_y$  have been studied by  $^{11}\text{B}$  NMR. The 3:1 material contains three-coordinate boron with a quadrupolar coupling constant  $Q_{\text{cc}} = 2.70$  MHz. In the 4:3

compound, four coordinate boron with  $Q_{cc} = 112$  kHz is found. A crystalline 1 : 1 material is shown to be a mixture of the 3 : 1 and 4 : 3 phases.<sup>322</sup> Slow decay of stimulated  $^{11}\text{B}$  spin echoes in borate glasses is associated with a randomness of spin detuning.<sup>323</sup>

Variable-angle sample-spinning (VASS) NMR is a recently introduced technique that permits observation of high-resolution spectra of nonintegral ( $I = \frac{3}{2}, \frac{5}{2}, \frac{7}{2}, \frac{9}{2}$ ) spin quadrupolar nuclei in solids since it averages second-order quadrupolar interactions. Use of high fields leads to narrow lines because the strength of this interaction is inversely proportional to the value of the field. However, nuclei with different quadrupolar coupling constants but similar chemical shifts may not be resolved. Since the shift of the ( $\frac{1}{2}, -\frac{1}{2}$ ) transition vanishes as the field approaches infinity. Resolution enhancement of  $^{11}\text{B}$  signals from a borosilicate glass, Pyrex 7740, has been achieved by obtaining VASS spectra at *lower* fields, in this case the spinning angle is  $75^\circ$  at 3.52 T. Under these conditions, separate resonances for tetrahedral  $\text{BO}_4$  and trigonal  $\text{BO}_3$  units are resolved and sideband features suppressed. The VASS technique may be generally useful in systems in which quadrupole-induced shift differences are greater than intrinsic shift differences.<sup>324</sup>

Contributions to wide-line spectra are associated with different electric field gradients and boron sites that are differentiated by chemical non-equivalence. Interaction of these gradients with the  $^{11}\text{B}$  quadrupole moment produces the observed spectral features. Thus wide-line  $^{11}\text{B}$  NMR indicates that glassy  $\text{B}_2\text{S}_3$  contains boron in three-coordinate  $\text{BS}_3$  groups.  $\text{Li}_2\text{S}-\text{B}_2\text{S}_3$  glasses are structurally different from the oxygen analogues  $\text{Li}_2\text{O}-\text{B}_2\text{O}_3$  in that the former maintains a higher fraction of four-coordinate boron.<sup>325</sup> Solid-state  $^{11}\text{B}$  NMR spectroscopy has been used to study various phases obtained in the systems, B-S, B-Se, B-S-Se and B-Te. In the first of these,  $\text{BS}_2$  and  $\text{B}_2\text{S}_3$  are observed and have  $Q_{cc} = 2.46$  and 2.16 MHz respectively. In the B-Se system  $\text{BSe}_2$ ,  $Q_{cc} = 2.07$  MHz, is formed. All the phases contain trigonal boron.<sup>326</sup> Studies of the  $^{11}\text{B}$  NMR spectra of the glass-forming systems  $\text{Li}_2\text{O}-\text{TeO}_2-\text{B}_2\text{O}_3$  and  $\text{TeO}_2-\text{B}_2\text{O}_3-\text{Al}_2\text{O}_3$  have been reported. Narrow and wide lines due to four- and three-coordinate boron are observed.<sup>327</sup>

$^{11}\text{B}$  MAS NMR data for  $\text{PCl}_x\text{Br}_{4-x}^+$  salts of  $\text{BCl}_n\text{Br}_{4-n}^-$  have been published. The chemical shifts for  $\text{BCl}_3\text{Br}^-$ ,  $\text{BCl}_2\text{Br}_2^-$ ,  $\text{BClBr}_3^-$  and  $\text{BBBr}_4^-$  are -6.1, -13.2, -21.5 and -30.6 ppm respectively; linewidths are all approx. 48 Hz.<sup>328</sup> The wide-line variable-temperature NMR spectrum of the intercalation compound  $\text{C}_{16}\text{BF}_4$ , formed from graphite,  $\text{BF}_3$  and  $\text{ClF}_3$  reveals a large  $^{11}\text{B}$  quadrupolar splitting, and so it is proposed that this material contains  $\text{B}_2\text{F}_7^-$ .<sup>329,330</sup>

$^{11}\text{B}$  spin-lattice relaxation times for the three isomers of  $\text{B}_{10}\text{C}_2\text{H}_{12}$  have

TABLE 44

Relaxation times and quadrupole coupling constants in isomers of  $\text{B}_{10}\text{C}_2\text{H}_{12}$ .

Compound	Position	$\delta^{11}\text{B } T_1$ (s)	$e^2qQ$ (kHz)
1,2- $\text{B}_{10}\text{C}_2\text{H}_{12}$	9, 12	0.0373	917
	8, 10	0.0488	801
	4, 5, 7, 11	0.0255	1109
	3, 6	0.0149	1451
1,7- $\text{B}_{10}\text{C}_2\text{H}_{12}$	5, 12	0.0370	921
	9, 10	0.0631	705
	4, 6, 8, 11	0.0351	946
	2, 3	0.026	1099
1,12- $\text{B}_{10}\text{C}_2\text{H}_{12}$	2-11	0.0399	887

been measured. The boron quadrupole coupling constants are calculated, ignoring asymmetry parameters, from the ration  $[1/T_1, ^{11}\text{B}]/[1/T_1, ^{13}\text{C}]$  [see Table 44).<sup>331</sup>

Quadrupolar coupling constants for the alkaline-earth hexaborides  $\text{EB}_6$  are  $1.26 \pm 0.02$ ,  $0.56 \pm 0.08$  and  $0.80 \pm 0.04$  MHz respectively for  $\text{E} = \text{Ca}$ ,  $\text{Sr}$  and  $\text{Ba}$ . The  $^{11}\text{B}$  chemical shifts correlate with the metallic radius of  $\text{E}$ .<sup>332</sup> Longitudinal dipolar fluctuations of rare-earth moments are found to be the main source of  $^{11}\text{B}$  spin-lattice relaxation times in doped rare-earth borides such as  $(\text{Y}_{1-x}\text{Gd}_x)\text{Rh}_4\text{B}_4$ . Variations of  $T_1$  in the superconducting states are associated with reduction of the electron-spin relaxation times.<sup>333</sup>

$^{11}\text{B}$  NMR has been used effectively to probe the symmetry of the boron environment in  $\text{Ni}_{100-x}\text{B}_x$  glasses ( $x = 40-18.5$ ). There is a relatively narrow range of electrostatic field gradient components, implying weak fluctuations in bond angles and distances and in coordination geometry. Comparison with cubic  $\text{Ni}_3\text{B}$  and  $\text{Ni}_4\text{B}_3$  indicates a trigonal prismatic arrangement of atoms around boron rather than the Archimedian antiprism found in cubic  $\text{NiB}_2$ .  $^{11}\text{B}$  spin-lattice relaxation times for the glassy metals and crystalline borides plotted as a function of  $x$ , with the exception of  $\text{c-NiB}_2$ , reside on a smooth curve.<sup>334</sup> Such studies promise to be quite helpful in understanding the structure of metallic glasses.

#### ACKNOWLEDGMENTS

The author is grateful to Ms Joan Piskura and Ms Pam Highstrom of the 3M Technical Library for providing access to the literature.

## REFERENCES

1. A. R. Siedle, *Ann. Rep. NMR Spectrosc.*, 1982, **12**, 177.
2. T. L. Venable, W. C. Hutton and R. N. Grimes, *J. Am. Chem. Soc.*, 1984, **106**, 29.
3. D. P. Burum, *J. Magn. Reson.*, 1984, **59**, 430.
4. X. L. R. Fontaine and J. D. Kennedy, *J. Chem. Soc. Chem. Commun.*, 1986, 779.
5. T. C. Gibb and J. D. Kennedy, *J. Chem. Soc. Faraday Trans. 2*, 1982, **78**, 525.
6. D. F. Gaines, C. K. Nelson, J. C. Kunz, J. H. Morris and D. Reed, *Inorg. Chem.*, 1984, **23**, 3252.
7. W. Jarvis, Z. T. Abdou and T. Onak, *Polyhedron*, 1983, **2**, 1067.
8. W. Biffar, H. Noth and D. Sedlak, *Organometallics*, 1983, **2**, 579.
9. G. W. Kabalka, U. Sastry, K. A. R. Sastry, F. F. Knapp and P. C. Srivastava, *J. Organomet. Chem.*, 1983, **259**, 269.
10. P. C. Keller, *Inorg. Chem.*, 1982, **21**, 444.
11. P. C. Keller, *Inorg. Chem.*, 1982, **21**, 445.
12. M. Kameda and G. Kodama, *Inorg. Chem.*, 1982, **21**, 1267.
13. M. Kameda and G. Kodama, *Inorg. Chem.*, 1984, **23**, 3710.
14. M. Kameda and G. Kodama, *Polyhedron*, 1983, **2**, 413.
15. M. Shimoi and G. Kodama, *Inorg. Chem.*, 1983, **22**, 3300.
16. H. Monegot and J. Atchekzai, *Bull. Soc. Chim. Fr.*, 1983, 1-70.
17. B. F. Speilvogel, F. U. Ahmed, G. L. Silvey, P. Wisian-Nelson and A. T. McPhail, *Inorg. Chem.*, 1984, **23**, 4322.
18. B. G. Speilvogel, F. U. Ahmed, K. W. Morse and A. T. McPhail, *Inorg. Chem.*, 1984, **23**, 1776.
19. V. M. Norwood and K. W. Morse, *Inorg. Chem.*, 1987, **26**, 284.
20. J. Bielawski, K. Niedenzu and J. S. Stewart, *Z. Naturforsch.*, 1985, **40b**, 389.
21. B. F. Speilvogel, F. U. Ahmed and A. T. McPhail, *J. Am. Chem. Soc.*, 1986, **108**, 3824.
22. B. F. Speilvogel, F. U. Ahmed, M. K. Das and A. T. McPhail, *Inorg. Chem.*, 1984, **23**, 3263.
23. P. Kolle and H. Noth, *Chem. Rev.*, 1985, **35**, 399.
24. H. Noth, B. Rasthofer and S. Weber, *Z. Naturforsch.*, 1984, **38b**, 1058.
25. H. Noth and S. Weber, *Z. Naturforsch.*, 1983, **38b**, 1460.
26. P. Kolle and H. Noth, *Chem. Ber.*, 1986, **119**, 3849.
27. C. K. Narula and H. Noth, *Z. Naturforsch.*, 1983, **38b**, 1161.
28. M. J. Farquharson and J. S. Hartman, *J. Chem. Soc. Chem. Commun.*, 1984, 256.
29. D. Y. Lee and J. C. Martin, *J. Am. Chem. Soc.*, 1984, **106**, 5745.
30. P. Paetzold and R. Truppat, *Chem. Ber.*, 1983, **116**, 1531.
31. H. U. Meier, P. Paetzold and E. Schroder, *Chem. Ber.*, 1984, **117**, 1954.
32. P. Paetzold, C. von Plotho, G. Schmid, R. Boese, B. Schraeder, D. Bougard, U. Pfeiffer, R. Gleiter and W. Schaeffer, *Chem. Ber.*, 1984, **117**, 1089.
33. P. Paetzold and C. von Plotho, *Chem. Ber.*, 1982, **115**, 2819.
34. M. Haase and U. Klingbiel, *Angew. Chem. Int. Ed. Engl.*, 1985, **24**, 324.
35. P. Paetzold, C. von Plotho, G. Schmid and R. Boese, *Z. Naturforsch.*, 1984, **39b**, 1069.
36. H. Noth and S. Weber, *Z. Naturforsch.*, 1983, **38b**, 1460.
37. B. Glaser and H. Noth, *Angew. Chem. Int. Ed. Engl.*, 1985, **24**, 416.
38. P. Paetzold, C. von Plotho, H. Schwan and H.-U. Meier, *Z. Naturforsch.*, 1984, **39b**, 610.
39. H. Noth and S. Weber, *Chem. Ber.*, 1985, **118**, 2144.
40. A. Brandl and H. Noth, *Chem. Ber.*, 1985, **118**, 3759.
41. J. R. Jennings, R. Snaith, M. M. Mahmoud, S. C. Wallwork, J. Halfpenny, E. A. Petch and K. Wade, *J. Organometal. Chem.*, 1983, **249**, C1.

42. R. A. Bartlett, X. Feng and P. P. Power, *J. Am. Chem. Soc.*, 1986, **108**, 6817.
43. X. Feng, M. M. Olmstead and P. P. Power, *Inorg. Chem.*, 1986, **25**, 4615.
44. H.-J. Bestman and T. Arenz, *Angew. Chem. Int. Ed. Engl.*, 1984, **23**, 381.
45. F. Dirschl, H. Noth and W. Wagner, *J. Chem. Soc. Chem. Commun.*, 1984, 1533.
46. H. Klusik and A. Berndt, *Angew. Chem. Int. Ed. Engl.*, 1983, **22**, 877.
47. R. Wehrman, H. Klusik and A. Berndt, *Angew. Chem. Int. Ed. Engl.*, 1984, **23**, 369.
48. R. Wehrman, H. Klusik and A. Berndt, *Angew. Chem. Int. Ed. Engl.*, 1984, **23**, 826.
49. C. Pues and A. Berndt, *Angew. Chem. Int. Ed. Engl.*, 1984, **23**, 313.
50. C. Habben and A. Meller, *Chem. Ber.*, 1984, **117**, 2351.
51. M. Hildenbrand, H. Pritzkow, U. Zenneck and W. Siebert, *Angew. Chem. Int. Ed. Engl.*, 1984, **23**, 371.
52. S. M. van der Kerk, P. M. H. Budzelaar, A. van der Kerk-van Hoof, G. J. M. van der Kerk and P. von R. Schleyer, *Angew. Chem. Int. Ed. Engl.*, 1983, **22**, 48.
53. R. Wherman, C. Pues, M. Kluski and A. Berndt, *Angew. Chem. Int. Ed. Engl.*, 1984, **23**, 372.
54. S. M. van der Kerk, P. M. H. Budzelaar, A. L. M. van Eekeren and G. J. M. van der Kerk, *Polyhedron*, 1984, **3**, 271.
55. B. Pachaly and R. West, *J. Am. Chem. Soc.*, 1985, **107**, 2987.
56. H. Klusik and A. Berndt, *J. Organometal. Chem.*, 1982, **234**, C17.
57. P. Kolle, H. Noth and R. T. Paine, *Chem. Ber.*, 1986, **119**, 2681.
58. H. E. Fisch, H. Pritzkow and W. Siebert, *Angew. Chem. Int. Ed. Engl.*, 1984, **23**, 608.
59. K. Niedenzu, P. M. Niedenzu and K. R. Warner, *Inorg. Chem.*, 1985, **24**, 1604.
60. C. M. Clarke, K. Niedenzu, P. M. Niedenzu and S. Trofimenko, *Inorg. Chem.*, 1985, **24**, 2648.
61. J. Bielawski and K. Niedenzu, *Inorg. Chem.*, 1986, **25**, 85.
62. J. Bielawski, M. K. Das, E. Hanecker, K. Niedenzu and H. Noth, *Inorg. Chem.*, 1986, **25**, 4623.
63. K. Niedenzu and P. M. Niedenzu, *Inorg. Chem.*, 1984, **23**, 3713.
64. J. Bielawski, T. G. Hodgkins, W. J. Layton, K. Niedenzu, P. M. Niedenzu and S. Trofimenko, *Inorg. Chem.*, 1986, **25**, 87.
65. E. Hanecker, T. G. Hodgkins, K. Niedenzu and H. Noth, *Inorg. Chem.*, 1985, **24**, 459.
66. W. J. Layton, K. Niedenzu, P. M. Niedenzu and S. Trofimenko, *Inorg. Chem.*, 1985, **24**, 1454.
67. K. Bielawski and K. Niedenzu, *Inorg. Chem.*, 1986, **25**, 1771.
68. K. Niedenzu and H. Noth, *Chem. Ber.*, 1983, **116**, 1132.
69. H. Fisch, H. Pritzkow and W. Siebert, *Angew. Chem. Int. Ed. Engl.*, 1984, **23**, 608.
70. B. M. Mikhailov, M. E. Gurskii and D. G. Pershin, *J. Organometal. Chem.*, 1983, **246**, 19.
71. M. E. Gurskii, S. V. Baranin, A. S. Shaskov, A. I. Lutsenko and B. M. Mikhailov, *J. Organometal. Chem.*, 1983, **246**, 129.
72. W. Siebert, U. Ender and W. Herter, *Z. Naturforsch.*, 1985, **40b**, 326.
73. B. Wrackmeyer, *Organometallics*, 1984, **3**, 1.
74. A. J. Ashe, S. T. Abu-Orabi, O. Eisenstein and H. F. Sandford, *J. Org. Chem.*, 1983, **48**, 901.
75. A. J. Ashe and F. J. Drone, *J. Am. Chem. Soc.*, 1987, **109**, 1879.
76. W. Haubold, J. Hrebicek and G. Sawitzki, *Z. Naturforsch.*, 1984, **39b**, 1027.
77. B. Lauer and G. Wulff, *J. Organometal. Chem.*, 1983, **256**, 1.
78. R.-J. Binnerwirtz, H. Klingenberg, R. Welte and P. Paetzold, *Chem. Ber.*, 1983, **116**, 1271.
79. R. Bravo and J.-P. Laurent, *J. Chem. Res. (S)*, 1983, 61.

80. R. Contreras, C. Garcia, T. Mancilla and B. Wrackmeyer, *J. Organometal. Chem.*, 1983, **246**, 213.
81. E. Hohaus, *Z. Anorg. allg. Chem.*, 1983, **506**, 185.
82. L. Horner, U. Kaps and G. Simons, *J. Organometal. Chem.*, 1985, **287**, 1.
83. W. Kliegel, D. Nanninga, S. J. Rettig and T. Trotter, *Can. J. Chem.*, 1983, **61**, 2329.
84. W. Maringele, G. M. Sheldrick, A. Meller and M. Noltemeyer, *Chem. Ber.*, 1984, **117**, 2112.
85. P. C. Keller, R. L. Marks and J. V. Rund, *Polyhedron*, 1983, **2**, 595.
86. R. Koster, G. Seidel, S. Kersch and B. Wrackmeyer, *Z. Naturforsch.*, 1987, **42b**, 191.
87. H.-O. Berger and H. Noth, *J. Organometal. Chem.*, 1983, **250**, 33.
88. R. Koster and G. Seidel, *Angew. Chem. Int. Ed. Engl.*, 1984, **23**, 155.
89. O. Graalman, U. Klingebiel, W. Clegg, M. Haase and G. M. Sheldrick, *Z. Anorg. allg. Chem.*, 1984, **519**, 87.
90. V. J. Heintz, W. A. Freeman and T. A. Keiderling, *Inorg. Chem.*, 1983, **22**, 2319.
91. M. Yalpani and R. Koster, *Chem. Ber.*, 1983, **116**, 3332.
92. M. Yalpani, R. Boese and D. Blaser, *Chem. Ber.*, 1983, **116**, 3338.
93. M. Yalpani, R. Koster and G. Wilke, *Chem. Ber.*, 1983, **116**, 1336.
94. H. Noth, *Z. Naturforsch.*, 1984, **39b**, 1463.
95. F. Santiesteban, M. A. Campos, H. Morales, R. Contreras and B. Wrackmeyer, *Polyhedron*, 1984, **3**, 589.
96. P. Idelmann, G. Muller, W. Scheidt, W. Schussler and R. Koster, *Angew. Chem. Int. Ed. Engl.*, 1984, **23**, 153.
97. H. Binder, W. Matheis, H.-J. Dieseroth and H. Fu-Son, *Z. Naturforsch.*, 1983, **38b**, 554.
98. M. Yalpani and R. Boese, *Chem. Ber.*, 1983, **116**, 3347.
99. M. Noltemeyer, G. M. Sheldrick, C. Habben and A. Meller, *Z. Naturforsch.*, 1983, **38b**, 1182.
100. C. Habben, A. Meller and G. M. Sheldrick, *Z. Naturforsch.*, 1986, **41b**, 1093.
101. K. Wolfer, H.-D. Hausen and H. Binder, *Z. Naturforsch.*, 1985, **40b**, 235.
102. L. Bhal, R. V. Singh and J. P. Tandon, *Synth. React. Inorg. Met.-Org. Chem.*, 1983, **13**, 613.
103. C. Habben and A. Meller, *Z. Naturforsch.*, 1984, **39b**, 1022.
104. B. Wrackmeyer, *Polyhedron*, 1986, **5**, 1709.
105. B. Wrackmeyer, *Z. Naturforsch.*, 1982, **37b**, 788.
106. R. Contreras and B. Wrackmeyer, *Spectrochim. Acta*, 1982, **38A**, 941.
107. H. C. Brown and P. K. Jadhav, *J. Am. Chem. Soc.*, 1983, **105**, 2092.
108. H. Klusik, C. Pues and A. Berndt, *Z. Naturforsch.*, 1984, **39b**, 1042.
109. B. Wrackmeyer, C. Bihlmeyer and M. Schilling, *Chem. Ber.*, 1983, **116**, 3182.
110. H. C. Brown, B. Basavalah and N. G. Bhat, *Organometallics*, 1983, **2**, 1468.
111. R. J. Binnerwitz, H. Klingenberger, R. Welte and P. Paetzold, *Chem. Ber.*, 1983, **116**, 1271.
112. N. S. Hosmane, N. N. Sirmokadam and M. N. Mollenhauer, *J. Organometal. Chem.*, 1985, **279**, 359.
113. W. Haubold, A. Gemmler and U. Kratz, *Z. Anorg. allg. Chem.*, 1983, **507**, 222.
114. H. C. Brown and T. E. Cole, *Organometallics*, 1983, **2**, 1316.
115. H. Burger, M. Grunwald and G. Pawelke, *J. Fluorine Chem.*, 1985, **28**, 183.
116. H. Noth and D. Sedlak, *Chem. Ber.*, 1983, **116**, 1479.
117. A. Fox, J. S. Hartman and R. E. Humphries, *J. Chem. Soc. Dalton Trans.*, 1982, 1275.
118. D. R. Martin, J. U. Mondal, R. D. Williams, J. B. Iwamoto, N. C. Massey, D. M. Nuss and P. L. Scott, *Inorg. Chim. Acta*, 1983, **70**, 47.
119. J. M. Miller, *Inorg. Chem.*, 1983, **22**, 2384.

120. B. Glaser and H. Noth, *Chem. Ber.*, 1986, **119**, 3253.
121. J.-M. Dupart, S. Pace and J. G. Riess, *J. Am. Chem. Soc.*, 1983, **105**, 1051.
122. H. Noth and W. Storch, *Chem. Ber.*, 1984, **117**, 2140.
123. L. Synoradzki, R. Mynott, J. Anbei, Y. Tsay and R. Koster, *Chem. Ber.*, 1984, **117**, 2863.
124. C. Eaborn, M. N. A. El-Kheli, P. B. Hitchcock and J. D. Smith, *J. Chem. Soc. Chem. Commun.*, 1984, 1673.
125. J. L. Atwood, S. G. Bott, C. Eaborn, M. N. A. El-Kheli and J. D. Smith, *J. Organomet. Chem.*, 1985, **294**, 23.
126. C. Eaborn, M. N. El-Kheli, N. Retta and J. D. Smith, *J. Organomet. Chem.*, 1983, **249**, 23.
127. C. Eaborn, N. Retta, J. D. Smith and P. B. Hitchcock, *J. Organomet. Chem.*, 1982, **235**, 265.
128. C. Eaborn, M. N. A. El-Kheli, P. B. Hitchcock and J. D. Smith, *J. Organomet. Chem.*, 1984, **272**, 1.
129. P. B. Hitchcock, H. A. Jasim, M. F. Lappert and H. D. Williams, *J. Chem. Soc. Chem. Commun.*, 1984, 662.
130. S. Kersch and B. Wrackmeyer, *J. Chem. Soc. Chem. Commun.*, 1986, 403.
131. H. E. Katz, *J. Am. Chem. Soc.*, 1985, **107**, 1420.
132. R. M. Farmer, Y. Sasaki and A. I. Popov, *Aust. J. Chem.*, 1983, **36**, 1785.
133. S. H. Lawrence, S. G. Shore, T. F. Koetzle, J. C. Huffman, C.-Y. Wei and R. Bau, *Inorg. Chem.*, 1985, **24**, 3171.
134. G. A. Olah, K. Laali and O. Farooq, *J. Org. Chem.*, 1984, **49**, 4951.
135. W. Totsch, H. Aichinger and F. Sladky, *Z. Naturforsch.*, 1983, **38b**, 332.
136. J. G. Dawber and S. I. E. Green, *J. Chem. Soc. Faraday Trans. 1*, 1986, **82**, 3407.
137. C. G. Salentine, *Inorg. Chem.*, 1983, **22**, 3920.
138. F. Teixidor, C. Vinas and R. W. Rudolph, *Inorg. Chem.*, 1986, **25**, 3339.
139. R. E. DePoy and G. Kodama, *Inorg. Chem.*, 1985, **24**, 2871.
140. W. Haubold and P. Jacob, *Z. Anorg. allg. Chem.*, 1983, **507**, 231.
141. N. E. Miller, *J. Organomet. Chem.*, 1984, **269**, 123.
142. B. Wrackmeyer, *Z. Naturforsch.*, 1982, **37b**, 412.
143. R. Schlögl and B. Wrackmeyer, *Polyhedron*, 1985, **4**, 885.
144. D. G. Meina, J. H. Morris and D. Reed, *Polyhedron*, 1986, **5**, 1639.
145. M. Arunchaiya, J. H. Morris, S. J. Andrews, D. A. Welch and A. J. Welch, *J. Chem. Soc. Dalton Trans.*, 1984, 2525.
146. M. Kameda, M. Shimoi and G. Kodama, *Inorg. Chem.*, 1984, **23**, 3705.
147. N. S. Hosmane, N. N. Sirmokadam and R. Herber, *Organometallics*, 1984, **3**, 1665.
148. N. S. Hosmane, P. de Heester, N. N. Maldar, S. B. Potts, S. S. C. Chu and R. Herber, *Organometallics*, 1986, **5**, 772.
149. J. A. Heppert and D. F. Gaines, *Inorg. Chem.*, 1983, **22**, 3155.
150. D. F. Gaines and D. E. Coons, *J. Am. Chem. Soc.*, 1985, **107**, 3266.
151. D. F. Gaines, J. A. Heppert and J. C. Kunz, *Inorg. Chem.*, 1985, **24**, 621.
152. D. F. Gaines, J. C. Kunz and M. J. Kulzick, *Inorg. Chem.*, 1985, **24**, 3336.
153. D. F. Gaines, J. A. Heppert, D. E. Coons and M. W. Jorgenson, *Inorg. Chem.*, 1982, **21**, 3663.
154. M. A. Nelson, M. Kameda, S. A. Snow and G. Kodama, *Inorg. Chem.*, 1982, **21**, 2898.
155. T. Davan, E. E. Corcoran and L. G. Sneddon, *Organometallics*, 1983, **2**, 1693.
156. D. F. Gaines and G. A. Steehler, *J. Chem. Soc. Chem. Commun.* 1984, 1127.
157. D. F. Gaines and D. E. Coons, *Inorg. Chem.* 1986, **25**, 364.
158. R. J. Astheimer and L. G. Sneddon, *Inorg. Chem.*, 1984, **23**, 3207.
159. J. H. Osborne, R. C. P. Hill and D. M. Ritter, *Inorg. Chem.*, 1986, **25**, 372.

160. Z. J. Abdou, M. Saltis, B. Oh, G. Siwap, T. Banuelos, W. Nam and T. Onak, *Inorg. Chem.*, 1985, **24**, 2363.
161. K. Fuller and T. Onak, *J. Organometal. Chem.*, 1983, **249**, C6.
162. G. Siwapinyoyos and T. Onak, *Inorg. Chem.*, 1982, **21**, 156.
163. W. Preetz and J. Fritze, *Z. Naturforsch.*, 1984, **39b**, 1472.
164. W. Preetz and J. Fritze, *Z. Naturforsch.*, 1987, **42b**, 287.
165. R. Koster, G. Seidel and B. Wrackmeyer, *Angew. Chem. Int. Ed. Engl.*, 1984, **23**, 512.
166. R. Koster, G. Seidel and B. Wrackmeyer, *Angew. Chem. Int. Ed. Engl.*, 1985, **24**, 326.
167. K. Base, S. Hermanek and F. Hanousek, *J. Chem. Soc. Chem. Commun.*, 1984, 299.
168. G. B. Jacobsen, J. H. Morris and D. Reed, *J. Chem. Soc. Dalton Trans.*, 1984, 415.
169. J. J. Briguglio, P. J. Carroll, E. W. Corcoran and L. G. Sneddon, *Inorg. Chem.*, 1986, **25**, 4618.
170. O. W. Howarth, M. J. Jaszal, J. G. Taylor and M. G. H. Wallbridge, *Polyhedron*, 1985, **4**, 1461.
171. B. Stibr, S. Hermanek, S. Janousek, Z. Plzak, J. Dolansky and J. Plesek, *Polyhedron*, 1982, **1**, 822.
172. J. R. Wermer, N. S. Hosmane, J. J. Alexander, U. Siriwardane and S. G. Shore, *Inorg. Chem.*, 1986, **25**, 4351.
173. B. Stibr, Z. Janousek, J. Plesek, T. Jelinek and S. Hermanek, *J. Chem. Soc. Chem. Commun.*, 1985, 1365.
174. T. L. Venable, R. B. Maynard and R. N. Grimes, *J. Am. Chem. Soc.*, 1984, **106**, 6187.
175. N. S. Hosmane, M. Dehghan and S. Davies, *J. Am. Chem. Soc.*, 1984, **106**, 6435.
176. K. Baesz, *Coll. Czech. Chem. Commun.*, 1983, **48**, 2593.
177. D. A. Saulys, N. A. Kutz and J. A. Morrison, *Inorg. Chem.*, 1983, **22**, 1821.
178. G. B. Jacobsen, D. G. Meina, J. H. Morris, C. Thomson, S. J. Andrews, D. Reed, A. J. Welch and D. F. Gaines, *J. Chem. Soc. Dalton Trans.* 1985, 1645.
179. G. B. Jacobsen, J. H. Morris and D. Reed, *J. Chem. Soc. Dalton Trans.*, 1984, 415.
180. D. Reed, *J. Chem. Res. (S)*, 1984, 198.
181. E. H. Wong, M. G. Gatter and R. M. Kabbani, *Inorg. Chem.* 1982, **21**, 4022.
182. A. Arafat, J. Baer, J. C. Huffman and L. J. Todd, *Inorg. Chem.*, 1986, **25**, 3757.
183. A. Arafat, G. D. Friesen and L. J. Todd, *Inorg. Chem.*, 1983, **22**, 3721.
184. C. Vinas, W. M. Butler, F. Teixidor and R. W. Rudolph, *Inorg. Chem.*, 1986, **25**, 4369.
185. D. C. Busby and M. F. Hawthorne, *Inorg. Chem.* 1982, **21**, 4101.
186. W. Preetz, H.-G. Srebny and H. C. Marsman, *Z. Naturforsch.*, 1984, **39b**, 6.
187. S. Wu and M. Jones, *Inorg. Chem.*, 1986, **25**, 4802.
188. F. Teixidor and R. W. Rudolph, *J. Organometal. Chem.*, 1983, **241**, 301.
189. E. H. Wong, L. Prasad, E. J. Gabe and M. C. Gatter, *Inorg. Chem.*, 1983, **22**, 1143.
190. C. T. Brewer, R. G. Swisher, E. Sinn and R. N. Grimes, *J. Am. Chem. Soc.*, 1985, **107**, 3558.
191. H.-G. Srebny, W. Preetz and H. C. Marsman, *Z. Naturforsch.*, 1983, **39b**, 189.
192. N. N. Greenwood, *Chem. Soc. Rev.*, 1984, **13**, 353.
193. N. N. Greenwood, *Pure Appl. Chem.*, 1983, **55**, 1415.
194. M. Mancini, P. Bougeard, R. C. Burns, M. Mlekuz, B. G. Sayer, J. I. A. Thompson and M. J. McGlinchey, *Inorg. Chem.*, 1984, **23**, 1072.
195. M. V. Baker and L. D. Field, *J. Chem. Soc. Chem. Commun.*, 1984, 996.
196. D. J. Wink and N. J. Cooper, *J. Chem. Soc. Chem. Commun.*, 1984, 1257.
197. M. F. Lappert, A. Singh, J. L. Atwood and W. E. Hunter, *J. Chem. Soc. Chem. Commun.*, 1983, 206.
198. M. V. R. Stainer and J. Takats, *J. Am. Chem. Soc.*, 1983, **105**, 410.

199. R. Shinomoto, J. G. Brennan, N. M. Edelstein and A. Zalkin, *Inorg. Chem.*, 1985, **24**, 2896.
200. G. V. Fazakerley, G. Folcher and H. Marquet-Ellis, *Polyhedron*, 1984, **3**, 457.
201. T. M. Gilbert, F. J. Hollander and R. G. Bergman, *J. Am. Chem. Soc.*, 1985, **107**, 3508.
202. R. L. Bausemer, J. C. Huffman and K. G. Caulton, *J. Am. Chem. Soc.*, 1983, **105**, 6163.
203. J. C. Vites, C. E. Housecroft, G. B. Jacobsen and T. P. Fehlner, *Organometallics*, 1984, **3**, 1591.
204. J. Vites, C. E. Housecroft, C. Eigenbrodt, M. L. Buhl, G. J. Long and T. P. Fehlner, *J. Am. Chem. Soc.*, 1986, **108**, 3304.
205. C. E. Housecroft and T. P. Fehlner, *Organometallics*, 1986, **5**, 379.
206. K. S. Wong, W. R. Scheidt and T. P. Fehlner, *J. Am. Chem. Soc.*, 1982, **104**, 1111.
207. W. F. McNamara, E. Duesler, R. T. Paine, J. V. Ortiz and H. Noth, *Organometallics*, 1986, **5**, 380.
208. G. A. Carriedo, G. P. Elliot, J. A. K. Howard, D. B. Lewis and F. G. A. Stone, *J. Chem. Soc. Chem. Commun.*, 1984, 1585.
209. D. Palladino and T. P. Fehlner, *Organometallics*, 1983, **2**, 1692.
210. J. Feilong, T. P. Fehlner and A. L. Rheingold, *J. Am. Chem. Soc.*, 1987, **109**, 1860.
211. S. A. Snow, M. Shimoi, C. D. Ostler, B. K. Thompson, G. Kodama and R. W. Parry, *Inorg. Chem.*, 1984, **23**, 511.
212. S. A. Snow and G. Kodama, *Inorg. Chem.*, 1985, **24**, 796.
213. R. P. Micciche, P. J. Carroll and L. G. Sneddon, *Organometallics*, 1985, **4**, 1619.
214. J. Bould, N. N. Greenwood and J. D. Kennedy, *J. Organometal. Chem.*, 1983, **249**, 11.
215. S. K. Boocock, M. A. Toft, K. E. Inkrott, L. Y. Hsu, J. C. Huffman and S. G. Shore, *Inorg. Chem.*, 1983, **23**, 3084.
216. N. S. Hosmane and N. N. Sirmokadam, *Organometallics*, 1984, **3**, 1119.
217. R. P. Micciche and L. G. Sneddon, *Organometallics*, 1983, **2**, 674.
218. T. G. Swisher, E. Sinn and R. N. Grimes, *Organometallics*, 1984, **3**, 599.
219. R. B. Maynard, R. G. Swisher and R. N. Grimes, *Organometallics*, 1983, **2**, 500.
220. R. Swisher, E. Sinn and R. N. Grimes, *Organometallics*, 1983, **2**, 506.
221. L. Barton and P. K. Rush, *Inorg. Chem.*, 1985, **24**, 3413.
222. L. Borodinsky and R. N. Grimes, *Inorg. Chem.*, 1982, **21**, 1921.
223. L. Borodinsky, E. Sinn and R. N. Grimes, *Inorg. Chem.*, 1982, **21**, 1928.
224. J. J. Briguglio and L. G. Sneddon, *Organometallics*, 1985, **4**, 721.
225. R. P. Micciche, J. J. Briguglio and L. G. Sneddon, *Organometallics*, 1984, **3**, 1396.
226. M. B. Fischer, D. F. Gaines and J. A. Ulman, *J. Organometal. Chem.*, 1982, **231**, 55.
227. N. W. Alcock, C. Parkhill and M. G. H. Wallbridge, *Acta Crystallogr.*, 1985, **41**, 716.
228. P. K. Rush and L. Barton, *Polyhedron*, 1985, **4**, 1741.
229. D. E. Coons and D. F. Gaines, *Inorg. Chem.*, 1985, **24**, 3774.
230. X. L. R. Fontaine, N. N. Greenwood, J. D. Kennedy, I. MacPherson and M. Thornton-Pett, *J. Chem. Soc. Dalton Trans.*, 1987, 476.
231. J. Bould, J. E. Crook, N. N. Greenwood and J. D. Kennedy, *J. Chem. Soc. Dalton Trans.*, 1984, 1903.
232. J. Bould, N. N. Greenwood and J. D. Kennedy, *J. Chem. Soc. Dalton Trans.*, 1984, 2477.
233. N. N. Greenwood, M. J. Hails, J. D. Kennedy and W. S. McDonald, *J. Chem. Soc. Dalton Trans.*, 1985, 953.
234. M. A. Beckett, J. E. Crook, N. N. Greenwood and J. D. Kennedy, *J. Chem. Soc. Dalton Trans.*, 1984, 1427.
235. C. T. Brewer and R. N. Grimes, *J. Am. Chem. Soc.*, 1985, **107**, 3552.
236. T. P. Hanusa, J. C. Huffman, T. L. Curtis and L. J. Todd, *Inorg. Chem.*, 1986, **24**, 787.
237. J. J. Briguglio and L. G. Sneddon, *Organometallics*, 1986, **5**, 327.

238. T. L. Venable, E. Sinn and R. N. Grimes, *Inorg. Chem.*, 1982, **21**, 887.
239. T. L. Venable, E. Sinn and R. N. Grimes, *Inorg. Chem.*, 1982, **21**, 904.
240. T. L. Venable, E. Sinn and R. N. Grimes, *Inorg. Chem.*, 1982, **21**, 895.
241. B. Stibr, Z. Janousek, K. Base, J. Dolansky, S. Hermanek, K. Solntsev, L. A. Butman, I. I. Kuznetsev and N. T. Kuznetsov, *Polyhedron*, 1982, **1**, 833.
242. G. K. Barker, N. R. Godfrey, M. Green, H. E. Parge, F. G. A. Stone and A. J. Welch, *J. Chem. Soc. Chem. Commun.*, 1983, 277.
243. G. K. Barker, M. Green, F. G. A. Stone and W. C. Wolsey, *J. Chem. Soc. Dalton Trans.*, 1983, 2063.
244. Z.-T. Wang, E. Sinn and R. N. Grimes, *Inorg. Chem.*, 1985, **24**, 826.
245. Z.-T. Wang, E. Sinn and R. N. Grimes, *Inorg. Chem.*, 1985, **24**, 834.
246. D. G. Mema and J. H. Morris, *J. Chem. Soc. Dalton Trans.*, 1985, 1903.
247. M. A. Beckett, N. N. Greenwood, J. D. Kennedy and M. Thornton-Pett, *J. Chem. Soc. Dalton Trans.*, 1985, 1119.
248. M. A. Beckett, N. N. Greenwood, J. D. Kennedy and M. Thornton-Pett, *J. Chem. Soc. Dalton Trans.*, 1986, 795.
249. X. L. R. Fontaine, H. Fowkes, N. N. Greenwood, J. D. Kennedy and M. Thornton-Pett, *J. Chem. Soc. Dalton Trans.*, 1986, 547.
250. R. P. Micciche, J. J. Briguglio and L. G. Sneddon, *Inorg. Chem.*, 1984, **23**, 3992.
251. N. N. Greenwood, M. J. Hails, J. D. Kennedy and W. S. McDonald, *J. Chem. Soc. Dalton Trans.*, 1985, 953.
252. R. T. Baker, M. S. Delaney, R. E. King, C. B. Knobler, J. A. Long, T. B. Marder, T. E. Paxson, R. G. Teller and M. F. Hawthorne, *J. Am. Chem. Soc.*, 1984, **106**, 2965.
253. W. C. Kalb, Z. Demidowicz, D. M. Speckman, C. Knobler, R. G. Teller and M. F. Hawthorne, *Inorg. Chem.*, 1982, **21**, 4027.
254. P. E. Behnken and M. F. Hawthorne, *Inorg. Chem.*, 1984, **23**, 3420.
255. L. Zheng, R. T. Baker, C. B. Knobler, J. A. Walker and M. F. Hawthorne, *Inorg. Chem.*, 1983, **22**, 3350.
256. J. A. Doi, E. A. Mizusawa, C. B. Knobler and M. F. Hawthorne, *Inorg. Chem.*, 1984, **23**, 1482.
257. R. E. King, S. B. Miller, C. B. Knobler and M. F. Hawthorne, *Inorg. Chem.*, 1983, **22**, 3548.
258. M. P. Garcia, M. Green, F. G. A. Stone, R. G. Somerville, A. J. Welch and D. M. P. Mingos, *J. Chem. Soc. Dalton Trans.*, 1985, 2343.
259. D. E. Smith and A. J. Welch, *Organometallics*, 1986, **5**, 760.
260. W. S. Rees, D. M. Schubert, C. B. Knobler and M. F. Hawthorne, *J. Am. Chem. Soc.*, 1986, **108**, 5367; 1987, **109**, 2861.
261. W. S. Rees, D. M. Schubert, C. B. Knobler and M. F. Hawthorne, *J. Am. Chem. Soc.*, 1986, **108**, 5369.
262. M. Green, J. A. K. Howard, A. P. James, A. N. Jelfs, C. M. Nunn and F. G. A. Stone, *J. Chem. Soc. Dalton Trans.*, 1987, 81.
263. M. Green, J. A. K. Howard, A. N. Jelfs, O. Johnson and F. G. A. Stone, *J. Chem. Soc. Dalton Trans.*, 1987, 73.
264. Y. Do, C. B. Knobler and M. F. Hawthorne, *J. Am. Chem. Soc.*, 1987, **109**, 1853.
265. N. N. Greenwood and J. D. Kennedy in *Metal Interactions with Boron Clusters* (R. N. Grimes, ed.), Plenum Press, New York, Chap. 2, p. 43.
266. J. D. Kennedy, *Prog. Inorg. Chem.* 1984, **32**, 519; *ibid.*, 1986, **32**, 211.
267. J. E. Crook, N. N. Greenwood, J. D. Kennedy and W. S. McDonald, *J. Chem. Soc. Dalton Trans.*, 1984, 2487.
268. M. A. Beckett, N. N. Greenwood, J. D. Kennedy and M. Thornton-Pett, *Polyhedron*, 1985, **4**, 505.

269. M. Elrington, N. N. Greenwood, J. D. Kennedy and M. Thornton-Pett, *J. Chem. Soc. Dalton Trans.*, 1986, 2277.
270. H. Fowkes, N. N. Greenwood, J. D. Kennedy and M. Thornton-Pett, *J. Chem. Soc. Dalton Trans.*, 1986, 517.
271. M. A. Beckett, J. D. Kennedy and O. W. Howarth, *J. Chem. Soc. Chem. Commun.*, 1985, 855. (This reference has been liberally quoted.)
272. N. N. Greenwood, M. J. Hails, J. D. Kennedy and W. S. McDonald, *J. Chem. Soc. Dalton Trans.*, 1985, 953.
273. X. L. R. Fontaine, H. Fowkes, N. N. Greenwood and J. D. Kennedy, *J. Chem. Soc. Chem. Commun.*, 1985, 1165.
274. M. Bown, X. L. R. Fontaine, N. N. Greenwood, J. D. Kennedy and M. Thornton-Pett, *J. Chem. Soc. Dalton Trans.*, 1987, 1169.
275. M. Bown, X. L. R. Fontaine, N. N. Greenwood, P. MacKinnon, J. D. Kennedy and M. Thornton-Pett, *J. Chem. Soc. Chem. Commun.*, 1987, 442.
276. A. J. Wynd, S. E. Robbin, D. A. Welch and A. J. Welch, *J. Chem. Soc. Chem. Commun.*, 1985, 819.
277. G. Ferguson, M. Parvez, J. A. MacCurtin, O. N. Dhubhghaill, T. R. Spalding and D. Reed, *J. Chem. Soc. Dalton Trans.*, 1987, 699.
278. M. Elrington, N. N. Greenwood, J. D. Kennedy and M. Thornton-Pett, *J. Chem. Soc. Dalton Trans.*, 1987, 451.
279. X. L. R. Fontaine, N. N. Greenwood, J. D. Kennedy, P. I. MacKinnon and M. Thornton-Pett, *J. Chem. Soc. Dalton Trans.*, 1986, 1111.
280. J. A. Heppert, M. A. Kuzlik and D. F. Gaines, *Inorg. Chem.*, 1984, **23**, 14.
281. E. W. Corcoran and L. G. Sneddon, *J. Am. Chem. Soc.*, 1984, **106**, 7793.
282. J. Kroner and B. Wrackmeyer, *J. Chem. Soc. Faraday Trans. 2*, 1976, **72**, 2283.
283. J. A. Anderson, R. J. Astheimer, J. D. Odom and L. G. Sneddon, *J. Am. Chem. Soc.*, 1984, **106**, 2275.
284. E. W. Corcoran and L. G. Sneddon, *J. Am. Chem. Soc.*, 1985, **107**, 7446.
285. Z. Janousek, J. Plesek, B. Stibr and S. Hermanek, *Coll. Czech. Chem. Commun.*, 1983, **48**, 228.
286. G. E. Herberich and H. Ohst, *Adv. Organomet. Chem.*, 1986, **25**, 199.
287. W. Siebert, *Angew. Chem. Int. Ed. Engl.*, 1985, **24**, 943.
288. T. Kuhlman, S. Roth, J. Roziere and W. Siebert, *Angew. Chem. Int. Ed. Engl.*, 1986, **25**, 105.
289. G. Schmid, O. Boltsch, D. Blaser and R. Bose, *Z. Naturforsch.*, 1984, **39b**, 1082.
290. G. Schmid, U. Hohner, D. Kampmann, D. Zaika and R. Bose, *J. Organometal. Chem.*, 1983, **256**, 225.
291. G. Schmid, D. Kampfelman, U. Hohner, D. Blaser and R. Bose, *Chem. Ber.*, 1984, **117**, 1052.
292. W. Siebert, M. E. El-Essawi, R. Full and J. Heck, *Z. Naturforsch.*, 1985, **40b**, 458.
293. J. J. Eisch, J. E. Gallo and S. Kozima, *J. Am. Chem. Soc.*, 1986, **108**, 379.
294. G. E. Herberich, W. Boveleth, B. Hessner, M. Hostalek, D. J. P. Koffer, H. Ohst and D. Sohnen, *Chem. Ber.*, 1986, **119**, 420.
295. G. E. Herberich, W. Boveleth, B. Hessner, M. Hostalek, D. J. P. Koffer and M. Negele, *J. Organometal. Chem.*, 1987, **319**, 311.
296. F. E. Herberich, B. Hessner and R. Saive, *J. Organometal. Chem.*, 1987, **319**, 9.
297. G. E. Herberich, W. Boveleth, B. Hessner, D. J. P. Koffer, M. Negele and R. Saive, *J. Organometal. Chem.*, 1986, **308**, 153.
298. G. E. Herberich and H. Ohst, *Chem. Ber.*, 1985, **118**, 4303.
299. G. E. Herberich, U. Buschges, B. Hessner and H. Luthe, *J. Organometal. Chem.*, 1986, **312**, 13.

300. G. E. Herberich, B. Hessner, J. A. K. Howard, D. J. P. Koffer and R. Bose, *Angew. Chem. Int. Ed. Engl.*, 1986, **25**, 165.
301. G. E. Herberich, J. Hengsbach, G. Huttner and U. Schubert, *J. Organometal. Chem.*, 1983, **246**, 141.
302. G. E. Herberich and H. Ohst, *Z. Naturforsch.*, 1983, **38b**, 1388.
303. R. Boese, N. Finke, J. Henkelman, G. Maier, P. Paetzold, H. P. Reisenauer and G. Schmid, *Chem. Ber.*, 1985, **118**, 1644.
304. R. Boese, N. Finke, T. Keil, P. Paetzold and G. Schmid, *Z. Naturforsch.*, 1985, **40b**, 1327.
305. G. E. Herberich and A. K. Naithani, *J. Organometal. Chem.*, 1983, **241**, 1.
306. G. E. Herberich, W. Boveleth, B. Hessner, W. Koch, E. Raabe and D. Schmitz, *J. Organometal. Chem.*, 1984, **265**, 225.
307. G. E. Herberich and D. Sohnen, *J. Organometal. Chem.*, 1983, **254**, 143.
308. G. E. Herberich, J. J. Becker and L. Zelenka, *J. Organometal. Chem.*, 1985, **280**, 147.
309. J. Edwin, M. C. Bohm, N. Chester, D. M. Hoffman, U. Pritzkow, W. Siebert, K. Stumpf and H. Wadepohl, *Organometallics*, 1983, 1666.
310. K. Stumpf, W. Siebert, R. Koster and G. Seidel, *Z. Naturforsch.*, 1987, **42b**, 186.
311. J. Edwin, M. Bockman, M. C. Bohm, D. E. Brennan, W. E. Geiger, C. Kruger, J. Pebler, H. Pritzkow, W. Siebert, W. Swiridoff, H. Wadepohl, J. Weiss and U. Zenneck, *J. Am. Chem. Soc.*, 1983, **105**, 2582.
312. H. Wadepohl, H. Pritzkow and W. Siebert, *Organometallics*, 1983, **2**, 1899.
313. M. Bochmann, K. Geilich and W. Siebert, *Chem. Ber.*, 1985, **118**, 401.
314. H. Wadepohl and W. Siebert, *Chem. Ber.*, 1985, **118**, 729.
315. H. Wadepohl and W. Siebert, *Z. Naturforsch.*, 1983, **39b**, 50.
316. T. Kuhlman and W. Siebert, *Z. Naturforsch.*, 1984, **39b**, 1046.
317. T. Kuhlman and W. Siebert, *Z. Naturforsch.*, 1985, **40b**, 167.
318. J. Edwin, W. Siebert and C. Kruger, *J. Organometal. Chem.*, 1985, **282**, 297.
319. W. J. Dell, P. J. Bray and S. Z. Xiao, *J. Non-Cryst. Solids*, 1983, **58**, 1.
320. T. Templeton and R. K. MacCrone, *J. Non-Cryst. Solids*, 1983, **56**, 387.
321. A. Magistris and G. Chiodelli, *J. Power Sources*, 1983, **9**, 379.
322. I. A. Harris and P. J. Bray, *Phys. Chem. Glasses*, 1984, **25**, 69.
323. M. Englesberg and N. M. Borges, *J. Phys.*, 1984, **C17**, 3633.
324. S. Schramm and E. Oldfield, *J. Chem. Soc. Chem. Commun.*, 1982, 980.
325. D. E. Hintenlang and P. J. Bray, *J. Non-Cryst. Solids*, 1985, **69**, 243.
326. H.-U. Hurter, B. Krebs, H. Eckert and W. Muller-Warmuth, *Inorg. Chem.*, 1985, **24**, 1288.
327. I. A. Harris and P. J. Bray, *Phys. Chem. Glasses*, 1984, **25**, 44.
328. R. K. Harris, A. Root and K. B. Dillon, *Spectrochim. Acta*, 1983, **39A**, 309.
329. L. B. Ebert, D. R. Mills, J. C. Scanlon and H. Selig, *Mater. Res. Bull.*, 1981, **16**, 831.
330. L. B. Ebert and H. Selig, *Synth. Metals*, 1981, **3**, 53.
331. A. J. Leffler, *J. Chem. Phys.*, 1984, **81**, 2574.
332. R. E. J. Sears, *J. Chem. Phys.*, 1982, **76**, 5651.
333. K. Kumagai and F. Y. Fradin, *J. Magnetism Magnetic Matls.*, 1983, **31-33**, 523.
334. P. Panissod, I. Bakonyi and R. Hasegawa, *Phys. Rev.* 1983, **B28**, 2374.
335. B. Krockert and P. Paetzold, *Chem. Ber.*, 1987, **120**, 631.
336. P. Jutzi, B. Krato, M. Hursthouse and A. J. Howes, *Chem. Ber.*, 1987, **120**, 565.
337. M. Yalpani, R. Boese and R. Koster, *Chem. Ber.*, 1987, **120**, 607.
338. S. Hermanek, T. Jelinek, J. Plesek, B. Stibr and J. Fusek, *J. Chem. Soc. Chem. Comm.*, 1987, 927.

# NMR Studies of Alkali Anions in Non-Aqueous Solvents

PETER P. EDWARDS, AHMED ELLABOUDY,  
DOLORES M. HOLTON and NICHOLAS C. PYPER

*University Chemical Laboratory, Lensfield Road,  
Cambridge CB2 1EW, UK*

I. Introduction . . . . .	315
II. Nuclear shielding in the alkali anions . . . . .	318
A. Assignment of the resonance . . . . .	318
B. Experimental nuclear shieldings relative to gaseous neutral atoms . . . . .	326
C. Reliable calculations of nuclear-shielding differences for gaseous alkali ions . . . . .	327
D. Deduction of the nature of $M^-$ in solution . . . . .	331
E. Summary . . . . .	332
III. Solution structure of $Na^-$ probed by nuclear relaxation measurements . . . . .	332
A. Experimental results . . . . .	332
B. Theoretical considerations . . . . .	334
C. Quadrupolar relaxation . . . . .	338
D. Summary . . . . .	346
IV. Chemical dynamics in alkali-metal solutions . . . . .	348
A. The sodium anion . . . . .	348
B. Caesium-based species . . . . .	357
V. Overall conclusions . . . . .	362
References . . . . .	364

## 1. INTRODUCTION

The chemistry<sup>1</sup> of the alkali elements is dominated by the occurrence of systems involving the alkali cation  $M^+$ . However, during the past four decades experimental evidence has accumulated for the existence of alkali anions  $M^-$  in both gaseous and condensed phases.<sup>2</sup> In the alkali anions two electrons occupy the  $ns^2$  valence orbital, the neutral atom having this orbital only singly occupied. The preparation and study of metal anions has its origins in investigations of metal-ammonia solutions, which were first examined by Sir Humphry Davy in 1807.<sup>3</sup> Alkali metals dissolve in anhydrous liquid ammonia to yield, at very low metal concentration, solvated electrons and solvated alkali cations.<sup>4</sup> As the metal content

is increased, these charged species aggregate to form a species of stoichiometry  $M$  whose spectral characteristics are remarkably insensitive to the particular alkali metal.<sup>4</sup> Thus it has been inferred from ESR and NMR studies of metal-ammonia solutions that the electron (spin) density at the alkali nucleus in the species of stoichiometry  $M$  is as low as 1% of that in the corresponding gaseous ground-state atom.<sup>5</sup> In slightly more concentrated solutions the possibility of interactions between the solvated electrons clearly arises. Magnetic-susceptibility experiments, first performed by Taylor and Lewis in 1925,<sup>6</sup> reveal the presence of high concentrations of diamagnetic species. The precise structure of the spin-paired species in metal-ammonia solutions is still controversial,<sup>7</sup> two possible contenders being the dielectron species  $e_2^{2-}$  (possibly in association with a cation) and the triple-ion species  $e^-M^+e^-$ .<sup>3</sup> An important feature of the available data for metal-ammonia solutions is the relative insensitivity of the spin-pairing process to the particular alkali metal used.<sup>7</sup>

In marked contrast, a different situation occurs in solutions of alkali metals in amines and ethers. Here the experimental evidence is for the occurrence of distinct species whose properties are markedly dependent upon the alkali metal they contain.<sup>3,8</sup> One striking example is the optical spectra of metal amine and ether solutions. In addition to an absorption due to the solvated electron, they show an intense metal-dependent band occurring at high energies.<sup>9</sup> This optical absorption shifts to higher energies as the atomic number of the alkali metal decreases.<sup>10</sup> A typical example, taken from Ref. 11, showing the optical absorption spectra of alkali metals in 12-crown-4 (12C4), is depicted in Fig. 1. The metal-, temperature- and solvent-dependences of these bands prompted Matalon, Ottolenghi and Golden<sup>12</sup> to suggest that the species responsible for spin pairing in alkali-amine solutions were alkali anions. Thus the optical transitions were charge-transfer-to-solvent (CTTS) bands, similar, in certain respects, to those observed for halide ions in solution.<sup>8</sup>

This postulation of alkali anions in non-aqueous solvents is not unreasonable when it is realized that these exist as stable species in the gas phase, having infinite lifetimes if left unperturbed. Indeed, the ionization potentials of the gaseous alkali anions, which are equal to the electron affinities of the corresponding neutral atoms, have been accurately measured from photodetachment experiments.<sup>13</sup> However, in these metal solutions it was not possible to deduce the precise nature of the diamagnetic species  $M^-$  from just these optical studies. In addition, a major experimental problem was the relatively low solubility of alkali metals in these low-dielectric solvents.<sup>9</sup> The situation was drastically changed in the early and mid-1970s by the seminal studies of Dye and coworkers.<sup>14-18</sup> The use of crown ethers and cryptands as cosolvents with amines and ethers provided

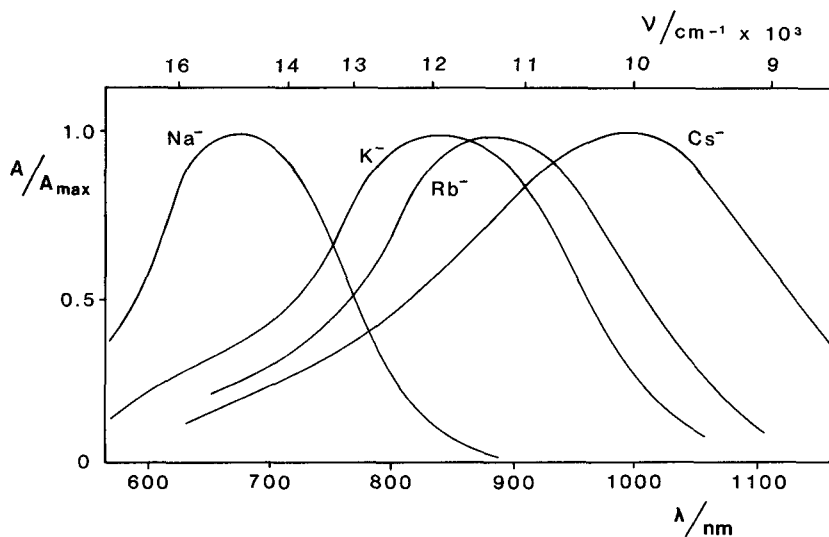


FIG. 1. Optical spectra (room temperature) of solutions of sodium, potassium, rubidium and caesium in 12-crown-4 (taken from Ref. 11 and used with permission).

the key to the preparation, isolation and identification of distinct alkali anions.<sup>2</sup> Thus in 1974 Dye *et al.*<sup>15,16</sup> reported the first crystal structure of a salt containing the sodium anion and a complexed sodium cation. This work was closely followed by the first observation of the  $^{23}\text{Na}$  NMR spectrum of  $\text{Na}^-$  in fluid solutions of sodium metal in ethylamine in the presence of the cryptand  $\text{C}_{222}$ .<sup>18</sup> More recently, Ellaboudy *et al.*<sup>19</sup> have reported  $^{23}\text{Na}$  magic-angle spinning NMR of crystalline salts of the sodium anion. The NMR spectra, in both liquid and solid states, have also been reported for species of stoichiometry  $\text{K}^-$ ,<sup>20,21</sup>  $\text{Rb}^-$ <sup>22-24</sup> and  $\text{Cs}^-$ .<sup>22,25</sup>

Recently attention has been focused on the use of liquid crown-ether solvents, whose structures are shown in Fig. 2, for the preparation of alkali anions.<sup>11,23,26-28</sup> It is known that these crown ethers form strong complexes with alkali cations.<sup>29</sup> The formation of such strong cationic complexes provides the driving force for the dissolution of alkali metals in these liquid crowns. This, coupled with the use of binary alkali-metal alloys, has led to the production of stable metal solutions containing high concentrations of alkali anions.<sup>21</sup> Moreover, the high concentrations of alkali-based species in these solutions have been exploited to carry out extensive magnetic resonance studies aimed at elucidating both the structure and microdynamical processes occurring in these metal solutions.<sup>26,28</sup> The primary aim of this review is to describe the progress that has been achieved

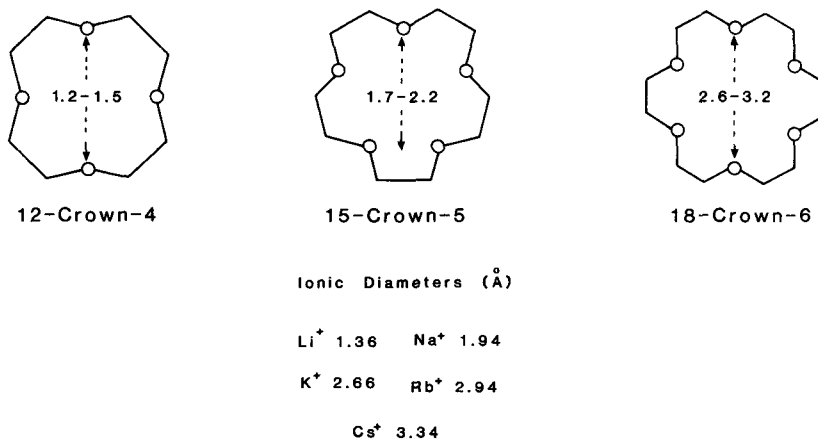


FIG. 2. A representation of the structures of 12-crown-4, 15-crown-5 and 18-crown-6. The dotted lines indicate the approximate cavity dimensions (as indicated).

to date in the study of alkali anions in liquid 12-crown-4 and 15-crown-5 (15C5).

## II. NUCLEAR SHIELDING IN THE ALKALI ANIONS

### A. Assignment of the resonance

The NMR spectra originating from the alkali-metal nuclei have been measured for a wide range of samples prepared by dissolving alkali metals in non-aqueous solvents. These signals have been observed from metal solutions prepared using both pure solvents<sup>23,26,28,30-32</sup> and solvent mixtures.<sup>20-22,24,25</sup> NMR spectra of these metal solutions, which show signals based on both the alkali cation and the alkali anion, are shown in Fig. 3. In the  $\delta$  scale of shielding used in the figure, the NMR signal from a solution of an aqueous cation at infinite dilution has zero shift ( $\delta = 0$ ). The shifts relative to this origin (taken as reference R) have the same sign as the frequency shifts, a negative value of  $\delta$  corresponding to a low-frequency shift and hence to an increase in the nuclear shielding. Thus one has  $\delta = 10^6 (v_S - v_R)/v_R = \sigma_R - \sigma_S$ ; where  $v_R$  and  $v_S$  are respectively the reference and sample frequencies while  $\sigma_R$  and  $\sigma_S$  are the absolute values of the shielding (screening) constants of the same nucleus.

In Fig. 3 the very small deviation of the high-frequency signals from the reference enables the former to be unambiguously identified as arising from a cation-based species, i.e. one of stoichiometry  $\text{M}^+$ . Furthermore, in all the

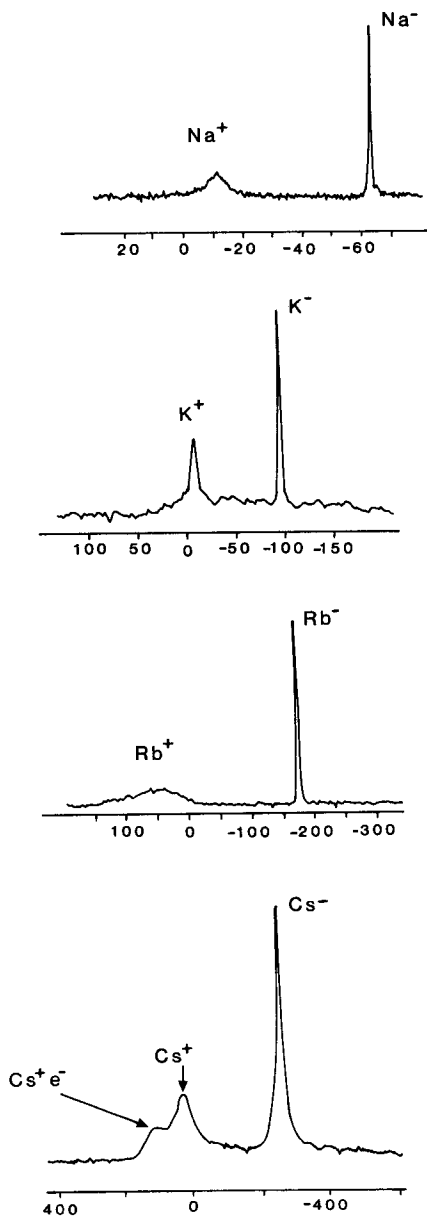


FIG. 3.  $^{23}Na$ ,  $^{39}K$ ,  $^{87}Rb$  and  $^{133}Cs$  NMR spectra from the cationic and ionic forms ( $M^+$  and  $M^-$ ) of the alkali metals in non-aqueous solutions containing crown ethers and cryptands:  $^{23}Na$ , Ref. 18;  $^{39}K$ , Ref. 20;  $^{87}Rb$ , Ref. 24;  $^{133}Cs$ , Ref. 25.

solutions prepared by dissolving Na or Cs metals, excepting those containing the complexing agent  $C_{222}$ , the deviations of the high-frequency signals from the appropriate reference are small.<sup>22,30,32</sup> It is thus clear that these signals also originate from some cation-based species. For the caesium solutions further experiments<sup>25</sup> described in Section IV.B not only confirm that this is indeed the case, but also yield further information concerning these cation-based species. Although for the solutions prepared in the presence of the reagent  $C_{222}$  the high-frequency signals are not inconsiderably shifted from the reference (Table 1), these signals can again be assigned to a cation-based species, albeit one strongly complexed by a  $C_{222}$  molecule. The  $\delta$  values of these cation signals are both temperature- and solvent-dependent (Table 1). This confirms the assignment to a cation-based species.

The NMR signals observed (Table 1) to low frequency of both the reference (R) and cation ( $M^+$ ) resonances, and therefore strongly *shielded* relative to the cation species in the same sample, could, in principle, arise from several different metal-based species. This large shielding relative to the  $M^+$  signal in the same sample means that one can immediately rule out some different, yet still cation-based, species. The chemical shifts of these non-cation-based species are found to be approximately temperature-independent. Furthermore, their chemical shifts (listed in Table 1) are seen to be relatively insensitive to the solvent, this insensitivity being especially marked for the sodium case. This table also contains the NMR linewidths (full width at half maximum height,  $\Delta\nu_{1/2}$ ), which are seen to be significantly narrower than those from the cationic signals in all the systems excepting Rb in 12C4. The temperature- and solvent-insensitivity of the shielded signals, coupled with their narrow linewidths, confirms that these resonances do not arise from a cation-based agglomerate, even in those systems for which *no* cation signal is observed.

One can envisage seven possible extreme limiting cases for the origins of these signals

- (i) A weighted time-average signal in the fast-exchange limit from a species of stoichiometry  $M^-$  and some other diamagnetic species.
- (ii) A loose triple ion in which two solvated electrons are complexed to a solvated cation.
- (iii) A spherically symmetrical dianion of the solvated cation. This is a species of stoichiometry  $M^-$  consisting of a central solvated cation surrounded by two electrons in a spherically symmetric orbital. However, since most of the electron density in this orbital is concentrated in spatial regions *outside* the solvent molecules complexed to the  $M^+$  cation, the orbital is very considerably expanded compared with the ns orbital in the isolated gaseous anion.

TABLE 1  
NMR data for  $M^+$  and  $M^-$  species ( $M = {}^{23}\text{Na}$ ,  ${}^{39}\text{K}$ ,  ${}^{87}\text{Rb}$  and  ${}^{133}\text{Cs}$ ) in solution and solid states.

Species	Solvent	Temperature (K)	Chemical shift		Linewidth (Hz)	Ref.
			$\delta$	$\sigma(\text{S})-\sigma(\text{M})_{\text{g}}$		
$\text{Na}^+(\text{NaCl})$ (infinite dilution)	$\text{H}_2\text{O}$	301	0	-60.5	14	33
$\text{Na}^+(\text{NaCl})$	$\text{H}_2\text{O}$	298	—	-60.5	5.2	22
$\text{Na}^+(\text{NaCl})$	$\text{D}_2\text{O}$	298	0	-60.5	32	30
$\text{Na}^+(\text{NaCl})$ (saturated solution)	$\text{H}_2\text{O}$	298		-61.2	8.0	22
$\text{Na}^+(\text{NaCl})$	HMPA	274	3.9	-64.4	30	30
$\text{Na}^+(\text{NaCl})$	HMPA	298	3.8	-64.3	30	30
$\text{Na}^+(\text{NaI})$	EA	298	13.9	-74.4	17.9	22
$\text{Na}^+(\text{NaI})$	MA	258	11.7	-72.2	9.0	22
$\text{Na}^+(\text{NaBPh}_4)$	THF	298	-7.6	-52.9	23.0	22
$\text{Na}^+(\text{NaBPh}_4)$	DEA	203	—	—	3500	31
$\text{Na}^+(\text{NaBPh}_4)$	DEA	250	-2.8	-57.7	310	32
$\text{Na}^+(\text{NaBPh}_4)$	DEA	279	-2.2	-58.3	110	32
$\text{Na}^+\text{C222}$	MA	258	-10.7	-49.8	30.8	22
$\text{Na}^+\text{C222}$	EA	256-274	-9.7	-50.8	120-170	22
$\text{Na}^+\text{C222}$	THF	269	-10.1	-50.4	51	22
$\text{Na}^+\text{18C6}$	THF	241	0	-60.5	—	22
$\text{Na}^-$	C222/MA	258	-61.9	1.4	11	22
$\text{Na}^-$	C222/EA	256-274	-62.1	1.6	6-9	22
$\text{Na}^-$	C222/THF	269	-62.8	2.3	<3	22

TABLE 1 (*cont.*)NMR data for  $M^+$  and  $M^-$  species ( $M = {}^{23}\text{Na}$ ,  ${}^{39}\text{K}$ ,  ${}^{87}\text{Rb}$  and  ${}^{133}\text{Cs}$ ) in solution and solid states.

Species	Solvent	Temperature (K)	Chemical shift		Linewidth (Hz)	Ref.
			$\delta$	$\sigma(\text{S})-\sigma(\text{M})_{\text{g}}$		
$\text{Na}^-(\text{Na})$	HMPA	263	-61.7	1.5	10	30
$\text{Na}^-(\text{Na})$	DEA	185	-62.3	1.8	45	32
$\text{Na}^-(\text{NaK})$	DEA	203	-62.4	1.9	8	32
$\text{Na}^-$	DPA	213	-62.4	1.9	20	32
$\text{Na}^-$	DMP	231	-62.0	1.5	14	22
$\text{Na}^-(\text{Na})$	12C4	300	-61.8	1.3	10	23
$\text{Na}^-(\text{NaK})$	12C4	285-300	-62	1.5	2.7-3.2	28
$\text{Na}^-(\text{NaRb})$	12C4	285-310	-62	1.5	6.2-7.3	28
$\text{Na}^-(\text{NaCs})$	12C4	260-300	-62	1.5	1.9-1.0	28
$\text{Na}^-$	15C5					
$\text{Na}^-(\text{Na})$	18C6/THF		-62	1.5		22
$\text{Na}^-$	$\text{Rb}^+18\text{C6}, \text{Na}^-$		-59.6		90	19
	$\text{Cs}^+18\text{C6}, \text{Na}^-$		-62.9		75	19
	$\text{Na}^+\text{C222}, \text{Na}^-$		-61.3		290	19
$\text{K}^+(15\text{C5})_2$	15C5/ $\text{Me}_2\text{O}$	220	-9.9			20
$\text{K}^-(\text{CsK})$	12C4/THF	250	-98.2	-2.8	180	21

K <sup>-</sup>	15C5/Me <sub>2</sub> O	220	-99.3	-1.7	20	20
K <sup>-</sup>	K <sup>+</sup> (15C5) <sub>2</sub> K <sup>-</sup>	180	-105	+4		20
Rb <sup>+</sup>	H <sub>2</sub> O	298	1.1	-212.7	158	22
	MeOH	298	-12.0	-199.6	300	22
Rb <sup>+</sup> C222	H <sub>2</sub> O	298	50.4	-262	1300	22
Rb <sup>+</sup> C222	MeOH	298	88.4	-300	4000	22
Rb <sup>-</sup>	EA	233	-185.4	-26.2	220	22
Rb <sup>-</sup>	THF	227	-197.2	-14.4	15	22
Rb <sup>-</sup>	12C4	300	-191.0	-20.6	1000	23
Cs <sup>+</sup> (CsI)	H <sub>2</sub> O	298	4.4	-348.4	3	22
Cs <sup>+</sup> (CsI)	MeOH	298	-28.7	-315.3	3	22
Cs <sup>+</sup> C222	THF	298	132.7	-476.7	30	22
Cs <sup>+</sup> halide <sup>-</sup>	12C4	193	-4	-340	50	25
Cs <sup>+</sup> (CsNa)	12C4/THF	198	-22.4	-321.6	95	25
Cs <sup>+</sup> (CsNa)	12C4/THF	243	-26.4	-317.6	720	25
Cs <sup>+</sup>	12C4/THF	193	1.9	-345.9	50	25
Cs <sup>+</sup>	15C5/THF	193	109	-453	—	25
Cs <sup>-</sup>	C222/THF	202	—	-52.3	10	22
Cs <sup>-</sup>	12C4/THF	193	-300	-44		25
Cs <sup>-</sup>	15C5/THF	193	-280	-64		25

---

- (iv) The contact triple ion. This is a non-spherically symmetric state of an  $M^-$  species with two electrons located on opposite sides of a cation  $M^+$ , this entire species then being solvated.
- (v) A solvated alkali anion. This is a distinct, spherically symmetric metal anion, either weakly or strongly interacting with the surrounding solvent but not with any cationic species.
- (vi) A spherically symmetric alkali anion  $M^-$  in a solvent-separated ion pair with some cationic species.
- (vii) A spherically symmetric alkali anion  $M^-$  in a contact ion-pair with some cationic species.

Figure 4 shows a representation of the structures envisaged as responsible in cases (ii)–(vii). Each of these seven possibilities is now discussed in turn; the first three can be eliminated for the reasons now presented.

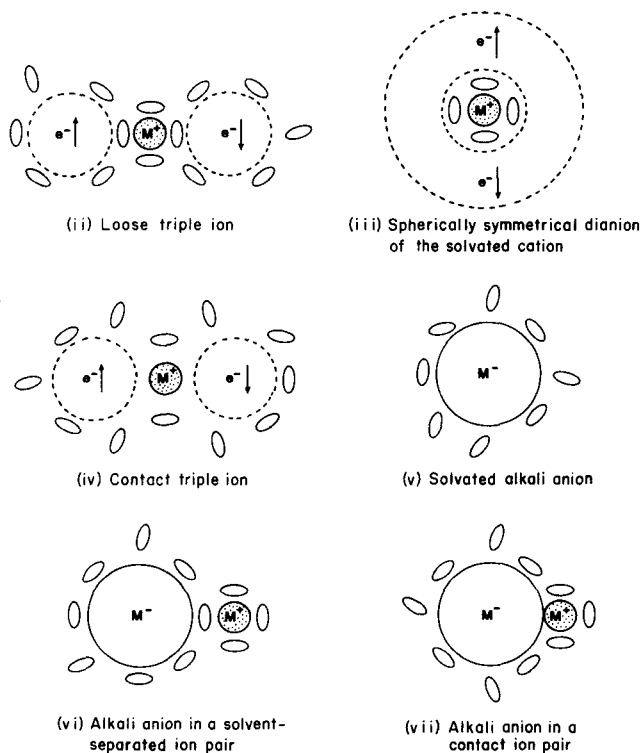


FIG. 4. Schematic representation of possible structures for the alkali anion in solution. The small ellipsoids represent solvent molecules.

Three arguments show that this low-frequency resonance does not arise from a time-average of the signal from a shielded species and a cation-based species, possibility (i). First, the observation of a distinct NMR signal from the metal cation in the spectra of the type shown in Fig. 3 trivially shows that the shielded signal does not involve an average with the observed cation signal. Secondly, the solvent-insensitivity of the resonance frequency of the shielded species suggests that, in those systems in which only this resonance is observed, it does not involve averaging with a cation-based signal. Thirdly, the shielded signals in the liquid-state samples occur at resonant frequencies close to those observed (Table 1) in the solid state from species of stoichiometry  $M^-$ . These solid-state spectra show signals attributable to  $M^-$  as well as deshielded signals attributable to  $M^+$ .

The metal-based entity (ii) is generally held responsible for the spin-pairing present in metal-ammonia solutions.<sup>3,7</sup> A considerable solvation of *both* electrons and cations occurs, and both electron spins are correlated (possibly via a superexchange-type interaction through the cation) to give a singlet electronic ground state located at an energy some 0.4 eV below the triplet excited state. The chemical shift of this triple-ion species would be so similar to that of the  $M^+$  cation that the former can be ruled out as a contender for the observed signal (Fig. 3).

The dianion of the solvated cation (iii) could be envisaged as arising as the limit of the process in which the two electrons in the loose triple ion are delocalized into a spherically symmetric orbital still encompassing both the  $M^+$  cation and its first solvation sheath. The metal NMR characteristics of this species would be even more similar to those of the solvated cation; hence one can dismiss the dianion of the solvated cation as a source of the NMR signal.

In order to distinguish between the contact triple ion (iv) and the solvated alkali anion (v), one needs to compare the observed chemical shift with that of a gaseous alkali anion as described in the next section. The presence or absence of ion pairs involving the solvated anion, (vi) and (vii), can be deduced by combining nuclear spin-lattice relaxation measurements with the rates of quadrupolar relaxation estimated from a simple electrostatic model. This is described in Section III.C.2.

It should be pointed out, however, that one can envisage passing continuously from the loose triple ion (ii) to the contact triple ion (iv) by moving the electrons towards the nucleus while simultaneously moving the solvation sheath away from the alkali cation. By a similar process, one can pass continuously from the dianion of the solvated cation (iii) to a free or weakly solvated spherically symmetric alkali anion (v). It is interesting to note that one can also envisage passing continuously from the spherically symmetric anion (v) to the contact triple ion (iv). Theoretical calculations<sup>33</sup>

predict the existence of excited  $np^2$  configurations of the alkali anions; the electronic charge distribution in the contact triple ion (iv) is qualitatively similar to that of the  $^1D$  state of the  $np^2$  excited electronic configuration.

Information concerning the location of the species of stoichiometry  $M^-$  in the continuous passage to (v) from both (iii) and (iv), as well as the strength of the interaction of the alkali anion (v) with its environment, can only be deduced from a detailed consideration of its chemical shift<sup>34</sup> and nuclear-relaxation<sup>26</sup> behaviour. In particular, one might expect that the nuclear-relaxation rates for a quadrupolar nucleus will decrease on passing from the non-spherically symmetric contact triple ion (iv) to the spherically symmetric gas-like anion (v). This approach of gleaning information about the microscopic structure of the species from relaxation measurements is described in Section III. In the following section we focus on the information to be obtained from nuclear-shielding considerations.

## B. Experimental nuclear shielding relative to gaseous neutral atoms

Optical-pumping,<sup>35,36</sup> atomic-beam<sup>37</sup> and NMR techniques<sup>38-41</sup> have established the shielding constants  $\sigma(M^+)_{aq}$  of the aqueous cations  $^{23}Na^+$ ,  $^{39}K^+$ ,  $^{87}Rb^+$  and  $^{133}Cs^+$  at infinite dilution relative to those of the corresponding gaseous metal atoms,  $\sigma(M)_g$ , with an accuracy of around 2%. We note that, as far as we can ascertain, NMR shielding constants for  $M^+$  are uncorrected for bulk-susceptibility effects. All of these alkali-cation resonances are deshielded (paramagnetically shifted) from those of the respective gaseous atoms by the values given in Table 2. These shielding differences are important in the present context since the aqueous solutions are the standard relative to which the shielding of the alkali containing species in solution is usually measured.<sup>18,22,23</sup> Hence the shielding of the anion in solution (uncorrected for solution bulk susceptibility), relative to that of the gaseous metal atom, can be measured experimentally.

TABLE 2

Experimentally derived shieldings of solvated aqueous cations at infinite dilution relative to those of the gaseous atoms.

Nucleus	$\sigma(M)_g - \sigma(M^+)_{aq(\infty)}$
$^{23}Na$	$60.5 \pm 1$
$^{39}K$	$101 \pm 5$
$^{87}Rb$	$211.6 \pm 1.2$
$^{133}Cs$	$344 \pm 5.8$

The shieldings  $\sigma(S)$  of the species listed in Table 1 relative to the corresponding gaseous metal atoms are reported in the fifth column of this table. These experimental chemical-shift differences  $\sigma(S) - \sigma(M)_g$  were derived from the shielding differences of column 4 of Table 1 by subtracting the shielding differences of Table 2. It should be noted that errors in Table 2 are necessarily propagated into the results assembled in the fifth column of Table 1.

The shielding differences relative to gaseous atoms (Table 1, column 5) are more readily interpreted theoretically than the corresponding shieldings relative to those of the solvated aqueous alkali cations. Indeed, it is well known that cation–water interactions in aqueous solutions cause the cation NMR signals to be very significantly deshielded (paramagnetically shifted) relative to those of the free cation. Similarly one would anticipate a significant paramagnetic shift of the NMR signal originating from the contact triple ion (iv) due to the asymmetric nature of the electronic charge distribution. The failure of the NMR signals from the species of stoichiometry  $M^-$  to display paramagnetic shifts of the magnitudes displayed by the solvated cations strongly suggests that contact triple ions are not responsible for the low-frequency NMR signals.

The nature of the alkali-metal anion in solution can only be deduced if reliable values are known for the nuclear-shielding difference  $\Delta\sigma_g^{(-)}(M)$  between the shielding for the gas-phase anion,  $\sigma(M^-)_g$ , and that,  $\sigma(M)_g$ , of the neutral alkali-metal atom. The shielding  $\sigma(M^-)_g$  for the closed-shell species  $M^-$  is defined to be positive as implied by the expression provided by the Ramsey theory of nuclear shielding,<sup>42</sup> so that

$$\Delta\sigma_g^{(-)}(M) = \sigma(M^-)_g - \sigma(M)_g. \quad (1)$$

However, it is shown in the next section that these shielding differences can be accurately calculated by adding the predictions computed from non-relativistic atomic Hartree–Fock wavefunctions to the (much smaller, but non-zero) contributions from electron–electron correlation. The latter can reliably be derived<sup>34,43</sup> from experimental data. Information concerning the alkali anion in solution is derived by comparing the gaseous shielding differences (1) with the experimental solution values listed in the fifth column of Table 1.

### C. Reliable calculations of nuclear-shielding differences for gaseous alkali ions

In the Ramsey theory<sup>42</sup> the total shielding of a nucleus is the sum of a diamagnetic part and a paramagnetic part. The paramagnetic contribution to the shielding of any isolated atomic S state vanishes if the gauge origin is

chosen at the nucleus.<sup>44</sup> The total shielding  $\sigma(S)$  of species  $S$  is equal to the diamagnetic contribution given in the point-charge point-dipole description of the nucleus in non-relativistic theory by

$$\sigma(S) = \frac{1}{3c^2} \left\langle \Psi_S(r_1, r_2, \dots, r_N) \left| \sum_{i=1}^N r_i^{-1} \right| \Psi_S(r_1, r_2, \dots, r_N) \right\rangle. \quad (2)$$

Here  $|\Psi_S(r_1, r_2, \dots, r_N)\rangle$  is the exact wavefunction for the  $N$ -electron system ( $S$ ) and  $c$  is the velocity of light in atomic units ( $\approx 137$ ).

Since the exact wavefunction cannot presently be accurately computed for atoms containing more than an extremely small number of electrons, it is useful to define the Hartree-Fock contribution  $\sigma_{\text{HF}}(S)$  to the shielding as that predicted by replacing the exact wavefunction by the Hartree-Fock wavefunction in (2). This wavefunction can be simply and exactly computed for all atoms by using a numerical Hartree-Fock program.<sup>45,46</sup> The difference between the exact and Hartree-Fock shielding defines the correlation contribution  $\sigma_{\text{corr}}(S)$  through

$$\sigma(S) = \sigma_{\text{HF}}(S) + \sigma_{\text{corr}}(S). \quad (3)$$

This separation is useful not only because  $\sigma_{\text{corr}}(S)$  is only a small fraction of  $\sigma(S)$ , but also because  $\sigma_{\text{corr}}(S)$  can be related,<sup>34,43,47,48</sup> by using the Hellmann-Feynman theorem, to the nuclear-charge dependence of the correlation energy; thus

$$\sigma_{\text{corr}}(S) = -\frac{1}{3c^2} \left( \frac{dE_{\text{corr}}(Z)}{dZ} \right)_{Z=Z_S}, \quad (4)$$

where the correlation energy  $E_{\text{corr}}(Z)$  of the system having nuclear charge  $Z$  and isoelectronic with  $S$  is the exact non-relativistic energy minus that predicted in the non-relativistic Hartree-Fock approximation. In (4)  $Z_S$  is the nuclear charge of the system  $S$ .

An expression for the difference  $\Delta\sigma(S)$  between the shielding of  $S$  and that,  $\sigma(S_1)$ , of the system ( $S_1$ ) obtained by ionization of one electron from  $S$  is derived<sup>34,43</sup> by subtracting the results (3) and (4) for the total shieldings. The result is

$$\Delta\sigma(S) = \sigma(S) - \sigma(S_1) = \Delta\sigma_{\text{HF}}(S) + \Delta\sigma_{\text{corr}}(S) \quad (5)$$

$$= \Delta\sigma_{\text{HF}}(S) + \frac{1}{3c^2} \left( \frac{dI_{\text{corr}}(Z)}{dZ} \right)_{Z=Z_S}, \quad (6)$$

where  $I_{\text{corr}}(Z)$  is the contribution, arising from electron correlation, to the ionization potential for the removal of an electron from the system of nuclear charge  $Z$  and isoelectronic with  $S$  to yield a system isoelectronic

with  $S_1$ . The result (6) is useful because the quantities  $I_{\text{corr}}(Z)$  can be evaluated<sup>34,43</sup> from experimental ionization potentials. Thus, after subtracting from each experimental ionization potential the small corrections that are computed to arise from relativistic effects and nuclear motion, one has the best available estimate of each ionization potential predicted from the exact non-relativistic wavefunction. The difference between this prediction and the ionization potential computed from the non-relativistic Hartree–Fock wavefunction is the correlation contribution  $I_{\text{corr}}(Z)$  to the ionization potential required in (4). The derivatives of  $I_{\text{corr}}(Z)$  with respect to  $Z$  are evaluated numerically from the four isoelectronic ionization processes in the alkali metals, the alkaline earths and the group IIIA and group IVA elements. The dominant source of error in the  $\Delta\sigma_{\text{corr}}(S)$  values arises from uncertainties in the numerical procedures used to evaluate the derivatives; these small numerical uncertainties have been discussed in detail elsewhere.<sup>34,43</sup> These errors can be estimated to be approximately  $\pm 0.03$  ppm by comparing the results of different numerical procedures.

The Hartree–Fock contributions  $\Delta\sigma_{\text{HF}}(S)$  to the shielding differences  $\Delta\sigma(S)$  have been calculated as the difference between the total shielding  $\sigma_{\text{HF}}(S)$  and  $\sigma_{\text{HF}}(S_1)$  of  $S$  and  $S_1$  computed by using the Hartree–Fock approximation to (2):

$$\Delta\sigma_{\text{HF}}(S) = \sigma_{\text{HF}}(S) - \sigma_{\text{HF}}(S_1). \quad (7)$$

For the case where  $S$  is an alkali-metal anion (i.e.  $S = M^-$ ), so that  $S_1 = M$  (the neutral alkali atom), the shielding difference  $\Delta\sigma(M^-)$  defined by (5) is  $\Delta\sigma_g^{(-)}(M)$  defined by (1). For the case  $S = M$  and  $S_1 = M^+$ ,  $\Delta\sigma(S)$  defined by (5) becomes  $\Delta\sigma_g^{(+)}(M)$ . Since the numerical errors in Hartree–Fock values  $\Delta\sigma_{\text{HF}}(S)$  will be  $10^{-5}$  ppm at most, the accuracy of the calculated values of  $\Delta\sigma_g^{(+)}(M)$  is determined by the errors ( $\pm 0.03$  ppm) in the correlation contribution.

The total computed shielding differences<sup>34,43</sup>  $\Delta\sigma_g^{(+)}(M)$  and  $\Delta\sigma_g^{(-)}(M)$  for the alkali-metal series Li to Cs are presented in Table 3. These results show that for each metal the contribution from electron–electron correlation, i.e. the difference between the exact result and the Hartree–Fock value (reported in parentheses), is small but not negligible. These calculations illustrate four points.

(i) The total shielding constants  $\sigma(M^+)_g$ ,  $\sigma(M)_g$  and  $\sigma(M^-)_g$ , of which the numbers in Table 3 are differences, are themselves very large, e.g.  $\sigma(\text{Cs})_g = 5780.2$  ppm. However, the overwhelming contribution in both cases arises from the core electrons, which make very similar contributions in  $M^+$ ,  $M$  and  $M^-$ . However, these core contributions do not cancel exactly. The core of each neutral atom is slightly contracted relative to that of the anion, thus

TABLE 3

Computed shielding of gaseous alkali cations and gaseous alkali anions relative to gaseous atoms.<sup>a</sup>

Metal (M)	$\sigma(M^+)_{\text{g}} - \sigma(M)_{\text{g}}^b$	$\sigma(M^-)_{\text{g}} - \sigma(M)_{\text{g}}^c$
Li	-6.07 (-6.046)	3.14 (2.743)
Na	-5.18 (-5.089)	2.88 (2.583)
K	-4.08 (-3.933)	2.38 (2.122)
Rb	-3.77 (-3.593)	2.27 (1.995)
Cs	-3.31 (-3.169)	2.08 (1.801)

<sup>a</sup> All results in ppm. Results not in parentheses are non-relativistic, but include effects of electron correlation. Errors arising from the correlation calculation are 0.03 ppm. Hartree-Fock results in parentheses are accurate to all figures quoted.

<sup>b</sup> From Ref. 43.

<sup>c</sup> From Ref. 34.

causing the core shielding difference to contribute minutely but negatively to  $\Delta\sigma_{\text{g}}^{(-)}(\text{M})$  to the extent of less than 0.004 ppm.

(ii) The values decrease smoothly as one proceeds down the group IA elements solely because the valence orbital, whose occupation varies from 0 to 2 as one goes from cation to neutral to anion, becomes more diffuse. It should be noted that the smooth variation in  $\Delta\sigma_{\text{g}}^{(-)}(\text{M})$  down the series (Table 3) contrasts markedly with the values ( $\Delta\sigma_{\text{g}}^{(-)}(\text{Rb}) = 54.7$  ppm;  $\Delta\sigma_{\text{g}}^{(-)}(\text{Cs}) = 232.1$  ppm) that would be deduced by taking the difference between the total shieldings estimated from a simple analytic function<sup>49</sup> constructed to reproduce the known Hartree-Fock shieldings in much lighter systems. The inappropriateness of using these estimates to calculate the small shielding differences of interest here has been fully discussed elsewhere.<sup>43</sup>

(iii) The values of  $\Delta\sigma_{\text{g}}^{(+)}(\text{M})$  are much smaller than the experimental values of the shieldings  $\sigma(M^+)_{\text{aq}}$  of the solvated aqueous cations measured relative to those of the gaseous metal atoms. This confirms the large solvent-induced paramagnetic deshieldings of these ions in aqueous solution.

(iv) For K, Rb and Cs the results of various atomic-beam magnetic resonance experiments have been combined to produce experimental values for  $\Delta\sigma_{\text{g}}^{(+)}(\text{M})$ . For Rb the experimental result<sup>50</sup> of  $3.8 \pm 2.6$  for  $\Delta\sigma_{\text{g}}^{(+)}(\text{Rb})$  agrees well with the theoretical value of 3.77 ppm, although the errors on the experimental value are not inconsiderable. However, it has been pointed out elsewhere<sup>43</sup> that the reported experimental values

of  $\Delta\sigma_g^{(+)}(\text{K})$ <sup>51</sup> and  $\Delta\sigma_g^{(+)}(\text{Cs})$ <sup>52</sup> are not credible and that these experiments need to be reexamined.

#### D. Deduction of the nature of $\text{M}^-$ in solution

Information concerning the nature of  $\text{M}^-$  in solution can be obtained by comparing the experimental shieldings of the alkali anions in solution reported in Table 1 (measured relative to the shielding of the gaseous atom) with the theoretical predictions for the gaseous anions (Table 3). It should also be noted that the experimental numbers in Table 1 have not been corrected for the bulk susceptibilities of the respective solutions. For solutions of sodium in hexamethylphosphoramide (Table 1), the volume susceptibility has been measured<sup>53</sup> to be  $-0.5 \times 10^{-6}$  cgs units, and incorporation of this correction yields<sup>34</sup> a "true" experimental value of  $\Delta\sigma^{(-)}(\text{Na})$  of 2.5 ppm, a correction of some 1 ppm to the measured nuclear-shielding difference.

Clearly for the sodide ion, the observed nuclear-shielding differences ( $\Delta\sigma^{(-)}(\text{Na})$ , Table 1) in the various metal solutions are, within experimental error ( $\pm 1$  ppm, see preceding comments), identical with that (2.88 ppm) calculated for the species  $^{23}\text{Na}^-$  in the gas phase. This, coupled with the remarkable insensitivity of  $\Delta\sigma^{(-)}(\text{Na})$  to the nature of the solvent in all systems examined, shows that the 2p orbitals are well screened from interactions with surrounding solvent or solute molecules by the presence of the filled 3s valence orbital, which itself is unaffected by its environment.

In contrast, the NMR signals of  $^{87}\text{Rb}^-$  and  $^{133}\text{Cs}^-$  in solution are very significantly deshielded relative to those of the corresponding gaseous atoms, as shown by the negative values of  $\Delta\sigma^{(-)}(\text{M})$ , reported in Table 1. The combination of these results with the reliable calculated values of  $\Delta\sigma_g^{(-)}(\text{M})$  shows that the  $\text{Rb}^-$  and  $\text{Cs}^-$  ions in solution are deshielded relative to the gaseous anions, although their deshielding with respect to the gaseous atoms is even more significant. In addition, the observed  $\Delta\sigma^{(-)}(\text{Rb})$  values show a solvent dependence in both the two- and three-component solutions. It is interesting to note, however, the similarity in shifts for  $^{87}\text{Rb}^-$  solutions of Rb in THF with added  $\text{C}_{222}$  (three-component metal solution) and solutions of Rb in the liquid crown 12C4 (a two-component system), both polycyclic ether solvents. This is to be contrasted with the significant influence that the presence of  $\text{C}_{222}$  has on the shielding of cationic Rb,  $\text{Rb}^+$  (Table 1). The negative experimental values of  $\Delta\sigma^{(-)}(\text{Rb})$  suggest that the ground-state wave function of the  $^{87}\text{Rb}^-$  ion is very considerably modified by the presence of the solvent.

The significant deshielding of both  $\text{Rb}^-$  and  $\text{Cs}^-$  signals could arise from two different factors. First, one can regard the anion as being of the type (v)

(Fig. 4), although the interaction with external solvent molecules has become sufficiently strong that it removes the spherical symmetry of the anion. Under these circumstances, where there is a slight asymmetry in the charge distribution, one can expect a non-negligible deshielding arising via the well-known mechanism that, for example, deshields solvated alkali cations. Secondly, the high-frequency shifts could arise if the true electronic structure of the species were intermediate between that (iii) (Fig. 4) of the dianion of the solvated cation and the spherically symmetric anion (v). Thus as one passes from (v) to (iii) the electronic structure acquires some of the character of that of the solvated cation. Since the signals from such cations are known to exhibit large high frequency shifts (Table 1) the observed deshieldings<sup>22-25</sup> of the  $\text{Rb}^-$  and  $\text{Cs}^-$  ions could thereby be explained.

The results<sup>20,21</sup> for  $^{39}\text{K}^-$  in solution suggest that this metal anion is considerably more gas-like than the rubidium anion, certainly in the liquid crown systems. However, the  $^{39}\text{K}^-$  ion does clearly suffer certain small perturbations on its gas-phase electronic structure. This can be gauged from the chemical-shift data in Tables 1 and 3, which indicate a small degree of deshielding in  $^{39}\text{K}^-$  as compared with the gas-phase anion.

## E. Summary

The nuclear-shielding differences between alkali anions and neutral atoms can now be calculated reliably by combining Hartree-Fock predictions with electron-electron correlation corrections derived from experimental ionization potentials. The close similarity between the calculated values and those measured in experiments on  $^{23}\text{Na}^-$  suggests that this species exists in solution as an essentially gas-like anion only weakly coupled to its environment. The large and negative experimental values for  $\Delta\sigma^{(-)}(\text{Rb})$  and  $\Delta\sigma^{(-)}(\text{Cs})$  for  $\text{Rb}^-$  and  $\text{Cs}^-$  in solution suggest that these species are significantly modified upon passing from the gaseous to the condensed phase.

## III. SOLUTION STRUCTURE OF $\text{Na}^-$ PROBED BY NUCLEAR RELAXATION MEASUREMENTS

### A. Experimental results

The measured<sup>26</sup> spin-lattice relaxation times  $T_{1n}$  for  $\text{Na}^-$  in 12C4 as a function of concentration, temperature and counterion are assembled in Table 4. The  $^1\text{H}$  and  $^{13}\text{C}$  relaxation times for pure 12C4 are also included. The  $T_{1n}$  data for this entire series of  $\text{Na}^-$  samples is also shown in Fig. 5.



It has been found<sup>26</sup> that, for a given metal solution, the effect of metal concentration on  $T_{1n}$  is small: increasing the concentration of  $\text{Na}^-$  in NaK/12C4 solutions by a factor of 57 only causes a drop in the value of  $T_{1n}$  of less than a factor of 3. This change is most probably attributable to the increase in viscosity of the concentrated solutions. For a given metal concentration, the spin-lattice relaxation time is virtually independent of the nature of the counterion. Arrhenius plots of the temperature dependence of  $T_{1n}$  have been used<sup>26</sup> to determine the activation energy  $E_a$  for the nuclear spin-lattice relaxation process in the metal solutions. Similarly, the activation energy and the appropriate correlation time for the neat solvent have been derived from the  $^1\text{H}$  and  $^{13}\text{C}$  spin-lattice relaxation data. The resulting activation energies, summarized in Table 4, show the activation energy for  $\text{Na}^-$  relaxation in 12C4 solution via the  $T_{1n}$  process to be the same as that for the neat solvent. Furthermore, the data show the activation energy to be essentially independent of both concentration and counteranion.

The field dependence of  $T_{1n}$  was checked<sup>26</sup> on one NaK/12C4 sample. The relaxation rates were found to be the same at 23.8 MHz (90 MHz proton frequency) and 66.1 MHz (250 MHz proton frequency). Also, decoupling the protons was found to have no effect on either the intensity of the  $\text{Na}^-$  signal or on the measured relaxation time.

## B. Theoretical considerations

### 1. Background

The interactions causing nuclear spin-lattice relaxation may be classified as either of one of two types depending on whether they involve coupling between the nuclear magnetic dipole moment and perturbing magnetic fields ("magnetic relaxation") or coupling between the nuclear electric quadrupole moment and fluctuating electric field gradients ("quadrupolar relaxation"). These two interactions have been considered in detail as possible spin-lattice relaxation mechanisms for the sodium anion in 12C4 solutions.<sup>26</sup> The same arguments may apply also to other metal solutions that have viscosities significantly lower than that of 12C4.

It should be noted that, although the rotational correlation time calculated using the Debye equation is not quantitatively accurate,<sup>54</sup> it has nevertheless been used to demonstrate that the extreme narrowing condition ( $\omega_0 \tau_c < 1$ ) is satisfied for the  $^{23}\text{Na}$  resonances in both 12C4 as well as the solvents of lower viscosity. Here  $\omega_0$  is the appropriate (nuclear) precession frequency and  $\tau_c$  is a characteristic correlation time governing nuclear relaxation. Use of the measured viscosity (9.98 cP) of 12C4 coupled

with an estimate of  $3.0 \text{ \AA}$  for the radius of 12C4 yielded a rotational correlation time of  $2.25 \times 10^{-10} \text{ s}$ . Use of the alternative form of the Debye equation in which the appearance of the molecular radius is replaced by that of the molar volume gave a correlation time of  $2.22 \times 10^{-10} \text{ s}$ . Use of the larger value of  $\tau_c$  showed  $\omega_0 \tau_c$  to be 0.03, thereby demonstrating the extreme narrowing condition is satisfied. The magnetic-field independence of the spin relaxation provided further evidence that this condition is fulfilled.

## 2. Magnetic relaxation

Fluctuating magnetic fields at the  $^{23}\text{Na}$  nucleus responsible for any magnetic relaxation could originate from the nuclear spins of surrounding species, from the spins of unpaired electrons, from the anisotropy of the  $^{23}\text{Na}$  nuclear-shielding tensor, or from spin-rotation interactions. The latter two mechanisms can only operate in a "strong-complex solvation model"<sup>59</sup> in which the sodium anion is so strongly complexed to another species that the entire complex reorients as a single rigid body. In the event that the second species is a cation, one has the contact ion pair introduced in Section II as possibility (vii) for the solution structure of  $\text{Na}^-$ , while the solvent-separated ion pair, the possibility (vi), would arise if the second body were to consist of a solvent molecule plus a cation.

In the "strong-complex solvation model" the dipole-dipole relaxation is caused by the modulation, arising from reorientation of the entire complex, of the through-space dipolar coupling between the  $\text{Na}^-$  nuclear spin and the nuclear spins of the complexed species. In the extreme-narrowing limit, applicable here, the rate  $(T_{1\text{Na}}^{\text{DDR}})^{-1}$  of  $^{23}\text{Na}$  spin-lattice relaxation caused by dipolar coupling to  $n_p$  protons is given by

$$(T_{1\text{Na}}^{\text{DDR}})^{-1} = \gamma_{\text{Na}}^2 \gamma_{\text{H}}^2 r_{\text{NaH}}^{-6} \hbar^2 \tau_c(\text{comp}) n_p, \quad (8)$$

where  $\gamma_X$  is the gyromagnetic ratio of nucleus X,  $r_{XY}$  is the distance between the nuclear spins X and Y, while  $\tau_c(\text{comp})$  is the correlation time for the reorientational motion responsible for the nuclear relaxation. The unknown distance  $r_{\text{NaH}}$  will be of the order ( $3.40 \text{ \AA}$ ) of the sum of the van der Waals radius ( $1.2 \text{ \AA}$ ) of a hydrogen atom plus the ionic radius ( $2.2 \text{ \AA}$ ) of the sodium anion deduced from the crystal structure of  $\text{Na}^+\text{C222.Na}^-$ .<sup>18</sup> The use of the covalent radius ( $0.28 \text{ \AA}$ ) of hydrogen will almost certainly yield an underestimate ( $2.84 \text{ \AA}$ ) for  $r_{\text{NaH}}$ . The Debye equation suggests that the correlation time  $\tau_c(\text{comp})$  for the entire complex in a solution of 12C4 can be related to the rotational correlation time  $\tau_c(\text{solv})$  of the pure solvent through

$$\tau_c(\text{comp}) = \tau_c(\text{solv}) (a_{\text{comp}}/a_{\text{solv}})^3, \quad (9)$$

where  $a_{\text{comp}}$  and  $a_{\text{solv}}$  are the radii of the complex and a single 12C4 molecule respectively. Although these parameters must clearly be subject to some uncertainty, use of standard values of C—C, C—O, C—H bond lengths and bond angles yields, after elementary trigonometry, the value  $a_{\text{solv}} = 3.0 \text{ \AA}$  and hence  $a_{\text{comp}} = 5.20 \text{ \AA}$ . Two values for the correlation time  $\tau_c(\text{solv})$  can also be deduced from the  $^1\text{H}$  and  $^{13}\text{C}$  spin-lattice relaxation times of pure 12C4 reported in Table 4. If the  $^1\text{H}$  relaxation is taken to arise entirely from the dipolar coupling between pairs of protons bonded to the same carbon atom, and the  $^{13}\text{C}$  relaxation is assumed to arise solely from dipolar coupling to the two protons to which it is directly bonded, then the rates  $(T_{\text{1solv}}^{\text{DDH}})^{-1}$  and  $(T_{\text{1solv}}^{\text{DDC}})^{-1}$  of  $^1\text{H}$  and  $^{13}\text{C}$  spin-lattice relaxation are given by

$$(T_{\text{1solv}}^{\text{DDH}})^{-1} = \frac{3}{2}\gamma_{\text{H}}^4 r_{\text{HH}}^{-6} \hbar^2 \tau_c(\text{solv}), \quad (10)$$

$$(T_{\text{1solv}}^{\text{DDC}})^{-1} = 2\gamma_{\text{C}}^2 \gamma_{\text{H}}^2 r_{\text{CH}}^{-6} \hbar^2 \tau_c(\text{solv}). \quad (11)$$

Combination of these equations with the value for  $r_{\text{HH}}$  deduced from  $r_{\text{CH}} = 1.073 \text{ \AA}$  assuming perfect tetrahedral hybridization yields  $\tau_c(\text{solv}) = 0.92 \times 10^{-10}$  and  $0.38 \times 10^{-10} \text{ s}$  respectively, from the  $^1\text{H}$  and  $^{13}\text{C}$  relaxation times at 293 K. Since the observed relaxation rates may have contributions neglected in the derivation of (10) and (11), these two values will be upper limits for  $\tau_c(\text{solv})$ . However, these values are consistent with those deduced from the measured viscosity using the Debye equation. Use of the larger value of  $\tau_c(\text{solv})$  in (9) yields  $\tau_c(\text{comp}) = 4.79 \times 10^{-10} \text{ s}$ , from which the value  $(T_{\text{1Na}}^{\text{DDR}})^{-1} = 0.008 n_{\text{p}} \text{ s}^{-1}$  is deduced from (8), taking  $r_{\text{NaH}}$  to be  $3.40 \text{ \AA}$ . The results show that in the "strong-complex solvation model"  $^{23}\text{Na}$ – $^1\text{H}$  dipolar coupling in the present system could not contribute significantly to the observed relaxation rate since  $n_{\text{p}}$ , the number of interacting protons, would have to be unrealistically large, namely of the order of 300–900, which corresponds to 20–55 crown molecules at a distance of  $3.40 \text{ \AA}$ . Evidence for the reliability of this estimate of  $(T_{\text{1Na}}^{\text{DDR}})^{-1}$  is provided by comparing observed and calculated rates of  $^7\text{Li}$  dipole–dipole relaxation in aqueous LiCl, for which the "strong-complex solvation model" is known to be appropriate. If the  $\text{Li}^+$ –O distance in the  $\text{Li}^+$ –water complex is taken to be  $2.0 \text{ \AA}$  by analogy with the  $\text{Li}$ – $\text{O}^{2-}$  distance of  $1.977 \text{ \AA}$ <sup>56</sup> in solid  $\text{Li}_2\text{O}$ , then the  $^7\text{Li}$ – $^1\text{H}$  internuclear distance is calculated to be  $2.694 \text{ \AA}$ . The correlation time  $(2.7 \times 10^{-12} \text{ s})$ <sup>57</sup> of pure water at  $25^\circ\text{C}$  shows, using a relation of the type (9) that the correlation time for the  $\text{Li}^+$ –water complex is  $1.56 \times 10^{-11} \text{ s}$  if the radii of the complex and of a water molecule are taken to be  $2.694 \text{ \AA}$  and  $1.5 \text{ \AA}$  respectively. If each  $\text{Li}^+$  is tetrahedrally coordinated by water molecules then the relation of the type (8) predicts the rate of  $^7\text{Li}$  dipole–dipole relaxation to be  $0.028 \text{ s}^{-1}$ , in qualitative agreement with

the experimental value extrapolated to infinite dilution of  $0.0352\text{ s}^{-1}$ .<sup>58</sup> Furthermore, a contribution of  $0.0089\text{ s}^{-1}$  is estimated to arise from the translational motion of water molecules outside the first solvation shell, leaving a contribution of  $0.0268\text{ s}^{-1}$  to arise from the reorientation of the complex.<sup>58</sup> The estimation via (9) of the rotational correlation time of the complex from an experimental correlation time of a related species in the same solvent has the advantage of not relying on the precise values of the constants of proportionality entering the Debye equation.

In the "weak solvation model"<sup>59,60</sup> the modulation of the  $^{23}\text{Na}$ - $^1\text{H}$  dipole-dipole coupling responsible for the relaxation arises from the relative translation motion of free sodium anions and independent 12C4 solvent molecules. An expression for the rate  $(T_{1\text{Na}}^{\text{DDT}})^{-1}$  of  $^{23}\text{Na}$  spin-lattice relaxation caused by this mechanism is given by modifying the result of Abragam<sup>61</sup> to take account of the different diffusion constants ( $D_{\text{Na}^-}$  and  $D_{\text{solv}}$  and gyromagnetic ratios for the sodium anion and the 12C4 solvent. After further introduction of a factor of 2/3, which arises because the  $^{23}\text{Na}$  relaxation is caused by coupling to an unlike rather than to a like spin, the rate is found to be

$$(T_{1\text{Na}}^{\text{DDT}})^{-1} = \frac{8\pi\gamma_{\text{Na}}^2\gamma_{\text{H}}^2\hbar^2 N}{15d(D_{\text{Na}^-} + D_{\text{solv}})}, \quad (12)$$

where  $N$  is the density of  $^1\text{H}$  spins and  $d$  is the closest distance of approach between a  $^{23}\text{Na}$  nucleus and a proton. A useful estimate of the ratio of the rates of relaxation predicted by the "weak" and "strong-complex solvation models" is derived by eliminating the diffusion constants from (12) by invoking the Stokes equation while eliminating  $\tau_{\text{c}}(\text{comp})$  from (8) by using the Debye equation. The result is

$$\frac{(T_{1\text{Na}}^{\text{DDT}})^{-1}}{(T_{1\text{Na}}^{\text{DDR}})^{-1}} = \frac{12\pi N r_{\text{NaH}}^6}{5d n_{\text{p}} a_{\text{comp}}^3 (a_{\text{Na}^-}^{-1} + a_{\text{solv}}^{-1})}, \quad (13)$$

where  $a_{\text{Na}^-}$  is the radius of the sodium anion. If the distance  $d$  is taken to be  $r_{\text{NaH}}$  and  $N$  is calculated from the density of 12C4, taking into account all 16 protons, then the ratio (13) is found to be  $1.56n_{\text{p}}^{-1}$ . This yields a value of the relaxation rate  $(T_{1\text{Na}}^{\text{DDT}})^{-1}$  of  $0.0125\text{ s}^{-1}$ , which is over two orders of magnitude smaller than the observed relaxation rate in the metal solution ( $\approx 3.3\text{ s}^{-1}$ ). In addition, the insensitivity of the  $\text{Na}^-$  linewidth, relaxation rate and signal intensity to proton decoupling rule out  $^{23}\text{Na}$ - $^1\text{H}$  dipole-dipole interactions as being responsible for the observed relaxation rates of  $\text{Na}^-$  in these liquid solutions. We note in passing that, in contrast, in the solid state these dipolar interactions contribute significantly to the  $^{23}\text{Na}$  spin-lattice relaxation.<sup>62</sup>

Rates of  $^{23}\text{Na}$  relaxation caused by dipolar interactions with the spins of the unpaired electrons, shown by ESR studies to be present in solution, would be proportional to the concentration of these unpaired spins. The concentration of the unpaired electrons would be expected to be closely related to that of the concentration of the  $\text{Na}^-$  in solution (which has been measured directly). It is unlikely that changing the  $\text{Na}^-$  ion concentration by a factor of 57 would only change the electron concentration by a factor of 3, the factor required if the nuclear relaxation originated solely from dipolar interaction with the unpaired electrons. It has been concluded from these results that the interaction with unpaired electron spins cannot be responsible for the observed relaxation data (Fig. 5).

Anisotropy of the nuclear shielding can only relax  $^{23}\text{Na}$  nuclei in sodium anions if they are incorporated into a complex having a symmetry sufficiently low that the  $^{23}\text{Na}$  shielding tensor is not isotropic. In any such low-symmetry complex there would be a significant electric field gradient at the  $^{23}\text{Na}$  nucleus whose interaction with the nuclear electric quadrupole moment would relax this nucleus at a rate much greater than that observed. Furthermore, the rate of relaxation by chemical-shielding anisotropy varies as the square of the applied field, while the observed relaxation rates are field-independent.

The observed  $^{23}\text{Na}$  relaxation cannot arise from the spin-rotation mechanism, because this relaxes nuclei more rapidly at higher temperatures, in contrast with the observed decrease in the spin-lattice relaxation rate as the temperature is increased (Table 4). These arguments provide further conclusive evidence that neither nuclear-shielding anisotropy nor spin-rotation interactions are responsible for the observed rates of  $^{23}\text{Na}$  spin-lattice relaxation for the sodium anion in solution.

It can therefore be concluded that none of these magnetic-relaxation mechanisms can be responsible for the observed<sup>26</sup> rates of  $^{23}\text{Na}$  spin-lattice relaxation in the sodium anion in 12C4 solutions.

### C. Quadrupolar relaxation in $\text{Na}^-$

#### 1. Deduction of mechanism

The quadrupole moment of  $^{23}\text{Na}$  ( $(0.14\text{--}0.15) \times 10^{-28} \text{ e m}^2$ ) and the temperature dependence of  $T_{1n}$  strongly suggest that the dominant relaxation process involves the fluctuating quadrupolar interactions caused by ionic and/or molecular motions in the liquid. The electric field gradient at the  $^{23}\text{Na}$  nucleus in  $\text{Na}^-$  vanishes identically for both the isolated species and that symmetrically tetrahedrally, or octahedrally, coordinated by static ions or solvent molecules as in the strong-complex solvation model.

Not only has the latter possibility been dismissed for the reasons already discussed, but also this model is inappropriate for the quadrupolar relaxation of other anions in solution.<sup>60</sup> Furthermore, it is shown in the next section that the observed linewidths are incompatible with ion-pair descriptions (Figs 4 (vi) and (vii)) for the Na<sup>-</sup> ion in the 12C4 solutions. In the weak solvation model, applicable here, the quadrupole relaxation arises from the time-dependent fluctuations in the electric field gradient at the <sup>23</sup>Na nucleus caused by the independent translation or rotational motion of the other ions or polar solvent molecules. However, the remarkable insensitivity of the NMR chemical shift of the sodium anion to counterion, composition and temperature in 12C4 solutions suggests that the "fully random distribution" (FRD)<sup>59</sup> subdivision of the weak solvation model is appropriate for Na<sup>-</sup> in these liquid crowns. In this model there is neither preferential orientation of solvent molecules nor a clearly identifiable first solvation shell.

The rate of quadrupolar spin-lattice relaxation is given exactly by<sup>61</sup>

$$(T_{1n})_{\text{quad}}^{-1} = \frac{3}{40} \frac{2I+3}{I^2(2I-1)} \left( \frac{eQ}{\hbar} \right)^2 \Xi, \quad (14)$$

with

$$\Xi = \int_0^\infty \overline{[F(t)F(t-\tau)]} d\tau, \quad (15)$$

where  $I$  and  $eQ$  are respectively the nuclear spin and quadrupole moment and  $F(t)$  is the electric field gradient at the <sup>23</sup>Na nucleus at time  $t$ . The bar denotes an ensemble average. Since the parameter  $\Xi$  is a measure of the strength of the interaction of the relaxing nucleus with its environment, it is of interest<sup>26,63</sup> to compare rates of nuclear relaxation that have been scaled for differences in the properties ( $I, eQ$ ) of each nucleus. The required values

TABLE 5

**Nuclear quadrupole moments and Sternheimer antishielding factors for cations and anions.**

Ion	$eQ$	$\beta_2$
<sup>23</sup> Na <sup>+</sup>	0.14	-5.073
<sup>23</sup> Na <sup>-</sup>	0.14	-15
<sup>35</sup> Cl <sup>-</sup>	-0.079	-69.14
<sup>81</sup> Br <sup>-</sup>	0.28	-123
<sup>127</sup> I <sup>-</sup>	-0.69	-138.4
<sup>133</sup> Cs <sup>+</sup>	-0.003	-102.5

of  $eQ$  are assembled in Table 5. Thus one defines a property  $(T_{1x})_{sn}^{-1}$  by

$$(T_{1x})_{sn}^{-1} = (T_{1x})_{meas} \left( \frac{eQ_{Na}}{eQ_x} \right)^2 \frac{I_x^2(2I_x - 1)}{2I_x + 3} \left( \frac{4}{3} \right). \quad (16)$$

In order to compare the microstructure and dynamics of  $Na^-$  with that of other commonly occurring ions, one compares the values of  $\Xi$  for the sodium anion with those for the other ions shown in Table 6. The resulting values of  $(T_{1x})_{sn}^{-1}$  reported in column 5 of Table 6 represent the nuclear-relaxation rates that would arise if all the ions all had the same quadrupole moment and nuclear spin as the  $^{23}Na$  nucleus. This scaling, from columns 4 to 5, uses theory of such firmly established validity that the scaled numbers can be regarded as experimental results. It is of interest to note that the value of  $\Xi$ , which is directly proportional to  $(T_{1x})^{-1}$ , is very much smaller for  $Na^-$  than that for any other ion except  $Cs^+$  examined in this table. It should also be noted that the scaled  $Cs^+$  value of 817 is much greater than that for  $Na^-$ , the smallness of the  $Cs^+$  rate of column 4 being caused by the small value of  $eQ$  for  $^{133}Cs$ .

The magnitude of the parameter  $\Xi$  in (15) depends both on the mean-square electric field gradient at the nucleus of interest and a characteristic timescale for the fluctuations in this field gradient. This timescale is most conveniently represented in terms of a single correlation time  $\tau_c$ . In a simple model of quadrupolar relaxation, in the extreme-narrowing limit, this

TABLE 6

Measured and scaled nuclear spin-lattice relaxation rates of ions in solution.

Ion	Solvent	$\tau_{solv}$ (ps)	$(T_{1x})_{meas}^{-1}$	$(T_{1x})_{sn}^{-1}$	$(T_{1x})_{sns}^{-1}$	$(T_{1x})_{snst}^{-1}$
$Na^+$	$H_2O$	3.5	16.2	16.2	191	7109
$Na^+$	12C4	3.5	3770	3770	44 450	44 450
$Na^-$	12C4	130.0	3.33	3.33	3.33	3.33
$Cl^-$	$H_2O$	3.5	25	39	1.66	61.71
$Cl^-$	MeOH	7.5	400	631	26.5	459
$Cl^-$	EtOH	15.6	1300	2047	86	7177
$Cl^-$	12C4	130.0	14 100	22 260	935	935
$Br^-$	MeOH	7.5	11 800	2950	38.8	673
$Br^-$	EtOH	15.6	43000	10 750	142	1180
$I^-$	$H_2O$	3.5	4600	346	3.58	133
$I^-$	MeOH	7.5	46 000	3460	35.8	620.5
$I^-$	EtOH	15.6	100 000	7520	78	650
$Cs^+$	$H_2O$	3.5	0.075	817	15.5	577

integral (15) is proportional to the mean-square value of the electric field gradient  $eq$  multiplied by  $\tau_c$ , so that<sup>61</sup>

$$\Xi = (eq)^2 \tau_c. \quad (17)$$

The electric field gradient  $(eq)_e$  at the nucleus generated by the environment external to the ion is magnified by a factor  $1 + \beta_2$ , the Sternheimer antishielding factor, to produce the total field gradient  $eq$ .<sup>64</sup> Thus

$$eq = (eq)_e(1 + \beta_2). \quad (18)$$

This antishielding originates from the additional electric field gradient generated by the electrons belonging to the ion. This in turn arises because the external environment distorts the electronic charge distribution of the ion away from spherical symmetry.<sup>64</sup> Table 5 shows values of  $\beta_2$  for the ions considered in Table 6. Since (17) and (18) show that the nuclear spin-lattice relaxation rate is proportional to  $(1 + \beta_2)^2$ , it is useful<sup>26,63</sup> to define the scaled relaxation rates

$$(T_{1x})_{\text{sns}}^{-1} = (T_{1x})_{\text{sn}}^{-1} \frac{(1 + \beta_2(\text{Na}^-))^2}{(1 + \beta_2(x))^2}. \quad (19)$$

The resulting values reported in column 6 of Table 6 therefore represent the nuclear relaxation rates that would arise if all the ions both had the same nuclear properties as the  $^{23}\text{Na}$  nucleus and had the same Sternheimer antishielding factor as  $\text{Na}^-$ . The resulting data (column 6 of Table 6) are genuine reflections of the differences in strengths of the interactions of each nucleus with its environment external to the ion. Thus these numbers now reflect the differences in the microscopic structure and microdynamics of the various ions in solution. The rate of  $\text{Na}^+$  relaxation relative to that of  $\text{Na}^-$  is increased markedly by this scaling because the value of  $\beta_2$  for  $\text{Na}^+$  is considerably less than that for  $\text{Na}^-$ . Although the scaled relaxation rate (column 6) of  $\text{Na}^-$  is comparable to that of the halide ions in water, it is still nevertheless much less than that for  $\text{Cl}^-$  in the same solvent (12C4).

In any theory of nuclear relaxation in liquids the microdynamical behaviour can be characterized by a correlation time  $\tau_c$  already introduced in (17). For all of the ions except  $\text{Cl}^-$  in 12C4 and  $\text{Na}^+$  in  $\text{H}_2\text{O}$  and 12C4, the molecules in the first solvation shell are known to reorientate independently both of the ion and of each other.<sup>59,60</sup> Since the  $T_{1n}^{-1}$  data for  $\text{Cl}^-$  in 12C4 have only recently been reported, the details of the microdynamics responsible for this relaxation have not yet been elucidated. For all of the  $\text{Na}^-$  solutions, differing in concentration and counteraction, the activation

energy ( $22 \pm 1 \text{ kJ mol}^{-1}$ ), for the process responsible for the  $\text{Na}^-$  spin-lattice relaxation was found<sup>26</sup> (Table 4) to be essentially identical with that ( $23 \pm 1 \text{ kJ mol}^{-1}$ ) for the process responsible for the  $^{13}\text{C}$  and  $^1\text{H}$  relaxation in the pure solvent. As the latter relaxation arises from reorientation of individual 12C4 molecules, the activation energies show that such independent solvent reorientation is the source of the fluctuations in the electric field gradient responsible for the  $\text{Na}^-$  spin-lattice relaxation. Hence the correlation time governing the  $\text{Na}^-$  relaxation is the same as that,  $\tau_{\text{solv}}$ , for the reorientation of individual uncomplexed solvent molecules in the neat liquid. The required value of  $\tau_{\text{solv}}$  at 303 K was derived<sup>26</sup> from the values of  $T_{1n}^{-1}$  for  $^{13}\text{C}$  and  $^1\text{H}$  as described above in Section III.B.2. As the correlation time for neat 12C4 thus derived, 130 ps, is much longer than either that (15.6 ps) of  $\text{C}_2\text{H}_5\text{OH}$  or that (3.5 ps) of  $\text{H}_2\text{O}$ , the scaled relaxation rates of column 7 in Table 6 for  $\text{Na}^-$  relaxation in 12C4 would be expected to be much greater than those for the ions in the other solvents if the strengths of the fluctuating electric field gradients were comparable. The much longer  $\tau_{\text{solv}}$  of 12C4 is consistent with the much greater viscosity (10 cP) compared with that of  $\text{H}_2\text{O}$  (1 cP).

The argument presented in the last paragraph shows that it is interesting to scale the data of Column 6 by a factor  $\tau(12\text{C4})/\tau_x$ , thereby generating the relaxation rates  $(T_{1x})_{\text{snsr}}^{-1}$  that the ions would have if they all had the same quadrupole moments, nuclear spins and Sternheimer antishielding factors as  $\text{Na}^-$ , and were all in solvents of the same viscosity as 12C4. Thus this scaled relaxation rate is given by

$$(T_{1x})_{\text{snsr}}^{-1} = (T_{1x})_{\text{sns}}^{-1} \frac{\tau(12\text{C4})}{\tau_x}. \quad (20)$$

This scaling markedly increases the rates of column 3 in Table 6, except those for  $\text{Na}^-$  and  $\text{Cl}^-$  in 12C4, yielding scaled relaxation rates, which illustrate that the strength of the fluctuations of the environment experienced by the  $\text{Na}^-$  ion is at least an order of magnitude smaller than those for all of the other systems. Note that the "raw" experimental relaxation rates of column 4 (which govern the NMR line width if  $T_{1n} = T_{2n}$ ) might be incorrectly interpreted as suggesting that the interaction of  $\text{Na}^+$  with its environment in  $\text{H}_2\text{O}$  is only slightly greater than that of  $\text{Na}^-$  with its environment in 12C4. However, the present scaled relaxation rates show that this is not the case, and they (column 7) provide the conclusive evidence<sup>63</sup> that the sodium anion in these systems is considerably more decoupled from its environment than any of the other common ions. In particular, the strength of the interaction of  $\text{Na}^-$  with its environment is about 280 times smaller than that of the  $\text{Cl}^-$  ion in the same solvent (12C4).

## 2. Modification of nuclear relaxation in $\text{Na}^-$ by ion-ion interactions

The contribution to the rate of quadrupole relaxation arising either from ion pairing or from the transient passage of ions can be calculated from (14) if the parameter  $\Xi$  can be estimated. If the perturbing ion carrying charge  $e$  is located at a distance  $r$  from the quadrupolar nucleus then the fluctuations in the electric field gradient have a mean-square magnitude  $4e^2r^{-6}$  if the Sternheimer antishielding factor of the ion being perturbed is neglected. If these fluctuations are characterized by a single correlation time  $\tau_c$  then  $\Xi$  is given by

$$\Xi = 4e^2[(1 + \beta_2)P]^2 r^{-6} \tau_c, \quad (21)$$

where  $P$  is the polarization factor, which takes account of the reduction of the electric field gradient caused by the polarization of the surrounding medium induced by the ion pair. This factor is given by<sup>60</sup>

$$P = (2\varepsilon_\infty + 3)/5\varepsilon_\infty, \quad (22)$$

where  $\varepsilon_\infty$  is the high-frequency dielectric constant, which is equal to the square of the refractive index extrapolated to infinite wavelength ( $n_\infty$ ). The fluctuations in the electric field gradient responsible for the relaxation arise from reorientation of the ion pair over timescales during which this reorients appreciably. Since the ion pair reorients independently of the surrounding molecules, any electric field gradient arising from any preferential orientation of these surrounding molecules does not fluctuate over this timescale and therefore does not contribute to the relaxation. This shows that the electric field gradient is not reduced by any factor involving the static dielectric constant because this constant arises from orientation of the surrounding molecules by the ion pair. However, the charge distributions of the electrons on surrounding molecules can readjust much more rapidly than the ion pair reorients. Therefore the electric field gradients at the nuclei in the ion pair will contain a contribution from the electronic polarization of the surrounding medium caused by the electric field gradient originating from the ion pair. This shows<sup>26</sup> that the polarization factor  $P$  should be calculated from the high-frequency rather than the static dielectric constant. The same considerations show that the electric field gradient arising from the passage of one ion past another ion containing a quadrupolar nucleus is also modified by the polarization factor in (22).

For the ion pairs in water or  $\text{MeNH}_2$  the rotational correlation time  $\tau_c$  has been calculated from Debye equation<sup>54</sup>

$$\tau_c = 4\pi(a_{\text{ip}})^3 \eta / 3kT, \quad (23)$$

where  $a_{ip}$  is the radius of the reorienting ion pair. However, for the ion pairs in 12C4,  $\tau_c$  can be calculated<sup>26</sup> using (9) from the correlation time of  $0.704 \times 10^{-10}$  s (deduced from measurements of the  $^1\text{H}$  relaxation in pure 12C4 at 303 K).

The correlation time  $\tau_c$  appropriate to the quadrupolar relaxation of a nucleus in species 1 of radius  $a_1$  caused by the electric field gradient originating from the independent passage of species 2 of radius  $a_2$  is given by

$$\tau_1 = \frac{(a_1 + a_2)^2}{6(D_1 + D_2)}, \quad (24)$$

where  $D_1$  is a diffusion constant of species 1. This result is derived<sup>26</sup> from the formula  $\tau_1 = r^2/12D$  by taking the closest distance of approach  $r$  to be  $a_1 + a_2$  and replacing the diffusion constant  $D$  for like molecules by  $\frac{1}{2}(D_1 + D_2)$ , as discussed by Abragam.<sup>61</sup> After introducing the Stokes equation for the diffusion constants,  $\tau_1$  can be expressed as

$$\tau_1 = \frac{\pi\eta a_1^3(1+R)^2}{kT(1+R^{-1})}, \quad (25)$$

with  $R = a_2/a_1$ . This can be expressed in terms of the correlation time  $\tau_{c,1}$  for the reorientation of the isolated system 1 by invoking the Debye equation to yield

$$\tau_1 = \frac{3}{4} \tau_{c,1} \frac{(1+R)^2}{1+R^{-1}}. \quad (26)$$

The expression (23) with  $\tau_c$  now replaced by  $\tau_1$ , (25), predicts the correct linewidths only if every ion in the solution experiences the transient passage of another ion. In dilute solutions these linewidth predictions should be reduced<sup>26</sup> by a factor equal to the fraction of the time during which an ion is perturbed by the passage of another ion. Linewidth predictions thus derived for a variety of systems are presented in Table 7.

The reliability of calculations using (21)–(23) has been tested<sup>26</sup> by predicting the width of the  $\text{Cl}^-$  resonance in the contact ion pair with  $\text{Et}_4\text{N}^+$  in water. The  $\text{N}^+-\text{Cl}^-$  distance  $r_{\text{N,Cl}}$  was taken to be equal to that (4.844 Å) measured for solid  $\text{Et}_4\text{NCl} \cdot \text{H}_2\text{O}$  by X-ray crystallography.<sup>65</sup> Measurement of a space-filling Corey–Pauling model of the ion pair  $\text{Et}_4\text{N}^+\text{Cl}^-$  yielded  $r_{\text{N,Cl}} = 4.8$  Å, in agreement with experiment, from which  $a = 4.25$  Å. Extrapolation to infinite wavelength of the water refractive indices of 1.329 at 7065 Å and 1.399 at 4358 Å through  $n_\lambda = n + B\lambda^{-2}$  yields  $n = 1.322$ . The halfwidth of the  $\text{Cl}^-$  resonance in a contact ion pair with  $\text{Et}_4\text{N}^+$  is predicted using  $\beta_2[\text{Cl}^-] = -69.1$  to be 579 Hz. This agrees well with the experimental value of  $598 \pm 195$  Hz deduced<sup>66</sup> from measurement of the

TABLE 7

Predicted NMR linewidths for  $\text{Na}^+$  and  $\text{Na}^-$  in various anion-cation aggregates.

Ion	System <sup>a</sup>	Solvent	$\Delta\nu_{1/2}/\text{Hz}$
$\text{Cl}^-$	cip $\text{Et}_4\text{N}^+$	$\text{H}_2\text{O}$	579
$\text{Na}^+$	cip $\text{Br}^-$	$\text{MeNH}_2$	11
$\text{Na}^+$	ssip $\text{Br}^-$	$\text{MeNH}_2$	1
$\text{Na}^+$	passed by $\text{Br}^-$	$\text{MeNH}_2$	1.8
$\text{Na}^+(\text{MeNH}_2)$	passed by $\text{Br}^-$	$\text{MeNH}_2$	0.1
$\text{Na}^+$	cip $\text{Na}^-$	$\text{MeNH}_2$	9
$\text{Na}^+$	ssip $\text{Na}^-$	$\text{MeNH}_2$	0.8
$\text{Na}^+$	passed by $\text{Na}^-$	$\text{MeNH}_2$	1.4
$\text{Na}^-$	cip $\text{Na}^+$	$\text{MeNH}_2$	106
$\text{Na}^-$	ssip $\text{Na}^+$	$\text{MeNH}_2$	10
$\text{Na}^-$	cip $\text{Na}^+(18\text{C}6)$	$\text{MeNH}_2$	10
$\text{Na}^-$	ssip $\text{Na}^+(18\text{C}6)$	$\text{MeNH}_2$	3
$\text{Na}^-$	passed by $\text{Na}^+$	$\text{MeNH}_2$	17
$\text{Na}^-$	passed by $\text{Na}^+(18\text{C}6)$	$\text{MeNH}_2$	1.6
$\text{Na}^-$	cip $\text{Na}^+$	$12\text{C}4$	2951
$\text{Na}^-$	cip $\text{Na}^+(12\text{C}4)_2$	$12\text{C}4$	237
$\text{Na}^-$	ssip $\text{Na}^+(12\text{C}4)_2$	$12\text{C}4$	51
$\text{Na}^-$	passed by $\text{Na}^+(12\text{C}4)_2$	$12\text{C}4$	38

<sup>a</sup> cip = contact ion pair; ssip = solvent-separated ion pair.

concentration dependence of the halfwidth of the  $\text{Cl}^-$  ion solvated solely by water molecules.

It has been suggested<sup>67</sup> that there is significant pairing of  $\text{Na}^+$  and  $\text{Br}^-$  ions in solutions of  $\text{NaBr}$  in  $\text{MeNH}_2$ , even though the halfwidth of the  $\text{Na}^+$  resonance is as small as 4.5 Hz. After introducing  $\beta_2[\text{Na}^+] = -5.073$ ,  $\text{Na}^+$  and  $\text{Br}^-$  ionic radii of 1.0 and 1.98 Å and the  $\text{MeNH}_2$  refractive index of 1.3491,<sup>68</sup> the linewidth of the  $\text{Na}^+$  resonance in the contact-ion pair is predicted<sup>26</sup> to be 11 Hz. This is reduced to 1 Hz in a solvent-separated ion pair, taking the radius of the  $\text{MeNH}_2$  molecule to be the 1.3 Å estimated from a Corey-Pauling model. These results suggest that, although the observed linewidth precludes the existence of contact ion pairs, they are consistent with the existence of solvent-separated ion pairs, which was indeed the hypothesis favoured by Phillips *et al.*<sup>67</sup> A prediction of a width of 1 Hz from ion-pairing is not inconsistent with experiment, because the  $\text{Na}^+$  resonance in water has a width of 5 Hz originating entirely from reorientation of the solvent. In this calculation<sup>26</sup> the entire ion pair consisting of the three species was taken to reorient as a single rigid body. It is debatable whether the concept of ion pair would be appropriate if either

ion moved independently, this essentially being similar to the independent motion of the counterion past the ion containing the quadrupolar nucleus.

The NMR signal of  $\text{Na}^+$  in solutions in  $\text{MeNH}_2$  containing 18-crown-6 (18C6) is also observed to be narrow,<sup>69</sup> having a width of 1–3 Hz despite the postulation of substantial ion-pairing in these solutions. The radius of an 18C6 molecule and hence of the  $\text{Na18C6}^+$  complex was estimated<sup>26</sup> to be 4.9 Å if all the C–O–C angles of the crown ring are taken to be 110°. The  $\text{Na}^+$  linewidths predicted for a contact ion pair with  $\text{Na18C6}^+$  and for independent translation of the complex cation are presented in Table 7. The observed  $\text{Na}^+$  linewidths suggested<sup>26</sup> that contact ion pairs are not formed, but are consistent with an ion pair between  $\text{Na}^+$  and  $\text{Na18C6}^+$  separated by a  $\text{MeNH}_2$  molecule. The calculations invoking free  $\text{Na}^+$ , although unrealistic for solutions containing 18C6, do show the marked reduction of the  $\text{Na}^+$  linewidths predicted to occur when the  $\text{Na}^+$  becomes complexed to 18C6.

In the 12C4 solutions studied previously both the high molar ratio of 12C4 to Na and the X-ray crystal structure of  $\text{Na(12C4)}_2^+\text{Cl}^- \cdot 5\text{H}_2\text{O}$  allowed rejection<sup>26</sup> of the hypothesis that 1 : 1 Na 12C4<sup>+</sup> complexes are formed. The radius of the  $\text{Na(12C4)}_2^+$  complexes present in solution is estimated to be 4.86 Å by assuming normal values for bond lengths and bond angles. This is consistent with the maximum radius of 5.45 Å predicted by adding one C–H bond length plus the van der Waals radius of a hydrogen atom to the  $\text{Na}^+$ –C distance measured by X-ray crystallography of solid  $\text{Na(12C4)}_2^+\text{Cl}^- \cdot 5\text{H}_2\text{O}$ .<sup>70</sup> It is also consistent with the minimum radius of 4.0 Å predicted by adding the van der Waals radius of oxygen (1.4 Å) to the  $\text{Na}^+$ –ring–C distance of 2.5 Å measured from the solid chloride hydrate. The  $\text{Na}^+$  resonance linewidths predicted from these data, with the value of 1.462<sup>71</sup> for the refractive index of 12C4, are presented in Table 7. The linewidths predicted either for contact or solvent-separated ion pairs are so much greater than the observed widths that it was concluded<sup>26</sup> that the  $\text{Na}^+$  ions do not exist as part of any ion pairs in these solutions. Similarly, the  $\text{Na}^+$  ions are not subject to the continual passage of diffusing  $\text{Na(12C4)}_2^+$  complexes. Since the observed line width of 3 Hz is approximately one tenth of the 38 Hz calculated for the continual passage of  $\text{Na}^+(\text{12C4})_2$  complexes, only a maximum of one tenth of the ions can be subjected to such a perturbation at any one instant.

#### D. Summary

The nuclear spin–lattice relaxation of  $\text{Na}^+$  in 12-crown-4 solutions has been found<sup>26</sup> to be essentially independent of the countercation and to depend only weakly on the concentration of the  $\text{Na}^+$  ions in solution. Furthermore,

the activation energies for the processes responsible for the  $\text{Na}^-$  nuclear spin-lattice relaxation are not only independent of metal concentration, and counteraction, but are the same as those observed for the processes governing the  $^1\text{H}$  and  $^{13}\text{C}$  relaxation in the pure 12-crown-4 solvent. It has been concluded<sup>26</sup> from these observations that the  $\text{Na}^-$  ion in solution is relaxed solely through a very inefficient quadrupole mechanism in which the electric field gradient responsible for the relaxation originates from the independent translation and/or rotational motion of surrounding 12-crown-4 molecules. Calculations of the NMR linewidth have shown<sup>26</sup> that the  $\text{Na}^-$  ion does not exist as a contact or solvent-separated ion pair with the sodium cation, and that, if the  $\text{Na}^-$  is past by a  $\text{Na}^+(\text{12C4})_2$  complex, then, at most, 10% of the  $\text{Na}^-$  ions at any one time will be participating in such an encounter. The  $\text{Na}^-$  ion in solution is therefore envisaged as having the structure shown in Fig. 6. This illustrates the  $\text{Na}^-$  ion surrounded by weakly interacting solvent molecules that, moreover, reorientate and translate independent of the  $\text{Na}^-$  ion, which itself retains the gas-phase  $3s^2$  electronic structure.

After scaling the rates of nuclear spin-lattice relaxation of commonly occurring cations and anions to take account of differences in nuclear spins,

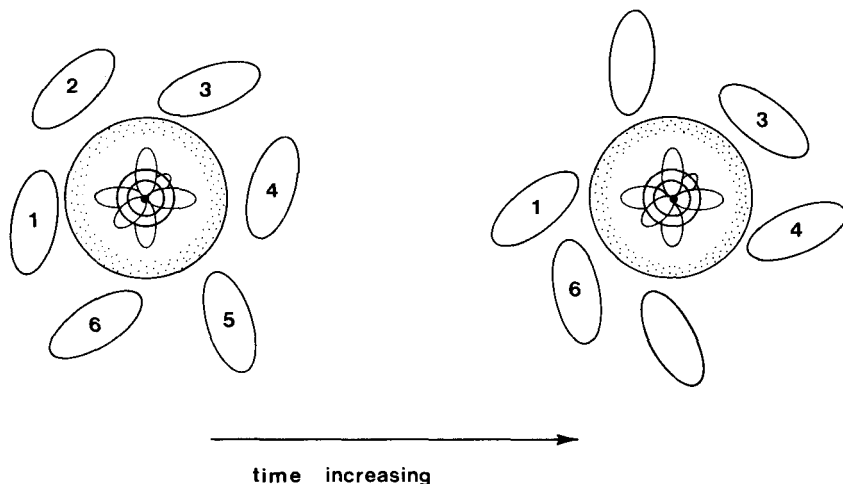


FIG. 6. A representation of the structure of the sodium anion in solution, based on information from chemical-shift and nuclear-relaxation measurements. Solvent molecules labelled 1-6; the drawings depict the situation around the  $\text{Na}^-$  ion as a function of time. The 12C4 molecules rotate and reorientate independently of the centrosymmetric  $\text{Na}^-$  ion. 12C4 solvent molecules that are not numbered represent those that have exchanged with the bulk solvent.

quadrupole moments, Sternheimer antishielding factors and solvent viscosities, the  $^{23}\text{Na}$  nuclear spin in  $\text{Na}^-$  is seen to be considerably more decoupled from its environment than any of the other centrosymmetric ions in solution.<sup>63</sup>

#### IV. CHEMICAL DYNAMICS IN ALKALI-METAL SOLUTIONS<sup>25,28</sup>

##### A. The sodium anion<sup>28</sup>

As we have seen (Section III), the Debye equation can be invoked to show that the extreme-narrowing condition is appropriate in the liquid crown systems: viz  $\omega_o \tau_c \ll 1$ . If this is the case then one expects an equality between

TABLE 8

Sodium-anion spin-lattice and spin-spin relaxation times for various sample compounds, temperatures and counteranions.<sup>a</sup>

NaK $[\text{Na}^-] = 0.11 \text{ mol dm}^{-3}$				NaK $[\text{Na}^-] = 0.17 \text{ mol dm}^{-3}$			
$T$	$T_{1n}$	$T_{2n}$	$\Delta\nu_{1/2}$	$T$	$T_{1n}$	$T_{2n}$	$\Delta\nu_{1/2}$
290	164	147	3.9	280	99	88	5.0
293	181	160	3.2	290	141	110	3.6
295	188	154	3.7	300	187	136	3.2
300	215	157	3.7				
305	250	181	3.4				
310	288	205	3.1				
NaRb $[\text{Na}^-] = 0.165 \text{ mol dm}^{-3}$							
$T$	$T_{1n}$	$T_{2n}$	$\Delta\nu_{1/2}$				
285	119	74	6.6				
290	129	72	6.3				
295	155	70	6.3				
300	177	65	6.2				
NaCs $[\text{Na}^-] = 0.02 \text{ mol dm}^{-3}$				NaCs $[\text{Na}^-] = 0.14 \text{ mol dm}^{-3}$			
$T$	$T_{1n}$	$T_{2n}$	$\Delta\nu_{1/2}$	$T$	$T_{1n}$	$T_{2n}$	$\Delta\nu_{1/2}$
270	89	79	6	285	112	69	6.8
280	121	109	4	290	136	75	6.5
290	191	130	3.4	295	167	86	6.1
300	228	167	1.9	300	210	94	5.3

<sup>a</sup> All  $T_{1n}$  and  $T_{2n}$  values in ms and all linewidths in Hz. All data from Ref. 28.

the spin-spin and spin-lattice relaxation rates, provided that these arise via the quadrupole mechanism that was shown in the last section to govern the spin-lattice relaxation. In the solutions prepared by dissolving NaK, NaRb and NaCs alloys in 12C4, the spin-spin and spin-lattice relaxation times of the  $\text{Na}^-$  ion have been measured<sup>28</sup> as functions of both temperature and composition (deduced from the integrated intensity of the  $\text{Na}^-$  signal). However, the observed  $^{23}\text{Na}$  spin-spin relaxation times are always shorter than the corresponding spin-lattice relaxation times, and this difference appears to be more pronounced at higher temperatures (Table 8 and Fig. 7). Therefore another nuclear spin-spin relaxation process must be augmenting the quadrupole relaxation contribution  $(T_{2n})_{\text{quad}}^{-1}$ . One can attribute this additional relaxation to chemical exchange processes that limit the lifetime of  $\text{M}^-$  in solution. Writing

$$(T_{2n})_{\text{total}}^{-1} = (T_{2n})_{\text{quad}}^{-1} + (T_{2n})_{\text{exch}}^{-1} \quad (27)$$

Equation (27) yields, via substitution, the exchange contribution  $(T_{2n})_{\text{exch}}^{-1}$  to the total relaxation rate. In Fig. 8 we present, for a range of solutions, the temperature variation of  $(T_{2n})_{\text{exch}}^{-1}$  in terms of Arrhenius-type plots, from which one can derive some activation energies for the processes responsible for the additional spin-spin relaxation.

In the case of mixed  $\text{Cs}^+\text{Na}^-$  samples the exchange rate was temperature-independent over the entire temperature range examined.

For the  $\text{Rb}^+\text{Na}^-$  and  $\text{K}^+\text{Na}^-$  systems the observed data suggest two processes; the first, occurring in the low-temperature regime, is markedly temperature-dependent, whereas in the high-temperature limit the  $\text{K}^+\text{Na}^-$  exchange rates become insensitive to temperature.

Since the signal for which the  $T_{1n}$  and  $T_{2n}$  values have been measured (Fig. 7) arises from just the  $\text{Na}^-$  ion, the signal from this species is in the slow-exchange limit. Hence the lifetime of the  $\text{Na}^-$  ion is equal to the value of  $(T_{2n})_{\text{ex}}$  deduced from (27). A typical value for this lifetime is that of 1.1 s for a 0.02 M  $\text{Na}^-\text{Cs}^+$  solution at 280 K.

At the highest temperatures the lifetime of  $\text{Na}^-$  in NaK solutions is temperature-independent and the process has no activation energy. In the case of the  $\text{Rb}^+\text{Na}^-$  solution the lifetime is very slightly more sensitive to temperature at low temperatures than at high temperatures; here it is not unreasonable to anticipate that the lifetime of  $\text{Na}^-$  would become temperature-independent if experiments could be performed at sufficiently higher temperatures. Thus the countercation very significantly influences both the high- and low-temperature exchange processes; that is, the mechanism limiting the lifetime of  $\text{Na}^-$  must therefore involve the countercations  $\text{K}^+$ ,  $\text{Rb}^+$  and  $\text{Cs}^+$ . The observation of temperature-independent lifetimes for  $\text{Na}^-$  suggested that the chemical-exchange process

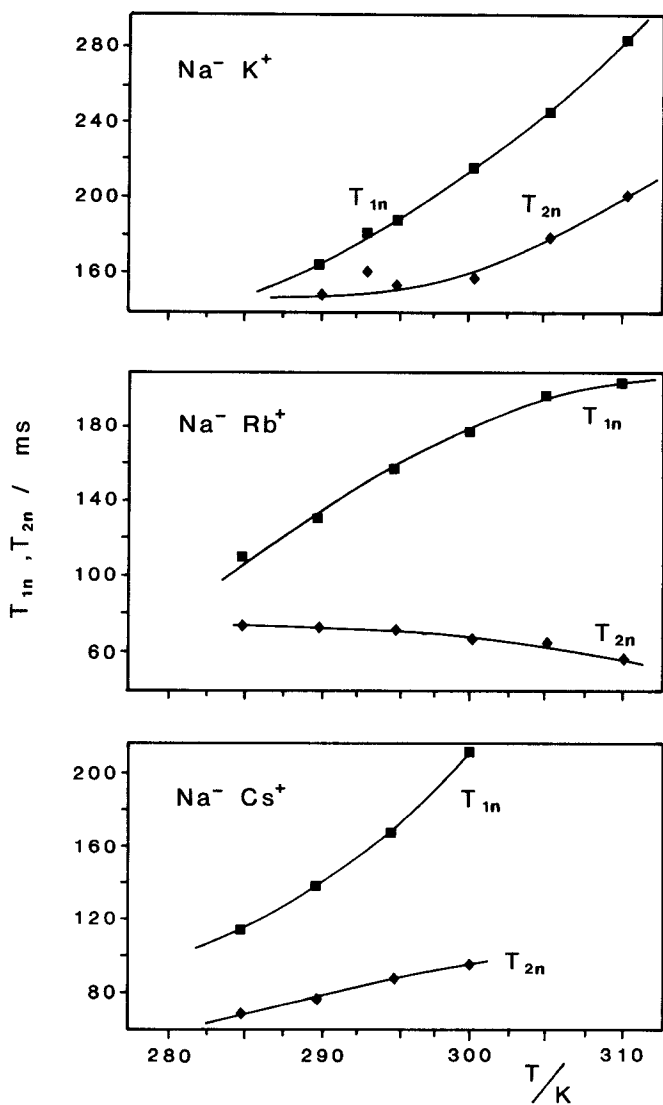


FIG. 7.  $^{23}\text{Na}$  nuclear spin-spin ( $T_{2n}$ ) and spin-lattice ( $T_{1n}$ ) relaxation times for solutions of mixed alkali-metal alloys in 12C4.

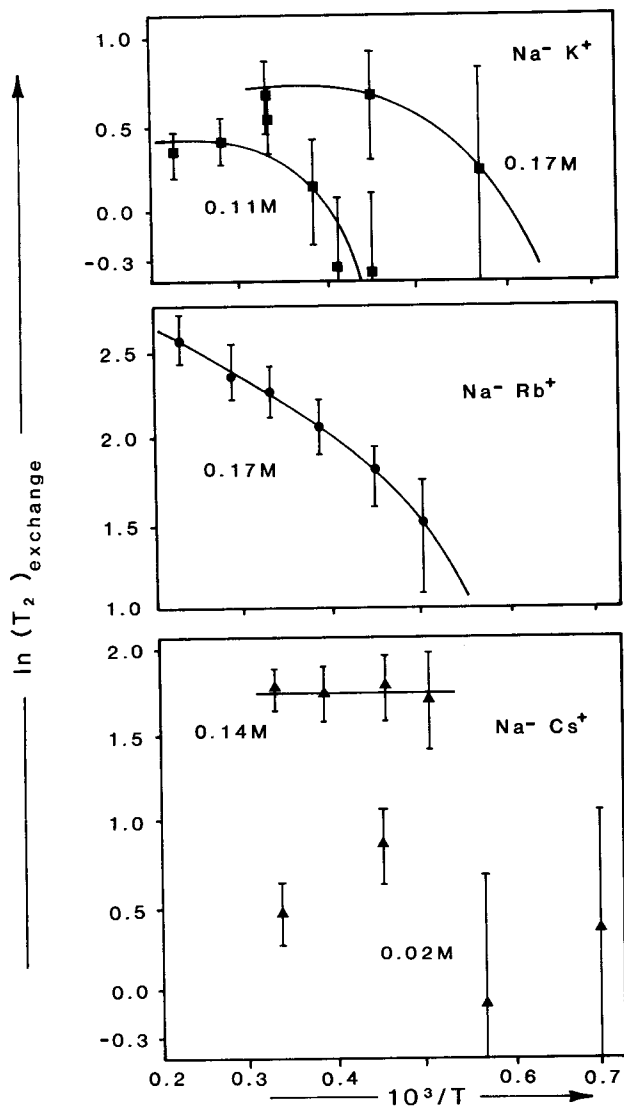


FIG. 8.  $^{23}\text{Na}$  spin-spin exchange rates  $(T_{2n})_{\text{exch}}^{-1}$  as functions of temperature for solutions of mixed alkali-metal alloys in 12C4.

dominating under these conditions has zero activation energy. Furthermore, the derived lifetimes for  $\text{Na}^-$  in solution are remarkably long compared with typical timescales ( $10^{-10}$  s) for processes occurring at a molecular level.

Since the observed rates are counteranion-dependent, the exchange processes cannot be unimolecular. In addition, most bimolecular processes have a rate depending upon temperature as  $A \exp(-E_a/kT)$ , and this can only yield a rate independent of temperature if  $E_a = 0$ . If the preexponential factor  $A$  were an expression of the rates of molecular collision then this would give a rate very much greater than the observed lifetime of  $\text{Na}^-$ . It has therefore been suggested<sup>28</sup> that the temperature-independent exchange process is due to quantum-mechanical tunnelling of electrons from  $\text{Na}^-$ . The rate of tunnelling would involve the amplitude of the tail of the  $\text{Na}^-$  wavefunction at some other site. Since this wavefunction decreases exponentially with increasing distance, then clearly for tunnelling onto sites at large distances, slow rates are possible. As the limiting (high-temperature) rates are also strongly metal-dependent (i.e. dependent upon the alkali counteranion  $\text{M}^+$ ), any tunnelling of an  $ns$  valence electron of  $\text{Na}^-$  must be onto a species containing a counteranion, as opposed to tunnelling onto a solvent molecule. Electron tunnelling from  $\text{Na}^-$  must therefore proceed to some vacant (accessible) orbital on the alkali cation. Clearly, a heavily complexed cation will have these  $s$  orbitals occupied via strong directional bonding of the lone pair of electrons from the crown solvent; see Section I. It has been proposed<sup>28</sup> that electron tunnelling from  $\text{Na}^-$  is only possible onto an "uncomplexed" cation. This uncomplexed cation is viewed as one that is partially solvated by the crown, but not one that forms a strong inclusive complex in which the cation is partly (or completely) enclosed either in the

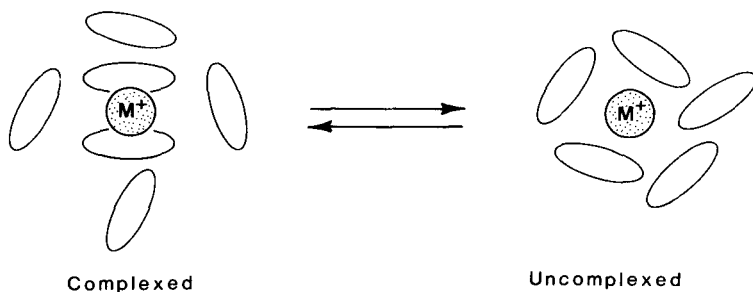
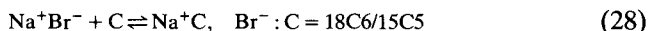


FIG. 9. A schematic representation of the difference between complexed and solvated alkali cations in 12C4; the former is representative of the situation at low temperatures in  $\text{Na}^+$ ,  $\text{K}^+$  and  $\text{Rb}^+$  samples; the solvated species are postulated for the high-temperature regime (see text).

cavity of the crown or as a sandwich complex, i.e.  $M^+C_2$  (Fig. 9). The latter possibilities arise in the crown solutions because the essentially 2D nature of the crown-ether molecule allows for strong interaction between the cations and the crown. Obviously, in the case of 12C4 and 15C5, liquids under ambient conditions, the crown is *both* the complexant *and* the solvent. This two-site equilibrium, (29) below, has been invoked<sup>28</sup> as the process responsible for the lifetime limitation of  $Na^-$  for those cases where this lifetime is strongly temperature-dependent. A representation of both complexed and uncomplexed cationic species is shown in Fig. 9. This equilibrium (29) can be expected to be temperature-dependent and to shift to the right with increasing temperature. In many ways, this model is similar to that recently advanced by Phillips *et al.*<sup>67</sup> for solutions of NaBr in ethylamine in the presence of a complexing agent, where the equilibrium is



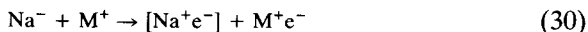
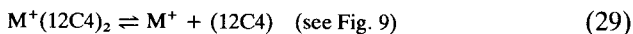
and where the solvent ( $EtNH_2$ ) is known also to solvate sodium cations. However, the equilibrium in the crowns does not involve a significant degree of ion-pairing, unlike the case of NaBr in ethylamine. The low-temperature exchange data (Fig. 8) strongly suggest that it is most difficult to form the uncomplexed potassium cation in these systems, followed by  $Rb^+$  and  $Cs^+$ .

A tunnelling process of the sort invoked here would be expected to be sensitive to the nature of the countercation over the entire range of temperature, and also to depend upon the countercation concentration at the lower temperature. The data plotted in Fig. 8 also show the concentration dependence of the  $Na^-$  ( $T_{2n}^{-1}$ )<sub>exch</sub> rate.

In the case of NaK solutions it has been proposed<sup>28</sup> that the transition to the (high-temperature) exchange process occurs when the equilibrium (29) is far enough to the right to yield the maximum number of uncomplexed  $K^+$  ions within some characteristic (diffusion or encounter) distance of the  $Na^-$  ion. Thus one predicts that on increasing the concentration of  $K^+$  one will go over to the quantum-mechanical tunnelling regime at a lower temperature. This is in qualitative accord with the concentration dependence of the exchange terms. Similarly, the exchange rate would be expected to be dependent on the concentration of  $Na^-$ , again as observed experimentally. In this view, the lifetime of  $Na^-$  will be determined by the number of uncomplexed alkali cations within the tunnelling distance. Thus, at low concentrations, at all temperatures there is an insufficient number of uncomplexed cations. Hence an increase in temperature leads to the formation of more uncomplexed cations and the exchange rate will increase accordingly. However, for the most concentrated solutions at the highest temperatures the concentration of  $K^+$  is sufficiently high that the lifetime-limiting step then becomes the tunnelling rate.

For NaCs solutions, increasing the concentration of  $\text{Cs}^+$  from 0.02 to 0.14 M increases the exchange rate by a factor of 3.6. It should be noted that these are relatively dilute solutions and that the rate does not increase by the factor of 7 increase of the concentration. Under these circumstances, once one has a number of uncomplexed cations sufficient to yield a significant tunnelling rate, increasing the concentration of metal in solution will only marginally affect the overall rate. The data suggest that the activation energy of the process (29) is zero for NaCs, so that increasing the temperature does not lead to changes in the total exchange rate  $(T_{2n}^{-1})_{\text{exch}}$ .

In summary, then, two processes for limiting the lifetime of  $\text{Na}^-$  in these solution have been proposed; for the case of 12C4



The species  $\text{M}^+\text{e}^-$  is a weak complex between a cation and an unpaired electron, and was envisaged to possess a small (<10%) atomic character, with both  $\text{M}^+$  and  $\text{e}^-$  being quite highly solvated.<sup>3</sup> Although the processes, as written, indicate that the paramagnetic "remnant"  $[\text{Na}^+\text{e}^-]$  of  $\text{Na}^-$  is also a weak complex, it was suggested that this species is instantaneously left in an electronic state approximating closely to that of a gas-phase sodium atom.

The above two processes cannot be the only ones occurring in these metal solutions, since in the absence of other processes, reactions (29) and (30) will lead, in time, to the depletion of  $\text{Na}^-$  while increasing both the  $\text{Na}^+\text{e}^-$  and  $\text{M}^+\text{e}^-$  concentrations. It has therefore been suggested that  $\text{Na}^-$  is regenerated through the process



The other possibility that  $\text{Na}^-$  is regenerated by a reaction of  $\text{Na}^+\text{e}^-$  with  $\text{M}^+\text{e}^-$  to yield  $\text{Na}^-$  and  $\text{M}^+$  has been rejected<sup>28</sup> because this process not only necessitates the ejection of an electron from  $\text{M}^+\text{e}^-$ , which requires work against the Coulombic interaction of  $\text{e}^-$  and  $\text{M}^+$ , but also  $\text{M}^+\text{e}^-$  is only present in concentrations much smaller than that of the free or solvated electron required in process (31). Further evidence in favour of the regeneration of  $\text{Na}^-$  via the process (31) comes from pulse-radiolysis studies<sup>72</sup> of metal solutions. These studies show that  $\text{Na}^-$  is formed from  $\text{Na}^+$  via a two-step process in which  $\text{Na}^+$  is first converted to  $\text{Na}^+\text{e}^-$ , which is then converted to  $\text{Na}^-$  in accordance with process (31). Clearly, the process (31) can only be held responsible for the regeneration of  $\text{Na}^-$  if there is a significant concentration of solvated electrons  $\text{e}^-$ . The major ESR signal observed<sup>11,73</sup> in the metal-liquid-crown solutions is an intense signal close to free spin, which is consistent with the idea of a high concentration of

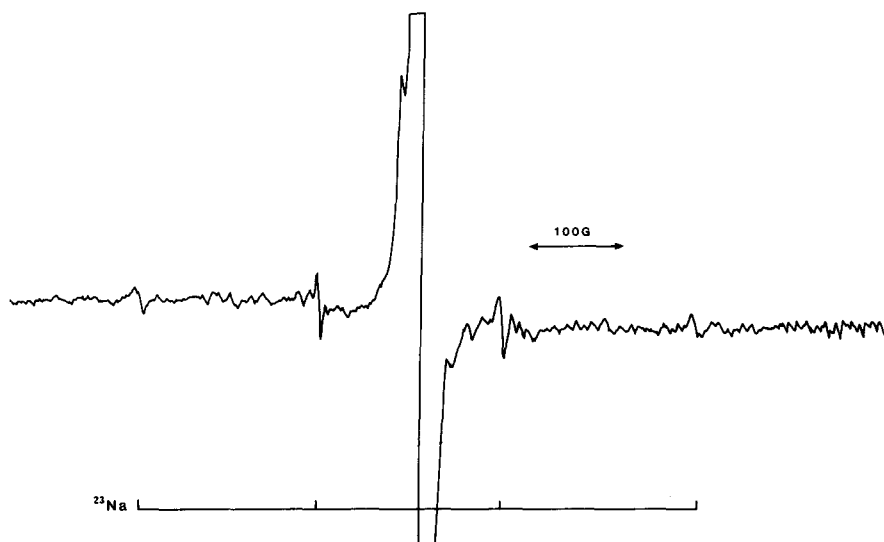
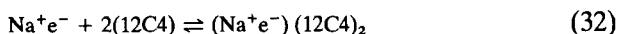


FIG. 10. ESR spectrum of a quenched solution of sodium-rubidium alloy in 12C4.

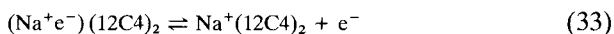
solvated electrons. Furthermore, ESR studies of the frozen solutions show a very strong absorption at free spin, as illustrated, for example, by the NaRb spectra shown in Fig. 10.

The fact that pure sodium metal dissolves in the pure crown solvents shows that the atom-like  $\text{Na}^+\text{e}^-$  species must be capable of undergoing further reaction with the crown solvent to yield some cation-based species. If this were not the case and the only reaction of  $\text{Na}^+\text{e}^-$  with  $\text{e}^-$  was to yield  $\text{Na}^-$  (as in (31)) then Na metal would not dissolve in a pure crown. Experimental evidence has been advanced<sup>74</sup> to show that the alkali anions are not formed in just one single step in the dissolution of alkali metals in solutions containing crown ethers. One can reject the possibility that  $\text{Na}^+\text{e}^-$  could lose an electron to form  $\text{Na}^+$  and a solvated electron because the experimental data have already shown that  $\text{Na}^-$  will not lose an electron onto the solvent, but requires the presence of an uncomplexed  $\text{M}^+$  ion. This process is expected, *a priori*, to be more facile in the anion than the corresponding loss of an electron from an atomic species  $\text{M}^+\text{e}^-$ . These considerations have led to the suggestion<sup>28</sup> that the  $\text{Na}^+\text{e}^-$  species undergoes the following process with the solvent:

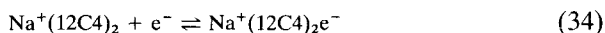


to yield a solvated sodium atom still having a high percentage atomic character. Since the crown ether is known to be a strong solvator of cations,

it has also been suggested that the solvated alkali atom can undergo the further reaction



to produce solvated electrons. This reaction can provide the source of the unpaired electrons that are required in process (31), which must occur when pure sodium metal is dissolved in a crown solvent to produce  $\text{Na}^-$  ions. Clearly, the  $\text{Na}^+$  complex has the possibility of forming a weak ion pair with a solvated electron:



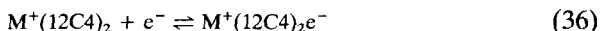
Evidence for the occurrence of these species comes from both ESR studies of quenched metal–12-crown-4 solutions<sup>11,28,73</sup> and similar studies of vitreous solids formed by rapid quenching of alkali hexamethylphosphoramide (HMPA) solutions.<sup>75</sup> A typical spectrum from a quenched NaRb solution in 12-crown-4 is shown in Fig. 10. Here the large hyperfine splitting due to  $^{23}\text{Na}$  is clearly observed, and this has been assigned to the solvated atomic species  $(\text{Na}^+\text{e}^-)(12\text{C}4)_2$  rather than to the  $\text{Na}^+\text{e}^-$  species because the former can be expected to occur in much higher concentration.<sup>28</sup> The isotropic hyperfine splitting  $A_{\text{iso}}$  corresponds to 65% occupancy of the Na 3s orbital. The same sodium-based signal has also been observed from a frozen NaK–12-crown-4 solution, the isotropic hyperfine splitting being the same as the NaRb case. Evidence for the existence of more than one species  $\text{Na}^+\text{e}^-$  of high percentage atomic character as postulated in the above schemes comes from ESR studies<sup>75</sup> of quenched solutions of sodium metal in HMPA. These studies showed the largest such signal to have approximately 64% atomic character, but with a number of other high-atomic-character species.

The species  $\text{Na}^+(12\text{C}4)_2\text{e}^-$  has also been identified from solid-state NMR studies, which showed the species to have less than  $10^{-3}\%$  atomic character.<sup>76</sup> The ESR signal given by such a species would be indistinguishable from that of a trapped electron not associated with a cation. Returning to the process (30), ESR studies<sup>11,73</sup> of the quenched metal–12-crown-4 solution also provide evidence for the existence of the  $\text{M}^+\text{e}^-$  species having a small ( $<10\%$ ) atomic character. The absorption in the  $g \approx 2$  region in Fig. 10 is a superposition of a strong signal at free spin and another signal whose width, moreover, in NaK and NaCs samples differs from that in the NaRb case. From an analysis<sup>11,73</sup> of the linewidths of this metal-dependant signal, it has been shown that this resonance can be assigned to the species  $\text{M}^+\text{e}^-$ , having approximately 1% atomic character. Since this species has a low percentage atomic character, it has been suggested<sup>28</sup> that it can also dissociate to produce free (or solvated) electrons,

according to the equilibrium



This reaction of  $M^+$  with the solvent to form the  $M^+(12C4)_2$  complex is simply the inverse of the reaction (29), postulated as the first step in the process limiting the lifetime of  $Na^-$  in solution. Clearly, the possibility exists that the  $M^+(12C4)_2$  complex will form a weak ion pair with the electron



For the solutions prepared by dissolving pure Cs metal in mixtures of 12-crown-4/15-crown-5 and THF there is NMR evidence<sup>25</sup> that both the species  $Cs^+L_2$  and  $Cs^+L_2e^-$  ( $L = 12C4, 15C5$ ) postulated in (36) are indeed present. This is discussed in the next section, in which the failure to detect any cation-based signals at ambient temperature from solutions prepared using only pure crown solvents is commented on.

It is important to note that equilibria involving electrons are envisaged as occurring within the Boron–Oppenheimer approximation, i.e. that the electron hops are much more rapid than any timescales for molecular motion. Thus the molecules are essentially stationary during the time when the electron moves from one site to another; processes in which both the electron and the arrangements of the molecules in space change simultaneously are not regarded as occurring with any significant degree of probability. This means that processes such as  $M^+e^- + L_2 \rightarrow M^+L_2e^-$  have not been invoked in the scheme of equilibria presented above.

## B. Caesium-based species<sup>25</sup>

In the last section the temperature, concentration and counterion dependence of the nuclear spin–lattice and spin–spin relaxation times of the alkali anion signals were described. In conjunction with ESR studies of quenched solutions, it was shown how these results could be used to deduce both the nature of the chemical species present and some of the equilibria they undergo. In particular, the species  $Na^+(12C4)_2$  and  $Na^+(12C4)_2e^-$  were postulated to play an important role in the scheme of equilibria limiting the lifetime of  $Na^-$ , even though no NMR signals based on any cation-based species were observed for systems prepared using either pure 12C4 or pure 15C5 as solvent. Similarly, no  $^{133}Cs$  NMR signals could be detected from solutions of caesium metal in the pure crown-ether solvents, 12C4 and 15C5, even though the optical spectra<sup>11,27,73</sup> of these blue solutions reveal the presence of the  $Cs^-$  ion. The failure to observe such signals suggests that they are broadened beyond detection either by chemical exchange processes or by a highly efficient relaxation mechanism.

It is the object of this section to describe further  $^{133}\text{Cs}$  NMR experiments that have recently been carried out<sup>25</sup> using mixed solvent systems. The results provide further evidence for the scheme of reactions presented in the last section. The failure to observe cation-based signals in metal solutions prepared using pure crown solvents could be caused by rapid rates of relaxation occurring at the relatively high temperatures at which the measurements necessarily had to be made. Unfortunately, these two liquid crown ethers have only a very narrow temperature range because of their relatively high freezing points ( $>260\text{ K}$ ). However, as illustrated by Dye and coworkers,<sup>2,15,18</sup> the accessible liquid temperature range can be increased by the addition of a cosolvent such as tetrahydrofuran (THF).

Figure 11 shows  $^{133}\text{Cs}$  NMR spectra at 198 K for three saturated caesium-metal solutions containing different proportions of the liquid crown ethers

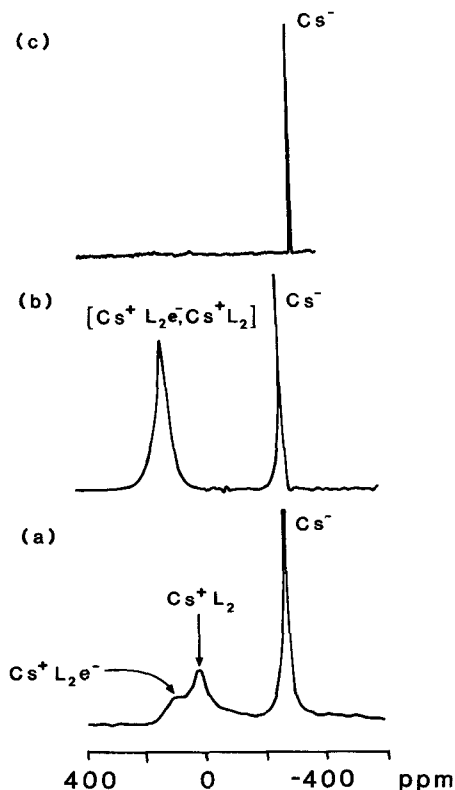


FIG. 11.  $^{133}\text{Cs}$  NMR spectra (52.485 MHz) of solutions of caesium metal in 12C4, 15C5/tetrahydrofuran mixtures (taken from Ref. 25 and used with permission). (a) 5% v/v 12C4/THF; (b) 5% v/v 15C5/THF; and (c) 20% v/v 12C4/THF mixtures. Chemical shifts measured relative to an infinitely dilute solution of  $\text{CsCl}$  in  $\text{D}_2\text{O}$ .

12C4 and 15C5 in THF. Solutions that contain low crown-ether content (<5% v/v) (Fig. 11) yield spectra that consist of either two or three signals. The chemical-shift data presented in Table 1 show that the signals at chemical-shifts of  $-278$ ,  $-280$  and  $-300$  ppm for the 12C4 and 15C5 solutions, (a), (b) and (c) respectively, can be assigned to the caesium anion  $\text{Cs}^-$ . For the caesium-THF solution containing 5% 12C4 (Fig. 11(a)) there are two signals, having chemical shifts of  $+1.9$  ppm and  $+65.9$  ppm, which have been assigned to cation-based species. The signal at  $+1.9$  ppm was assigned to the species  $\text{Cs}^+(\text{12C4})_2$  consisting of a  $\text{Cs}^+$  ion complexed by two 12C4 molecules. The assignment was unambiguous because signals having very similar chemical shifts ( $\delta = -4$  ppm) and linewidths of approximately 50 Hz are observed (Table 1) from solutions of caesium halides ( $\text{CsX}$ ;  $\text{X} = \text{Cl}, \text{Br}, \text{I}$ ) in neat liquid 12C4. There are two compelling reasons for assigning the broader signal located at  $+65.9$  ppm to the paramagnetic complex  $\text{Cs}^+(\text{12C4})_2\text{e}^-$ . First, the NMR signal from the solid electride  $\text{Cs}^+(\text{12C4})_2\text{e}^-$ , whose crystal structure has been characterized, occurs at almost the identical chemical shift.<sup>76</sup> Secondly, the shift difference between the  $\text{Cs}^+(\text{12C4})_2$  and  $\text{Cs}^+(\text{12C4})_2\text{e}^-$  signals is a Knight shift  $\mathcal{K}$ , which originates from the Fermi contact interaction with the unpaired electron. The shift difference is given by<sup>57</sup>

$$\mathcal{K} = -\frac{g_e}{g_n} \frac{\beta_e}{\beta_n} \frac{A}{4kT}, \quad (37)$$

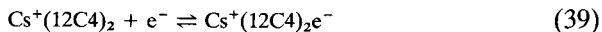
where  $A$  is the metal hyperfine coupling constant,  $g_e$  and  $g_n$  are the electronic and nuclear  $g$  factors while  $\beta_e$  and  $\beta_n$  are the Bohr and nuclear magnetons. Using this equation, it has been predicted from the observed Knight shift of 64 ppm that  $A = 20\,000$  Hz. In the liquid state one expects<sup>61</sup> to observe a single NMR signal from the species  $\text{Cs}^+(\text{12C4})_2\text{e}^-$  if  $T_{1e}^{-1}$ , the inverse of the electron spin-lattice relaxation time, is much greater than  $A$ . If the nuclear relaxation of  $^{133}\text{Cs}$  in  $\text{Cs}^+(\text{12C4})_2\text{e}^-$  is dominated by the modulation of the hyperfine coupling by the electron spin-lattice relaxation then the width of the NMR signal is given by<sup>61</sup>

$$\Delta\nu_{1/2} = \pi A^2 T_{1e}. \quad (38)$$

An experimentally derived value for  $T_{1e}$  of  $3 \times 10^{-8}$  s at 190 K for this solution, when combined with the above  $A$  value of 20 000 Hz, has been used<sup>25</sup> to predict from (38) that the width of the NMR signal from  $\text{Cs}^+(\text{12C4})_2\text{e}^-$  is 38 Hz. The contribution to the observed linewidth arising from other processes, such as quadrupole relaxation, can be expected to be similar to these occurring for the diamagnetic species  $\text{Cs}^+(\text{12C4})_2$ . It has been found experimentally<sup>25</sup> that the NMR linewidth of  $\text{Cs}^+(\text{12C4})_2\text{e}^-$  is some 30 Hz greater than that of the  $\text{Cs}^+(\text{12C4})_2$  signal. The close similarity

between the experimental result and the calculated width has been taken to provide compelling evidence for the assignment.

On raising the temperature, the signals from  $\text{Cs}^+(12\text{C4})_2\text{e}^-$  and  $\text{Cs}^+(12\text{C4})_2$  broaden rapidly and finally coalesce to form a single broad line at 200 K. The averaging of these two NMR signals has been ascribed to the equilibrium.



This is just the process (36). At higher temperatures the signal broadens very rapidly to become unobservable. The failure of the averaged signal to sharpen with increase in temperature has been ascribed to an extremely efficient nuclear spin-relaxation mechanism, whose rate increases very rapidly with temperature.

The dynamical processes responsible for broadening the  $\text{Cs}^+$  based signals can also be enhanced by the addition of further 12C4. Thus the nuclear relaxation processes responsible for the failure to observe cation-based signals in the 5% v/v 12C4 solution at high temperatures are also the cause of the absence of similar signals in the system containing 20% v/v 12C4 (Fig. 11c), even at the lowest temperatures.

The  $^{133}\text{Cs}$  NMR spectra at various temperatures from a solution of Cs metal in 5% v/v mixture of 15C5 and THF are shown in Fig. 12. In the lowest-temperature spectrum the signal at  $\delta = +109$  ppm has been assigned largely, if not entirely, to the species  $\text{Cs}^+(15\text{C5})_2\text{e}^-$ , because this shift is very similar to that measured for the solid electride  $\text{Cs}^+(15\text{C5})_2\text{e}^-$ .<sup>76</sup> If this signal does not arise entirely from this paramagnetic species, but rather represents a time-average of signals from both  $\text{Cs}^+(15\text{C5})_2\text{e}^-$  and  $\text{Cs}^+(15\text{C5})_2$ , then the observed shift suggests that the equilibrium (39) is well over to the right for the heavier inonophore. The spectrum at 193 K shows that the cation signal at  $\delta = 109$  ppm has an integrated area  $x$  ( $x > 5$ ) times greater than that of the  $\text{Cs}^-$  signal at  $\delta = -280$  ppm. Hence the contributions to the widths of these peaks arising from lifetime limitation in the classic two-site exchange process would be in the ratio 1 :  $x$ . Therefore, the major contribution to the width of the cation signal at this temperature cannot arise from direct exchange between the cation-based species and the  $\text{Cs}^-$  ion. On increasing the temperature, the cation signal broadens much more rapidly than the anion signal. If this broadening were to arise from the direct exchange process then the anion signal would have to broaden at a rate  $x$  times greater than the cation signal. This is not observed experimentally. Indeed, at 213 K the anion signal has almost the same width at that at 193 K, while the cation signal has broadened by some 50%. It has been concluded that the broadening of both cation and anion peaks over the entire temperature range does not arise from a classic two-site exchange process.

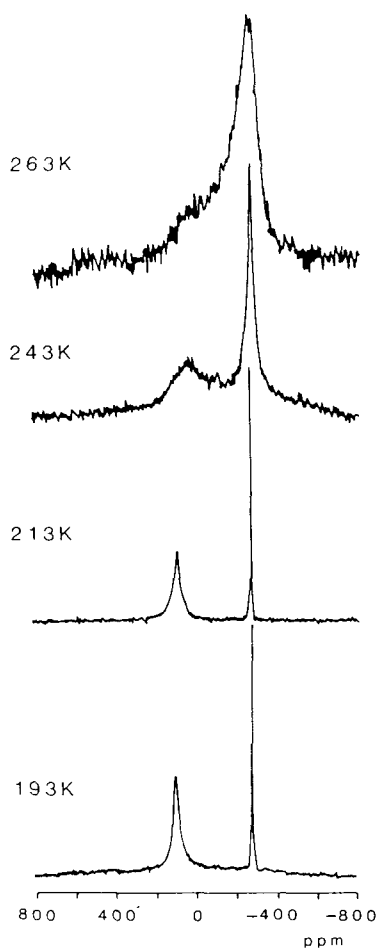


FIG. 12. Variable-temperature  $^{133}\text{Cs}$  NMR spectra of solutions of caesium in a 15C5/tetrahydrofuran mixture (taken from Ref. 25 and used with permission).

Solutions that contain mixed alkali metals  $\text{CsM}$  ( $\text{M} = \text{Na}$ ,  $\text{K}$  and  $\text{Rb}$ ) in crown-ether (L)-THF solvent mixtures show  $^{133}\text{Cs}$  NMR spectra that consist of only a single NMR line due to the complex cation  $\text{Cs}^+\text{L}_2$ . Furthermore,  $^{23}\text{Na}$ ,  $^{39}\text{K}$ ,  $^{85}\text{Rb}$  and  $^{87}\text{Rb}$  NMR studies of the same solutions showed the presence of the  $\text{Na}^-$ ,  $\text{K}^-$  and  $\text{Rb}^-$  ions. This clearly reflects the greater thermodynamic stability, in these solutions, of each species  $(\text{Cs}^+\text{L}_2)\text{M}^-$  compared with  $(\text{M}^+\text{L}_2)\text{Cs}^-$ . The temperature dependences of

the NMR characteristics ( $\sigma$ ,  $\Delta\nu_{1/2}$  and  $T_{1n}$ ) of the  $\text{Cs}^+$  signals in these mixed-metal solutions were consistent with the assignment to  $\text{Cs}^+\text{L}_2$ . Increasing the temperature leads to a substantial increase in the linewidth of the cation signal coupled with a very small low-frequency shift and decrease in the spin-lattice relaxation rates. For example, the  $\text{Cs}^+(\text{12C4})_2$  NMR signal observed from CsNa solutions in 12C4/THF solvent mixture has  $\delta = -22.4$  ppm,  $\Delta\nu = 97$  Hz and  $T_{1n} = 8.4$  ms at 198 K changing to  $\delta = -26.4$  ppm,  $\Delta\nu = 716$  Hz and  $T_{1n} = 35.8$  ms at 243 K. No signal has been detected above 250 K. The decrease in the spin-lattice relaxation rate at higher temperatures is consistent with quadrupole relaxation for the cation-based signal in this system. However, the substantial increase in the linewidth suggests the presence of exchange processes. Clearly, direct exchange between  $\text{Cs}^+$  and, for example,  $\text{Na}^+$  is ruled out in these mixed-metal solutions.

## V. OVERALL CONCLUSIONS

Both pure alkali metals and binary alloys formed from them dissolve in a wide range of non-aqueous solvents. In this work we have reviewed the NMR evidence for the existence of species of stoichiometry  $\text{M}^-$  in solutions prepared using either crown ethers or cryptands, possibly in association with another solvent.

The measurement of the chemical shift of the resonance of the species of stoichiometry  $\text{M}^-$  relative to that of the corresponding gaseous atom yields information on the nature of the species in solution. For all the members of a wide range of systems containing  $\text{Na}^-$  the chemical shifts are found to be identical with the completely reliable value computed for the gaseous sodium anion.

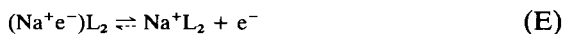
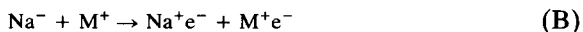
The agreement to within  $\pm 1$  ppm of the measured shielding in solution and the corresponding gaseous phase value provides very strong evidence that the  $\text{Na}^-$  ion in solution interacts only very weakly with its environment. This is especially noticeable when it is remembered that the corresponding cation resonances in a wide range of solutions are deshielded with respect to the gaseous cation by some 62 ppm.

By contrast, the resonances assigned to the species  $\text{K}^-$ ,  $\text{Rb}^-$  and  $\text{Cs}^-$  are deshielded with respect to the corresponding gaseous anions, and the deshielding increases as one passes down the group 1A elements. The very appreciable deshielding of  $\text{Rb}^-$  and  $\text{Cs}^-$  with respect to the gaseous anions is evidence that both these species interact significantly with their environment.

For solutions of sodium metal and sodium/alkali alloys in 12-crown-4, an extensive series of measurements of the  $\text{Na}^-$  nuclear spin-lattice relaxation time as a function of temperature and composition revealed that the inefficient (quadrupole-dominated) nuclear relaxation originated from the fluctuations in the electric field gradients caused by the independent translational and reorientational motions of individual solvent molecules around the anion. In particular, the activation energies for the process governing the  $\text{Na}^-$  spin-lattice relaxation in all the 12-crown-4 solutions studied are identical, to within experimental error, with the activation energy governing both the  $^1\text{H}$  and  $^{13}\text{C}$  nuclear spin relaxation in the pure solvent. It was also deduced that, for solutions in 12-crown-4, each  $\text{Na}^-$  ion does not exist as part of an ion pair and that the sodium anion is not subject to the continuous passage of other ions.

Comparison of the experimental spin-lattice relaxation times for  $\text{Na}^-$  with rates of relaxation for other ions, suitably scaled to take account of differences in nuclear spins, quadrupole moments, Sternheimer antishielding factors and solvent viscosities, provides powerful evidence that  $\text{Na}^-$  in these metal solutions is more decoupled from its environment than any of the other ions considered. This comparison, taken in conjunction with the chemical-shift evidence, shows that  $\text{Na}^-$  exists in these solutions as a state very closely approximating to that of the gaseous species, the anion interacting only minimally with its surroundings.

For all the wide variety of sodium and sodium-alloy solutions in 12-crown-4, the spin-spin relaxation rates are considerably greater than the spin-lattice relaxation rates, and these differences in rates are used to deduce the lifetime of  $\text{Na}^-$  in these solutions as a function of temperature, composition and counteraction. It is deduced from these measurements that the lifetime of  $\text{Na}^-$  is limited by quantum-mechanical tunnelling of one of the 3s valence electrons onto an uncomplexed alkali cation. The non-trivial temperature and counterion dependence of this process suggests that this lifetime limitation arises from the interplay between the first two of a number of equilibria envisaged as occurring in these metal solutions: these equilibria may be summarized as follows:





The third process is simply the regeneration of  $Na^-$ . This, as well as the processes (D)–(F) describing the other reactions undergone by sodium-based species, also occurs during the process of dissolving pure sodium metal in a crown solvent. Finally, the last two reactions (G) and (H) describe the fate of the species  $M^+e^-$ , having approximately 1% atomic character.

Although there is ESR evidence for both the atomic and the cation-based species postulated in the above equilibria, no NMR signals from such species have been detected from solutions in the neat 12-crown-4 solvent. However, NMR experiments on caesium metal dissolved in mixtures of 12-crown-4 and 15-crown-5 in tetrahydrofuran reveal the presence of both  $Cs^+L_2e^-$  as well as  $Cs^+L_2$  in these metal solutions.

In this review we hope to have illustrated the power of magnetic resonance techniques, both NMR and ESR, in gleanng information about the structure and dynamics of these intriguing alkali anions in solution.

## ACKNOWLEDGMENT

We thank SERC for financial support.

## REFERENCES

1. N. N. Greenwood and A. Earnshaw, *Chemistry of the Elements*, Pergamon Press, Oxford, 1984.
2. J. L. Dye, *Prog. Inorg. Chem.*, 1984, **32**, 327.
3. P. P. Edwards *Adv. Inorg. Chem. Radiochem.*, 1982, **25**, 135.
4. J. C. Thompson, *Electrons in Liquid Ammonia*, Clarendon Press, Oxford, 1976.
5. R. Catterall, in *Metal Ammonia Solutions* (J. J. Lagowski and M. J. Sienko eds), p. 105, Butterworth, London, 1970.
6. N. W. Taylor and G. N. Lewis, *Proc. Natl Acad. Sci. USA*, 1925, **11**, 456.
7. J. L. Dye, in *Metal Ammonia Solutions* (J. J. Lagowski and M. S. Sienko eds), p. 1, Butterworth, London, 1970.
8. J. L. Dye, in *Electrons in Fluids* (J. J. Jortner and N. R. Kestner, eds), p. 77, Springer-Verlag, Berlin, 1972.
9. J. L. Dye, *Angew. Chem. Int. Ed. Engl.*, 1979, **18**, 587.
10. R. R. Dewald and J. L. Dye, *J. Phys. Chem.*, 1964, **68**, 121.
11. R. N. Edmonds, D. M. Holton and P. P. Edwards, *J. Chem. Soc. Dalton Trans.*, 1986, 323.
12. S. Matalon, S. Golden and M. Ottolenghi, *J. Phys. Chem.*, 1969, **73**, 3098.
13. T. A. Patterson, H. Hotop, A. Kashdan, D. W. Norcross and W. C. Lineberger, *Phys. Rev. Lett.*, 1974, **32**, 189.

14. J. L. Dye, M. T. Lock, F. J. Tehan, R. B. Coolen, N. Papadakis, J. M. Ceraso and M. G. De Backer, *Ber. Bungen Gesell. Physik. Chem.*, 1971, **75**, 659.
15. J. L. Dye, J. M. Ceraso, M. T. Cok, B. L. Barnett and F. J. Tehan, *J. Am. Chem. Soc.*, 1974, **96**, 608.
16. F. J. Tehan, B. L. Barnett and J. L. Dye, *J. Am. Chem. Soc.*, 1974, **96**, 7203.
17. J. L. Dye, C. W. Andrews and S. E. Mathews *J. Phys. Chem.*, 1975, **79**, 3065.
18. J. M. Ceraso and J. L. Dye, *J. Phys. Chem.*, 1974, **61**, 1585.
19. A. S. Ellaboudy, M. O. Tinkham, B. Vaneck, J. L. Dye and P. B. Smith, *J. Phys. Chem.*, 1984, **88**, 3852.
20. M. L. Tinkham and J. L. Dye, *J. Am. Chem. Soc.*, 1985, **107**, 6129.
21. P. P. Edwards, A. S. Ellaboudy and D. M. Holton, *Nature*, 1985, **317**, 242.
22. J. L. Dye, C. W. Andrews and J. M. Ceraso, *J. Phys. Chem.*, 1975, **79**, 3076.
23. D. M. Holton, P. P. Edwards, D. C. Johnson, C. J. Page, W. McFarlane and B. Wood, *J. Chem. Soc.*, 1984, 740.
24. M. L. Tinkham, A. S. Ellaboudy, J. L. Dye and P. B. Smith, *J. Phys. Chem.*, 1986, **90**, 14.
25. A. S. Ellaboudy, N. C. Pyper and P. P. Edwards, 1987, *J. Am. Chem. Soc.*, 1987, in press.
26. D. M. Holton, A. Ellaboudy, N. C. Pyper and P. P. Edwards, *J. Chem. Phys.*, 1986, **84**, 1089.
27. A. S. Ellaboudy, D. M. Holton, R. N. Edmonds and P. P. Edwards, *J. Chem. Soc. Chem. Commun.*, 1986, 1444.
28. A. S. Ellaboudy, D. M. Holton, N. C. Pyper and P. P. Edwards, *J. Phys. Chem.*, 1987, submitted.
29. C. J. Pederson, *J. Am. Chem. Soc.*, 1967, **89**, 7017.
30. P. P. Edwards, S. C. Guy, D. M. Holton and W. McFarlane, *J. Chem. Soc. Chem. Commun.*, 1981, 1185.
31. P. P. Edwards, S. C. Guy, D. M. Holton, D. C. Johnson, W. McFarlane and B. Wood, *J. Phys. Chem.*, 1983, **87**, 4362.
32. D. M. Holton, P. P. Edwards, D. C. Johnson, C. J. Page, W. McFarlane and B. J. Wood, *J. Am. Chem. Soc.*, 1987, **107**, 6499.
33. W. Hotop and W. C. Lineberger, *J. Phys. Chem. Ref. Data*, 1975, **4**, 539, and refs. therein.
34. N. C. Pyper and P. P. Edwards, *J. Am. Chem. Soc.*, 1986, **108**, 78.
35. C. W. White, W. M. Hughes, G. S. Hayne and H. G. Robinson, *Phys. Rev.*, 1968, **174**, 23.
36. G. S. Hayne, C. W. White, W. M. Hughes and H. G. Robinson, *Bull. Am. Phys. Soc.*, 1968, **13**, 20.
37. A. Beckmann, K. D. Bolken and D. Elke *Z. Phys.*, 1974, **270**, 173.
38. O. Lutz, *Phys. Lett.*, 1967, **25A**, 440.
39. O. Lutz, *Z. Naturforsch. Tech.*, 1968, **23a**, 1202.
40. O. Lutz and A. Schweuk, *Phys. Lett.*, 1967, **24A**, 122.
41. C. Deverell and R. E. Richards, *Mol. Phys.*, 1966, **10**, 551.
42. N. F. Ramsey, *Phys. Rev.*, 1950, **78**, 699.
43. N. C. Pyper, *J. Phys.*, 1985, **B18**, 1317.
44. E. A. Hylleraas and S. Skavlem, *Phys. Rev.*, 1950, **79**, 117.
45. C. Froese-Fischen, *The Hartree-Fock Method for Atoms*, Wiley, New York, 1977.
46. I. P. Grant, B. J. McKenzie, P. H. Nomington, D. F. Mayers and N. C. Pyper, *Comp. Phys. Commun.*, 1980, **21**, 207.
47. A. Mazziotti, *Chem. Phys. Lett.*, 1970, **5**, 343.
48. A. Mehrotra and K. M. S. Saxena, *Can. J. Phys.*, 1976, **53**, 97.
49. G. L. Malli and S. Fraga, *Theoret. Chim. Acta*, 1966, **5**, 275.

50. S. J. Davis, J. J. Wright and L. C. Balling, *Phys. Rev.*, 1974, **A9**, 1494.
51. E. I. Obiajunwa, S. A. Adebisi, E. A. Togun and A. F. Oluwale, *J. Phys.*, 1983, **B16**, 2733.
52. A. F. Oluwale, *Physica Scripta*, 1977, **15**, 339.
53. R. N. Edmonds, S. C. Guy, P. P. Edwards and D. C. Johnson, *J. Phys. Chem.*, 1984, **88**, 3764.
54. J. A. Pople, W. G. Schneider, and H. J. Bernstein, *High Resolution Nuclear Magnetic Resonance*, McGraw Hill, New York, 1959.
55. R. K. Harris and B. E. Mann, *NMR and the Periodic Table*, Academic Press, London, 1978.
56. Landolt-Bornstein, 1973, Series 3, Vol. 7, Part b.
57. A. Carrington and A. D. McLachan, *The Principles of Magnetic Resonance*, 1967.
58. F. W. Wehroli, *J. Magn. Reson.*, 1976, **23**, 527.
59. H. G. Hertz, *Ber. Bunsenges. Phys. Chem.*, 1973, **77**, 531.
60. C. A. Melendres and H. G. Hertz, *J. Chem. Phys.*, 1974, **61**, 4156.
61. A. Abragam, *The Principles of Nuclear Magnetism*, Oxford University Press, 1961.
62. A. S. Ellaboudy and J. L. Dye, *J. Magn. Reson.*, 1986, **66**, 491.
63. A. S. Ellaboudy, D. M. Holton, N. C. Pyper, P. P. Edwards, B. Wood and W. McFarlane, *Nature*, 1986, **321**, 684.
64. R. M. Steinheimer, *Phys. Rev.*, 1966, **146**, 140.
65. J. H. Loehlin and A. Kwick, *Acta Crystallogr.*, 1978, **B34**, 3488.
66. M. Yukasaka, J. Sugawara, H. Iwamura and J. Fujiyama, *Bull. Chem. Soc. Jpn.*, 1981, **54**, 1933.
67. R. C. Phillips, S. Khazasli and J. L. Dye, *J. Phys. Chem.*, 1985, **89**, 600.
68. R. D. Dreisback, *Physical Properties of Chemical Compounds—III*, p. 289, Advances in Chemistry Series No. 29, American Chemical Society, Washington, D.C., 1961.
69. R. C. Phillips, S. Khazaeli and J. L. Dye, *J. Phys. Chem.*, 1985, **89**, 606.
70. J. P. Van Remoortere, and J. P. Bres, *Inorg. Chem.*, 1974, **13**, 2071.
71. *The Aldrich Library of NMR Spectra* 1983, 2nd Edn. (C. J. Puche, ed.), Vol. I, p. 211.
72. J. W. Fletcher and W. A. Seddon, *J. Phys. Chem.*, 1975, **79**, 3055.
73. D. M. Holton, A. S. Ellaboudy, R. N. Edmonds and P. P. Edwards, *Proc. R. Soc. Lond.*, 1987, in press.
74. Z. Jedlinski, A. Stolarzewicz, Z. Grobelny and M. Szwarc, *J. Phys. Chem.*, 1984, **88**, 6094.
75. R. Catterall and P. P. Edwards, *J. Phys. Chem.*, 1975, **79**, 3010.
76. A. S. Ellaboudy and J. L. Dye, Private communication, 1987.

# Index

- Acer pseudoplatanus*, 38  
<sup>27</sup>Al NMR, 65, 66, 168–169  
 Alkali anions ( $M^-$ ) in non-aqueous solvents  
   chemical dynamics  
     caesium-based species, 357–362  
     sodium anion, 348–357  
   nuclear shielding, 318–332  
     assignment of the resonance, 318–326  
     deduction of nature of  $M^-$  in solution, 331–332  
     gaseous alkali ions, 327–331  
     gaseous neutral atoms, 326–327  
     summary, 332  
   solution structure of  $Na^-$ , 332–348  
     experimental results, 332–334  
     quadrupolar relaxation, 338–346  
     theoretical considerations, 334–338  
     summary, 346–348  
 Alkali cations, complexed/  
   uncomplexed, 352  
 Alkali metals, optical absorption spectra, 316–317  
 Ammonium nitrate solutions, proton exchange, 42  
 ATP consumption, assessment, 50  
 ATP synthesis, 34–37  
   and  $P_i$  consumption, 51  
   in yeast, 51  
 ATP-ase, inhibition by DCCD, 36–37
- BAPTA, 22–26  
   and 5FBAPTA, 27, 33  
 Beads, microcarrier, 5  
<sup>9</sup>Be NMR, 168  
 Block equations, 44  
 Boltzmann equilibrium, 44  
<sup>10</sup>Boron  
   boranes, 168–169  
   NMR, 168–169  
   nuclear referencing, 66
- <sup>11</sup>Boron  
   alkenylborane-metal complexes, 150–151  
   alkylboranes, 225–229  
   alkylborohydride, 231  
   (amine)<sub>2</sub>  $BF_2^+$  cations, 211  
   amino-acid analogues, 209  
   aminoboron cations, 70  
   amino-diorganylboranes, 87–90  
   amino(methylene)borane, 73  
   analogues, pharmacologically-active compounds, 209  
   bis(amido)boron, nuclear shielding, 73  
   bis(chloroboryl)alkanes, 228  
   1-bora-adamantanes and nonanes, 220  
   borabenzene-metal complexes, 152–153  
   boranes  
     <sup>10</sup>B, <sup>27</sup>Al and <sup>71</sup>Ga, 168–169  
     bridging ligands, 71  
     <sup>13</sup>C, 169–173  
     <sup>19</sup>F, <sup>35</sup>Cl and <sup>37</sup>Cl, 180  
     <sup>6</sup>Li and <sup>7</sup>Li, 168  
     <sup>14</sup>N and <sup>15</sup>N, 175–177  
     <sup>17</sup>O and <sup>77</sup>Se, 178–179  
     <sup>31</sup>P, 178  
     <sup>29</sup>Si, <sup>119</sup>Sn and <sup>207</sup>Pb, 174–175  
     shifts in heteroatom boranes, 233  
     transition metal, 181  
   borates, 149  
     with boron-element bonds, 145–147  
   borirane-2-ylideneborane, 73  
   borole-metal complexes, 154–156  
   boron-containing heterocycles, 219–225  
   boron-element complexes, 158  
   boronium salts, chemical shifts, 210  
   borylidene-boriranes, 71  
   carbaboranes  
     classical/non-classical bonding, 70  
   cationic boron compounds, 209–211  
   tetra co-ordinate, 141

- <sup>11</sup>Boron (*cont.*)  
  chelate complexes, 139–140  
  compounds, frequently encountered nuclei (table), 66  
  coupled boranes and carboranes, 294–298  
  diborabenzene-metal complexes, 153–154  
  diboranes, 114–117, 125–127  
    compounds, 227  
    diboranes (6) and  $\mu$ -diboranes, 127, 148  
  1,3-diborole-, 1,2,5-thiadiborole and 1,2-azaborole-metal complexes, 156–158  
  1,3-dihydro-1,3-diborettes, 71  
  dimeric and trimeric boranes, 137–138  
  diorganylboron compounds, 119–122  
    -halides, 83–84  
    -hydrides, 82  
    -oxygen, 84–85  
    -selenium, 86  
    sulphur, 86  
  halides, and amine complexes, 230–231  
  halogeno-organylboranes, 90–91  
  iminoboranes, 69, 72  
    adducts, shifts, 214  
  Lewis-base-borane adducts, 128–136, 148–149  
  metal borates, 147–148, 149  
  metalloboranes, metallocarboranes  
    B<sub>1</sub>, 254–259  
    B<sub>2,3,4</sub>, 259–263  
    B<sub>5,7,8</sub>, 263–274  
    B<sub>9</sub>, 275–285  
    B<sub>10</sub> and larger, 285–298  
  metalloboranes  
    NMR data, 281–282  
  metallocarboranes  
    <sup>1</sup>H and <sup>11</sup>B correlations, 277–278  
    NMR data, 281  
    structures, 274, 275, 280, 281  
  monoorganyl boranes, 122–125  
  multiple bonds to boron, 212–217  
  NMR, 63–65  
    analytical applications, 208  
    chemical shifts, 68–71  
    classical/non-classical, 71  
    indirect nuclear spin-spin couplings, 160–168  
    linewidths, 67  
    magnitude of substituent effects, 71–160  
    and <sup>14</sup>N, iminoboranes, 72  
    referencing, 63–64  
    studies of solids, 302–305  
    two-dimensional NMR spectroscopy, 206–208, 288  
  one-boron compounds, 209–232  
    alkylboranes, 225–229  
    analogues of pharmacologically active compounds, 209  
    boron-containing heterocycles, 219–225  
    cationic boron compounds, 209–211  
    compounds with multiple bonds, 212–217  
    pyrazaboles, 217–219  
    other one-boron compounds, 229–232  
  organofluorohydroxyborane, 231  
  organylborane adducts, 227  
  organylborates and zwitterionic adducts, 142–144  
  organylboron-oxygen compounds, 92–93  
  organyl-selenium compounds, 94  
  organyl-sulphur compounds, 94  
  organylboron  $\pi$  complexes, 149–160  
  organylboron-nitrogen compounds  
    cyclic, 96–101  
    non-cyclic, 95–96  
  phosphorylaminoboranes, 231  
  polyboranes and carboranes  
    B<sub>2,3</sub>, 233–235  
    B<sub>4</sub>, 235–237  
    B<sub>5</sub>, 237–240  
    B<sub>6,8,9</sub>, 240–251  
    B<sub>10,11,12</sub>, 251–254  
  pyrazaboles, 217–219  
  silicon-containing substituents, 231  
  silylboranes, 74  
  small-ring boron compounds, 212–217  
  stannacarboranes, 237  
  tetracoordinate boron, 127, 148–149, 159–160  
  three-coordinate boron, 74, 118–127  
    boranes, diboranes, 125–127  
    monorganylboranes, 122–125  
    diorganylboranes, 119–112

- <sup>11</sup>Boron (*cont.*)  
    triorganylboranes, 74, 118  
    transition-metal complexes, boron-containing heterocycles, 299–302  
    trigonal boranes without B—C bonds, 102–114, 125  
    BX<sub>3</sub>, 102–104  
    BX<sub>2</sub>Y, BXY<sub>2</sub>, BXYZ, 105–112  
    triorganylboranes, 75–82, 227  
    two-coordinate, 72–74  
Brain tissue  
    damage, in neonates, 41  
    superfusion, 43–46
- <sup>13</sup>C NMR, 64–65, 169–173  
    boranes  
        alkenyl-, 172  
        alkynyl-, 172  
        organo-, 170–172  
        phenyl-, 172  
    <sup>1</sup>H-decoupled, 173  
    titratable resonances, 32  
Calcium indicators, 22–26  
Carnosine, as pH indicator, 32–33  
*Catharanthus roseus*, 38  
Cations, intracellular, determination, 21–22  
Cells, sample preparation, 3–7  
*Chlorella fusca*, compartmentation, pH, 39  
<sup>35</sup>Cl, <sup>37</sup>Cl NMR, 180  
    nuclear referencing, 66  
<sup>59</sup>Co, nuclear referencing, 66  
COSY  
    correlations, 234–235  
    2D COSY decoupling, 243, 248  
Creatine kinase, magnetization-transfer methods, 49–50  
Creatine phosphotransferase  
    determination, 43–46  
Crown-ethers, 316–318  
<sup>133</sup>Cs NMR, 357–362  
    M<sup>+</sup>/M<sup>-</sup>, 319, 321–324  
    nuclear shielding, 326, 330
- D<sub>2</sub>O, as solvent, 41–42  
DANTE pulse sequence, 46–47  
Debye equation, 337, 348
- Depth-resolved surface-coil spectroscopy (DRESS), 17  
*Dictostelium discoideum*, 38  
Dicyclohexylcarbodiimide (DCCD)  
    sensitivity of ATP, 36, 42  
Difluoromethylalanine, 32–33
- Enzyme kinetics  
    inversion-transfer experiments, 46–47  
    magnetization-transfer methods, 42, 49–51  
    saturation-transfer methods, 42, 43–46  
    two-dimensional exchange experiments, 47–48  
Erich ascites tumour cells, 23, 24  
Erythrocytes, NAD concentrations, 41–42  
*Escherichia coli*  
    phosphorylations, 32  
    Pi consumption, 42  
EXORCYCLE scheme, 16
- <sup>19</sup>F  
    NMR, 22, 32–33, 66, 180  
    pH indicator, 32–33  
    spin-½ nuclei, 65  
*Fasciola hepatica*, 7  
FCCP, uncoupling effect, 37  
Field focusing nuclear magnetic resonance (FONAR), 14  
Fourier imaging methods, 19–21
- <sup>71</sup>Ga NMR, 168, 169
- <sup>1</sup>H NMR, 3  
    nuclear referencing, 66  
    spin-echo, 41  
Halogens  
    nuclear quadrupole moments, 339  
    Sternheimer antishielding factors, 339, 341  
    spin-lattice relaxation rates, 340  
Hartree-Fock wave-functions, 327–330

- Heart  
 anoxia and acidosis, 41  
 creatine kinase rate constants, 50  
 perfusion techniques, 9–12  
 resting  $\text{Ca}^{2+}$  levels, 25  
 saturation-transfer methods, 49  
*see also* Organs
- Hellmann–Feynman theorem, 328
- Heptamethylbenzenonium, 48
- Image selective *in vivo* spectroscopy (ISIS), 19
- INDO calculations, 70
- INEPT pulse sequence, 65
- Inversion-transfer experiments, 42, 46–47
- $^{39}\text{K}$  in living systems, 28–30
- $^{39}\text{K}$  NMR, 28  
 $\text{M}^+/\text{M}^-$ , 319, 321–324  
 nuclear shielding, 326, 330
- Kidney, perfusion techniques, 10–11  
*see also* Organs
- Lactate dehydrogenase (LDH),  
 reaction, 41–42
- $^7\text{Li}$  NMR, 168  
 nuclear referencing, 66  
 nuclear shielding, 330
- Liver, perfusion techniques, 10–11  
*see also* Organs
- Living systems  
 enzyme kinetics, 41–51  
 localization methods, 13–21  
 measurement of intracellular cations, 21–41  
 sample preparation, 3–12
- Localized spectroscopy, 14–19  
 surface coils, 14–16  
 topical magnetic resistance, 16–17  
 volume-selective excitation, 17–19
- Lolium multiflorum*, 38
- McArdle's syndrome, 40
- Magnetic-resonance imaging (MRI)  
 clinical uses, 39–41  
 development, 2
- Magnetization-transfer methods, 42, 49–51  
 mitochondrial/myofibril compartmentation, 49
- Metal ion measurement, living systems, 21–41
- $^{25}\text{Mg}$  NMR, 26  
 indicators, 26–28
- Microcarrier beads, 5
- Mitchell hypothesis, 33, 34
- Muscle  
 anaerobic exercise, 40  
 phosphorylase kinase deficiency, 41  
 sample preparation, 7–12  
*see also* Organs
- $^{14}\text{N}$  NMR, 65, 175–177  
 iminoboranes, 72  
 nuclear referencing, 66
- $^{15}\text{N}$  NMR, 175–177
- $^{23}\text{Na}$  NMR, 28–30  
 $\text{M}^+/\text{M}^-$ , 319, 321–324  
 nuclear shielding, 326, 330
- $\text{Na}^-/\text{Na}^+$ , NMR line widths, 345
- $\text{Na}^-$   
 chemical dynamics, 348–357  
 quadrupolar relaxation, 338–348  
 solution structure, 332–348  
 spin-lattice relaxation times, 333  
 spin-lattice/spin-spin relaxation times, 348–351  
 structure in solution (diagram), 347
- NAD-dependent conversions, 41
- Narrowband localization of excitation (NOBLE), 16
- Neonatal brain damage, 41
- Nicotiana tabacum*, 38
- Nuclear magnetic resonance (NMR)  
 metal-ammonia solutions, 315–317  
 nuclear properties, etc. (table), 66  
 transition metal nuclei, 181  
 variable-angle sample-spinning (VASS), 304  
*see also* specific elements
- Nuclear-spin relaxation, 65–68
- $^{17}\text{O}$ , NMR, 65, 178–179  
 nuclear referencing, 66

- Organs, and intact animals  
  localization methods, 13–21  
  non-perfusion techniques, 7–8  
  perfusion techniques, 9–12  
  sample preparation, 7–12  
  spectroscopic imaging, 19–21  
    intracellular cations, measurement, 21–41
- $^{31}\text{P}/^{15}\text{N}$  double resonance spin-echo, 42
- $^{31}\text{P}$  NMR, 30–32, 40, 178  
  clinical spectroscopy, 40  
  nuclear referencing, 66  
  physiological measurement, 77  
  spin- $\frac{1}{2}$  nuclei, 65
- $^{207}\text{Pb}$  NMR, 66, 175
- pH  
  artificial probes, 32  
  gradient, light-induced, in bacteria, 36–37  
  homeostasis and compartmentation, 37–39  
  intra-cellular measurements, 30–33  
  measurement in tissues, 39–41
- Phosphate, inorganic ( $P_i$ ), 30–32  
   $\gamma$ -ATP exchange, 51  
  consumption, unidirectional rate, 42, 49–51  
  in mitochondrial matrix, 38  
  vacuolar resonance, 38–39
- Phosphocreatine resonance, 45, 47  
  ‘shuttle’ hypothesis, 49–50
- Phosphorylase-a deficiency, 40
- $P_i$ , *see* Phosphate, inorganic
- Proton pumps, 33–37
- $^{195}\text{Pt}$  NMR, 66, 181  
  metalloboranes, 292, 295
- Ramsey theory  
  nuclear shielding, 327–328  
  terminology, 5, 68
- $^{87}\text{Rb}$  NMR  
   $M^+/M^-$ , 319, 321–324  
  nuclear shielding, 326, 330
- $^{103}\text{Rh}$  nuclear referencing, 66
- Rhodopseudomonas sphaeroides*, 36, 37
- Saturation-transfer methods, 42, 43–46  
  creatine kinase studies, 49–50  
  multiple saturation-transfer, 50–51
- $^{77}\text{Se}$  NMR, 66, 179
- ‘Shuttle’ hypothesis, 49
- $^{29}\text{Si}$  NMR, 174
- $^{119}\text{Sn}$  NMR, 174, 175
- Sodium NMR, in living systems, 28–30  
  *see also*  $\text{Na}^+$ ;  $\text{Na}^-$
- Spin polarization-transfer techniques, 65
- Sternheimer antishielding factors, 339, 341
- Stokes equation, 337
- Surface coils, 14–16
- $^{125}\text{Te}$ , nuclear referencing, 66
- Tissue superfusion apparatus, 4
- Topical magnetic resonance (TMR), 16–17
- Transition metals, NMR, 181
- Transplant organs, 7
- Two-dimensional exchange experiments, 47–48
- Volume-selective excitation, 17–19
- Zinc indicators, 22–25

This Page Intentionally Left Blank

## **Cumulative index of topics covered in Volumes 11–20 of this series**

Alkali anions in non-aqueous solvents, NMR studies of, **20**, 315  
Alkaloids, NMR of, **13**, 60  
Amino acids, NMR of, **11A**, 2, **16**, 2  
Boron compounds containing two-, three-, and four-coordinate boron, NMR spectroscopy of, **20**, 61  
Boron-11 NMR spectroscopy, **12**, 177, **20**, 205  
Calcium, NMR in chemistry of biology, **11A**, 183  
Carbon–carbon coupling constants: discussion, **11A**, 66  
data, **11A**, 99  
Carbon-13 NMR spectroscopy of Group VIII metal complexes, **11A**, 227  
Cyclophosphazenes, NMR of, **19**, 175  
Dynamic NMR spectroscopy in inorganic and organometallic chemistry, **12**, 263, **19**, 79  
Fluorine-19 NMR spectroscopy (1979–1981), **14**, 3  
Gases, high-resolution NMR of, **19**, 35  
Group VIII metal complexes, carbon-13 NMR of, **11A**, 227  
Haem proteins, paramagnetic, NMR spectroscopy of, **17**, 79  
High-resolution NMR, of liquids and gases: effects of magnetic-field-induced molecular alignment, **19**, 35  
of solids, **12**, 1  
Isomerization processes involving N–X bonds, **16**, 187  
Isotope effects on nuclear shielding, **15**, 106  
theoretical aspects of, **17**, 1  
Liquids, high-resolution NMR of, **19**, 35  
Living systems, NMR spectroscopy of, **20**, 1  
Macromolecules in solution, nuclear magnetic relaxation and models for backbones, motions of, **17**, 179  
Magnesium NMR in chemistry and biology, **11A**, 183  
Monosaccharides, NMR spectroscopy in the study of, **13**, 2  
Multiple resonance, **16**, 293  
Nitrogen NMR spectroscopy, **11B**, 2, **18**, 3  
Non-aqueous solvents, NMR studies of alkali anions in, **20**, 315  
Nuclear magnetic relaxation, and models for backbone motions of macromolecules in solutions, **17**, 179  
rotational correlation times in, **13**, 320  
Nuclear shielding, isotope effects on, **15**, 106  
substituent effects on, **15**, 2  
theoretical aspects of isotope effects on, **17**, 1  
Nuclear spin-spin couplings, calculations of, **12**, 82  
N–X bonds, isomerization processes involving, **16**, 187  
Oligosaccharides, NMR spectroscopy in the study of, **13**, 2  
Organic compounds adsorbed on porous solids, NMR of, **15**, 291  
Paramagnetic haem proteins, NMR spectroscopy of, **17**, 79  
Peptides, NMR of, **11A**, 2, **16**, 2

- Platinum NMR spectroscopy, **17**, 285
- Porous solids, NMR of organic compounds adsorbed on, **15**, 291
- Proteins, NMR of, **11A**, 2, **16**, 2
- Quadrupolar nuclei, less common, NMR of, **17**, 231
- Rotational correlation times in nuclear magnetic relaxation, **13**, 320
- Silicon-29 NMR spectroscopy, recent advances in, **15**, 235
- Solids, high-resolution NMR of, **12**, 1
- Sulphur-33 NMR spectroscopy of, **19**, 1
- Thallium NMR spectroscopy, **13**, 211
- Tin-119 NMR parameters, **16**, 73

## **Cumulative index of authors who have contributed to Volumes 11–20**

- Bastiaan, E. W., **19**, 35  
Bock, K., **13**, 2  
Boéré, R. T., **13**, 320  
Bothner-By, A. A., **19**, 35  
Briggs, R. W., **13**, 211
- Crabb, T. A., **13**, 60  
Craik, D. J., **15**, 2
- Deiningner, D., **15**, 291  
Drakenberg, T., **17**, 231
- Edwards, P. P., **20**, 315  
Ellaboudy, A., **20**, 315
- Forsén, S., **11A**, 183  
Fyfe, C. A., **12**, 1
- Hansen, P. E., **11A**, 66, 99, **15**, 106  
Heatley, F., **17**, 179  
Hinton, J. F., **13**, 211, **19**, 1  
Holton, D. M., **20**, 315
- Jameson, C. J., **17**, 1
- Kidd, R. G., **13**, 320  
Kowalewski, J., **12**, 82  
Krishnamurthy, S. S., **19**, 175
- Lindman, B., **11A**, 183
- Mann, B. E., **12**, 263  
Martin, G. J., **16**, 187
- Martin, M. L., **16**, 187  
McFarlane, W., **16**, 293  
McLean, C., **19**, 35  
Meiler, W., **15**, 291  
Metz, K. R., **13**, 211  
Morris, P. G., **20**, 1
- Orrell, K. G., **19**, 79  
Osten, H. J., **17**, 1
- Pfeifer, H., **15**, 291  
Pregosin, P. S., **11A**, 227, **17**, 285  
Pyper, N. C., **20**, 315
- Rattle, H. W. E., **11A**, 2, **16**, 2  
Rycroft, D. S., **16**, 293
- Satterlee, J. D., **17**, 79  
Siedle, A. R., **12**, 177, **20**, 205  
Sik, V., **19**, 79  
Stefaniak, L., **11B**, 2, **18**, 3  
Sun, X. Y., **16**, 187
- Thøgersen, H., **13**, 2
- van Zijl, P. C. M., **19**, 35
- Wasylishen, R. E., **12**, 1  
Webb, G. A., **11B**, 2, **18**, 3  
Williams, E. A., **15**, 235  
Witanowski, M., **11B**, 2, **18**, 3  
Woods, M., **19**, 175  
Wrackmeyer, B., **16**, 73, **20**, 61  
Wray, V., **11A**, 99, **14**, 3

This Page Intentionally Left Blank